

# **Instrumentation, Monitoring, and Testing at the CUY-90-15.24 Central Viaduct Project**

**By**

**Robert Y. Liang  
Department of Civil Engineering  
The University of Akron  
Akron, Ohio 44325-3905**

**Submitted to**

**The Ohio Department of Transportation  
and  
The U.S. Department of Transportation, Federal Highway Administration**



**Department of Civil Engineering  
The University of Akron  
Akron, OH 44325 - 3905**

**June 2000**

14685



1. Report No. FHWA/OH-2000/009	2. Government Accession No.	3. Recipient's Catalog No.	
4. Title and Subtitle INSTRUMENTATION, MONITORING, AND TESTING AT THE CUY-90-15.24 CENTRAL VIADUCT PROJECT		5. Report Date June, 2000	
		6. Performing Organization Code	
7. Author(s) Robert Y. Liang		8. Performing Organization Report No.	
9. Performing Organization Name and Address The University of Akron Department of Civil Engineering Akron, OH 44325		10. Work Unit No. (TRIS)	
		11. Contract or Grant No. State Job No. 14685(0)	
12. Sponsoring Agency Name and Address Ohio Department of Transportation 1600 West Broad Street Columbus, OH 43223		13. Type of Report and Period Covered Final Report	
		14. Sponsoring Agency Code	
15. Supplementary Notes Prepared in cooperation with the U.S. Department of Transportation, Federal Highway Administration			
16. Abstract A research project has been carried out to ensure construction safety and verification of design assumptions, and to gain insights on the foundation structure behavior of Bridge CUY-90-15.24, the Central Viaduct, also known as the Inner Belt Bridge, which is part of the Interstate Highway System in Cleveland, Ohio. The objectives include: (i) providing real-time measurements to allow project engineers to make sensible but critical decisions, (ii) long-term monitoring as part of bridge maintenance program to assess maintenance needs, (iii) re-assess design assumptions so that new knowledge can be gained and applied for future projects, (iv) Advance the knowledge on soil structure interactions and slope stabilization techniques, (v) form valuable database for current FHWA development of LRFD (Load Resistance Factor Design) for substructures, (vi) Perform FEM (Finite element Method) Simulation (Verified with Field Measurements) to provide further details of substructure behavior. During the course of the project, the following tasks have been successfully accomplished. (a) A series of analyses were performed for the existing slope condition to assess the strength parameters of the soil, in particular, the strength parameters of the slip surfaces. (b) As part of the planning process, the instrumentation plan of various types of sensors was developed and incorporated in the final design plan. (c) Real-time monitoring of all sensors has been successfully carried out. (f) As part of the study, a FEM program PLAXIS was employed to perform a numerical simulation. The FEM simulation process involved the calibration of soil properties to match the initial inclinometer reading from B-103 during initial site excavation. (g) After the installation of the drilled shafts, a lateral load test on drilled shafts # 1 and # 3 was successfully conducted. (h) Instrumented anchors # 1, # 8, and # 17 were performance tested. Instrumented anchor # 9 was creep tested. (i) The measured data, together with detailed FEM simulation results, have provided a powerful and insightful picture of the behavior of the slope and the foundation structures.			
17. Key Words Instrumentation, Monitoring, Slope, Stabilization, Foundation		18. Distribution Statement No Restrictions. This document is available to the public through the National Technical Information Service, Springfield, Virginia 22161	
19. Security Classif. (of this report) Unclassified	20. Security Classif. (of this page) Unclassified	21. No. of Pages	22. Price



# **Instrumentation, Monitoring, and Testing at the CUY-90-15.24 Central Viaduct Project**

**By**

**Robert Y. Liang  
Department of Civil Engineering  
The University of Akron  
Akron, Ohio 44325-3905**

Submitted to

The Ohio Department of Transportation  
and  
The U.S. Department of Transportation, Federal Highway Administration



**Department of Civil Engineering  
The University of Akron  
Akron, OH 44325 - 3905**

**June, 2000**

1  
2  
3  
4  
5  
6  
7  
8  
9  
10  
11  
12  
13  
14  
15  
16  
17  
18  
19  
20  
21  
22  
23  
24  
25  
26  
27  
28  
29  
30  
31  
32  
33  
34  
35  
36  
37  
38  
39  
40  
41  
42  
43  
44  
45  
46  
47  
48  
49  
50  
51  
52  
53  
54  
55  
56  
57  
58  
59  
60  
61  
62  
63  
64  
65  
66  
67  
68  
69  
70  
71  
72  
73  
74  
75  
76  
77  
78  
79  
80  
81  
82  
83  
84  
85  
86  
87  
88  
89  
90  
91  
92  
93  
94  
95  
96  
97  
98  
99  
100

### **DISCLAIMER STATEMENT**

The contents of this report reflect the views of the author who is responsible for the facts and the accuracy of the data presented herein. The contents do not necessarily reflect the official views or policies of the Ohio Department of Transportation or the Federal Highway Administration. This report does not constitute a standard, specification or regulation.

8  
1  
2  
3  
4  
5  
6  
7  
8  
9  
10  
11  
12  
13  
14  
15  
16  
17  
18  
19  
20  
21  
22  
23  
24  
25  
26  
27  
28  
29  
30  
31  
32  
33  
34  
35  
36  
37  
38  
39  
40  
41  
42  
43  
44  
45  
46  
47  
48  
49  
50  
51  
52  
53  
54  
55  
56  
57  
58  
59  
60  
61  
62  
63  
64  
65  
66  
67  
68  
69  
70  
71  
72  
73  
74  
75  
76  
77  
78  
79  
80  
81  
82  
83  
84  
85  
86  
87  
88  
89  
90  
91  
92  
93  
94  
95  
96  
97  
98  
99  
100



## EXECUTIVE SUMMARY

Bridge CUY-90-15.24, the Central Viaduct, also known as the Inner Belt Bridge, is part of the Interstate Highway System in Cleveland, Ohio. The structure carries up to eight traffic lanes, over many streets, the Cuyahoga River, Conrail tracks, the N-S Trestle, Cleveland Rapid Transit tracks, among others. The roadway carries an average of 134,660 vehicles per day. About nine percent of the traffic is heavy trucks. Since 1988, Richland Engineering Limited has inspected the bridge annually. In addition, beginning in 1991, detailed substructure stability study was carried out. From these studies, general observations revealed that: (a) Pier 1 has moved about 0.6 to 0.8 feet toward the river, and (b) The west end pier has moved about 0.3 to 0.4 feet toward the river. As an initial step to stabilize the slopes and piers, the grading and drainage improvements were completed in 1995. As a permanent stabilization to the upper slope, the CUY-90-15.24 project (PID No. 12374) has been approved. The stabilization scheme involved the use of drilled shafts, rock anchors, tiebacks, and driven piles. Because of unique features (extremely long drilled shafts, high capacity rock anchors) and the uncertainties of design assumptions (mechanisms of the slope stabilization), engineers have put into the plans a special item for instrumentation, testing, and long-term monitoring. The University of Akron was the designated research team to carry out the tasks involved in this special item.

The main objectives of the project are two fold: (a) ensure construction safety and verification of design assumptions, and (b) gain insights on the foundation structure behaviors. Specifically, the objectives include the following: (1) ensure safety (during construction and service) of the bridge, (2) measure stress and deformation of substructures used for slope stabilization to confirm both safety (limiting stresses) and serviceability (limiting deformations), (3) provide real-time measurements to allow project engineers to make sensible but critical decisions, (4) long-term monitoring as part of bridge maintenance program to assess maintenance needs, (5) re-assess design assumptions so that new knowledge can be gained and applied for future projects, (6) Advance the knowledge on soil structure interactions and slope stabilization techniques, (7) form valuable database for current FHWA development of LRFD (Load Resistance Factor Design) for substructures, (8) Perform FEM (Finite element Method) Simulation (Verified with Field Measurements) to provide further details of substructure behavior.

During the course of the project, the following tasks have been successfully accomplished. (a) A series of analyses were performed for the existing slope condition to assess the strength parameters of the soil, in particular, the strength parameters of the slip surfaces. (b) As part of the planning process, the instrumentation plan of various types of sensors was developed and incorporated in the final design plan. (c) All instrumentation sensors were individually calibrated and checked prior to field deployment. (d) All planned sensors were successfully installed during construction according to the design plans. (e) Real-time monitoring of all sensors has been successfully carried out. (f) As part of the study, a FEM program PLAXIS was employed to perform a numerical simulation. The FEM simulation process involved the calibration of soil properties to match the initial inclinometer reading from B-103 during initial site excavation. (g) After the installation of the drilled shafts, a lateral load test on drilled shafts # 1 and # 3 was successfully conducted. (h) Each rock anchor at the project

site was proof tested in accordance with the Post Tensioning Institute (PTI) specifications except the instrumented ones. Instrumented anchors # 1, # 8, and # 17 were performance tested. Instrumented anchor # 9 was creep tested. Detailed test results of this rock anchor has been discussed in chapter IV. The test results indicated that the anchor met the creep criteria set forth in the PTI specifications. Furthermore, the strain gage readings during testing and after anchor lock-off showed that the bond length was adequate, as the gages located at the end of the bond zone registered zero load transfer. (i) The measured data, together with detailed FEM simulation results, have provided a powerful and insightful picture of the behavior of the slope and the foundation structures. (j) The global stability of the slope with constructed foundation structures has been assessed from two vantage points: The measured slope movement and the calculated stress ratios at the slip surfaces. (k) The FEM simulation was carried out for a hypothetical case in which the unit weight of the soil above the slip surfaces had been artificially increased by 20 percent. The purpose of the artificial overloading in the FEM simulation was to facilitate additional slippage along the slip surface and to provide references for long-term monitoring.

Based on the experiences gained from field instrumentation and monitoring results, coupled with the detailed FEM simulation analysis results, the following conclusions can be made. (a) Construction itself can cause significant slope instability, particularly when activities such as excavation at the toe of the slope, pile driving, and boring holes for cast-in-place shafts. Therefore, it is imperative that engineers pay attention to these construction activities during remediation of a slope stability problem. (b) The design of drilled shafts for stabilizing the slope was based on the assumption that active earth pressure could have developed and fully thrust upon the shafts. This may be a very conservative approach, as it ignores the arching developed behind the drilled shafts. It also appears that if rock anchors are used at the site, the tensioning force would reduce the amount of earth thrust acting on the drilled shafts as well. (c) The design of geotechnical structures usually involves uncertainties about soil profile, soil properties, and mechanisms of the soil-structure interaction; therefore, it is prudent to incorporate the concept of structure redundancy. (d) Instrumentation and monitoring of geotechnical structures in the project has provided very useful factual data and important insights on the behavior of the slope, thus assisting the project engineers to make time-sensitive, critical decisions during construction. (e) This project clearly demonstrated that instrumentation and monitoring can serve the purpose of construction quality assurance as well. (f) The technology of vibrating-wire based strain gages has been shown to provide long-term, reliable strain measurements in a very difficult construction site. The planning, hands-on experiences, dedication of engineers, cooperation from contractors, and efficient data reduction software all played important role to ensure the success of the field instrumentation/monitoring project. (g) A combined technique involving field instrumentation/monitoring and FEM simulation provides a powerful tool for design verification. This is particularly important for projects involving innovative/new designs, unknown/uncertain soil properties, and lack of existing design/analysis methodology. (h) The deployment of instrumentation sensors during the construction (birth) of the foundation structure can be used throughout its life for diagnostics of any maintenance needs.

## ACKNOWLEDGMENT

The completion of this study comes as a result of the efforts of numerous individuals and organizations. The Ohio Department of Transportation (ODOT) is gratefully acknowledged for providing financial support for this work.

The author also is indebted to the following individuals and organizations for their technical support:

Kirk Gegick, Mike Karahan, Randy Ovell, and George Macky of ODOT District 12; Vik Dalal of ODOT Research and Development; Richard Engel, Jawdat Siddiqi of ODOT Structures Division; Mohamed Riaz of M.S. Consultants; Dean Palmer of Richland Engineering, Ltd.; Stuart Ravary of BBC&M Engineering, Ltd.; The Great Lakes Construction Company; AGRA Foundations; Schnabel Foundation Company; The department of Civil Engineering at the University of Akron, for providing services of Roger Buck, engineering technician.

Special thanks go to Dr. Jamal Nusairat for leading the field instrumentation team, Sanping Zeng for the Finite Element Simulation, and the graduate students at the University of Akron who assist in the field testing.



# Table of Contents

Section	Title	Page
	LIST OF TABLES .....	v
	LIST OF FIGURES .....	vi
I.	INTRODUCTION .....	I-1
I.1	Introduction .....	I-1
I.2	Objectives .....	I-2
I.3	Organization of the report .....	I-1
II.	HISTORICAL BACKGROUND OF THE PROJECT .....	II-1
II.1	Introduction .....	II-1
II.2	Nature of the problem .....	II-2
II.3	Existing conditions before project start .....	II-4
II.4	Pre-construction analysis and design .....	II-5
II.4.1	General subsurface conditions .....	II-6
II.4.2	Existing data .....	II-7
II.4.2.1	Borings and soil testing .....	II-7
II.4.2.2	Bridge deformation information .....	II-8
II.5	Preconstruction analysis and design .....	II-8
II.5.1	Preliminary slope stability analysis .....	II-8
II.5.1.1	Analysis by BBC&M Engineering, Inc. ....	II-8
III.	INSTRUMENTATION/MONITORING PROGRAM .....	III-1
III.1	Introduction .....	III-1
III.2	Slope movement monitoring .....	III-1
III.3	Foundation structure behavior .....	III-2
III.3.1	Driven piles .....	III-2
III.3.2	Drilled shafts .....	III-3
III.3.3	Ground anchors .....	III-4
III.3.4	Instrumentation of tie beams .....	III-4

<b>Section</b>	<b>Title</b>	<b>Page</b>
III.3.5	Instrumentation of drilled shaft cap .....	III-5
III.4	Instrumentation installation details .....	III-5
III.4.1	Sequence of installation .....	III-5
III.4.2	Techniques of installing instruments and monitoring .....	III-8
III.5	Data acquisition plans .....	III-10
IV.	SHORT AND LONG TERM MONITORING RESULTS .....	
IV.1	Overview of collected information before commencement of construction .....	IV-1
IV.2	Excavation for driven piles and pile driving .....	IV-3
IV.3	Drilled shafts construction .....	IV-6
IV.4	Rock anchor construction .....	IV-7
IV.5	Drilled shafts cap .....	IV-7
IV.6	Tie beams .....	IV-8
IV.7	Tensioning of rock anchors .....	IV-8
IV.8	Grouting of tie beams and backfilling of slope .....	IV-9
IV.9	Long-term monitoring results .....	IV-10
IV.10	Comments on the results of monitoring .....	IV-11
V.	FINITE ELEMENT ANALYSIS ON REINFORCED SLOPE .....	V-1
V.1	Introduction .....	V-1
V.2	Finite element modeling of CUY-90 Project .....	V-2
V.3	Material properties .....	V-3
V.3.1	Soil .....	V-3
V.3	Stabilization structures .....	V-3
V.4	Three-dimensional effect of existing pile supported pier .....	V-4
V.5	Calibration study to determine slip surface properties .....	V-7
V.6	Simulation of construction processes .....	V-8
V.7	FEM analysis results and discussion .....	V-10
V.7.1	Stresses and deformations in soil mass .....	V-10

<b>Section</b>	<b>Title</b>	<b>Page</b>
V.7.2	Force in structure members .....	V-10
V.7.2.1	Temporary retaining wall structure .....	V-11
V.7.2.2	Driven piles .....	V-11
V.7.2.3	Drilled shafts .....	V-11
V.7.2.4	Tie-beams .....	V-11
V.7.2.5	Ground anchors .....	V-11
VI	BACK CALCULATION OF P-Y CURVES UNSING INCLINOMETER DATA .....	VI-1
VI.1	Introduction .....	VI-1
VI.2	Back calculation of p-y curves from inclinometer data .....	VI-3
VI.2.1	General principle .....	VI-3
VI.2.2	Governing equation for soil-shaft interaction .....	VI-3
VI.2.3	Determination of the problem .....	VI-4
VI.2.4	Method of solution .....	VI-5
VI.3	Application to load test results .....	VI-6
VII.	OBSERVATIONS OF FIELD PEROFRMANCE .....	VII-1
VII.1	Stage I: Existing stress field prior to construction .....	VII-1
VII.2	Stage II: Excavation to pile cap elevation (9/23/97) and beginning of pile driving (10/3/98) .....	VII-2
VII.3	Stage III: Complete pile driving (1/19/98), Complete pile cap (2/11/98), backfill portion of the slope (2/23/98), and excavation for drilled shafts and tie beams .....	VII-3
VII.4	Stage IV: Drilled Shafts Construction (8/14/98~12/10/98) .....	VII-4
VII.5	Stage V: Lateral load test of drilled shafts #1 and #3 (1/13/99) .....	VII-4
VII.6	Stage VI: Installation of rock anchors (12/12/98 ~ 2/18/98), installation of tiebeams (3/1/99 ~ 3/25/99), tensioning of rock anchors (4/7/99 ~ 4/14/99), and grouting of the corrugated tubes (4/20/99). .....	VII-5
VII.7	Stage VII: Final stage of backfilling to final grade (4/23/99 ~ 5/7/99) .	VII-6
VII.8	Lessons learned from the project .....	VII-8

<u>Section</u>	<u>Title</u>	<u>Page</u>
VII.9	Telltale signs for long-term monitoring .....	VII-9
VIII	SUMMARY AND CONCLUSIONS .....	VIII-1
VIII.1	Summary of tasks accomplished .....	VIII-1
VIII.2	Conclusions .....	VIII-5
VIII.2	Conclusions .....	VIII-5
IX	REFERENCES .....	IX-1
 APPENDICES		
A.	Detailed information about the soil borings for inclinometers and piezometers installed by BBC&M, Inc. in 1994. ....	A-1
B.	Sequence of installation and detailed inspection of the drilled shafts. .	B-1
C.	Dynamic test results of Pile # 18. ....	C-1



## List of Tables

Table	Title	Page
2.1	Soil parameters used in the slope stability analysis .....	II-11
4.1	Major construction events .....	IV-2
4.2	Blow count vs. depth for test pile # 18 .....	IV-5
5.1	Soil properties .....	V-3
5.2	Properties of reinforcement structures .....	V-4
5.3	Properties of pile and cap .....	V-5
5.4	Properties of soil .....	V-5
5.5	Typical combination of strength reduction factors $R_{inter}$ .....	V-8
5.6	Incremental steps for nonlinear calculation .....	V-10
7.1	Comparisons between calculated and measured results for tiebeams after completion of anchor tensioning .....	VII-5
7.2	Comparison between calculated and measured results for tiebeam after backfill .....	VII-6
7.3	Comparison between measured and ultimate capacity of each structure .....	IV-7
7.4	Stresses in each foundation structure before and after the 20% increase in unit weight of the soil .....	VII-10

## List of Figures

Figure	Title	Page
1.1	Site condition prior to construction .....	I-5
1.2	Site condition prior to construction .....	I-6
1.3	Elevation view of the proposed stabilization scheme .....	I-7
1.4	Team members responsible for the successful completion of the project .....	I-8
2.1	Elevation view of the bridge .....	II-12
2.2	Location of inclinometers installed by ODOT .....	II-13
2.3	STABL model used in the analysis .....	II-14
2.4	Locations of inclinometers and piezometers installed by BBC&M. ....	II-12
3.1	Plan showing the entire stabilization system and the locations of instrumented elements of the system. ....	III-11
3.2	Location of earth inclinometers. ....	III-12
3.3	Location of instrumented piles and gages numbering. ....	III-13
3.4	Gages installed and covers on the pile flanges. ....	III-14
3.5	Gages being installed on piles 17, 18, and 19. ....	III-15
3.6	Gages being covered with protection stainless steel. ....	III-16
3.7	Ground being filled to the final grade for the pile cap construction. ....	III-17
3.8	Instrumented piles after completion of backfilling. ....	III-18
3.9	Instrumentation of drilled shaft cap for long-term monitoring. ....	III-19
3.10	Instrumentation of shafts 1 and 3 for lateral load test. ....	III-20
3.11	Sister bar strain gage installed on the cage. ....	III-21
3.12	Instrumented sections of the cages loaded on trucks. ....	III-22
3.13	Gages installed and wires run to the top of the section and the PVC housing tube for inclinometer. ....	III-23
3.14	Splicing the two segments of the girder, the cage, and the PVC tube. ....	III-24
3.15	Inclinometers in shafts #8, #9, and #10 and the wires from gages in shaft #9. ....	III-25
3.16	Schematic diagram of the lateral load test at CUY-90 project. Side View. ....	III-26

## List of Figures (Cont)

Figure	Title	Page
3.17	Setup for the lateral load test. ....	III-27
3.18	Setup for the lateral load test (Continued). ....	III-29
3.20	Reference beams and dial gage locations. ....	III-30
3.21	Instrumentation of shafts 8, 9, and 10 for long-term monitoring. ....	III-31
3.22	Details of anchor instrumentation and final setup. ....	III-32
3.23	Drilling for rock anchors. ....	III-33
3.24	Casing driven in the ground to support the free length for the anchor. ....	III-34
3.25	Setup for installation of the anchor. ....	III-35
3.26	Lowering the anchor in the hole. ....	III-36
3.27	Strand gage ready to be mounted. ....	III-37
3.28	Strand gage installed. ....	III-38
3.29	Installation of the load cell and bearing plates for testing and long term monitoring. ....	III-39
3.30	Anchor testing. ....	III-40
3.31	Location of gages on the tie beams. ....	III-41
3.32	Welding end blocks for strain gages on tiebeams. ....	III-42
3.33	Installation and testing of vibrating wire strain gages on the tiebeam. ....	III-43
3.34	Installed gages on the middle tiebeams. ....	III-44
3.35	Tiebeam gage wires run through conduit to the shaft cap. ....	III-45
3.36	Tiebeam gages run to the datalogger in the temporary wood box. ....	III-46
3.37	Bi-axial tiltmeter installed on the shaft cap (10' from each end). ....	III-47
3.38	Data collection boxes (final location). ....	III-48
4.1	Locations of earth inclinometers installed in 1994. ....	IV-16
4.2	Cross section geometry at the centerline of the project. ....	IV-17
4.3	Monitoring of deflection since 5/15/96 for B-103 Inclinometer at CUY-90 Project - A - Direction (Down Slope) ....	IV-18
4.4	Monitoring of deflection since 5/15/96 for B-103 Inclinometer at CUY-90 Project - B - Dir. ....	IV-19
4.5	Monitoring of deflection since 5/15/96 for B-104 Inclinometer at CUY-90 Project - A - Dir. ....	IV-20

## List of Figures (Cont)

Figure	Title	Page
4.6	Monitoring of deflection since 5/15/96 for B-104 Inclinometer at CUY-90 Project - B - Dir. ....	IV-21
4.7	Monitoring of deflection since 5/15/96 for B-103 Inclinometer at CUY-90 Project - A - Direction (Down Slope). Last reading before resuming pile driving.....	IV-22
4.8	Monitoring of deflection since 5/15/96 for B-103 Inclinometer at CUY-90 Project - B - Dir. Last reading before resuming pile driving .....	IV-23
4.9	Cut trench for pile driving. ....	IV-24
4.10	Pile driving. ....	IV-25
4.11	Partial backfilling of the slope to install temporary support for slope during pile driving. ....	IV-26
4.12	Drilled shafts installation for temporary slope support .....	IV-27
4.13	Monitoring of deflection since 5/15/96 for B-103 Inclinometer at CUY-90 Project - A - Direction (Down Slope). Last reading before resuming pile driving.....	IV-28
4.14	Monitoring of deflection since 5/15/96 for B-103 Inclinometer at CUY-90 Project - B - Dir. Last reading before resuming pile driving.....	IV-29
4.15	Monitoring of deflection since 5/15/96 for B-103 Inclinometer at CUY-90 Project - A - Direction (Down Slope). Last reading after resuming pile driving.....	IV-30
4.16	Monitoring of deflection since 5/15/96 for B-104 Inclinometer at CUY-90 Project - B - Dir. Last reading after resuming pile driving.....	IV-31
4.17	Monitoring of deflection since 5/15/96 for B-104 Inclinometer at CUY-90 Project - A - Dir. Last reading after completion of pile driving .	IV-32
4.18	Monitoring of deflection since 5/15/96 for B-104 Inclinometer at CUY-90 Project - B - Dir. Last reading after completion of pile driving ..	IV-33
4.19	Results of measured force, calculated capacity based on RA2 method and energy measured against blow count from PDA .....	IV-34

## List of Figures (Cont)

Figure	Title	Page
4.20	Results of measured force, calculated capacity based on RA2 method and energy measured against blow count from PDA for the bottom 8 feet of penetration .....	IV-35
4.21	Pile gages installation .....	IV-36
4.22	Pile gages installation and protection mounting.....	IV-37
4.23	Pile gages installed and soil compacted around piles .....	IV-38
4.24	Cross section of the slope partial backfilling after anchor cap completion .....	IV-39
4.25	Cross section of the slope partial backfilling after anchor cap completion	IV-40
4.26	Slope partial backfilling after anchor cap completion .....	IV-41
4.27	Long-term monitoring of strain in Pile # 1 in the anchor cap structure (2/12/98 ~ 6/30/98).....	IV-42
4.28	Long-term monitoring of stress in Pile # 1 in the anchor cap structure (2/12/98 ~ 6/30/98).....	IV-43
4.29	Long-term monitoring of strain in Pile # 17 in the anchor cap structure (2/12/98 ~ 6/30/98).....	IV-44
4.30	Long-term monitoring of stress in Pile # 17 in the anchor cap structure (2/12/98 ~ 6/30/98) .....	IV-45
4.31	Long-term monitoring of strain in Pile # 18 in the anchor cap structure (2/12/98 ~ 6/30/98).....	IV-46
4.32	Long-term monitoring of stress in Pile # 18 in the anchor cap structure (2/12/98 ~ 6/30/98) .....	IV-47
4.33	Long-term monitoring of strain in Pile # 19 in the anchor cap structure (2/12/98 ~ 6/30/98).....	IV-48
4.34	Long-term monitoring of stress in Pile # 19 in the anchor cap structure (2/12/98 ~ 6/30/98) .....	IV-49
4.35	Long-term monitoring of strain in Pile # 34 in the anchor cap structure (2/12/98 ~ 6/30/98).....	IV-50
4.36	Long-term monitoring of stress in Pile # 34 in the anchor cap structure (2/12/98 ~ 6/30/98) .....	IV-51

## List of Figures (Cont)

Figure	Title	Page
4.37	Monitoring of deflection since 5/15/96 for B-103 Inclinometer at CUY-90 Project - A - Direction (Down slope). Last reading on 6/30/1998 .....	IV-52
4.38	Monitoring of deflection since 5/15/96 for B-103 Inclinometer at CUY-90 Project - B - Dir. Last reading on 6/30/1998 .....	IV-53
4.39	Monitoring of deflection since 5/15/96 for B-104 Inclinometer at CUY-90 Project - A - Dir. Last reading on 6/30/1998 .....	IV-54
4.40	Monitoring of deflection since 5/15/96 for B-104 Inclinometer at CUY-90 Project - B - Dir. Last reading on 6/30/1998 .....	IV-55
4.41	Installation of inclinometers inside the PVC tubes in the drilled shafts ....	IV-56
4.42	Schematic diagram of the lateral load test - top view. ....	IV-57
4.43	Schematic diagram of the lateral load test - side view. ....	IV-58
4.44	Lateral load test, shaft # 1, measured and calculated deflection at shaft top. ....	IV-59
4.45	Lateral load test, shaft # 3, measured and calculated deflection at shaft top. ....	IV-60
4.46	Lateral load test, shaft # 1, measured deflection vs. depth using inclinometer. ....	IV-61
4.47	Lateral load test, shaft # 3, measured deflection vs. depth using inclinometer. ....	IV-62
4.48(a)	Lateral load test, shaft # 1, reduced strain vs. depth on tension side (loading from 0 to 400 Kips). ....	IV-63
4.48(b)	Lateral load test, shaft # 1, reduced strain vs. depth on tension side (loading from 400 to 800 Kips). ....	IV-64
4.49(a)	Lateral load test, shaft # 1, reduced strain vs. depth on compression side (loading from 0 to 400 Kips). ....	IV-65
4.49(b)	Lateral load test, shaft # 1, reduced strain vs. depth on compression side (loading from 400 to 800 Kips). ....	IV-66
4.50	Lateral load test, tilt in degrees at the jacking point in shafts # 1 and # 3 .	IV-67

## List of Figures (Cont)

Figure	Title	Page
4.51	Long-term monitoring of strain in pile # 1 in the anchor cap structure (6/30/98 ~ 12/31/98).....	IV-68
4.52	Long-term monitoring of stress in pile # 1 in the anchor cap structure (6/30/98 ~ 12/31/98).....	IV-69
4.53	Long-term monitoring of strain in pile # 17 in the anchor cap structure (6/30/98 ~ 12/31/98).....	IV-70
4.54	Long-term monitoring of stress in pile # 17 in the anchor cap structure (6/30/98 ~ 12/31/98).....	IV-71
4.55	Long-term monitoring of strain in pile # 18 in the anchor cap structure (6/30/98 ~ 12/31/98).....	IV-72
4.56	Long-term monitoring of stress in pile # 18 in the anchor cap structure (6/30/98 ~ 12/31/98).....	IV-73
4.57	Long-term monitoring of strain in pile # 19 in the anchor cap structure (6/30/98 ~ 12/31/98).....	IV-74
4.58	Long-term monitoring of stress in pile # 19 in the anchor cap structure (6/30/98 ~ 12/31/98).....	IV-75
4.59	Long-term monitoring of strain in pile # 34 in the anchor cap structure (6/30/98 ~ 12/31/98).....	IV-76
4.60	Long-term monitoring of stress in pile # 34 in the anchor cap structure (6/30/98 ~ 12/31/98).....	IV-77
4.61	Rock anchor drilling operation.....	IV-78
4.62	Strand gage mounted on one of the anchor strands.....	IV-79
4.63	Drilling and installation of rock anchors.....	IV-80
4.64	Lowering the coiled tendon in the hole.....	IV-81
4.65	Drilled shaft cap after concrete was cast.....	IV-82
4.66	Installed tiltmeters on the side of the drilled shaft cap....	IV-83
4.67	Strain gages mounted on the tie beams....	IV-84
4.68	Sleeves housing the tie beams for subsequent grouting.....	IV-85
4.69	Permanent vibrating-wire based load cell installed between the bearing plates and the anchor head to measure the applied load on the anchor....	IV-86

## List of Figures (Cont)

Figure	Title	Page
4.70	Anchor load test setup and testing assembly.....	IV-87
4.71	Anchor # 8 performance test, Load vs. movement at the anchor head.....	IV-88
4.72(a)	Anchor # 8 performance test results, gage # 1.....	IV-89
4.72(b)	Anchor # 8 performance test results, gage # 2.....	IV-90
4.72(c)	Anchor # 8 performance test results, gage # 3.....	IV-91
4.72(d)	Anchor # 8 performance test results, gage # 4.....	IV-92
4.72(e)	Anchor # 8 performance test results, gage # 5.....	IV-93
4.73	Anchor # 17 performance test, Load vs. movement at the anchor head...	IV-94
4.74	Anchor # 1 performance test, Load vs. movement at the anchor head.....	IV-95
4.75(a)	Anchor # 17 performance test results, gage # 1.....	IV-96
4.75(b)	Anchor # 17 performance test results, gage # 2.....	IV-97
4.75(c)	Anchor # 17 performance test results, gage # 3.....	IV-98
4.75(d)	Anchor # 17 performance test results, gage # 5.....	IV-99
4.76(a)	Anchor # 1 performance test results, gage # 1.....	IV-100
4.76(b)	Anchor # 1 performance test results, gage # 2.....	IV-101
4.76(c)	Anchor # 1 performance test results, gage # 3.....	IV-102
4.76(d)	Anchor # 1 performance test results, gage # 5.....	IV-103
4.77	Anchor # 9 creep test, Load vs. movement at the anchor head.....	IV-104
4.78(a)	Anchor # 9 creep test results, gage # 1.....	IV-105
4.78(b)	Anchor # 9 creep test results, gage # 2.....	IV-106
4.78(c)	Anchor # 9 creep test results, gage # 3.....	IV-107
4.78(d)	Anchor # 9 creep test results, gage # 4.....	IV-108
4.78(e)	Anchor # 9 creep test results, gage # 5.....	IV-109
4.79	Inclinometer # 8 Displacement in the A+ Direction, downslope (River direction), Base line reading 12/11/1998.....	IV-110



## List of Figures (Cont)

Figure	Title	Page
4.80	Inclinometer # 9A Displacement in the A+ Direction, downslope (River direction), Base line reading 12/11/1998.....	IV-111
4.81	Inclinometer # 9B Displacement in the A+ Direction, downslope (River direction), Base line reading 12/11/1998.....	IV-112
4.82	Inclinometer # 10 Displacement in the A+ Direction, downslope (River direction), Base line reading 12/11/1998.....	IV-113
4.83	Inclinometer # 1 Displacement in the A+ Direction, downslope (River direction), Base line reading 12/11/1998.....	IV-114
4.84	Inclinometer # 3 Displacement in the A+ Direction, downslope (River direction), Base line reading 12/11/1998.....	IV-115
4.85	Inclinometer # 8 Displacement in the A+ Direction, downslope (River direction), Base line reading 12/11/1998.....	IV-116
4.86	Inclinometer # 9A Displacement in the A+ Direction, downslope (River direction), Base line reading 12/11/1998.....	IV-117
4.87	Inclinometer # 9B Displacement in the A+ Direction, downslope (River direction), Base line reading 12/11/1998.....	IV-118
4.88	Inclinometer # 10 Displacement in the A+ Direction, downslope (River direction), Base line reading 12/11/1998.....	IV-119
4.89	Inclinometer # 17 Displacement in the A+ Direction, downslope (River direction), Base line reading 12/11/1998.....	IV-120
4.90	Tie-beam # 1, strain from gages on driven pile cap side .....	IV-121
4.91	Tie-beam # 1, strain from gages on drilled shaft cap side .....	IV-122
4.92	Tie-beam # 12, strain from gages on driven pile cap side .....	IV-123
4.93	Tie-beam # 12, strain from gages on drilled shaft cap side .....	IV-124
4.94	Tie-beam # 13, strain from gages on driven pile cap side .....	IV-125
4.95	Tie-beam # 13, strain from gages on drilled shaft cap side .....	IV-126
4.96	Tie-beam # 14, strain from gages on driven pile cap side .....	IV-127
4.97	Tie-beam # 14, strain from gages on drilled shaft cap side .....	IV-128
4.98	Tie-beam # 26, strain from gages on driven pile cap side .....	IV-129

## List of Figures (Cont)

Figure	Title	Page
4.99	Tie-beam # 26, strain from gages on drilled shaft cap side .....	IV-130
4.100	Shaft 1, strain vs. time from gages 9.5 feet below top of shaft cap .....	IV-131
4.101	Shaft 1, strain vs. time from gages 16 feet below top of shaft cap .....	IV-132
4.102	Shaft 1, strain vs. time from gages 22.5 feet below top of shaft cap.... .....	IV-133
4.103	Shaft 1, strain vs. time from gages 29 feet below top of shaft cap.... .....	IV-134
4.104	Shaft 1, strain vs. time from gages 35.5 feet below top of shaft cap.... .....	IV-135
4.105	Shaft 1, strain vs. time from gages 42 feet below top of shaft cap.... .....	IV-136
4.106	Shaft 1, strain vs. time from gages 47.33 feet below top of shaft cap.... .....	IV-137
4.107	Shaft 1, strain vs. time from gages 54.83 feet below top of shaft cap.... .....	IV-138
4.108	Shaft 1, strain vs. time from gages 64.83 feet below top of shaft cap.... .....	IV-139
4.109	Shaft 1, strain vs. time from gages 74.83 feet below top of shaft cap.... .....	IV-140
4.110	Shaft 1, strain vs. time from gages 84.83 feet below top of shaft cap.... .....	IV-141
4.111	Shaft 1, strain vs. time from gages 94.83 feet below top of shaft cap.... .....	IV-142
4.112	Shaft 1, strain vs. time from gages 115 feet below top of shaft cap.... .....	IV-143
4.113	Shaft 1, strain vs. time from gages 135 feet below top of shaft cap.... .....	IV-144
4.114	Shaft 9, strain vs. time from gages 11 feet below top of shaft cap.... .....	IV-145
4.115	Shaft 9, strain vs. time from gages 17.5 feet below top of shaft cap.... .....	IV-146
4.116	Shaft 9, strain vs. time from gages 24 feet below top of shaft cap.... .....	IV-147
4.117	Shaft 9, strain vs. time from gages 30.5 feet below top of shaft cap.... .....	IV-148
4.118	Shaft 9, strain vs. time from gages 37 feet below top of shaft cap.... .....	IV-149
4.119	Shaft 9, strain vs. time from gages 43.5 feet below top of shaft cap.... .....	IV-150
4.120	Shaft 9, strain vs. time from gages 50 feet below top of shaft cap.... .....	IV-151
4.121	Shaft 9, strain vs. time from gages 60 feet below top of shaft cap.... .....	IV-152
4.122	Shaft 9, strain vs. time from gages 70 feet below top of shaft cap.... .....	IV-153
4.123	Shaft 9, strain vs. time from gages 80 feet below top of shaft cap.... .....	IV-154

## List of Figures (Cont)

Figure	Title	Page
4.124	Shaft 9, strain vs. time from gages 95 feet below top of shaft cap....	IV-155
4.125	Shaft 9, strain vs. time from gages 115 feet below top of shaft cap....	IV-156
4.126	Shaft 9, strain vs. time from gages 135 feet below top of shaft cap....	IV-157
4.127	Long-term monitoring of strain in pile # 1 in the anchor cap structure (1/1/99 ~ 6/30/99).....	IV-158
4.128	Long-term monitoring of stress in pile # 1 in the anchor cap structure (1/1/99 ~ 6/30/99).....	IV-159
4.129	Long-term monitoring of strain in pile # 17 in the anchor cap structure (1/1/99 ~ 6/30/99).....	IV-160
4.130	Long-term monitoring of stress in pile # 17 in the anchor cap structure (1/1/99 ~ 6/30/99).....	IV-161
4.131	Long-term monitoring of strain in pile # 18 in the anchor cap structure (1/1/99 ~ 6/30/99).....	IV-162
4.132	Long-term monitoring of stress in pile # 18 in the anchor cap structure (1/1/99 ~ 6/30/99).....	IV-163
4.133	Long-term monitoring of strain in pile # 19 in the anchor cap structure (1/1/99 ~ 6/30/99).....	IV-164
4.134	Long-term monitoring of stress in pile # 19 in the anchor cap structure (1/1/99 ~ 6/30/99).....	IV-165
4.135	Long-term monitoring of strain in pile # 34 in the anchor cap structure (1/1/99 ~ 6/30/99).....	IV-166
4.136	Long-term monitoring of stress in pile # 34 in the anchor cap structure (1/1/99 ~ 6/30/99).....	IV-167
4.137	Long-term monitoring of strain in Pile # 1 in the anchor cap structure (2/12/98 ~ 6/30/99).....	IV-168
4.138	Long-term monitoring of stress in Pile # 1 in the anchor cap structure (2/12/98 ~ 6/30/99).....	IV-169
4.139	Long-term monitoring of strain in Pile # 17 in the anchor cap structure (2/12/98 ~ 6/30/99).....	IV-170
4.140	Long-term monitoring of stress in Pile # 17 in the anchor cap structure (2/12/98 ~ 6/30/99).....	IV-171

## List of Figures (Cont)

Figure	Title	Page
4.141	Long-term monitoring of strain in Pile # 18 in the anchor cap structure (2/12/98 ~ 6/30/99).....	IV-172
4.142	Long-term monitoring of stress in Pile # 18 in the anchor cap structure (2/12/98 ~ 6/30/99) .....	IV-173
4.143	Long-term monitoring of strain in Pile # 19 in the anchor cap structure (2/12/98 ~ 6/30/99).....	IV-174
4.144	Long-term monitoring of stress in Pile # 19 in the anchor cap structure (2/12/98 ~ 6/30/99) .....	IV-175
4.145	Long-term monitoring of strain in Pile # 34 in the anchor cap structure (2/12/98 ~ 6/30/99).....	IV-176
4.146	Long-term monitoring of stress in Pile # 34 in the anchor cap structure (2/12/98 ~ 6/30/99) .....	IV-177
4.147	Shaft # 1, South side, strain vs. depth for major events after tensioning rock anchors. ....	IV-178
4.148	Shaft # 1, North side, strain vs. depth for major events after tensioning rock anchors. ....	IV-179
4.149	Shaft # 9, Tension side, strain vs. depth for major events after tensioning rock anchors. ....	IV-180
4.150	Shaft # 9, Compression side, strain vs. depth for major events after tensioning rock anchors. ....	IV-181
4.151	Anchor # 1, long-term monitoring of load from load cell at anchor head. ....	IV-182
4.152	Anchor # 8, long-term monitoring of load from load cell at anchor head. ....	IV-183
4.153	Anchor # 9, long-term monitoring of load from load cell at anchor head. ....	IV-184
4.154	Anchor # 17, long-term monitoring of load from load cell at anchor head. ....	IV-185
4.155	Anchor # 1, movement at each gage location in the bonded length.....	IV-186
4.156	Anchor # 8, movement at each gage location in the bonded length.....	IV-187
4.157	Anchor # 9, movement at each gage location in the bonded length.....	IV-188
4.158	Anchor # 17, movement at each gage location in the bonded length.....	IV-189
4.159	Angle of tilt in degrees for tiltmeter 878. ....	IV-190

## List of Figures (Cont)

Figure	Title	Page
4.160	Angle of tilt in degrees for tiltmeter 879. ....	IV-191
4.161	Angle of tilt in degrees for tiltmeter 880. ....	IV-192
4.162	Angle of tilt in degrees for tiltmeter 881. ....	IV-193
4.163	Force diagram for the major events after tensioning the rock anchors. ....	IV-194
5.1	Centerline cross-section of CUY-90 project. ....	V-12
5.2	Calculation model. ....	V-13
5.3	Finite element mesh. ....	V-14
5.4	Soil layering information. ....	V-15
5.5	Cross-section of Pier 1 foundation. ....	V-16
5.6	FLPIER finite element mesh of 9 × 9-pile pier. ....	V-17
5.7	FLPIER finite element mesh of 9 × 36-pile pier. ....	V-18
5.8	Calculated load vs. deflections of 9 × 9-pile pier and 9 × 36-pile pier. ....	V-19
5.9	Calculated load vs. deflections of 9 × 9-pile pier and 9 × 36-pile pier with modified stiffness. ....	V-20
5.10	Comparison of soil movement along bore hole ZB103. ....	V-21
5.11	Soil displacement vectors due to phase 1. ....	V-22
5.12	Soil displacement contours due to phase 1. ....	V-23
5.13	Principal stress direction and magnitude due to phase 1. ....	V-24
5.14	: Mean effective stress contours after phase 1. ....	V-25
5.15	Relative shear stress ratio contours after phase 1. ....	V-26
5.16	Soil displacement vectors due to phase 2. ....	V-27
5.17	Soil displacement contours due to phase 2. ....	V-28
5.18	Principal stress direction and magnitude due to phase 2. ....	V-29
5.19	Mean effective stress contours after phase 2. ....	V-30
5.20	Relative shear stress ratio contours after phase 2. ....	V-31
5.21	Soil displacement vectors due to phase 3. ....	V-32

## List of Figures (Cont)

Figure	Title	Page
5.22	Soil displacement contours due to phase 3. ....	V-33
5.23	Principal stress direction and magnitude due to phase 3. ....	V-34
5.24	Mean effective stress contours after phase 3. ....	V-35
5.25	Relative shear stress ratio contours after phase 3. ....	V-36
5.26	Soil displacement vectors due to phase 4. ....	V-37
5.27	Soil displacement contours due to phase 4. ....	V-38
5.28	Principal stress direction and magnitude due to phase 4. ....	V-39
5.29	Mean effective stress contours after phase 4. ....	V-40
5.30	Relative shear stress ratio contours after phase 4. ....	V-41
5.31	Soil displacement vectors due to phase 5. ....	V-42
5.32	Soil displacement contours due to phase 5. ....	V-43
5.33	Principal stress direction and magnitude due to phase 5. ....	V-44
5.34	Mean effective stress contours after phase 5. ....	V-45
5.35	Relative shear stress ratio contours after phase 5. ....	V-46
5.36	Soil displacement vectors due to phase 6. ....	V-47
5.37	Soil displacement contours due to phase 6. ....	V-48
5.38	Principal stress direction and magnitude due to phase 6. ....	V-49
5.39	Mean effective stress contours after phase 6. ....	V-50
5.40	Relative shear stress ratio contours after phase 6. ....	V-51
5.41	Soil displacement vectors due to phase 7. ....	V-52
5.42	Soil displacement contours due to phase 7. ....	V-53
5.43	Principal stress direction and magnitude due to phase 7. ....	V-54
5.44	Mean effective stress contours after phase 7. ....	V-55
5.45	Relative shear stress ratio contours after phase 7. ....	V-56
5.46	Soil displacement vectors due to phase 8. ....	V-57

## List of Figures (Cont)

Figure	Title	Page
5.47	Soil displacement contours due to phase 8. ....	V-58
5.48	Principal stress direction and magnitude due to phase 8. ....	V-59
5.49	Mean effective stress contours after phase 8. ....	V-60
5.50	Relative shear stress ratio contours after phase 8. ....	V-61
5.51	Soil displacement vectors due to phase 9. ....	V-62
5.52	Soil displacement contours due to phase 9. ....	V-63
5.53	Principal stress direction and magnitude due to phase 9. ....	V-64
5.54	Mean effective stress contours after phase 9. ....	V-65
5.55	Relative shear stress ratio contours after phase 9. ....	V-66
5.56	Soil displacement vectors due to phase 10. ....	V-67
5.57	Soil displacement contours due to phase 10. ....	V-68
5.58	Principal stress direction and magnitude due to phase 10. ....	V-69
5.59	Mean effective stress contours after phase 10. ....	V-70
5.60	Relative shear stress ratio contours after phase 10. ....	V-71
5.61	Soil displacement vectors due to phase 11. ....	V-72
5.62	Soil displacement contours due to phase 11. ....	V-73
5.63	Principal stress direction and magnitude due to phase 11. ....	V-74
5.64	Mean effective stress contours after phase 11. ....	V-75
5.65	Relative shear stress ratio contours after phase 11. ....	V-76
5.66	Horizontal deflection of temporary shoring wall due to phase 6. ....	V-77
5.67	Bending moment along the depth of driven piles due to anchor tension (phase 10). ....	V-78
5.68	Bending moment along the depth of driven piles due to anchor tension and backfill (phase 11). ....	V-79
5.69	Axial force along the depth of driven piles due to anchor tension (phase 10). ....	V-80
5.70	Axial force along the depth of driven piles due to anchor tension and backfill (phase 11). ....	V-81

## List of Figures (Cont)

Figure	Title	Page
5.71	Deflection of driven piles due to anchor tension (phase 10). .....	V-82
5.72	Deflection of driven piles due to anchor tension and backfill (phase 11). .....	V-83
5.73	Bending moment along the shaft length for the drilled shaft #9 due to anchor tension (phase 10). .....	V-84
5.74	Bending moment along the shaft length for the drilled shaft #10 due to anchor tension (phase 10). .....	V-85
5.75	Bending moment along the shaft length for the drilled shaft #9 due to anchor tension and backfill (phase 11). .....	V-86
5.76	Bending moment along the shaft length for the drilled shaft #10 due to anchor tension and backfill (phase 11). .....	V-87
5.77	Axial force along the shaft length for the drilled shaft #9 due to anchor tension (phase 10). .....	V-88
5.78	Axial force along the shaft length for the drilled shaft #10 due to anchor tension (phase 10). .....	V-89
5.79	Axial force along the shaft length for the drilled shaft #9 due to anchor tension and backfill (phase 11). .....	V-90
5.80	Axial force along the shaft length for the drilled shaft #10 due to anchor tension and backfill (phase 11). .....	V-91
5.81	Deflection of drilled shaft #9 due to anchor tension (phase 10). .....	V-92
5.82	Deflection of drilled shaft #10 due to anchor tension (phase 10). .....	V-93
5.83	Deflection of drilled shaft #9 due to anchor tension and backfill (phase 11). ..	V-94
5.84	Deflection of drilled shaft #10 due to anchor tension and backfill (phase 11). ..	V-95
5.85	Bending moment along the beam axis for the tie-beam due to anchor tension (phase 10). .....	V-96
5.86	Bending moment along the beam axis for the tie-beam due to anchor tension and backfill (phase 11). .....	V-97
5.87	Shear force distribution for the tie-beam due to anchor tension (phase 10). ...	V-98
5.88	Shear force distribution for the tie-beam due to anchor tension and backfill (phase 11). .....	V-99
5.89	Axial force distribution for the tie-beam due to anchor tension (phase 10). ....	V-100



## List of Figures (Cont)

<b>Figure</b>	<b>Title</b>	<b>Page</b>
5.90	Axial force distribution for the tie-beam due to anchor tension and backfill (phase 11). .....	V-101
5.91	Axial force along the bond length of ground anchor after tension (phase 10).	V-102
6.1	The shaft geometry showing p-y curve positions (Shaft #1 at CUY-90-15.24 Project). .....	VI-8
6.2	P-Y curves derived from different methods (Shaft #1, depth = 92 in). .....	VI-9
6.3	P-Y curves derived from different methods (Shaft #1, depth = 405 in). .....	VI-10
6.4	P-Y curves derived from different methods (Shaft #1, depth = 711 in). .....	VI-11
6.5	P-Y curves derived from different methods (Shaft #1, depth = 1024 in). .....	VI-12
6.6	Comparison of deflections (Shaft #1, 100 kips). .....	VI-13
6.7	Comparison of deflections (Shaft #1, 300 kips). .....	VI-14
6.8	Comparison of deflections (Shaft #1, 500 kips). .....	VI-15
6.9	Comparison of deflections (Shaft #1, 600 kips). .....	VI-16
6.10	Comparison of deflections (Shaft #1, 680 kips). .....	VI-17
6.11	Comparison of pile head movement (Shaft #1). .....	VI-18
7.1	Monitoring of deflection since 5/15/96 for B-103 inclinometer, A-Direction	VII-11
7.2	Stability Evaluation and slip surfaces. .....	VII-12
7.3	Soil properties model. .....	VII-13
7.4	Stress ratio at shallow slip plane prior to construction (stage I). .....	VII-14
7.5	Stress ratio at deep slip plane prior to construction (stage I). .....	VII-15
7.6	Stress ratio at shallow slip plane after excavation to pile cap elevation (stage II) .....	VII-16
7.7	Stress ratio at deep slip plane after excavation to pile cap elevation (stage II) .....	VII-17
7.8	Deformation filed due to excavation. .....	VII-18
7.9	Deflection vs. depth (stage II) .....	VII-19
7.10	Stress ratio contour (stage II) .....	VII-20

## List of Figures (Cont)

Figure	Title	Page
7.11	Inclinometer reading after pile driving is completed till before start of shaft construction (stage III) .....	VII-21
7.12	Horizontal deflection of temporary retaining structure from FEM (stage III) .....	VII-22
7.13	Slurry tanks and shafts drilling .....	VII-23
7.14	Use of polymer slurry .....	VII-24
7.15	Inclinometer casing in drilled shafts. ....	VII-25
7.16	Slope movement after completion of shaft installation, inclinometer B-303 (stage IV) .....	VII-26
7.17	Calculated pile deflection after anchor tensioning (stage VI) .....	VII-27
7.18	Calculated pile bending moment after anchor tensioning (stage VI) .....	VII-28
7.19	Bending moment calculated by FEM vs. measured in shafts after anchor tensioning (Case VI) .....	VII-29
7.20	Deflection of shafts calculated by FEM vs. measured after anchor tensioning (stage VI) .....	VII-30
7.21	Soil movement at B-303 after finishing anchors tensioning (stage VI) .....	VII-31
7.22	Stress ratio at shallow slip plane after anchor tensioning (stage VI) .....	VII-32
7.23	Stress ratio at deep slip plane after anchor tensioning (stage VI) .....	VII-33
7.24	Deflection of driven piles after backfilling to final grade (stage VI) .....	VII-34
7.25	Driven piles bending moment after backfilling the slope (stage VII) .....	VII-35
7.26	Drilled shaft deflection after backfilling the slope (stage VII) .....	VII-36
7.27	Drilled shaft #9 bending moment after backfilling the slope (stage VII) .....	VII-37
7.28	Schematic of gage locations on the rock anchor. ....	VII-38
7.29	Comparison between measured and calculated axial force along bond length of the anchor .....	VII-39
7.30	Stress ratio at shallow slip plane (stage VII) .....	VII-40
7.31	Stress ratio at deep slip plane (stage VII) .....	VII-41
7.32	Soil movement at B-303 at the end of monitoring phase I. ....	VII-42

## List of Figures (Cont)

<u>Figure</u>	<u>Title</u>	<u>Page</u>
7.33	Force diagram at the end of monitoring phase I on 6/30/1999. ....	VII-43
7.34	Displacement and displacement contour due to overload .....	VII-44



# CHAPTER I

## INTRODUCTION

### I.1 Introduction

Bridge CUY-90-15.24, the Central Viaduct, also known as the Inner Belt Bridge, is part of the Interstate Highway System in Cleveland, Ohio. The structure carries up to eight traffic lanes, over many streets, the Cuyahoga River, Conrail tracks, the N-S Trestle, Cleveland Rapid Transit tracks, among others. The roadway carries an average of 134,660 vehicles per day. About nine percent of the traffic is heavy trucks. Since 1988, Richland Engineering Limited has inspected the bridge annually. In addition, beginning in 1991, detailed substructure stability study was carried out. From these studies, general observations revealed that: (a) Pier 1 has moved about 0.6 to 0.8 feet toward the river, and (b) The west end pier has moved about 0.3 to 0.4 feet toward the river. Figs. 1.1 and 1.2 show the site condition prior to construction. As an initial step to stabilize the slopes and piers, the grading and drainage improvements were completed in 1995. As a permanent stabilization to the upper slope, the CUY-90-15.24 project (PID No. 12374) has been approved. The stabilization scheme involved the use of drilled shafts, rock anchors, tiebacks, and driven piles. Fig. 1.3 shows the elevation view of the proposed stabilization scheme. However, because of unique features (extremely long drilled shafts, high capacity rock anchors) and the uncertainties of design assumptions (mechanisms of the slope stabilization), engineers have put into the plans a special item for instrumentation, testing, and long-term monitoring. The University of Akron was the designated research team to carry out the tasks involved in this special item.

Other team members responsible for the successful completion of the project are depicted in Fig. 1.4.

## **I.2 Objectives**

The main objectives of the project are two fold: (a) ensure construction safety and verification of design assumptions, and (b) gain insights on the foundation structure behaviors. Specifically, the objectives include the following:

1. Ensure safety (during construction and service) of the bridge.
2. Measure stress and deformation of substructures used for slope stabilization to confirm both safety (limiting stresses) and serviceability (limiting deformations).
3. Provide real-time measurements to allow project engineers to make sensible but critical decisions.
4. Long-term monitoring as part of bridge maintenance program to assess maintenance needs.
5. Re-assess design assumptions so that new knowledge can be gained and applied for future projects.
6. Advance the knowledge on soil structure interactions and slope stabilization techniques
7. Form valuable database for current FHWA development of LRFD (Load Resistance Factor Design) for substructures.
8. Perform FEM (Finite element Method) Simulation (Verified with Field Measurements) to provide further details of substructure behavior.

### **I.3 Organization of the Report**

Chapter I provides an introduction, scope of the work, objectives of the project, and outline of the final report.

Presented in chapter II is a brief summary of background information prior to the start of the construction. The background information included a discussion of the nature of the problem, quantitative data of past inclinometer data, and stability analysis of the problem slope.

Chapter III provides a detailed description of the instrumentation plan, types of sensors used, locations of the sensors and inclinometer casing, and the special load test plan. As installation of sensors took place while construction was progressing, a more detailed discussion was presented for the sensor installation techniques for different structures.

Chapter IV consists of the bulk of measured data prior to and during the construction. For easy reference, the measured data (such as strains, stresses, and deflections) have been plotted as a function of time to provide a time-history of structure responses at different construction stages. In addition, the measured data have been plotted as a function of locations, providing a spatial picture of the structure response with different construction stages as well. Together, these comprehensive plots of a wealth of measured data formed the basis for interpreting the structure behavior and verification of design assumptions.

Chapter V presents a detail description of using the FEM simulation technique to gain further insights on the slope stabilization mechanisms. The FEM program, PLAXIS, was employed to determine the stress and deformation fields of the slopes at various stages of construction, as well as structural behavior (stress, strain, deflection) of each substructure. The technique for representing the 3-dimensional pile group in a two-dimensional FEM

analysis was explained in this chapter as well. When applicable, a comparison was made between the computed results and the actual measured results. A good match was observed between the computed and the measured, lending strong credibility to the FEM PLAXIS simulation technique.

Chapter VI provides a brief summary of a back calculation technique to derive site-specific p-y curves for laterally loaded drilled shafts. As shown in the report, the back-calculation technique can allow engineers to obtain more representative p-y curves, which in turn can facilitate accurate predictions of the drilled shaft's behavior under the applied lateral loads.

Chapter VII presents observations of field performance, based on both field measurements and FEM simulation results.

Finally, chapter VIII provides summaries and conclusions of the project.



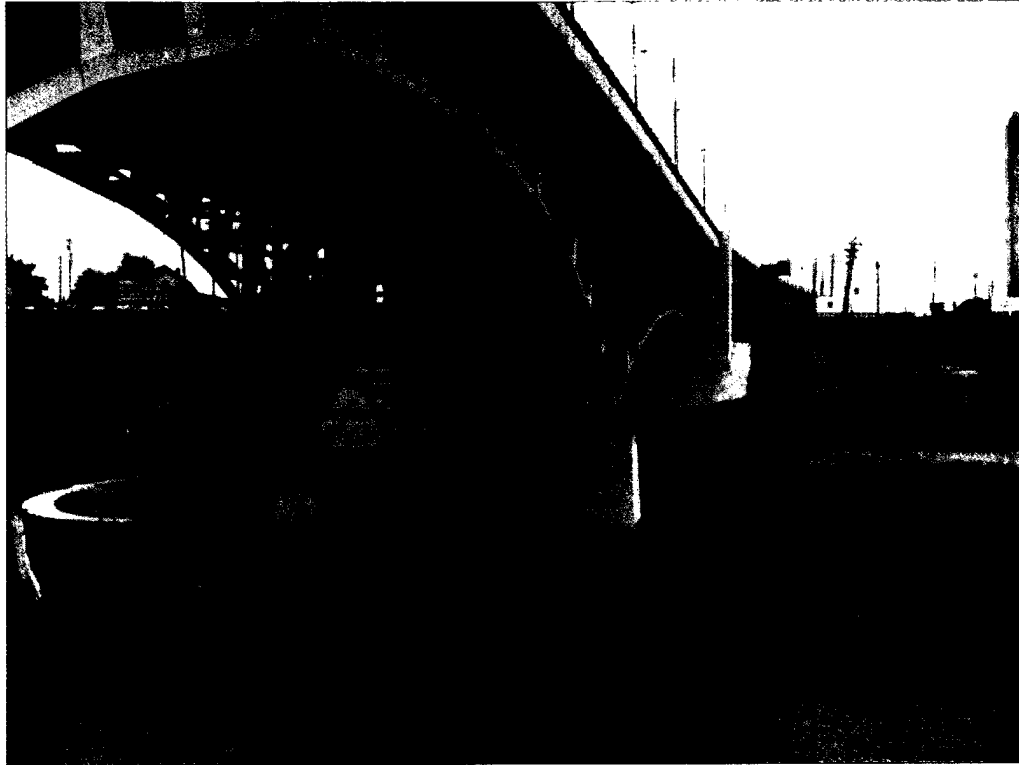


Fig. 1.1: Site condition prior to construction.



Fig. 1.2: Site condition prior to construction.

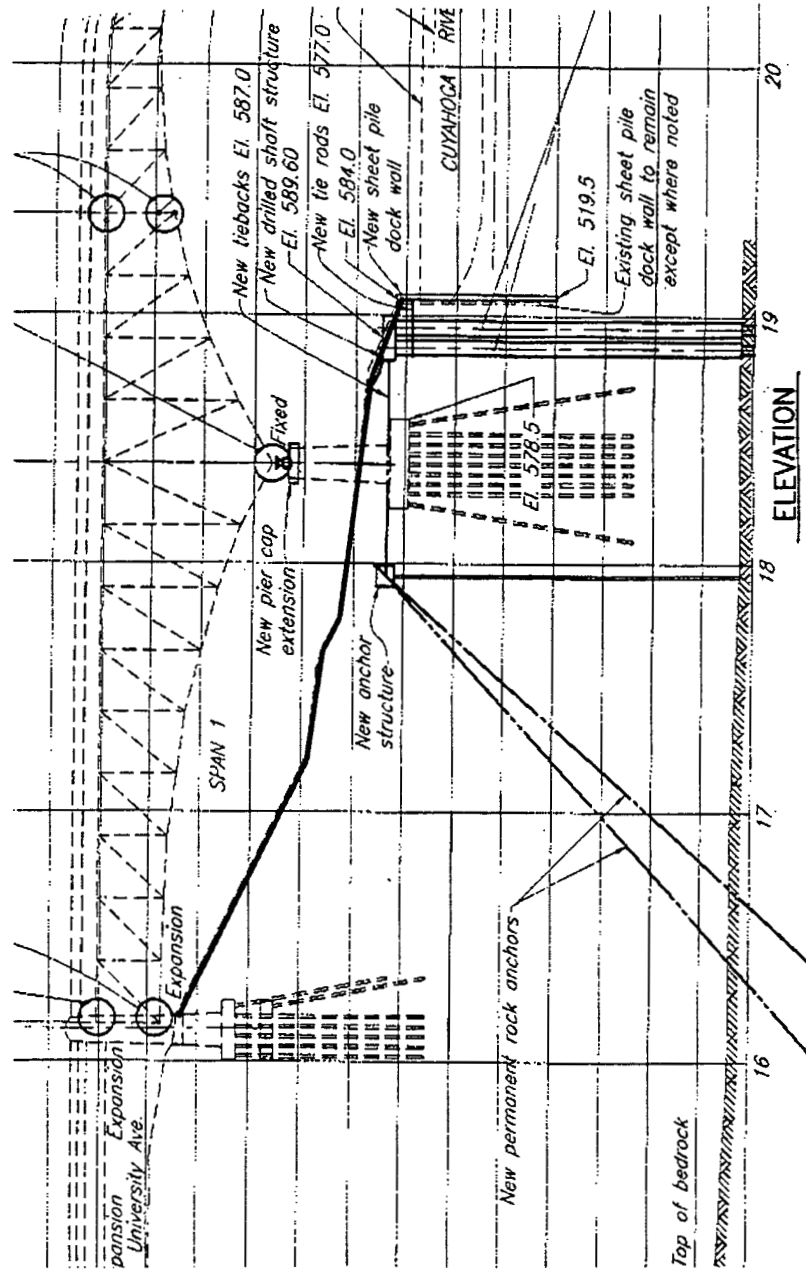


Fig. 1.3: elevation view of the proposed stabilization scheme.

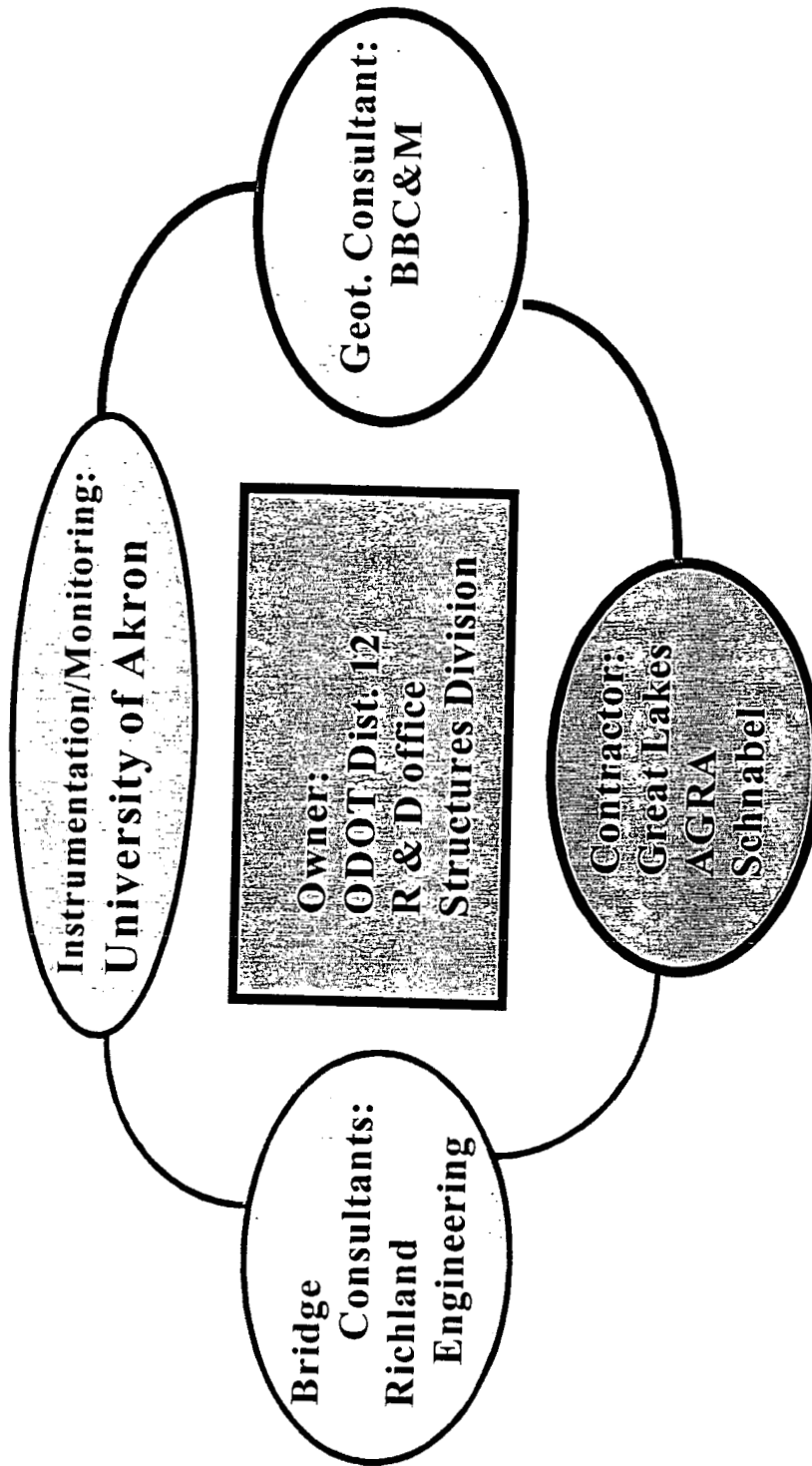


Fig. 1.4: Team members responsible for the successful completion of the project.

## CHAPTER II

### HISTORICAL BACKGROUND OF THE PROJECT

#### II.1 INTRODUCTION

Bridge CUY-90-1524, the Central Viaduct, also known as the Inner Belt Bridge, is part of the Interstate Highway System in Cleveland, Ohio. The bridge was completed and opened to traffic in 1959. The structure in the approach span areas consists of two separate reinforced concrete decks and safety walks carried by continuous steel beam spans, supported on separate reinforced concrete substructure units. The railing is a concrete parapet and aluminum tube on the exterior of the structures. A concrete safety shape is the common median barrier.

The main truss spans are a reinforced concrete deck, with steel curbs, safety walks and railing, and a concrete safety shape median, supported by steel stringers and floor beams carried by cantilevered, arched deck trusses. The piers are hollow reinforced concrete pedestals. A steel fascia girder was added to support the widening of ramp W- I in spans 1 and 2 in 1984. All substructure units except the rear abutment are founded on piling. The main truss spans consist of nine cantilever truss spans of 227', 400', 250', 400', 248', 348', 248', 349', and 251'. The overall length of the mainline structure is 5,080 feet. Fig. 2.1 shows the elevation view of the bridge.

Richland Engineering Limited (REL) has inspected the bridge annually since 1988, and previously in 1970 and 1974. There is evidence that span 1, the west end pier

and pier 1 of the main truss spans of the bridge are not in the position where they were originally constructed. There is distress at the superstructure expansion joint in span 2, and at the rockers at the west end pier.

## **II.2 NATURE OF THE PROBLEM**

The earliest physical conditions survey reports prepared for this structure included hints of substructure problems. In the 1970 report, the joint opening measurement table included a finger joint gap of zero inches in span 2. An upgrading project in 1973 included resetting the span 2 finger expansion joint opening to more than the original design. Reviewing the pictures taken in 1975, there appears to be an excessive lean in the roller nest for the south bearing at the west end pier. The openings of the expansion joints have been recorded since 1970. Measurements of the roller nest lean have been recorded since 1981.

In 1985, the west end pier, pier 1 and pier 2 were monumented and measured with electronic distance measuring equipment. Since 1985, these measurements have been repeated with each consultant inspection. These measurements have shown that there has been movement of pier 1 and the west end pier. To further study the movement, inclinometers were installed in 9 locations by crews from the Ohio Department of Transportation's Testing Lab. The locations of these inclinometer holes are shown in Fig. 2.2. The inclinometers were read at intervals of 1 to 3 months from 1990 to 1993. The readings have shown some subsurface movement. Since the inclinometers were not socketed into bedrock, the reliability of the data collected was questionable.

The data collected through these various monitoring methods was compiled and interpreted through an REL Substructure Stability Study that began in 1991. This study was presented to ODOT in March 1993. The data gathered shows movement of the west end pier and the movement of pier 1, both longitudinally eastward. This corresponds to the west end pier finger joints openings more than design, the closed finger joint at span 2 openings less than design, and the resetting of span 2 finger joint openings to more than design. This also explains the extreme tilt of the rocker bearings on the west end pier. The change in the relative span lengths and pier locations since 1988 also supports this explanation. Because of these results, the Substructure Stability Study concluded that the area below spans 1 and 2 was not stable, and probably was not stable when the bridge was built. In addition, the rate of movement of the piers increased when the area was converted from a railroad yard to a material storage area for asphalt production about 1988.

The impact of REL's Substructure Stability Study was two fold. The first action was that REL was authorized to continue studying the stability of the slope. BBC&M, as sub-consultant to REL, has done a preliminary slope stability evaluation based on existing soil data. The purpose of the preliminary slope stability analyses was to determine the probable locations of the failure planes to aid in the layout of the field investigation program. As part of this study, BBC&M Engineering, Inc. installed 10 new inclinometers and 12 pneumatic piezometers in 5 holes in 1994 and performed a Slope Stability Evaluation. Slope stability calculations for the slope below span 1 indicated that a stability factor of safety of 1.27 for the upper slope, 0.90 for the lower slope, and 1.17

for the entire slope. An acceptable factor of safety for long term stability is typically from 1.3 to 1.5.

The second result of the 1993 Substructure Stability Study was that REL was authorized to prepare plans for stabilizing the slopes and piers and realigning the superstructure. This project has two phases. Phase I, the grading and drainage improvements, was completed in 1995. The goal of this phase was to increase the slope stability safety factor for the upper slope and to stop the area below span 1 from being used for material storage. The work done at Phase I has stabilized the west end pier in the upper slope. Phase II, which was intended to stabilize the entire slope and pier 1 as well as reposition the span 1 structure, began in July 1997.

### **II.3 EXISTING CONDITIONS BEFORE PROJECT START**

Detailed existing conditions are documented in Richland Engineering's 1995 Physical Conditions Report for the bridge and BBC&M's Phases 2 and 3 Stability Evaluation Report (part of the Preliminary Design Report, CUY-90-15.24 Central Viaduct, PID No. 12374, Stabilize Pier 1 and relocate span 1, January 96). The movement of pier 1 has closed the expansion joint at span 2. The clearance between the truss members has closed to zero. The built-up steel truss verticals grate on each other as traffic vibrates the structures. Currently, the guide plates and bars are tearing and cutting. The loads being resisted by the truss are unknown. The pier might not be capable of transferring enough force from the ground movement to the steelwork to damage the truss members. But, further longitudinal movement by pier 1 may cause distress in the truss. The truss might arch, bracing might buckle, or members may start



to break. The bolster on pier 1 needs to be moved to the south to open the closed joint. The bearings at the west end pier need to be reset to be vertical at 60°F.

The relationship and relative positions of the piers, bearings, truss joints and deck joints were monitored. The measured and calculated distances do not agree from location to location because of the size of the structure and variables in obtaining data. The following general observations were drawn from the data:

- The north and south sides have not moved the same amount or direction.
- Pier 1 has moved about 0.6 to 0.8 feet toward the river.
- The west end pier has moved about 0.3 to 0.4 feet toward the river.
- The pier movement correlates with the deck expansion joint changes when the expansion rocker positions are included.

#### **II.4 PRE-CONSTRUCTION ANALYSIS AND DESIGN**

A four-phase detailed study was carried out by BBC&M to investigate the site conditions and to study the stability of the slope. The scope in Phases 1 & 2 included the subsurface investigation, testing and analysis of the soil conditions in the general area of Pier 1, West End Pier, and Pier 1A of the bridge. Recommendations for stabilization were made based upon the short-term data collected. Phases 3 & 4 included the 3 year monitoring of instrumentation installed at the slope and recommendations based upon the results of that monitoring.

The scope of Phase I was specifically to review readily available geotechnical data and perform preliminary slope stability analysis. The results of the slope stability analysis would assist in the selection of additional boring locations, sample depths and

types, and type of instrumentation needed for the field portion of the program contained in Phase 2.

#### **II.4.1 GENERAL SUBSURFACE CONDITIONS**

Part of Interstate Route 90 crosses the Cuyahoga River Valley at approximately one mile from the shore of Lake Erie. The surficial deposits along the shore line of Lake Erie are mostly lake plain deposits of glacial origin and extend from 2 to 10 miles from the lake southward into the City. The lake plain deposits are predominately sand and gravel deposits that are interbedded with till above the shale bedrock. The lake plain is dissected at the major river valleys such as the Rocky River, the Cuyahoga River and Euclid Creek. The Cuyahoga River Valley is deeply cut into the bedrock that underlies the plain and is 2.5 to 4 miles wide across the top and has a relief of over 400 feet.

Bedrock elevations range from 600 feet at the west side of the valley to 0 feet at the east side of the valley which indicates that the preglacial bedrock valley is located east of the present surficial river valley. The existing valley is a relatively minor depression of the ground surface compared to a much more impressive valley in the bedrock surface.

Much of the bedrock valley is filled with deposits of clay till and of glacial lacustrine clay or silty clay. These deposits extend upward to about Elev. 560. They are overlain by sand and silty sand.

Changing lake levels led to the alternate downcutting and deposition of delta materials at the mouth of the river. The deposited materials were silty and sometimes organic. It would be expected that the soil deposits at the bridge are horizontally

stratified, variable with depth and overlying a deep bedrock surface which continues to dip to the east well beyond the immediate location of the bridge structure. As a result, a detailed boring and testing program is necessary to sufficiently characterize the stratified deposits. The stability analysis of the bridge must take into account weak and possibly thin layers of material which may exist and govern the overall stability of the structure.

## **II.4.2 EXISTING DATA**

### **II.4.2.1 Borings and Soils Testing**

Four borings were obtained by ODOT in the area of the West End Pier and Pier No. 1 as part of the original soils investigation in 1954. These borings show standard penetration numbers and the distinction between surficial granular materials and underlying clays, but provided limited detail information. In 1990, nine borings (B-1 thru B-9) were obtained by ODOT while installing inclinometers. In 1992 an additional boring was obtained (B-10) by ODOT. These borings provided more detailed descriptions, soil classifications, grain size analysis and Atterburg Limits. Samples from B-10 were sent to BBC&M by Richland Engineering, Ltd. for strength testing which was completed in January, 1993. All of these borings were clustered directly under the bridge and did not extend to bedrock. The borings, in general, substantiate what would be expected in this geomorphic regime and include granular materials consisting of gravelly sands and sandy silts overlying cohesive deposits of gray silty clay.

The locations of these borings, as well as the boring logs are contained in the March, 1993, Richland Engineering report and they are reproduced in the Appendix A.

These borings were used to model the general site conditions for the preliminary stability analyses.

#### **II.4.2.2 Bridge Deformation Information**

Deformation information detailed in Richland's Report including expansion joint measurements, roller bearing tilt measurements and pier movements, indicate that Pier No. 1 has moved east between 2 and 3 inches and that the West End Pier has moved east up to 1 inch. As is to be expected, some conflicting information exists concerning the exact magnitude of movement, depending upon the three types of measurements examined. Nevertheless, all data substantiates that both the West End Pier and Pier No. 1 had moved east and that Pier No. 1 has moved substantially more than the West End Pier.

### **II.5 PRECONSTRUCTION ANALYSIS AND DESIGN**

#### **II.5.1 Preliminary Slope Stability Analysis**

##### **II.5.1.1 Analysis by BBC&M Engineering, Inc.**

BBC&M Engineering, Inc., performed preliminary slope stability analyses to determine the probable location(s) of the failure plane to aid in the layout of the field investigation program. Analyses were performed with an assumption that the slope was near a factor of safety of one since movement had already been mobilized. Shear strength parameters for the soil strata were then back calculated using on a factor of safety near one. For each analysis, the resulting failure plane yields a probable failure plane location for the slope at incipient failure. These information assisted in the selection of slope

inclinometer, pneumatic piezometer, and shelly tube sample locations for later field work.

Stability analyses were performed using the PC STABL 5, a slope stability analysis program developed by Purdue University. This program can rapidly model a variety of failure slope surfaces for a given set of strength parameters. An approximate soil profile is modeled using available boring information and shear strength parameters for the soils are chosen, by successive trials, which yield factors of safety near one. Slide surface initiation and termination points are specified based upon educated assumptions about probable slide plane shapes. The details of these results are summarized in REL report (Preliminary Design Report, CUY-90-15.24 Central Viaduct, PID No. 12374, Stabilize Pier 1 and relocate span 1, January 96)

It was stated in the report that it was not necessary, in that phase of the project, to establish the shear strength parameters which yield a factor of safety exactly equal to one, as long as the location of the failure plane is not overly sensitive to small changes in the shear strength parameters. Analyses were performed with a range of realistic strength parameters (based on the test data and experience) which yielded factors of safety above, near, and below unity.

To model the soil layers for slope stability analysis, a simplified soil profile was developed based upon the results of the 1990 and 1992 borings and the 1993 shear strength tests. The surface geometry was based upon the centerline profile as shown in the Richland Engineering drawing, "Slope Stability Analysis" dated March 1993. The profile consisted of a shallow granular soil with a friction angle of 39 degrees overlying a cohesive soil extending to bedrock. Bedrock is known to exist at Elev. 428 feet near Pier

No. 1. The bedrock surface was assumed to be horizontal for the purposes of this analysis.

The cohesive soil was modeled in several ways: with frictional characteristics only, varying from 13 to 23 degrees; and with undrained shear strength characteristics varying from 1000 psf to 2500 psf. An angle of internal friction of 23 degrees was computed as the average of the residual strengths obtained in the January, 1993 shear strength testing performed by BBC&M Engineering.

Three different slide scenarios (locations) were modeled. These scenarios represent the following: (1) Deep seated slide extending from the river side of the bulkhead to the landward side of the West End Pier, (2) Shallow slide extending from the river side of the bulkhead to the landward side of Pier No. 1, and (3) Shallow slide extending from the toe of the slope just downslope of the West End Pier to the top of the slope located upslope of the West End Pier.

Two different types of analysis methods were utilized, modified Bishop analysis with circular slip surface, and Janbu analysis with a block failure surface. Pier loads of 2000 psf were assumed to be distributed across the pier foundation width at the surface of the slope. The STABL model used in the analyses along with the locations of the most critical slide planes is shown in Fig. 2.3 and the soil strength parameters are presented in Table 2.1.

The possibility of deep seated movement occurring over a large Aerial extent requires that the boring program extend from the bulkhead along the west side of the Cuyahoga River to the landward side of Pier 1A. The geometry of the slide planes makes borings and monitoring of the east side of the Cuyahoga River unnecessary unless a related slide is

occurring at that location. The Richland Engineering Report did not include any information which suggest that movement on the east side of the river was occurring. Since the lateral extent of the slide is unknown, some boring information should be obtained beyond the immediate limits of the bridge in both the upriver and downriver directions. A total of 15 boreholes were proposed and completed in August 1994. 10 of which for inclinometers, and 5 for pneumatic piezometers. The locations of these borings are shown in Fig. 2.4. The detailed information about these borings are provided in Appendix A.

Table 2.1: Soil parameters used in the slope stability analysis

Soil type No.	Total unit weight (pcf)	Sat. unit weight (pcf)	Cohesion intercep (psf)	Friction angle $\phi$ (deg.)
1	100	120	0	35
2	100	120	0	34
3	110	130	0	21
4	90	120	0	21
5	105	130	0	21
6	95	115	0	37
7	110	130	0	30
8	150	160	5000	0

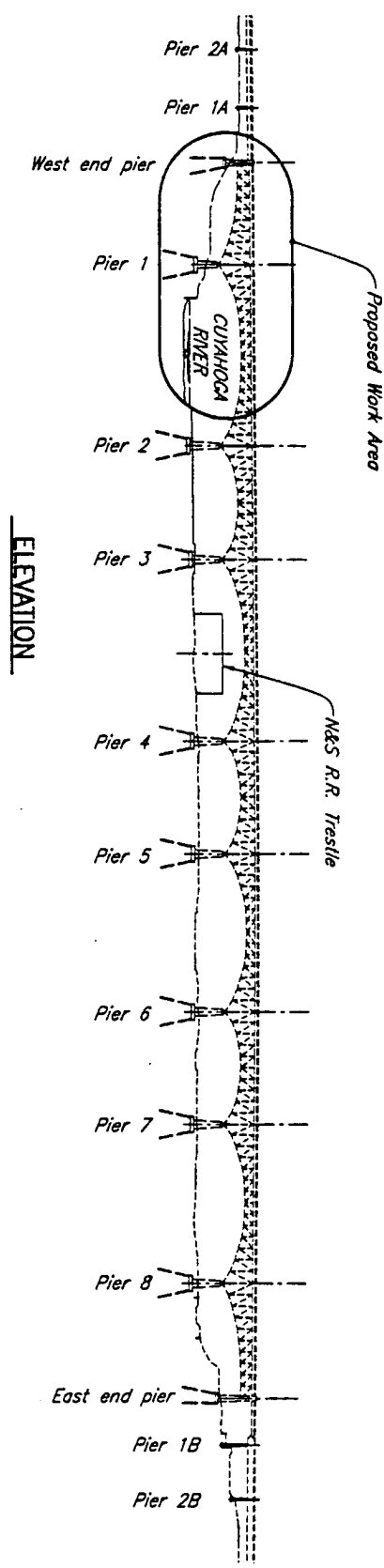


Fig. 2.1: Elevation view of the bridge.



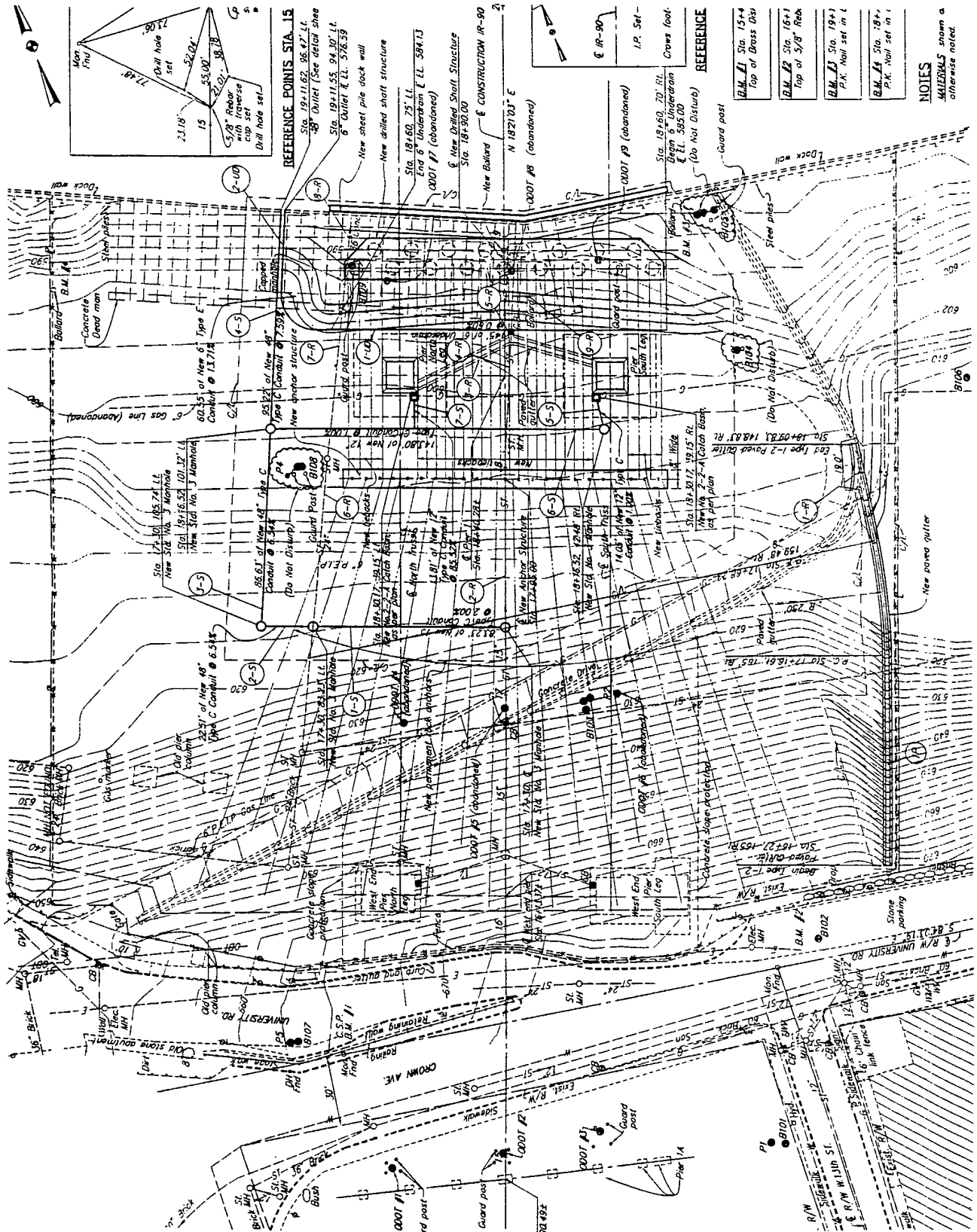


Fig. 2.2: Location of inclinometers installed by ODOT.



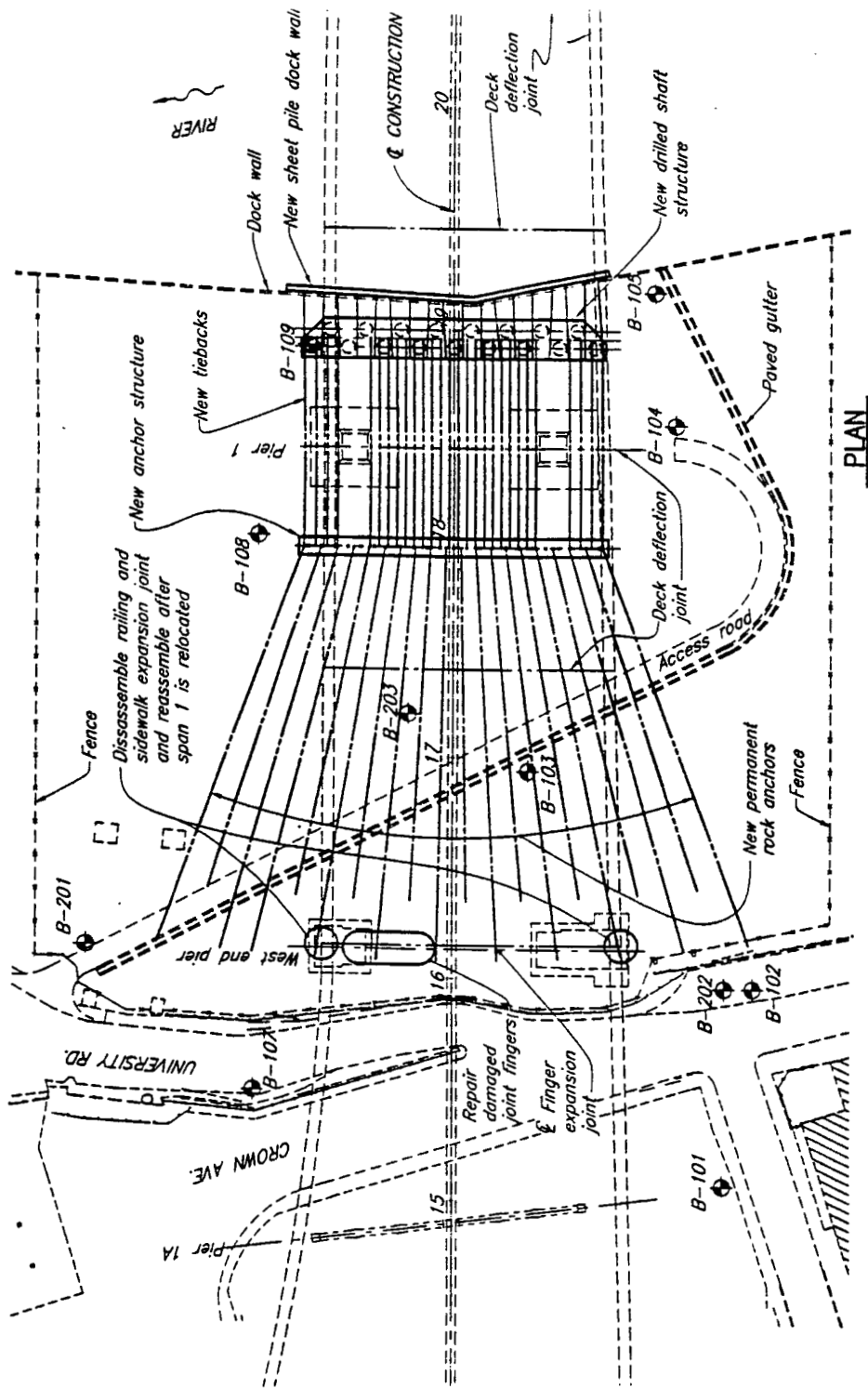


Fig. 2.4: Location of inclinometers and piezometers installed by BBC&M.



## **CHAPTER III**

### **INSTRUMENTATION/MONITORING PROGRAM**

#### **III.1 INTRODUCTION**

Instrumentation and monitoring of the behavior of the slope stabilization of the bridge piers was necessary to be able to measure the stress and deformations of the stabilized structure and the stabilizing elements. The instrumentation designed for this project was based on questions raised during the analysis about the behavior of each of the instrumented elements. Instruments were installed in the slope, on the driven piles for the anchor cap, on the rock anchors, and on the drilled shafts. The plan on the entire stabilizing system and the locations of the instrumented elements are shown in Fig. 3.1.

The instruments were installed per manufacturer recommendation and were monitored since then.

#### **III.2 SLOPE MOVEMENT MONITORING**

The movement of the slope was monitored by BBC&M Engineering, Inc. since 1994. They installed 10 inclinometers to depths below the rock elevation to be able to identify the deep slip plane location. These inclinometers were read quarterly and the locations of the slip planes were identified. The locations of the 10 inclinometers are shown in Fig. 3.2. Inclinometer readings done since 1994 were transferred from BBC&M

and reduced by the University of Akron team. The detailed plots of these 10 inclinometer readings are presented in chapter IV.

### **III.3 FOUNDATION STRUCTURE BEHAVIOR**

The study of the behavior of the stabilized foundation of the bridge required instrumentation of some elements of the stabilizing structure. Detailed information about each instrumented structure are summarized below.

#### **III.3.1 Driven Piles**

Five driven piles were instrumented, each with four vibrating wire strain gages (Geokon, model VSM 4000). Four gages were mounted 3' from the top of the pile (Elev. 583). Piles #1, #17, #18, #19, and #34 were instrumented. The detailed locations of these instrumented piles are shown in Fig. 3.3. In addition Fig. 3.4 to Fig. 3.8 show the pictures of gages attached 3 feet from the pile top. The gages were hooked to the data acquisition system (Geokon, model MICRO-10) right before the pile cap concrete was poured, and the collection of the data started at that time on 2/12/98.

Moreover, prior to installing the pile gages, during pile driving, a dynamic load test was conducted on pile #18. The Pile Driving Analyzer (PDA) owned by ODOT was used to conduct the test. The results of the testing and analysis are documented in Chapter IV.

### III.3.2 Drilled Shafts

During the course of instrumentation, six drilled shafts were instrumented for two purposes: first, to conduct a lateral load test to study the lateral response of the shafts, and second, to monitor the response of the shafts during construction and long term loading. Fig. 3.9 shows the plan location of those instrumented shafts.

For the purpose of lateral load testing, shafts # 1 and # 3 were instrumented. Shaft # 1 was instrumented with an inclinometer and 28 sister bar strain gages (Geokon, model 4911). Fig. 3.10 shows the instrumentation of shaft # 1. Figs. 3.11 to 3.14 present pictures of installation of strain gages and inclinometers. Shaft # 3 was instrumented with an inclinometer only. The locations of the two inclinometers installed in shaft #9 are shown in the picture presented in Fig. 3.15. During the lateral load test, which was conducted on January 13, 1999, two tiltmeters were mounted on the jacking level, one on each of the shafts, to measure the angle of rotation of the shaft at that point. Two teams were mobilized to take the inclinometer readings: The University of Akron team read inclinometer #1 and ODOT crew read inclinometer #3. The strain gages and tiltmeters were hooked to the data acquisition system where the data was collected. The jack used in the testing was with 500 tons capacity and 10 inches stroke. The capacity of the load cell used was 400 tons. The testing setup is shown in Fig. 3.16. In addition, Figs. 3.17 to 3.20 document the pictures of the setup and the testing.

For the purpose of long term monitoring, in addition to shafts #1 and #3, four shafts were instrumented. Shaft #8 was instrumented with an inclinometer, Shaft #9 with an inclinometer and 28 sister bar strain gages (Geokon, model 4911), shaft #10 with an inclinometer, and shaft #17 with an inclinometer as shown in Fig. 3.9. The gages in shaft

#9 were installed on both sides of the shaft in the direction of slope movement. The locations of the strain gages are shown in Fig. 3.21.

### **III.3.3 Ground Anchors**

A total of four ground anchors were instrumented for long term monitoring of the stresses and force in the anchors. The anchors were inclined at 45 and 47 degrees from horizontal. Anchor #1 is in the zone of shaft #1. Anchors #8 and #9 are in the zone of shafts #8, #9, and #10. Anchor #17 is in the zone of shaft #17. Anchors #1 and #17 were instrumented to check on the axial force in the edge anchors. Fig. 3.1 shows the approximate location of these anchors in the plan. Anchors #1, #8, #9, and #17 were instrumented each with five strand meters (Geokon, model 4410) and a vibrating wire load cell (Geokon, model 4900-6-750) with 750 Kips capacity as shown in Fig. 3.22. The construction procedure, installation of the strand gages, and testing is illustrated in pictures as shown in Figs. 3.23 to 3.30.

### **III.3.4 Instrumentation of Tie Beams**

Five tie beams were instrumented at two location on each. Location one is 3 feet from the drilled shaft cap, and location two is 3 feet from the driven piles cap. A total of four vibrating wire strain gages model Geokon 4000 were used at each location on the tie beam, with a total of 40 gages on the five tiebeams. The details of the location of the gages on the tie beams are shown in Fig. 3.31. In the initial instrumentation design submitted to Richland Engineering, Ltd., three tiebeams were instrumented. After a detailed review of the objectives of the instrumentation, it was found that it is necessary



to instrument the exterior tiebeams (i.e. the extreme left and extreme right ones). The data from those gages on the tie beams is been collected since 3/27/1999. The strain gages installation and the tiebeams entire structure are illustrated in pictures as shown in Figs. 3.32 to 3.36.

### **III.3.5 Instrumentation of Drilled Shaft Cap**

The cap was instrumented with 4 vibrating wire in-place tiltmeters to measure the rotation of the shaft cap and compare it with the rotation from the inclinometers. The locations of those tiltmeters are shown in Fig. 3.37 and a picture showing one set of bi-axial teltmeters is shown in Fig. 3.38.

## **III.4 INSTRUMENTATION INSTALLATION DETAILS**

### **III.4.1 Sequence of Installation**

The installation of the instruments were on with the construction progress. A time-line plot showing the construction progress is shown in Fig. 3.39. The driven piles were the first to be instrumented in the first week of February 1998. The drilled shafts were to follow during the period from August 4, 1998 to December 10, 1998. The gages and the 4 inch diameter PVC pipe to in-house the inclinometer for shaft #1 were mounted to the main bars on 10/11/98, then the steel cage was lowered in the hole and the concrete was poured on 10/13/98. For shaft #3, drilling started on 11/9/98 the cage was prepared and the PVC pipe was attached to the main steel and lowered in the hole. The shaft was concerted on 11/12/98. Drilling for shaft #8 started on 8/24/98 and the shaft was

completed on 9/8/98. The PVC pipe for inclinometer was mounted to the main steel and lowered in the hole. The diameter of the hole above and below bedrock elevation was 72 inches. During drilling for shaft #8, at a depth of 65', an H-pile (stub) was found and the contractor have to core through the pile and that is the reason behind the long period for completion of the shaft. Drilling for shaft #10 started on 8/13/98 and the shaft was completed on 8/20/98. The diameter of the hole above and below bedrock elevation was 72 inches. The PVC pipe for inclinometer was mounted to the main steel and lowered in the hole. Drilling for shaft #9 started on 10/30/98 and the shaft was completed on 11/19/98. The gages and PVC pipe for inclinometer was mounted to the main steel and lowered in the hole. The diameter of the hole above and below bedrock elevation was 72 inches. During drilling for shaft #9, at a depth of 48', an H-pile was found and the contractor have to core through the pile and that is the reason behind the long period for completion of the shaft. Drilling for shaft #17 started on 11/20/98 and the shaft was completed on 11/23/98. The PVC pipe for inclinometer was mounted to the main steel and lowered in the hole. The diameter of the hole above and below bedrock elevation was 72 inches. During drilling for shaft #8, at a depth of 48', an H-pile was found and the contractor have to core through the pile.

A complete tabulation of the sequence of installation for all the 17 drilled shafts and the detailed inspection information about each shaft are given in Appendix B. Moreover, a concrete curve showing the actual vs. the theoretical volume of concrete for every shaft are given in Appendix B.

The installation of the rock anchors started on 1/20/99 and was completed on 2/15/99. Four anchors were instrumented each with 5 strand gages. The hole for each

anchor was drilled and cased to the shale elevation. The casing was forwarded 5' into shale. On the day of installing each anchor, the shale part was drilled and cleaned. The tendon was then lowered in the hole and grouted. For the instrumented tendons (#1, #8, #9 and #17), the gages were installed on the stands during lowering of the tendon. The gages were tested before mounting to the strand, after mounting, after lowering in the hole, and after grouting was completed.

The installation of the tie-beams started after completion of rock anchor installation around 2/20/99. A total of 26 tie beams were constructed and were completed on 3/25/99. The installation of the strain gages on the tie beams started on 3/25/99 and was completed on 3/26/99. The gages were then connected to the data acquisition system, and the monitoring was commenced since. The next step was installing the tiltmeters on the drilled shaft cap. Two bi-axial tilt meters were installed. One 10' from the north side of the cap and one 10' from the south end of the cap as shown in Fig. 3.37.

After installing the tiltmeters, the stressing of the rock anchors started on 4/5/99, and was completed on 4/14/99. Anchors #1, #8 and #7 were performance tested and anchor #9 was creep tested. The results of testing are included in Chapter IV. The sheetings around the tie beams were grouted on 4/20/99. On 4/25/99, the second data logger was relocated and the wires from the load cells mounted on the instrumented anchors were wired to the data logger. The wiring of the gages to the data loggers was completed on 5/1/99. Backfilling the slope started on 4/28/99 and was completed on 5/7/99.

### **III.4.2 Techniques of Installing Instruments and Monitoring**

The state-of-the-art techniques were used in the installation of the instruments. The instruments consist of vibrating wire sensors that are considered to be the most reliable long-term monitoring gages. The gages for the driven piles were mounted to end blocks (Geokon, Model VSM-4000). The end blocks were welded first, then the gages were attached and calibrated. The gages were then covered with a steel protection cover to safeguard them during backfill. The gages used for drilled shafts were vibrating wire sister bars (Geokon, Model 4911). These gages were tied to the main reinforcement bars using the tie wires. The gages were checked then mounted on both sides of the cage, as shown in Figs. 3.10 to 3.15.

Rock anchor gages were vibrating wire strand type gages (Geokon, Model 4410). At the tendon manufacturing plant, each gage was put in a 1 inch diameter PVC pipe at the pre-selected location, and the electrical wires were run through the internal grout tube of the anchor. This is to protect the gages wires from potential damage during transportation. Fig. 3.27 shows the pre-installed vibrating wire gages in the spool of the tendon. At the day of installation, during lowering the tendon in the hole, the gages were mounted to the 7-wire strand following the installation procedure recommended by the manufacturer. The installation started by taking the 1 inch PVC pipe off the gage, then one end block was mounted to the strand. After that, the second end block is mounted loose, and the spacer bar is used to have exact distance between the blocks equal to the length of the gage and the end block was tightened. Then, the grease tube is put between the blocks and the gage was inserted and the screws were tightened at the end that is to the side of the wire. A screw was screwed to the other end and the gage wire was hooked

to the readout device to calibrate it. The screw was pulled till the gages reading is close to the required reading at the time of installation. When the reading was reached, the tiny screws on the other end block were tightened. A waterproof tape was wrapped around the end blocks to prevent grout from entering the gage. Then, grease was pumped through the grease fit into the pipe and the installation was complete. The gages were read every time they lower the tendon to install another gage, to make sure that the gages were working fine. The procedure is documented in pictures as shown in Figs. 3.26 to 3.28. The gages were installed at the following locations: 5', 15', 25', 35', and 45' from the bottom end of tendon. At each anchor head, a 750 Kips capacity vibrating wire 6-gage load cell was mounted to measure the anchor force during testing and long-term monitoring. The anchor head assembly is shown in Fig. 3.22 and a picture showing the details is presented in Fig. 3.29.

The tie beam gages were of vibrating wire type (Geokon, Model VSM-4000). They were mounted to the beams by first welding the end blocks, then installing and calibrating the gage. Four gages were used at each instrumented section on each beam, where they were welded to the flanges. Figs. 3.32 to 3.36 show the pictures of tie beams before and after strain gage installation. Each of the five instrumented beams was instrumented with a total of 8 gages: four of them were mounted 3 feet from the anchor cap and the other four were 3 feet from the drilled shaft cap. The gages wires were routed through the sleeve that encloses the tie beam to the drilled shaft cap, where they were routed through a PVC conduit to the data acquisition system.

In addition to the above instrumentation, two bi-axial tiltmeters were mounted on the drilled shaft cap on the riverside. Fig. 3.9 shows the locations of the tiltmeters being

mounted on the concrete cap, and the picture of the location of those tiltmeters is shown in Fig. 3.37. These tiltmeters were monitored continuously from the time before the anchor stressing started.

#### **III.4 DATA ACQUISITION PLANS**

The data collection was done by using the Geokon Model 6020 data acquisition systems. The sensors were first hooked to the multiplexers, and then the multiplexers were connected to the main data acquisition box. At the start of construction, one data acquisition was on site, where the pile gages were connected. The time interval for data collection was 5 minutes for the first 3 days, 10 minutes for 10 days, and half-an-hour afterwards. After completion of the tie beam gages installation, all the gages from the drilled shafts and the tie beams were connected to the second data acquisition system. A total of 96 gages were hooked to the second data acquisition (40 from tie beams and 56 from drilled shafts 1 and 9). The permanent location for the data acquisitions is on the drilled shafts cap. After relocating the first data logger to the final location, the gages from the rock anchors and the load cells were connected to the same data acquisition (20 gages from pile gages, 24 gages from the four load cells at anchor heads, and 18 gages from the rock anchors). The data collection interval for both systems is half-an-hour through the project duration. The pictures showing the final location and the collection boxes are presented in Figs. 3.39 and 3.40.

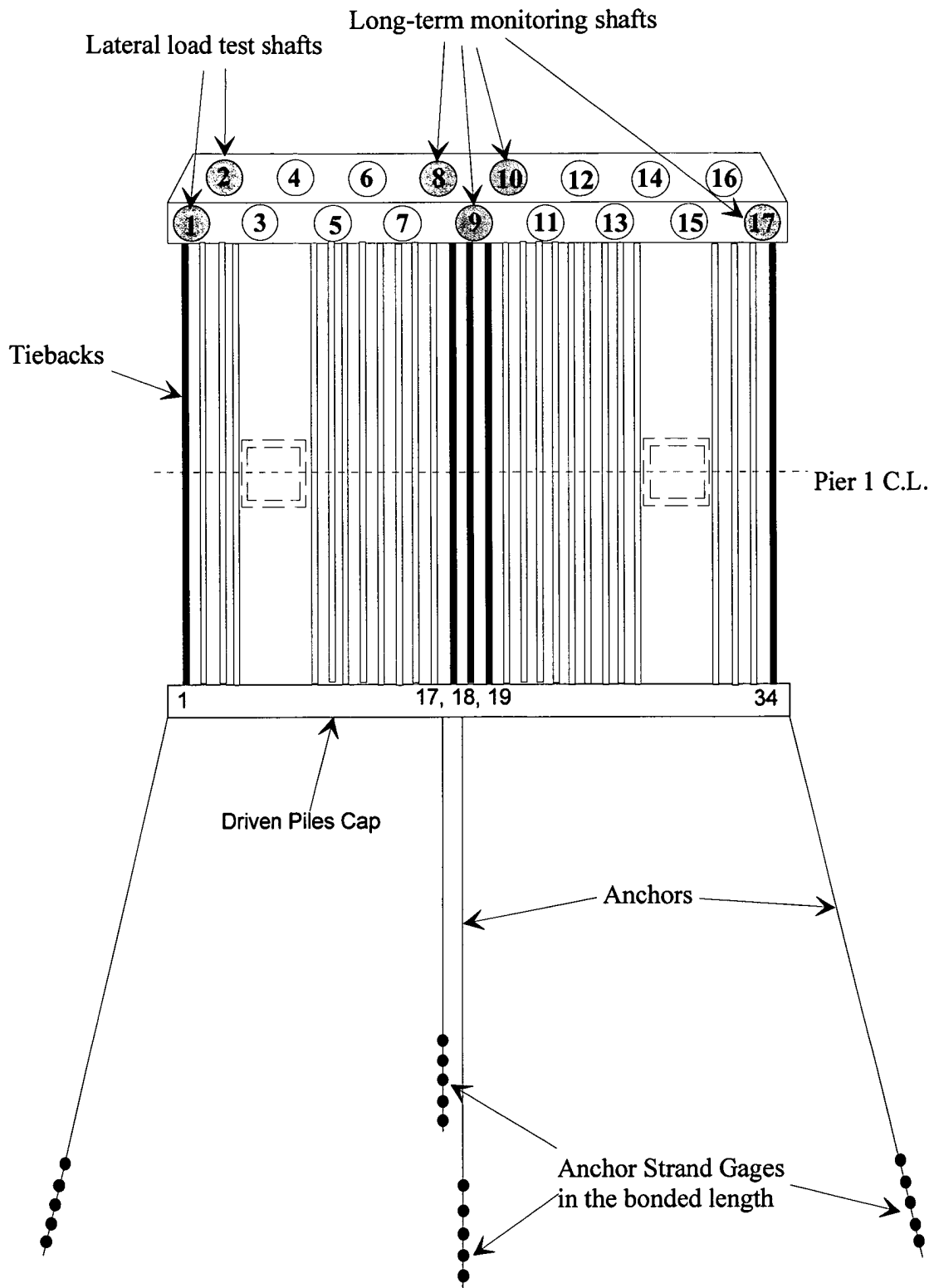


Fig.3.1: Plan Showing the entire stabilization system and the locations of instrumented elements of the system.

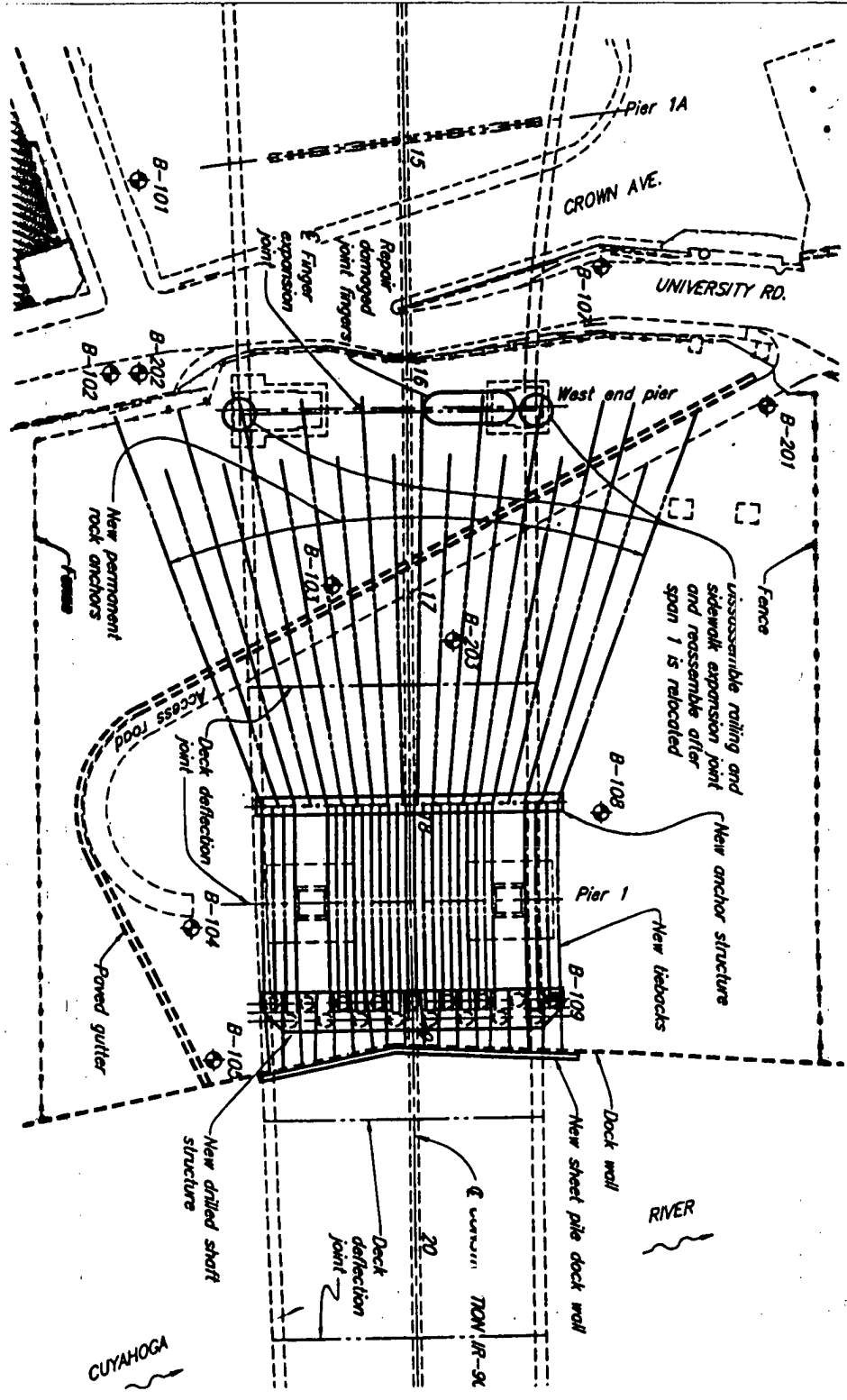


Fig. 3.2: Locations of earth inclinometers.



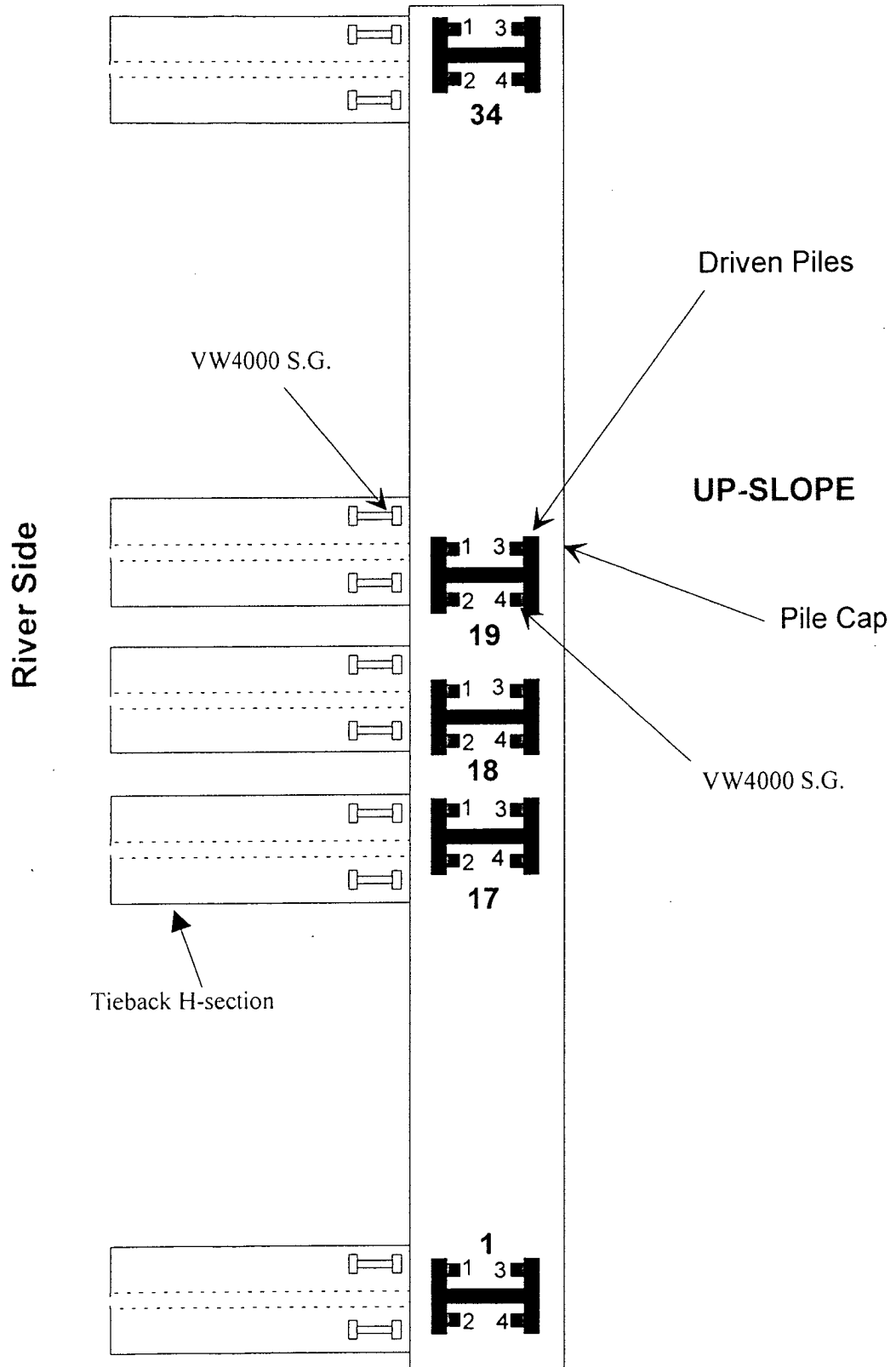
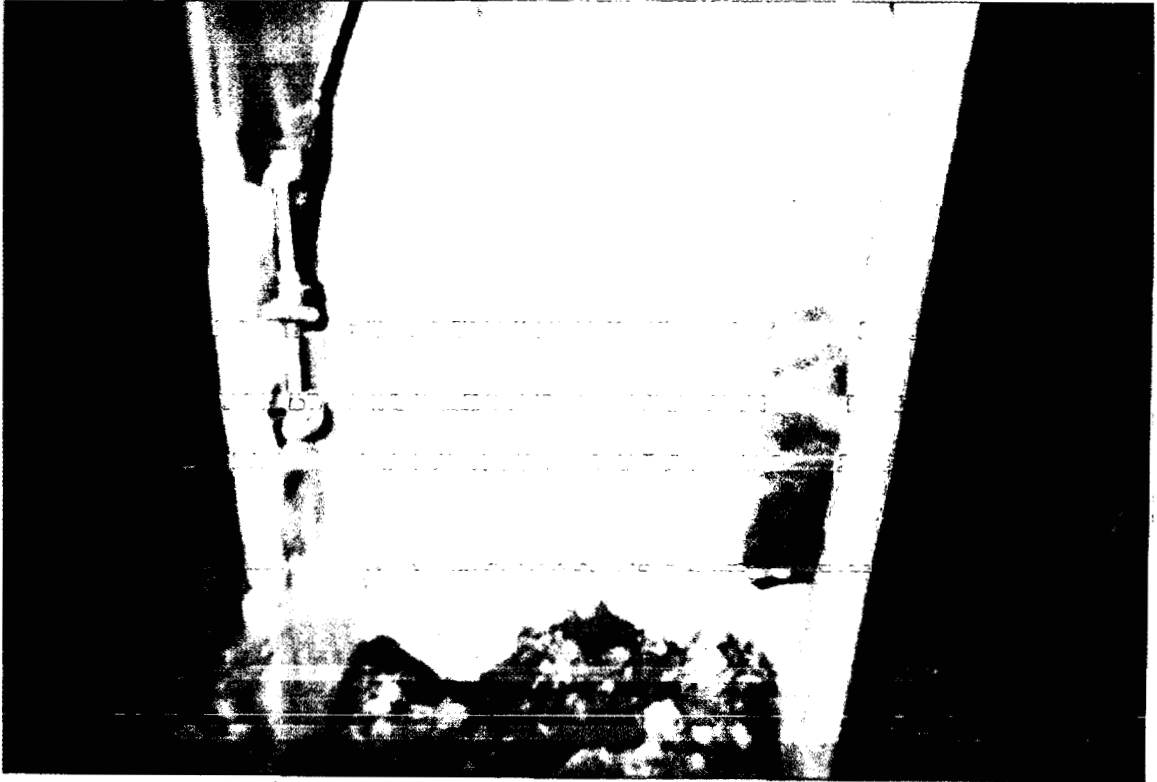


Fig. 3.3: Locations of instrumented piles and gages numbering.



Fig, 3.4: Gages installed and covers on the pile flanges.



Fig. 3.5: Gages being installed on piles 17, 18, and 19.



Fig. 3.6: Gages been covered with protection stainless steel



Fig. 3.7: Ground being filled to the final grade for the pile cap construction.

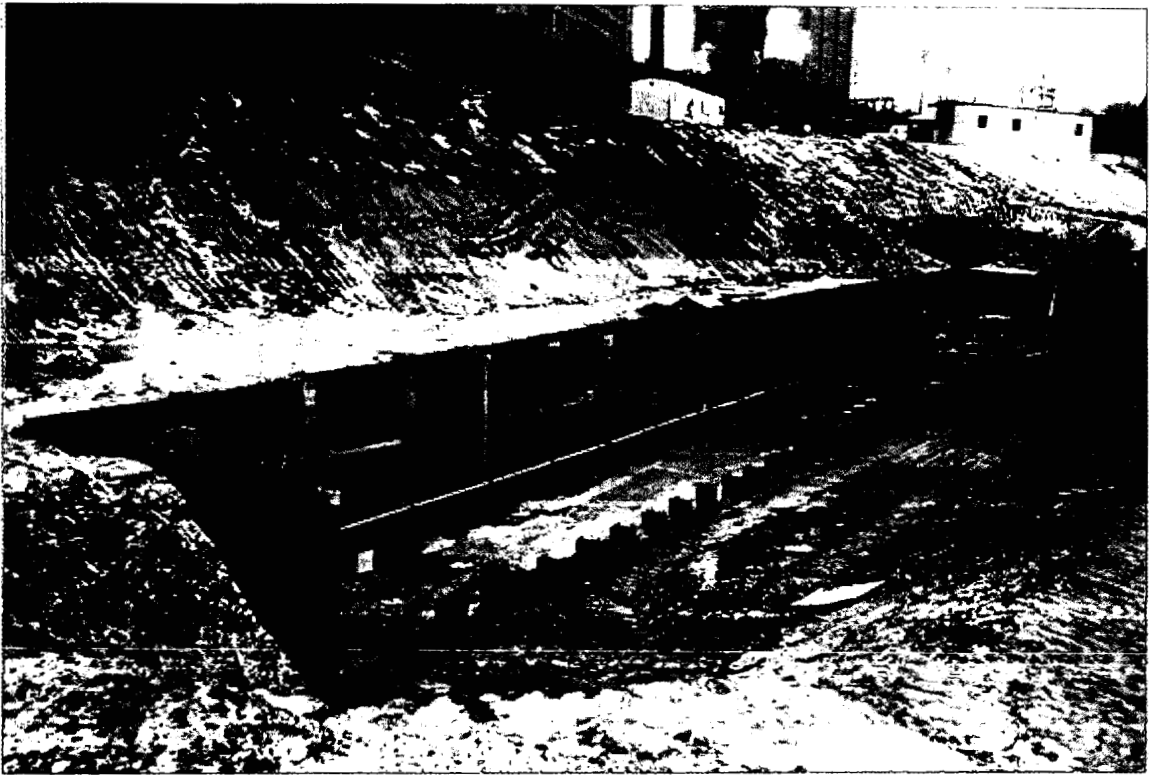


Fig. 3.8: Instrumented piles after completion of backfilling.

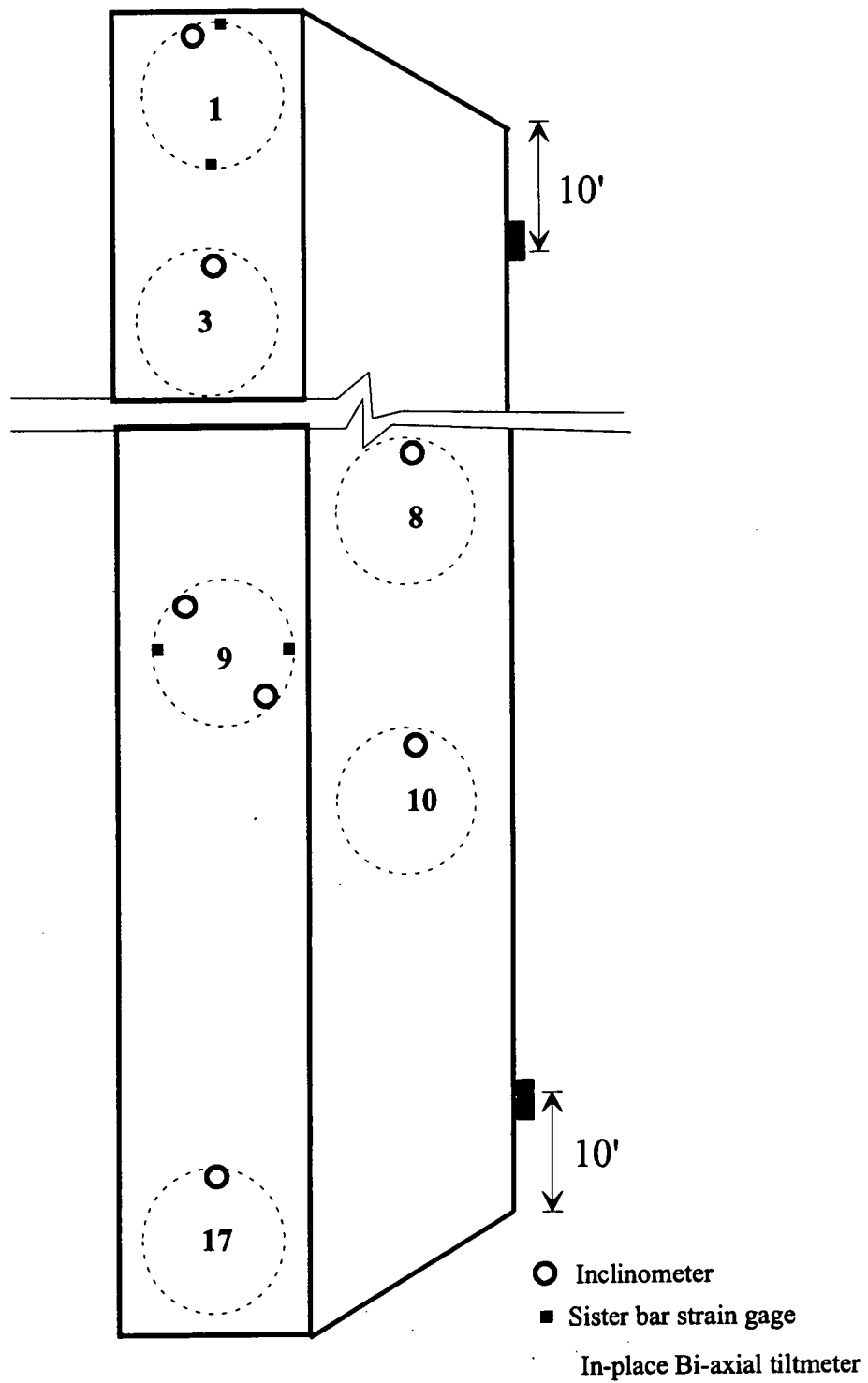


Fig. 3.9: Instrumentation of drilled shaft cap for long-term monitoring.

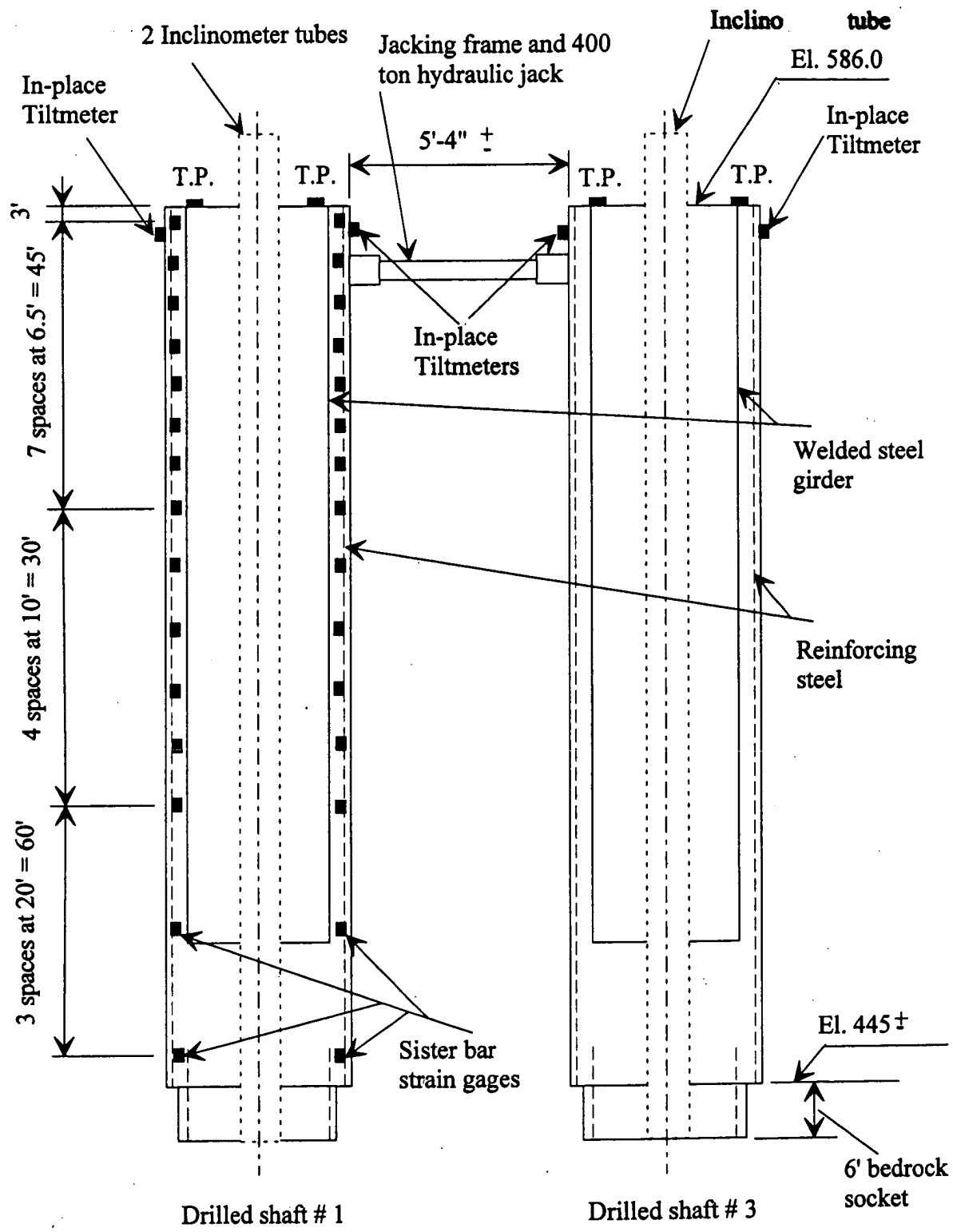


Fig. 3.10: I      tation of S      1 and 3 for Lateral Load Test





Fig. 3.11: Sister bar strain gage installed on the cage.

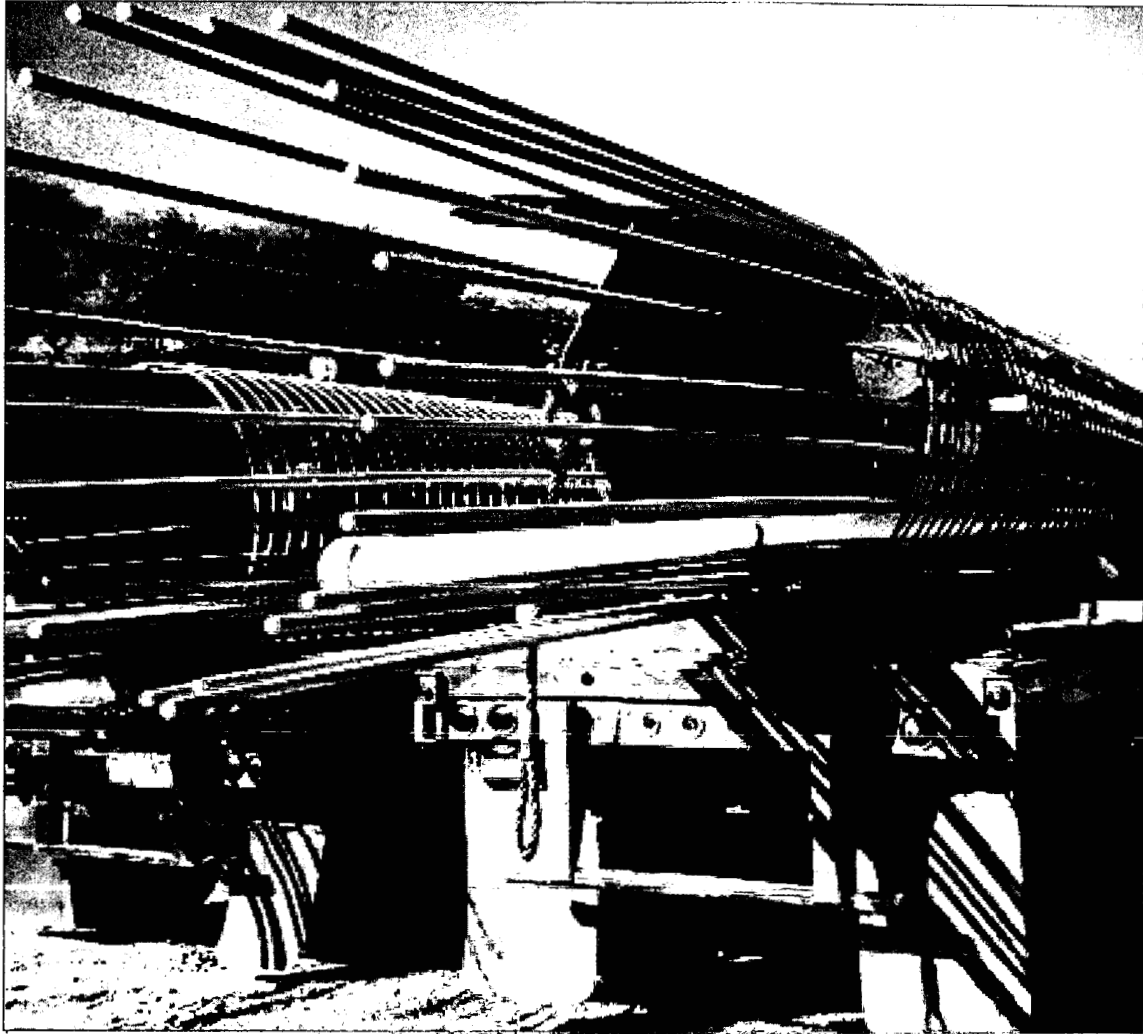


Fig. 3.12: Instrumented sections of the cages loaded on trucks.

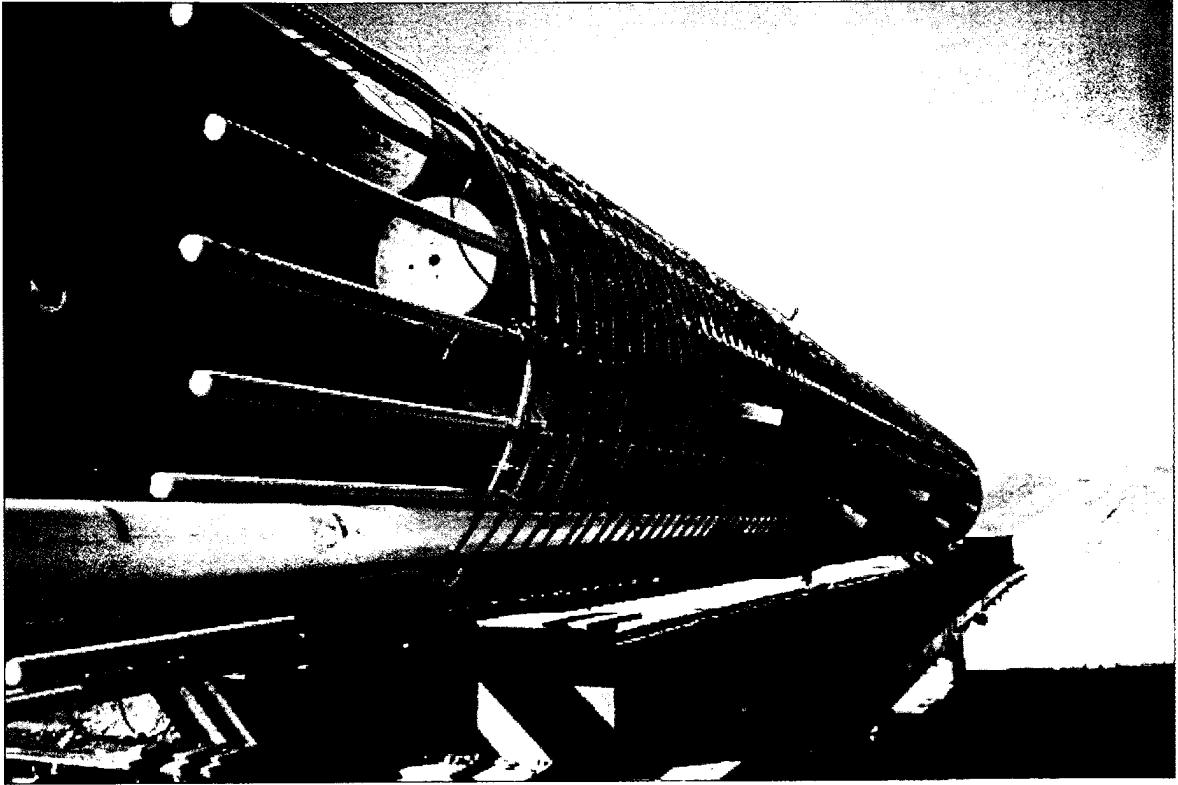


Fig. 3.13: Gages installed and wires run to the top of the section and the PVC housing tube for inclinometer.



Fig. 3.14: Splicing the two segments of the girder, the cage, and the PVC tube.



Fig. 3.15: Inclinometers in shafts #8, #9, and #10 and the wires from gages in shafts #9.

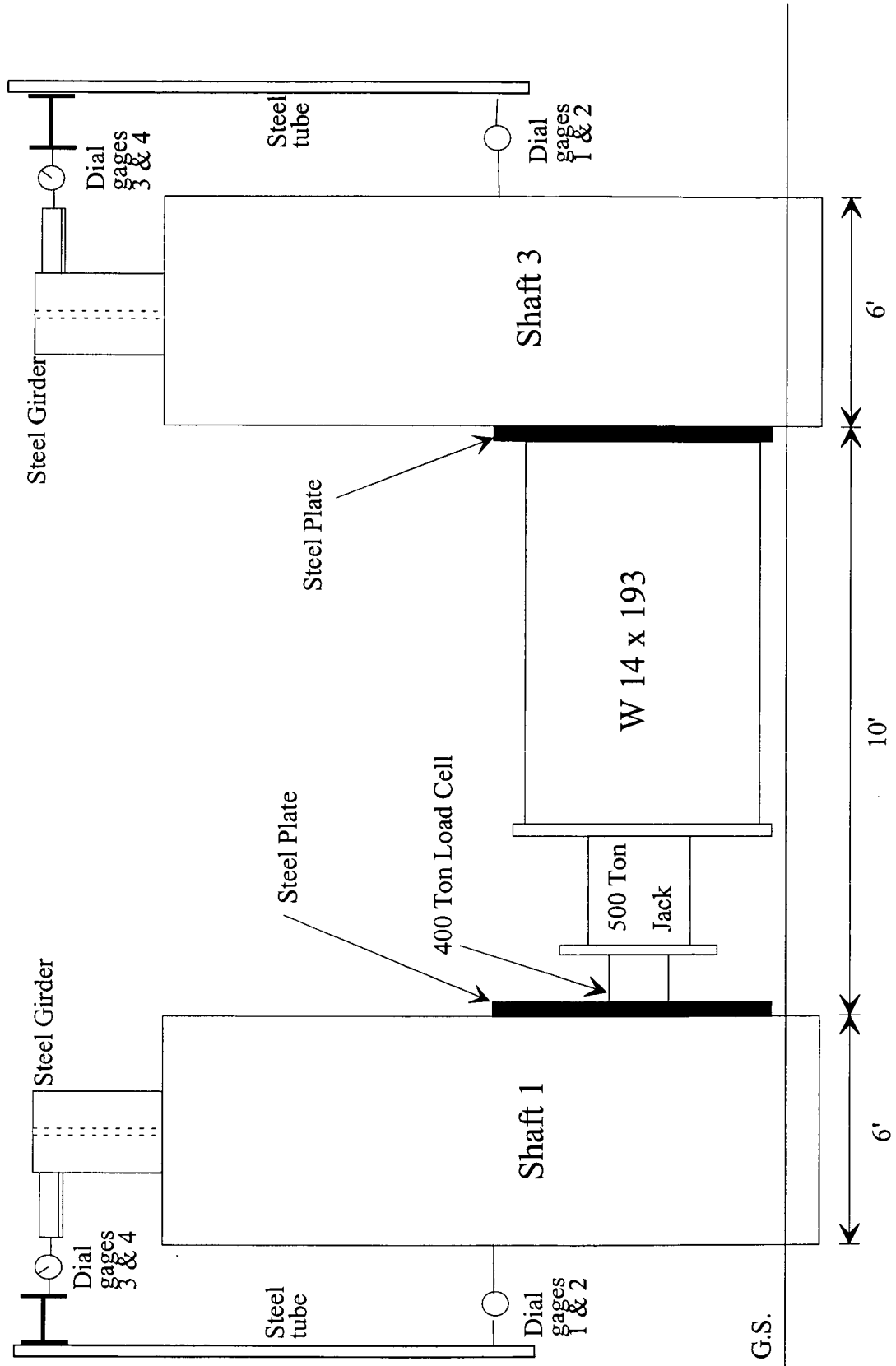


Fig. 3.16: Schematic diagram of the lateral load test at CUY-90 Project: SIDE VIEW.



Fig. 3.17: Setup for the lateral load test

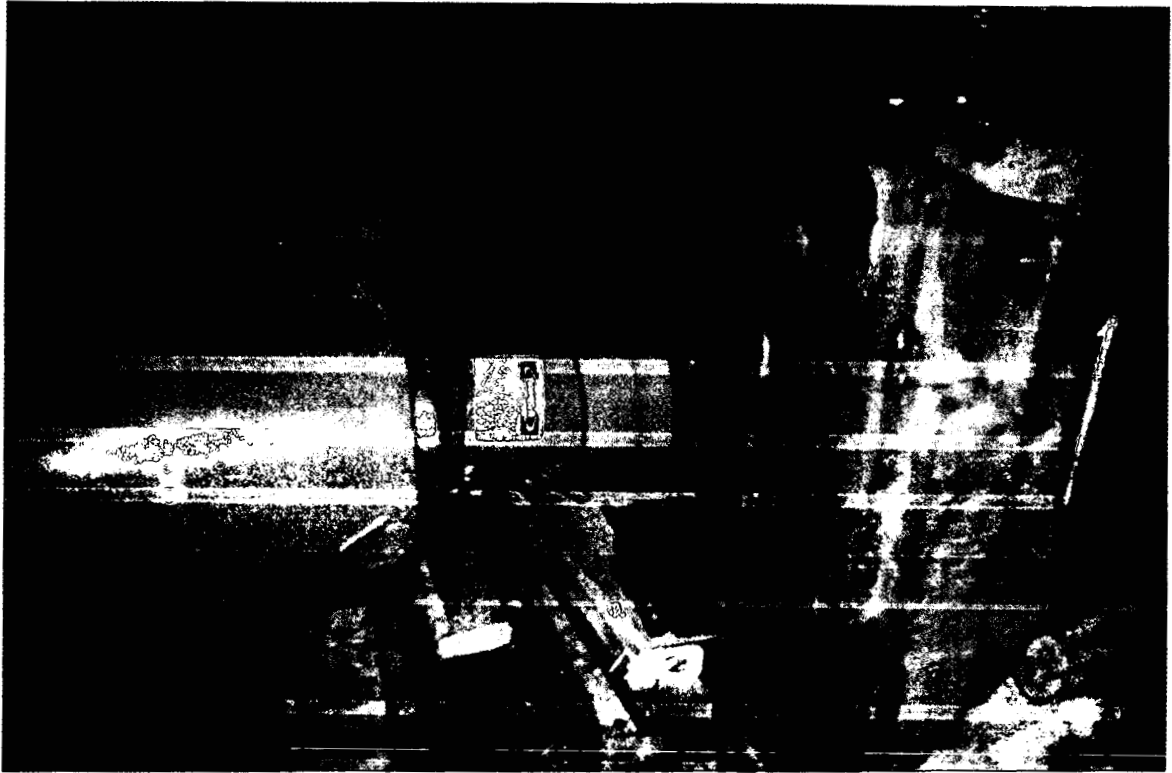


Fig. 3.18: Setup for the lateral load test (Continued)



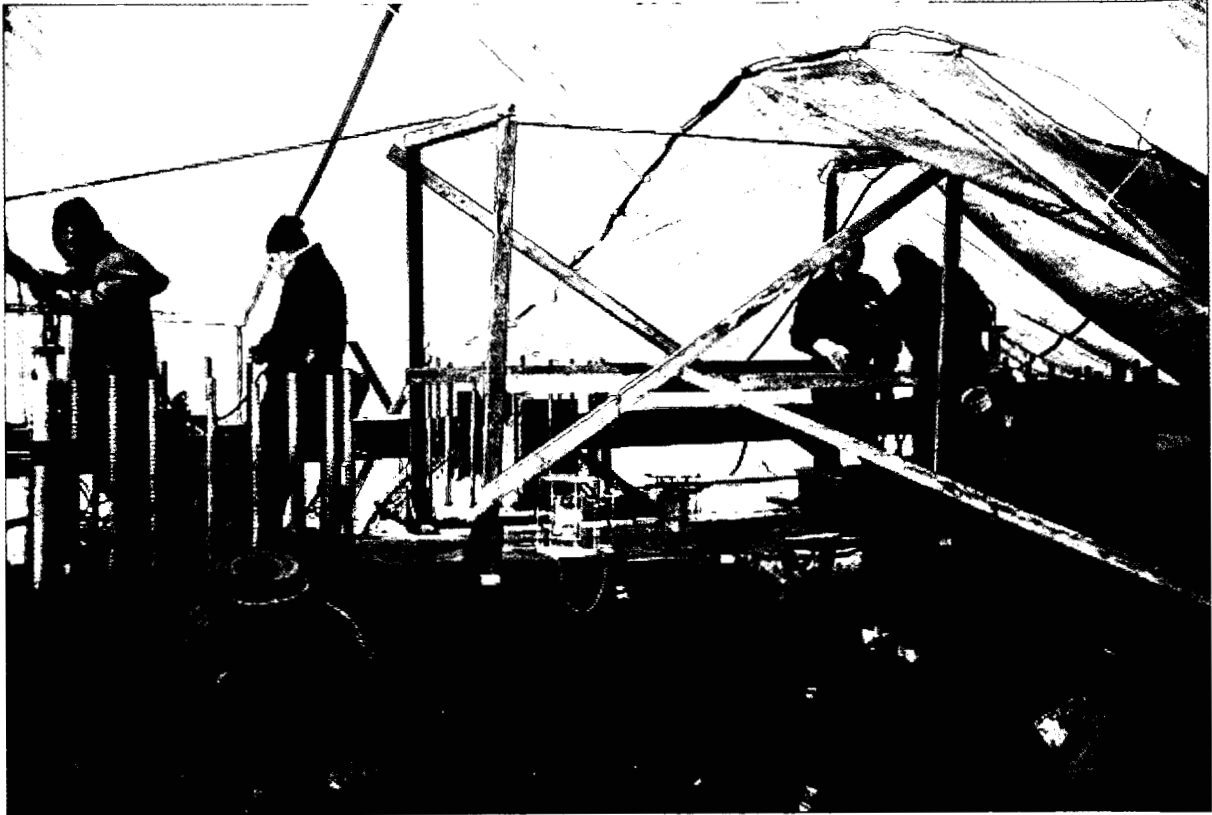


Fig. 3.19: Lateral load test undergoing.



Fig. 3.20: Reference beams and dial gage locations.

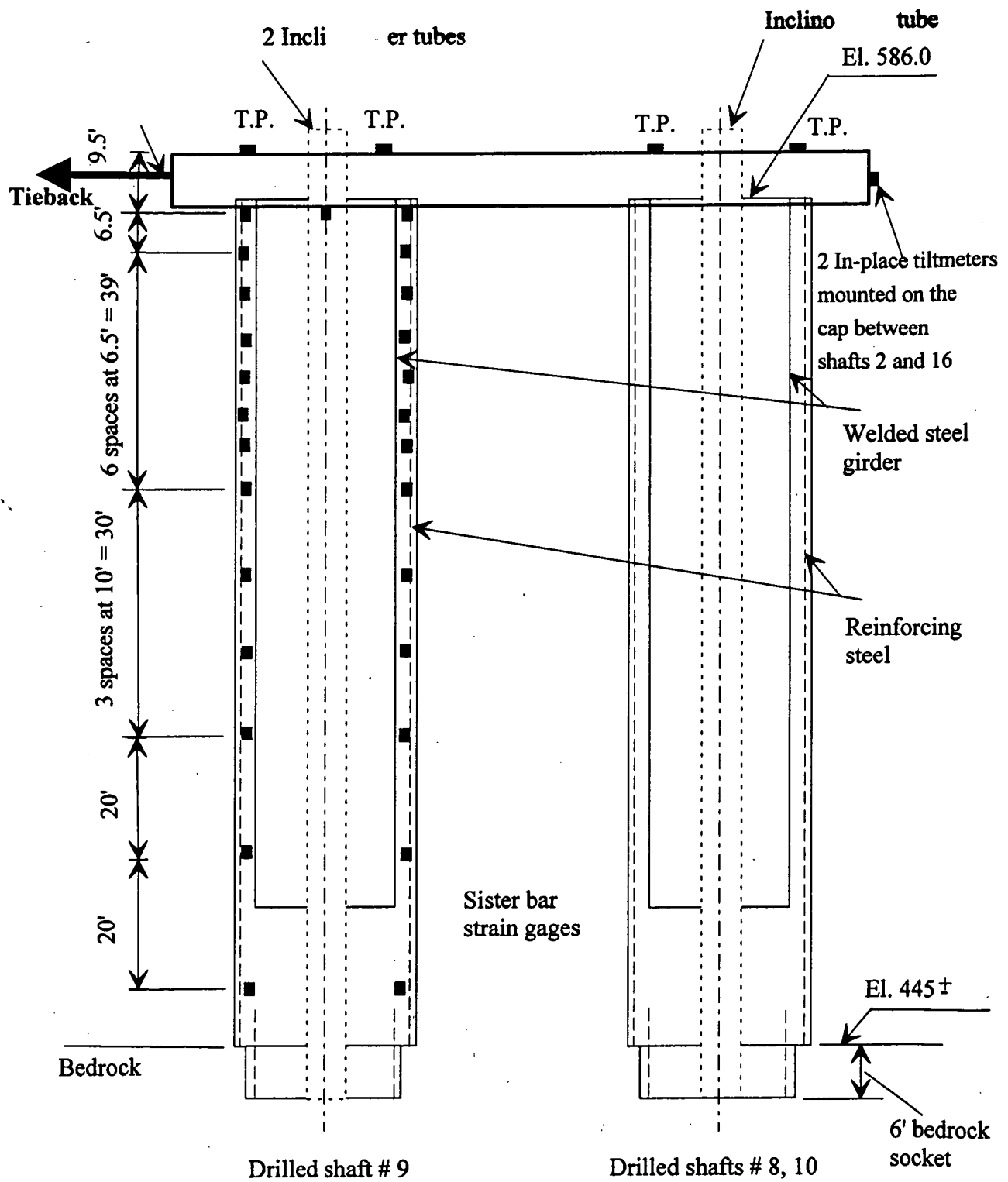


Fig. 3.21: Instrumentation of Shafts 8, 9 and 10 for long-term monitoring

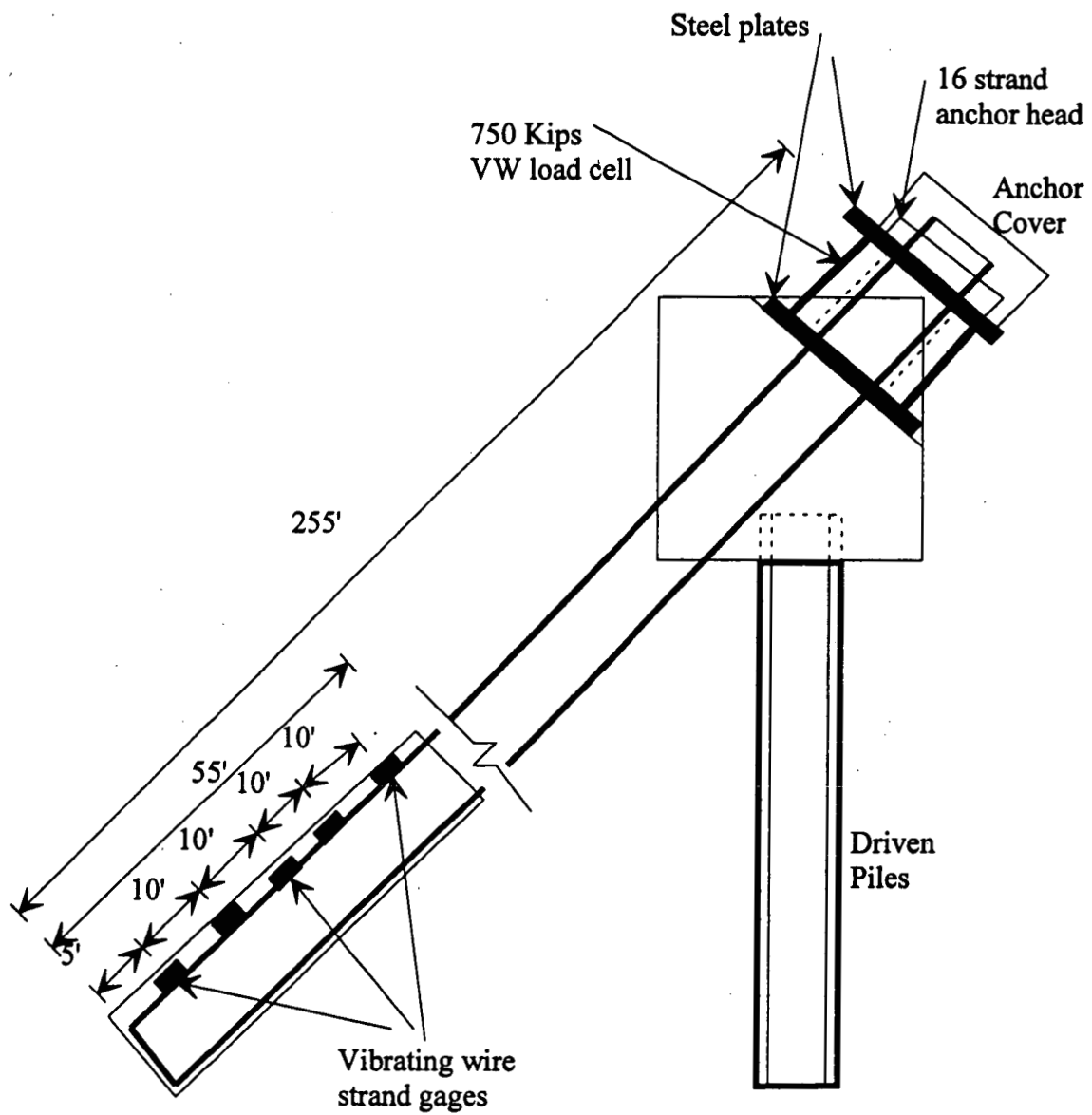


Fig. 3.22: Details of anchor instrumentation and final setup.



Fig. 3.23: Drilling for rock anchors

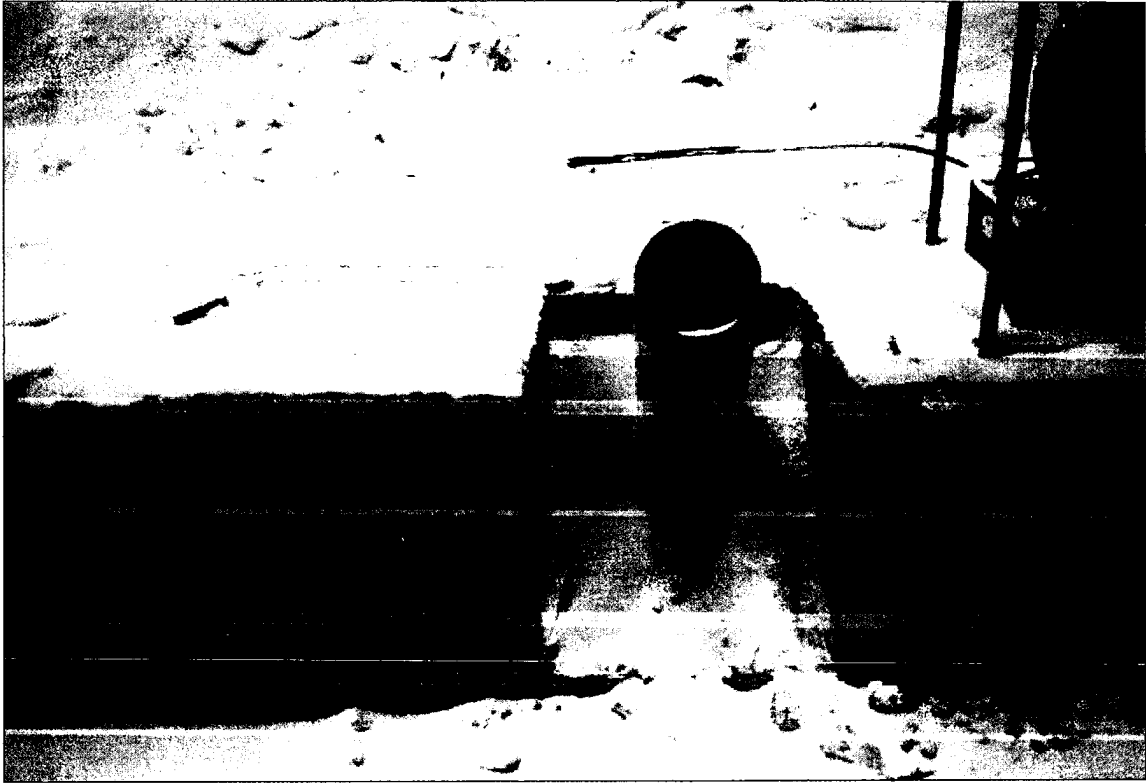


Fig. 3.24: Casing driven in the ground to support the free length of the anchor



Fig. 3.25: Setup for installation of the anchor.



Fig. 3.26: Lowering the anchor in the hole.





Fig. 3.27: Strand gage ready to be mounted.

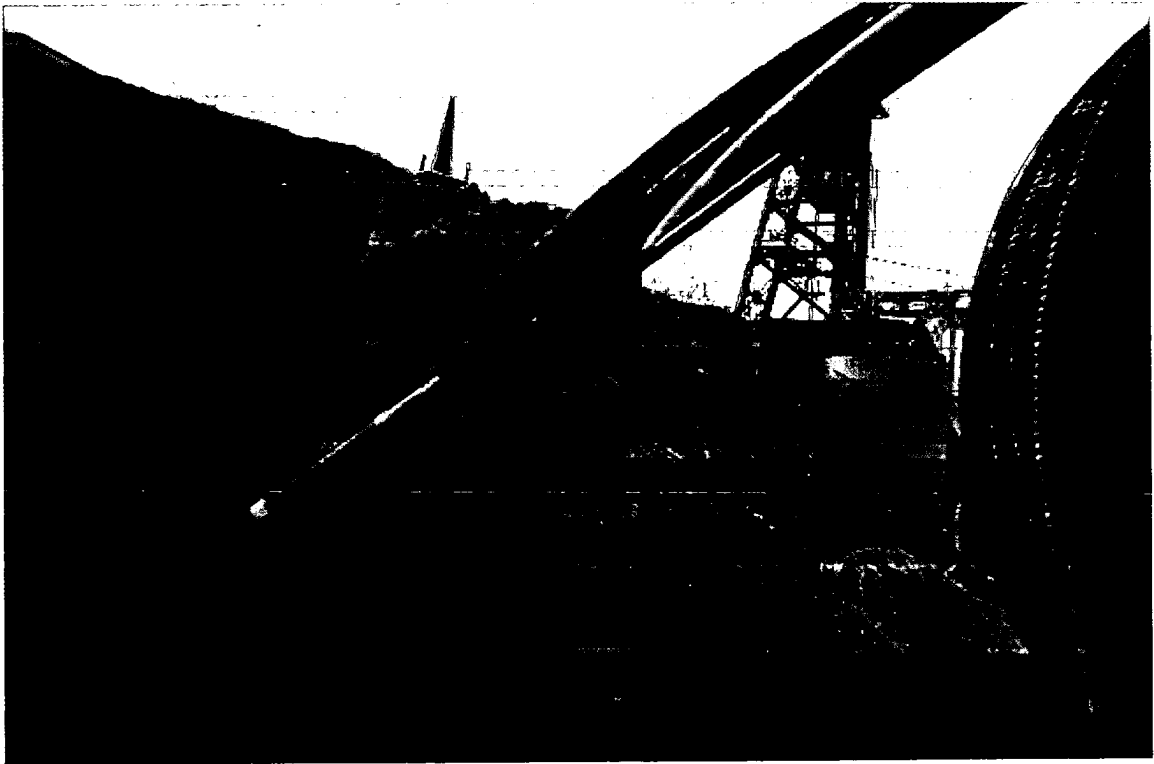


Fig. 3.28: Strand gage installed.



Fig. 3.29: Installation of the load cell and bearing plates for testing and long term monitoring.



Fig. 3.30: Anchor testing.

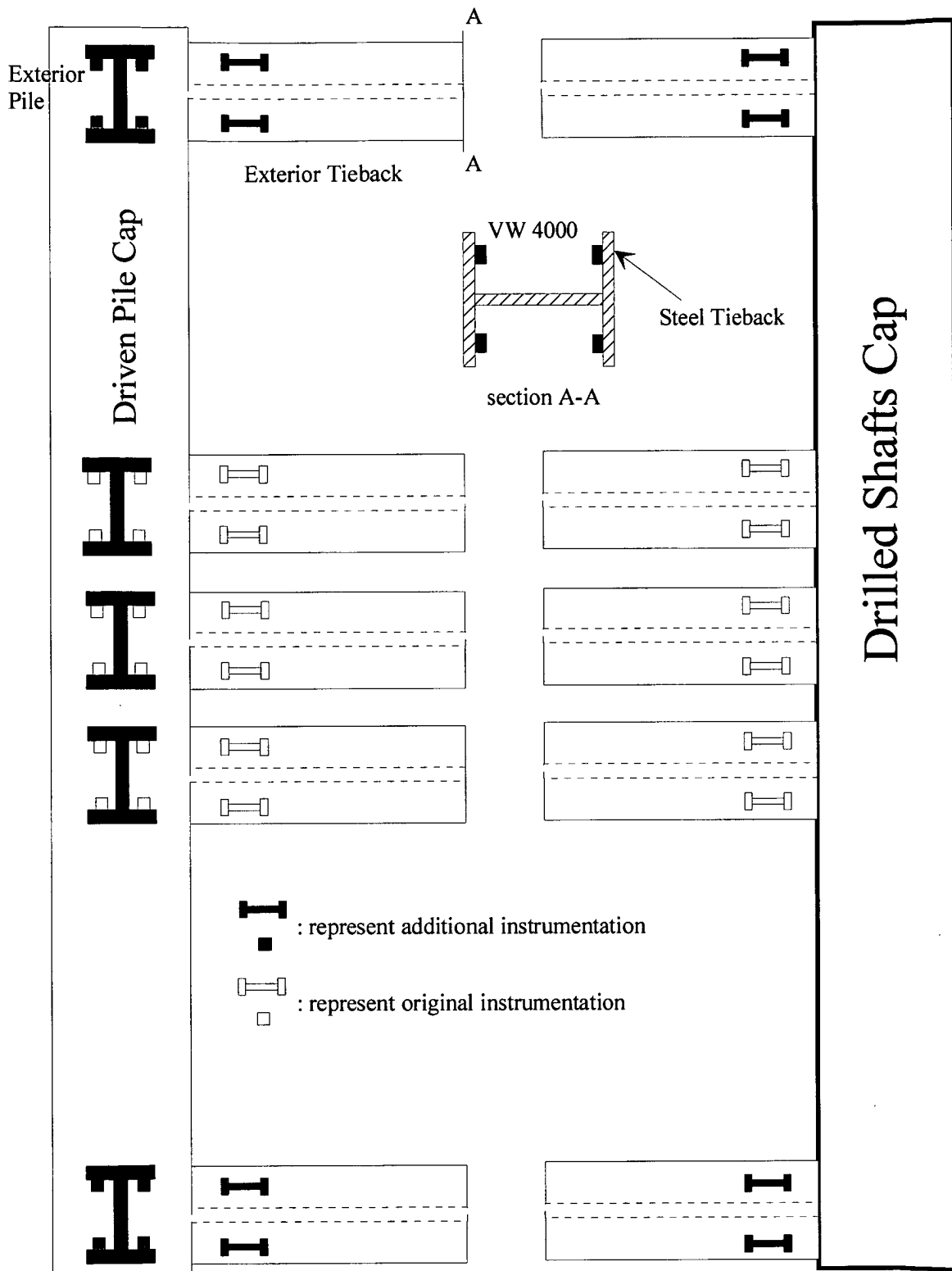


Fig. 3.31: Locations of gages on the tie beams



Fig. 3.32: Welding end blocks for strain gages on tiebeams



Fig. 3.33: Installation and testing of vibrating wire strain gages on the tiebeam.



Fig. 3.34: Installed gages on the middle tiebeams.



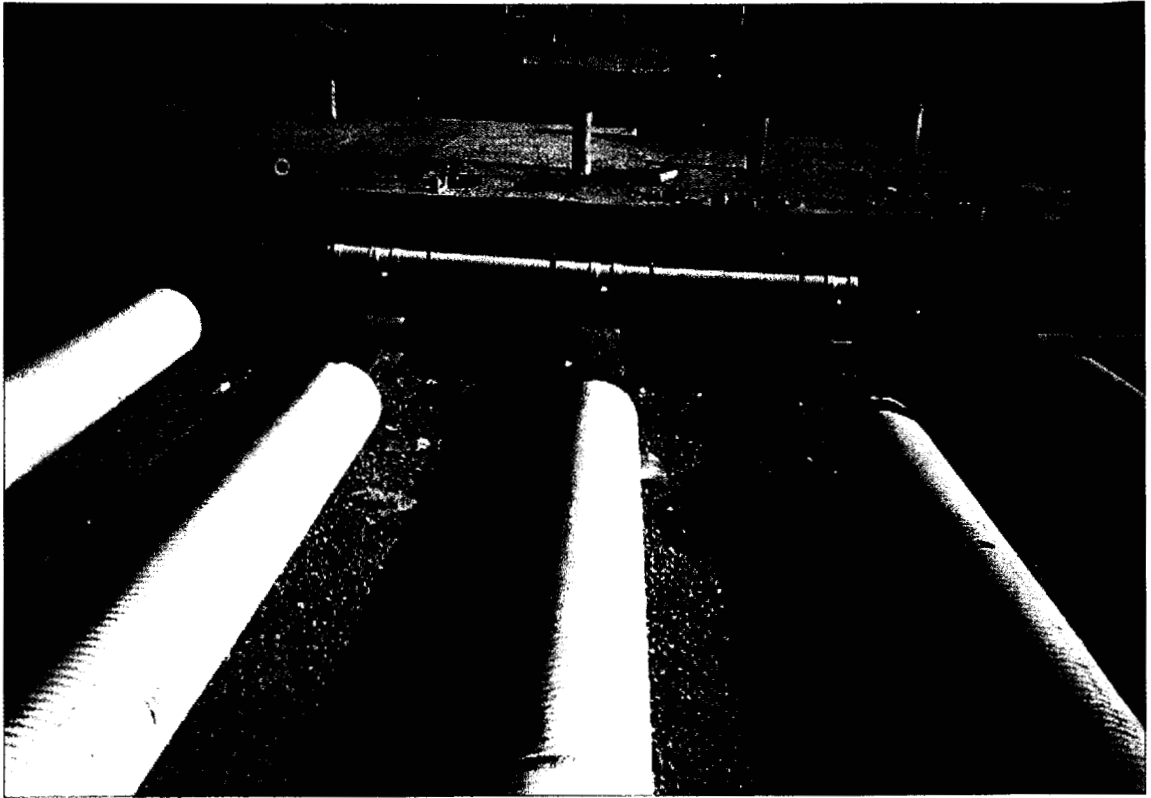


Fig. 3.35: Tiebeam gage wires run through conduit to the shaft cap.

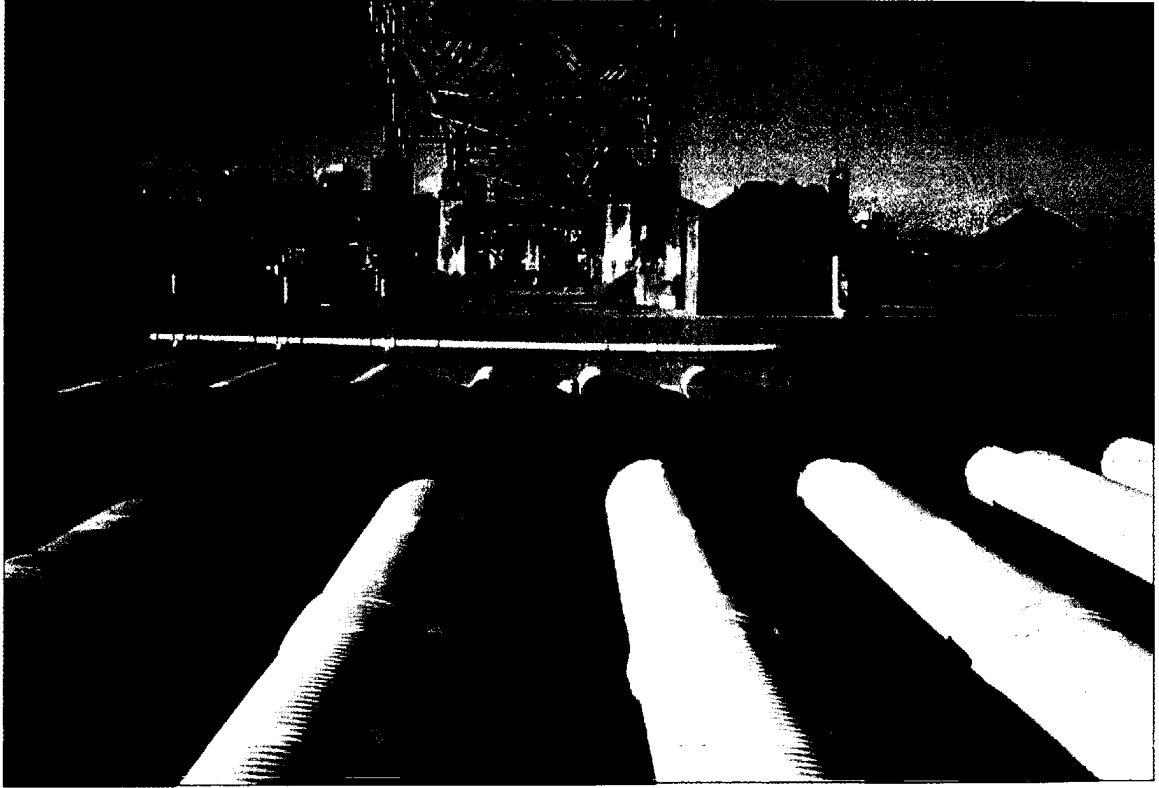


Fig. 3.36: Tiebeam gages run to the datalogger in the temporary wood box.

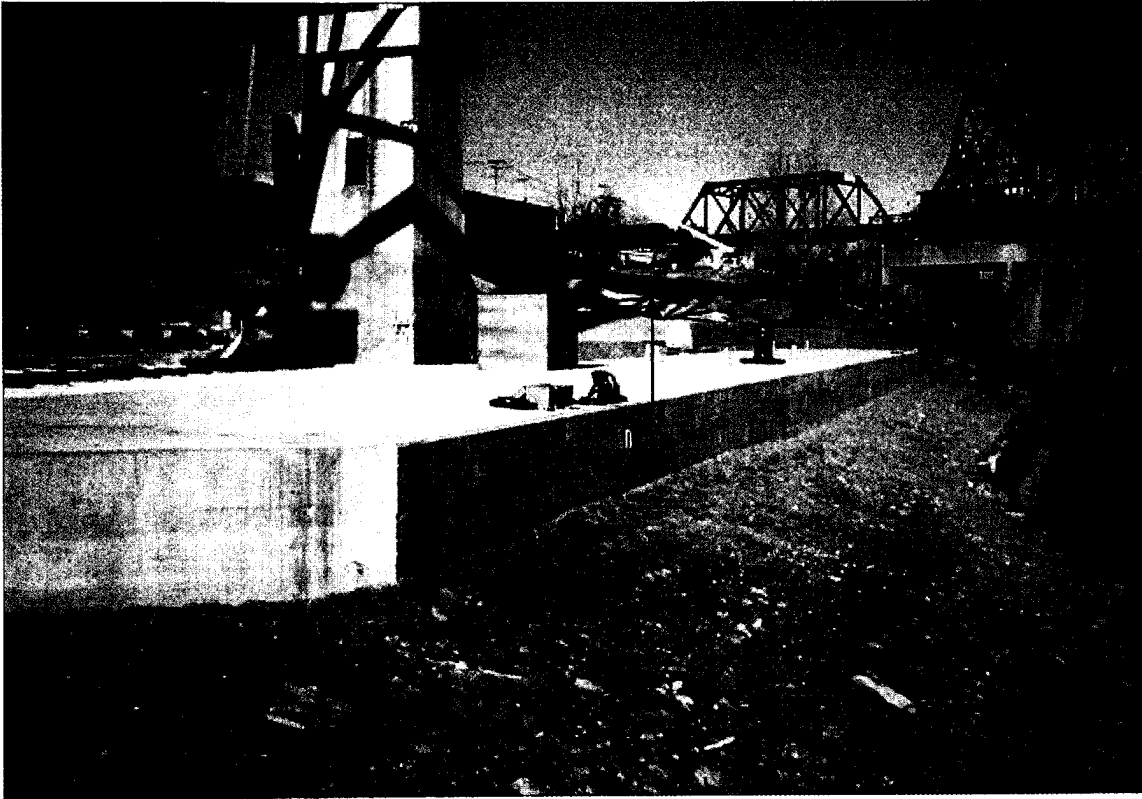


Fig. 3.37: Bi-axial tiltmeters installed on the shaft cap (10' from each end)



Fig. 3.38: Data collection boxes (final location).

## CHAPTER IV

### SHORT AND LONG TERM MONITORING RESULTS

#### IV.1 OVERVIEW OF COLLECTED INFORMATION BEFORE COMMENCEMENT OF CONSTRUCTION

Since the beginning of this research project, BBC&M, Inc., has kindly provided the University of Akron's team with all the inclinometer readings collected since 1994. The locations of these inclinometers are shown in Fig. 4.1. The slope cross-section geometry at the centerline of the bridge is shown in Fig. 4.2. The data collected since May 15, 1996 has been compiled and reduced into tables and graphs. For the purpose of documentation of slope movement in this report, the readings taken on May 15, 1996 were used as the base line for subsequent data reduction. Borehole inclinometer readings for B103 and B104 are used as representative data to show the amount of slope movement prior to the commencement of construction (around October 1997). The inclinometer measurements at the location of B103 is shown in Fig. 4.3 for the direction toward the down slope (A+ direction) and Fig. 4.4 for the direction 90° clockwise of the A+ direction (B+ direction). Similarly, for B-104, the inclinometer data for A direction and B direction are plotted in Figs. 4.5 and 4.6, respectively. The two particular dates noted on Figs. 4.3 through 4.6 are May 23, 1997 and October 9, 1997, which represent the last set of readings prior to construction, and the first set of readings after pile driving has taken place. As can be seen, significant slope movements have occurred between these two dates, indicating slope instability due to pile driving. For clarity of data

presentation, the major construction stages are summarized in Table 4.1 and the corresponding instrument monitoring results are presented in the remaining part of the chapter.

Table 4.1: Major construction events.

Event #	Event Description	Date
1	Excavation for anchor pile cap structure	9/23/1997
2	Start of pile driving	10/3/1997
3	Stop of pile driving to install the temporary drilled shafts and lagging	10/30/1997
4	Resume pile driving	12/11/1997
5	Pile driving completed	1/19/1998
6	Pour anchor cap concrete	2/11/1998
7	Backfill part of the cut trench on the anchor cap to flatten the slope and help reduce the slope movement	2/23/1998
8	Drilled shafts installation was started	8/4/1998
9	Drilled shafts installation was completed	12/10/1998
10	Lateral load test on shafts 1 & 3	1/13/1999
11	Rock anchor installation was started	12/12/1998
12	Drilled shaft cap was completed	2/19/1999
13	Rock anchor installation was finished	2/18/1999
14	Installation of tie beams was started	3/15/1999
15	Installation of tie beams was completed	4/1/1999
16	Start of tensioning rock anchors	4/6/1999
17	Tensioning of rock anchors was complete	4/14/1999
18	Grouting of the corrugated housing tubes of tie beams	4/20/1999
19	Start of backfilling the slope to the proposed final grade	4/23/1999
20	Backfilling the slope was completed	5/7/1999
21	Final reading of field instruments	6/30/1999

## **IV.2 EXCAVATION FOR DRIVEN PILES AND PILE DRIVING**

Excavation of the trench for pile driving started on 9/23/1997. Pile driving started on 10/3/1997. A set of inclinometer readings was taken on 10/9/1999, where a movement of 0.35" was noticed in inclinometer B-103 at a depth of 58' and 0.1" at a depth of 90'. While the pile driving was continuing, BBC&M took another set of readings on 10/29/1997, in which the slope showed additional movement of about 0.2" at a depth of 58' and 0.15" at a depth of 90'. Due to the measured high rate of slope movement, pile driving was stopped on 10/30/1997. The measured movements in inclinometer B-103 before and after this stage of construction are shown in Figs. 4.7 and Fig. 4.8 for A+ and B+ directions, respectively. The pictures of the cut trench and pile driving activities are shown in Figs. 4.9 and 4.10, respectively.

The proposed plan by BBC&M to stabilize the slope movement consisted of backfilling the slope around 10 ft. (from elev. 584 to elev. 594) and installing a row of 30 inch diameter drilled shafts, with bottom elevation at 564 and top elevation at 584. These drilled shafts were reinforced with H piles to hold the lagging with top elevation of 594, as shown in Figs. 4.11 and 4.12. The drilled shafts installation started on 11/24/1997, and was completed on 12/9/1997. During the period from 10/30/1997 and 12/8/1997, a weekly reading of inclinometer B-103 was taken and the results are plotted in Figs. 4.13 and 4.14, for A+ and B+ direction, respectively.

Pile driving was resumed on 12/9/1997 and completed on 1/19/1998. As shown in Figs. 4.15 through 4.18, a dynamic pile test was conducted on pile #18 on 12/16/1997. An additional 0.3 inches of slope movement was recorded upon completion of pile driving. The pile driving analyzer (PDA) was used to check on the drivability and





capacity of the pile and the stresses induced during driving. The blow-count vs. depth of the pile is represented in Table 4.2. The measured force, the calculated capacity based on RA2 method, and energy measured are shown in Fig. 4.19 against the blow count number. The same quantities for the last 8 feet of penetration are shown in Fig. 4.20. The CAPWAP analysis, as shown in Appendix C, yields a pile capacity of 636 Kips at the end of driving. As seen in Table 4.2, at a penetration depth of 115 feet, the setup due to a rest period of one night is significant. The pile capacity was believed to reach more than 700 Kips (2 times the design load) after setup.

The strain gages were mounted on the piles during the week of 1/23/1998. The installations of strain gages at various stages are shown in Figs. 4.21 to 4.23. The anchor cap forming started after completion of strain gage installation and the cap was poured on 2/12/1998, as shown in Fig. 4.24. The data from the pile gages was monitored since then, and the stresses and strains on the piles were evaluated.

Upon curing of the pile cap, on 2/23/1999, the slope of the trench was reduced by adding additional backfill as shown in Fig. 4.25. Fig. 4.26 shows a picture of the flattened slope of the trench. The measured responses from the pile strain gages due to the curing of the concrete in the pile cap and the added fill are presented in Figs. 4.27 to 4.36 for the period between 2/12/98 to 6/30/1998. For each instrumented pile, two graphs were presented. One graph shows the actual measured strain, and the other graph shows the reduced stress. The inclinometer readings from B-103 and B-104 are shown in Fig. 4.37 to Fig. 4.40 for the period between 10/9/97 and 6/30/98. It appears that the slope continued to move and exerted earth thrust force on the pile cap.

Table 4.2: Blow count vs. depth for test pile # 18

Penetration (ft)	Blow per ft	Penetration (ft)	Blow per ft	Penetration (ft)	Blow per ft
1-10	7	82	24	111	42
11-20	13	88	22	112	46
21-30	68	84	25	113	52
31-35	121	85	23	114	55
36-45	---	86	27	115	53
46-50	63	87	24	116	100
51-55	70	88	26	117	70
56-60	75	89	25	118	53
61	16	90	26	119	63
62	14	91	23	120	58
63	18	92	18	121	65
64	21	99	20	122	58
65	21	94	20	123	60
66	20	95	28	124	55
67	23	96	26	125	55
68	21	97	27	126	56
69	20	98	32	127	51
70	21	99	33	128	54
71	22	100	30	129	55
72	23	101	32	130	55
77	21	102	31	131	73
74	20	103	36	132	72
75	22	104	33	133	82
76	21	105	35	134	94
77	22	106	38	135	98
78	22	107	36	136	120
79	25	108	34	137	152
80	22	109	35	138	182
81	23	110	38	139	22 (0.08ft)

### IV.3 DRILLED SHAFTS CONSTRUCTION

Construction of the drilled shafts started on 8/4/1998 and completed on 12/31/1998. The Polymer slurry was used during the construction to hold the hole open during drilling and pouring the concrete. It was the first job in Ohio in which Polymer slurry was used. During the period of drilled shafts construction, the earth inclinometers were read weekly. As part of instrumentation plan, the sister bar strain gages were mounted to the steel cages and the inclinometers housing (5" diameter PVC tubes) were installed. After completion of drilled shaft construction, the inclinometer casing were installed inside the PVC tubes and the annulus were grouted as shown in Fig. 4.41. A lateral load test was performed on shafts #1 and #3 on 1/13/1999. The schematics of the testing setup and the measuring devices are shown in Figs. 4.42 and 4.43 for top view and section view, respectively. The measured deflection at the jacking point are plotted together with the type A prediction and they are shown in Figs. 4.44 and 4.45 for shaft #1 and #3, respectively. The measured deflection versus depth for shaft #1 and shaft #3 are presented in Figs. 4.46 and 4.47, respectively. The strain data for shaft # 1 were reduced and the strain versus depth were plotted in Fig. 4.48(a) and (b) for loads between 0 and 400 Kips and 400 Kips and 800 Kips, respectively. Similarly, strain readings for shaft # 3 are shown in Fig. 4.49 (a) and (b). In addition, the tilt in degrees at the jacking point in shafts # 1 and # 3 are presented in Fig. 4.50.

It is noted that the deflections of the shafts as measured are compatible with each other. The Type A predictions made by the PI, using the correlations between the standard penetration number and the soil parameters for p-y curves (Liang, 1997), agree

with measured up to 400 Kips of the applied load. The shaft nonlinear EI and constant EI when used in COM624 Program, tends to produce softer response.

To evaluate the effect of drilled shafts construction on the piles, the strain gages reading from 6/30/98 to 12/31/98 were shown in Figs. 4.51 to 4.60. In general, it can be seen that there have been continuous changes of the measured strains in that period of time. Of particular interest is that some of the gages showed significant oscillations, indicating the effect of heavy construction equipment movement.

#### **IV.4 ROCK ANCHOR CONSTRUCTION**

A total of seventeen rock anchors were installed. The casing was installed to a depth of 5 ft. into the shale to support the opening from collapsing due to overburden soil weight. The average free length of the anchors is about 200 ft. and the bonded length is 55 ft. Four rock anchors were instrumented each with 5 vibrating wire strand meters (Geokon Model 4410). The gages were read before and after installation. In addition, a total of four anchors were instrumented with a permanent load cell to measure the load at the anchor during tensioning and service life of the structure. Three of the instrumented anchors (anchors #1, #8, and #17) were performance tested and one anchor (anchor #9) was creep tested. The pictures showing the sequence of anchor hole drilling and installation of tendons are shown in Figs. 4.61 to 4.64.

#### **IV.5 DRILLED SHAFTS CAP**

The cap of the drilled shafts was formed and concrete was poured on Feb 9, 1999. The initial set of readings from the shaft inclinometers was taken on March 25, 1999,

which was before the start of tensioning the rock anchors. At the same time, the inclinometers in the slope were read. A total of two bi-axial tiltmeters were installed on the east side (river side) of the drilled shaft cap on April 7, 1999. The purpose of these tiltmeters was to monitor the rotation of the cap during various stages of construction, such as tensioning of the anchors, backfilling the slope, and long-term behavior monitoring. Fig. 4.65 shows the cap after concrete was cast and Fig. 4.66 shows the installed tiltmeters on the side of the cap.

#### **IV.6 TIE BEAMS**

The tie beams were installed during the period from Feb. 19, 1999 to March 20, 1999. Instrumentation of the tie beams was started on March 25, 1999. Fig. 4.67 shows a close-up of the installed strain gages on the beam. Fig. 4.68 depicts the sleeves housing the tie beams for subsequent grouting. The initial reading from the gages was recorded. After completion of gage installation, they were connected to the data acquisition system along with the strain gages from the drilled shafts (a total of 96 strain gages that are the capacity of the first datalogger), and monitoring of these strain gages in the beams was started on April 1, 1999.

#### **IV.7 TENSIONING OF ROCK ANCHORS**

The tensioning of rock anchors was started on April 7, 1999. Anchor #8 was performance tested. A total of five strand gage cables were connected to the data acquisition system. The sampling rate was set at a 1-minute interval. A permanent vibrating-wire based load cell was installed between the bearing plate and the anchor

head to measure the applied load on the anchor as shown in Fig. 4.69. The anchor head movement was recorded using a dial gage, in accordance with standard performance test procedure. The load test setup and testing assembly are shown in Fig. 4.70. The plot of the load versus dial gage reading is presented in Fig. 4.71. The strain readings versus time is plotted in Figs. 4.72(a) ~ (e) for each of the five strain gages.

On April 8, 1999, two performance tests were conducted on anchors #17 and #1. The same setup and testing procedure as for anchor #8 was followed. The head movement for anchor #17 and anchor #1 are presented in Figs. 4.73 and 4.74, respectively. The strain data from anchor #17 and anchor #1 are presented in Figs. 4.75(a)~(d) and 4.76(a)~(d), respectively.

A creep test was conducted on anchor #9 on April 14, 1999. The anchor head movement is presented in Fig. 4.77. The jack pressure and the load from the load cell were recorded. The strain data from the strand gages were reduced and plotted in Fig. 4.78(a)~(e).

Upon completion of anchor tensioning, a partial set of inclinometer readings was taken on 4/16/1999. The readings were from inclinometers #8, #9, and #10. The inclinometers showed a movement in the average of 0.3 inches up slope due to anchor tensioning as shown in Figs. 4.79 to 4.82. Moreover, the data from the tie beams gages, the drilled shafts gages, and the pile gages were collected on a half an hour interval.

#### **IV.8 GROUTING OF TIE BEAMS AND BACKFILLING OF SLOPE**

Upon completion of anchor tensioning, the area between the anchor cap and the drilled shafts cap was backfilled for 18 inch to the elevation near the top of the sleeves.

The tie beam sleeves were then grouted on April 20, 1999. The backfilling of the slope to the proposed final grade was finally completed on May 7, 1999. One week after completion of slope backfilling, a complete set of inclinometer readings was taken on May 17, 1999. The plots of deflection versus depth from the shaft inclinometers are shown in Figs. 4.83 to 4.89.

The data from tie beam gages is shown in Figs. 5.90 to 5.99 for tie beams #1, #12, #13, #14, and #26, respectively. For shaft gages, the data is presented in Figs. 4.100 to 4.113 for shaft #1, and in Figs. 4.114 to 4.126 for shaft #9. The data obtained from the pile gages up to 6/30/1999 is presented in Figs. 4.127 to 4.136.

#### **IV.9 LONG-TERM MONITORING RESULTS**

After completion of grouting the tie-beams sleeves, the electrical wires from the pile gages, the rock anchor gages and the load cells of the rock anchors were run through a PVC pipe to the permanent cabinet located on the drilled shafts cap. All the wires were connected to the dataloggers and long-term monitoring of the entire instruments was on-line on May 1, 1999.

The collected data till the end of monitoring phase on 6/30/1999 from all sensors are presented. Stresses and strain from pile gages since 2/12/1998 are presented in Figs. 4.137 to 4.146. Strains in drilled shaft #1 at each gage location are presented in Figs. 4.100 to 4.113, and in drilled shaft #3 at each gage location are presented in Figs. 4.114 to 4.126. Moreover, the strains with depth for the major events after tensioning of the rock anchors are presented in Figs. 4.147 to 4.150 for shafts #1 and #3, respectively. Tie

beams strains are presented in Figs. 4.90 to 4.99. The load from the load cell at each anchor head is presented in Figs. 4.151 to 4.154. The movement in the bonded length of each instrumented anchor at the location of every strand gage is presented in Figs. 4.155 to 4.158. The bi-axial tilt of the anchor cap measured with the vibrating wire in-place tiltmeters is presented in Figs. 4.159 to 4.162.

The force diagrams showing the forces in the main stabilizing elements after each stage of construction are presented in Fig. 4.163. The center line section including (i) drilled shaft #9, (ii) driven piles #17, #18 and #19, (iii) tie beams #12, #13, and #14, and (iv) rock anchors # 8 and #9, were used to construct the force diagrams.

#### **IV.10 COMMENTS ON THE RESULTS OF MONITORING**

From the data presented in this chapter, it can be seen that the rate of movement of the slope decreases dramatically after completion of the stabilization structure. The drilled shafts cap moved around 0.35" up slope after completion of anchor tensioning and slope backfilling.

The force in anchor #1 at lock-off on 4/7/1999 was 490 Kips, and dropped to 460 Kips after completion of tensioning all the anchors on 4/14/1999. During the period of backfilling the slope, the force was varying between 200 Kips and 400 Kips till 5/23/1999. After that the force went back to a steady value of around 450 Kips except during the period from 6/10/1999 to 6/17/1999. Regarding anchor #1 strand gages, the readings were steady showing no further movement after tensioning the anchors till the end of monitoring period. The bottom three gages that are mounted on the bottom 35 feet of the bonded length showed no movement.



The force in anchor #8 at lock-off on 4/8/1999 was 560 Kips, and dropped to 480 Kips after completion of tensioning all the anchors on 4/14/1999. The force in the anchor dropped down to 390 Kips during the period from 4/14 to 5/1/1999. During the period of backfilling the slope, the force was varying between 240 Kips and 490 Kips till 5/23/1999. After that the force went back to a steady value of around 480 Kips except during the period from 6/14/1999 to 6/17/1999, where the reading dropped to less than 200Kips and went back to 480 Kips. Regarding anchor #8 strand gages, the readings from gages #4 and #5 in the upper part of the bonded length were steady showing no further movement after tensioning the anchors till the end of monitoring period. Gages # 2 which was mounted 15 feet from the bottom of the bonded length showed decrease in the reading which means that the force in the anchor dropped till 5/20/1999. After that the reading stayed constant.

Anchor #9 was creep tested on 4/14/1999. The lock-off load was 590 Kips, and dropped to 520 during the period from 4/14 to 5/1/1999. During the period of backfilling the slope, the force varying between 300 Kips and 570 Kips till 5/23/1999. After that the force went back to a steady value of around 570 Kips except during the period from 6/4/1999 to 6/10/1999, where the reading dropped to less than 250Kips and went back to 560 Kips. Regarding anchor #9 strand gages, the readings from gages #4 and #5 in the top part of the bonded length were steady showing very little variation in the displacement reading. This was confirming the load holding at the anchor head. No further movement after tensioning the anchors till the end of monitoring period. Gage # 3 which was mounted 25 feet from the top of the bonded length showed some noisy data since 5/1/99 till 6/30/99. The lower two gages showed no movement.

Anchor #17 was performance tested on 4/9/1999. The lock-off load was 500 Kips, and dropped to 470 Kips by 4/14/1999. During the period from 4/14 to 5/1/1999, the force dropped to 450 Kips. During the period of backfilling the slope, the force was holding almost constant till 5/24/99. During the period from 5/24/99 to 5/27/99, the force dropped dramatically to less than 0 Kips. After 5/28/1999, the force went back to a steady value of around 460 Kips except during the period from 6/2/1999 to 6/5/1999, where the reading dropped to less than 300Kips, then it went back to 460 Kips. Regarding anchor #17 strand gages, the readings from gage #5 in the top part of the bonded length were steady showing very little variation in the displacement reading. This was confirming the load holding at the anchor head. No further movement after tensioning the anchors till the end of monitoring period. Bottom 3 gages mounted on the lower 35 feet of the bonded length show no movement since 5/1/99 till 6/30/99.

The strain gages mounted on the driven piles were monitored every ½ hour. The strains and stresses due to heat of hydration and transfer of the weight of the cap to the piles and surrounding soils is shown in Figs. 4.27 to 4.36. The data shows a variation in the strain in the range of 200  $\mu$ s. The strains started to decrease and it went down to around 30 to 50  $\mu$ s by the time the forms were took off the cap and the partial backfilling behind the cap started. After completion of backfilling, strains start developing with a rate of about 70  $\mu$ s a month. It can be noted that the variation in the strain in the piles was not uniform. The readings showed that there is a bi-axial state of stress in the piles except the center pile #19. Exploring the data thoroughly, it can be seen that the slope is moving in an angle to the north east of the bridge.

From the piles strain data, it can be seen that the rate of strain build up slowed down to almost zero upon starting drilled shafts construction. The rate decreased in piles #17, #18 and #19 upon starting rock anchors installation. After tensioning the rock anchors, the strains in the piles are all in tension. Pile #1 (the extreme north pile) shows an increase in strain in the range of 400  $\mu\text{s}$  in gages 1 and 2. The strain in gages 3 and 4 went from -400  $\mu\text{s}$  to about +50  $\mu\text{s}$ . Pile #34 (the extreme south pile) shows an increase of almost the same amount as pile #1 on both sides. The middle piles #17, #18, and #19 showed increase in the strain after tensioning of the rock anchors and the behavior of the piles turn to be a uniaxial bending. The build-up of the strains in the piles on tension side (gages #1 and #2) was in the range of +500  $\mu\text{s}$ , and on the compression side (gages #3 and #4) was in the range of +300  $\mu\text{s}$ .

The inclinometers installed in the drilled shafts showed a movement in the range of 0.4 inches at the shaft cap elevation. The movement was mainly in the upper 60 feet of the shaft. From the readings on 5/17/99, after completion of backfilling the slope, it can be seen that an additional 0.1 inch of upslope movement was recorded. This movement showed that the backfill was carried by the grouted tie beams, which caused the tie beams to bend and pull the shafts cap upslope.

The tie beams were carrying around 85 Kips of tensile force upon completion of the anchor tensioning. During backfilling, the force increased with time and reached around 105 Kips by the day backfilling was completed. The buildup of force was due to compaction and arching of soil between the tie beams grouted sleeves. The force decreased slightly and stayed close to about 100 Kips. The data in Figs. 4.90 to 4.99 support this conclusion.

The drilled shafts strain gage data shows maximum strain in the shafts at a depth of 30 feet from the top of the shaft cap. Figs. 4.147 to 4.150 shows that the shafts were subjected to an increase in the strains in the range of 50  $\mu$ s in compression due to tensioning of the rock anchors. The compression is due to the fact that the shafts moved up slope and the strains in the up slope side are in compression. The strain increased to about 70  $\mu$ s in compression by the time they finish backfilling the slope. Upon completion of monitoring phase, the strain relief to about 50  $\mu$ s. The existence of the cap restrains the top of the shafts from deflecting and the strains were close to zero at the top of the shafts due to fixity.

The bi-axial tiltmeters attached to the river side of the drilled shafts cap showed a higher rotation in the north side of the cap. Titlmeter # 878 showed a negative angle of tilt which means that the cap rotated in the up slope direction. Titlmeter # 879 showed a negative angle of tilt indicating movement to the north side of the cap. The titlometers attached to the south side of the cap showed angle of rotation in the range of 35% of the tilt in the north side of the cap.

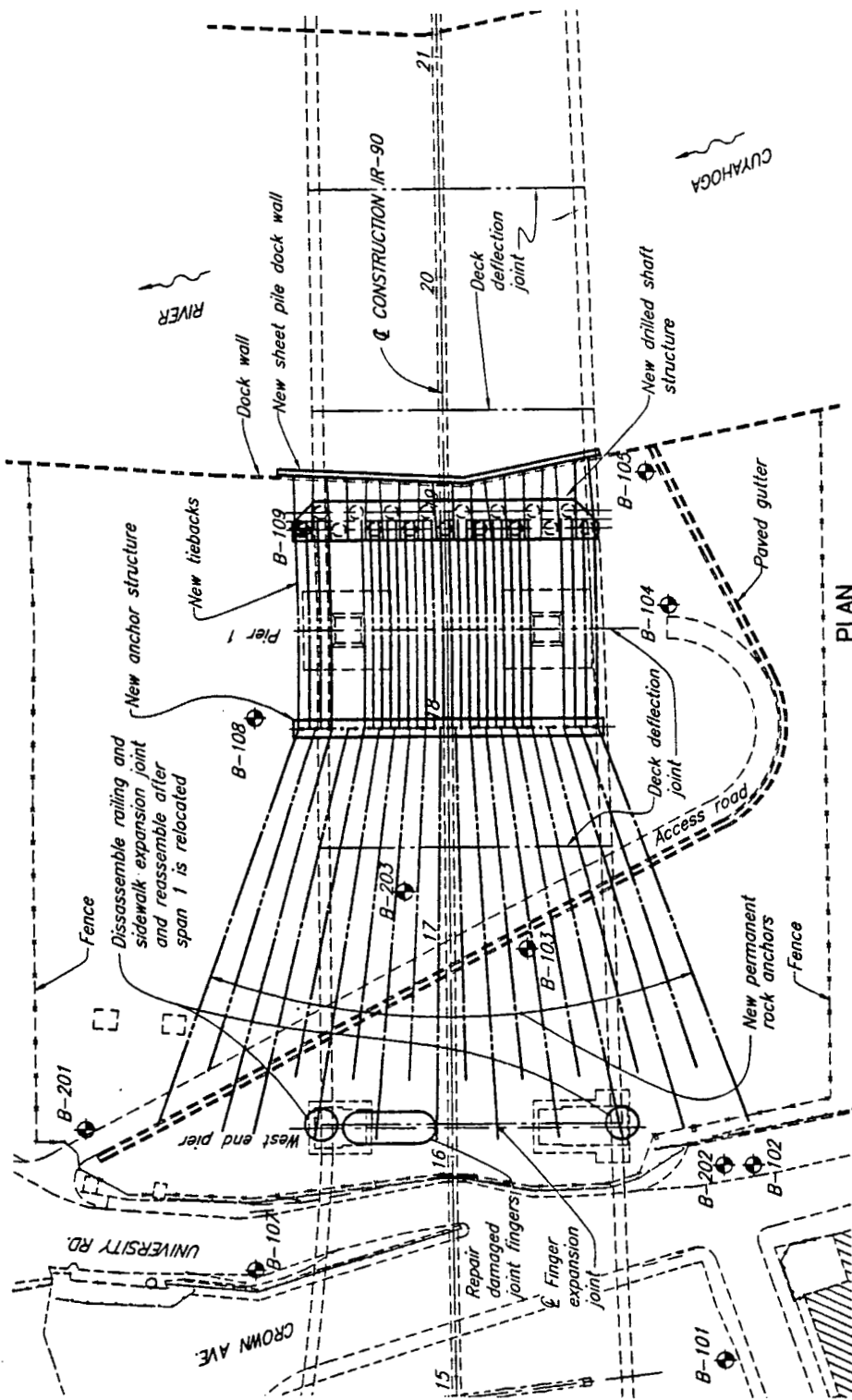


Fig. 4.1: Locations of earth inclinometers installed in 1994.

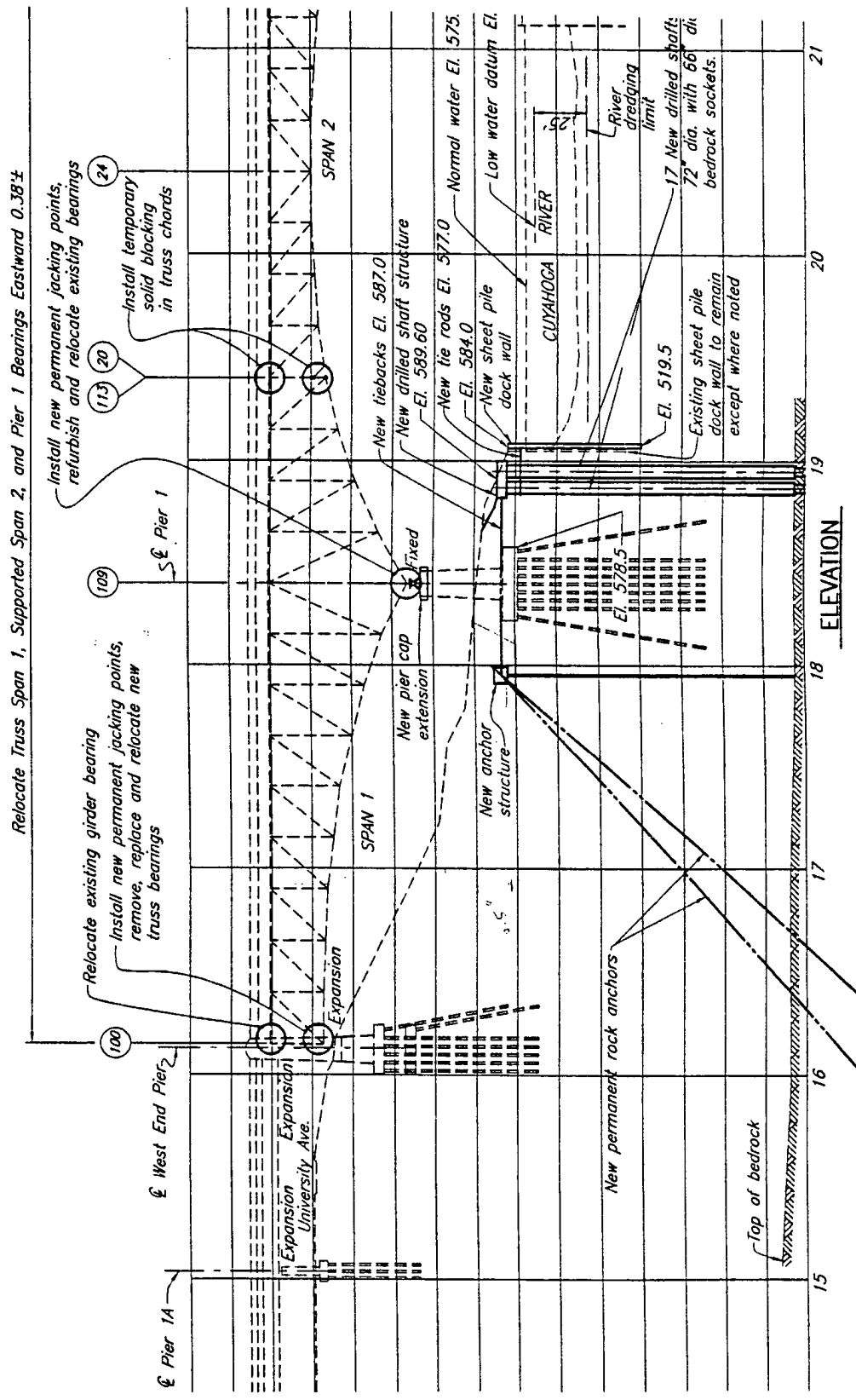


Fig. 4.2: Cross section geometry at the centerline of the project.

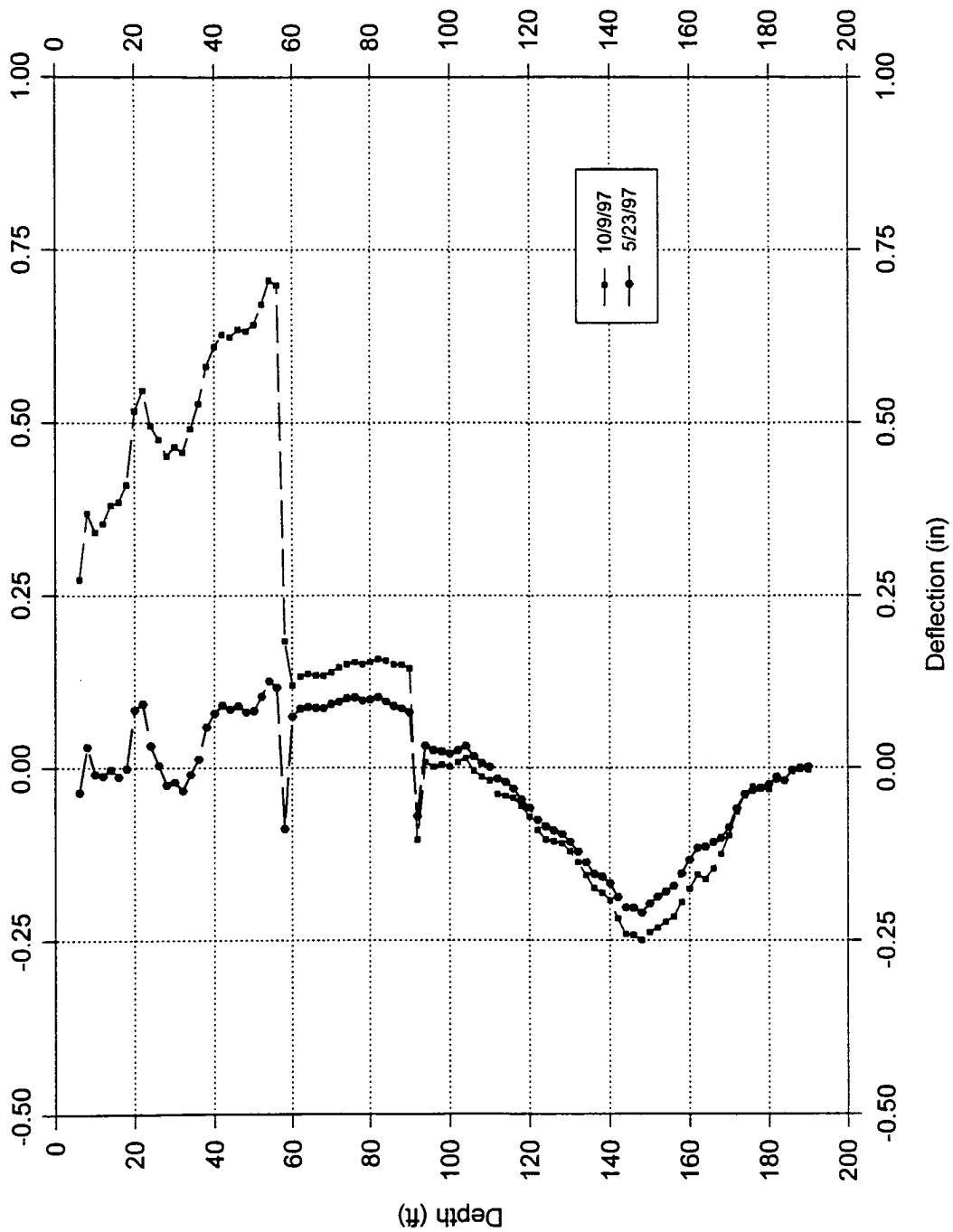


Fig. 4.3: Monitoring of deflection since 5/15/96 for B-103 Inclinator at CUY-90 Project-A-Direction(Down Slope).

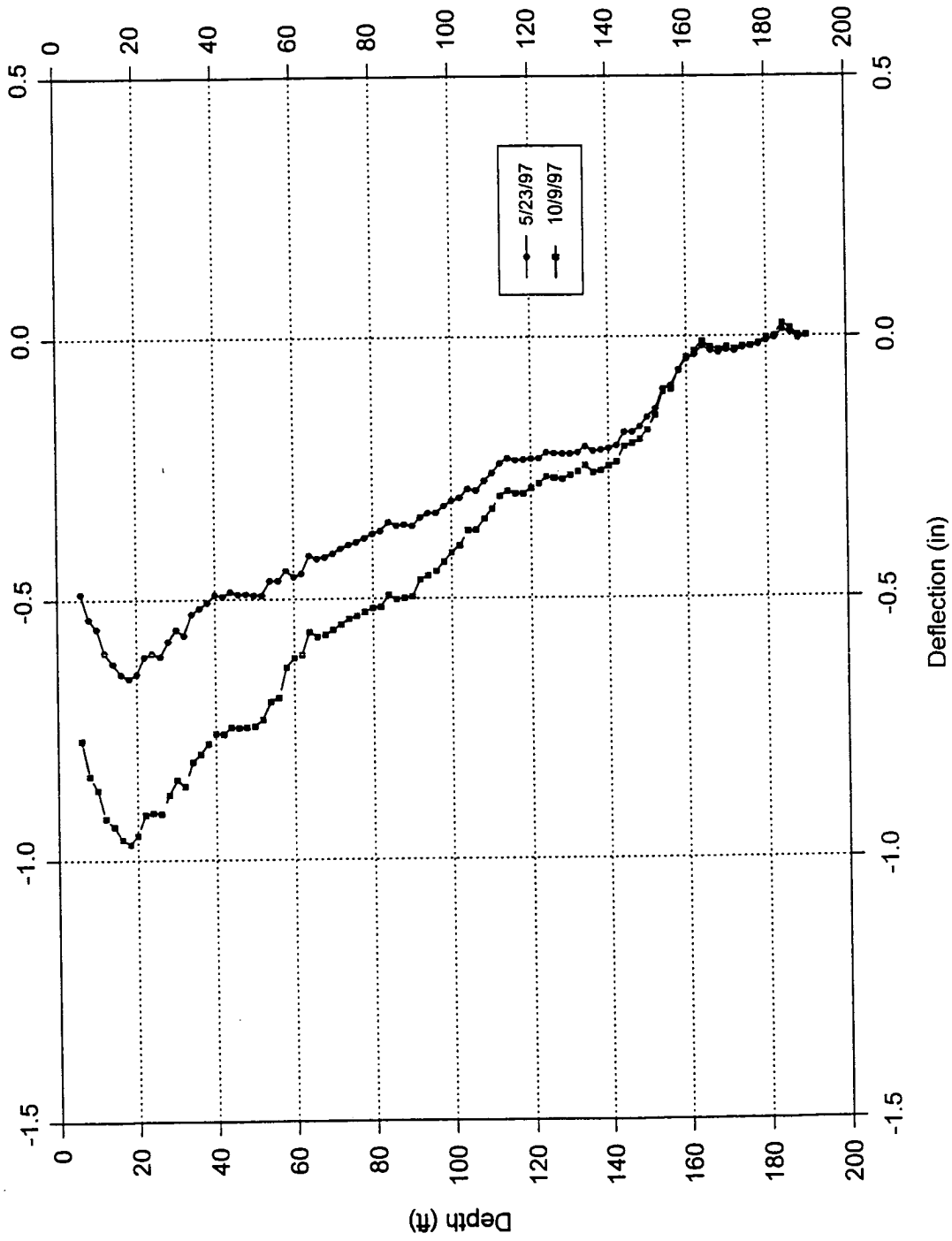


Fig. 4.4: Monitoring of deflection since 5/15/96 for B-103 Inclinator at CUY-90 Project - B-Dir



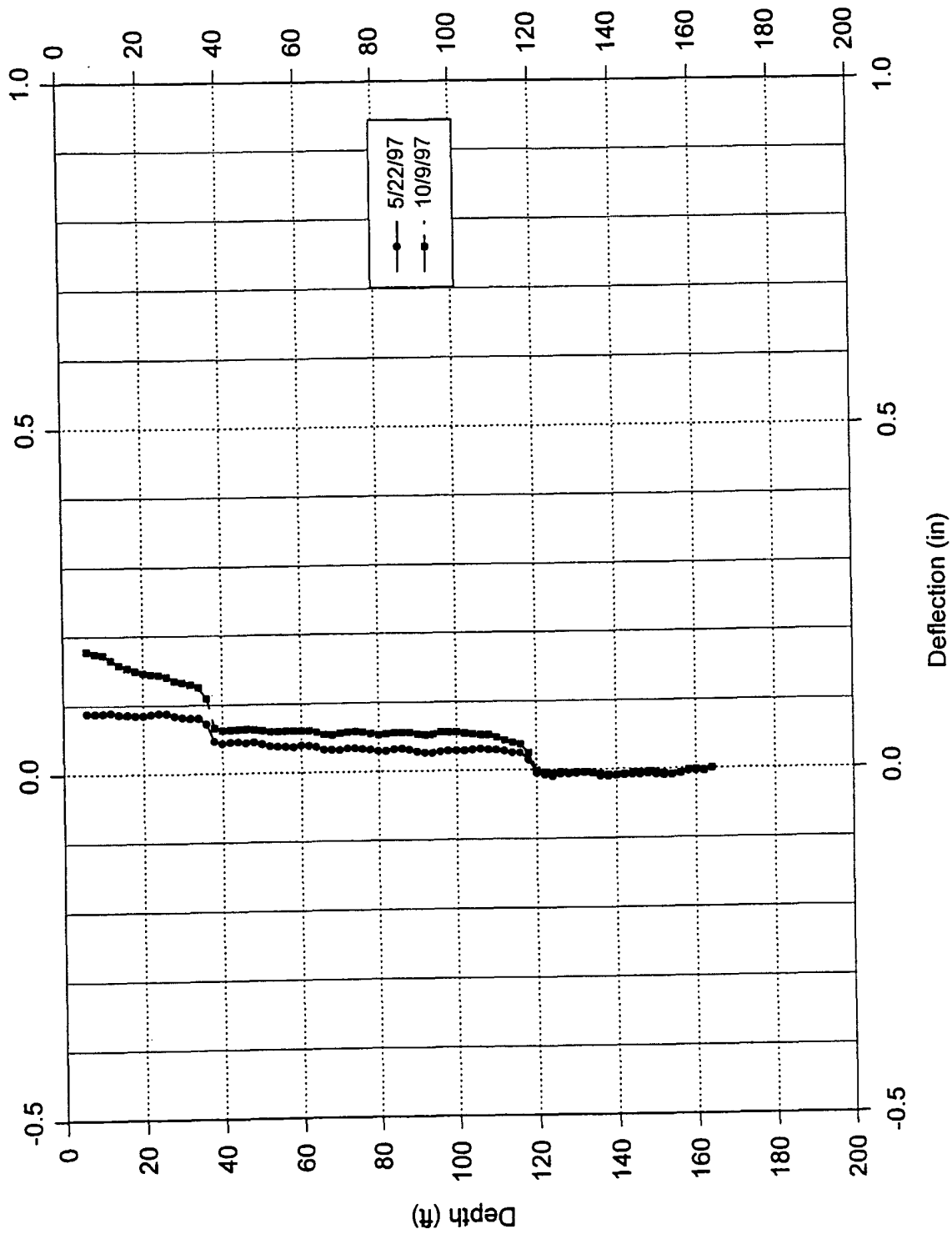


Fig. 4.5: Monitoring of deflection since 5/15/96 for B-104 Inclinator at CUY-90 Project - A-Dir

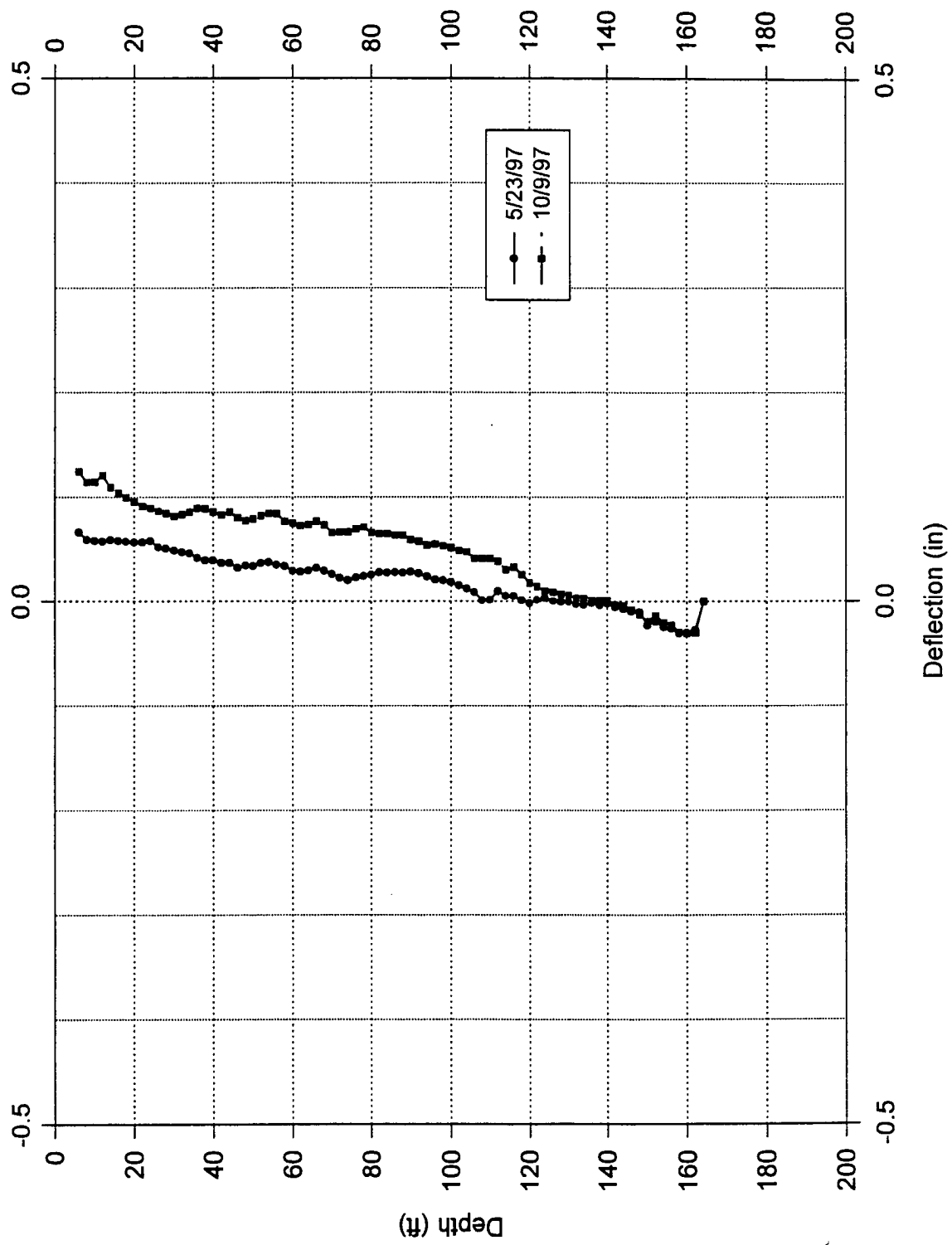


Fig. 4.6: Monitoring of deflection since 5/15/96 for B-104 Inclinator at CUY-90 Project - B-Dir

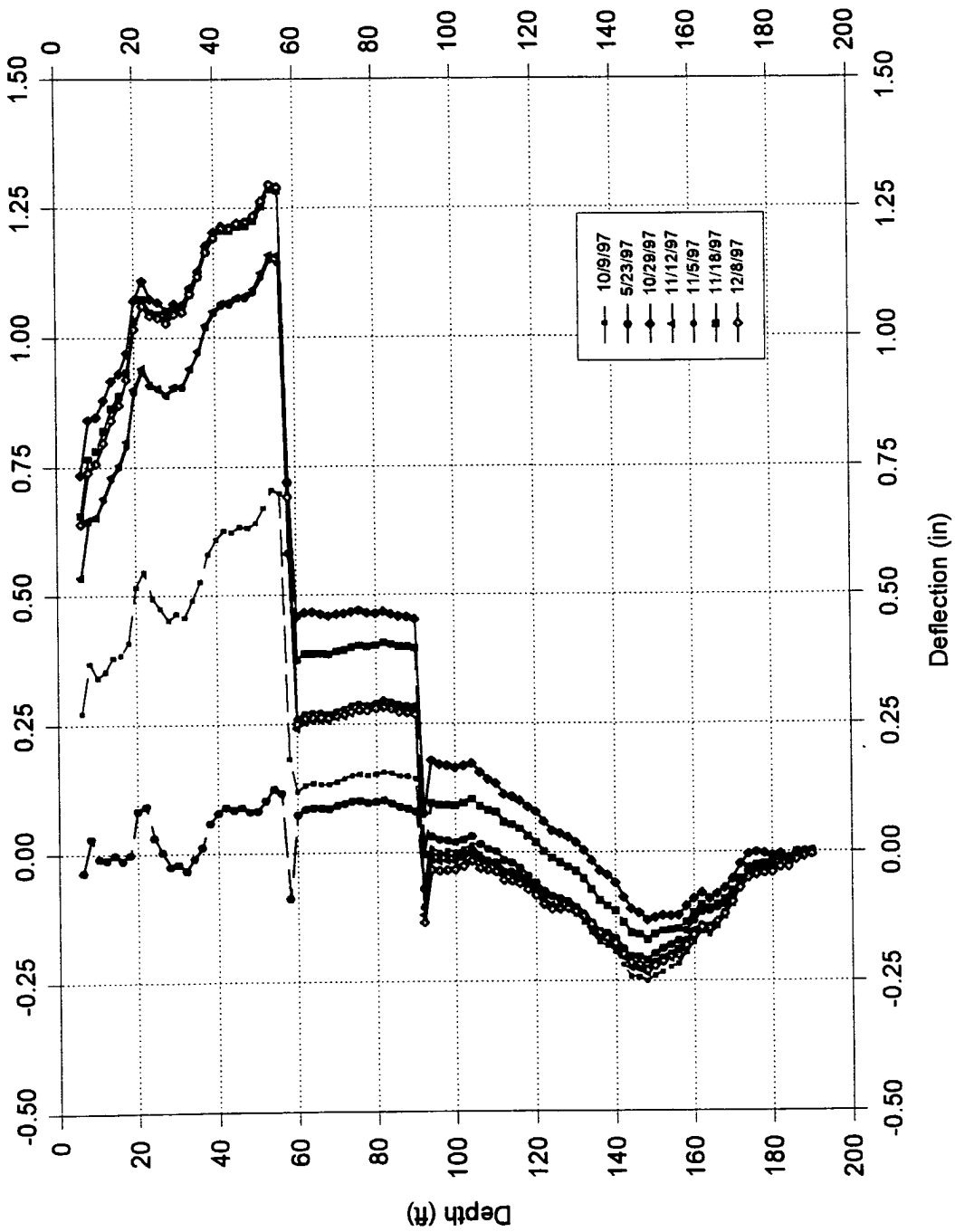


Fig. 4.7: Monitoring of deflection since 5/15/96 for B-103 Inclinometer at CUY-90 Project-A-Direction(Down Slope).  
Last reading before resuming pile driving.

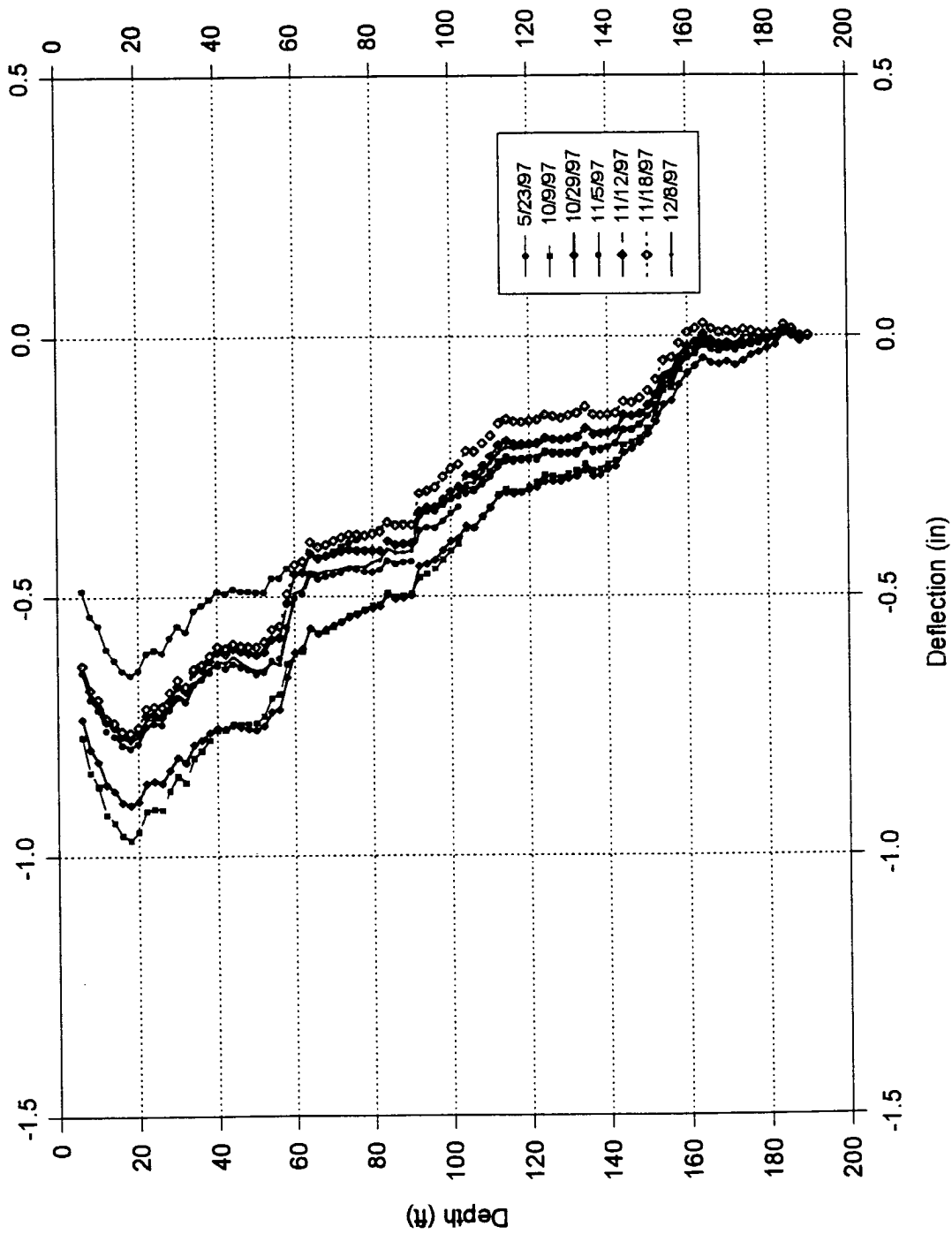


Fig. 4.14: Monitoring of deflection since 5/15/96 for B-103 Inclinometer at CUY-90 Project - B-Dir  
Last reading before resuming pile driving

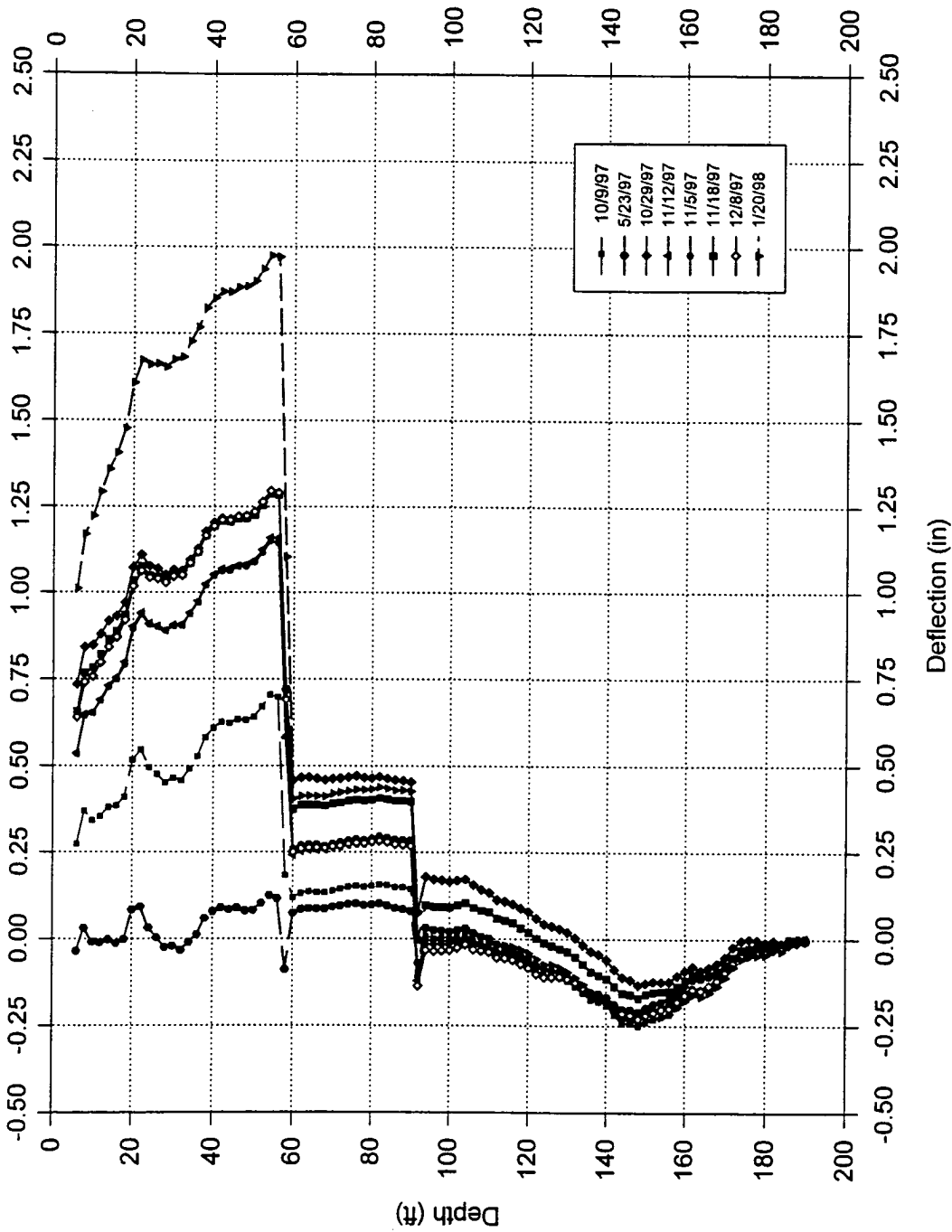


Fig. 4.15: Monitoring of deflection since 5/15/96 for B-103 Inclinometer at CUY-90 Project-A-Direction(Down Slope).  
 Last reading after completion of pile driving.

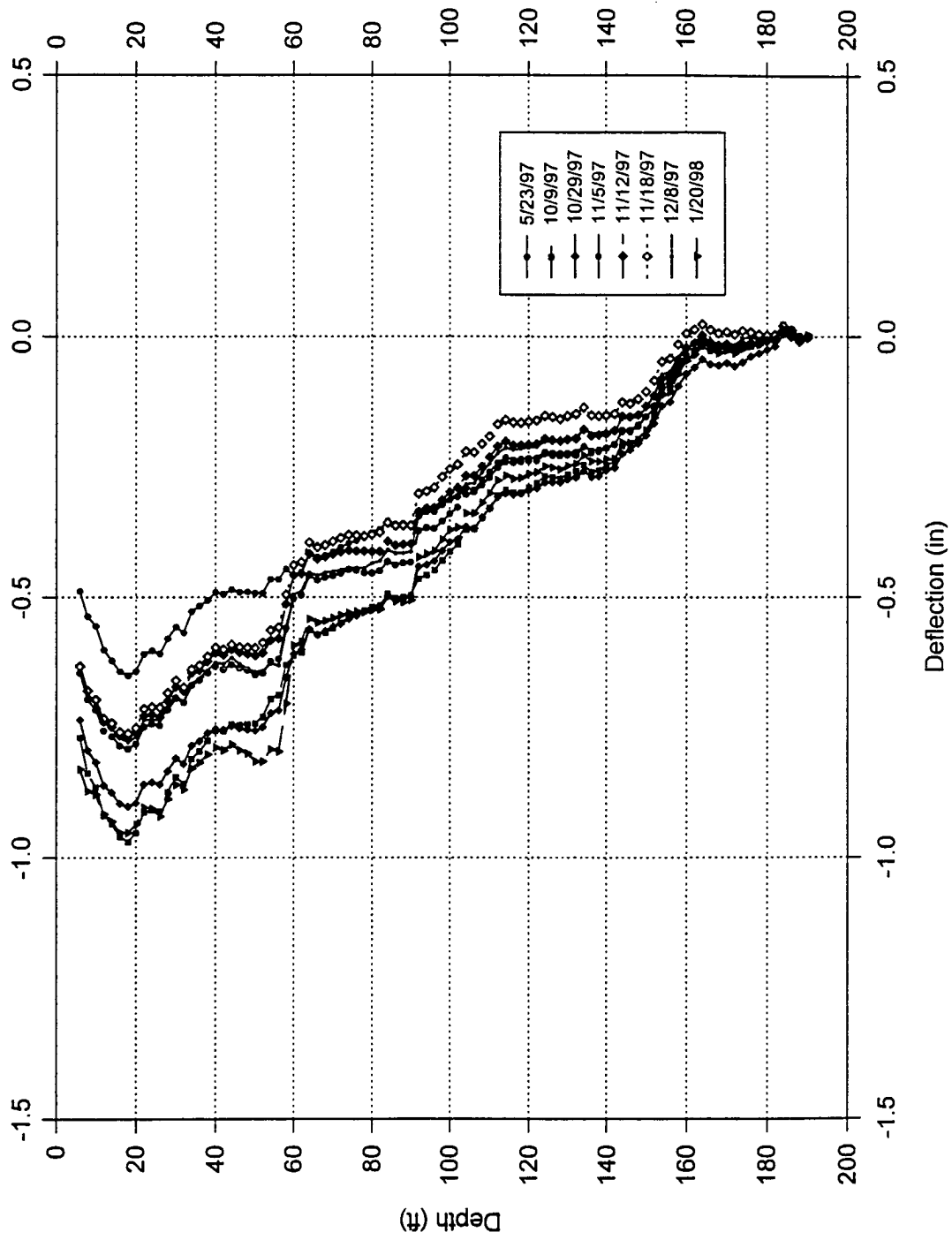


Fig. 4.16: Monitoring of deflection since 5/15/96 for B-103 Inclinator at CUY-90 Project - B-Dir  
 Last reading after completion of pile driving

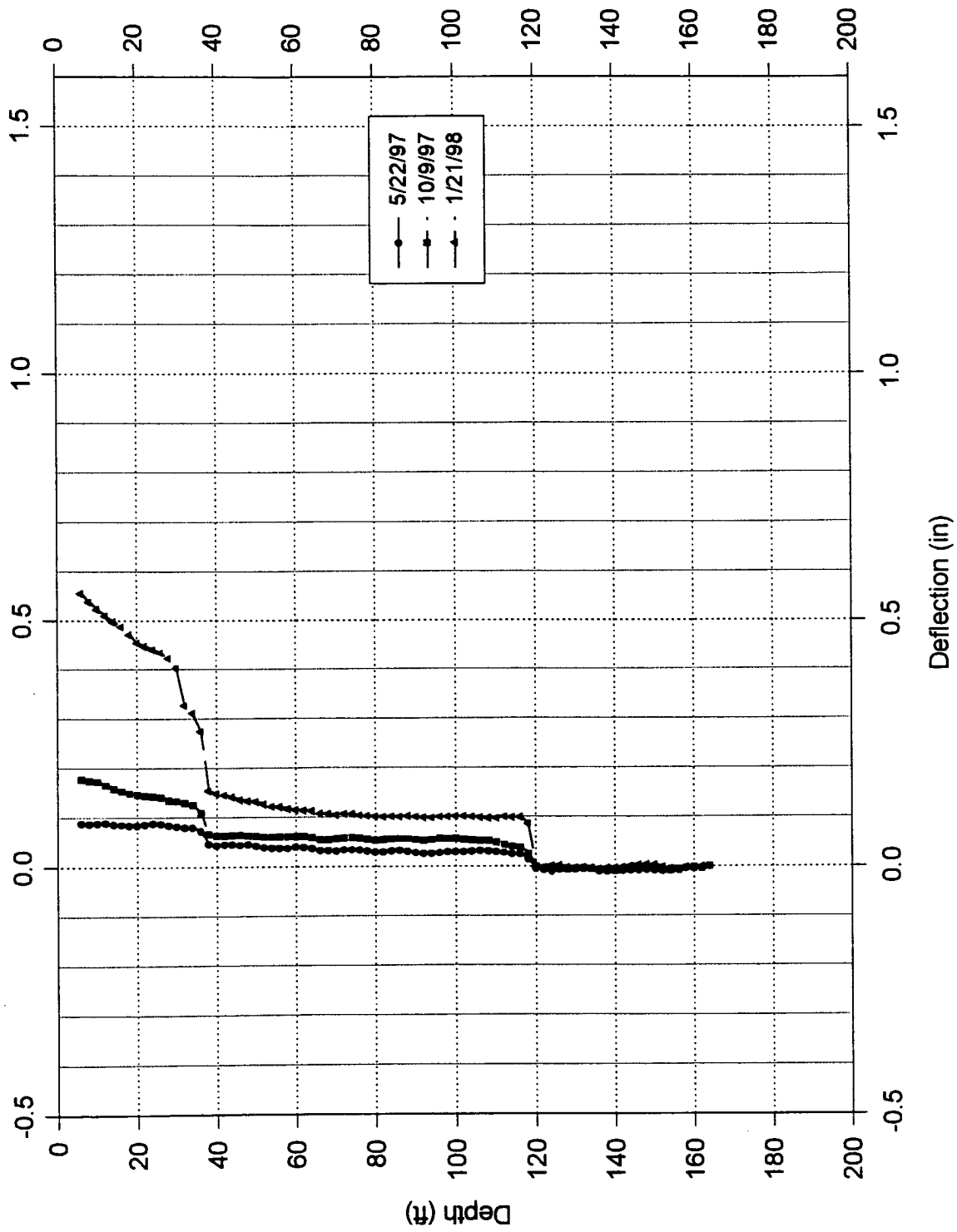


Fig. 4.17: Monitoring of deflection since 5/15/96 for B-104 Inclinometer at CUY-90 Project - A-Dir  
 Last reading after completion of pile driving.

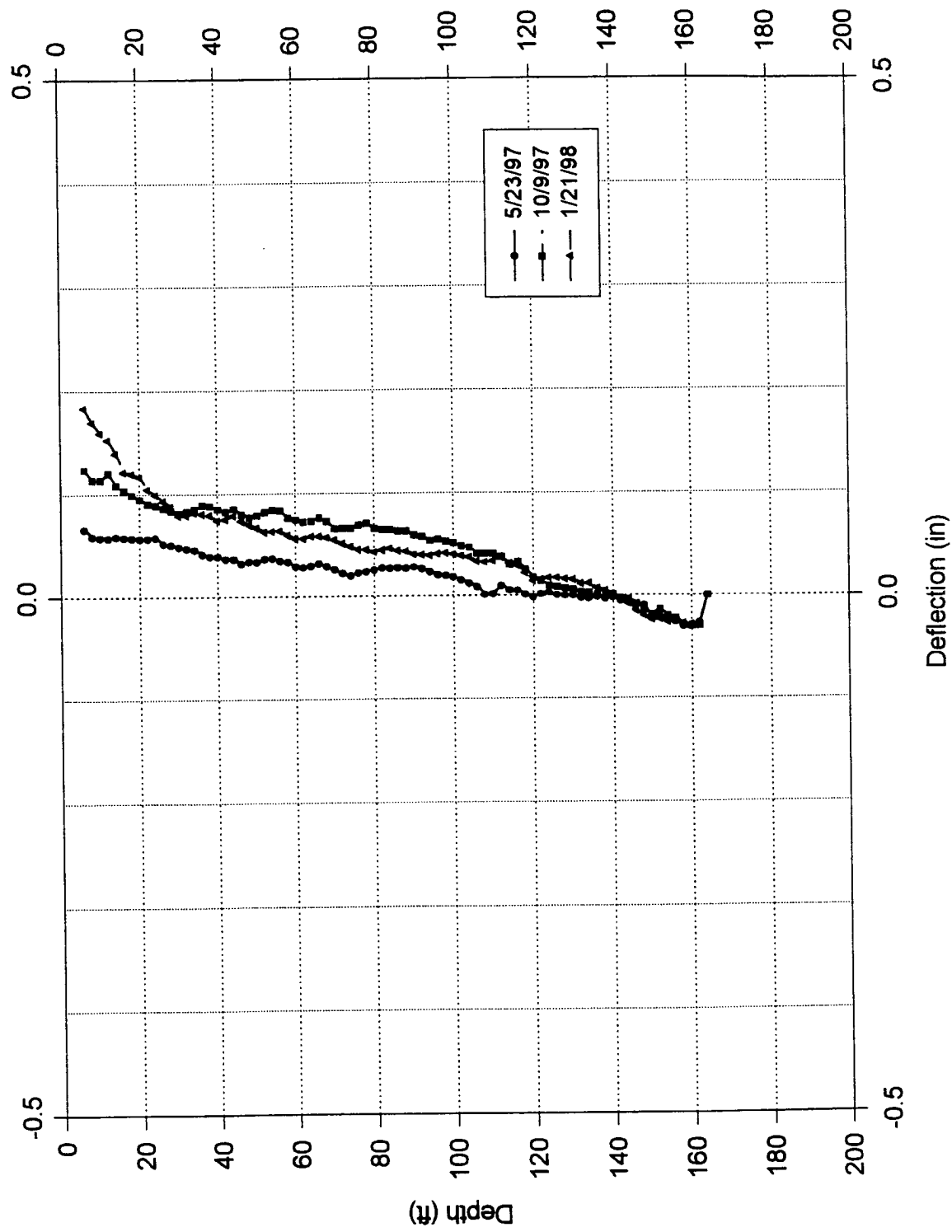


Fig. 4.18: Monitoring of deflection since 5/15/96 for B-104 Inclinometer at CUY-90 Project - B-Dir  
 Last reading after completion of pile driving.



I90, PN18, ICE- 80-S: OED

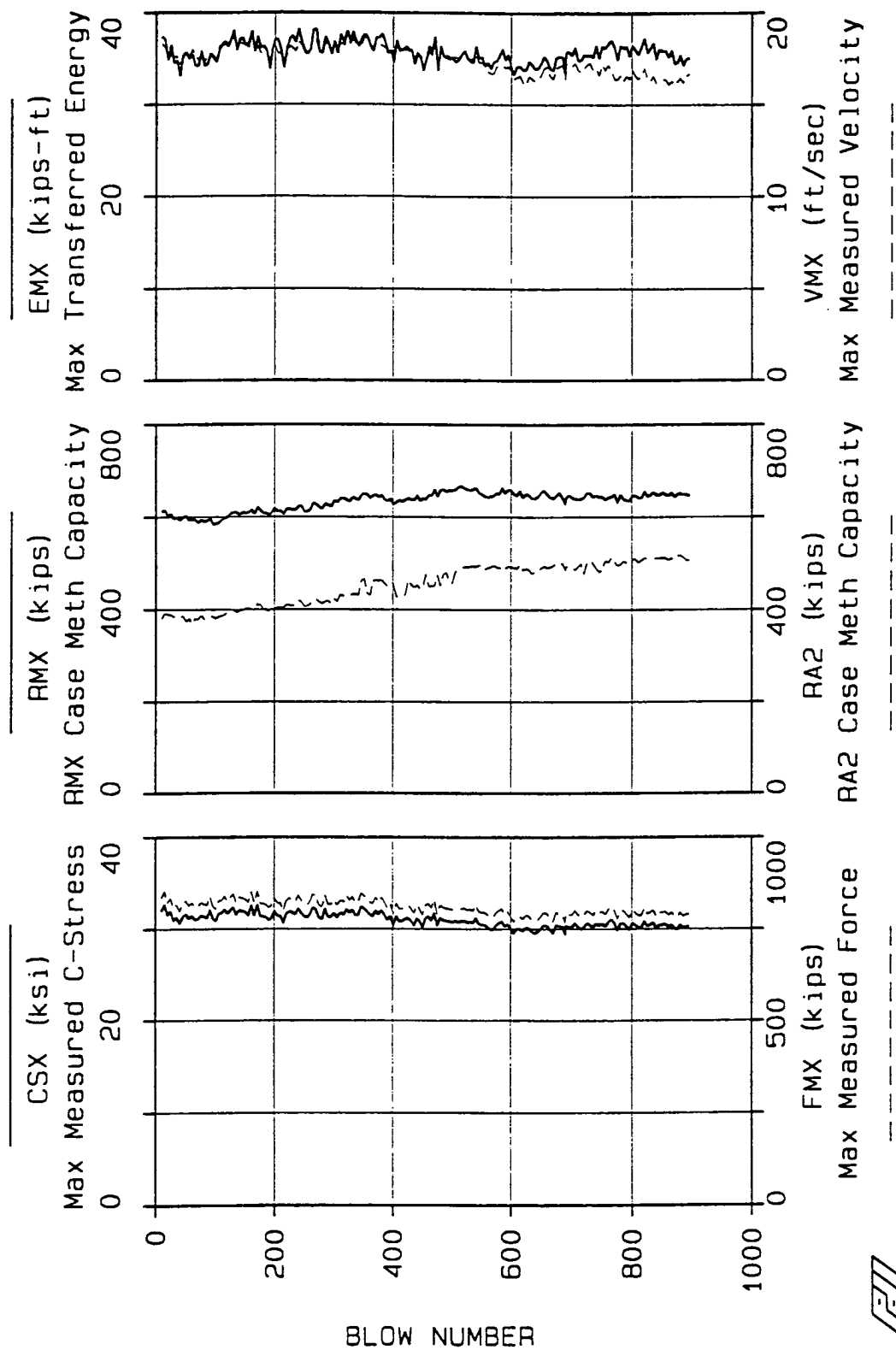


Fig. 4.19: Results of measured force, calculated capacity based on RA2 method and energy measured against blow count from PDA.

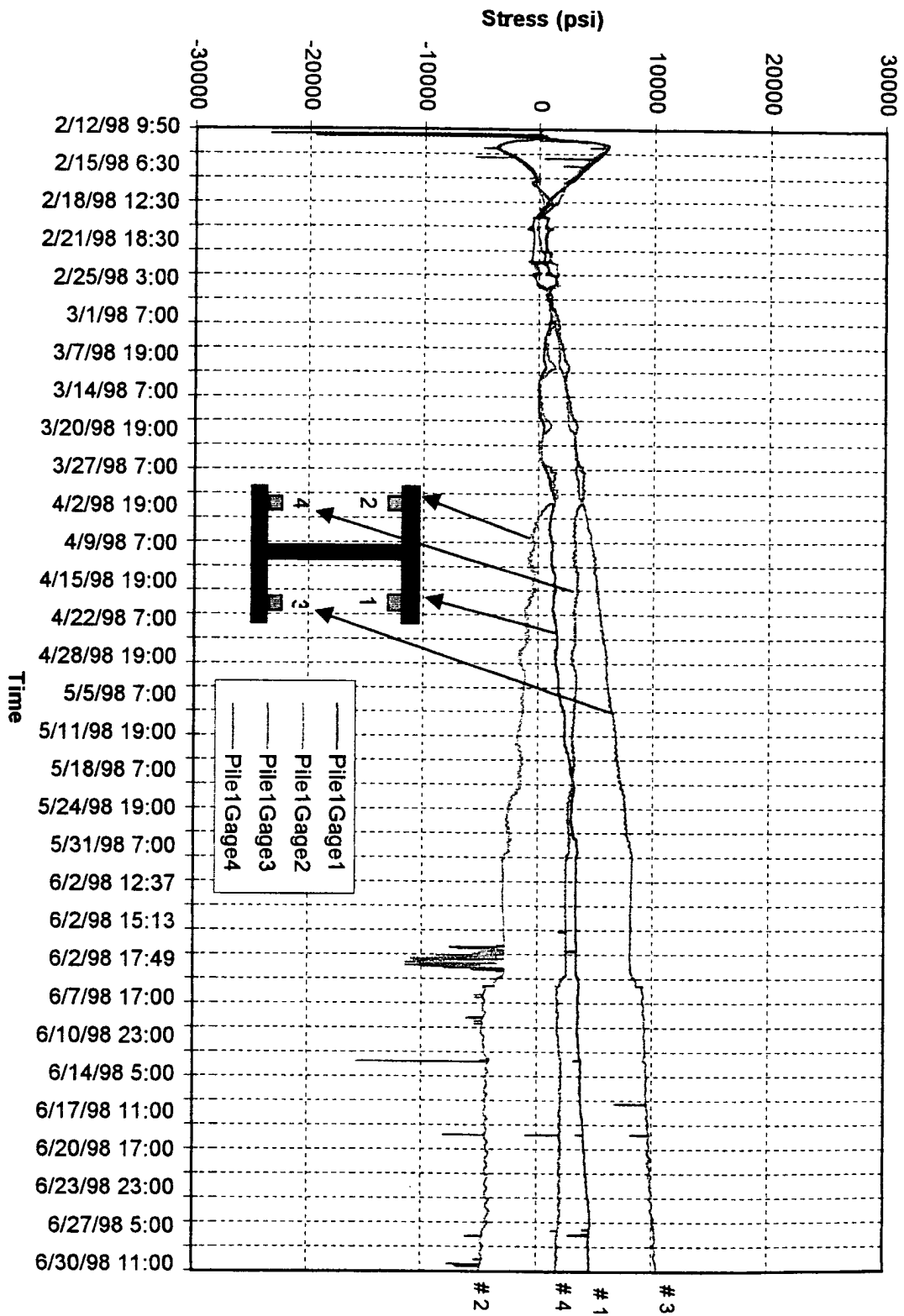


Fig. 4.28: Long-term monitoring of stress in Pile # 1 in the anchor cap structure (2/12/98 ~ 6/30/98)

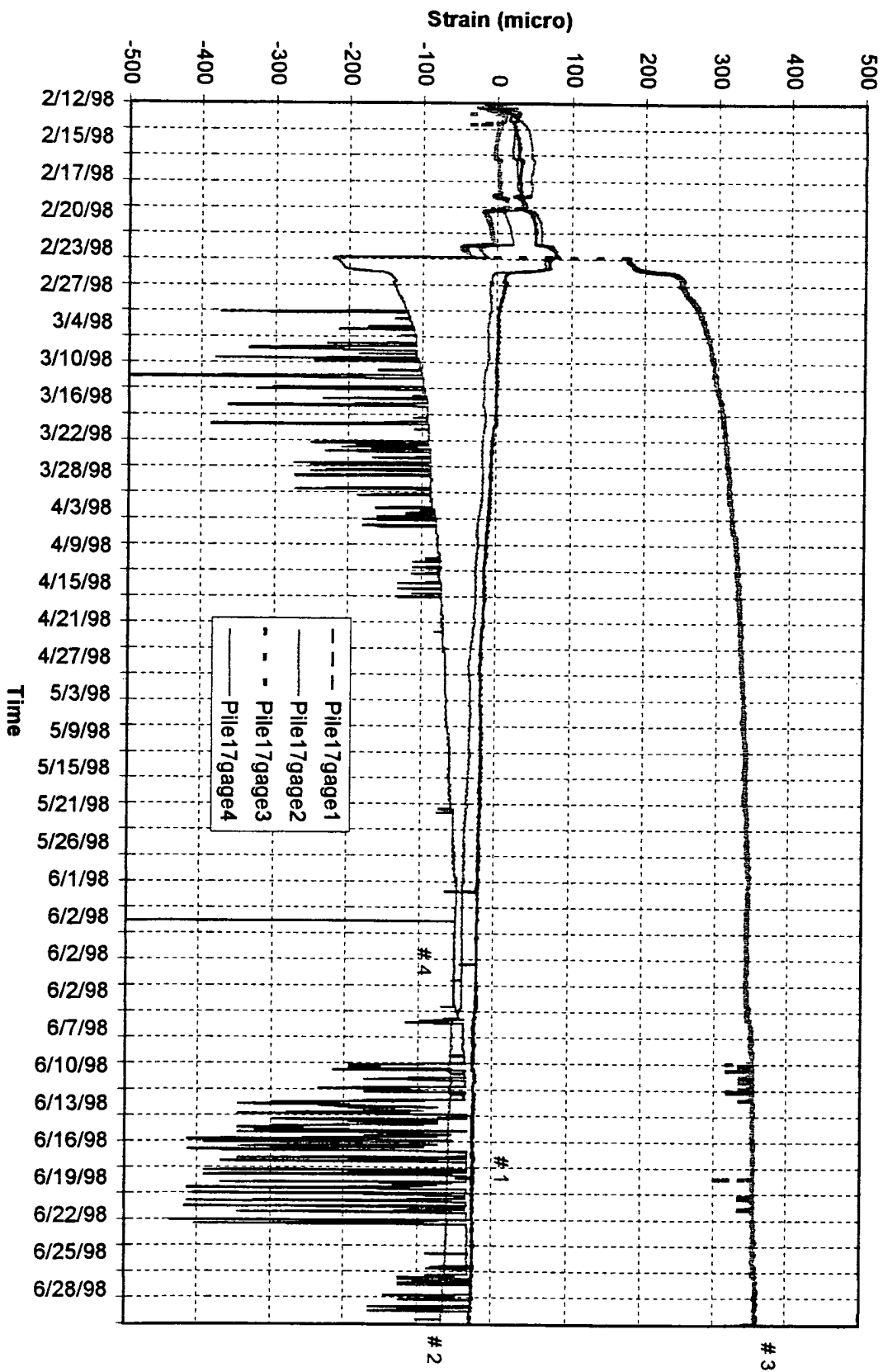


Fig. 4.29: Long-term monitoring of strain in Pile # 17 in the anchor cap structure (2/12/98 ~ 6/30/98)

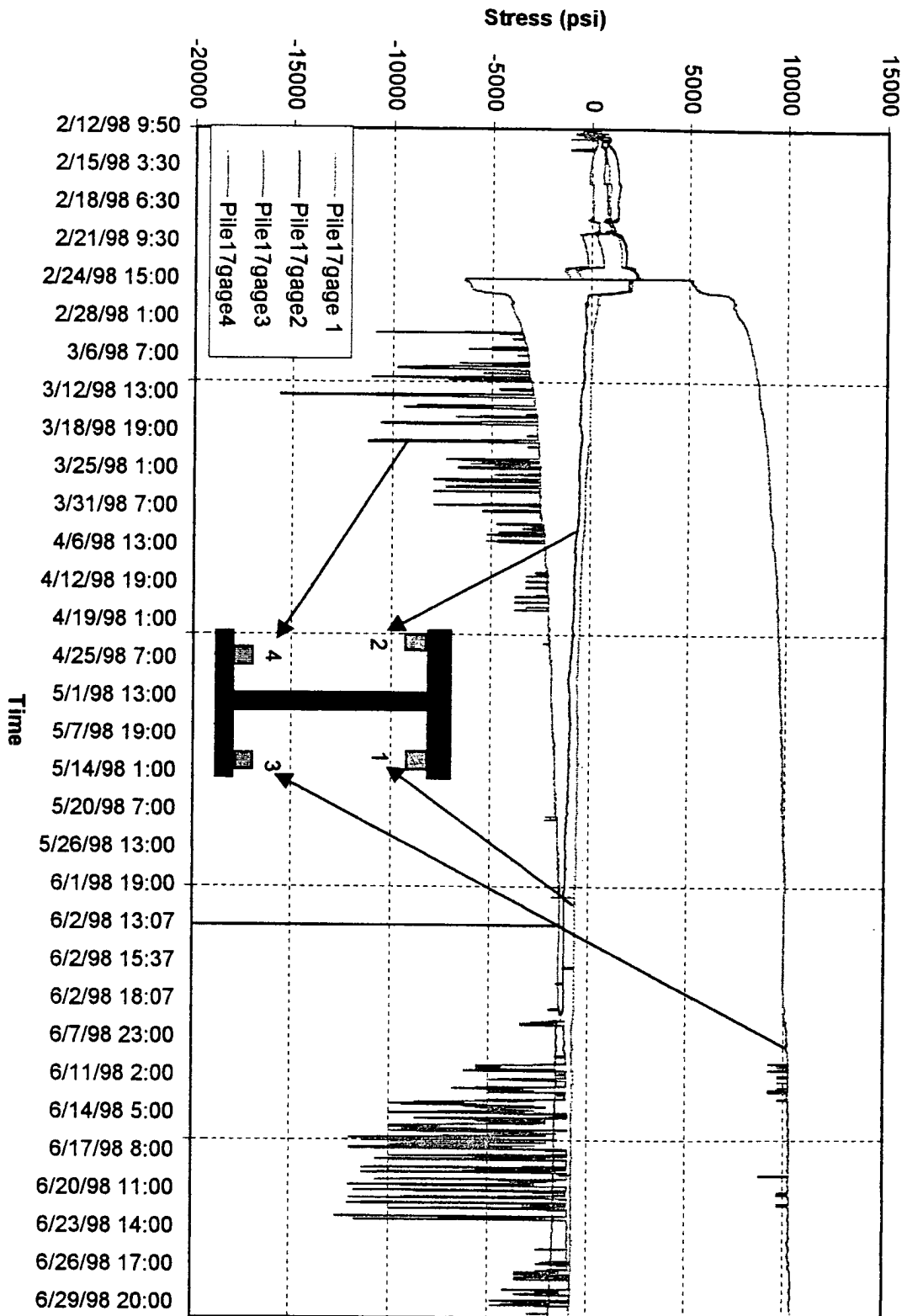


Fig. 4.30: Long-term monitoring of stress in Pile # 17 in the anchor cap structure (2/12/98 ~ 6/30/98)

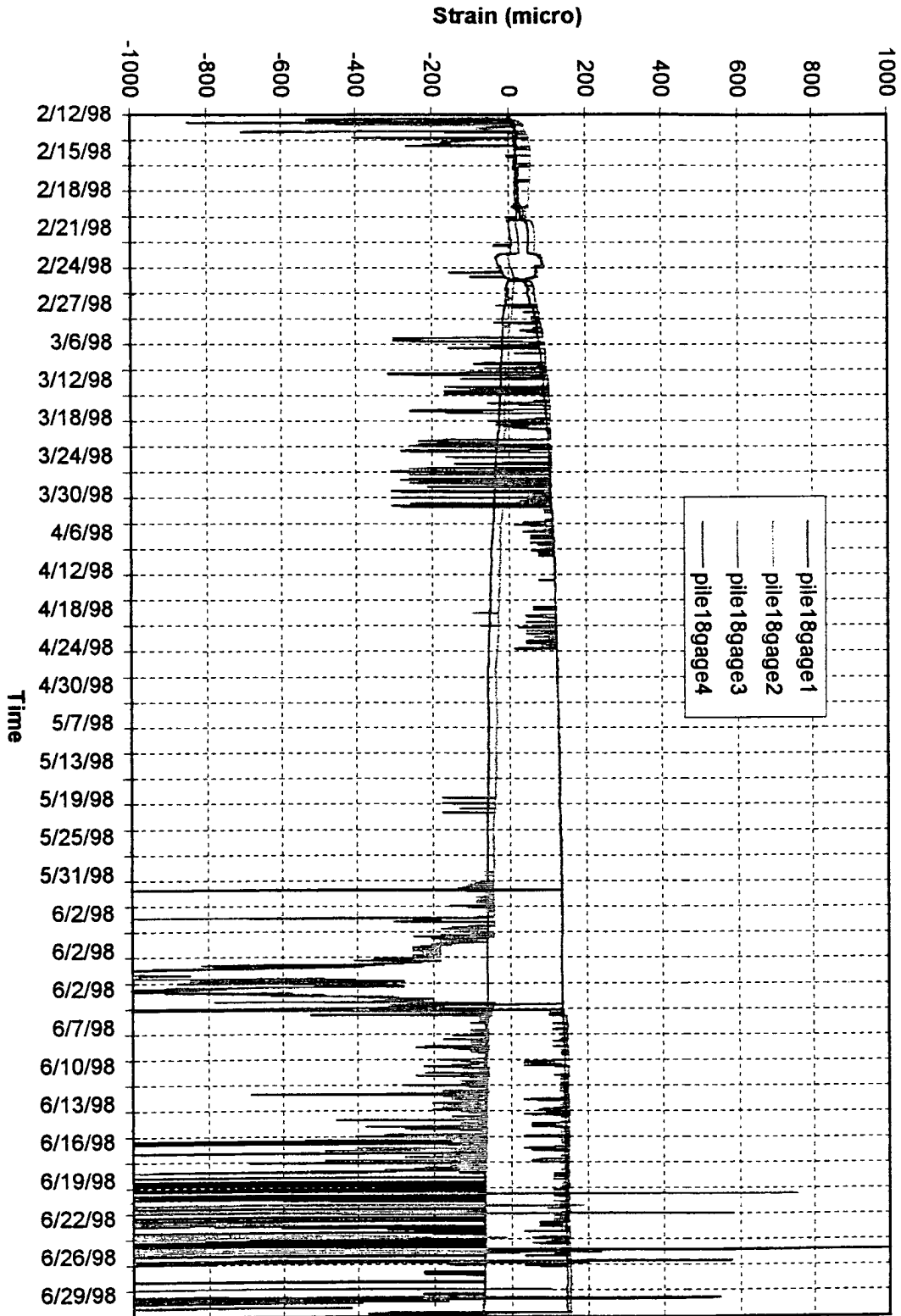


Fig. 4.31: Long-term monitoring of strain in Pile # 18 in the anchor cap structure (2/12/98 ~ 6/30/98)

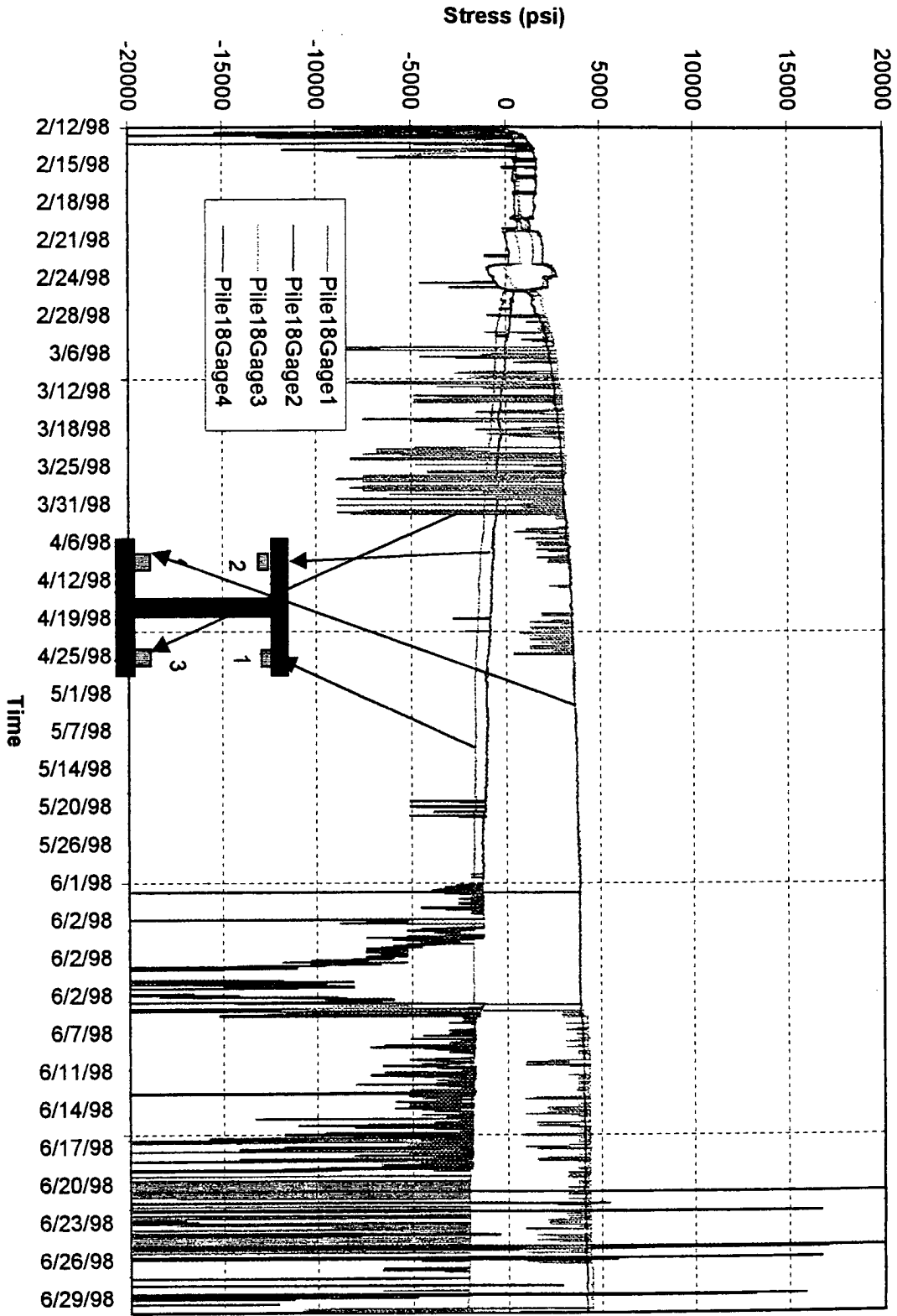


Fig. 4.32: Long-term monitoring of stress in Pile # 18 in the anchor cap structure (2/12/98 ~ 6/30/98)

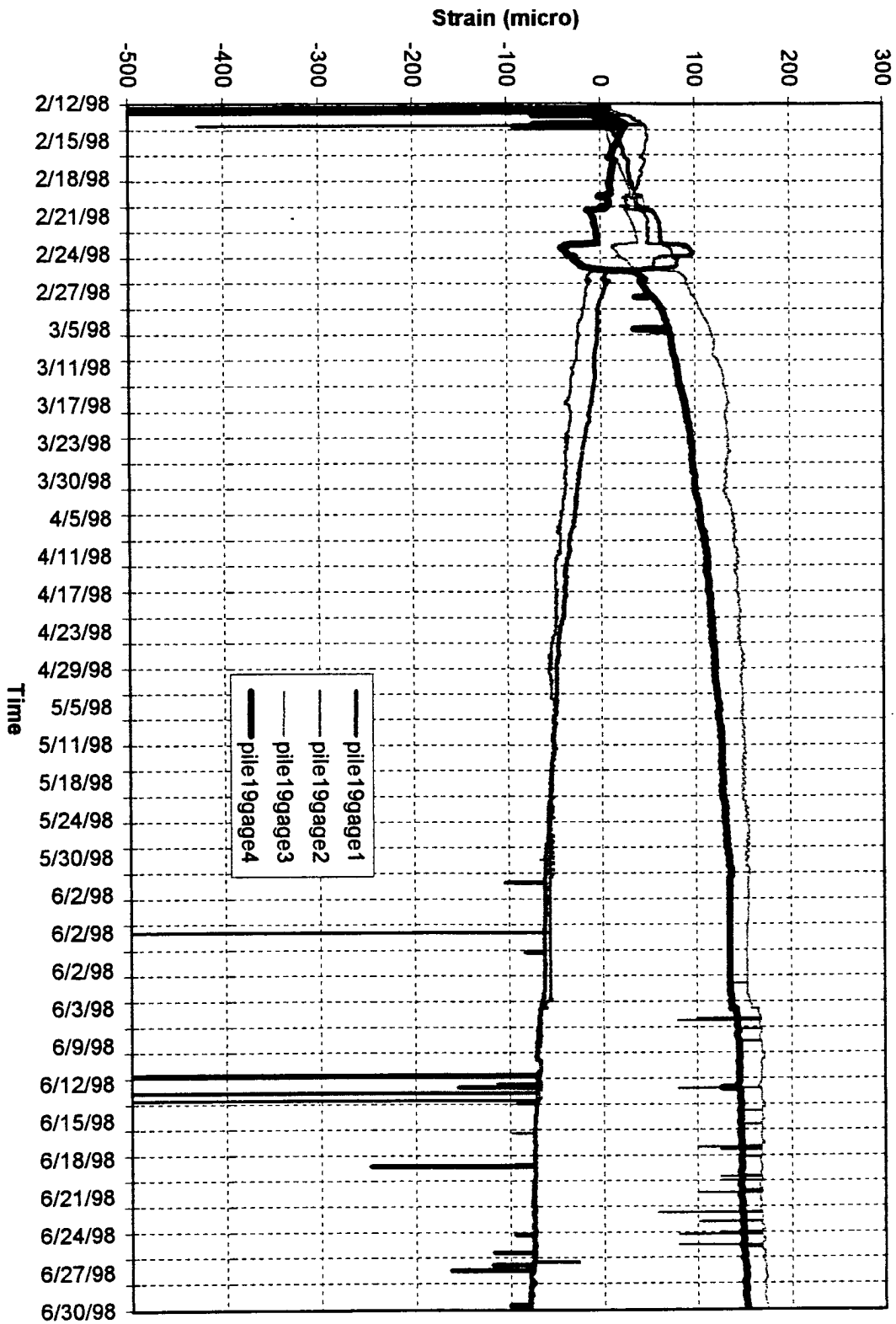


Fig. 4.33: Long-term monitoring of strain in Pile # 19 in the anchor cap structure (2/12/98 ~ 6/30/98)

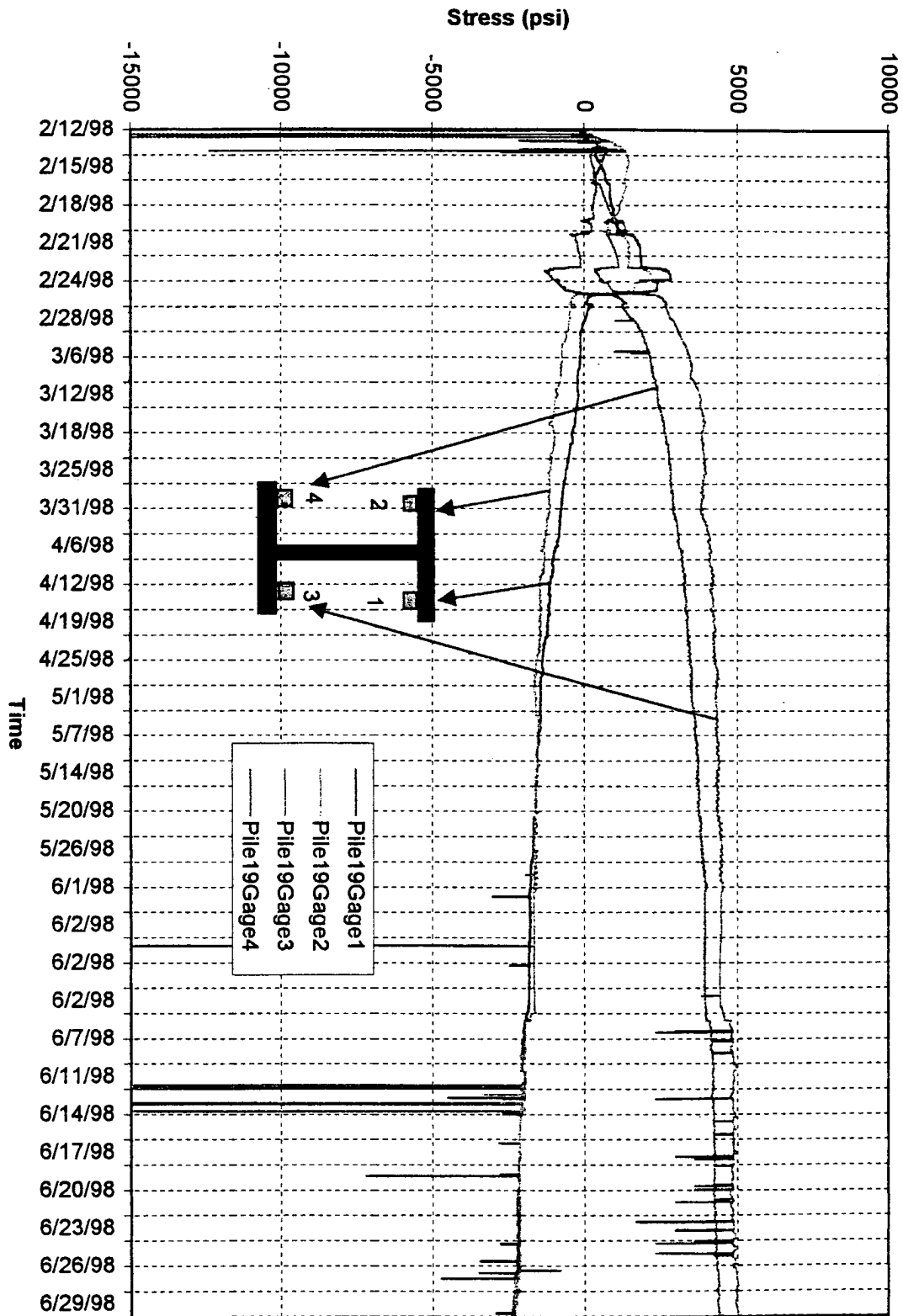


Fig. 4.34: Long-term monitoring of stress in Pile # 19 in the anchor cap structure (2/12/98 ~ 6/30/98)



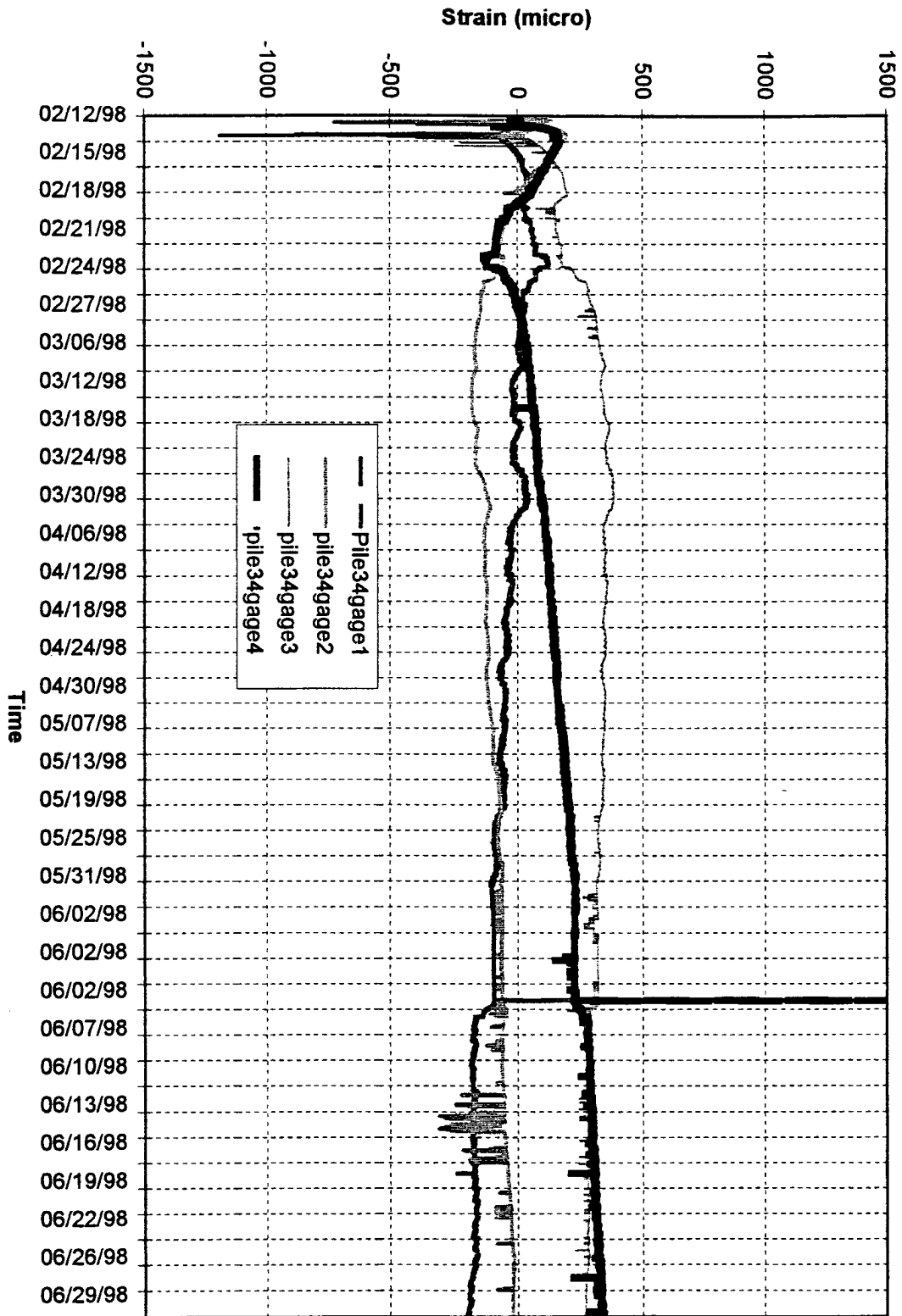


Fig. 4.35: Long-term monitoring of strain in Pile # 34 in the anchor cap structure (2/12/98 ~ 6/30/98)

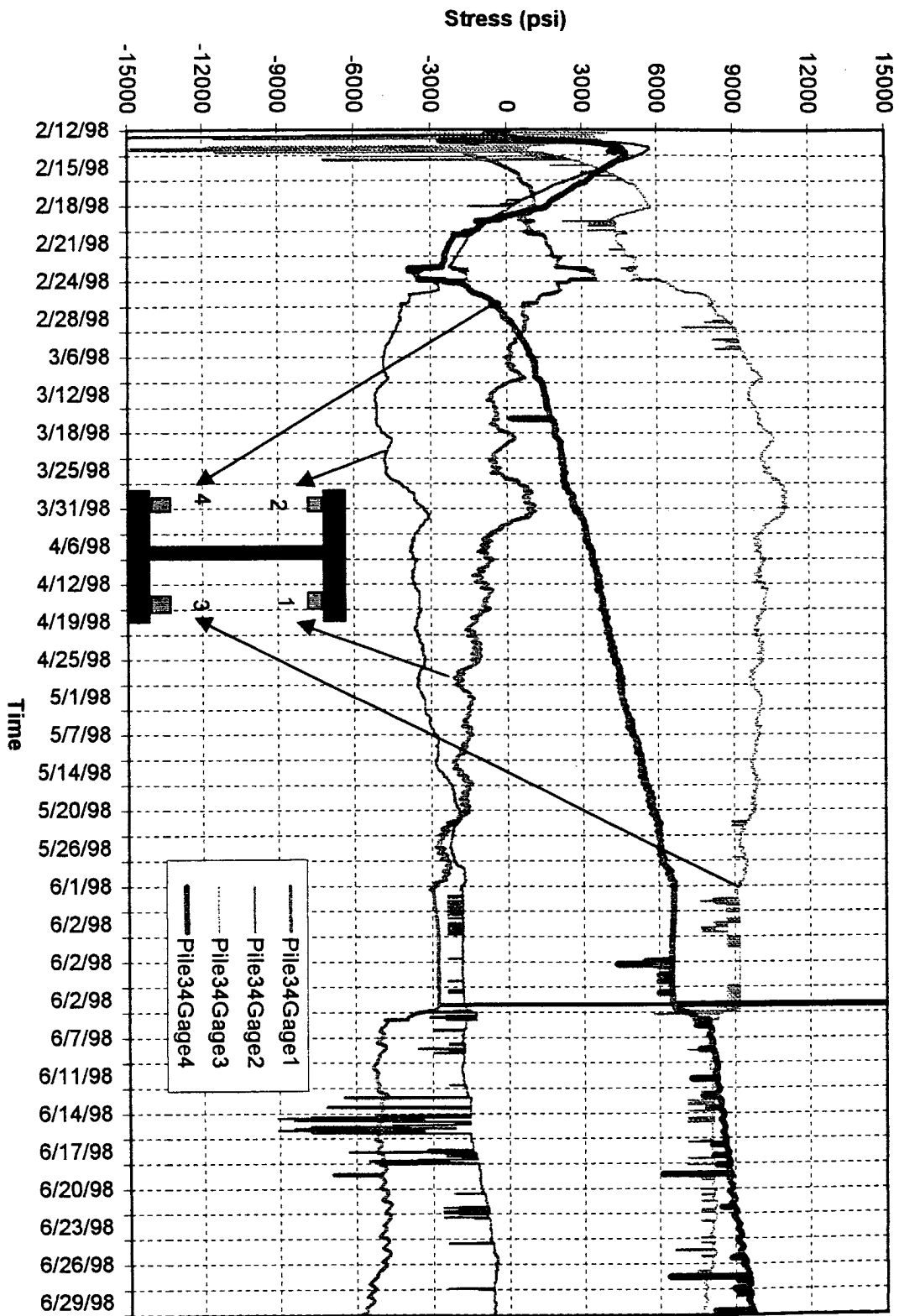


Fig. 4.36: Long-term monitoring of stress in Pile # 34 in the anchor cap structure (2/12/98 ~ 6/30/98)

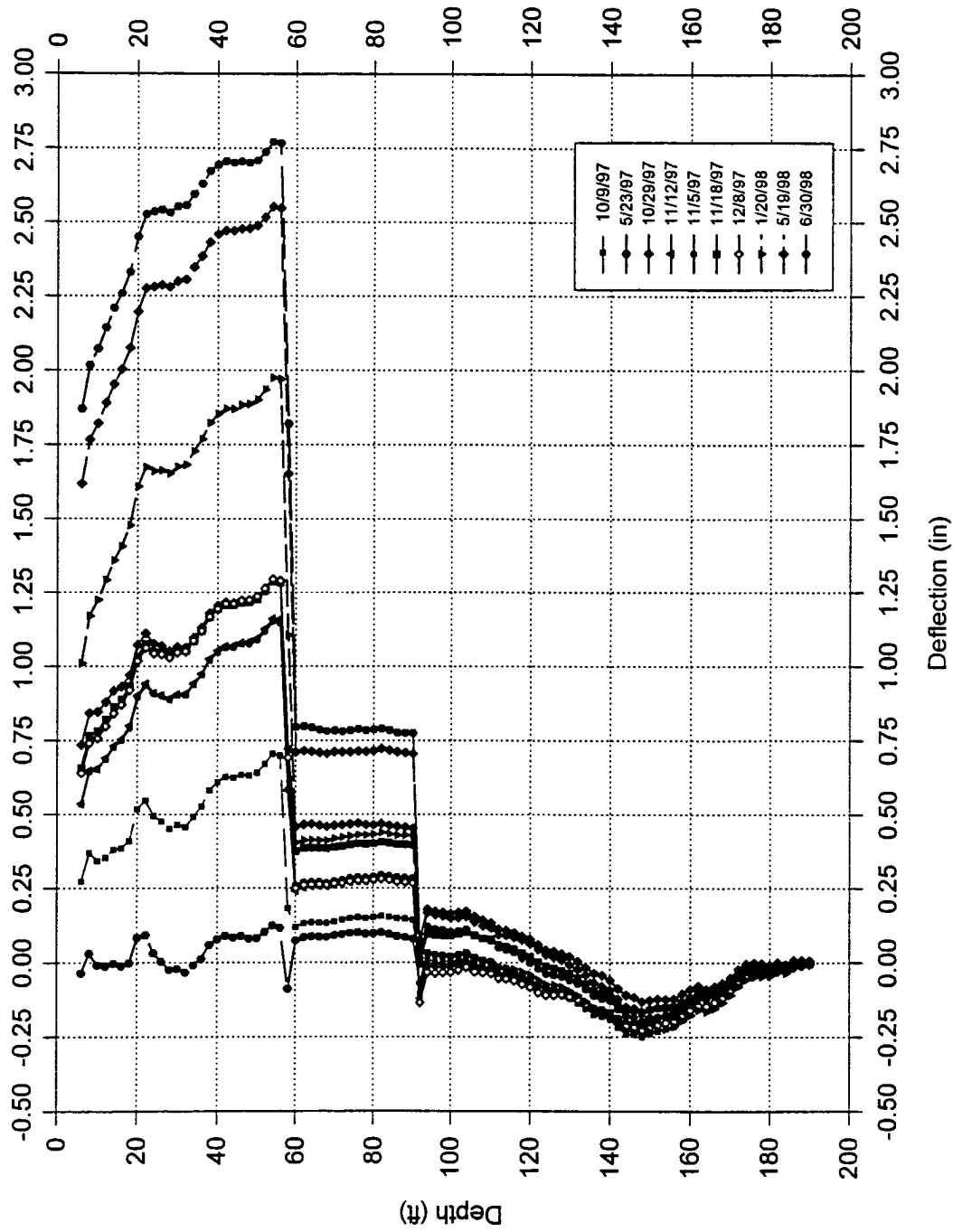


Fig. 4.37: Monitoring of deflection since 5/15/96 for B-103 Inclinator at CUY-90 Project-A-Direction(Down Slope).  
 Last reading on 6/30/1998.

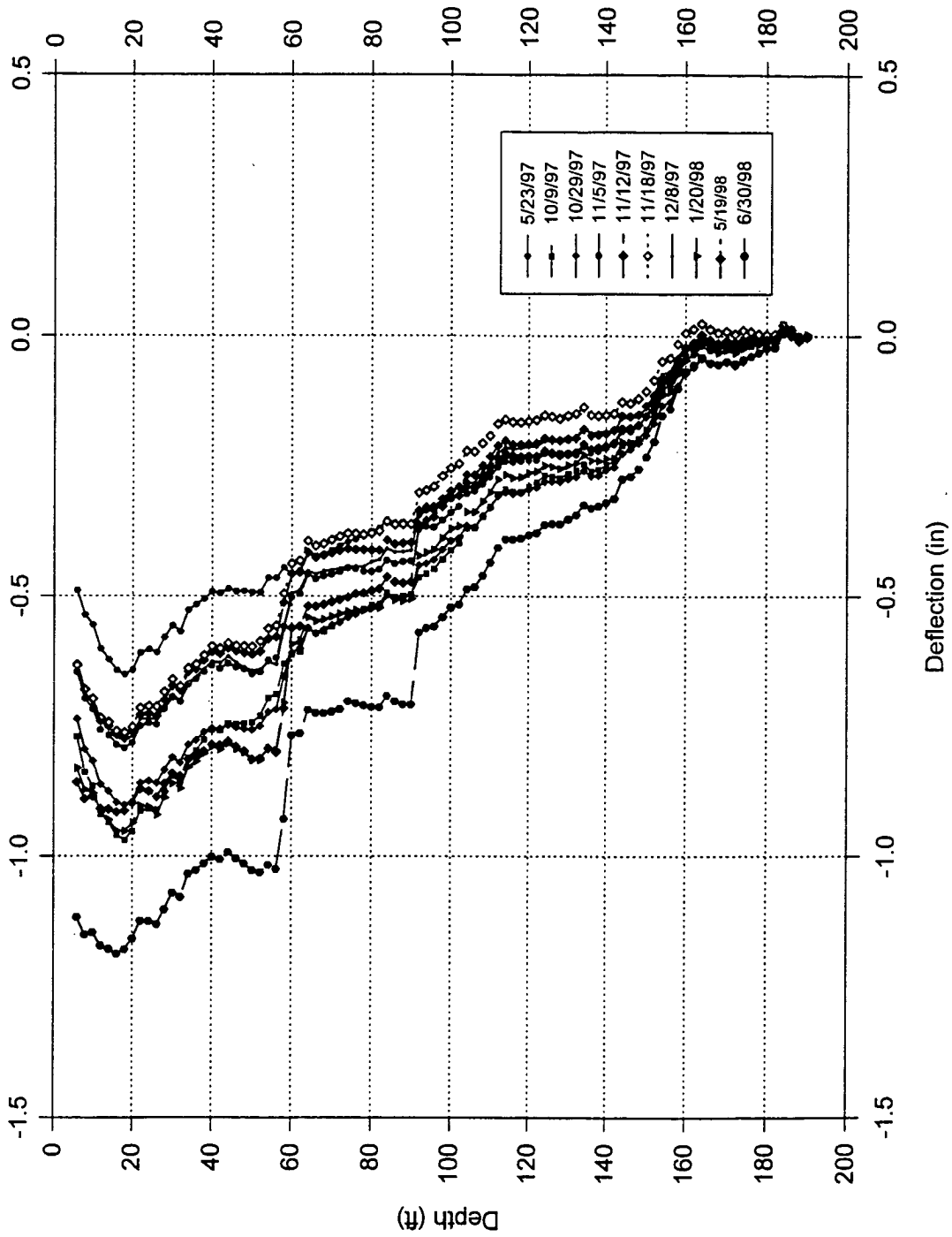


Fig. 4.38: Monitoring of deflection since 5/15/96 for B-103 Inclinometer at CUY-90 Project - B-Dir  
 Last reading on 6/30/98.

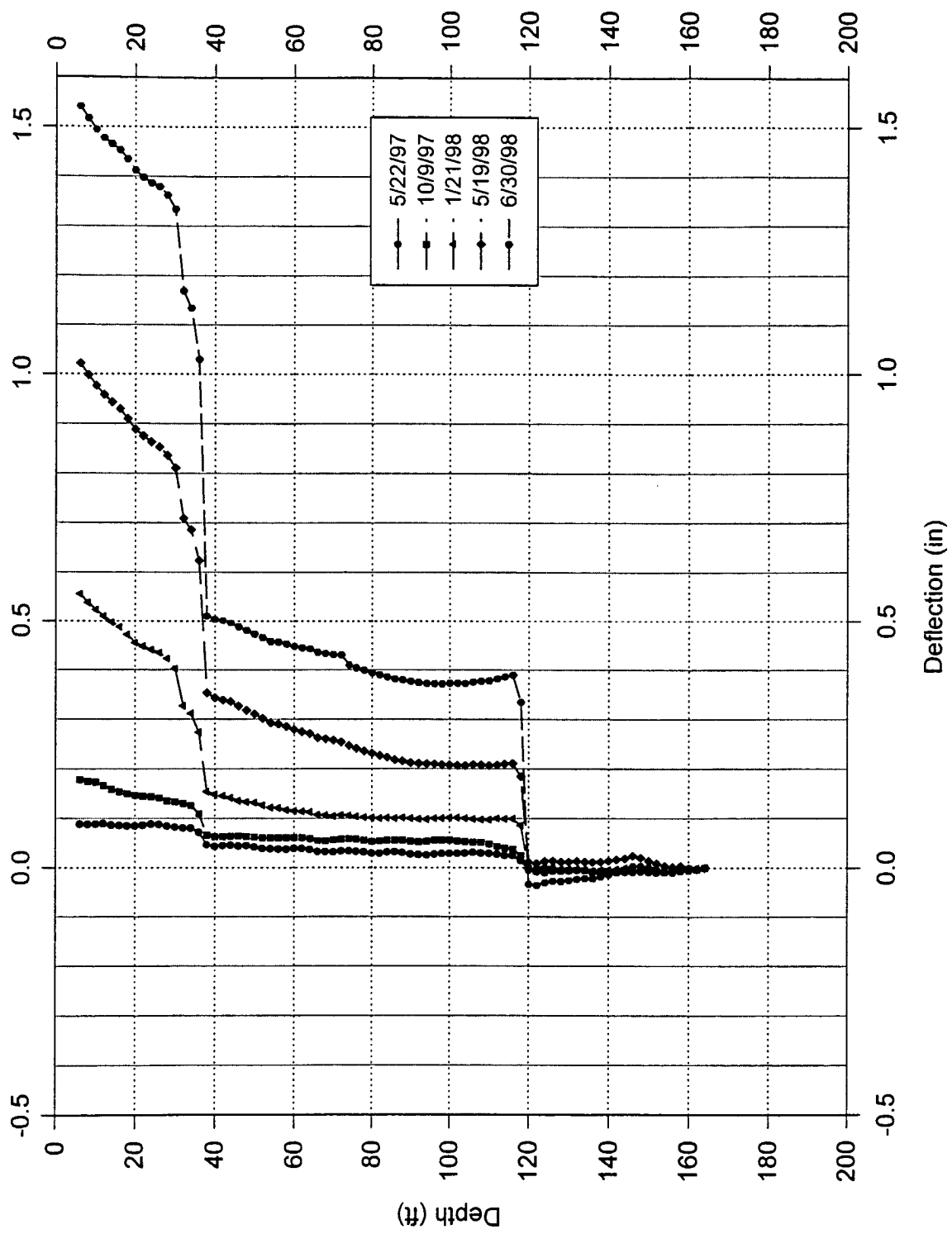


Fig. 4.39: Monitoring of deflection since 5/15/96 for B-104 Inclinator at CUY-90 Project - A-Dir  
Last reading 6/30/98.

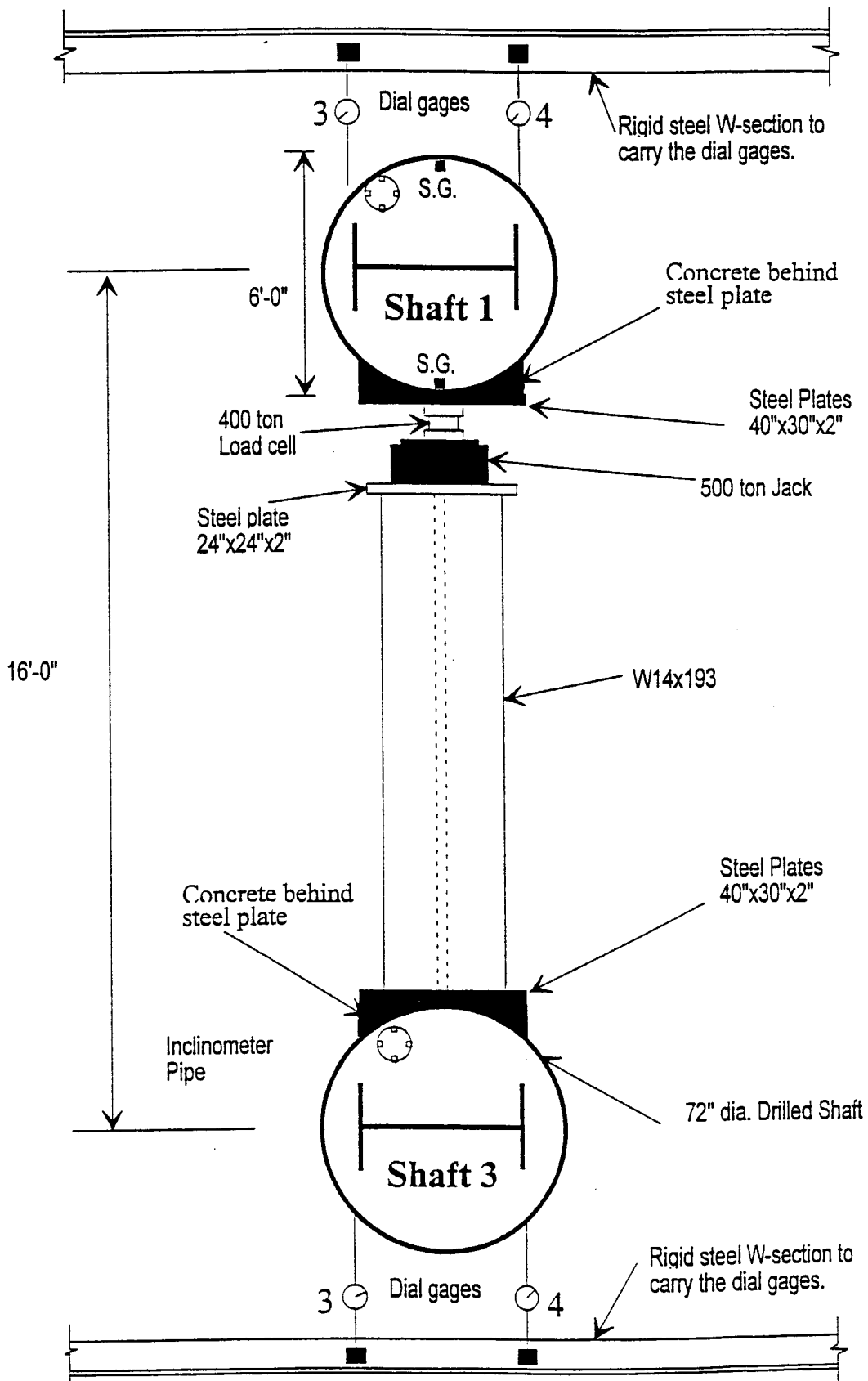


Fig. 4.42: Schematic diagram of the lateral load test – top view.

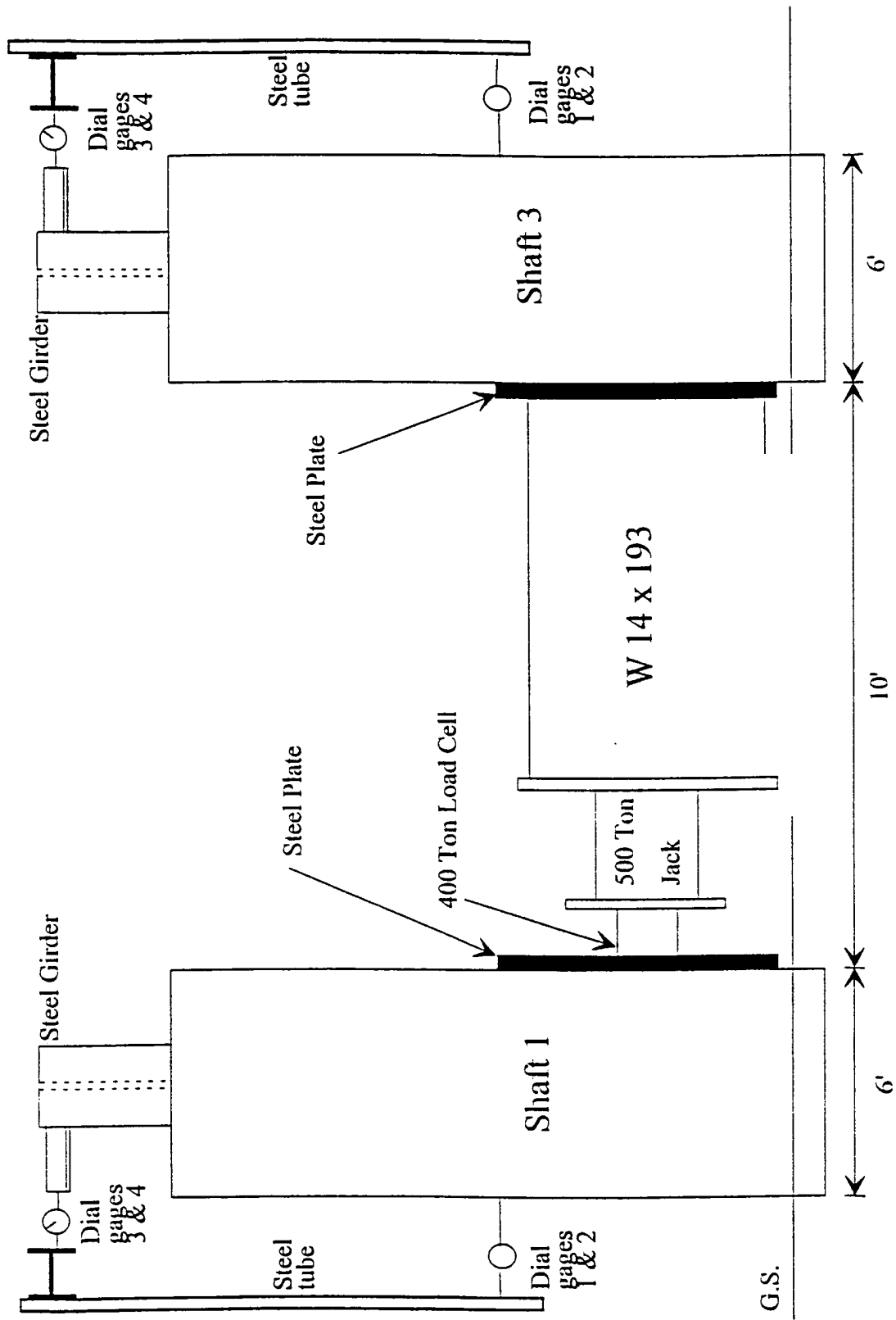


Fig. 4.43: Schematic diagram of the lateral load test – side view.

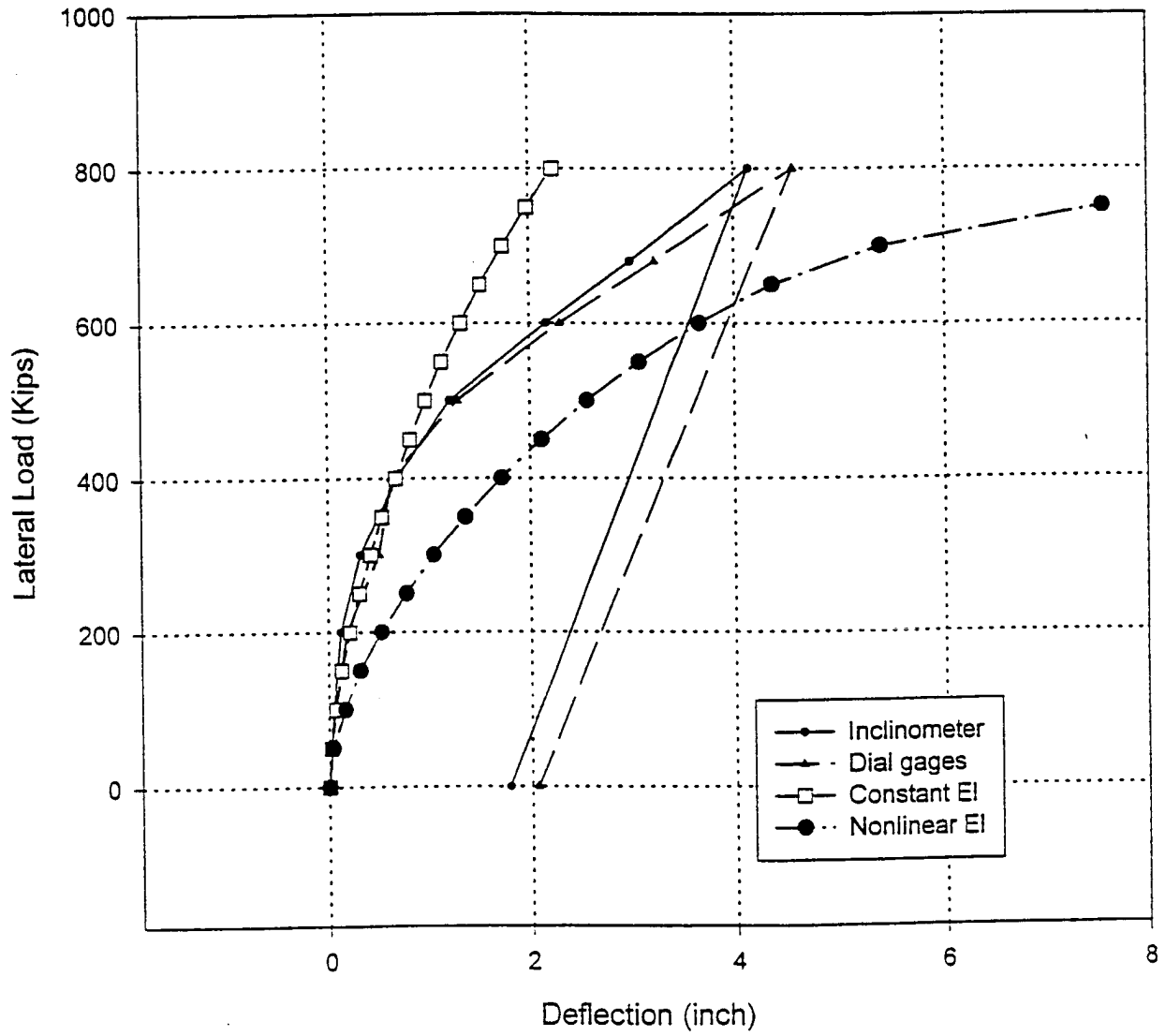


Fig. 4.44: Lateral load test, shaft # 1, measured and calculated deflection at shaft top.



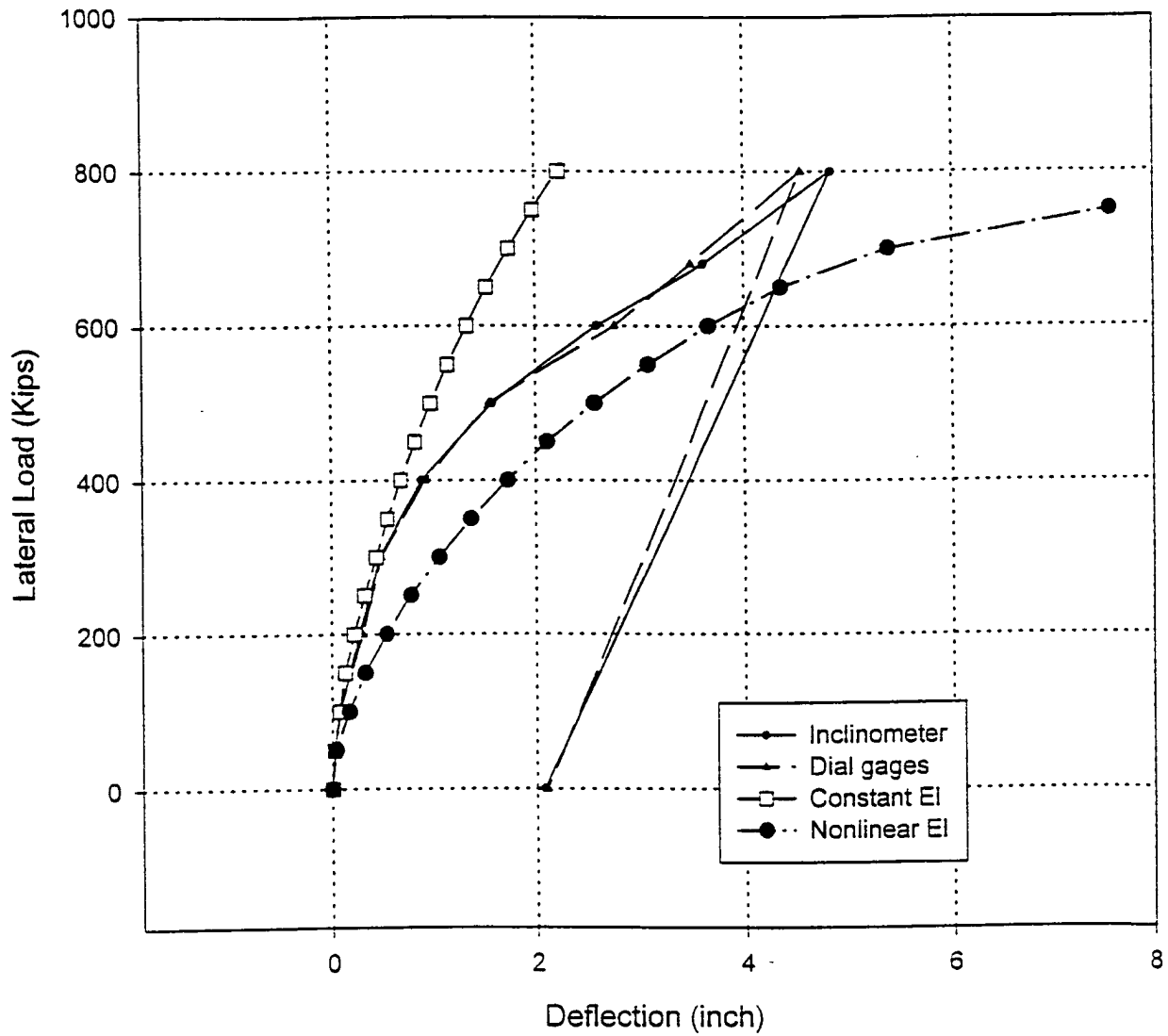


Fig. 4.45: Lateral load test, shaft # 3, measured and calculated deflection at shaft top.

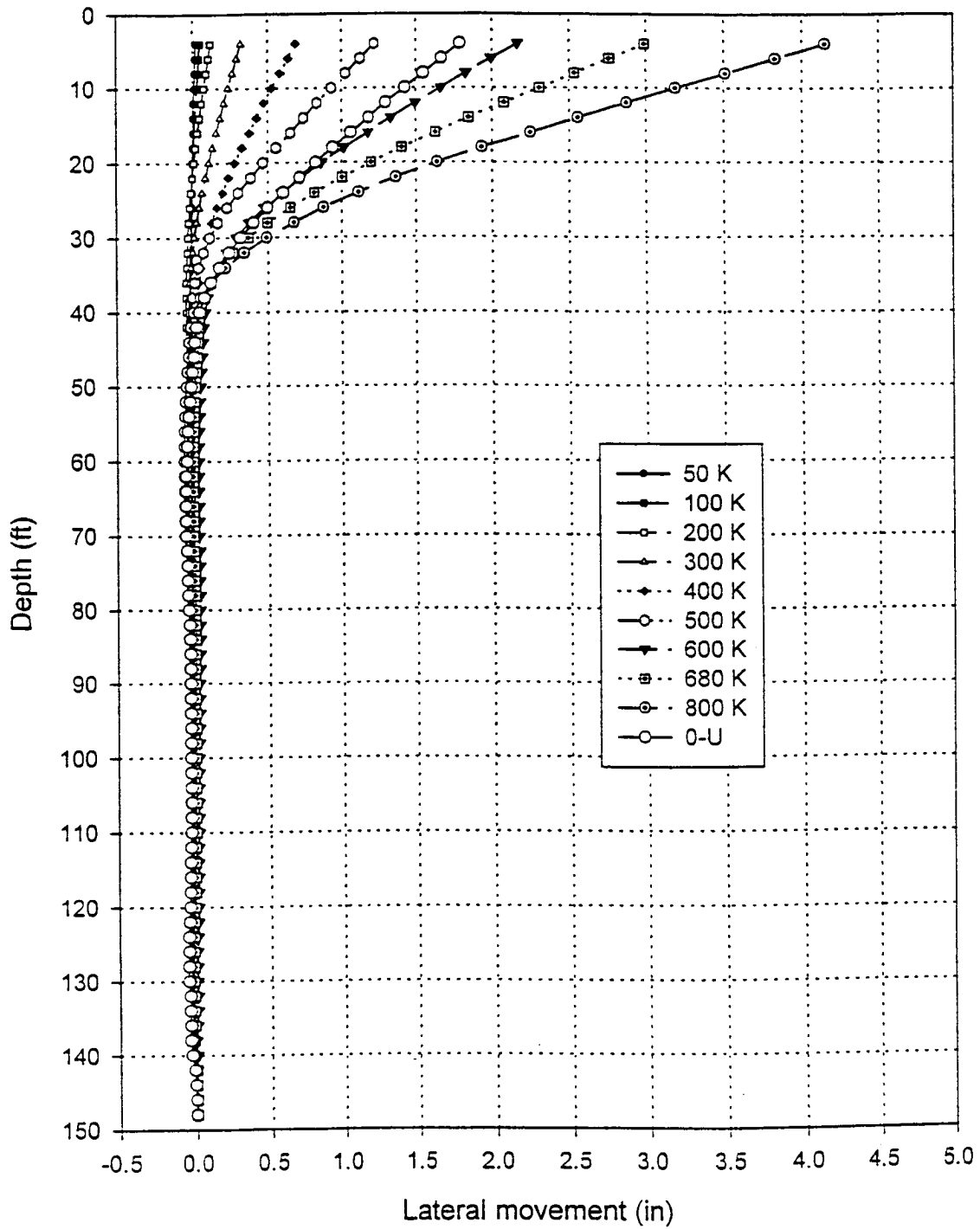


Fig. 4.46: Lateral load test, Shaft # 1, measured deflection vs. depth using inclinometer.

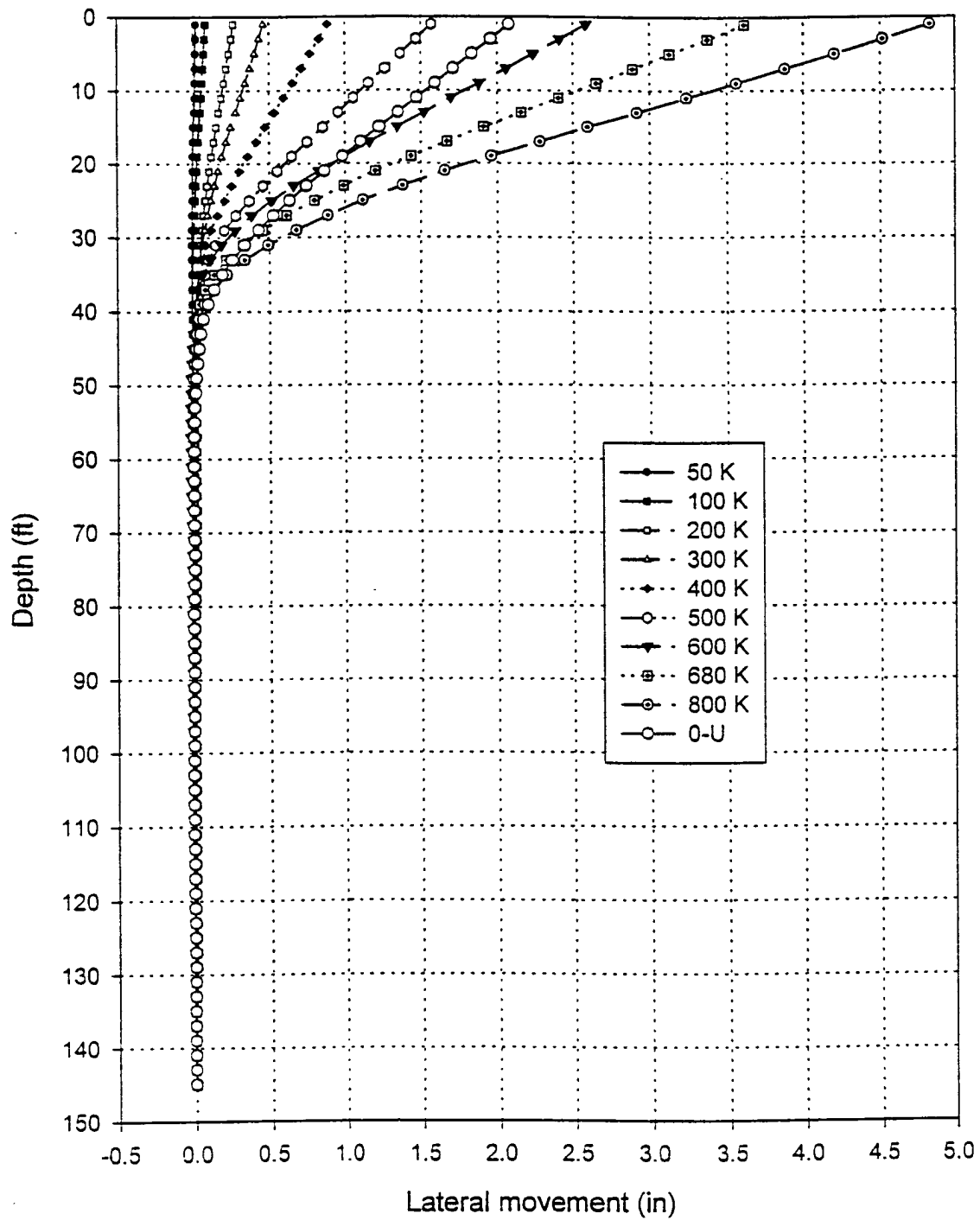


Fig. 4.47: Lateral load test, Shaft # 3, measured deflection vs. depth using inclinometer.

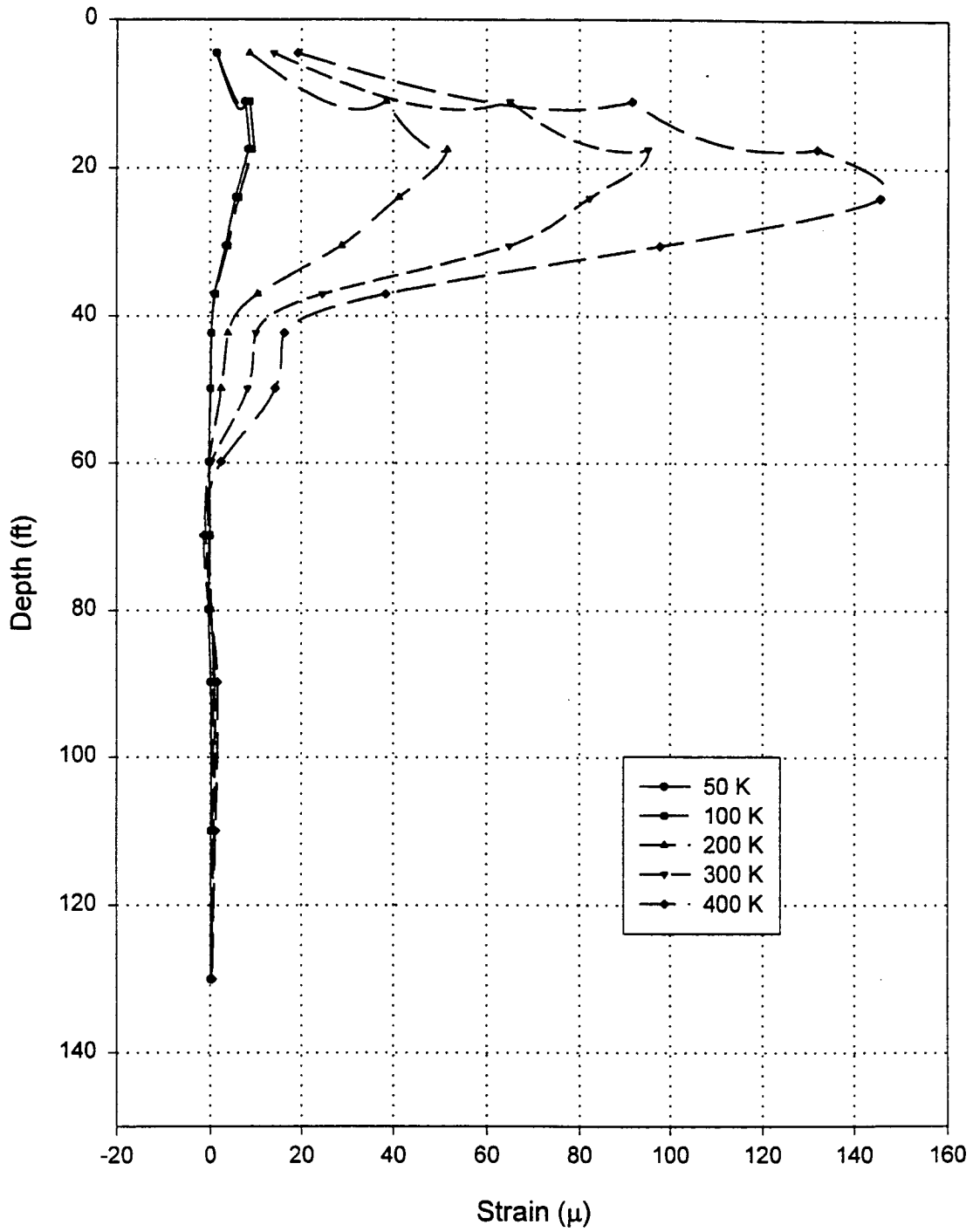


Fig. 4.48(a): Lateral load test, Shaft # 1, reduced strain vs. depth on tension side (loading from 0 to 400 Kips).

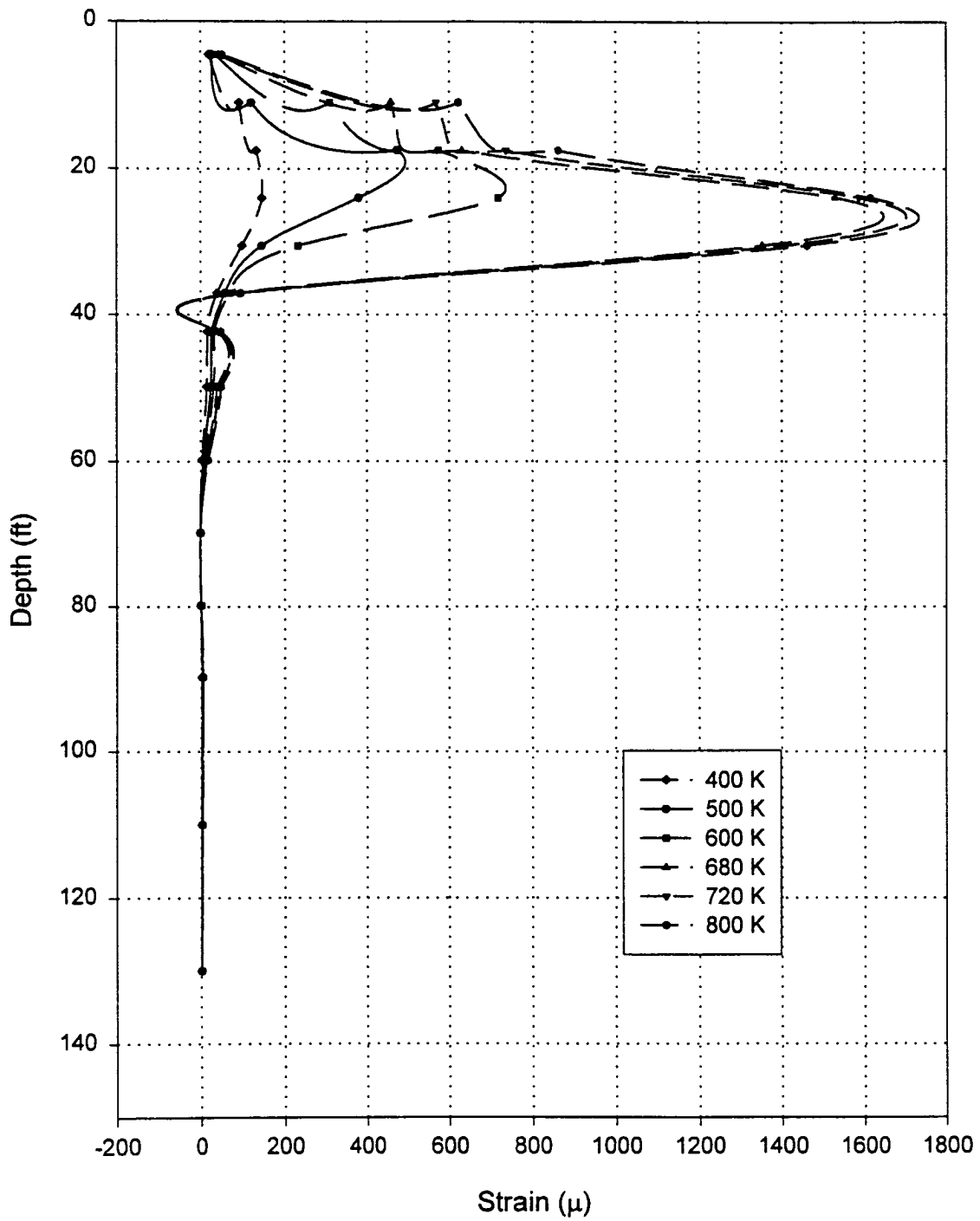


Fig. 4.48(b): Lateral load test, Shaft # 1, reduced strain vs. depth on tension side (loading from 400 to 800 Kips).

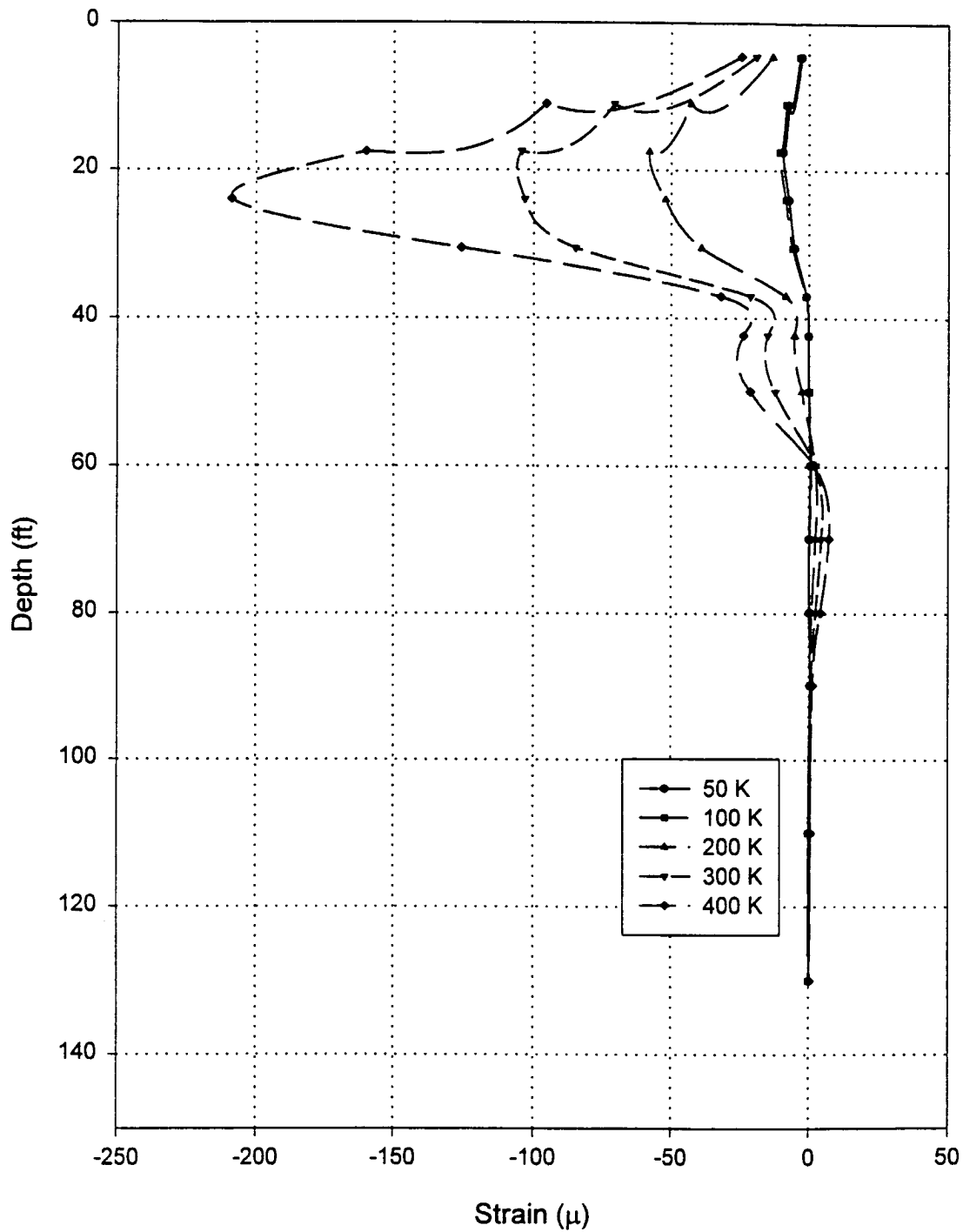


Fig. 4.49(a): Lateral load test, Shaft # 1, reduced strain vs. depth on compression side (loading from 0 to 400 Kips).

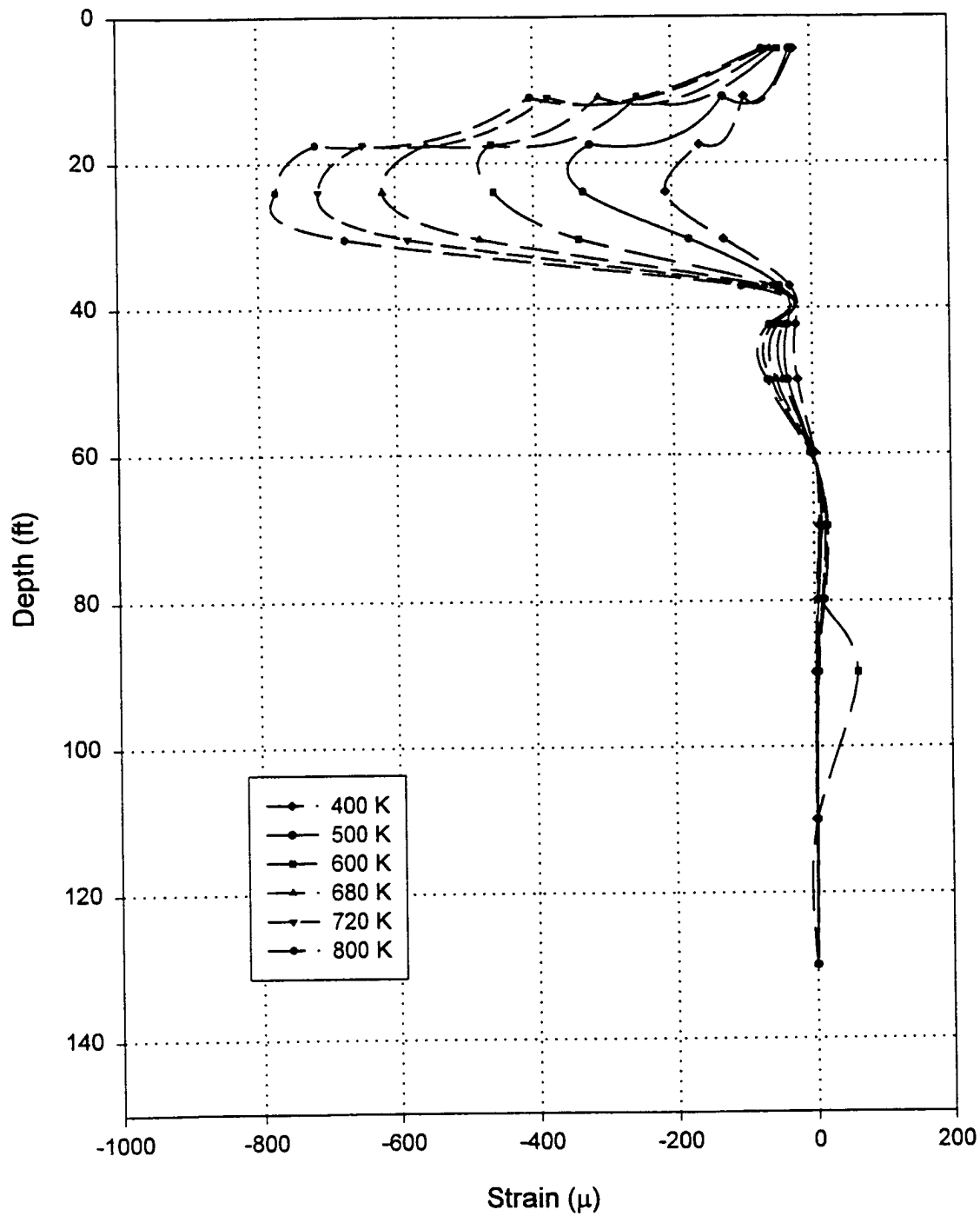


Fig. 4.49(b): Lateral load test, Shaft # 1, reduced strain vs. depth on compression side (loading from 400 to 800 Kips).

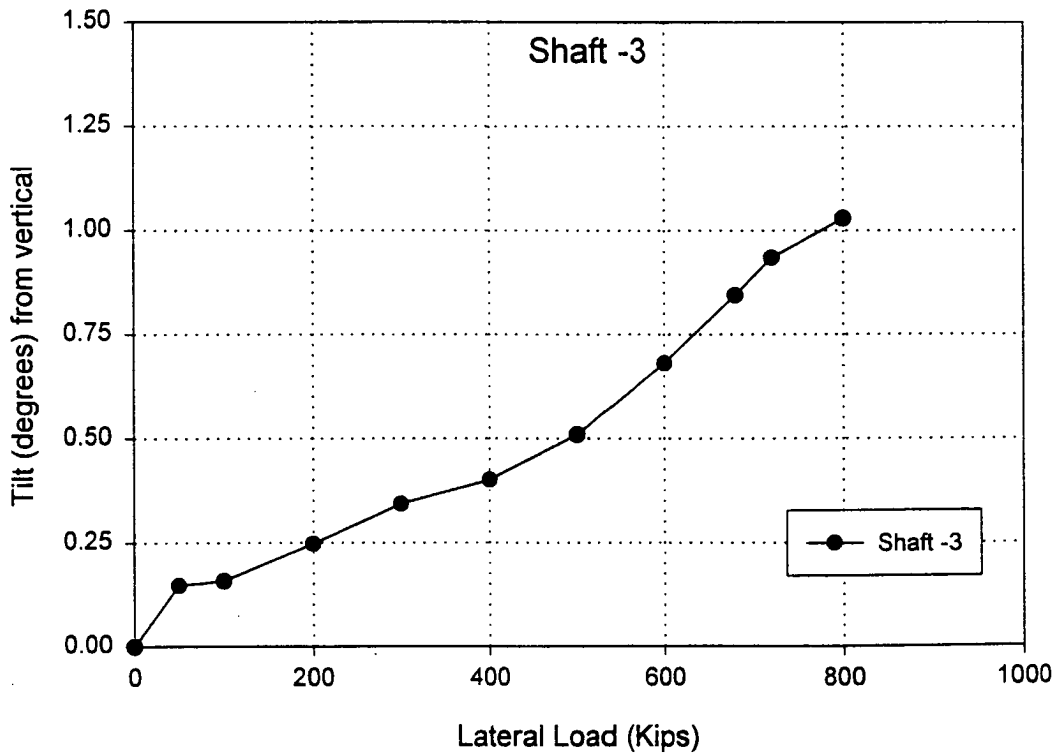
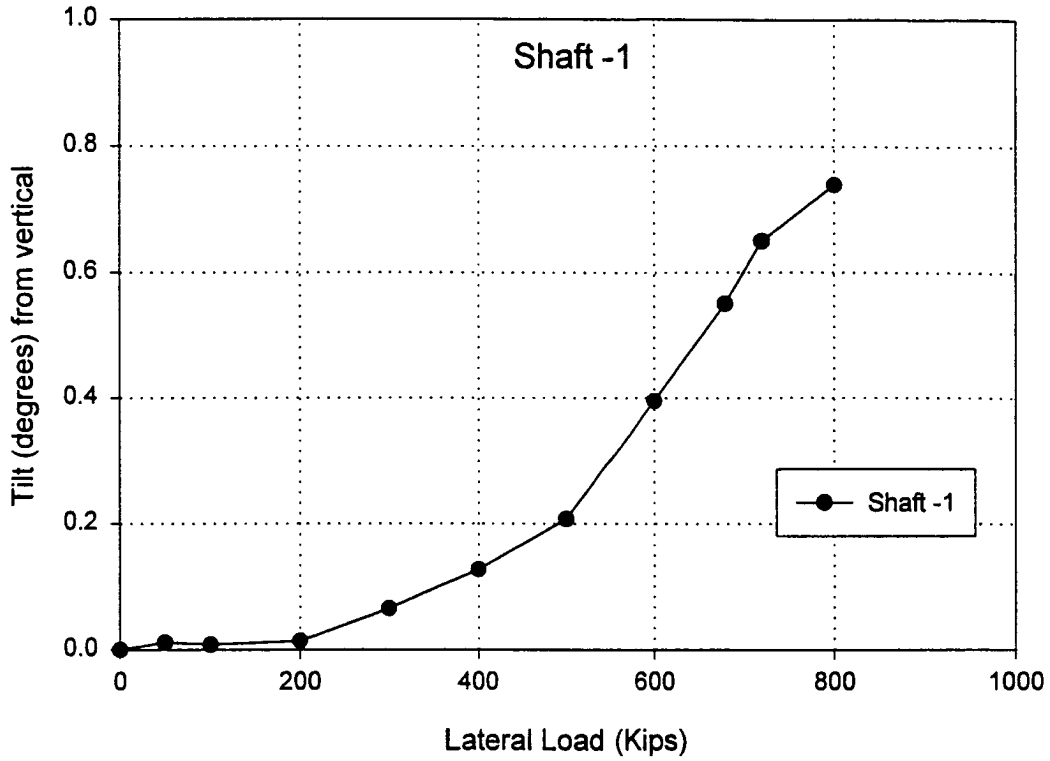


Fig. 4.50: Lateral load test, tilt in degrees at the jacking point in shafts #1 and #3.



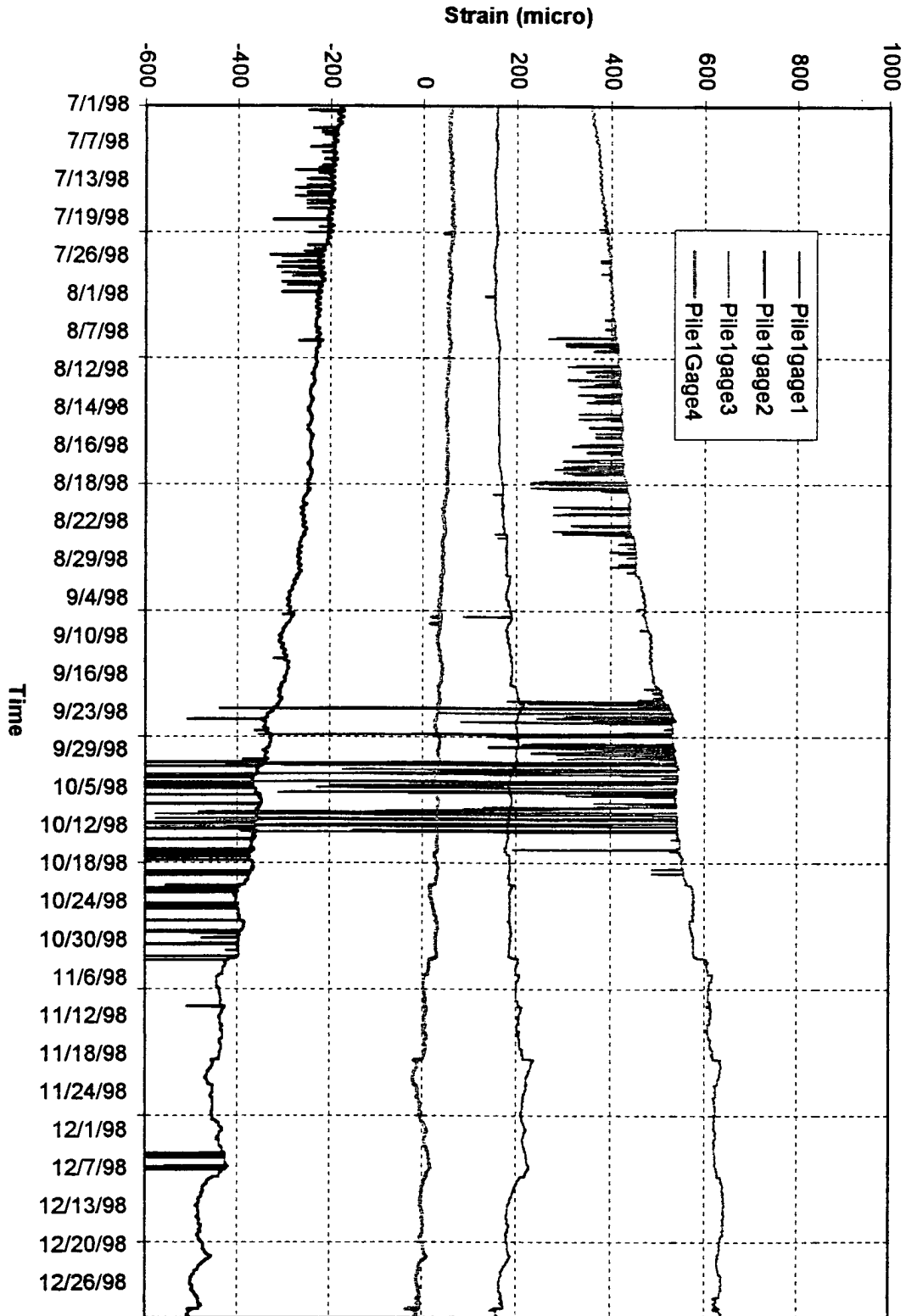


Fig. 4.51: Long-term monitoring of strain in Pile # 1 in the anchor cap structure (6/30/98 ~ 12/31/98)

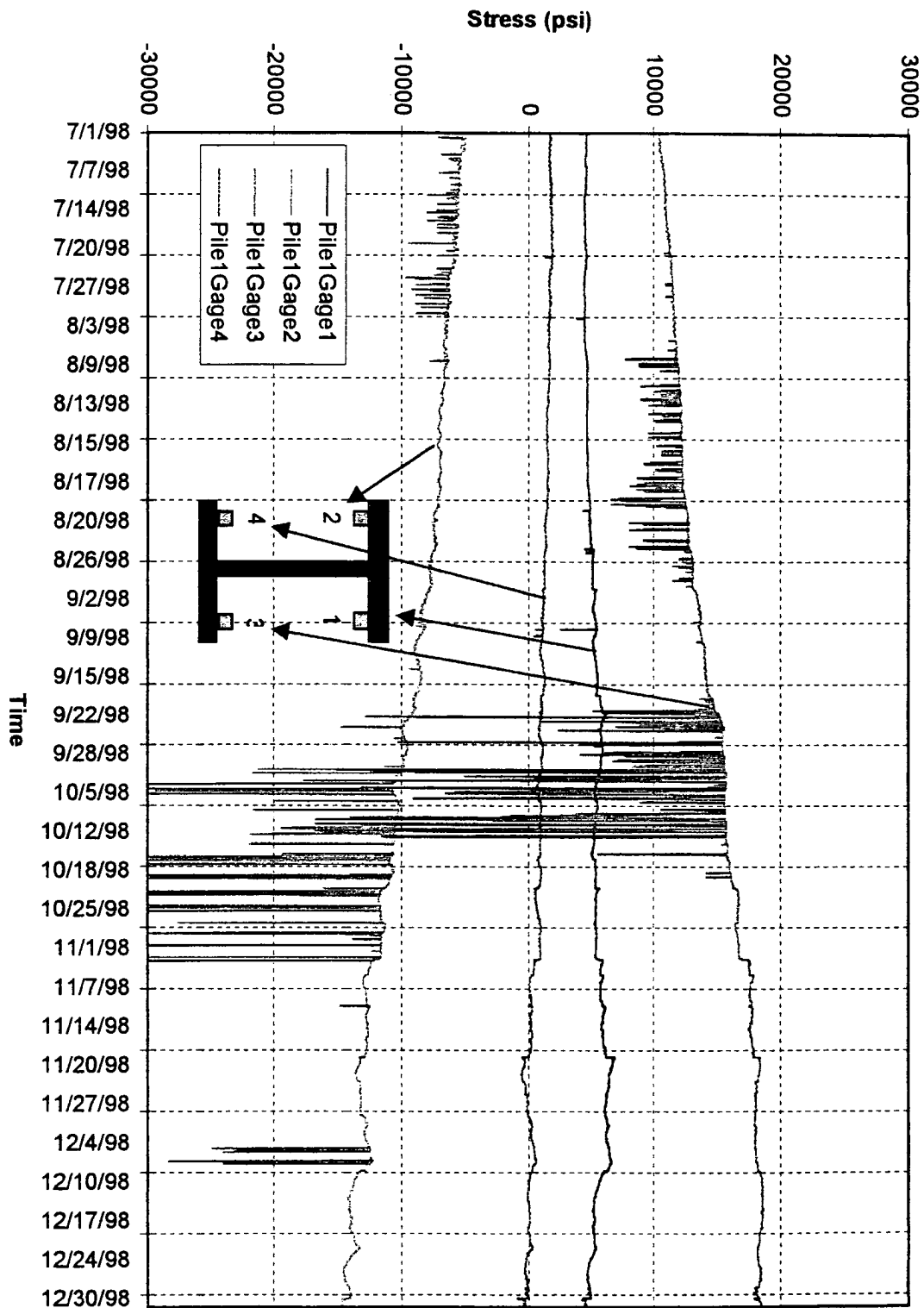


Fig. 4.52: Long-term monitoring of stress in Pile # 1 in the anchor cap structure (6/30/98 ~ 12/31/98)

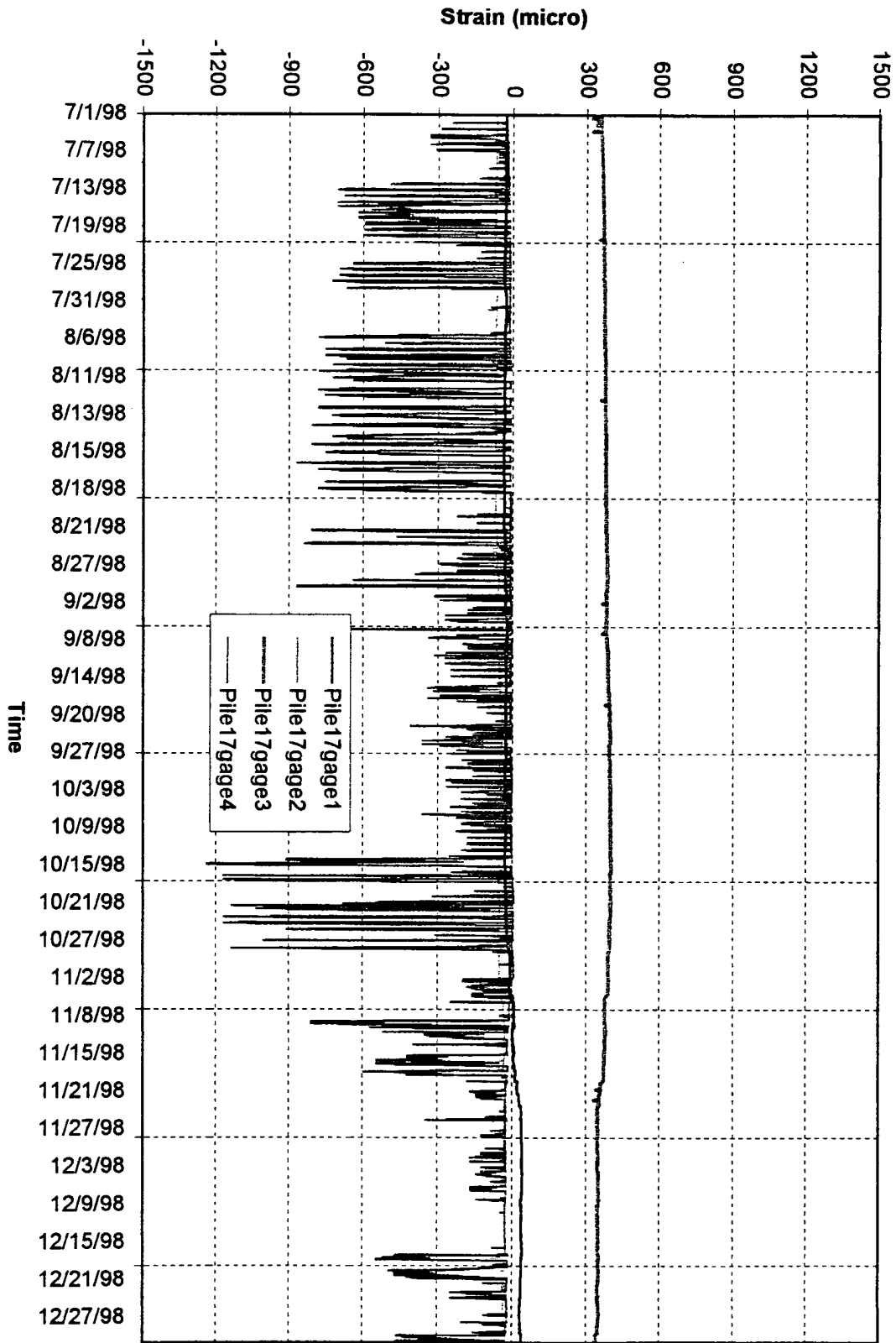


Fig. 4.53: Long-term monitoring of strain in Pile # 17 in the anchor cap structure (6/30/98 ~ 12/31/98)

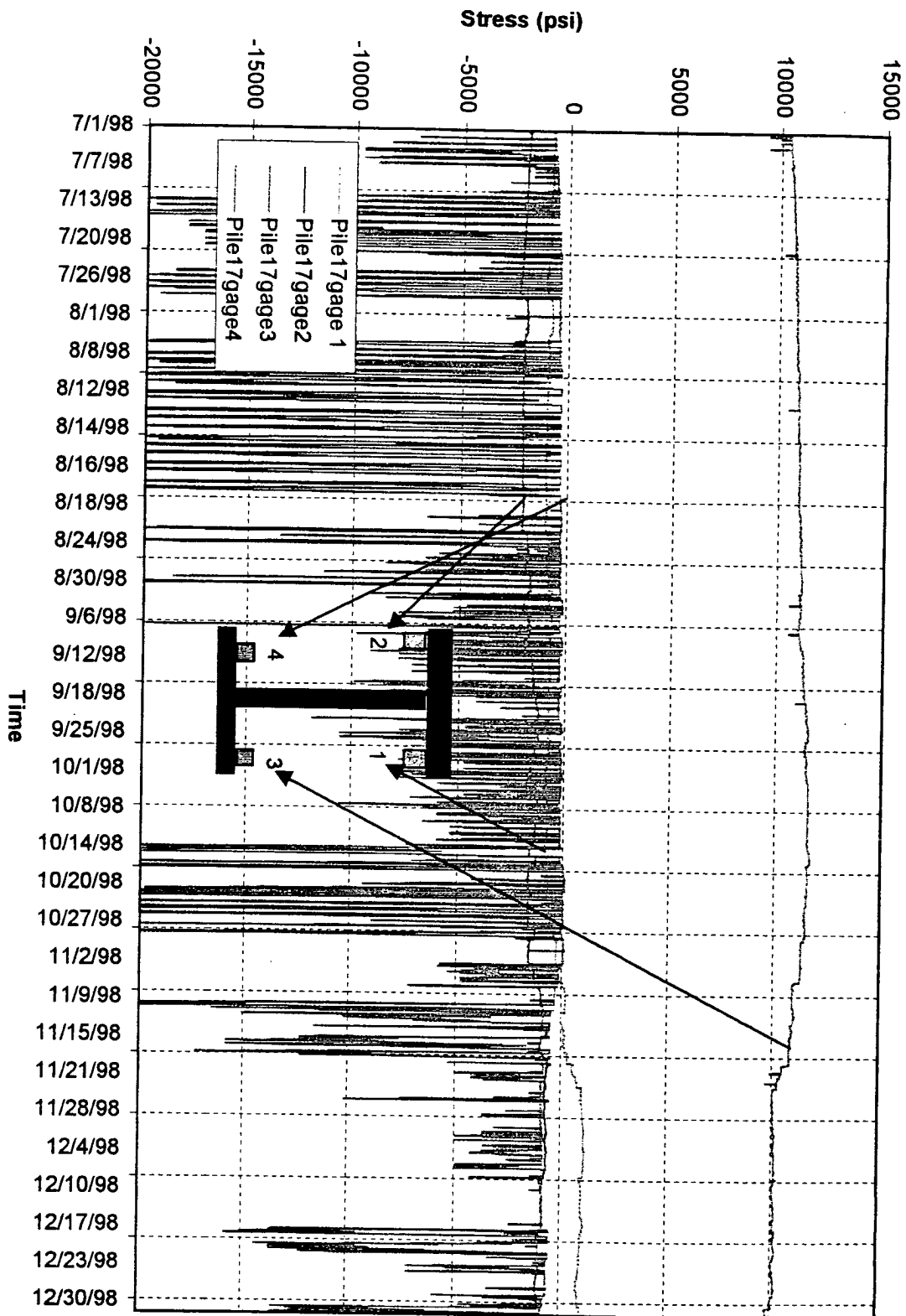


Fig. 4.54: Long-term monitoring of stress in Pile # 17 in the anchor cap structure (6/30/98 ~ 12/31/98)

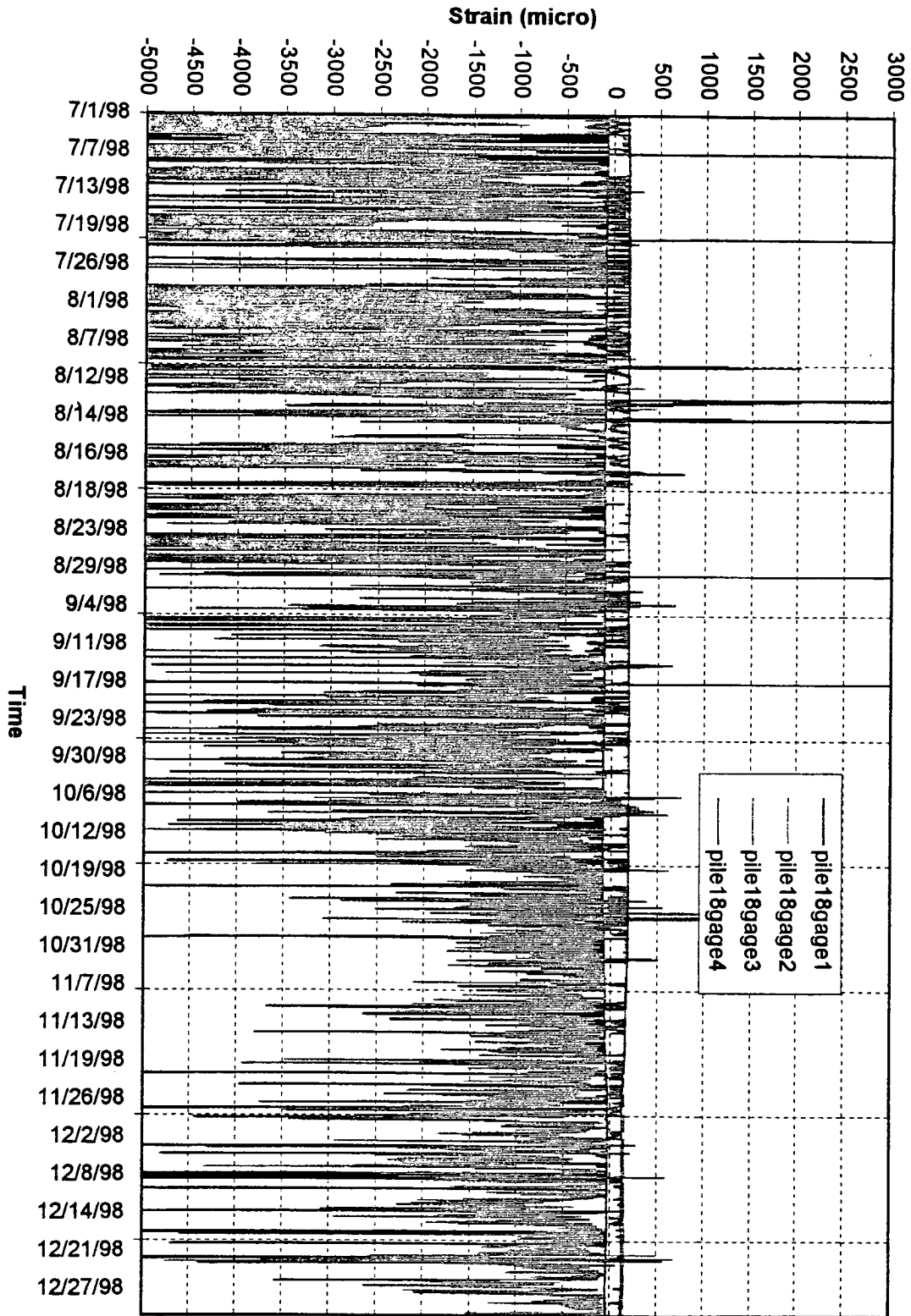


Fig. 4.55: Long-term monitoring of strain in Pile # 18 in the anchor cap structure (6/30/98 ~ 12/31/98)

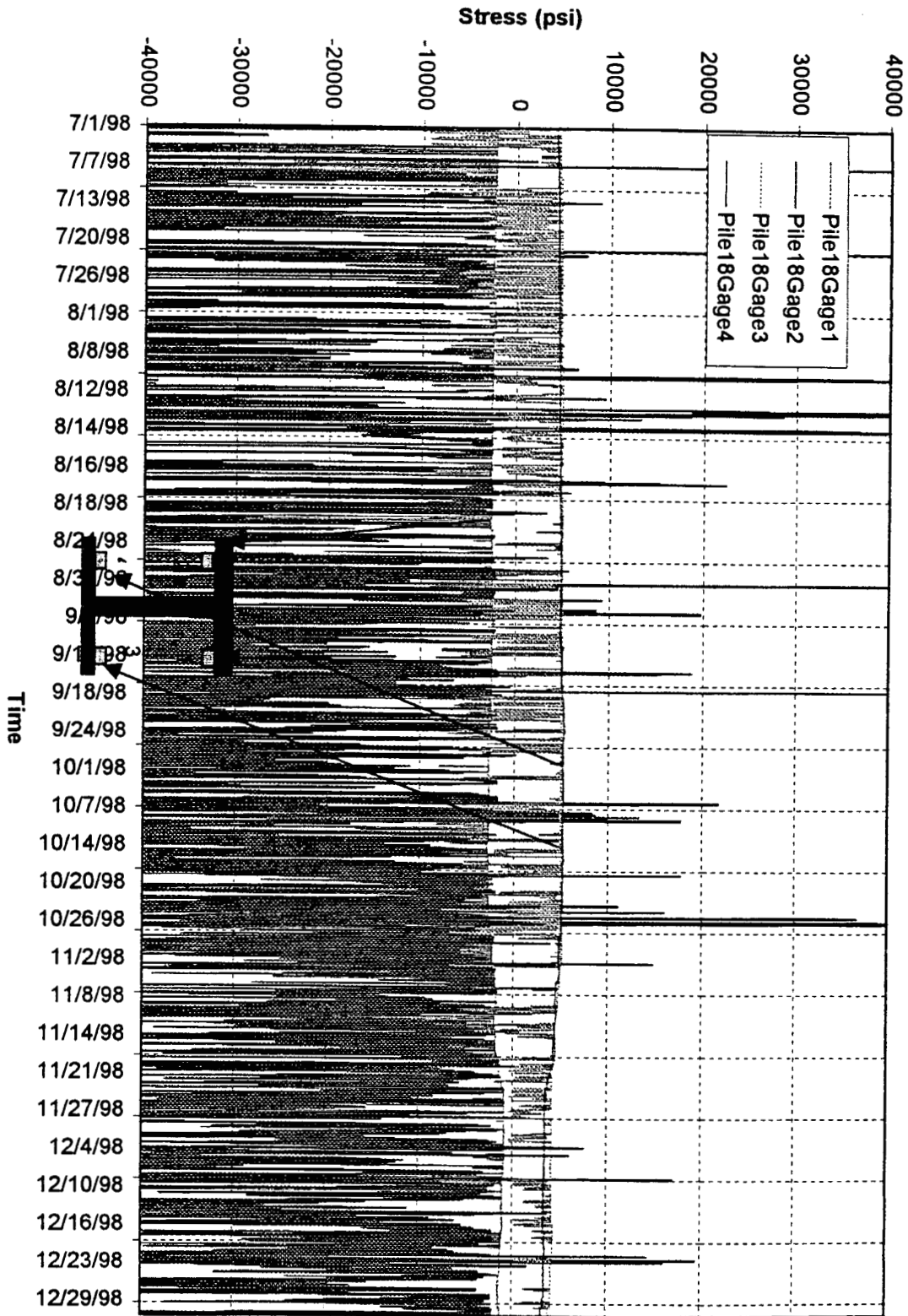


Fig. 4.56: Long-term monitoring of stress in Pile # 18 in the anchor cap structure (6/30/98 ~ 12/31/98)

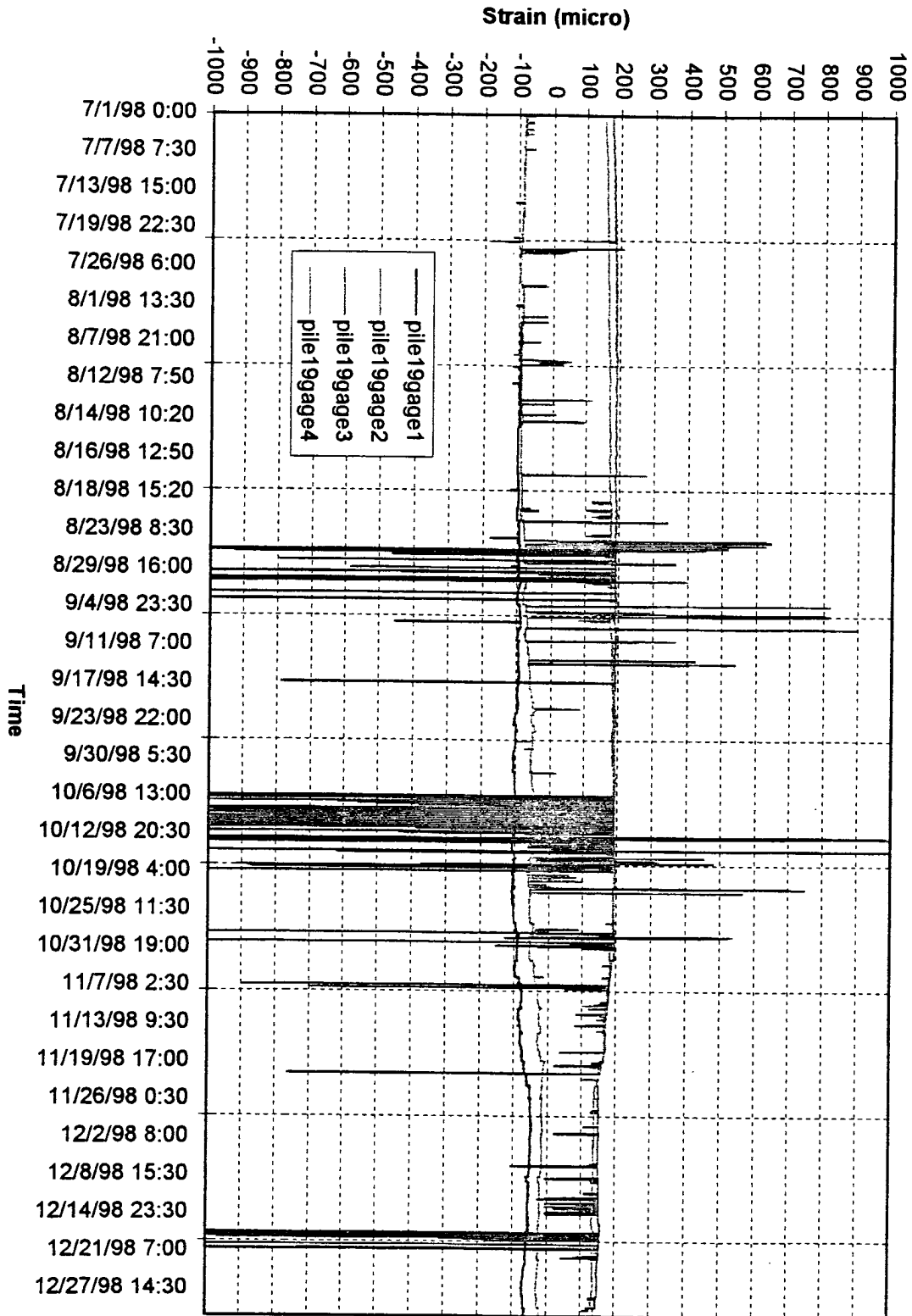


Fig. 4.57: Long-term monitoring of strain in Pile # 19 in the anchor cap structure (6/30/98 ~ 12/31/98)

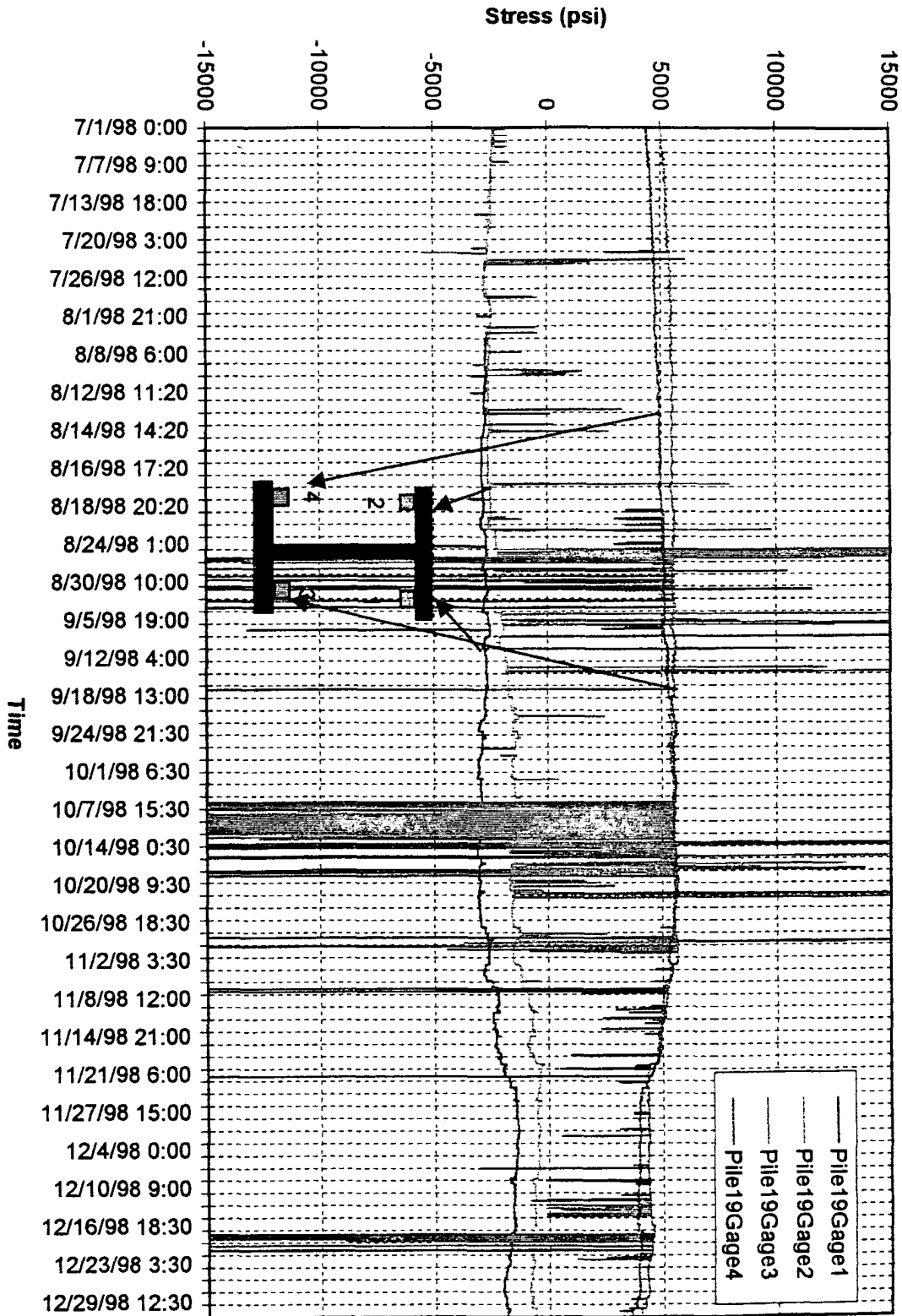


Fig. 4.58: Long-term monitoring of stress in Pile # 19 in the anchor cap structure (6/30/98 ~ 12/31/98)



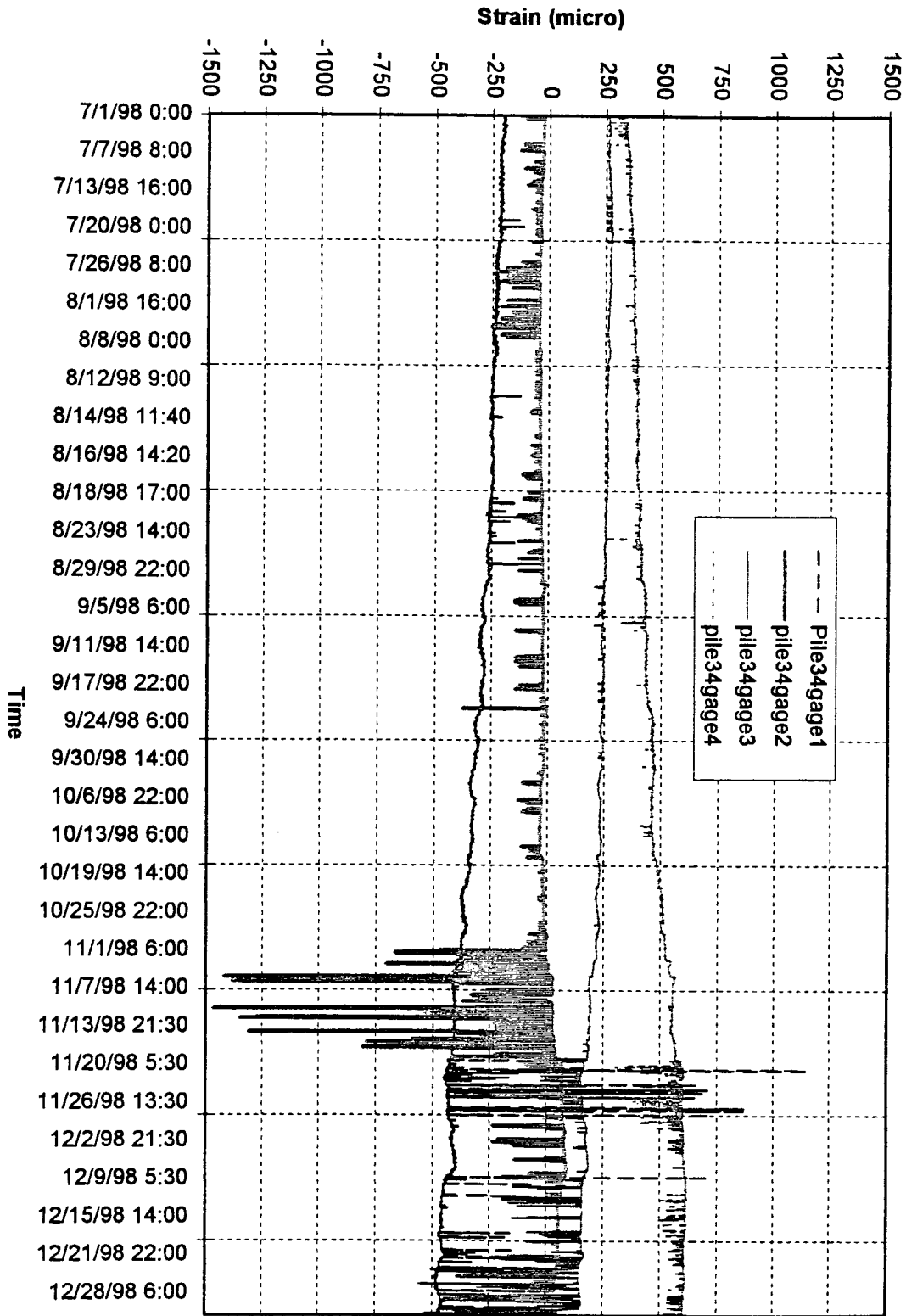


Fig. 4.59: Long-term monitoring of strain in Pile # 34 in the anchor cap structure (6/30/98 ~ 12/31/98)

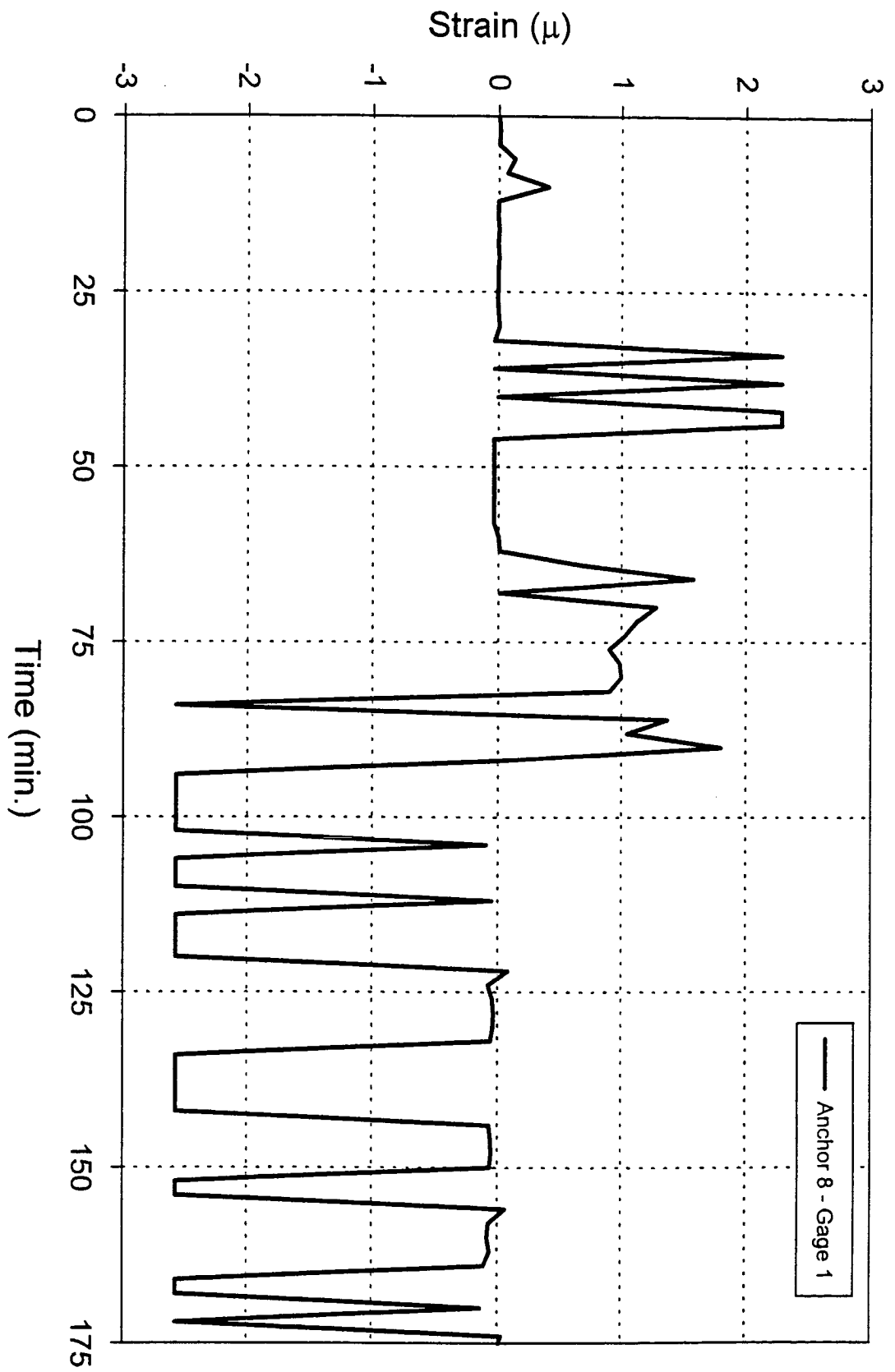


Fig. 4.72(a): Anchor # 8 performance test results, gage # 1.

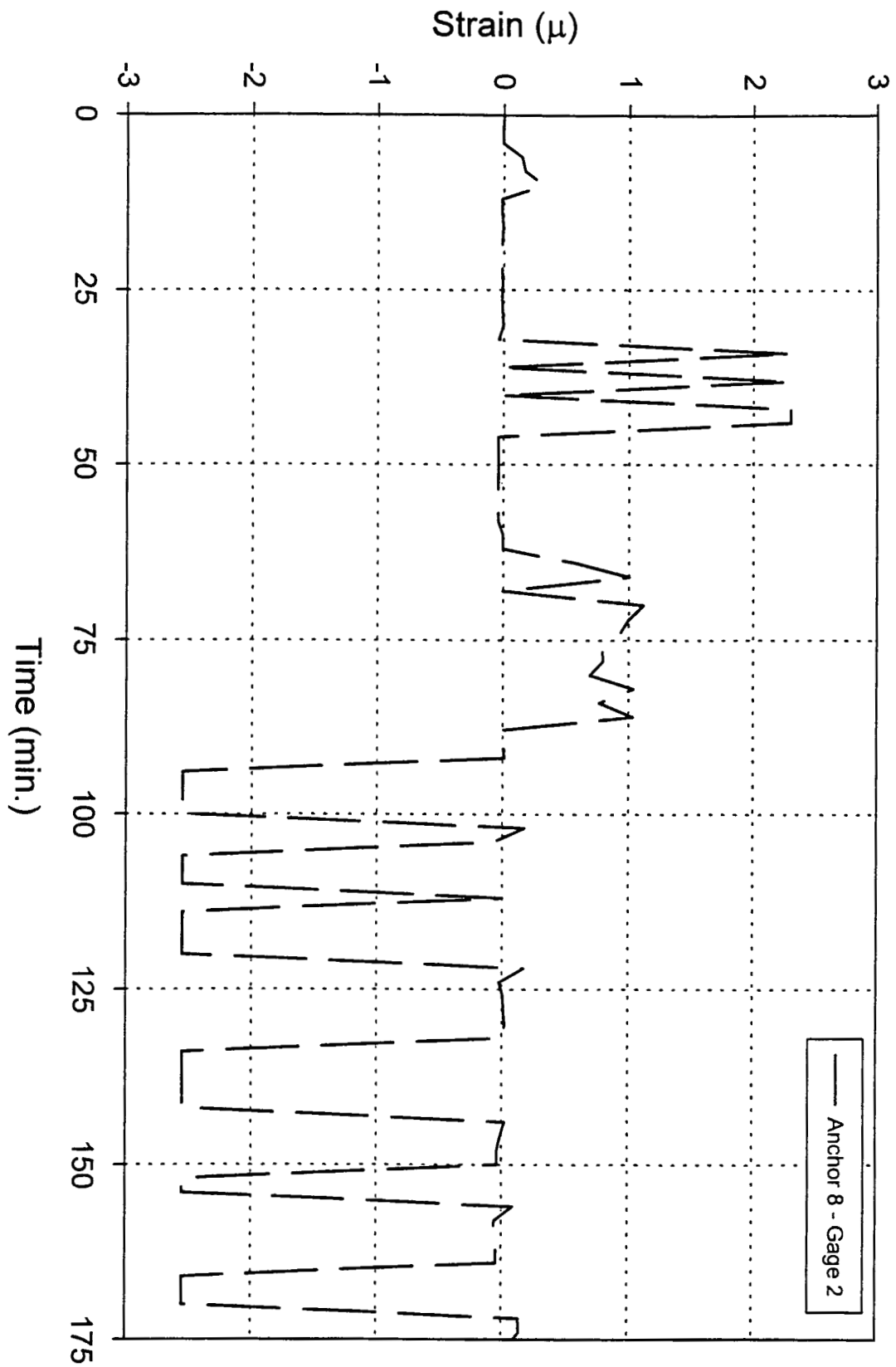


Fig. 4.72(b): Anchor # 8 performance test results, gage # 2.

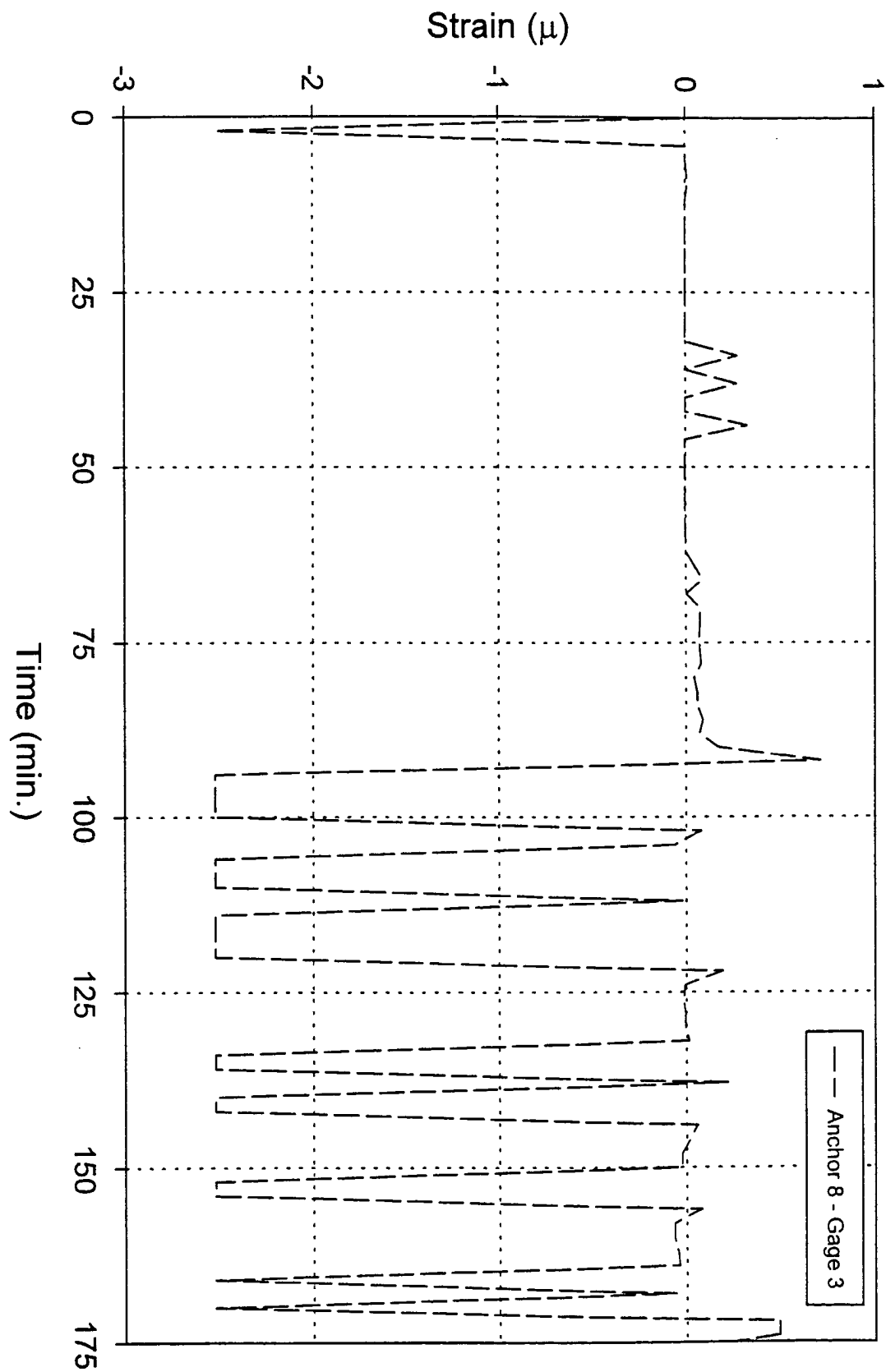


Fig. 4.72(c): Anchor # 8 performance test results, gage # 3.

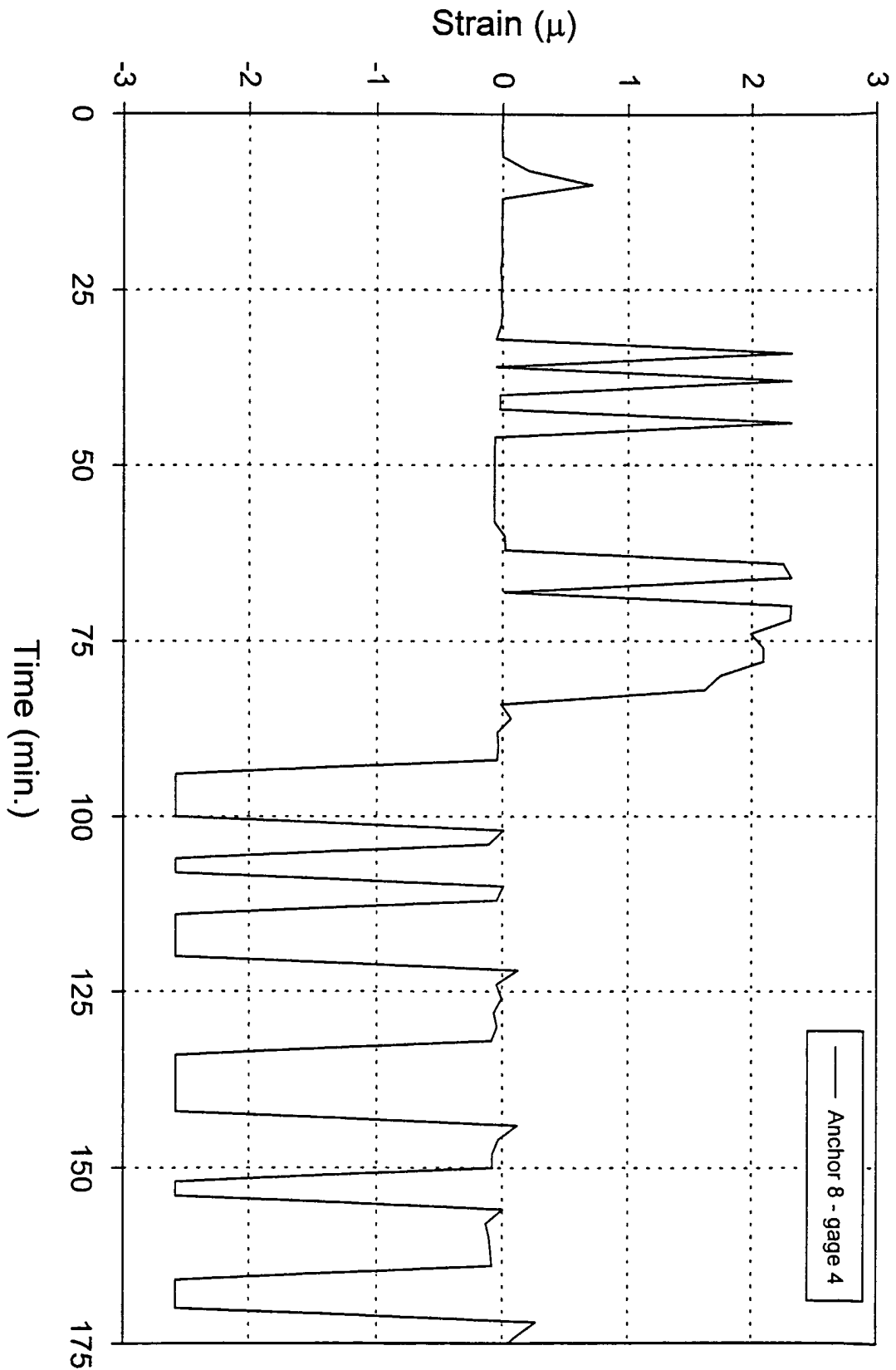


Fig. 4.72(d): Anchor # 8 performance test results, gage # 4.

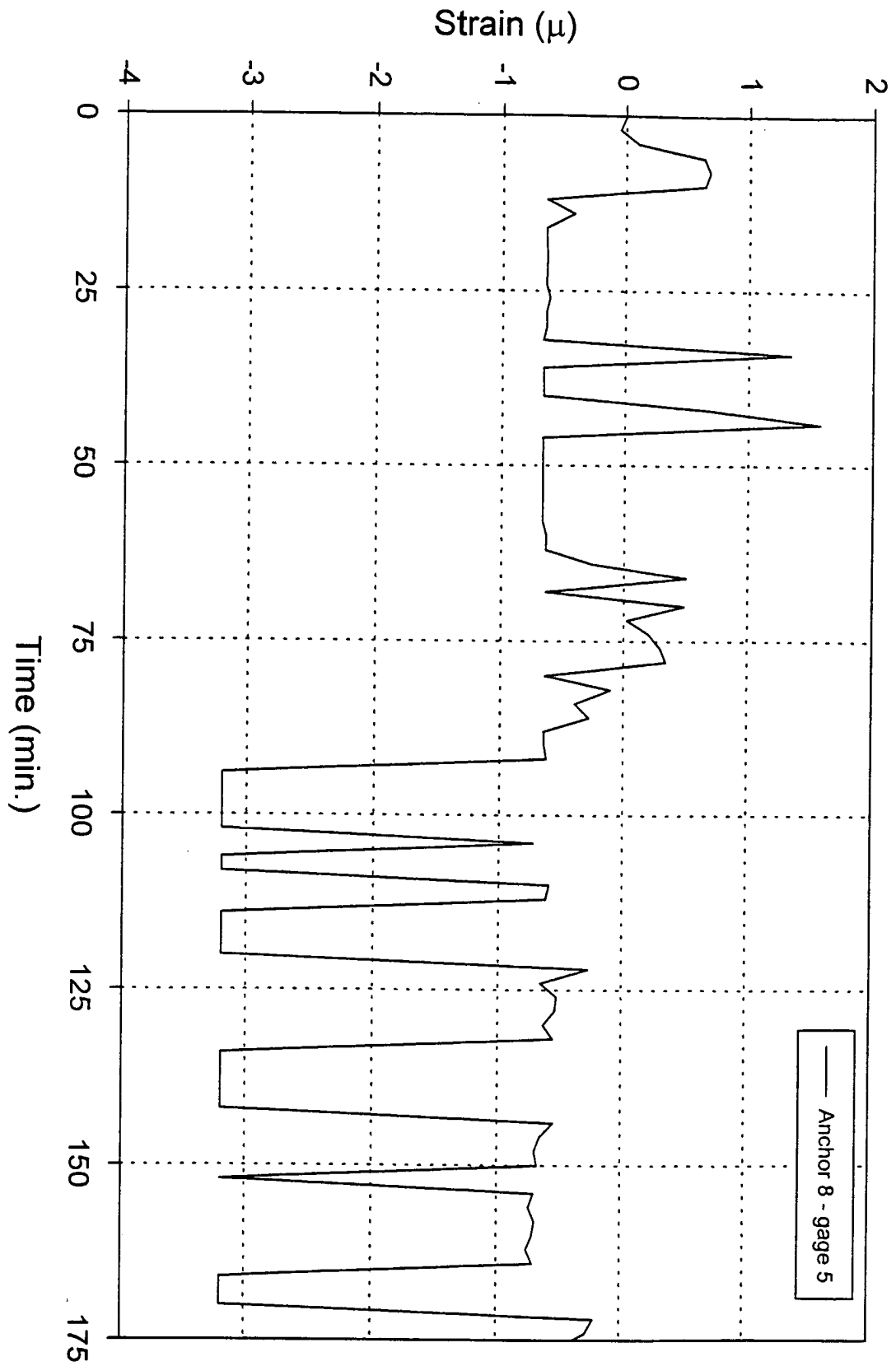


Fig. 4.72(e): Anchor # 8 performance test results, gage # 5.

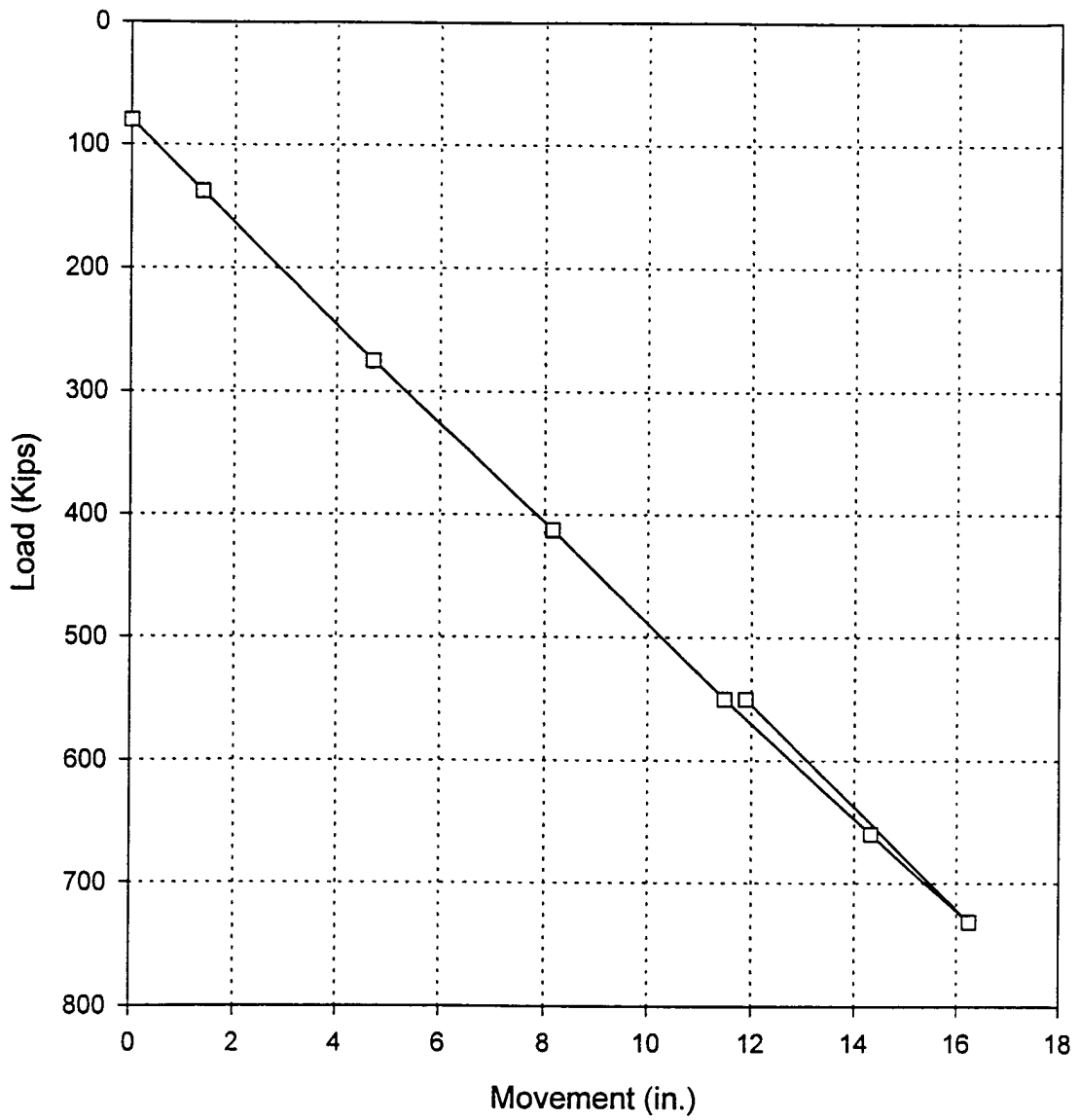


Fig. 4.73: Anchor #17 performance test, Load vs. movement at the anchor head

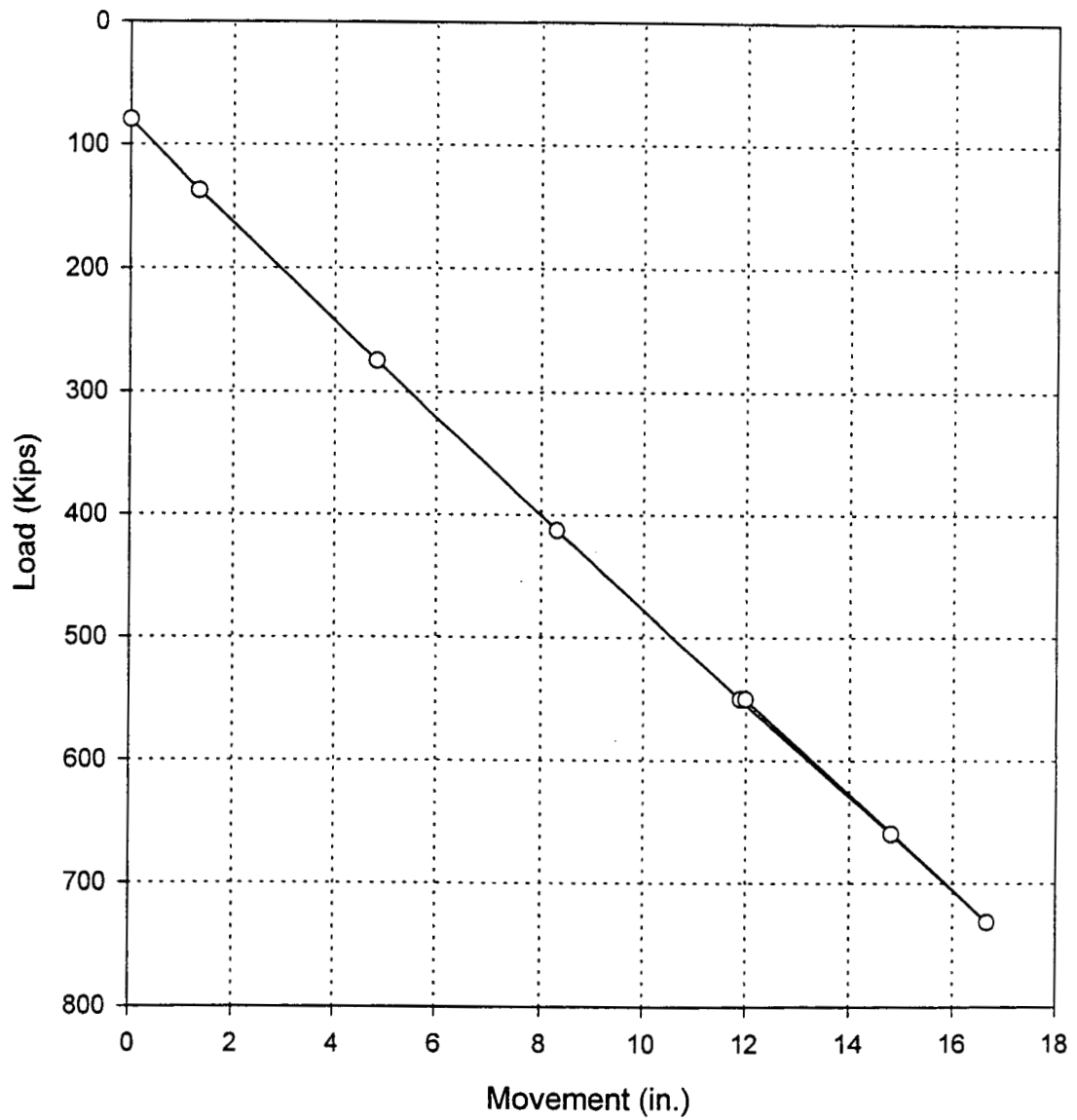


Fig. 4.74: Anchor #1 performance test, Load vs. movement at the anchor head



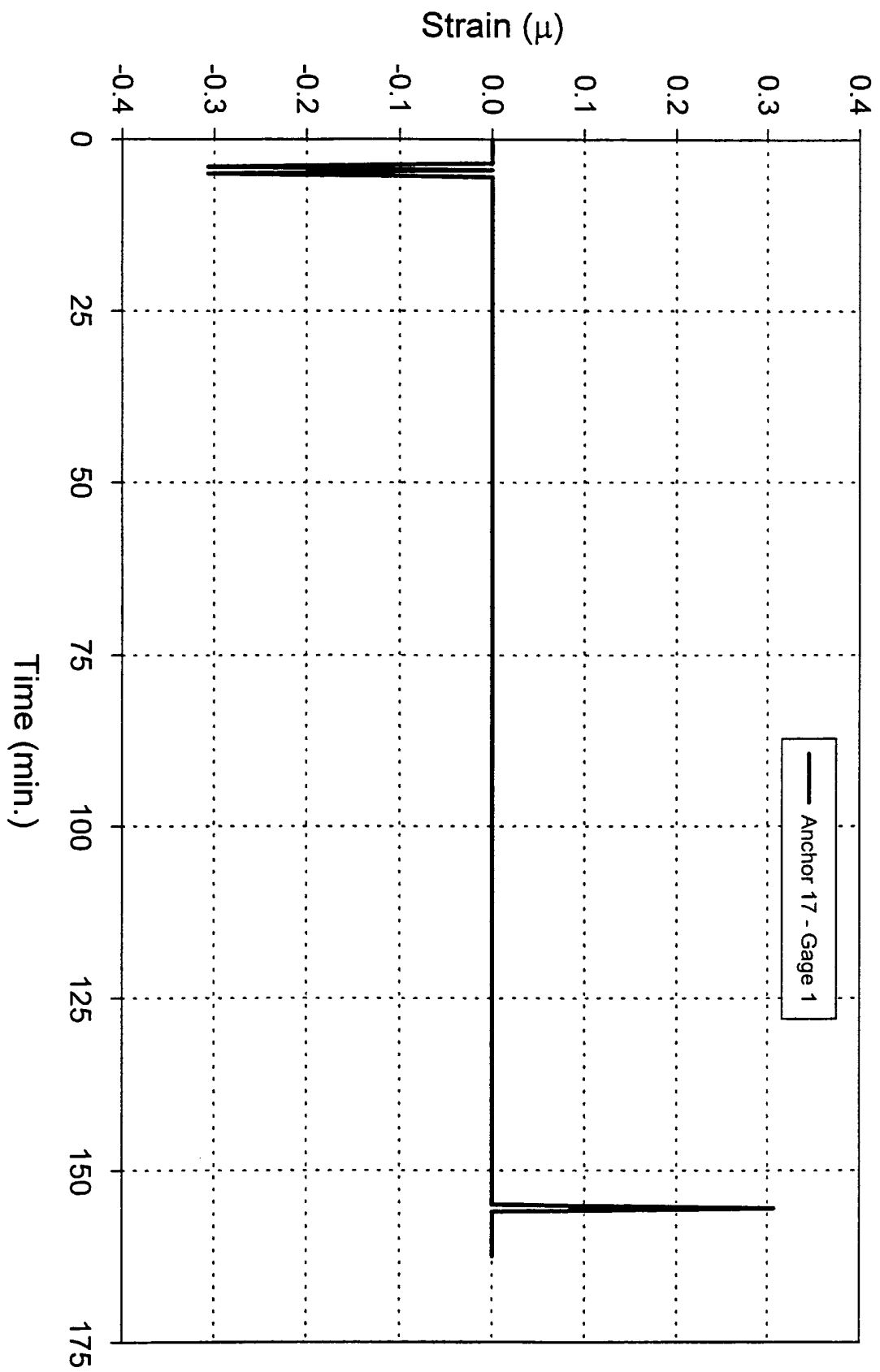


Fig. 4.75(a): Anchor # 17 performance test results, gage # 1.

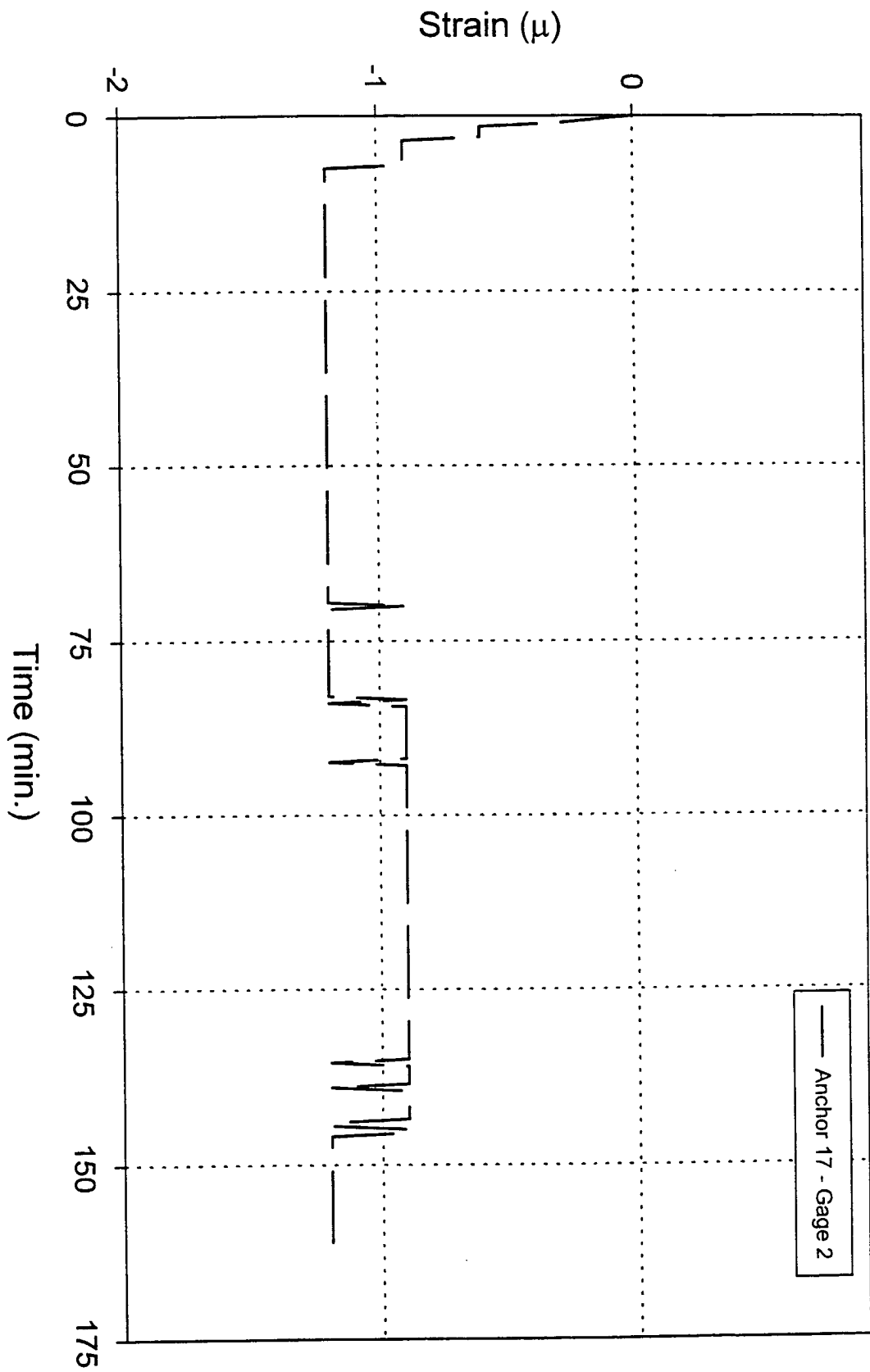


Fig. 4.75(b): Anchor # 17 performance test results, gage # 2.

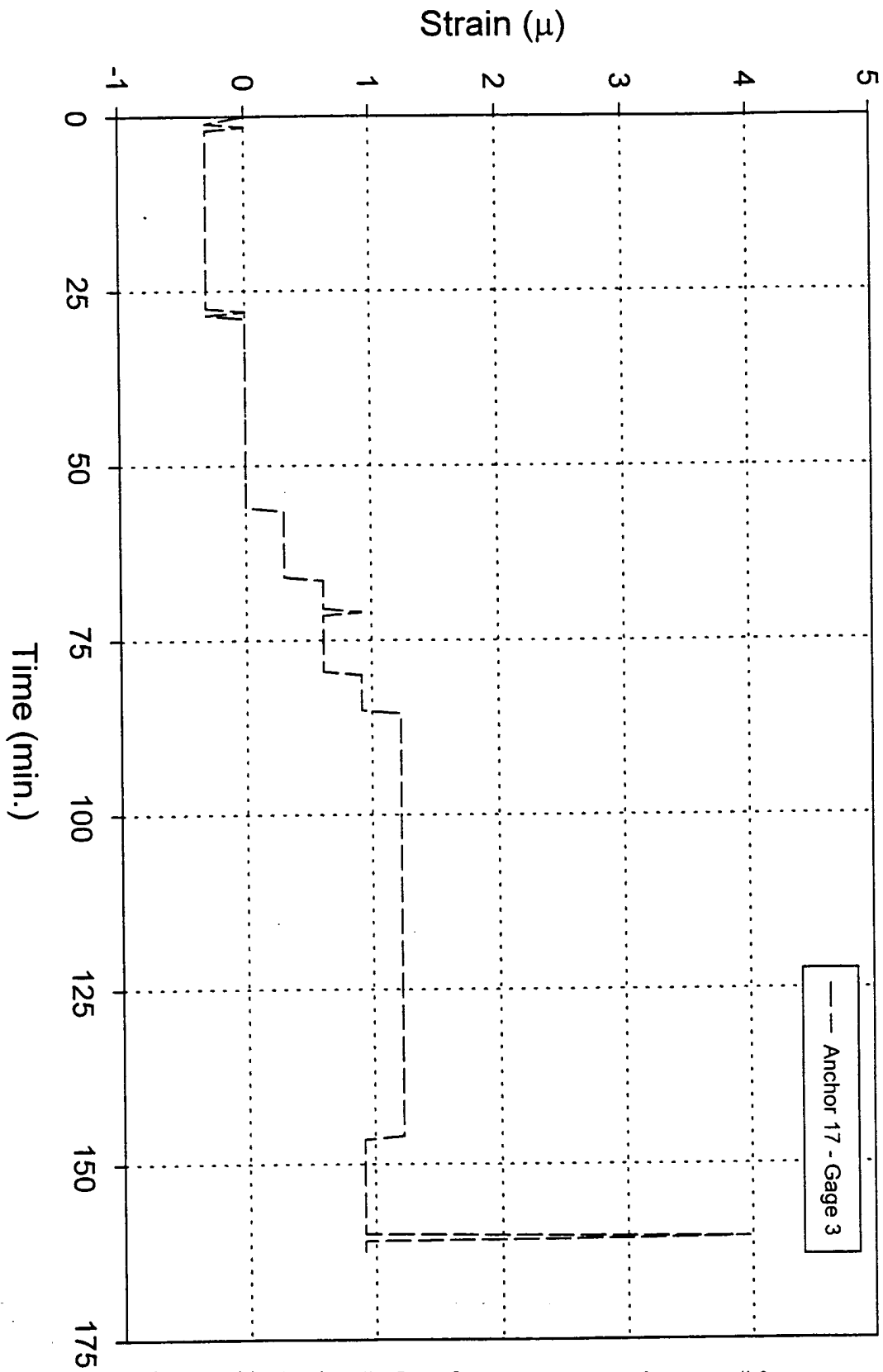


Fig. 4.75(c): Anchor # 17 performance test results, gage # 3.

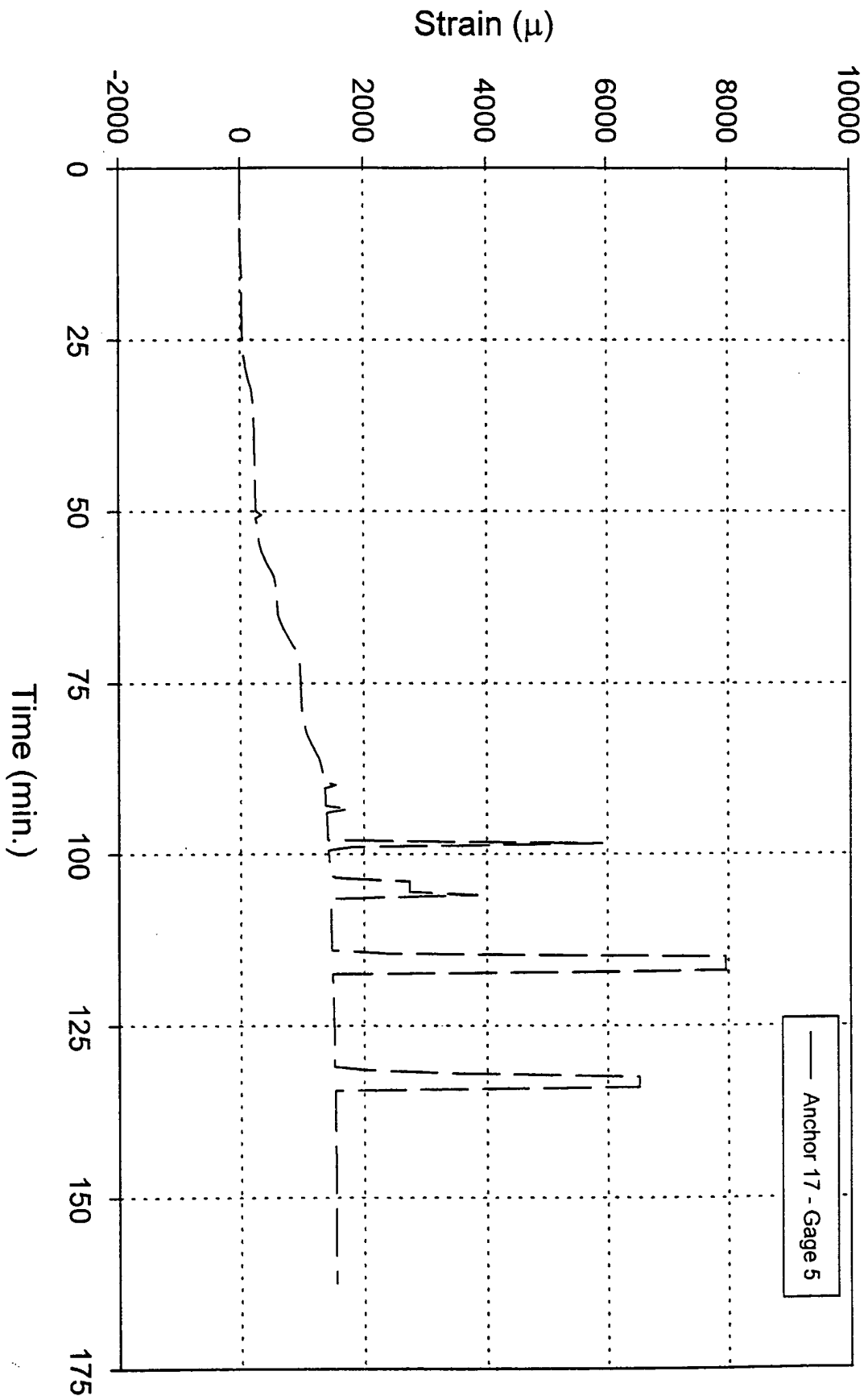


Fig. 4.75(d): Anchor # 17 performance test results, gage # 5.

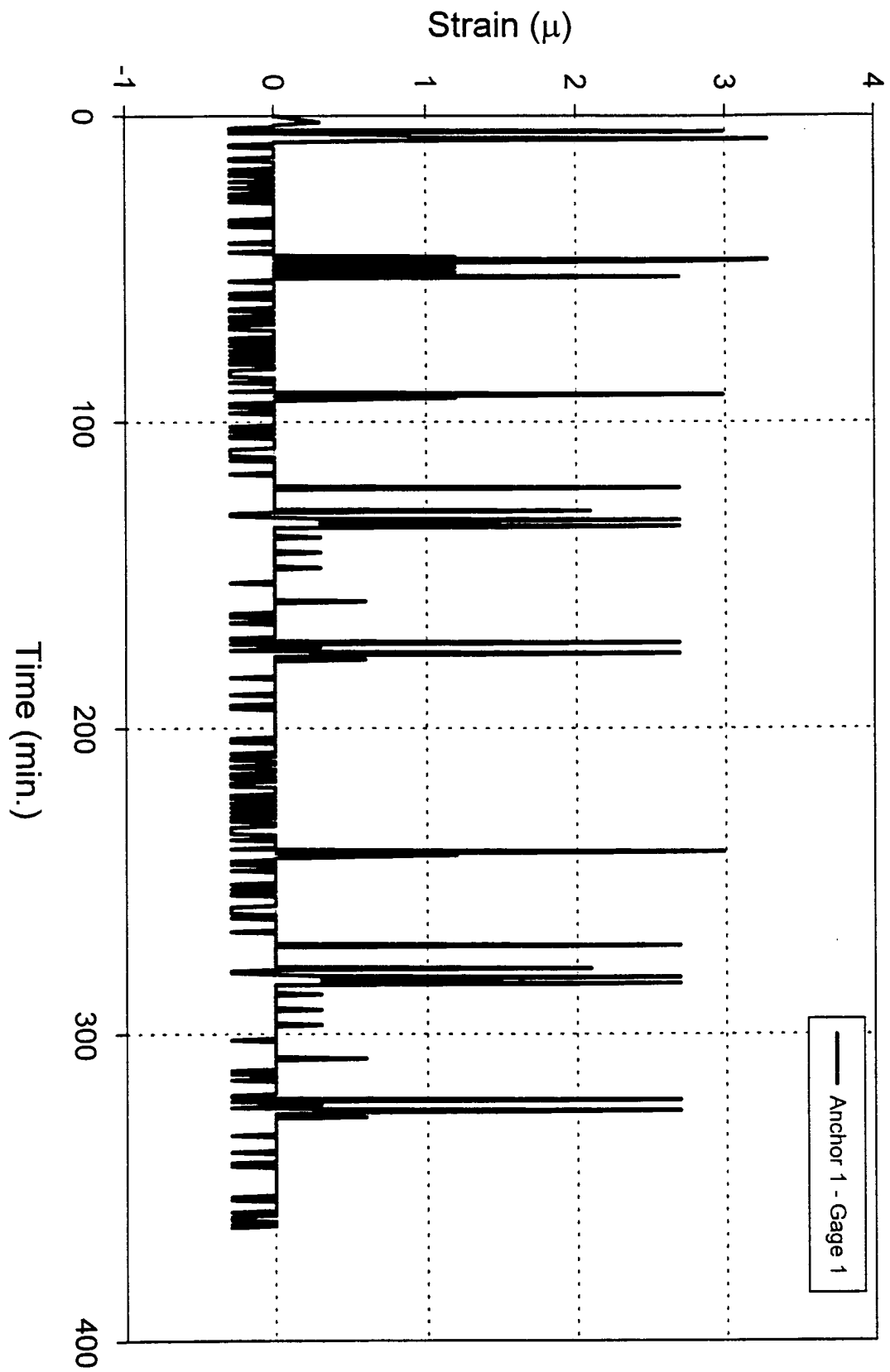


Fig. 4.76(a): Anchor # 1 performance test results, gage # 1.

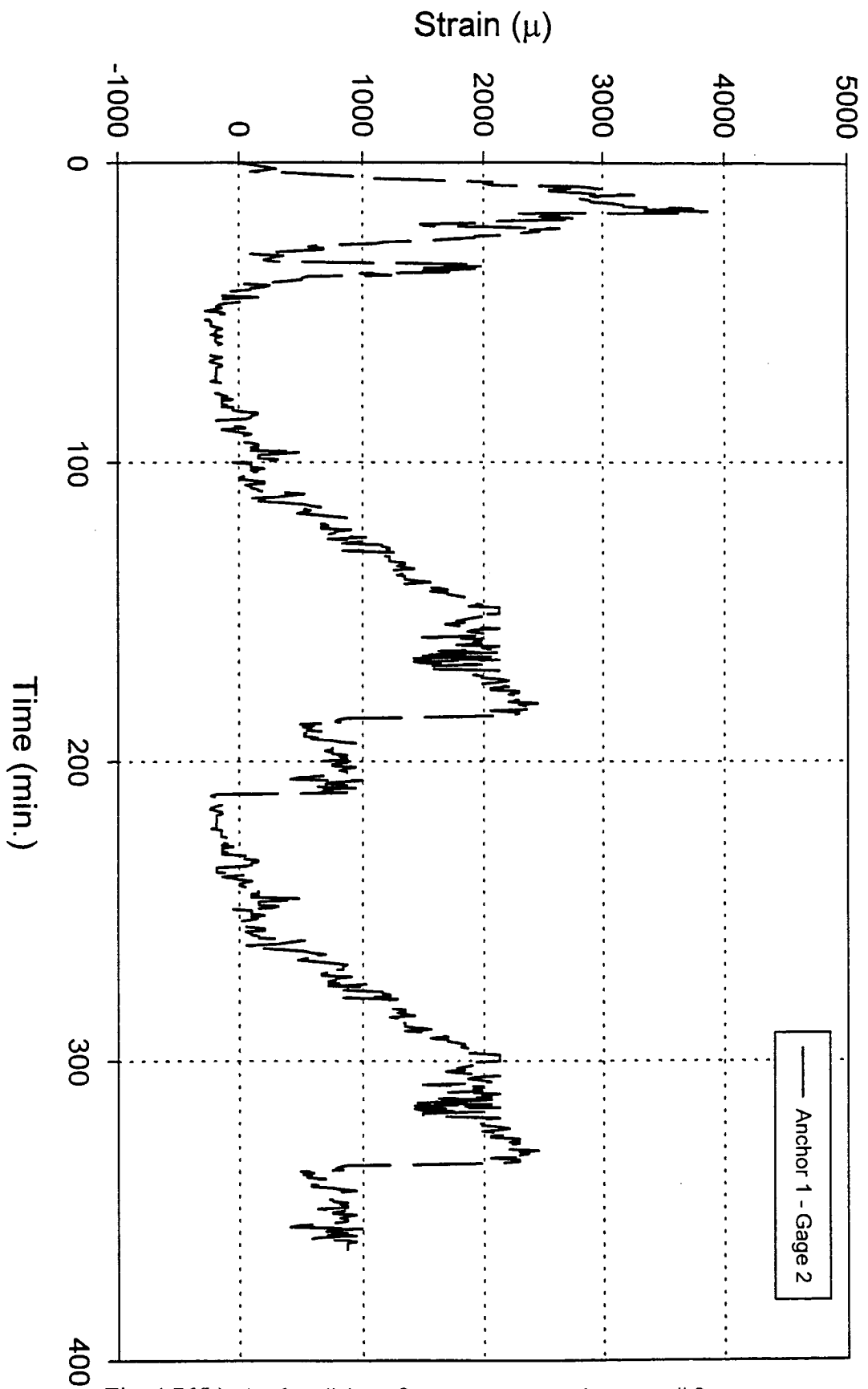


Fig. 4.76(b): Anchor # 1 performance test results, gage # 2.

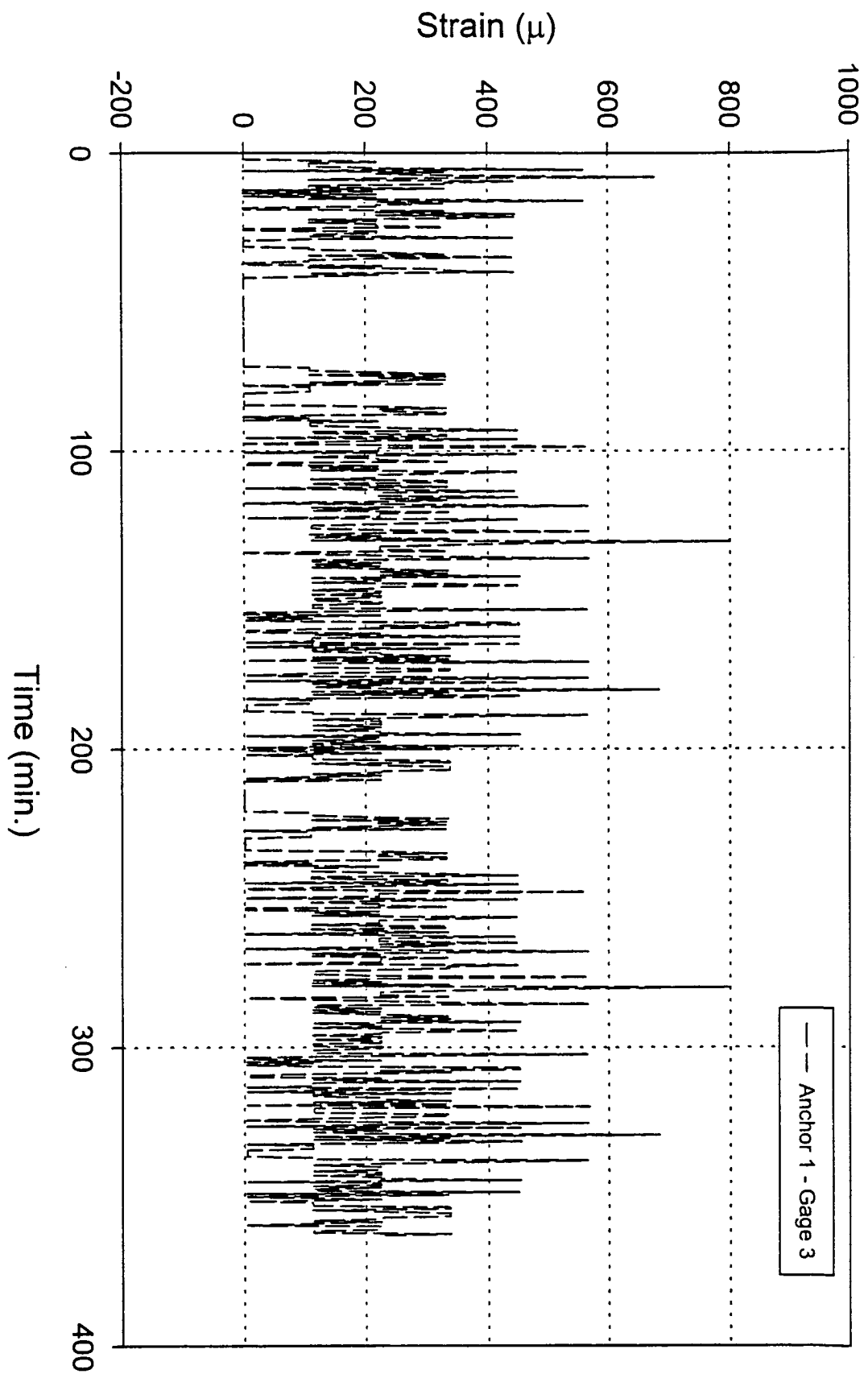
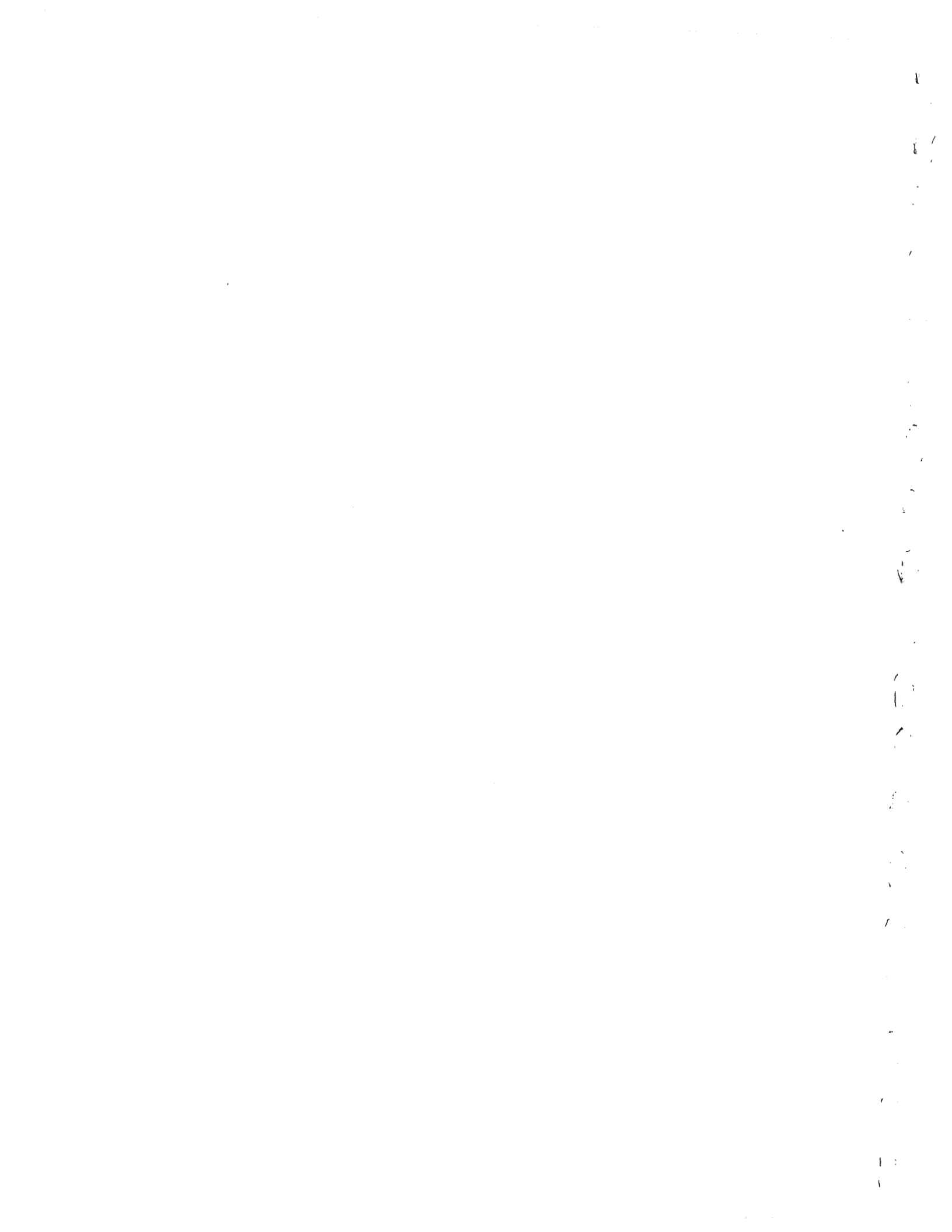


Fig. 4.76(c): Anchor # 1 performance test results, gage # 3.





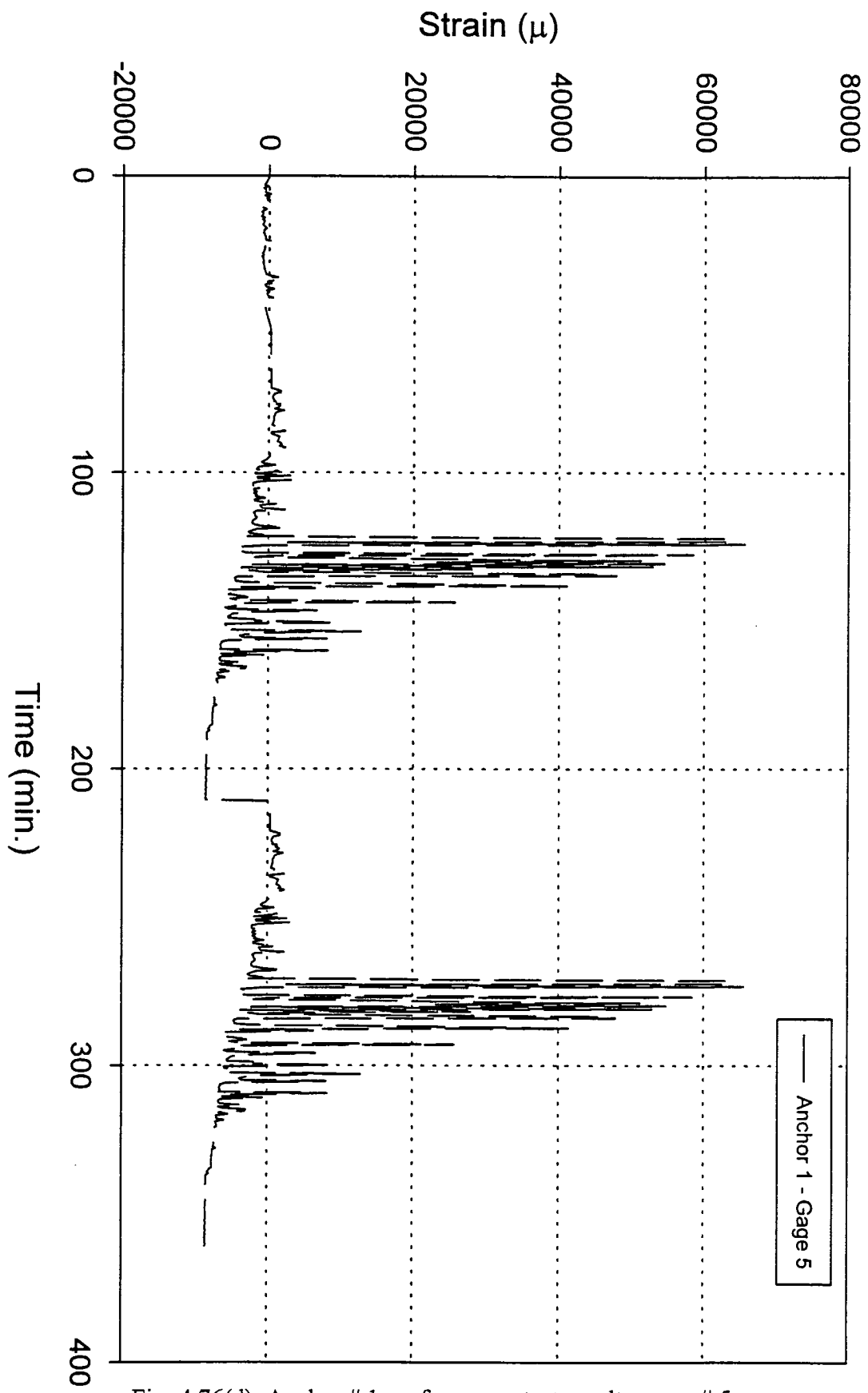


Fig. 4.76(d): Anchor # 1 performance test results, gage # 5.

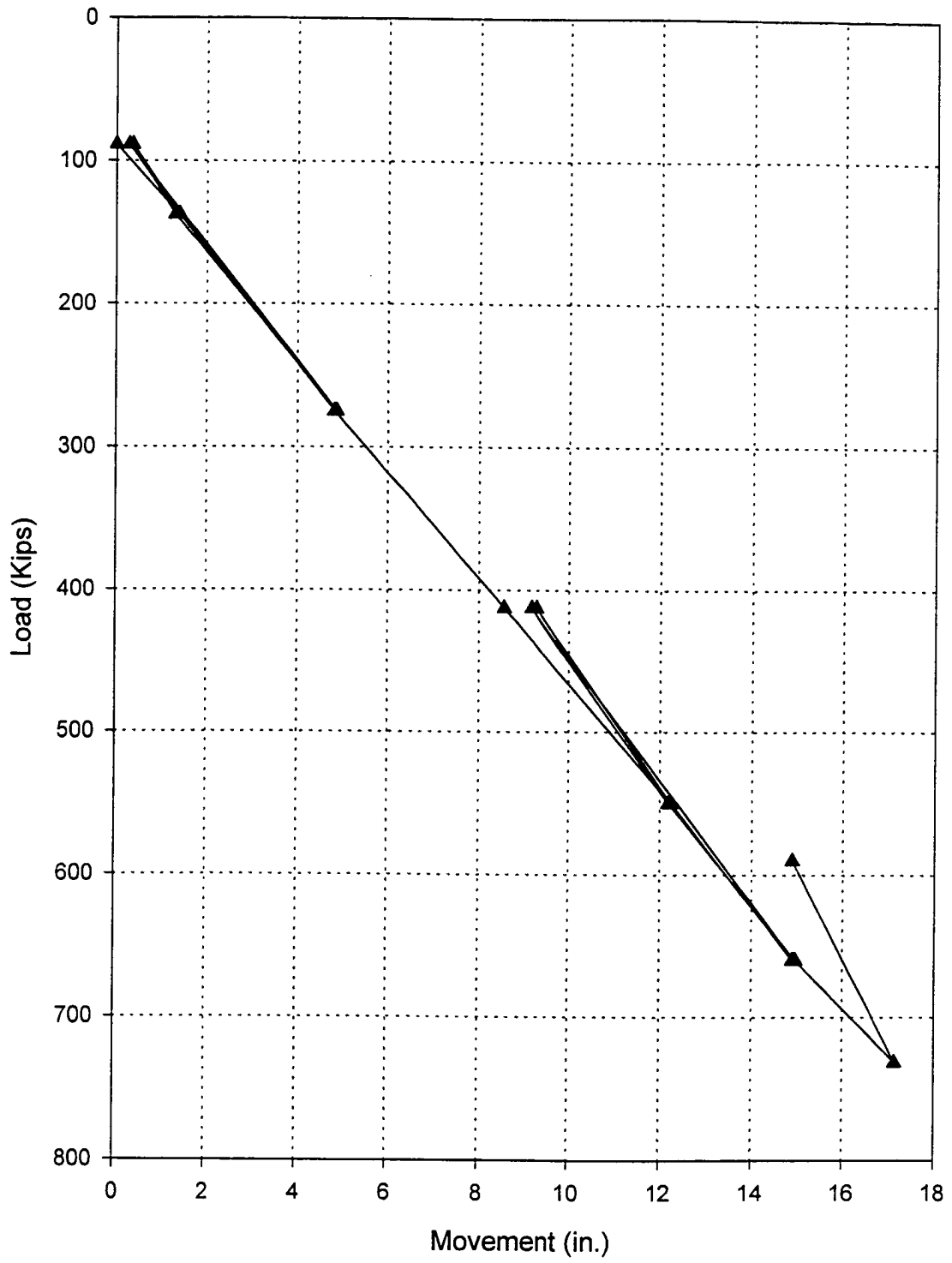


Fig. 4.77: Anchor #9 creep test, Load vs. movement at the anchor head

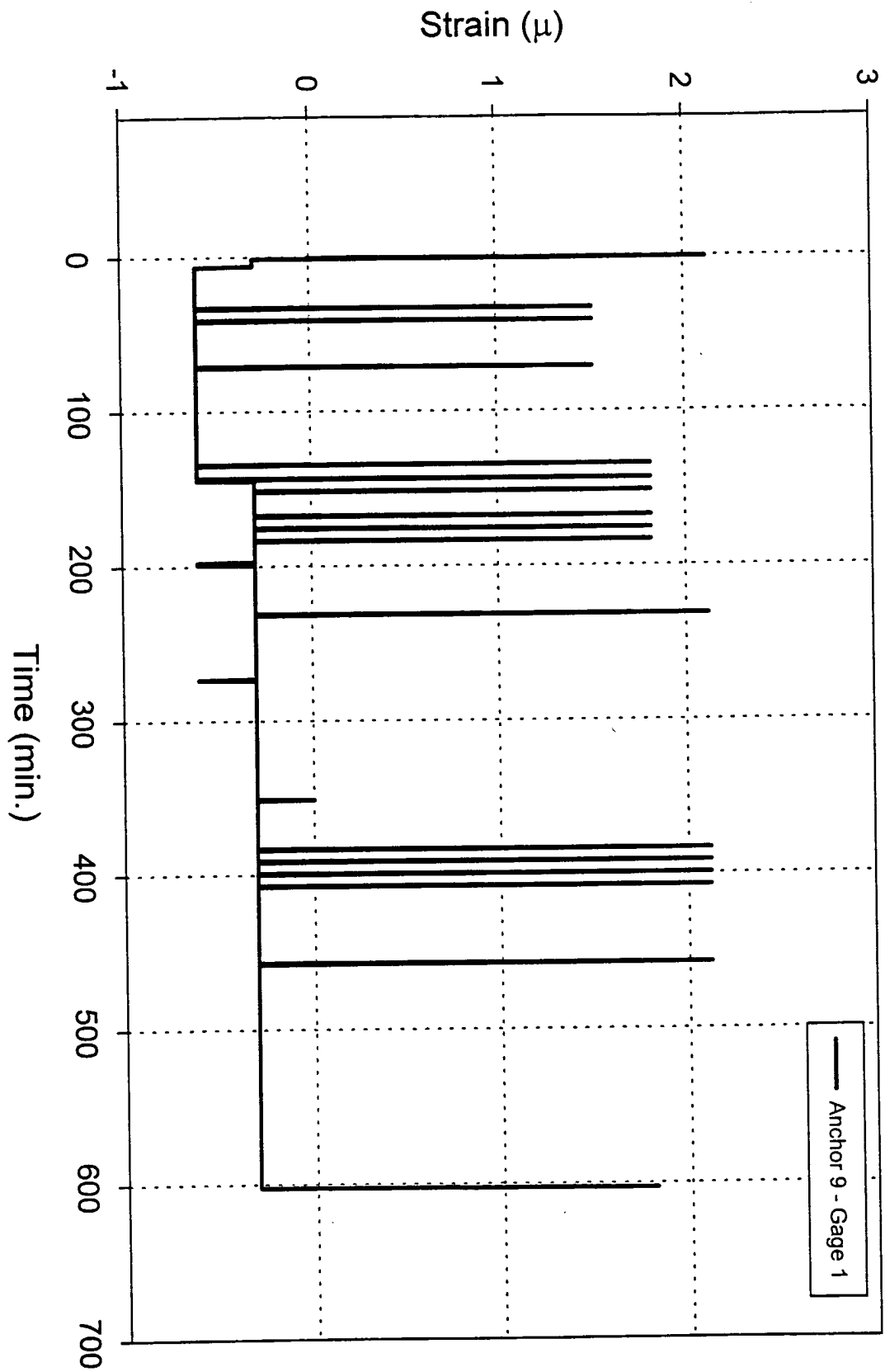


Fig. 4.78(a): Anchor # 9 creep test results, gage # 1.

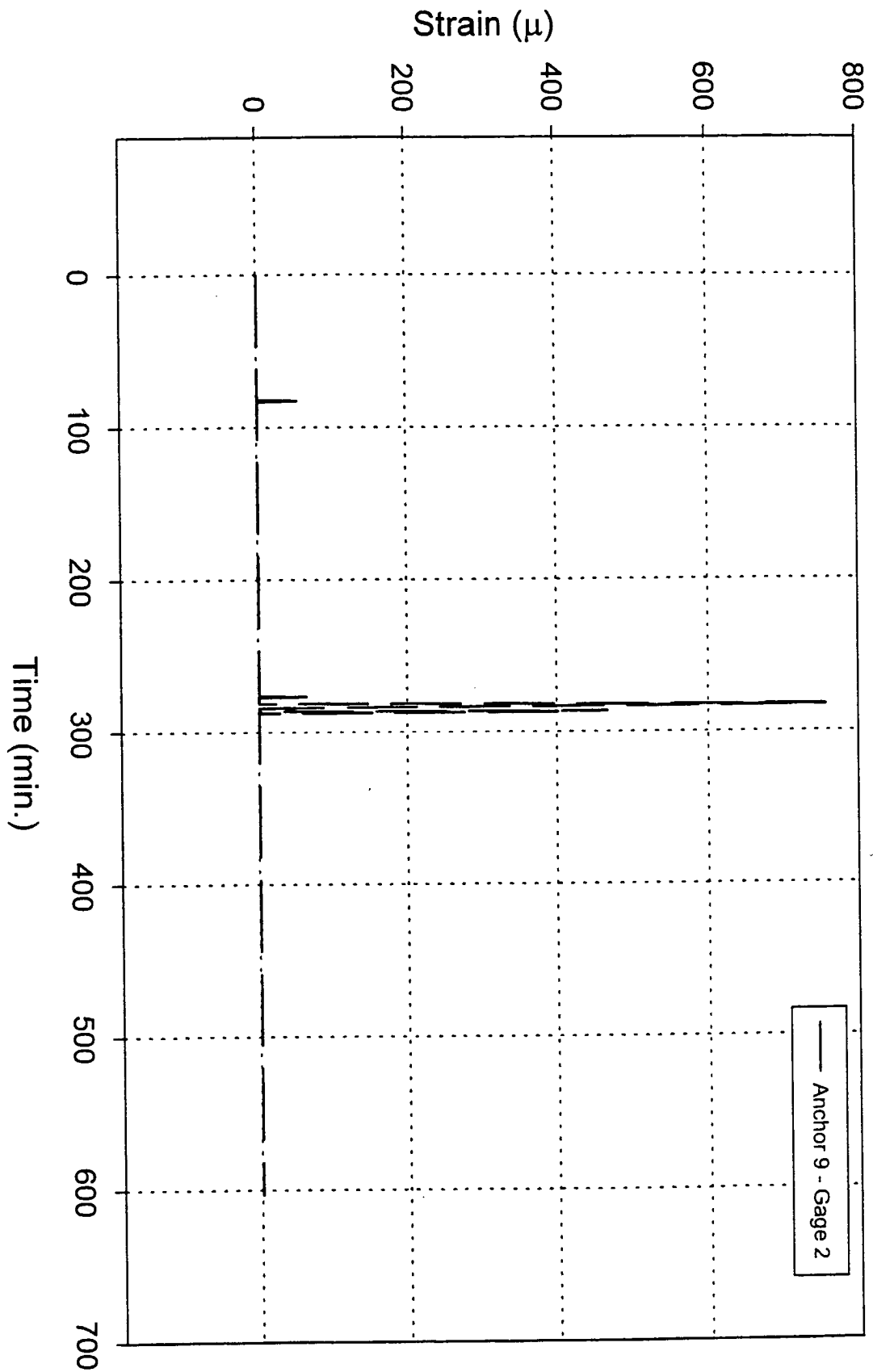


Fig. 4.78(b): Anchor # 9 creep test results, gage # 2.

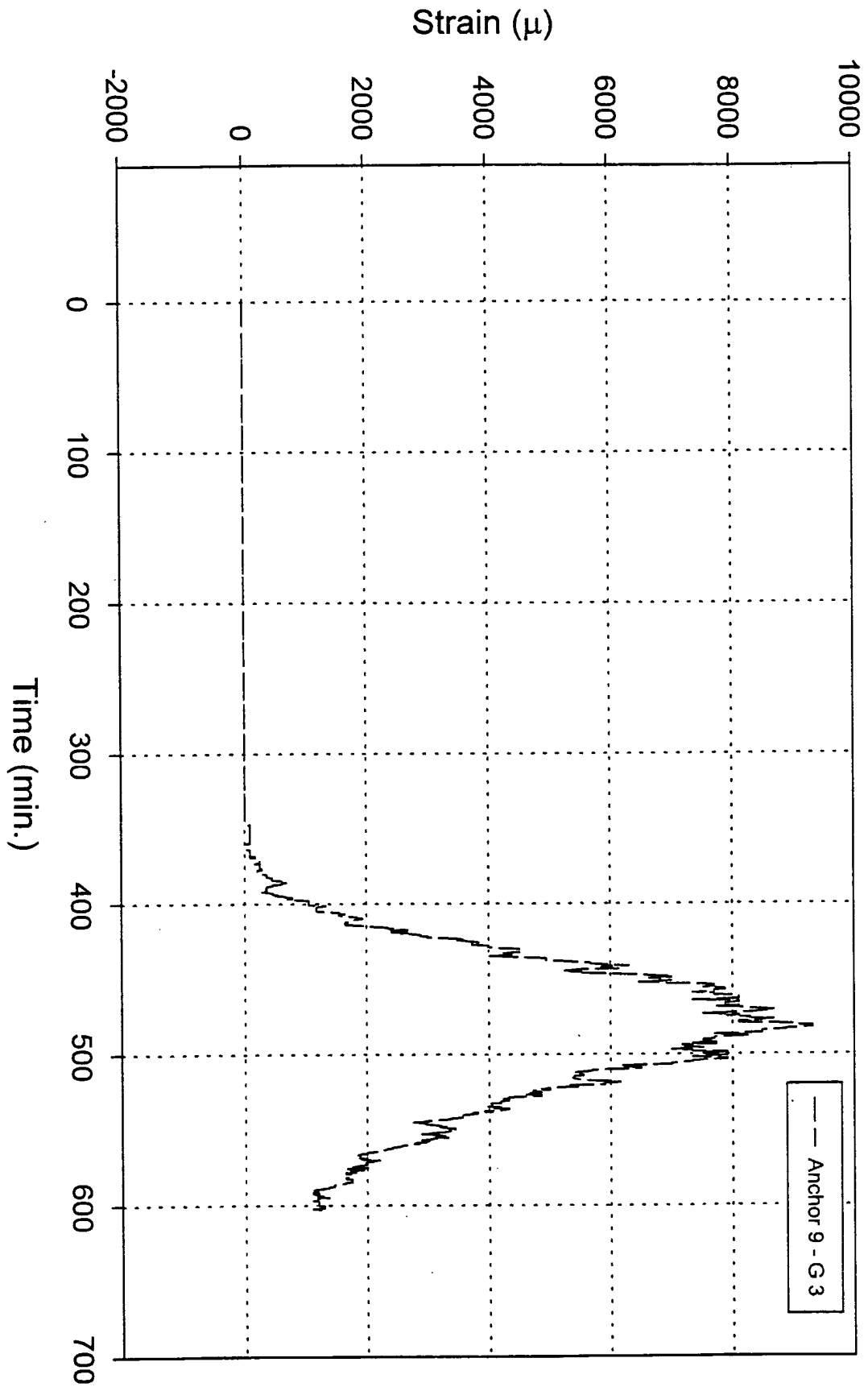


Fig. 4.78(c): Anchor # 9 creep test results, gage # 3.

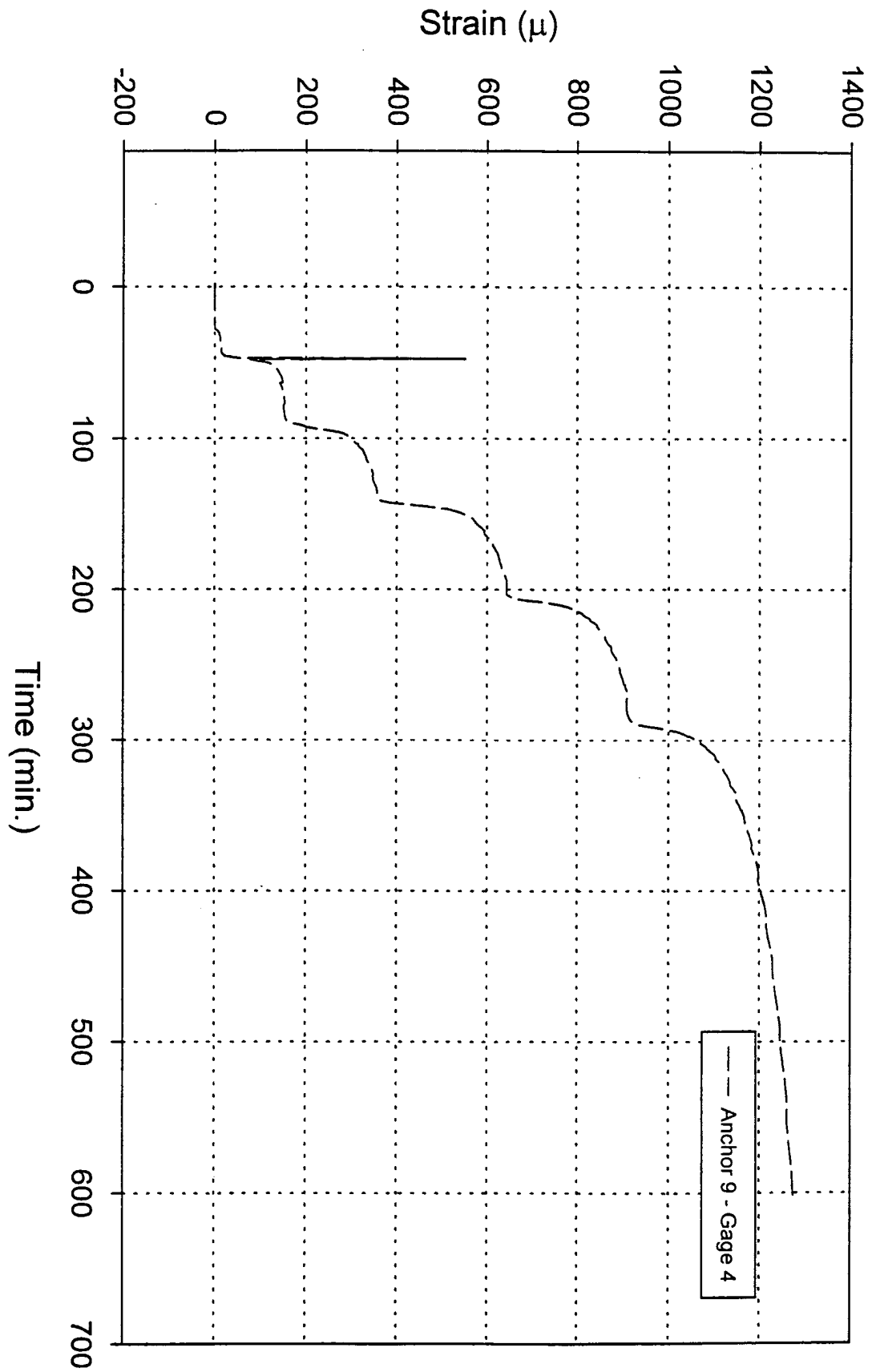


Fig. 4.78(d): Anchor # 9 creep test results, gage # 4.

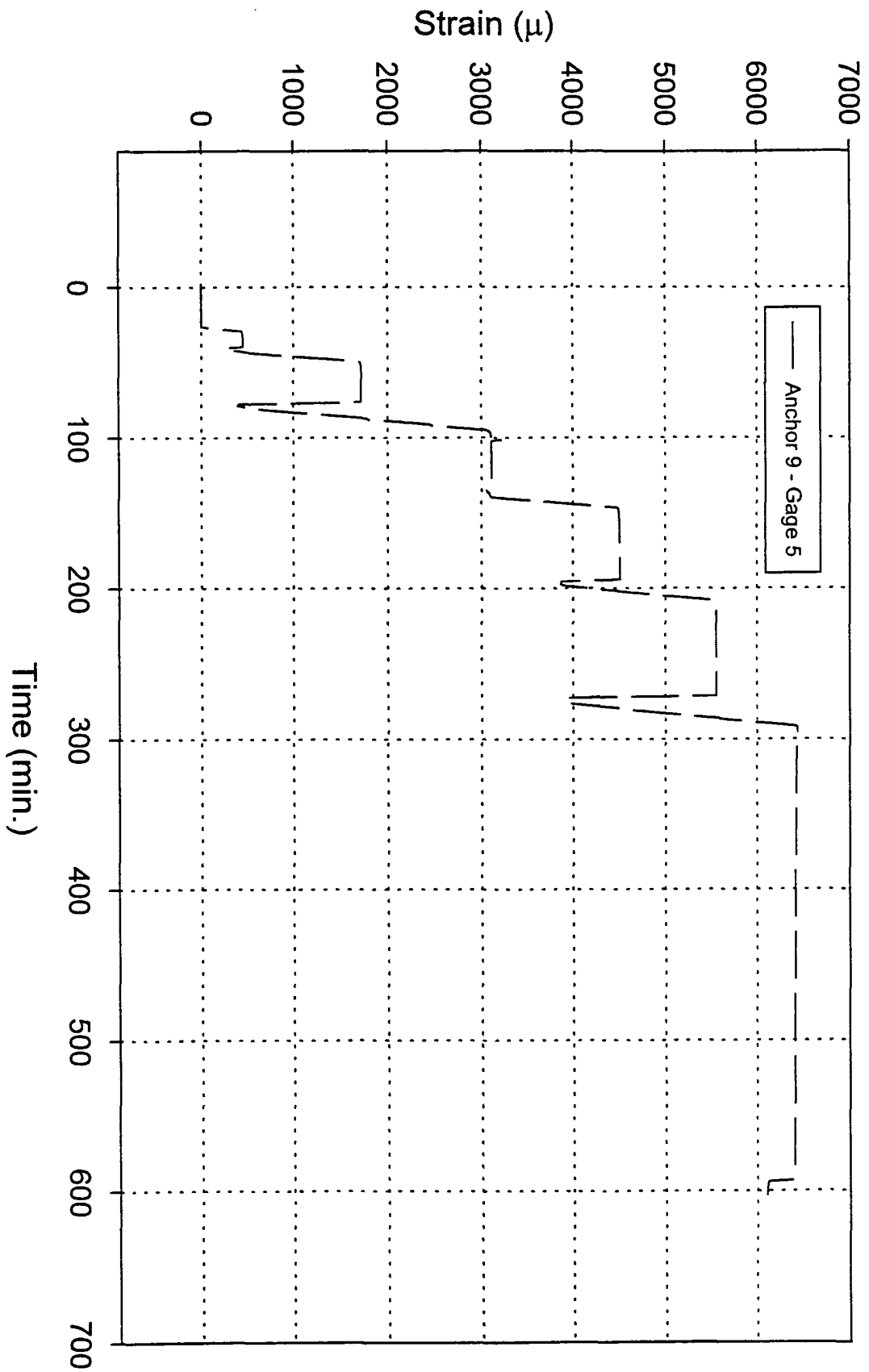


Fig. 4.78(e): Anchor # 9 creep test results, gage # 5.

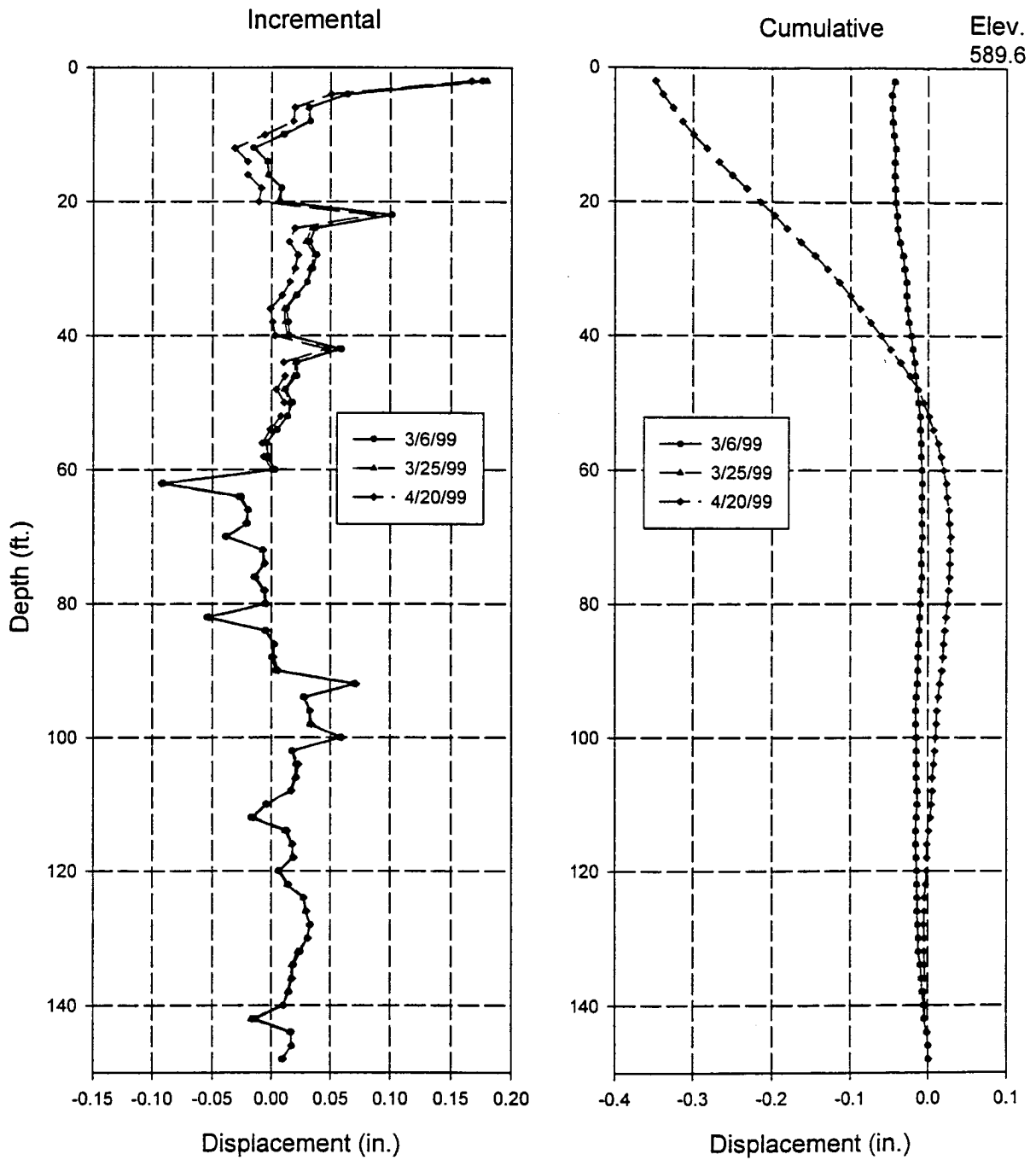


Fig. 4.79: Inclinometer # 8 Displacement in the A + Direction, downslope (River direction)  
 Base line reading 12/11/1998



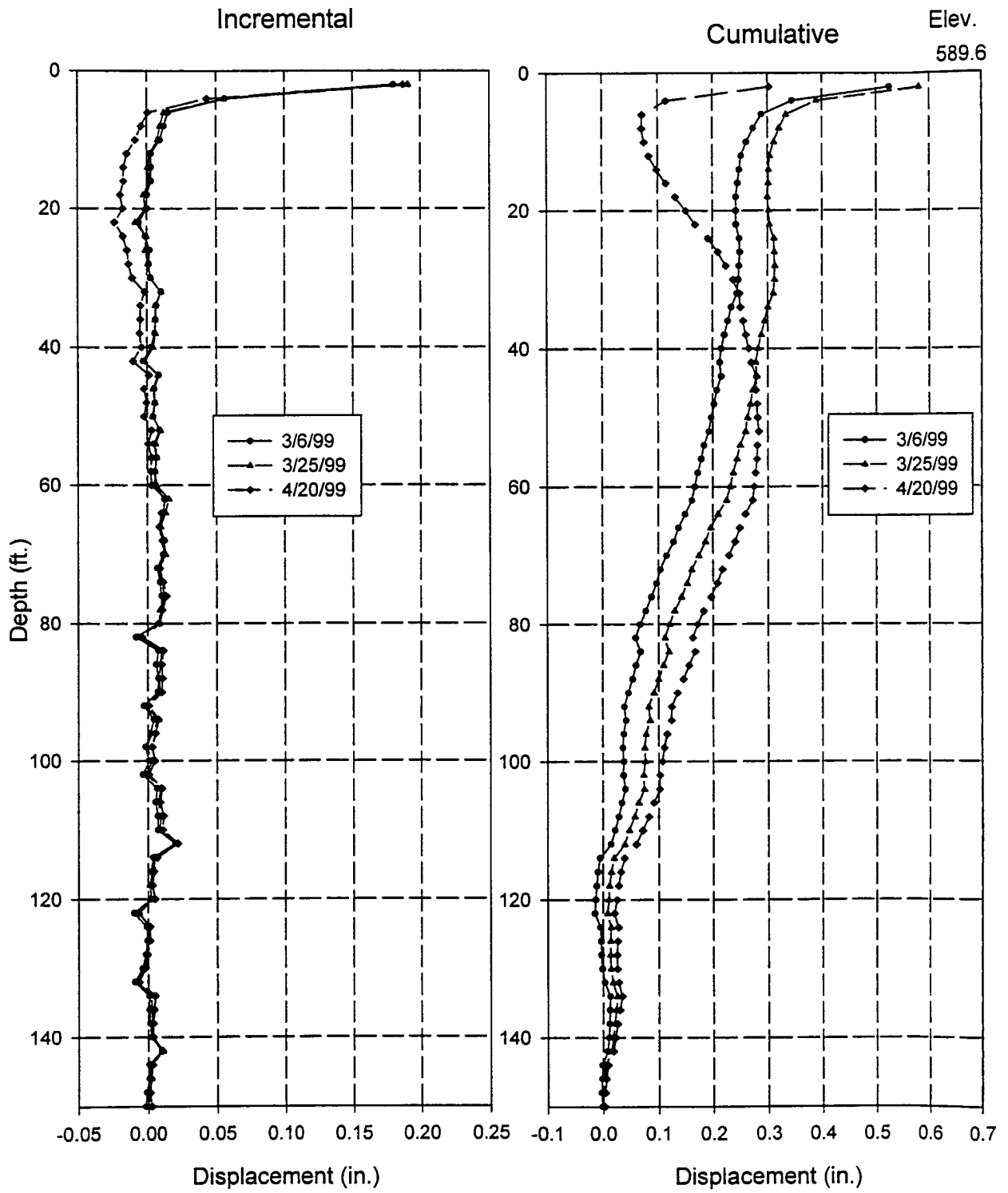


Fig. 4.80: Inclimometer # 9A Displacement in the A + Direction, downslope (River direction)  
Base Line reading 12/11/1998

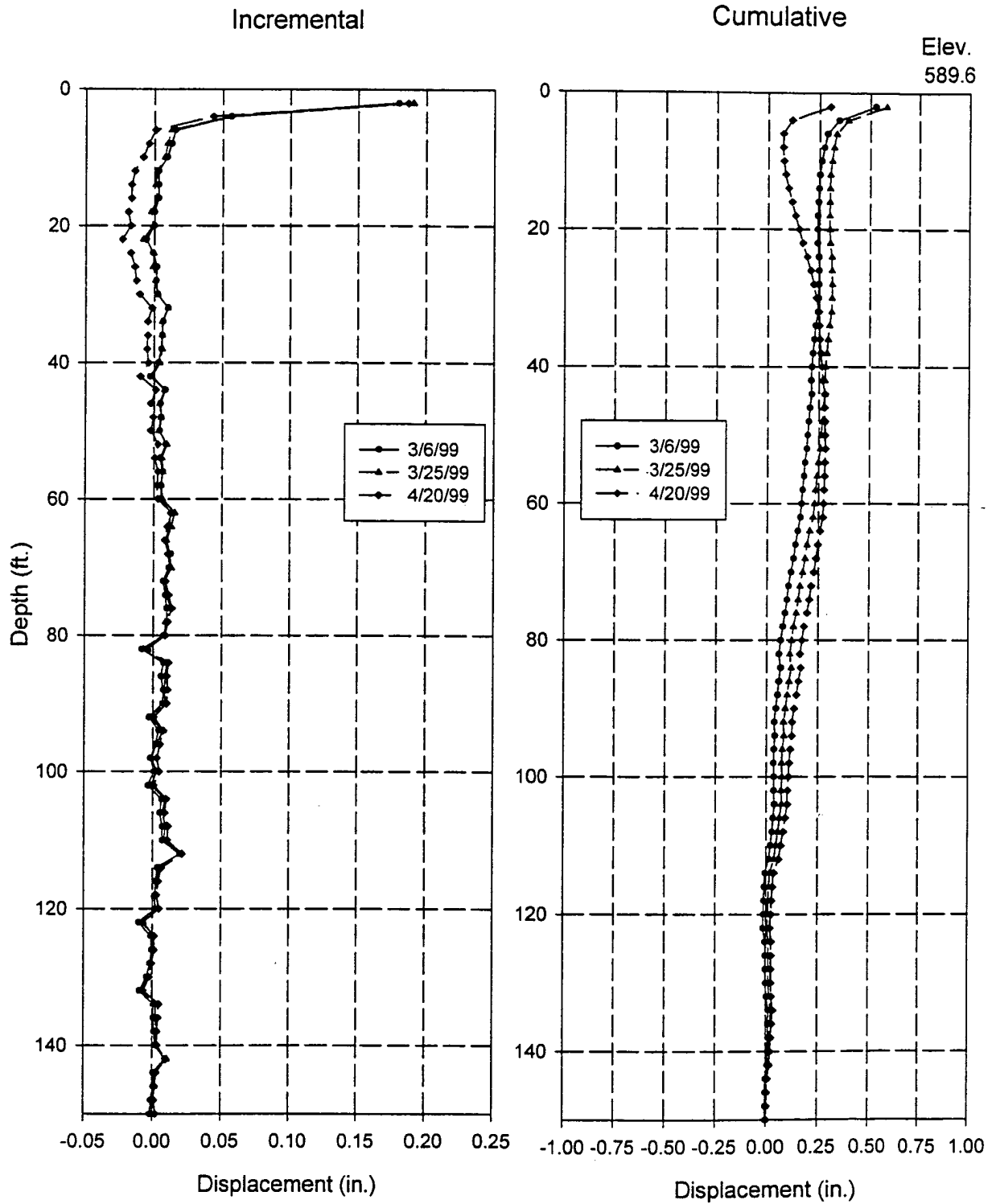


Fig. 4.81: Inclimometer # 9B Displacement in the A + Direction, downslope (River direction)  
Base Line reading 12/11/1998

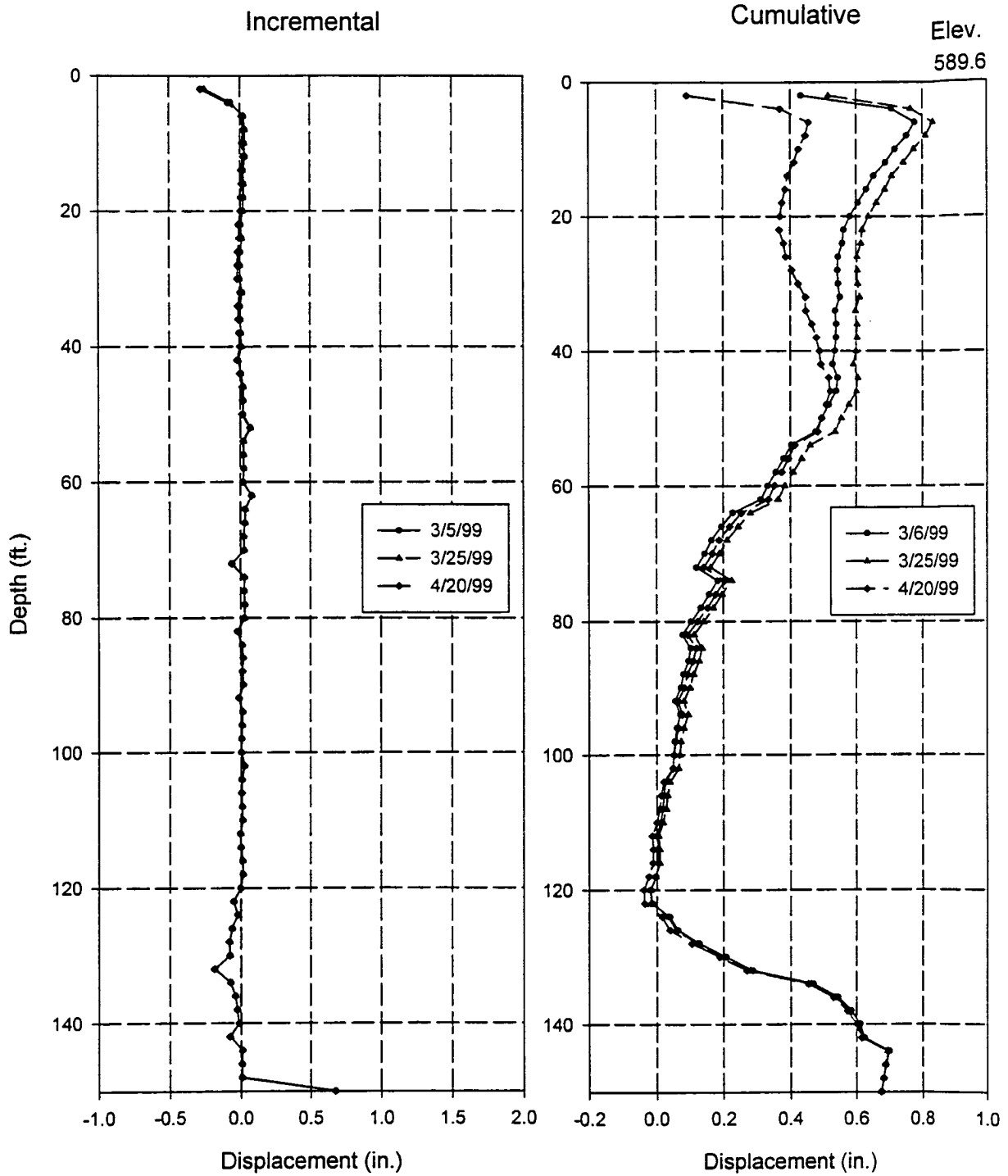


Fig. 4.82: Inclinometer # 10 Displacement in the A + Direction, downslope (River direction)  
Base Line reading 12/11/1998

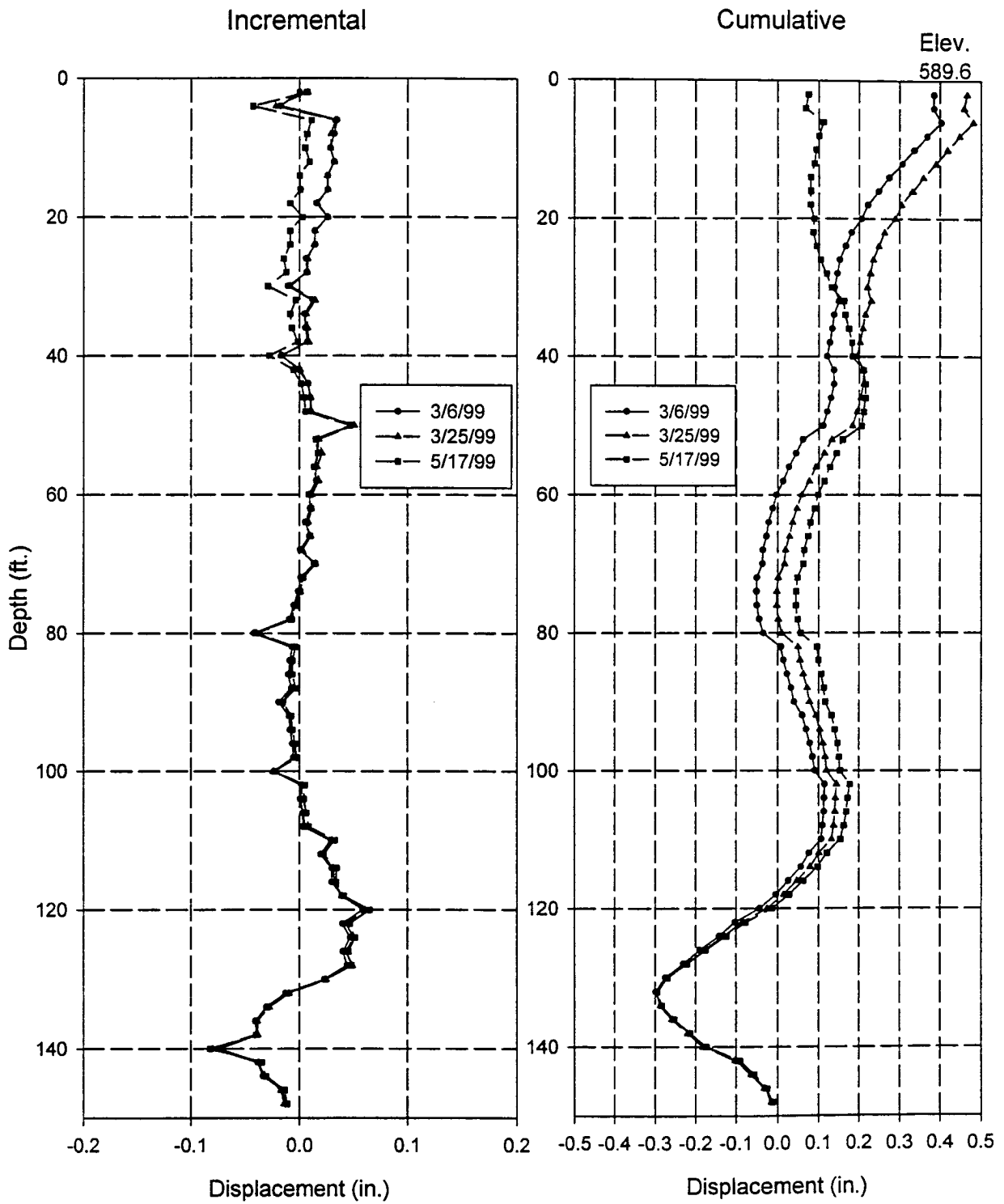


Fig. 4.83: Inclimometer # 1 Displacement in the A + Direction, downslope (River direction)  
Base Line reading 12/11/1998

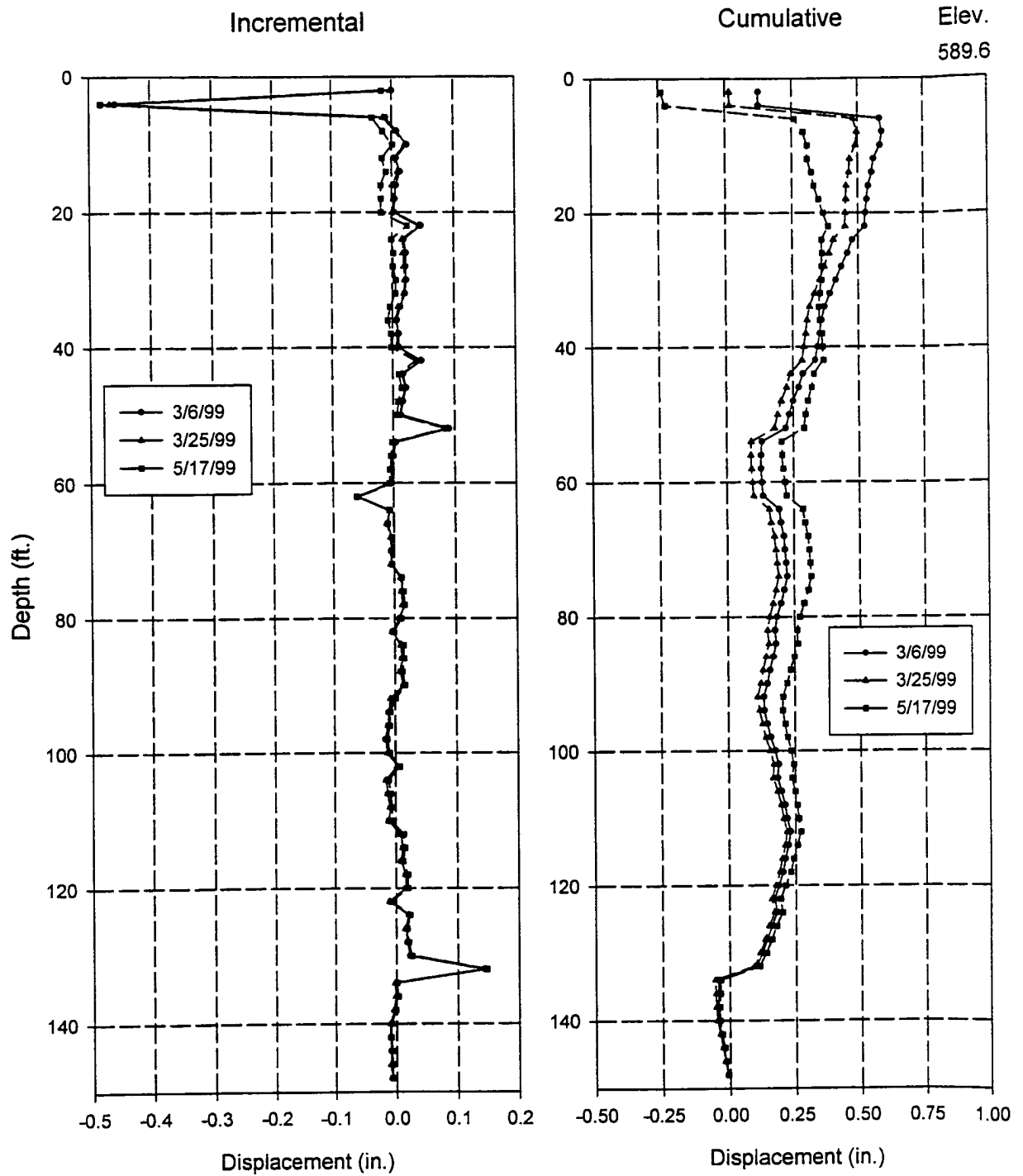


Fig. 4.84: Inclimometer # 3 Displacement in the A + Direction, downslope (River direction)  
Base Line reading 12/11/1998

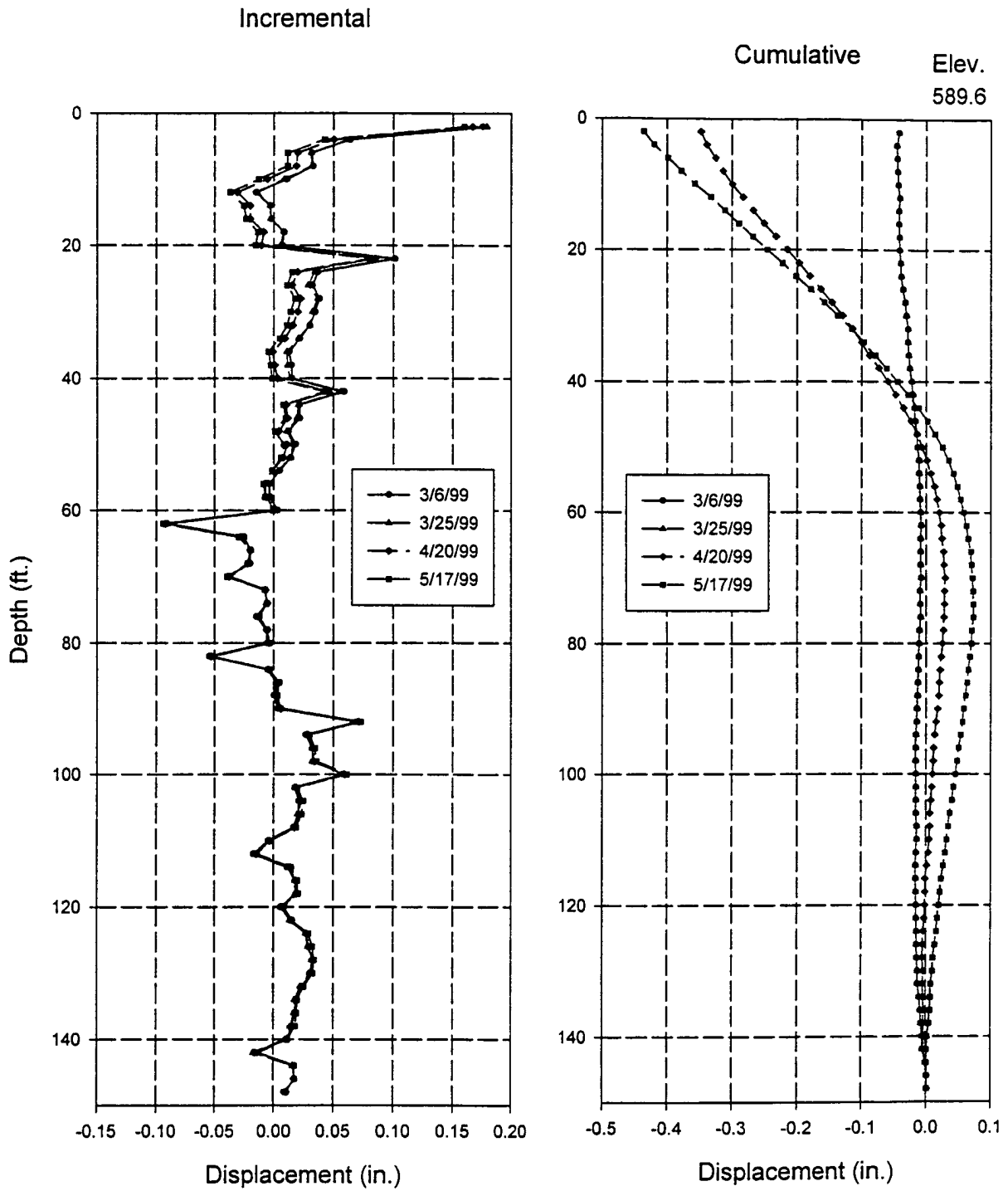


Fig. 4.85: Inclimometer # 8 Displacement in the A + Direction, downslope (River direction)  
Base Line reading 12/11/1998

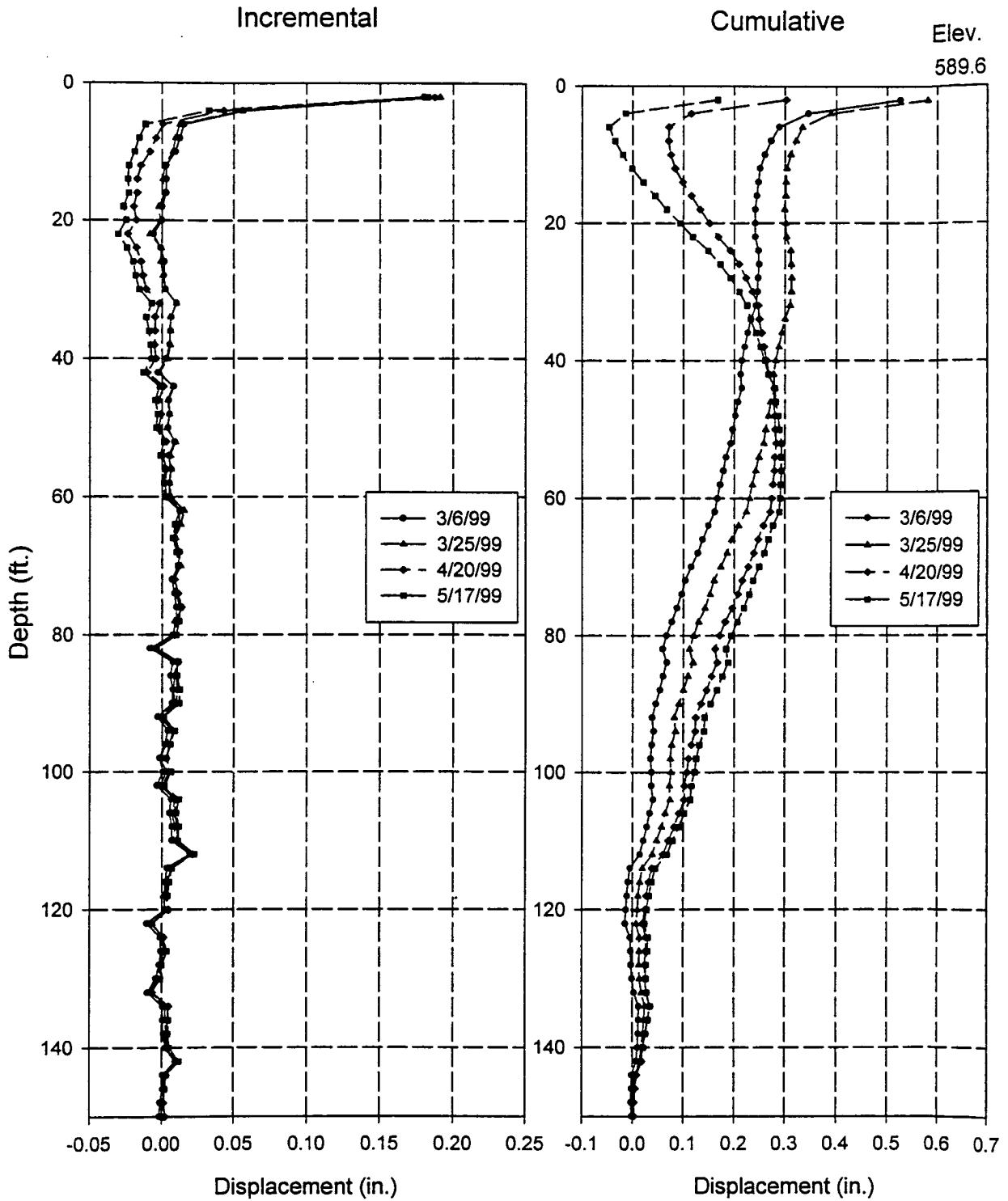


Fig. 4.86: Inclimometer # 9A Displacement in the A + Direction, downslope (River direction)  
Base Line reading 12/11/1998

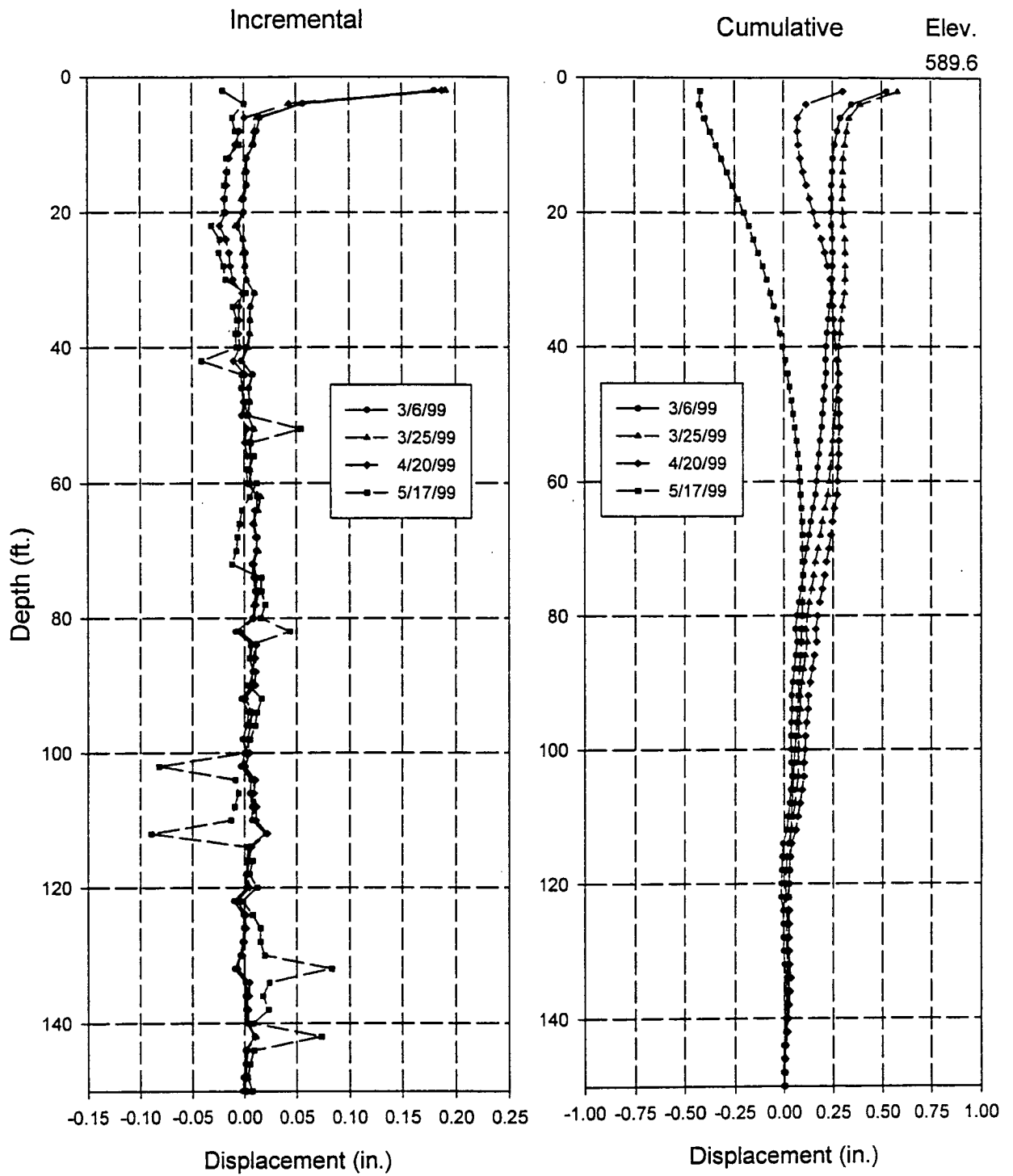


Fig. 4.87: Inclimometer # 9B Displacement in the A + Direction, downslope (River direction)  
Base Line reading 12/11/1998



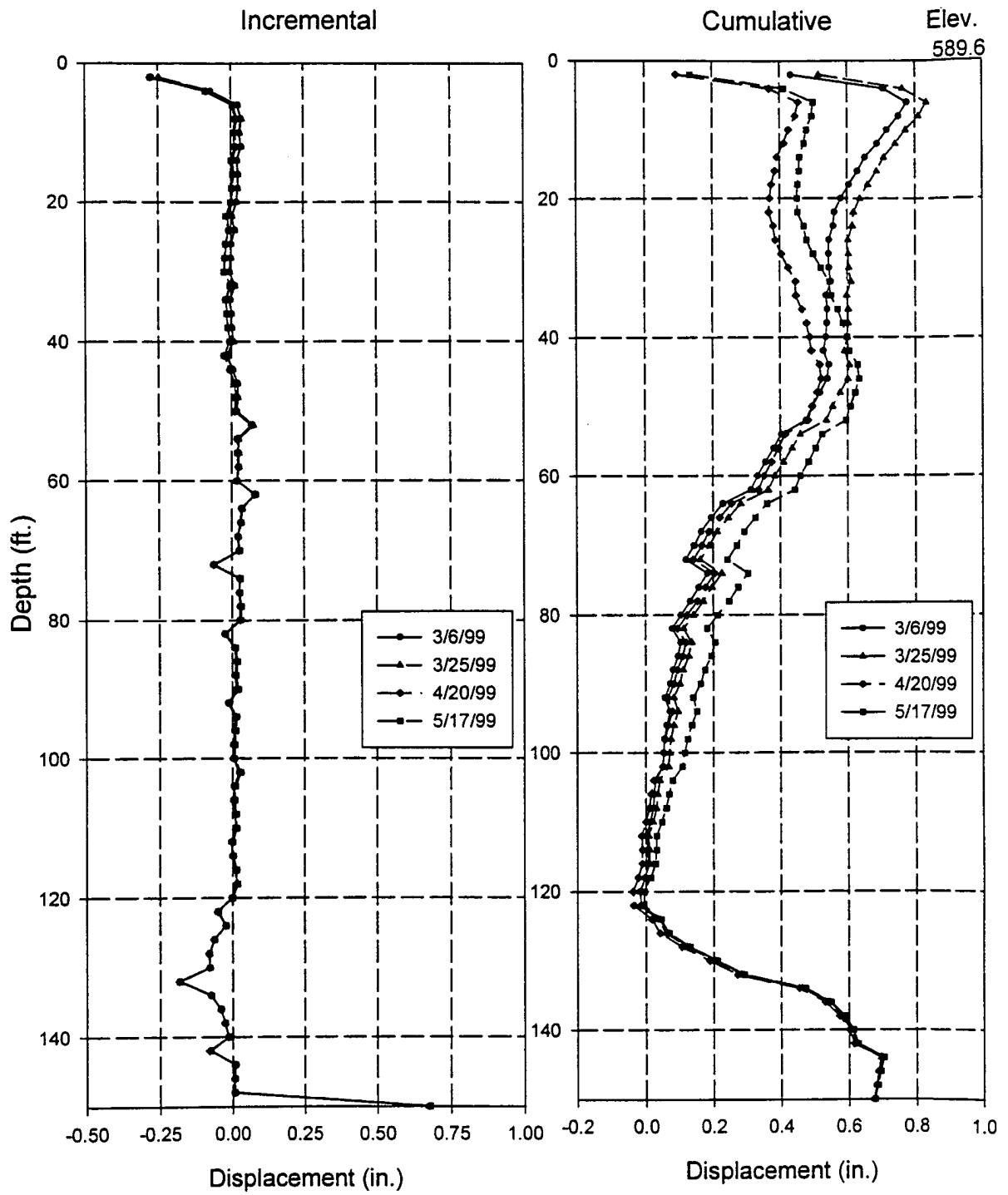


Fig. 4.88: Inclimometer # 10 Displacement in the A + Direction, downslope (River direction)  
Base Line reading 12/11/1998

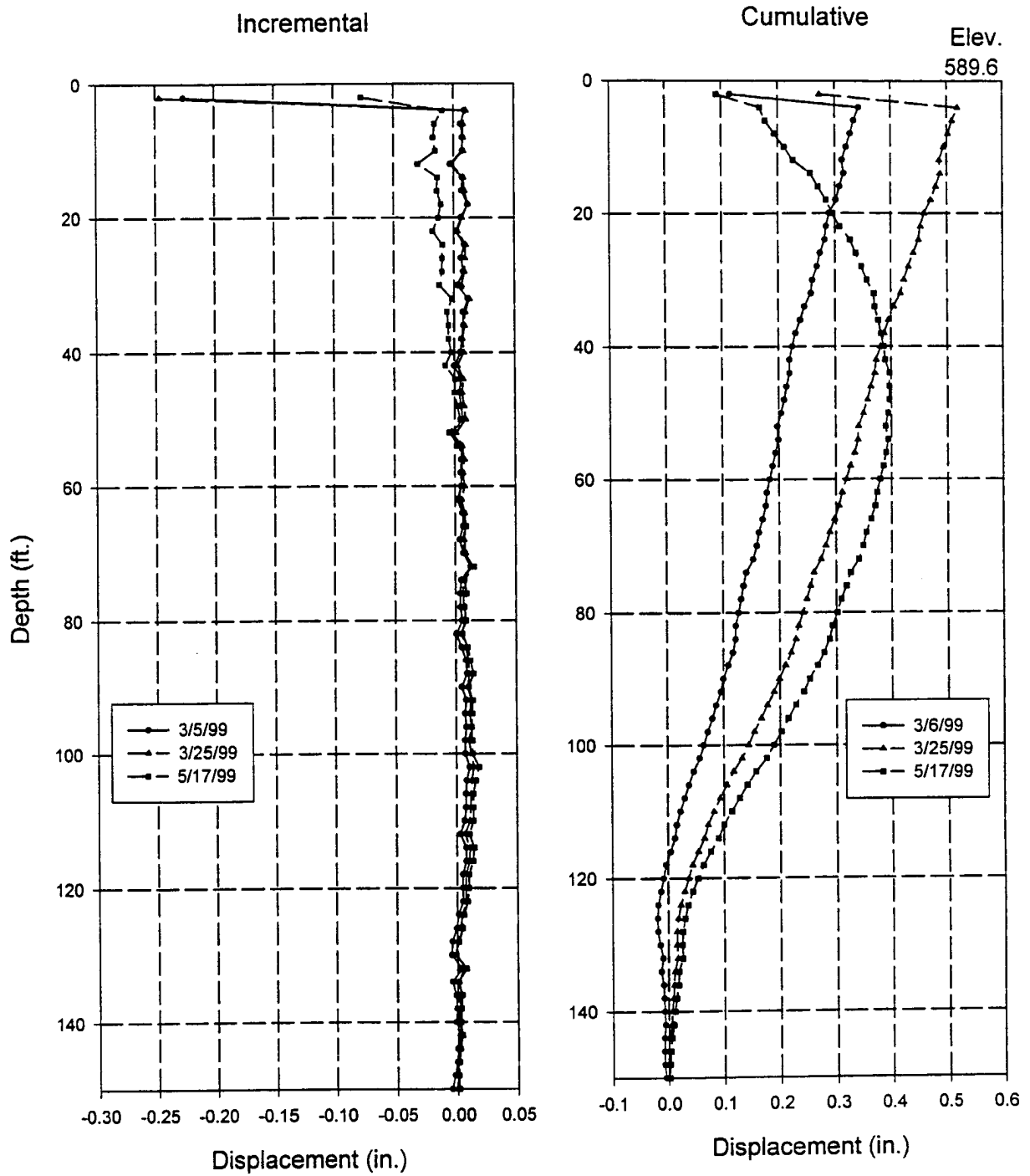


Fig. 4.89: Inclimometer # 17 Displacement in the A + Direction, downslope (River direction)  
Base Line reading 12/11/1998

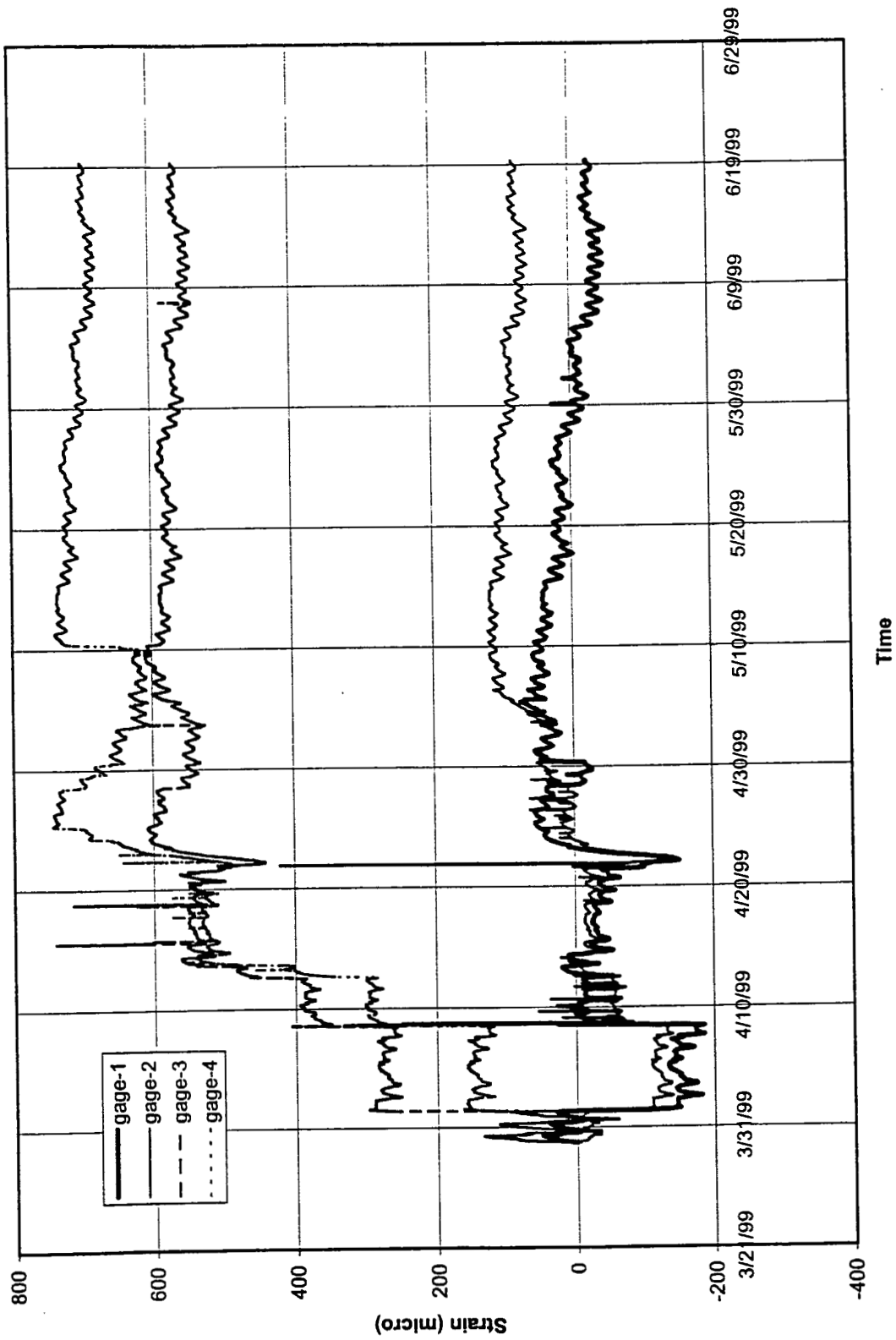


Fig. 4.90: Tie-beam #1, Strain from gages on driven pile cap side.

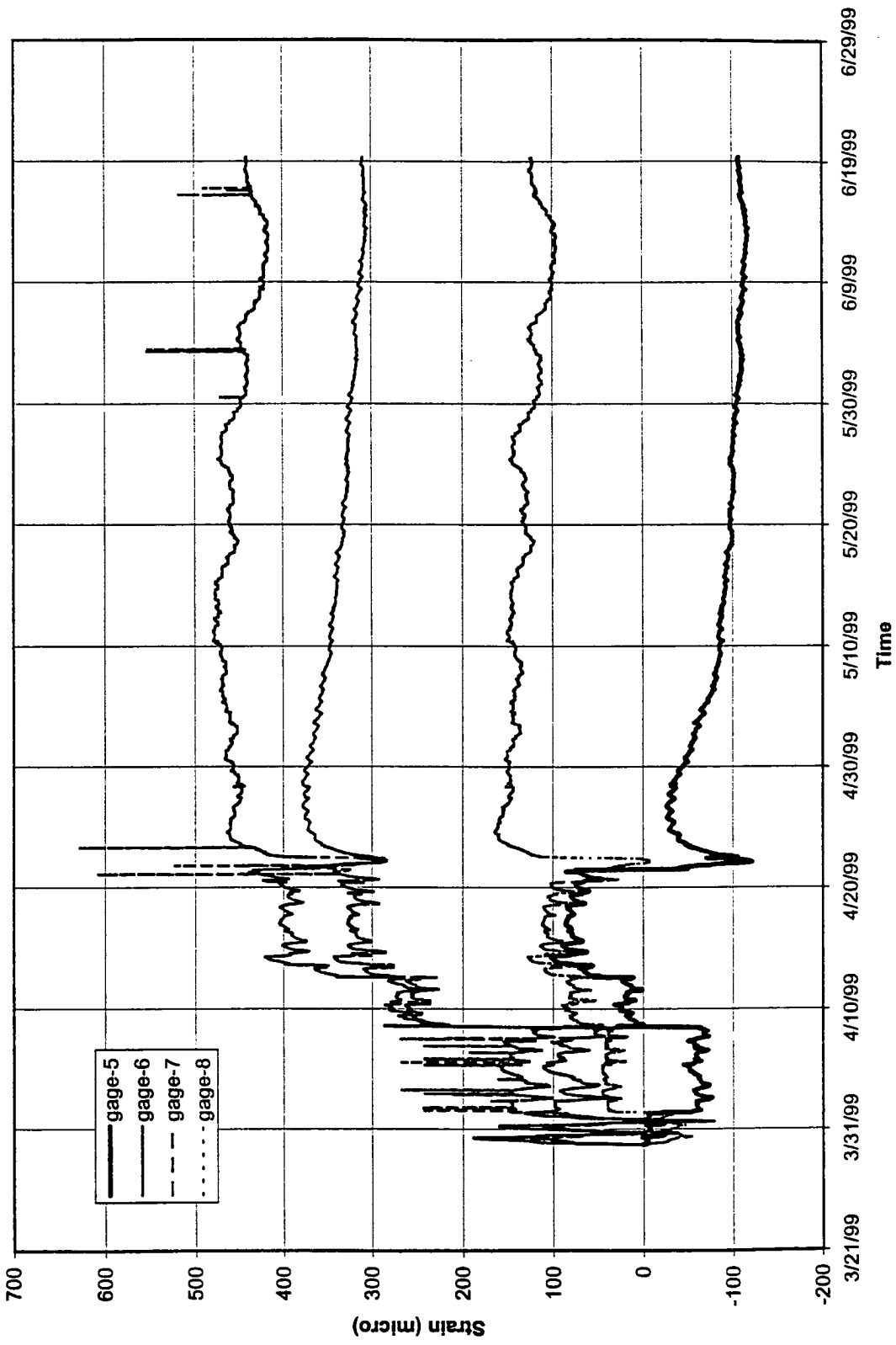


Fig. 4.91: Tie-beam #1, Strain from gages on drilled shaft cap side.

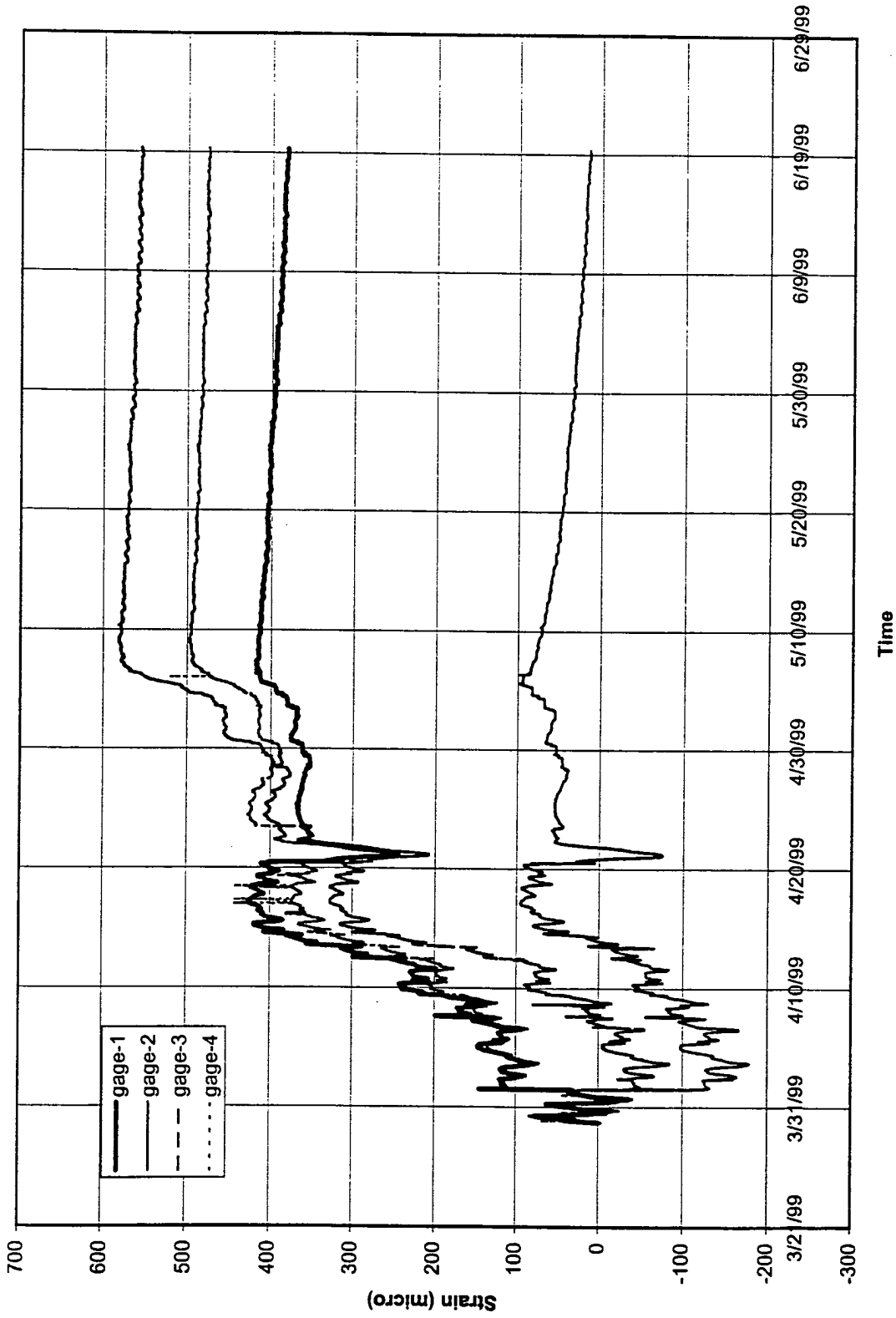


Fig. 4.92: Tie-beam #12, Strain from gages on driven pile cap side.

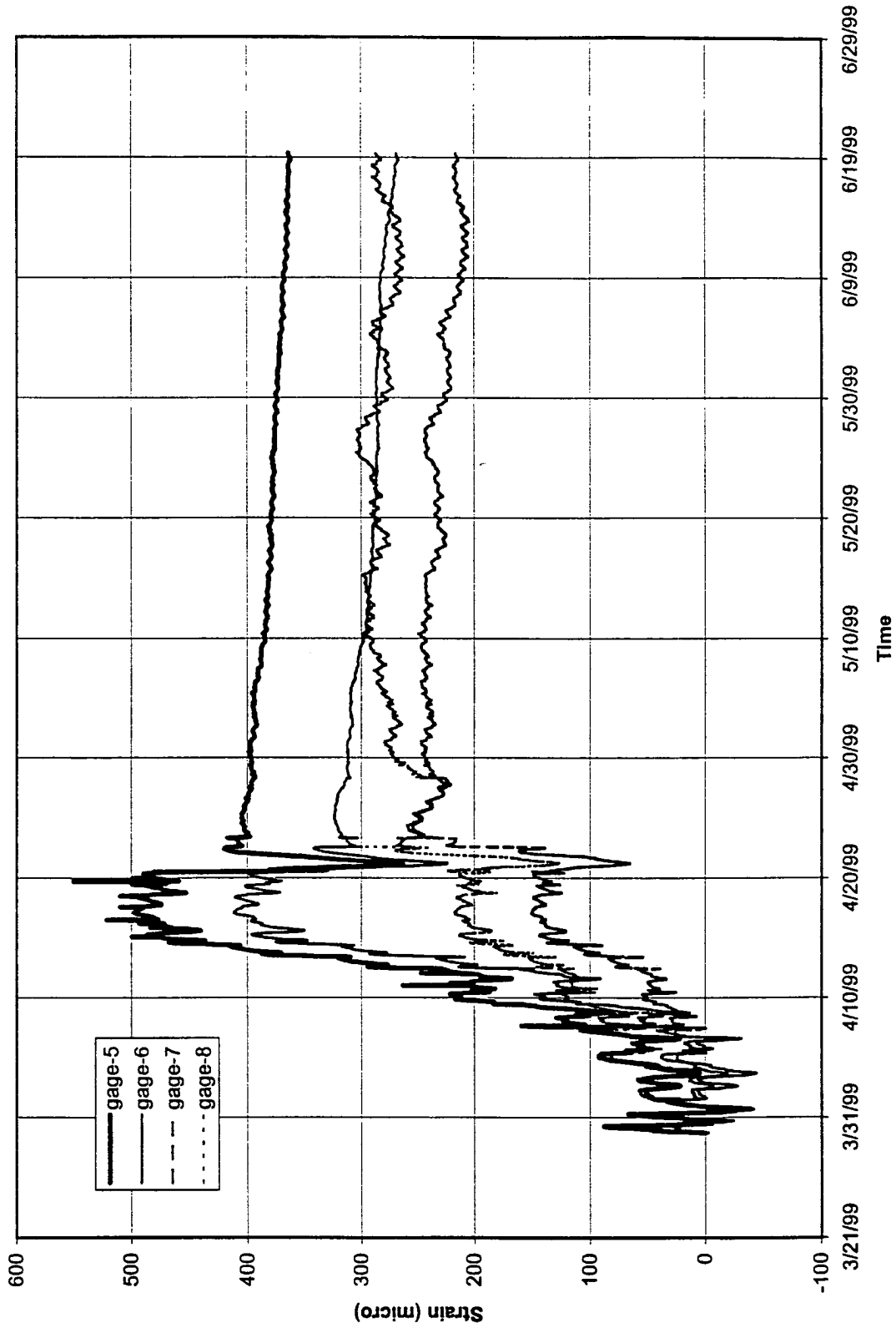


Fig. 4.93: Tie-beam #12, Strain from gages on drilled shaft cap side.

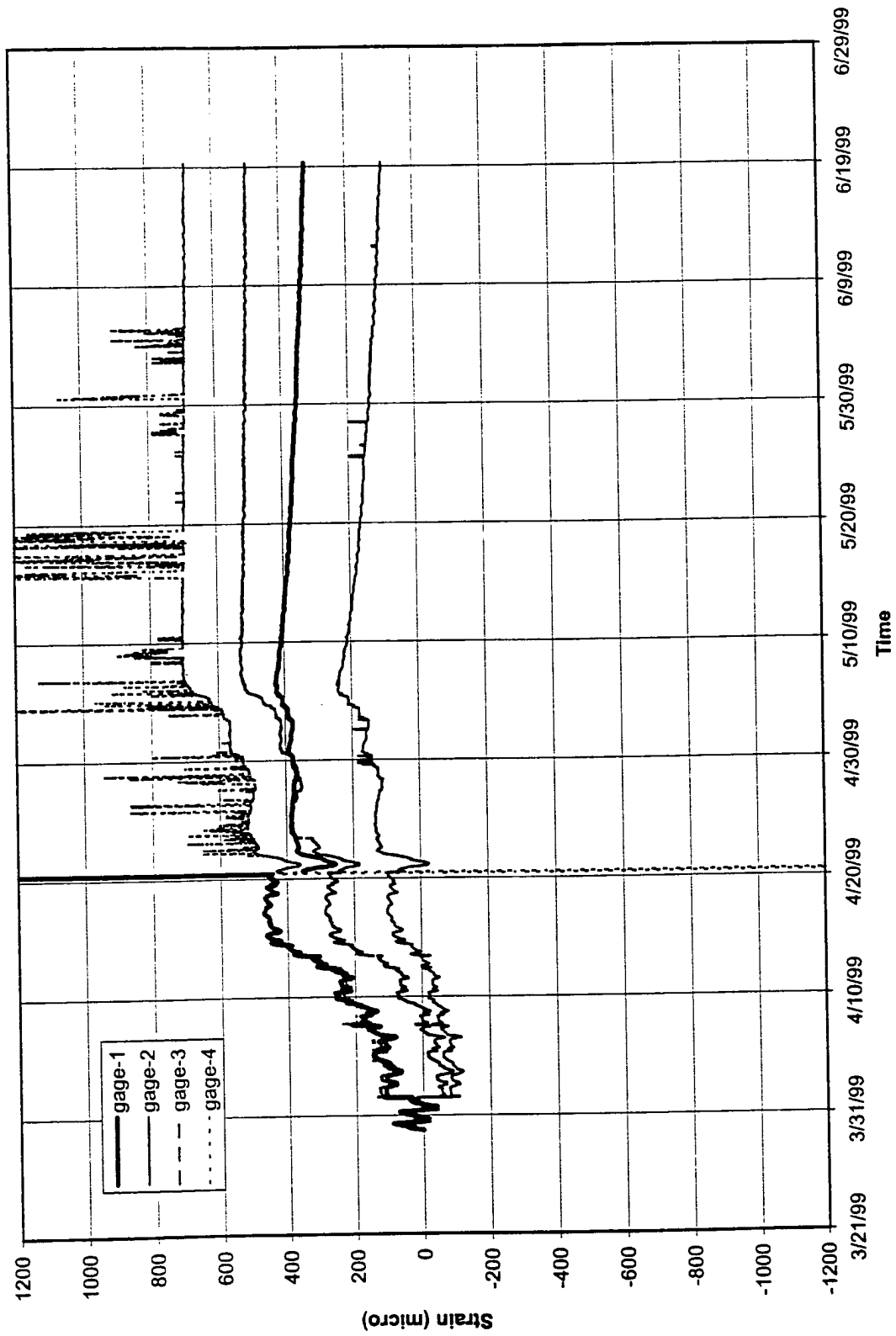


Fig. 4.94: Tie-beam #13, Strain from gages on driven pile cap side.

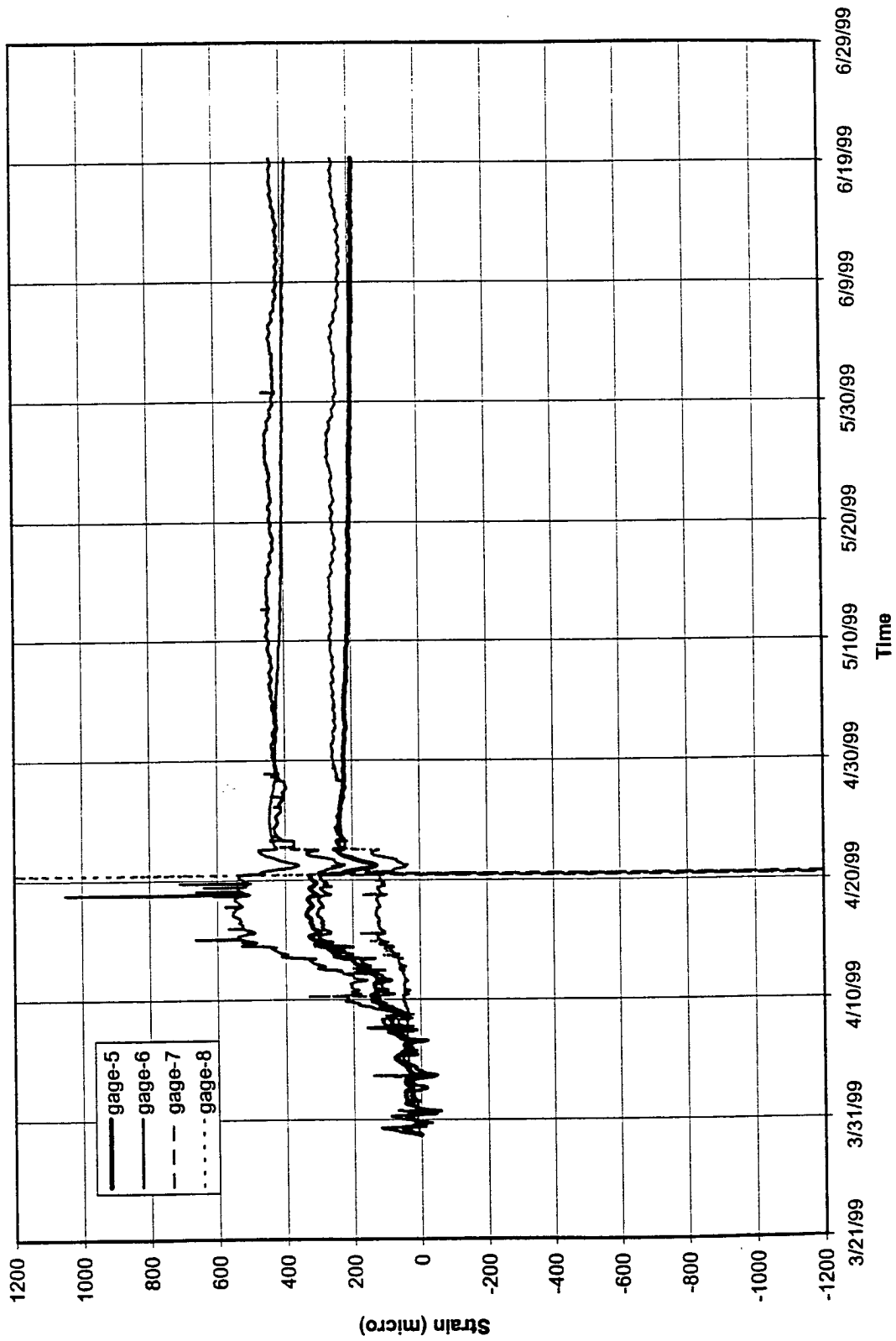


Fig. 4.95: Tie-beam #13, Strain from gages on drilled shaft cap side.



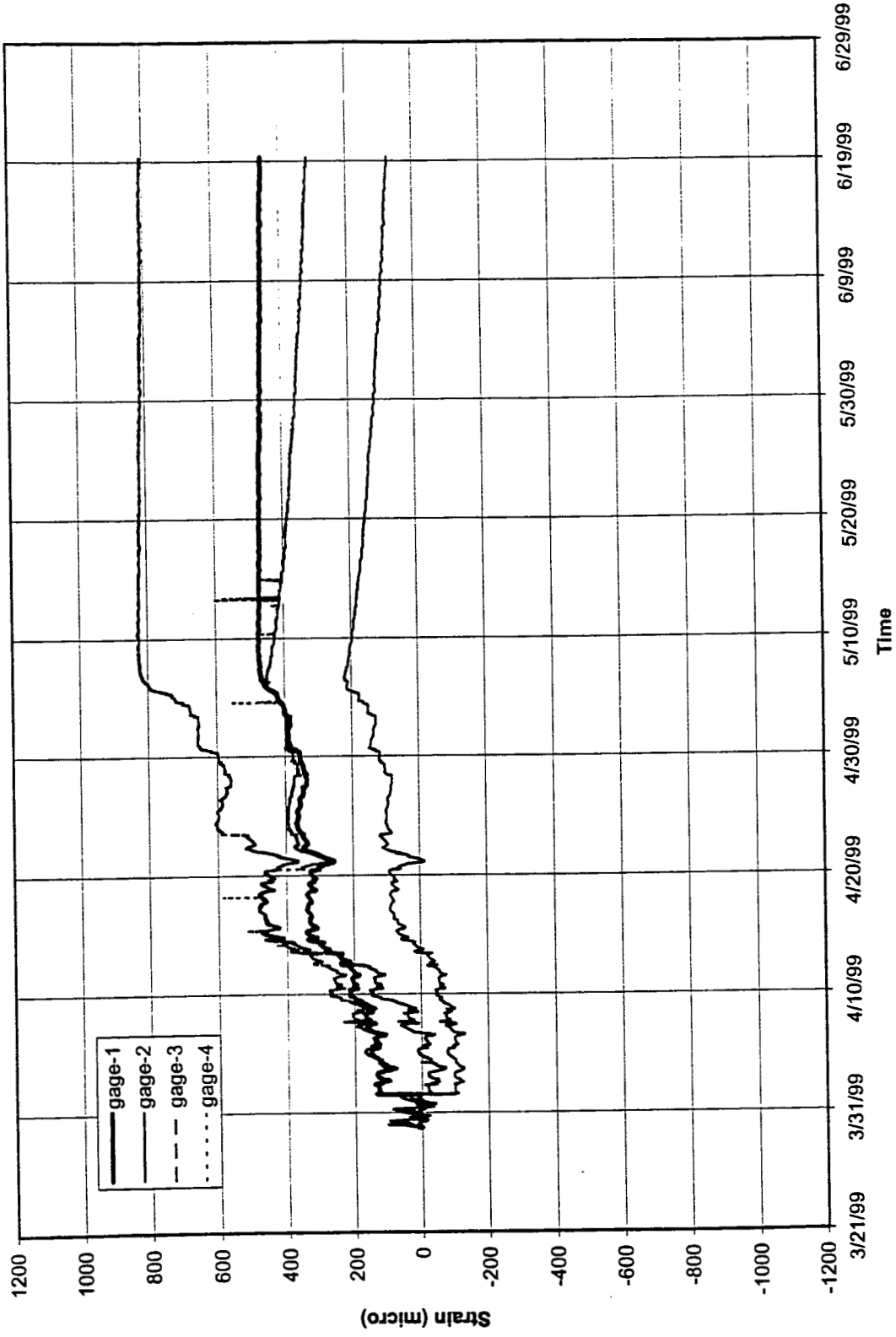


Fig. 4.96: Tie-beam #14, Strain from gages on driven pile cap side.

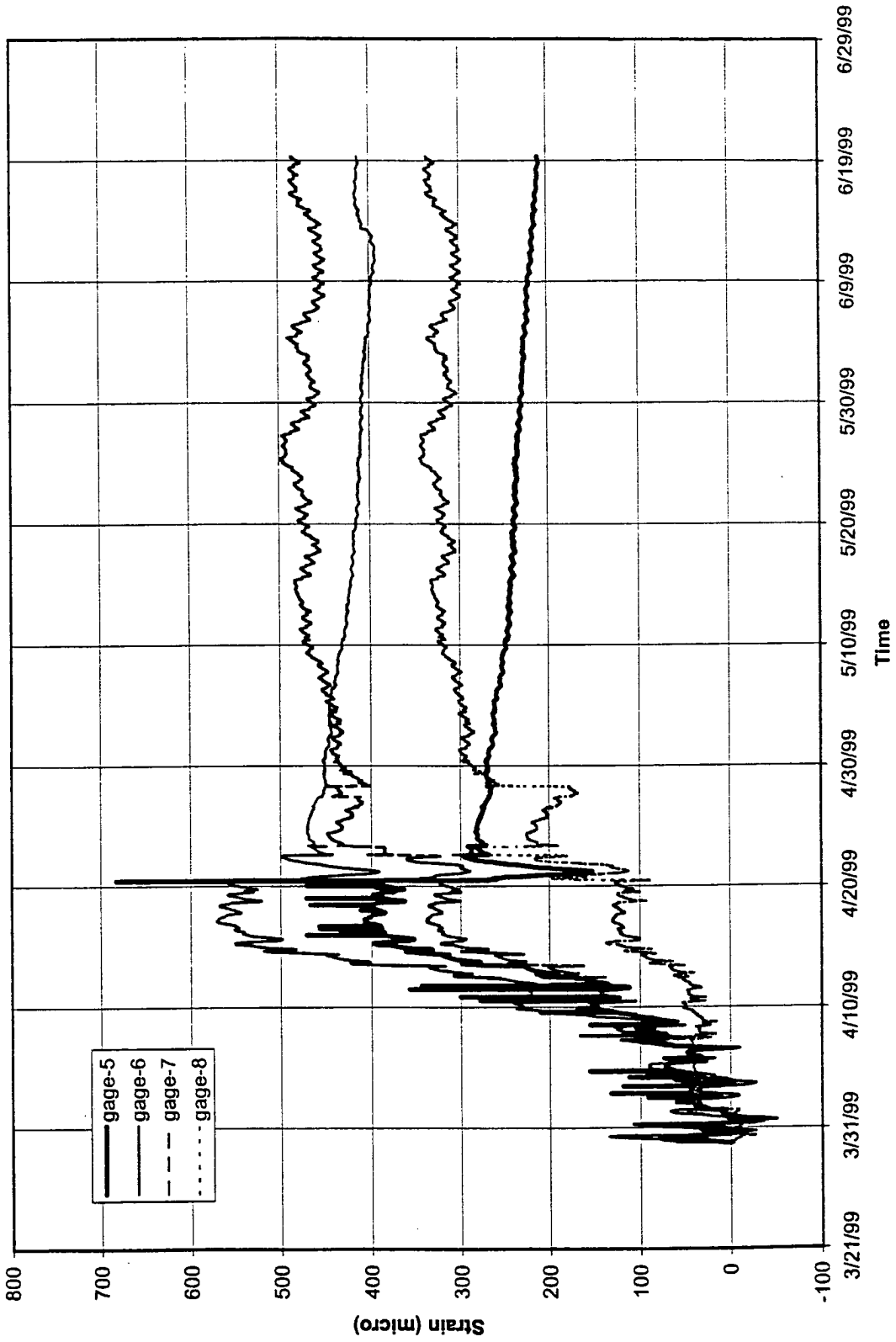


Fig. 4.97: Tie-beam #14, Strain from gages on drilled shaft cap side.

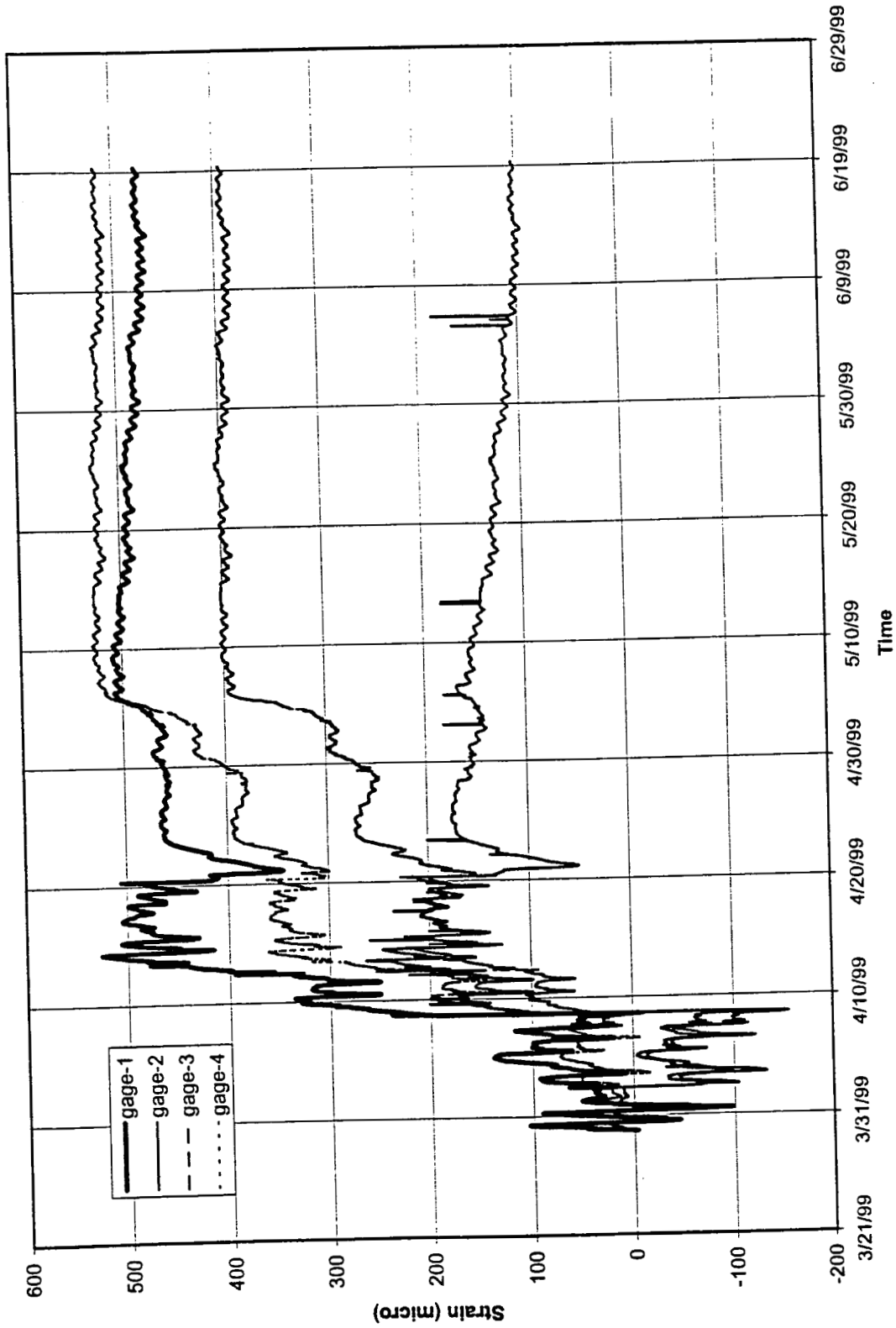


Fig. 4.98: Tie-beam #26, Strain from gages on driven pile cap side.

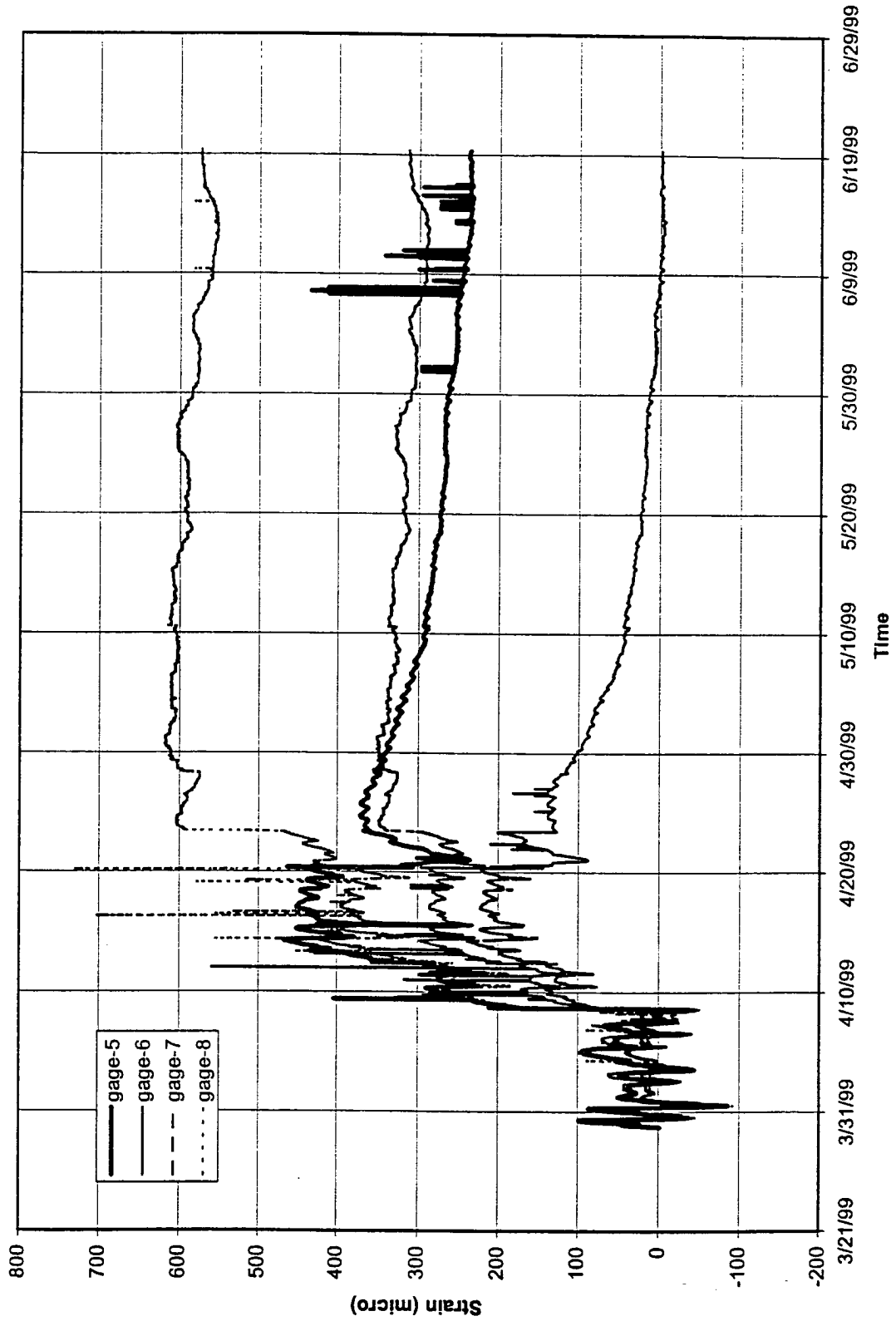


Fig. 4.99: Tie-beam #26, Strain from gages on drilled shaft cap side.

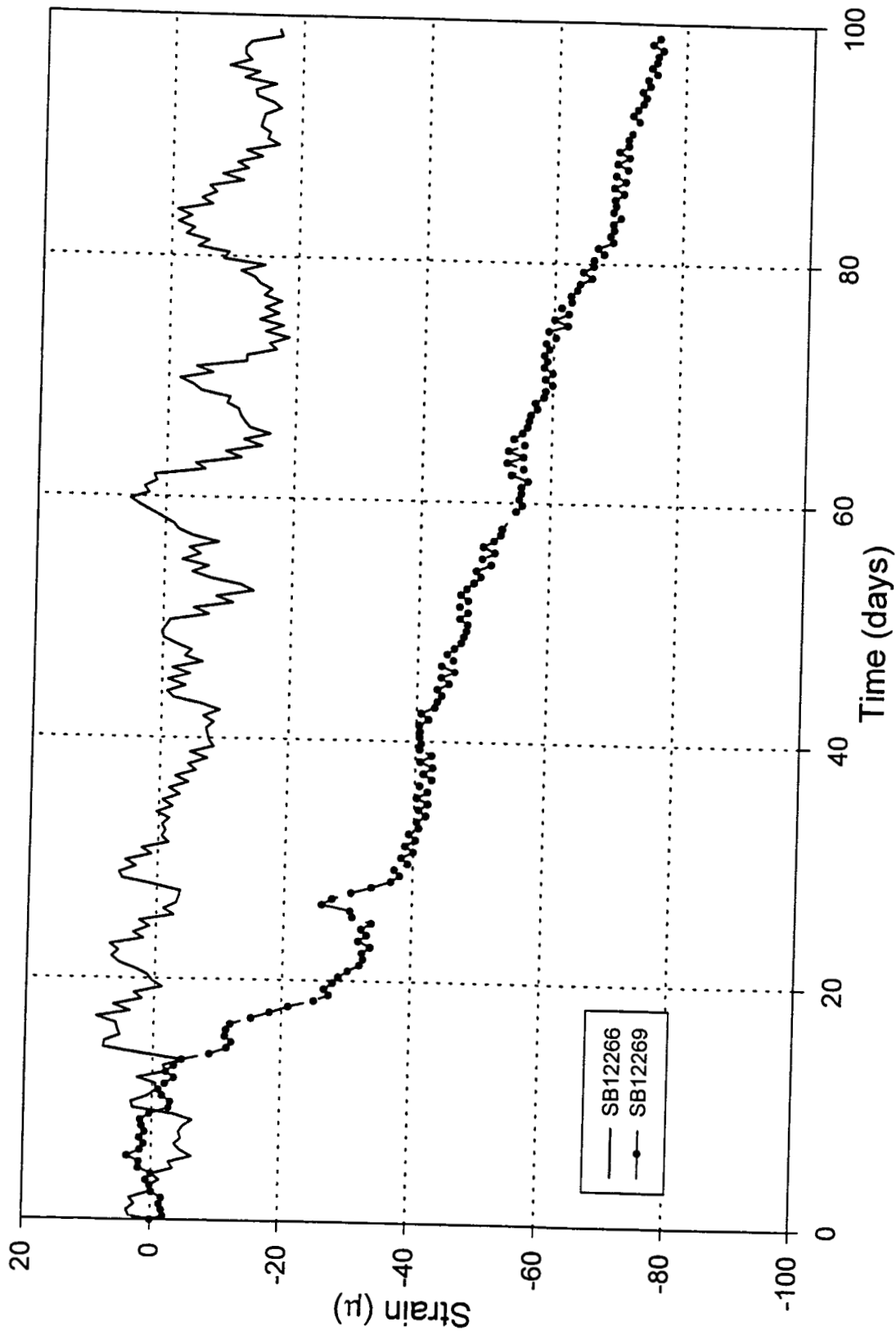


Fig. 4.100: Shaft 1, strain vs. time from gages 9.5 feet below top of shaft cap.

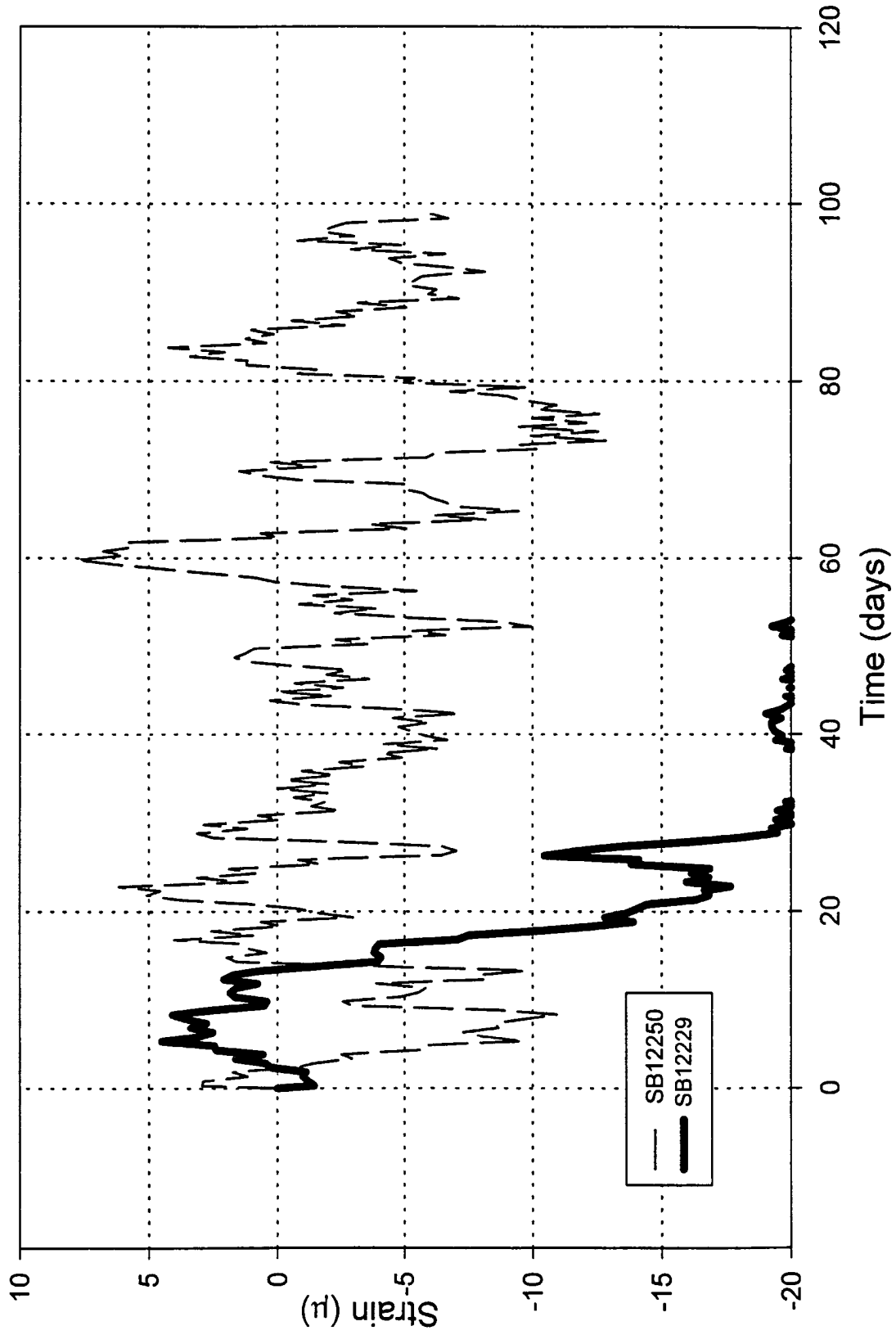


Fig. 4.101: Shaft I, strain vs. time from gages 16 feet below top of shaft cap.

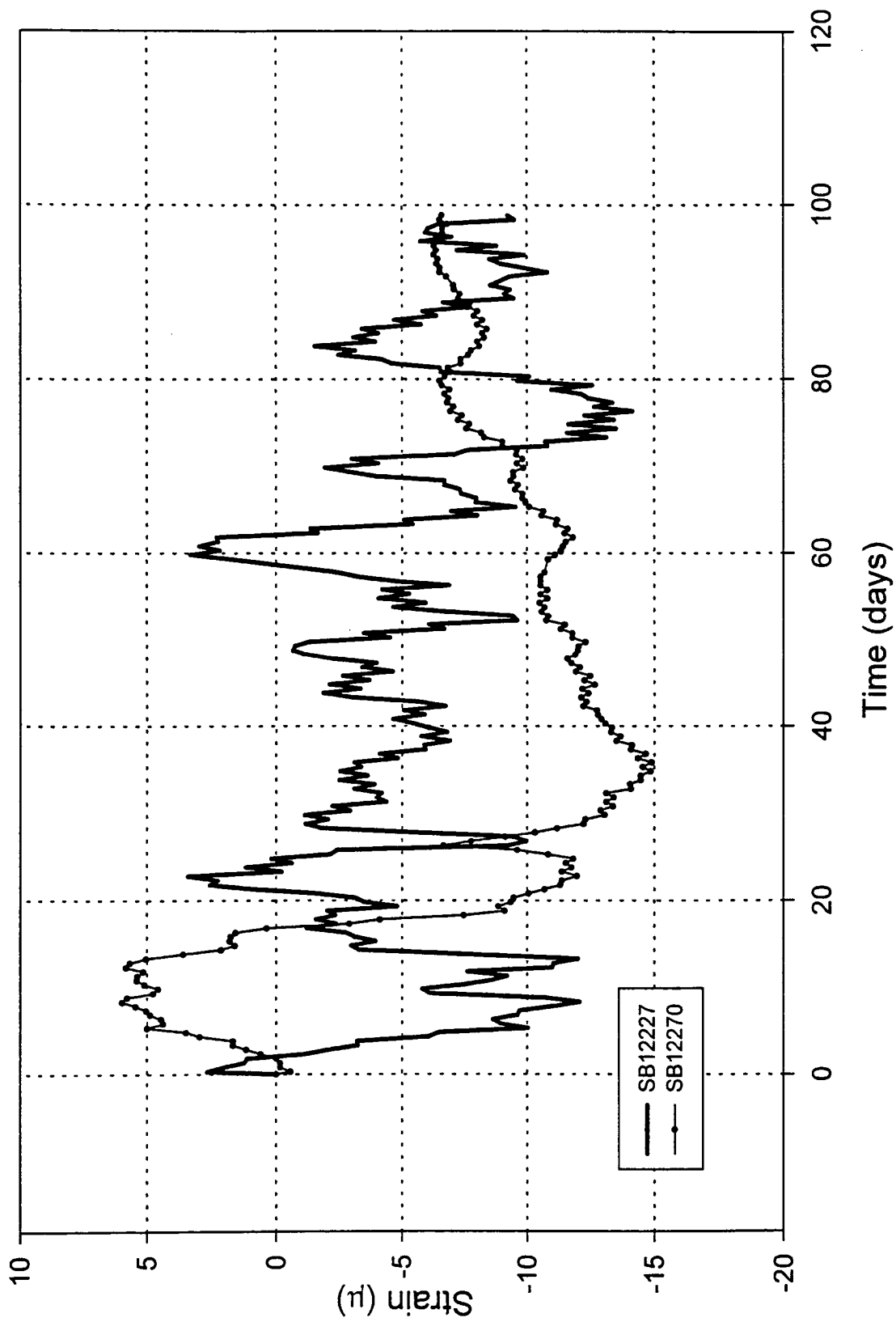


Fig. 4.102: Shaft 1, strain vs. time from gages 22.5 feet below top of shaft cap.

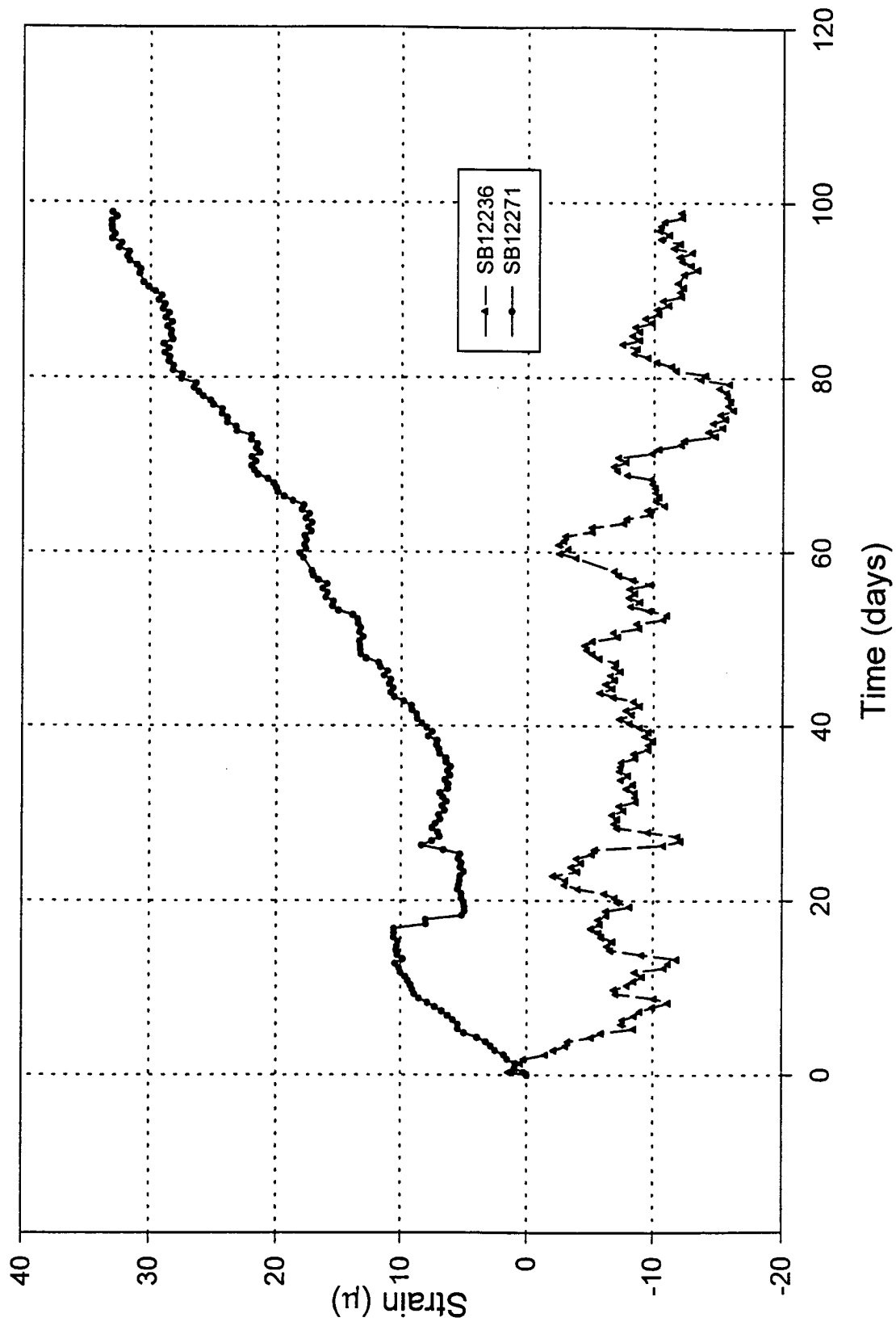


Fig. 4.103: Shaft 1, strain vs. time from gages 29 feet below top of shaft cap.



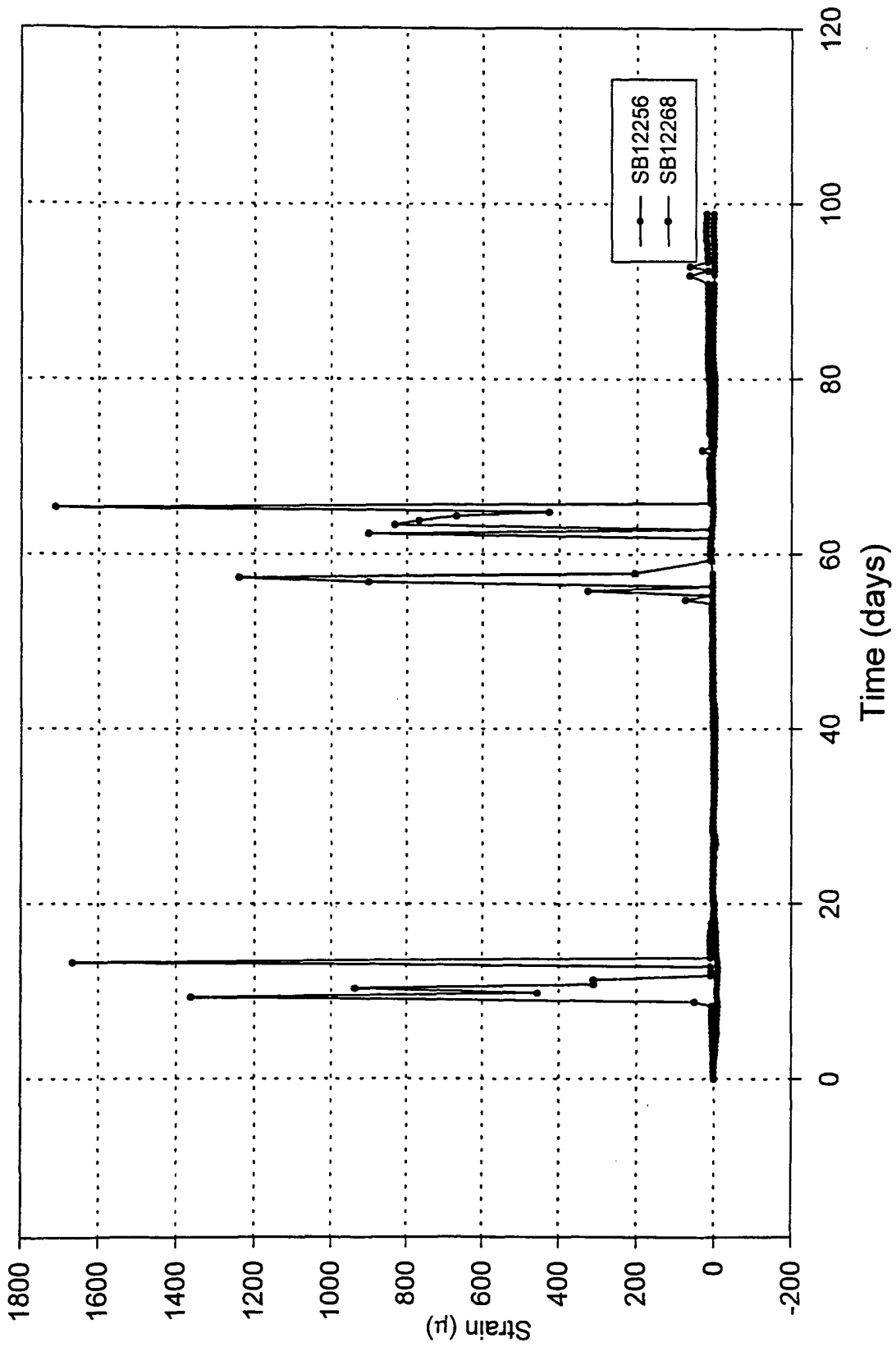


Fig. 4.104: Shaft 1, strain vs. time from gages 35.5 feet below top of shaft cap.

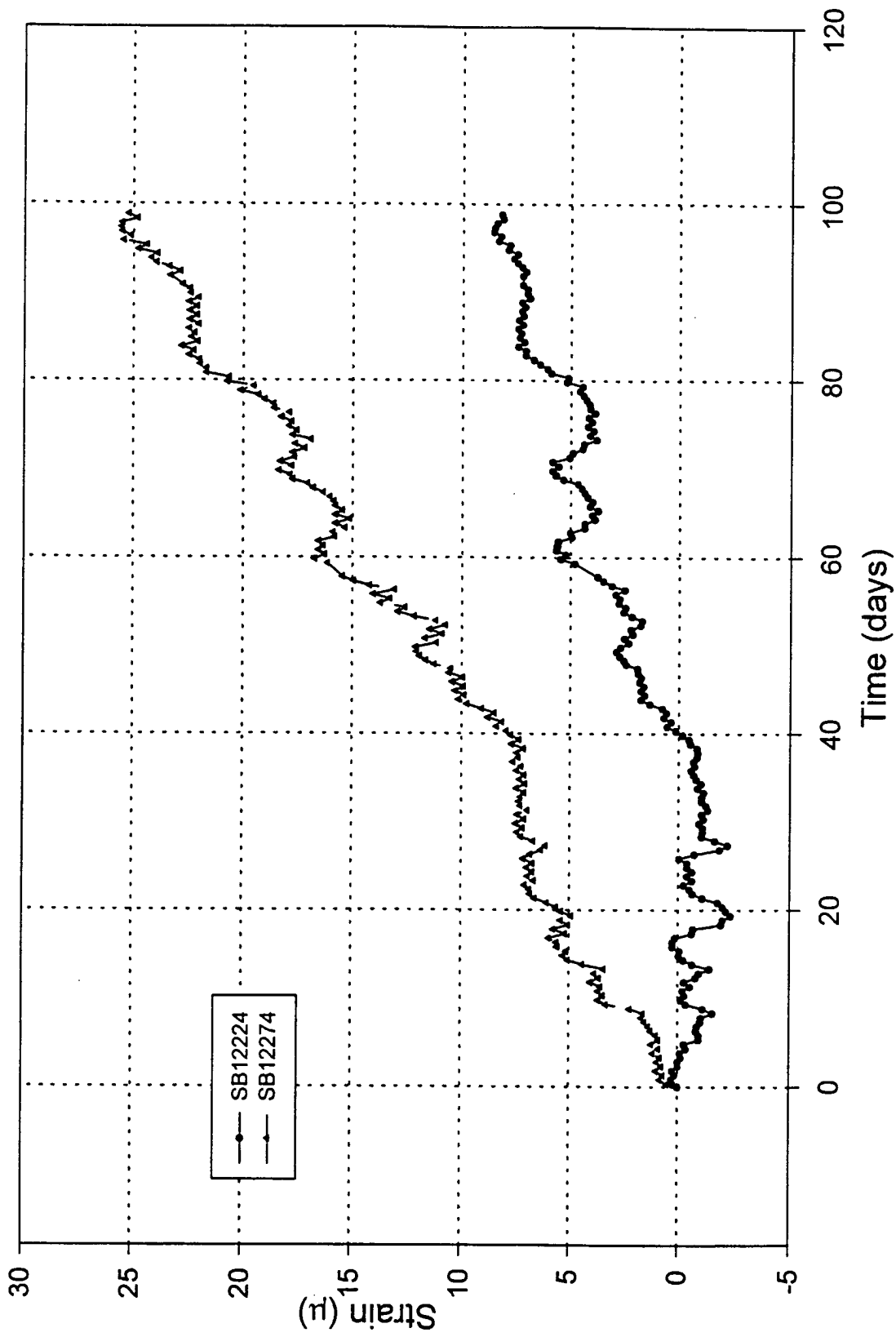


Fig. 4.105: Shaft 1, strain vs. time from gages 42 feet below top of shaft cap.

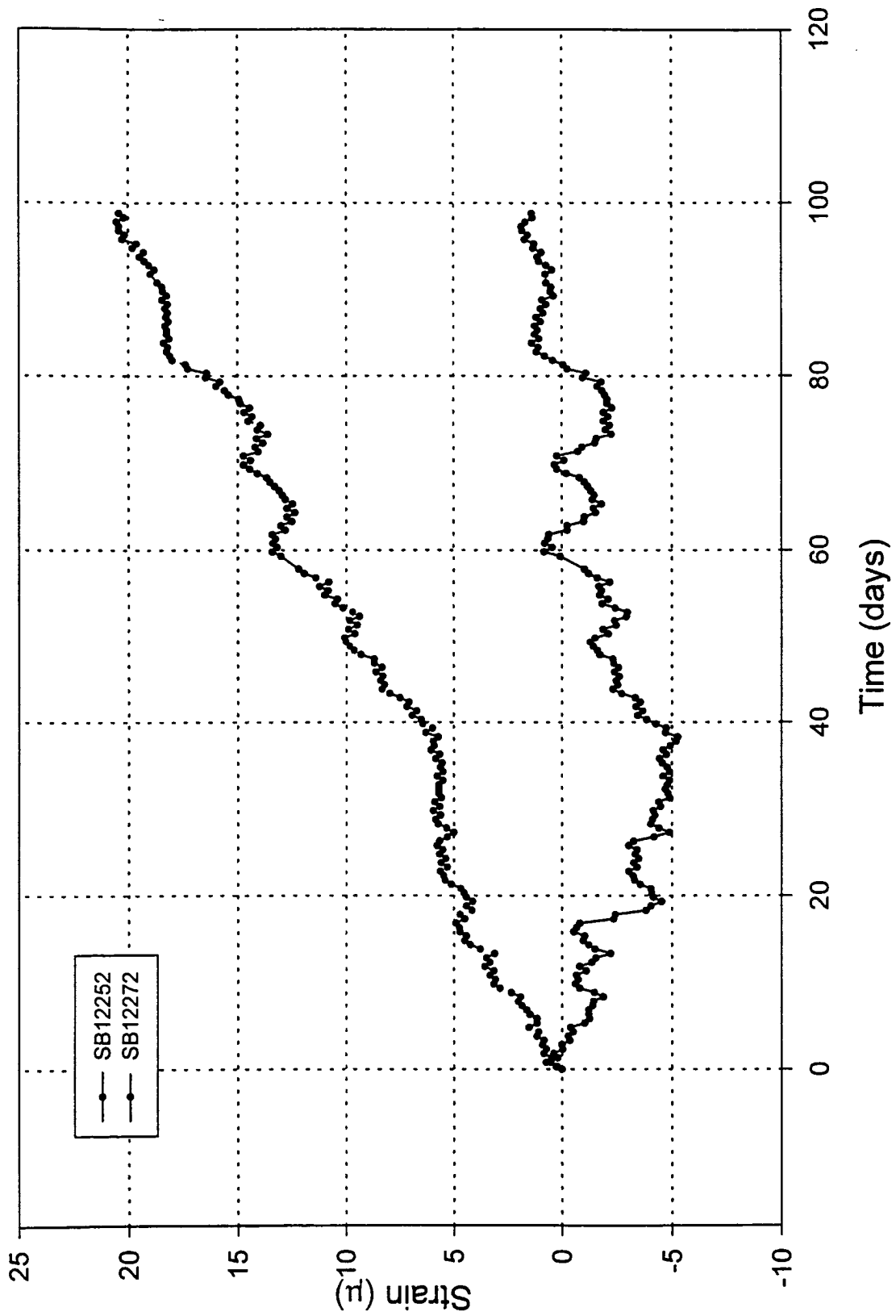


Fig. 4.106: Shaft 1, strain vs. time from gages 47.33 feet below top of shaft cap.

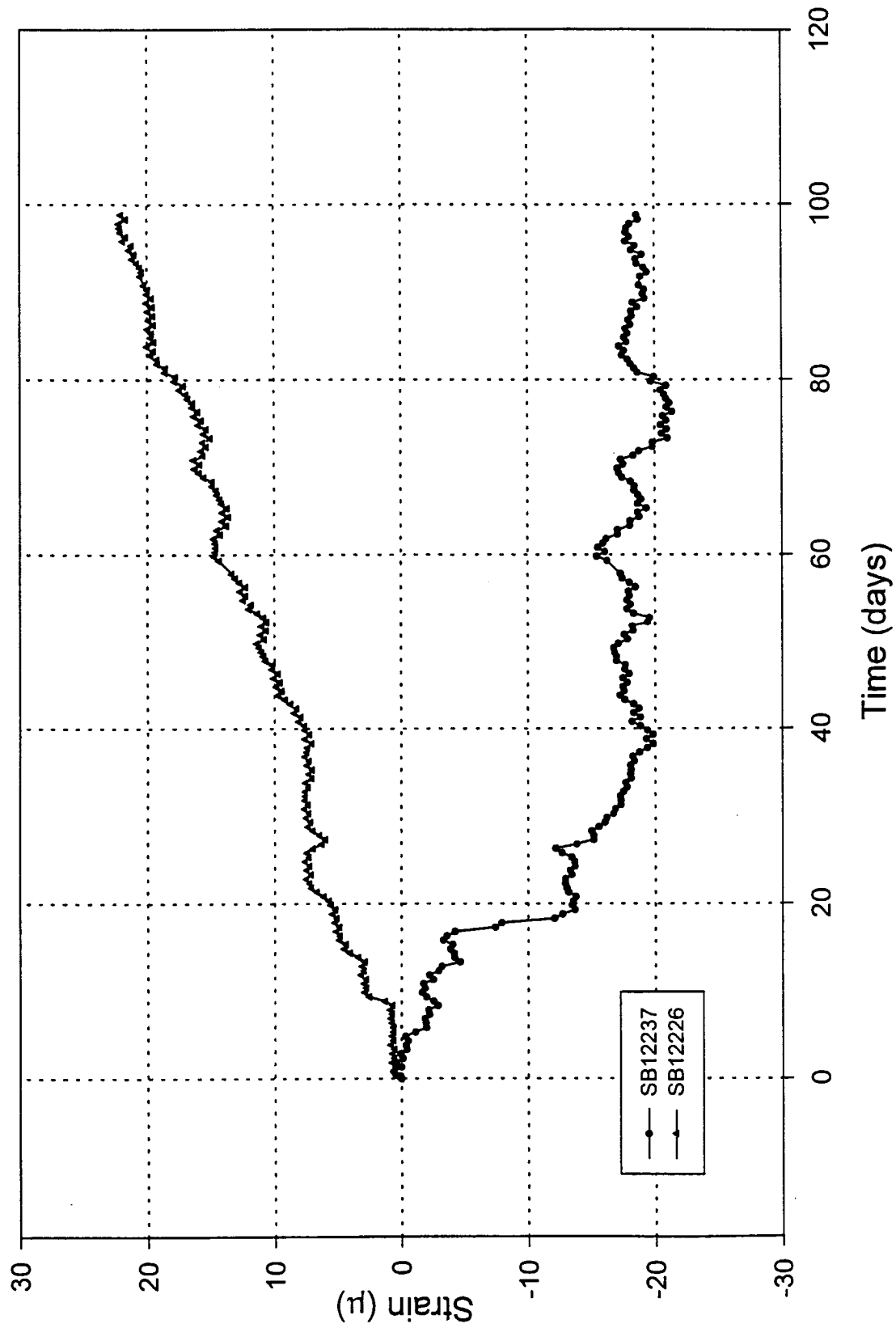


Fig. 4.107: Shaft 1, strain vs. time from gages 54.83 feet below top of shaft cap.

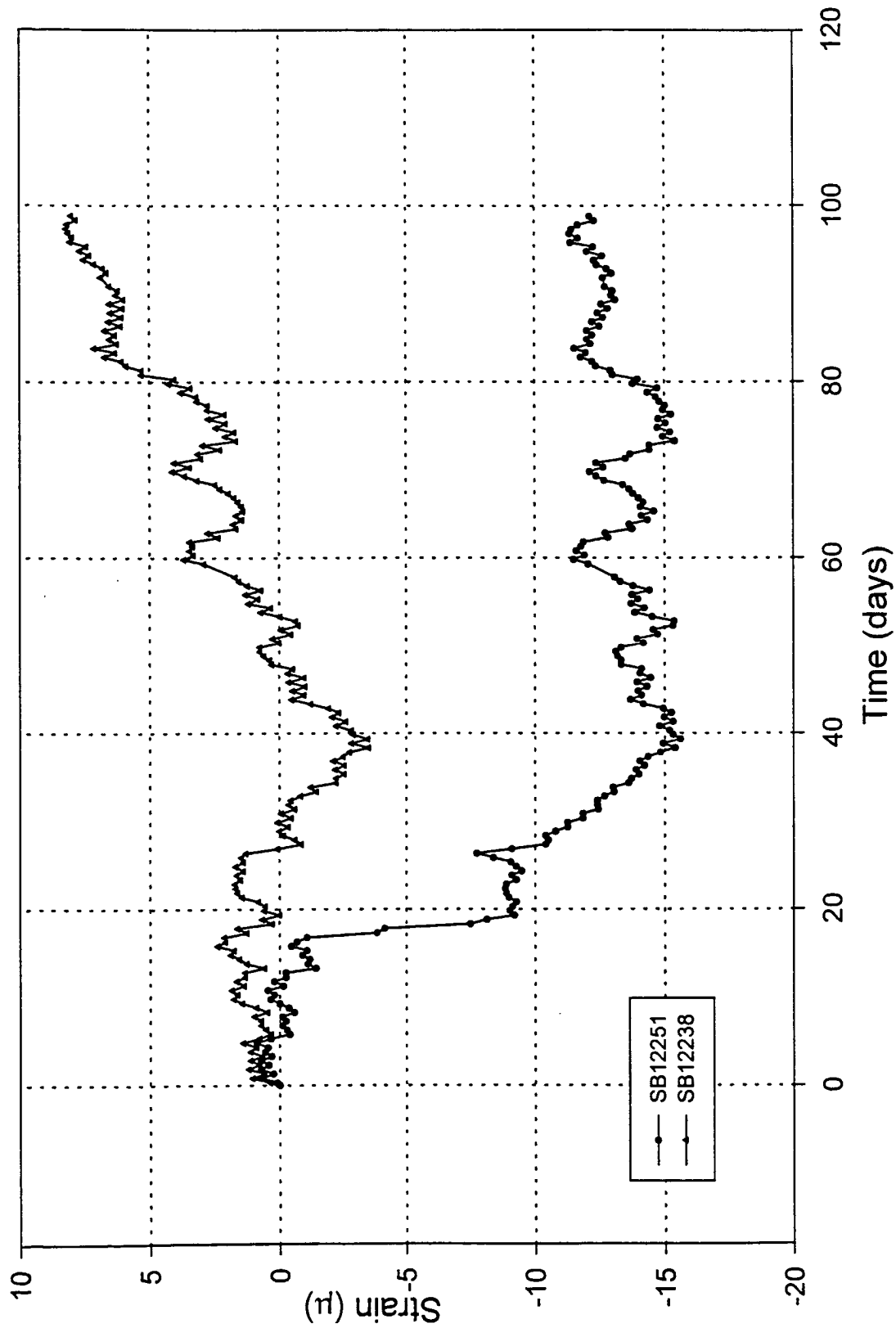


Fig. 4.108: Shaft 1, strain vs. time from gages 64.83 feet below top of shaft cap.

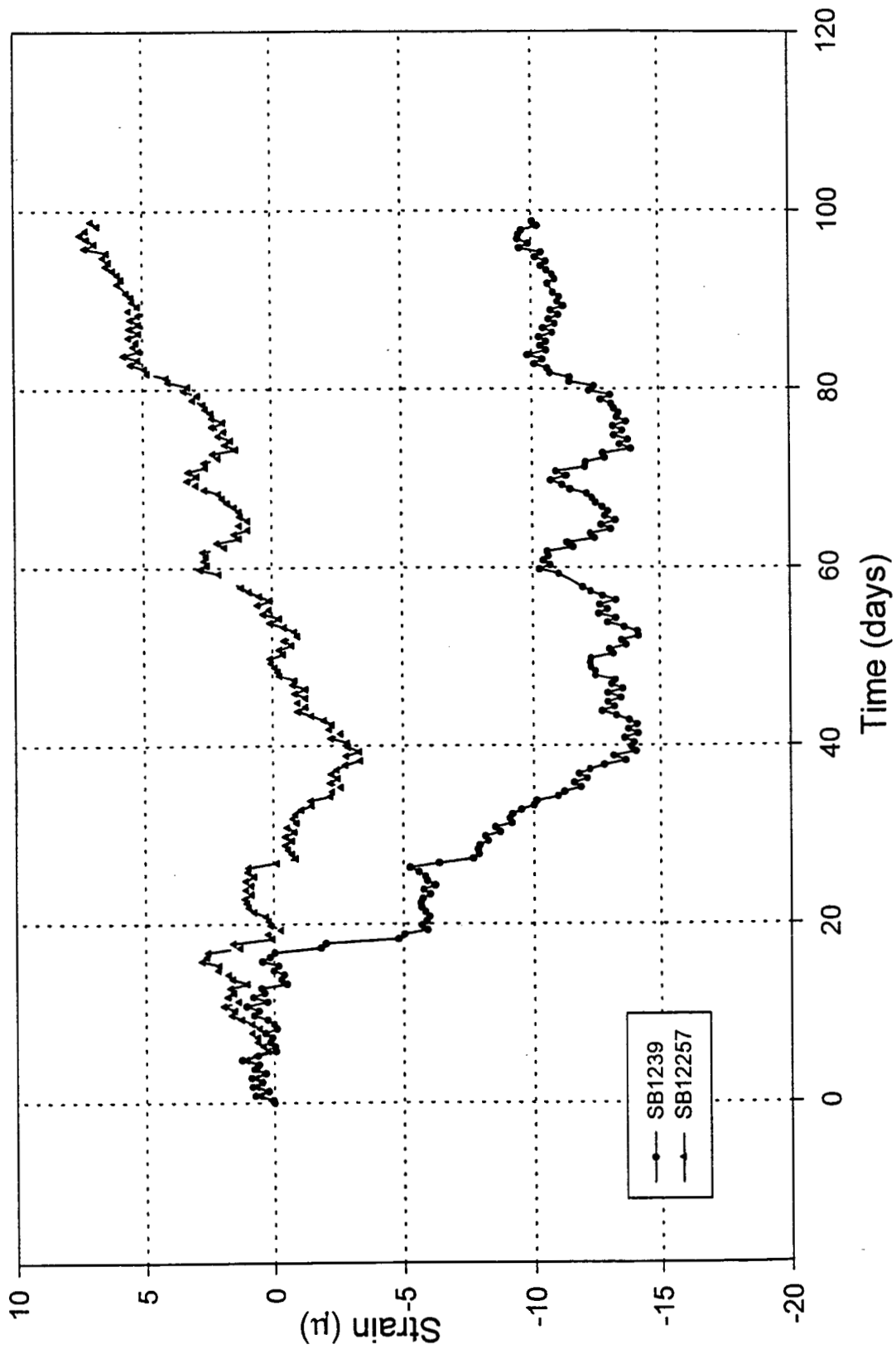


Fig. 4.109: Shaft 1, strain vs. time from gages 74.83 feet below top of shaft cap.

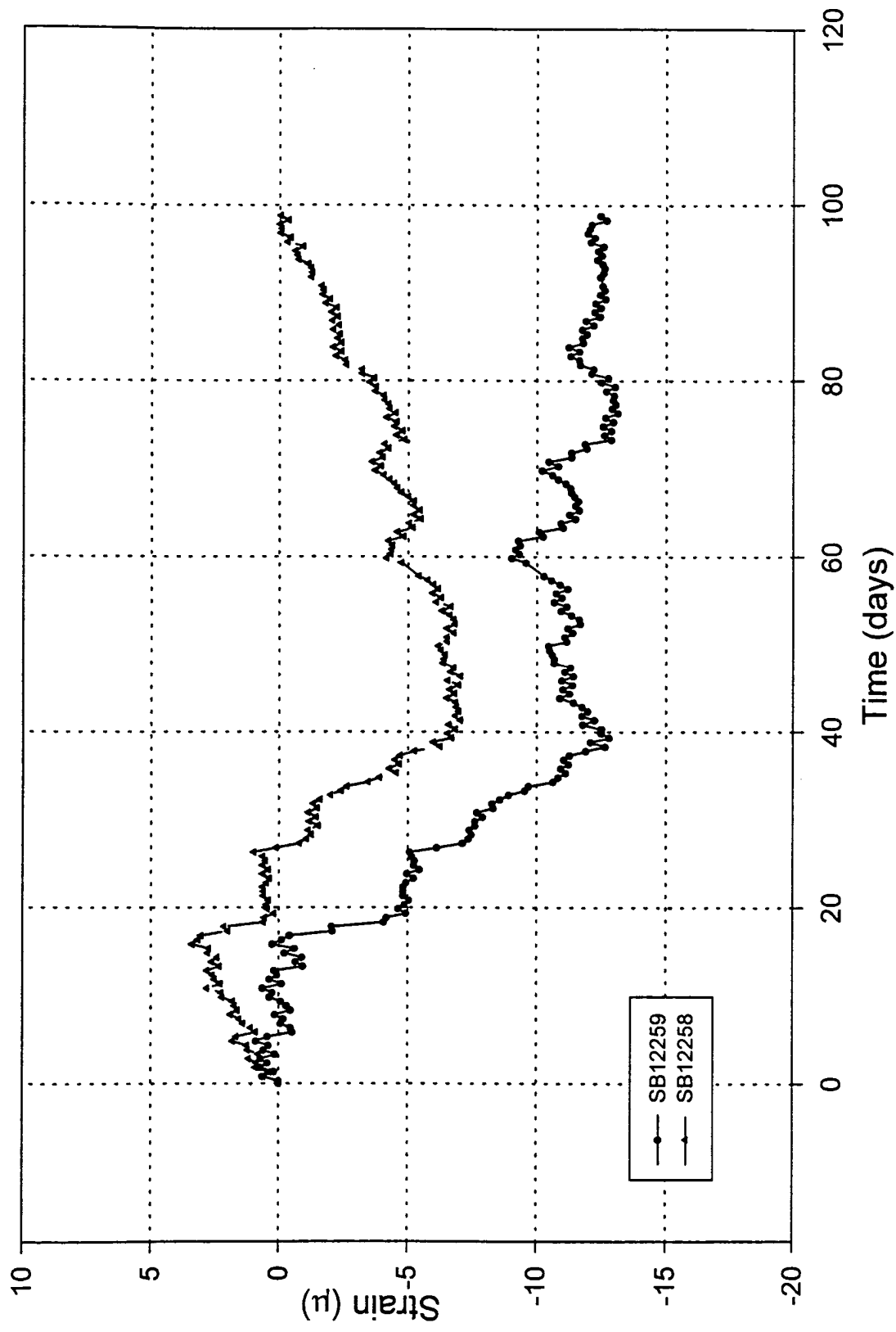


Fig. 4.110: Shaft 1, strain vs. time from gages 84.83 feet below top of shaft cap.

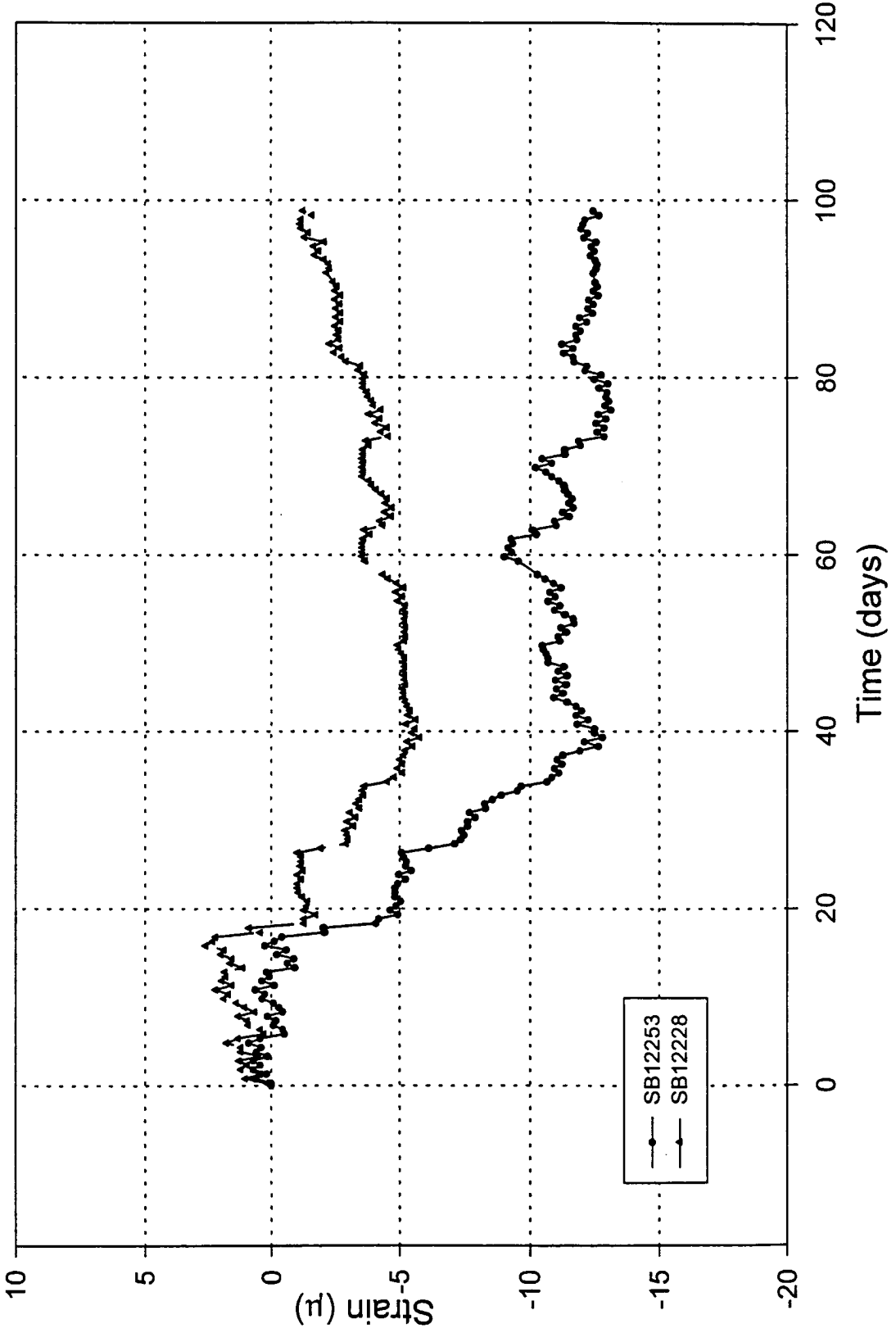


Fig. 4.111: Shaft 1, strain vs. time from gages 94.83 feet below top of shaft cap.



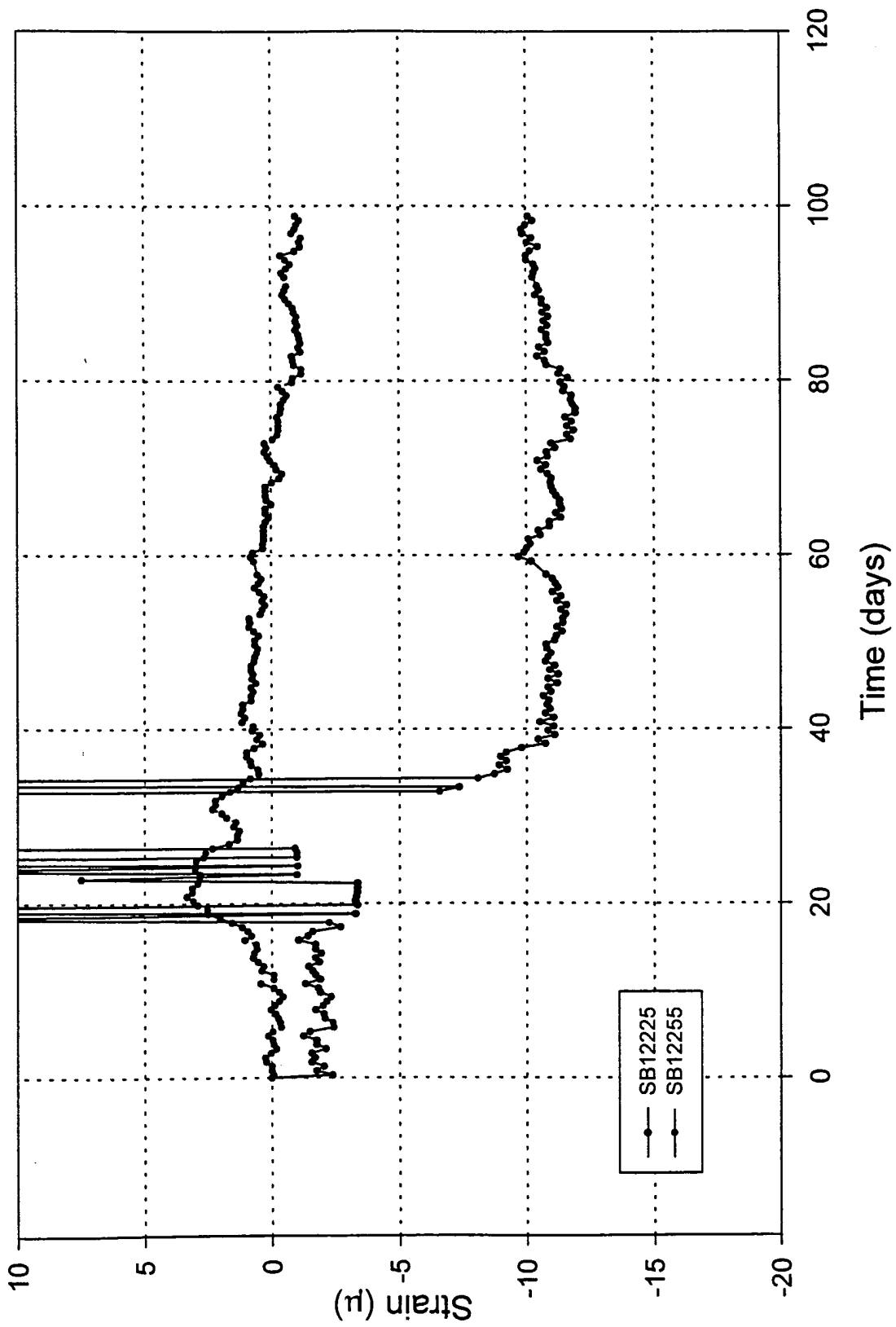


Fig. 4.112: Shaft 1, strain vs. time from gages 115 feet below top of shaft cap.

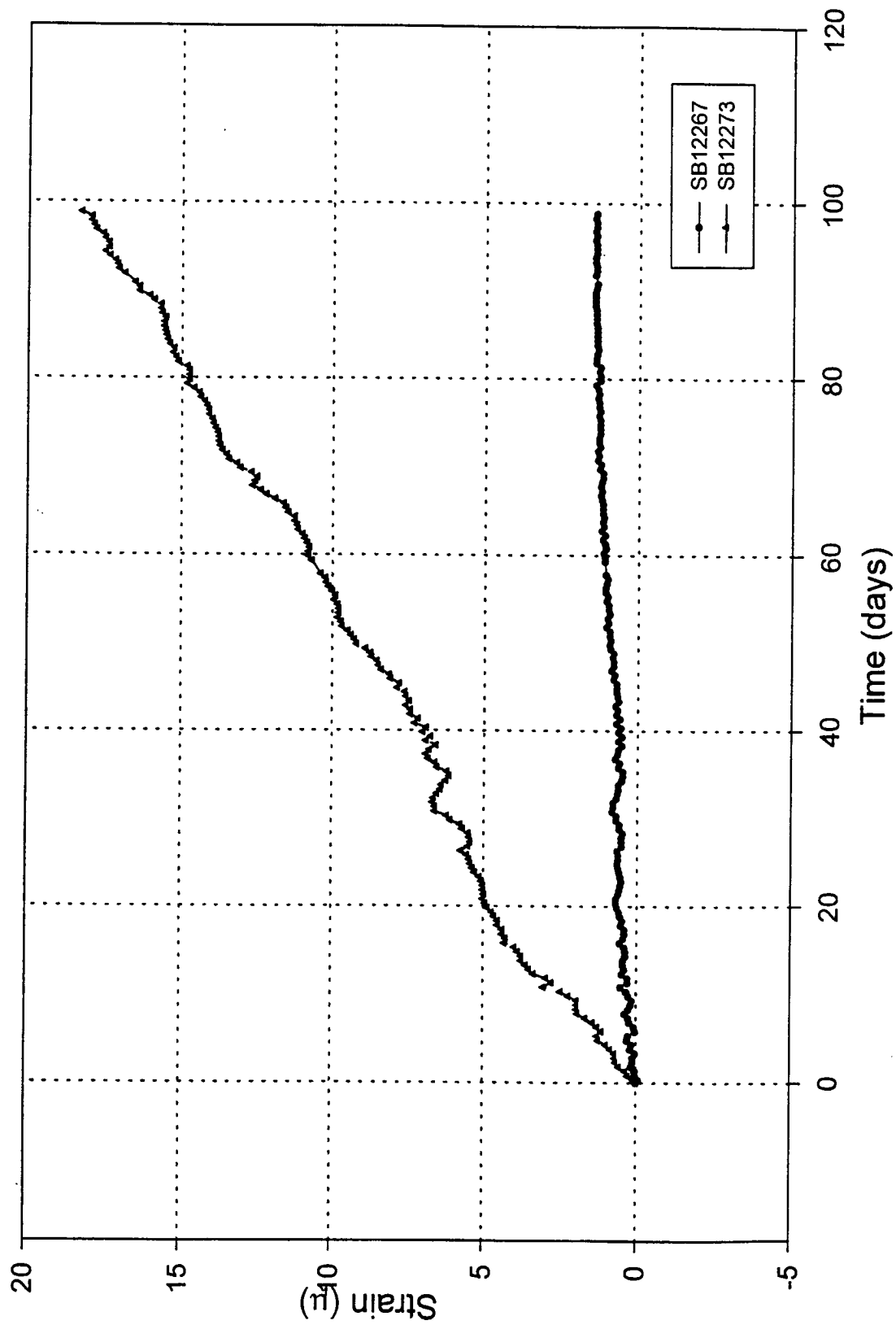


Fig. 4.113: Shaft 1, strain vs. time from gages 135 feet below top of shaft cap.

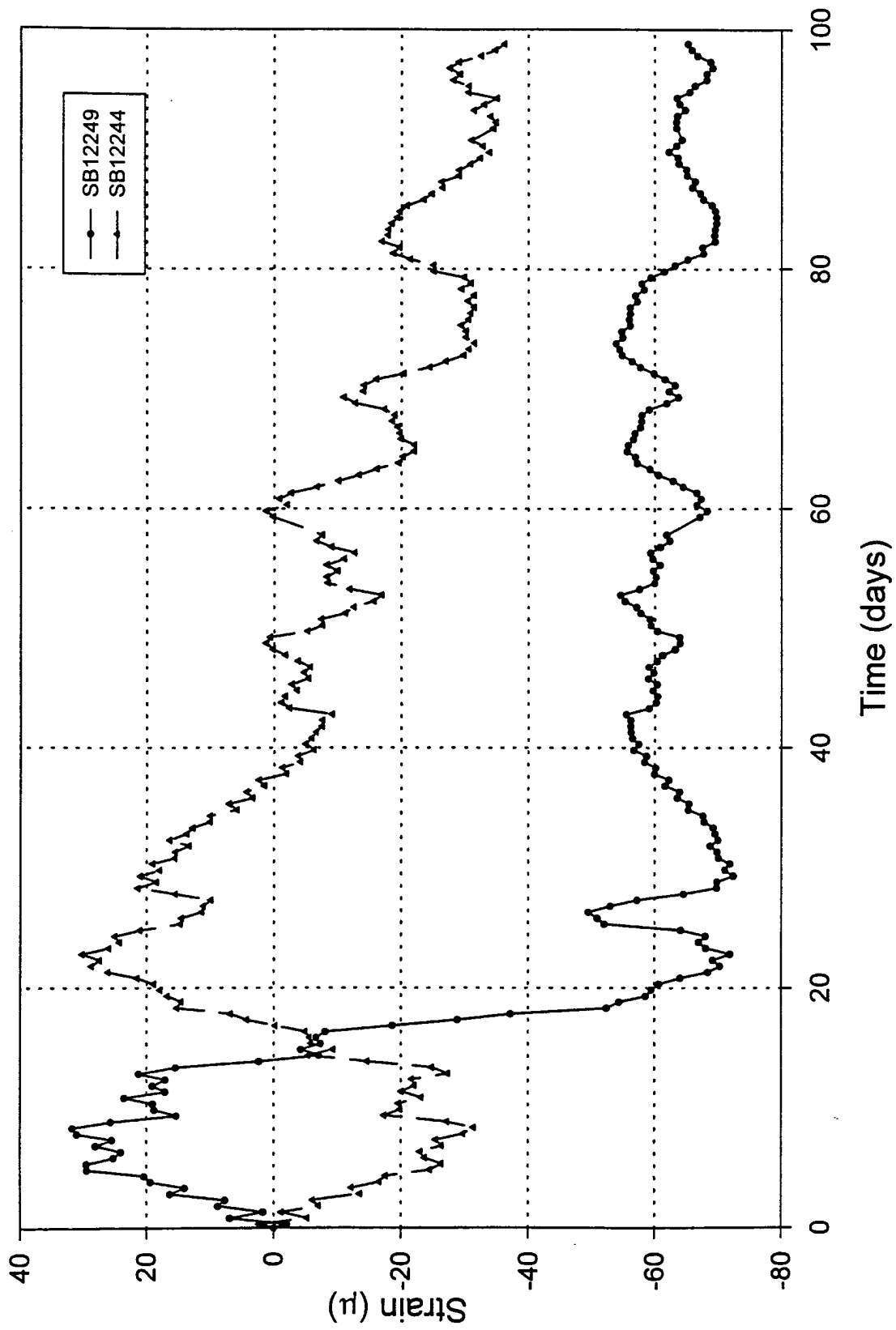


Fig. 4.114: Shaft 9, strain vs. time from gages 11 feet below top of shaft cap.

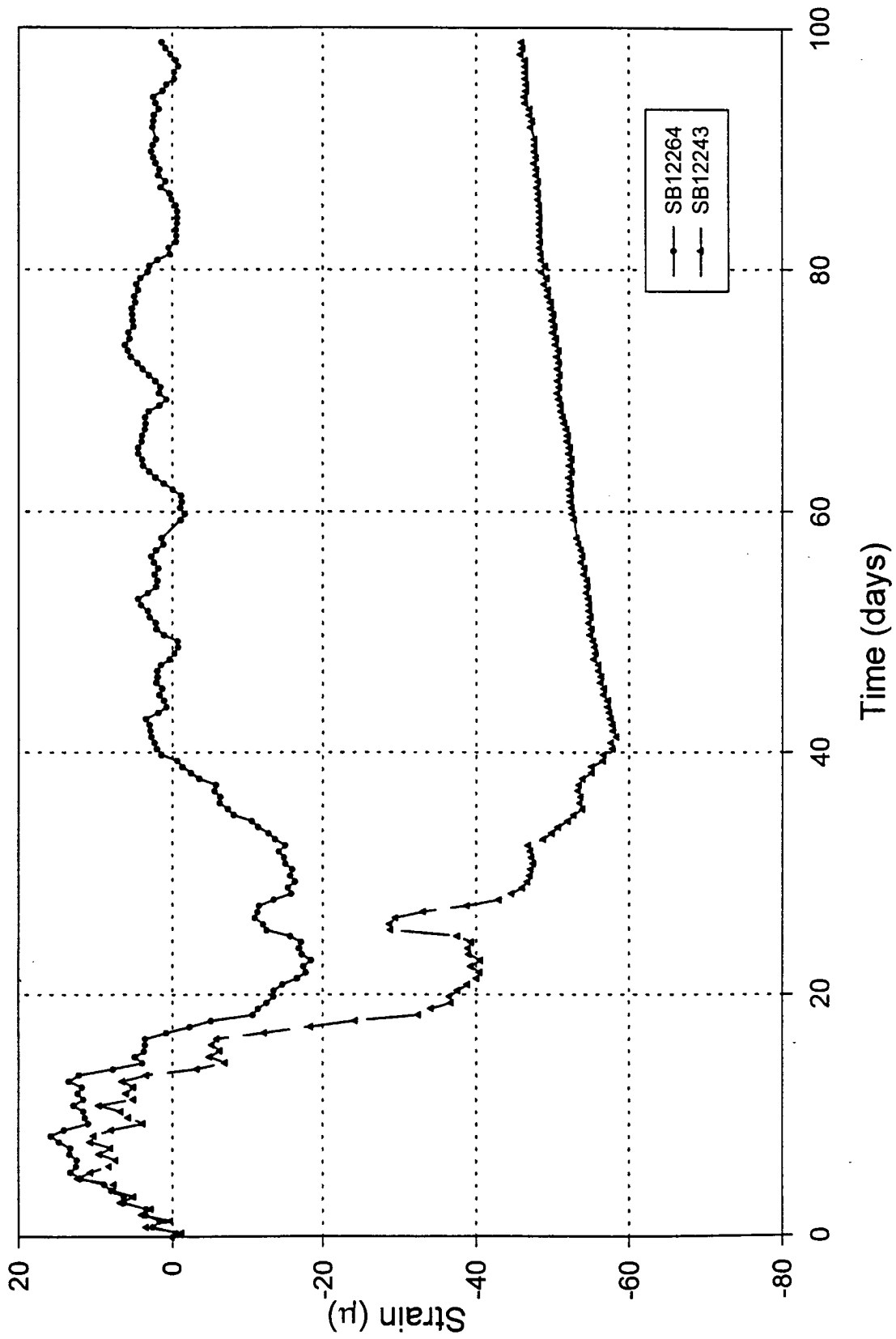


Fig. 4.115: Shaft 9, strain vs. time from gages 17.5 feet below top of shaft cap.

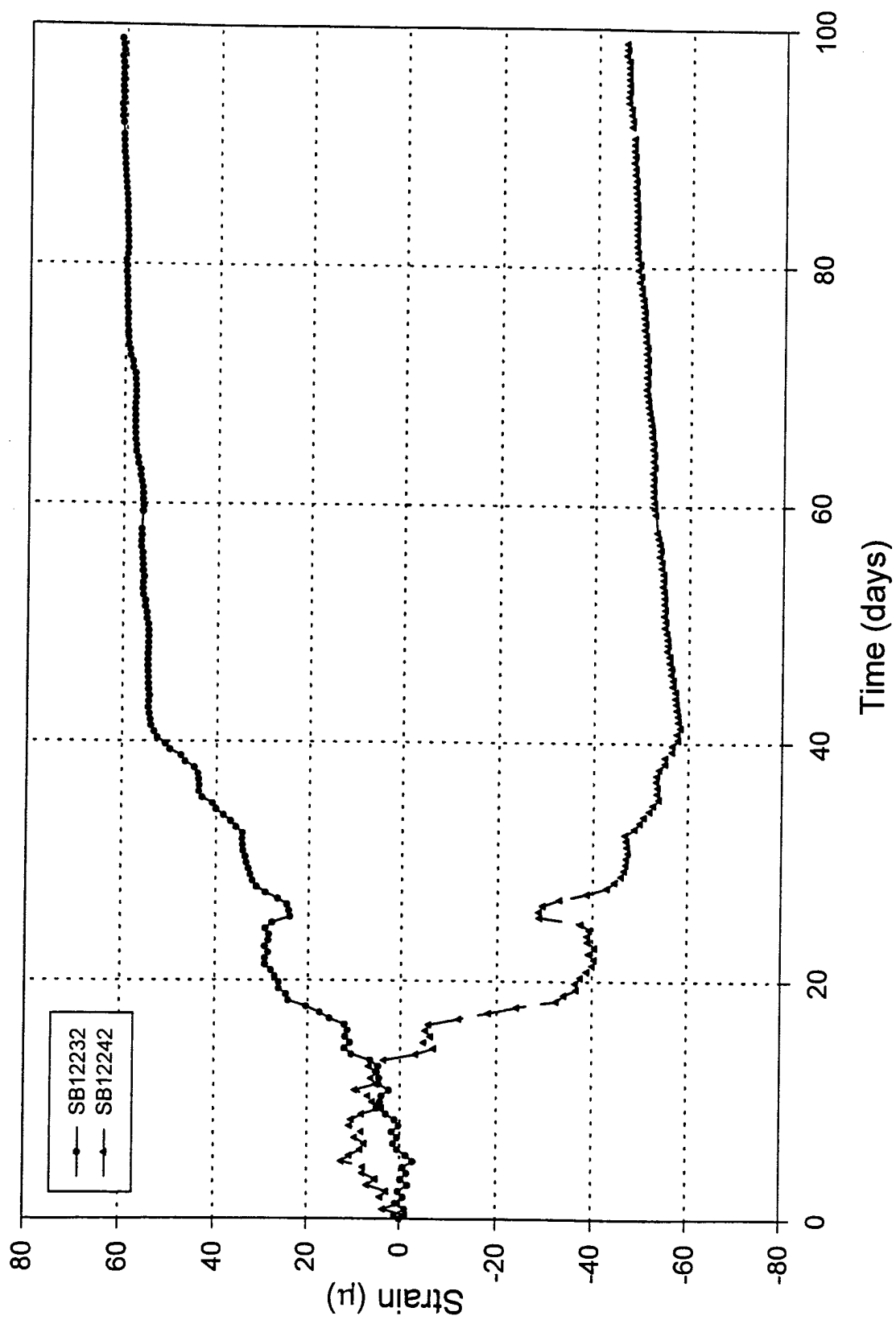


Fig. 4.116: Shaft 9, strain vs. time from gages 24 feet below top of shaft cap.

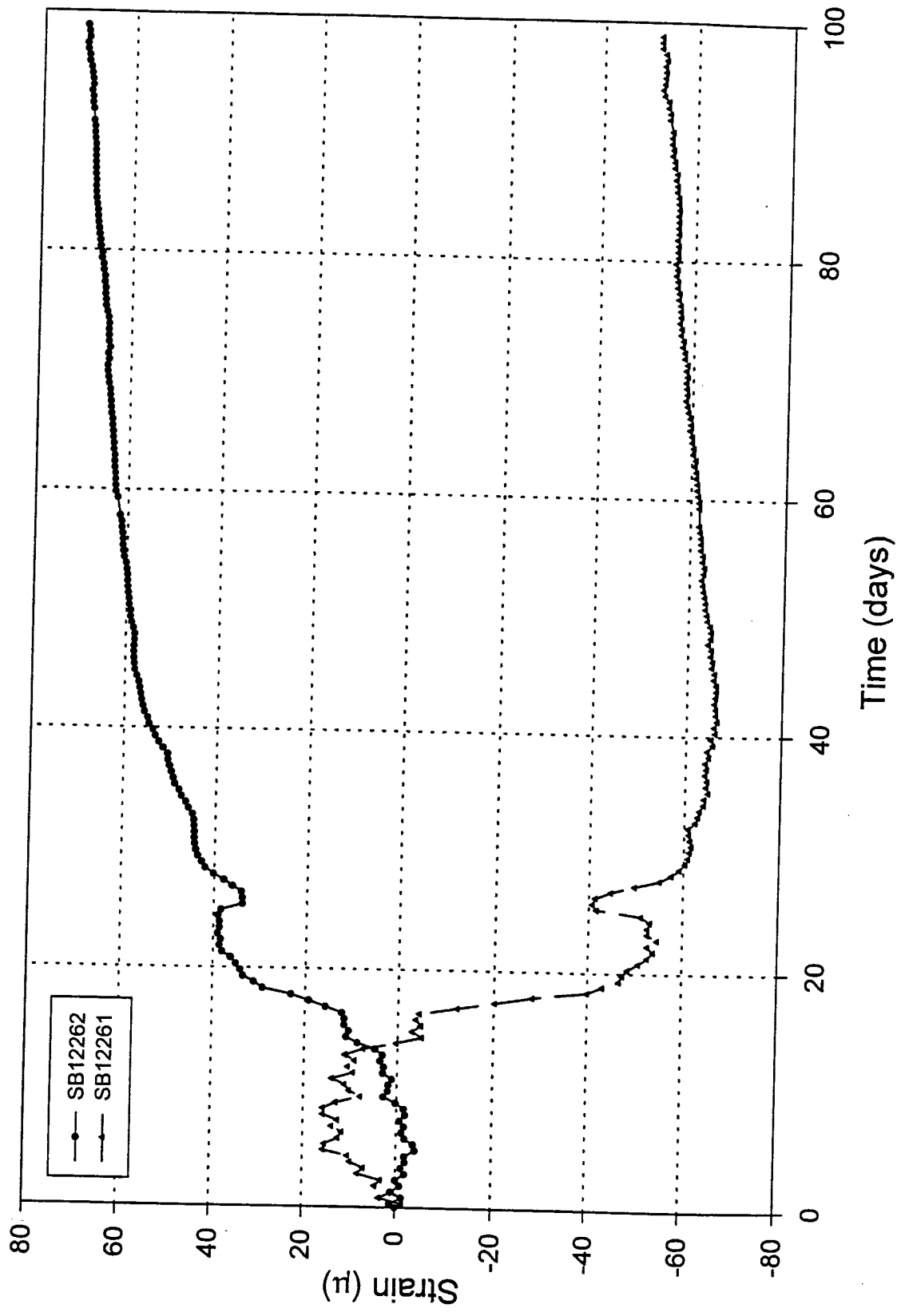


Fig. 4.117: Shaft 9, strain vs. time from gages 30.5 feet below top of shaft cap.

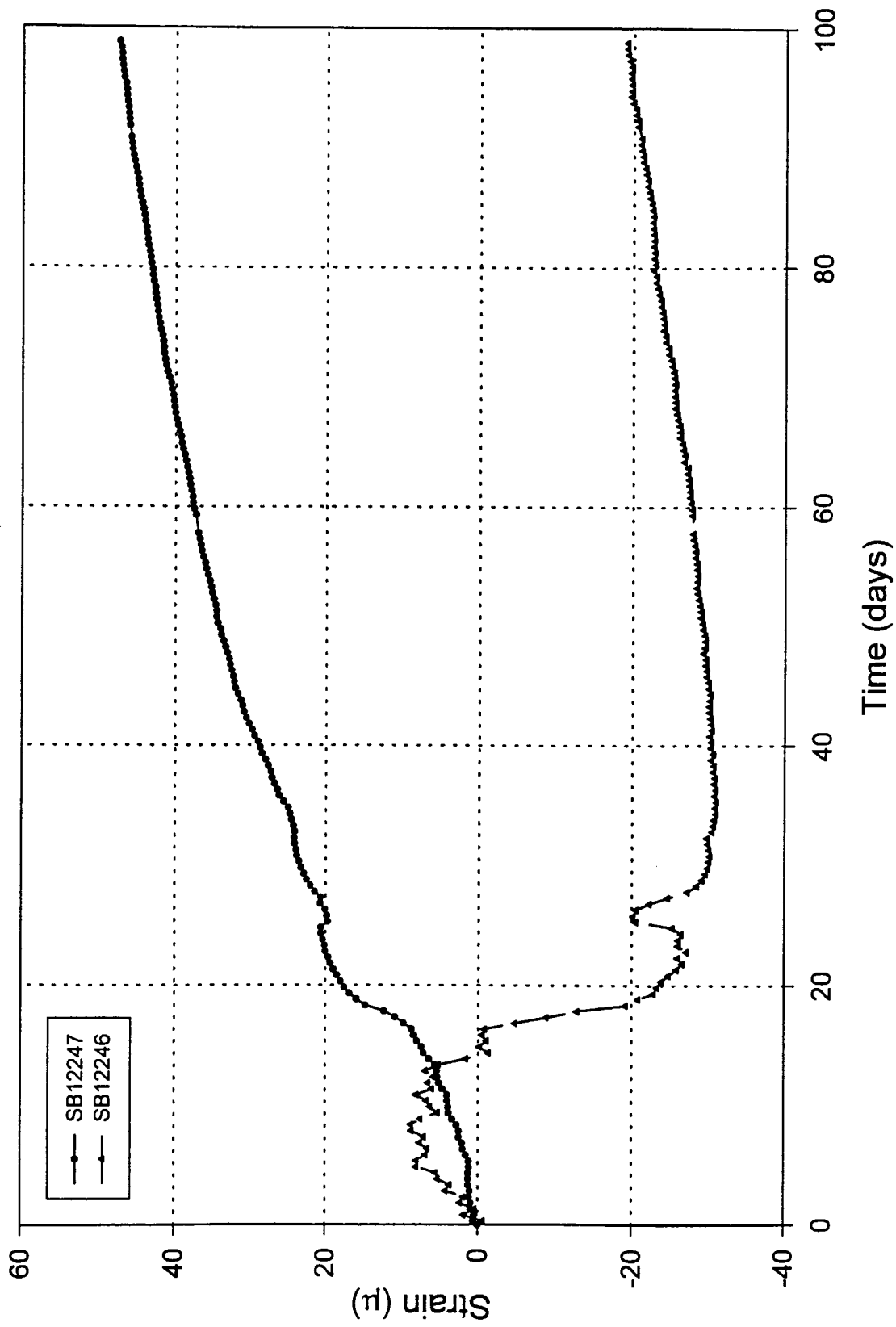


Fig. 4.118: Shaft 9, strain vs. time from gages 37 feet below top of shaft cap.

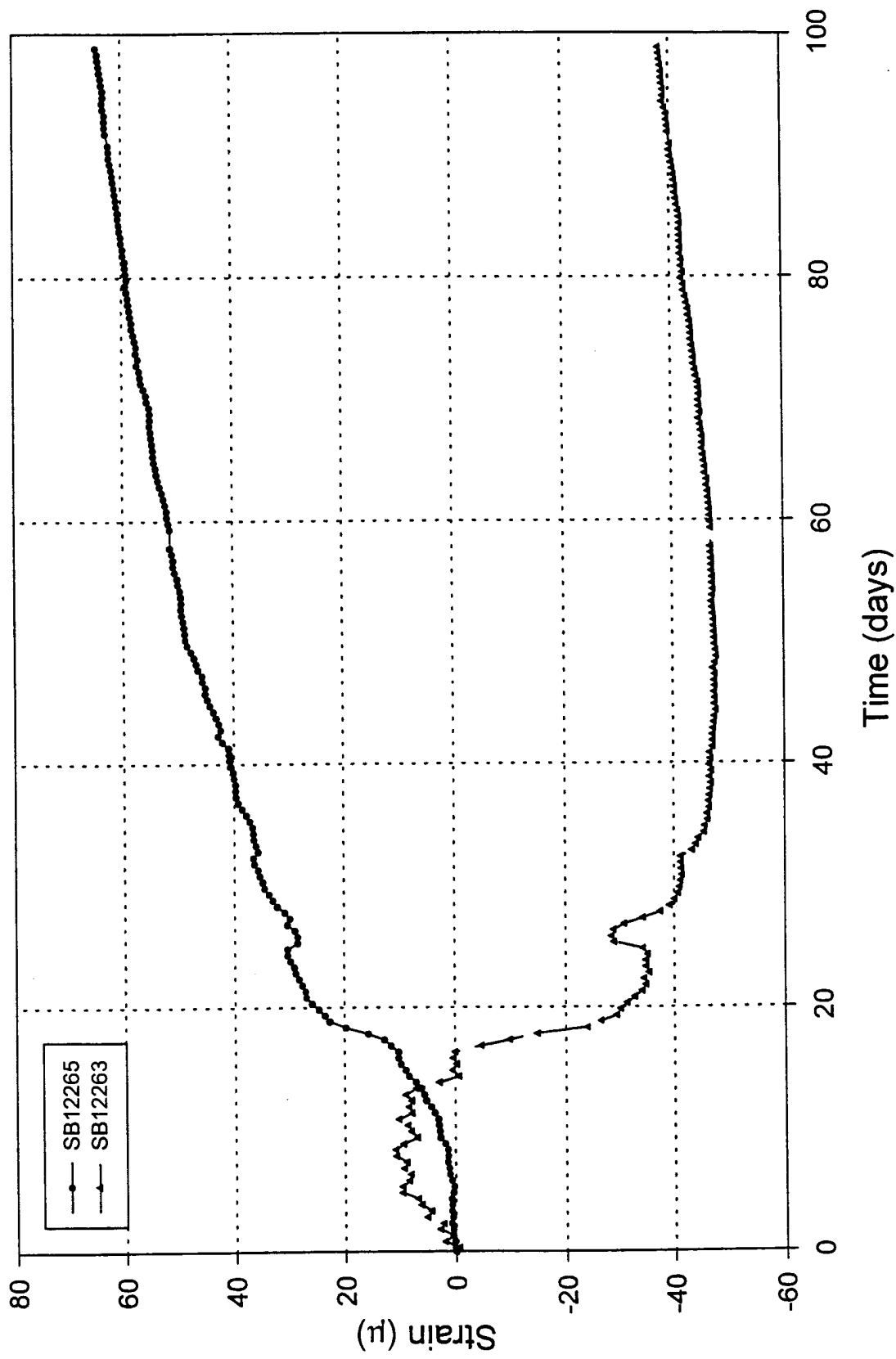


Fig. 4.119: Shaft 9, strain vs. time from gages 43.5 feet below top of shaft cap.



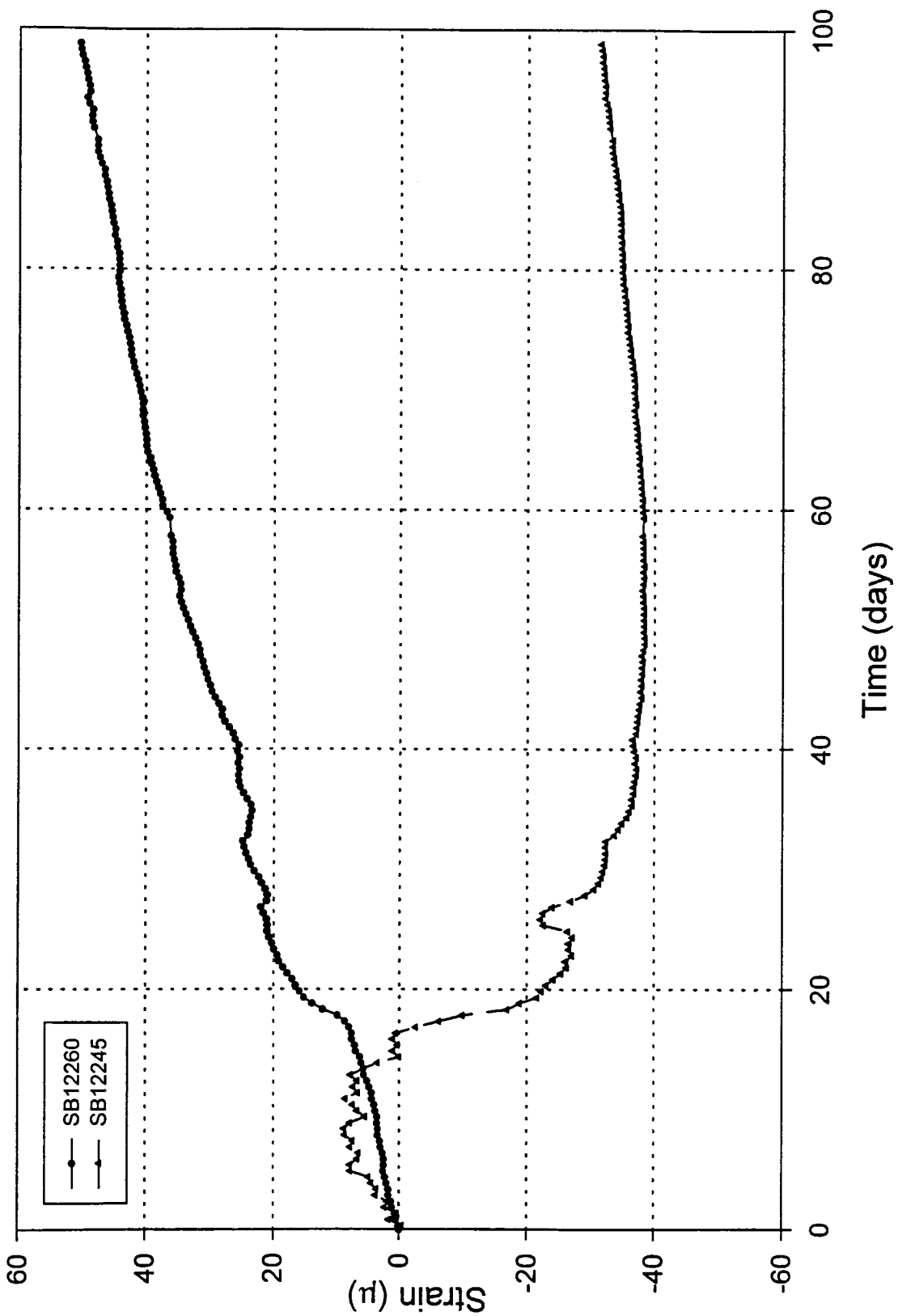


Fig. 4.120: Shaft 9, strain vs. time from gages 50 feet below top of shaft cap.

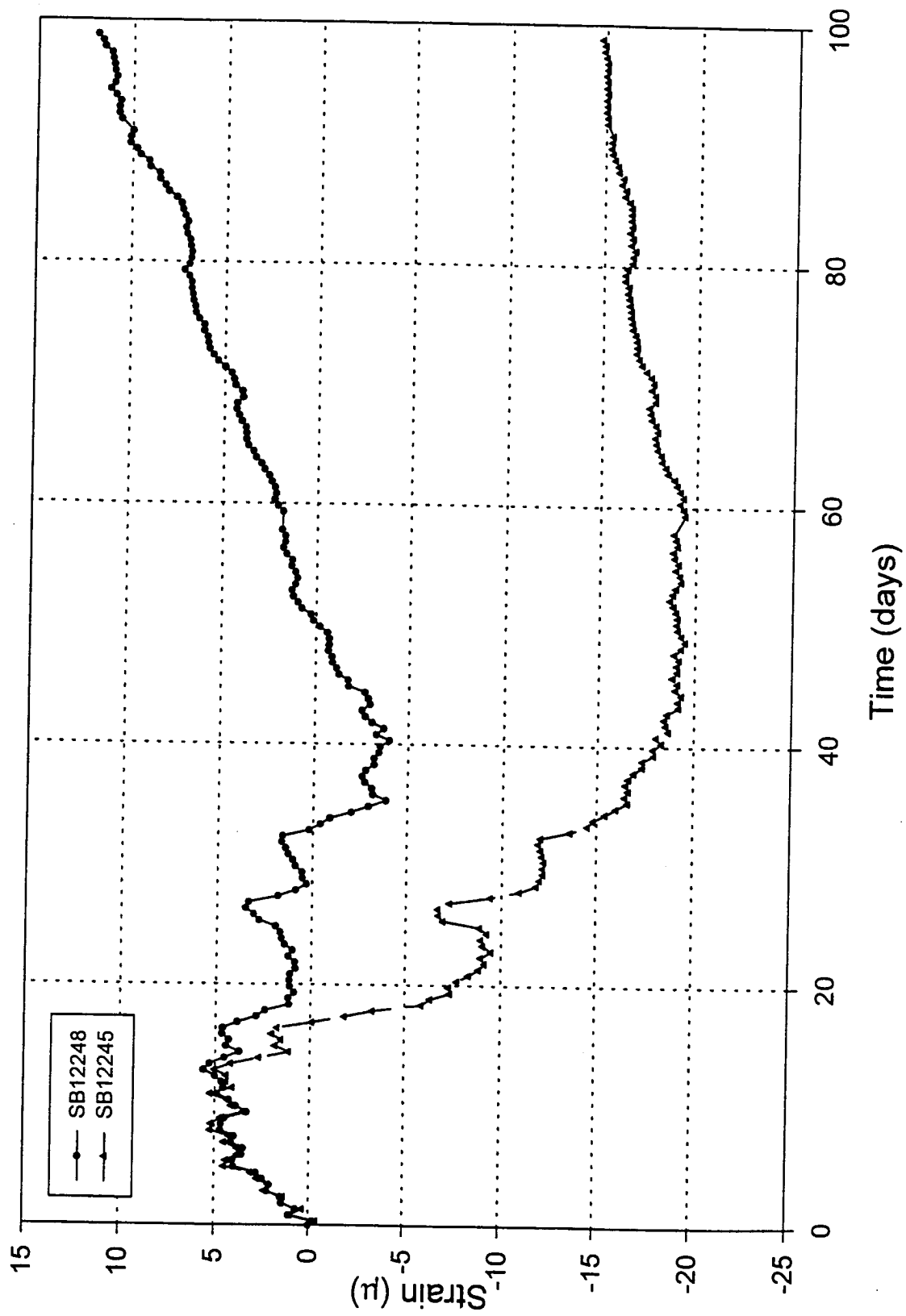


Fig. 4.121: Shaft 9, strain vs. time from gages 60 feet below top of shaft cap.

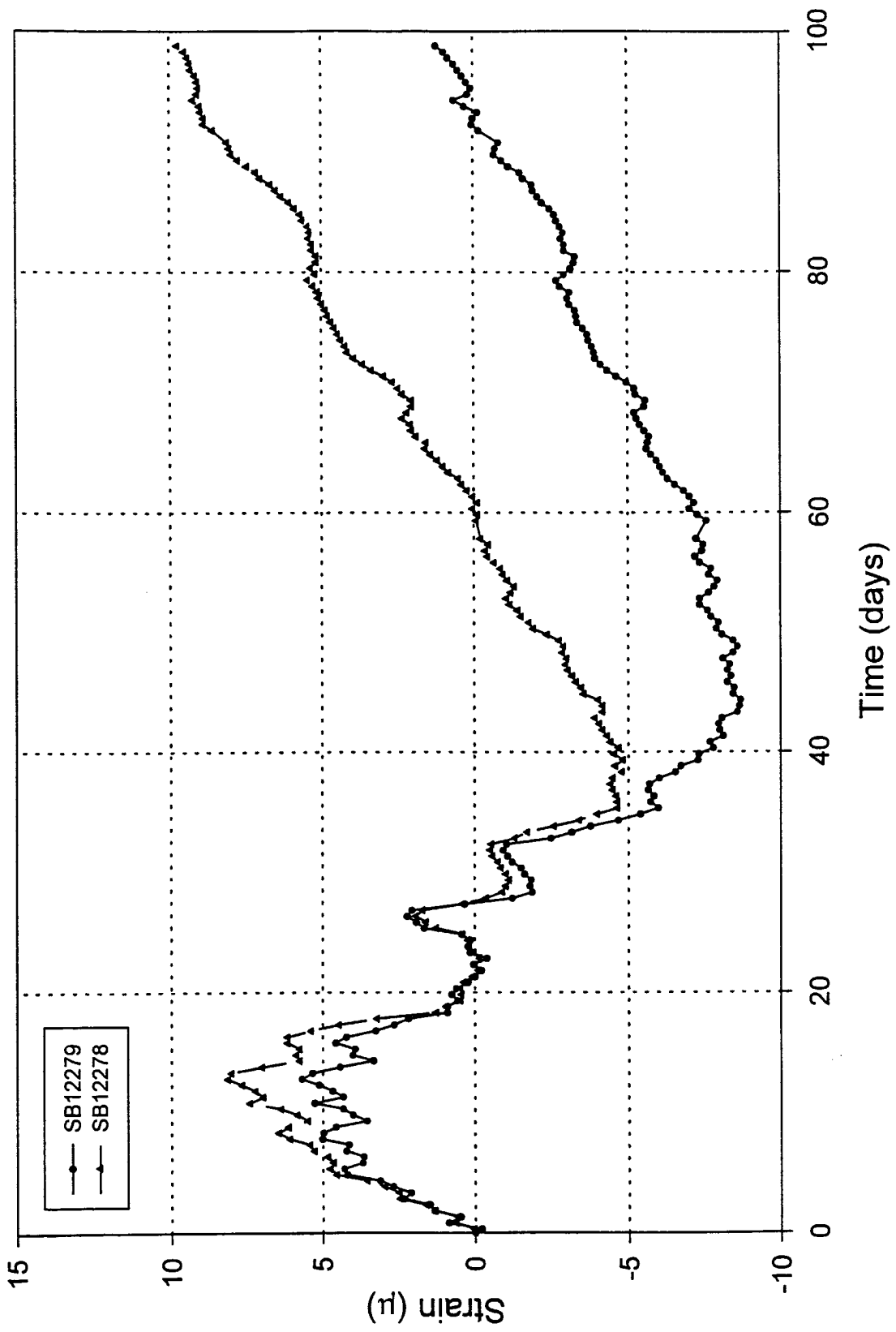


Fig. 4.122: Shaft 9, strain vs. time from gages 70 feet below top of shaft cap.

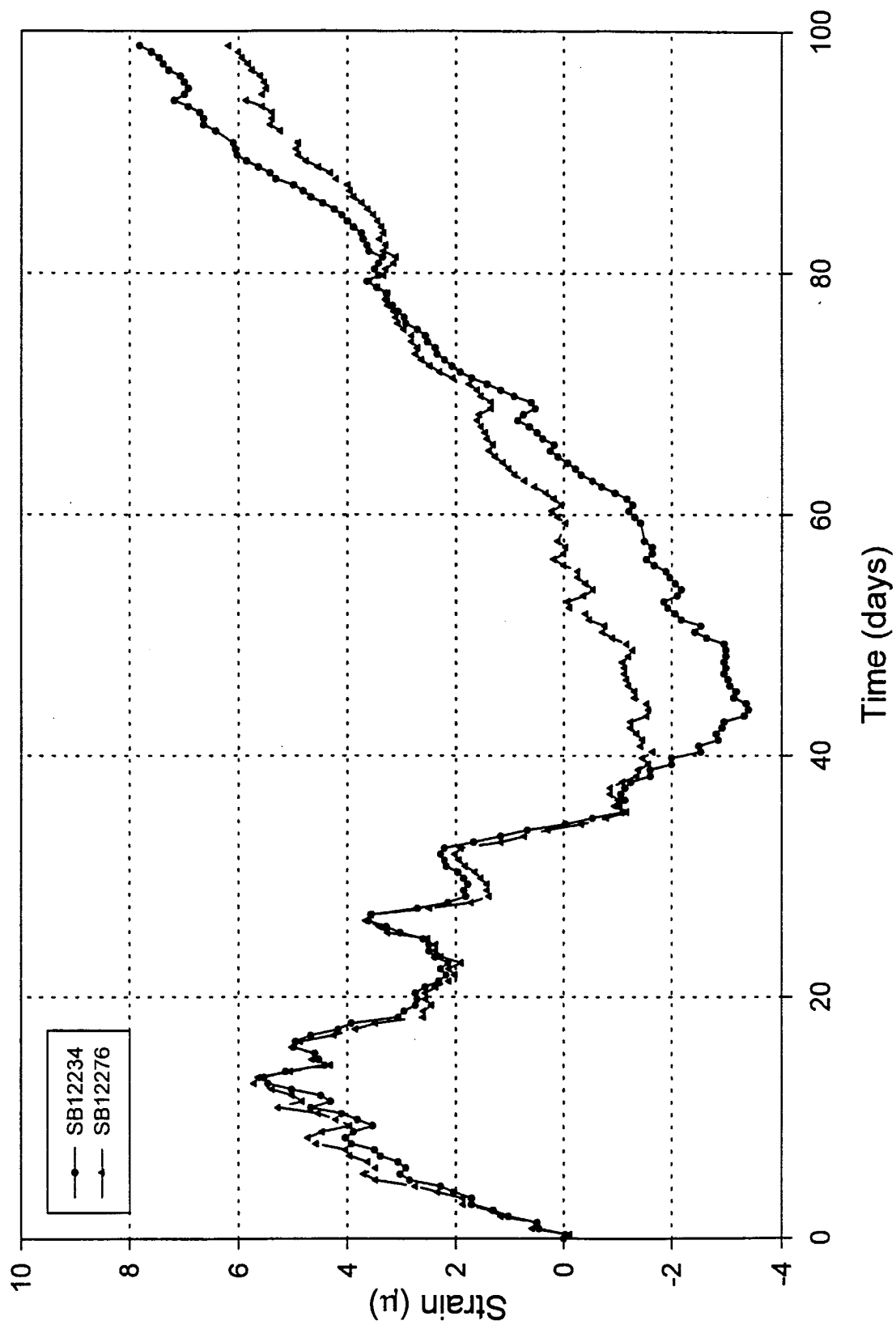


Fig. 4.123: Shaft 1, strain vs. time from gages 80 feet below top of shaft cap.

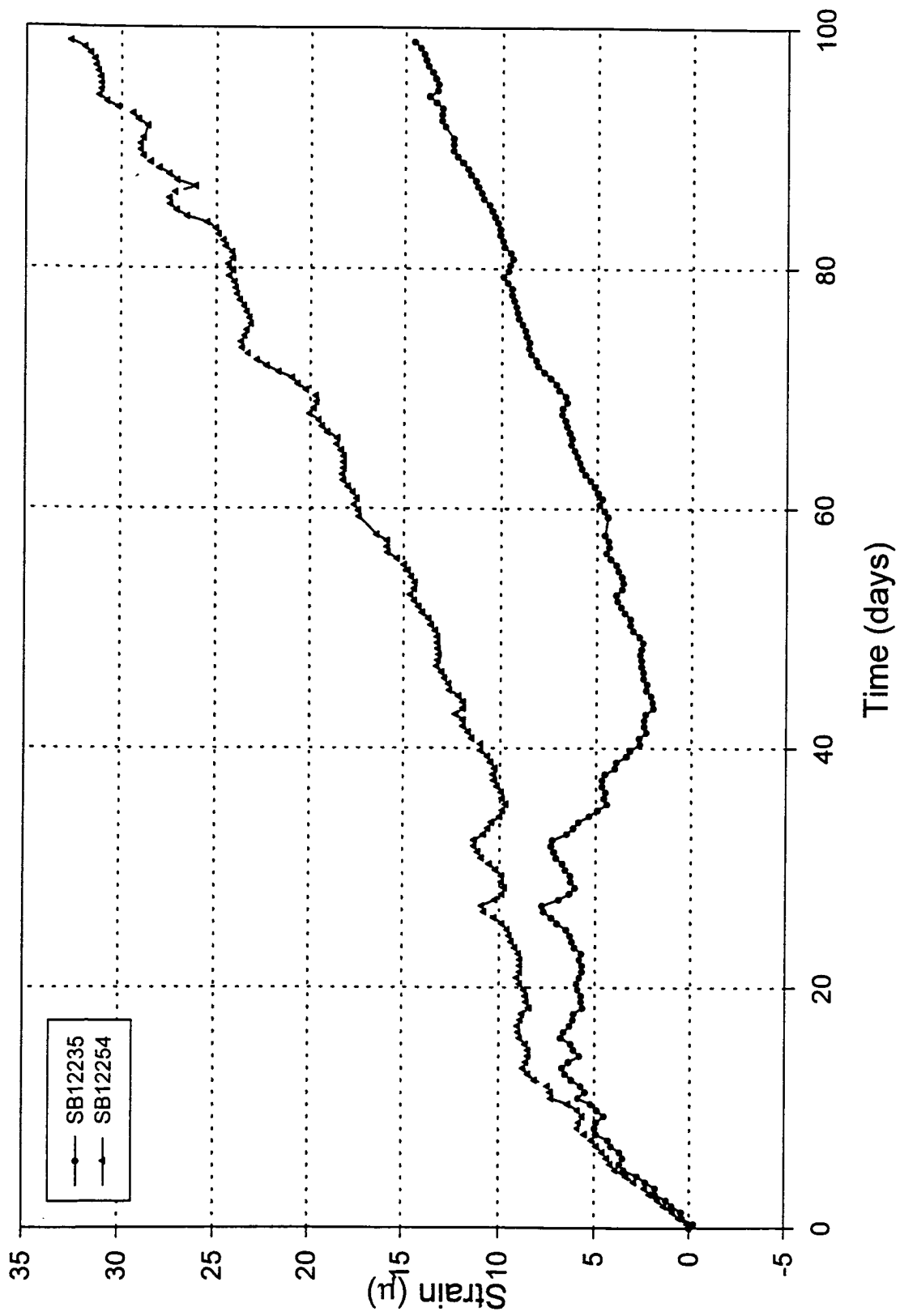


Fig. 4.124: Shaft 9, strain vs. time from gages 95 feet below top of shaft cap.

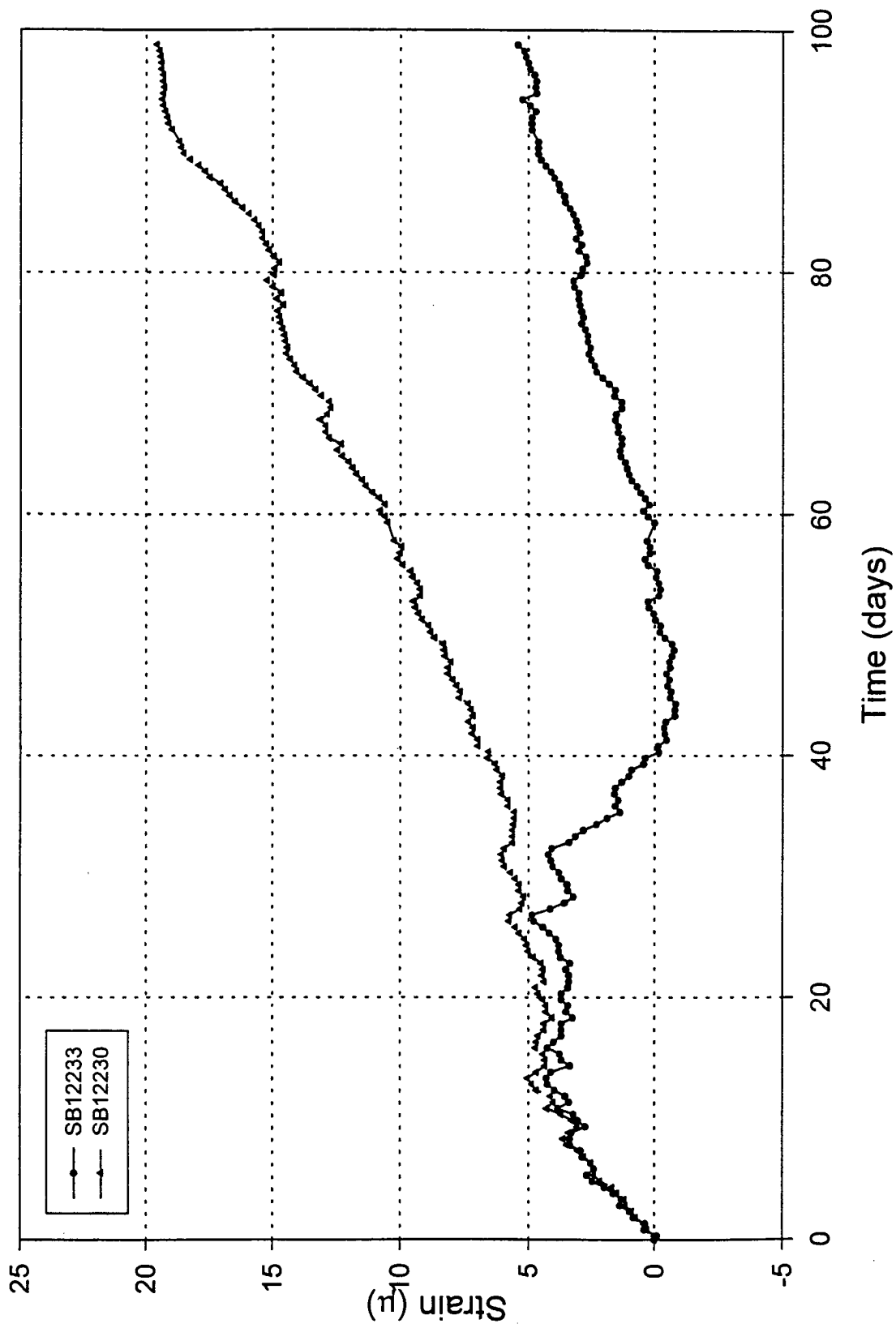


Fig. 4.125: Shaft 9, strain vs. time from gages 115 feet below top of shaft cap.

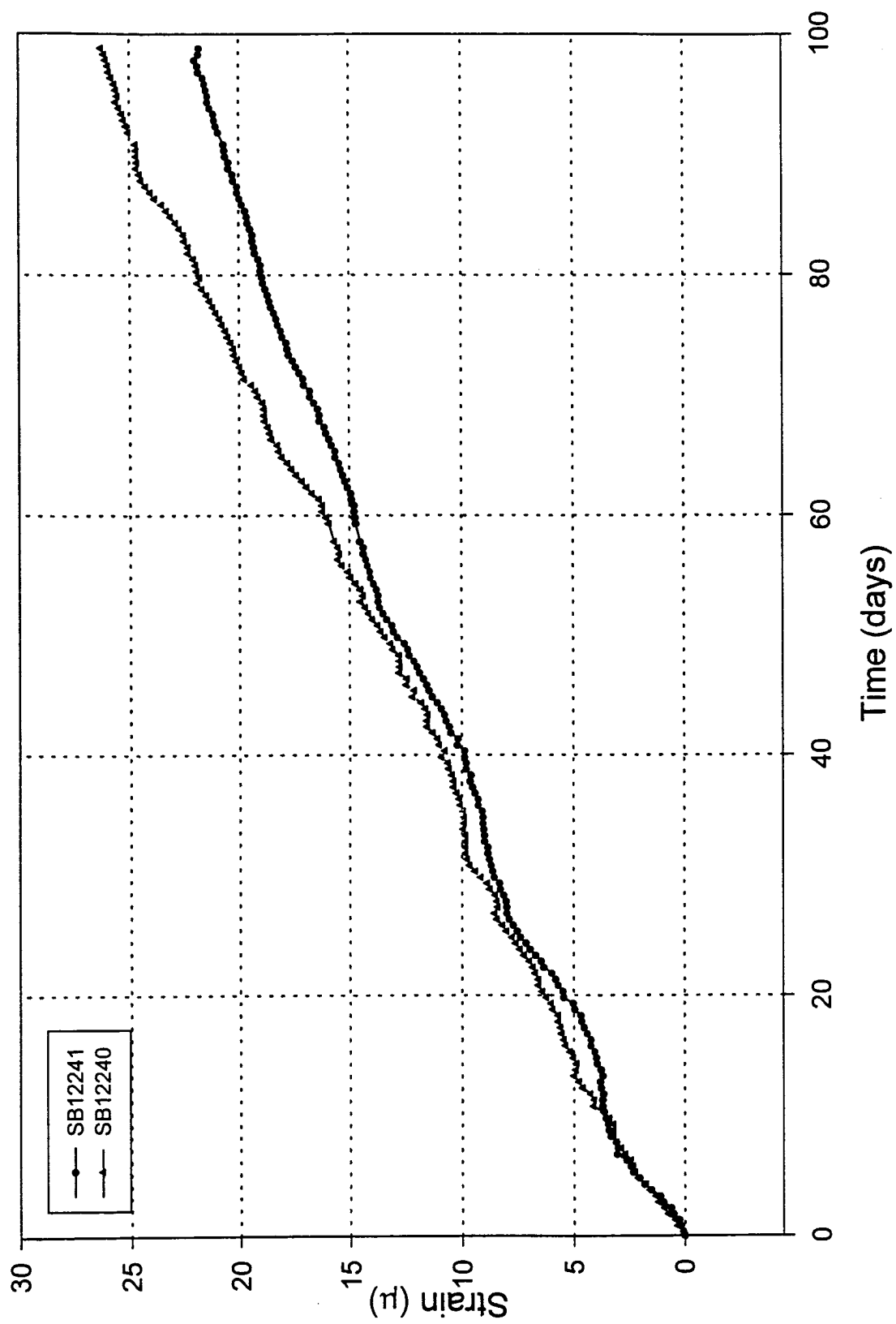


Fig. 4.126: Shaft 1, strain vs. time from gages 135 feet below top of shaft cap.

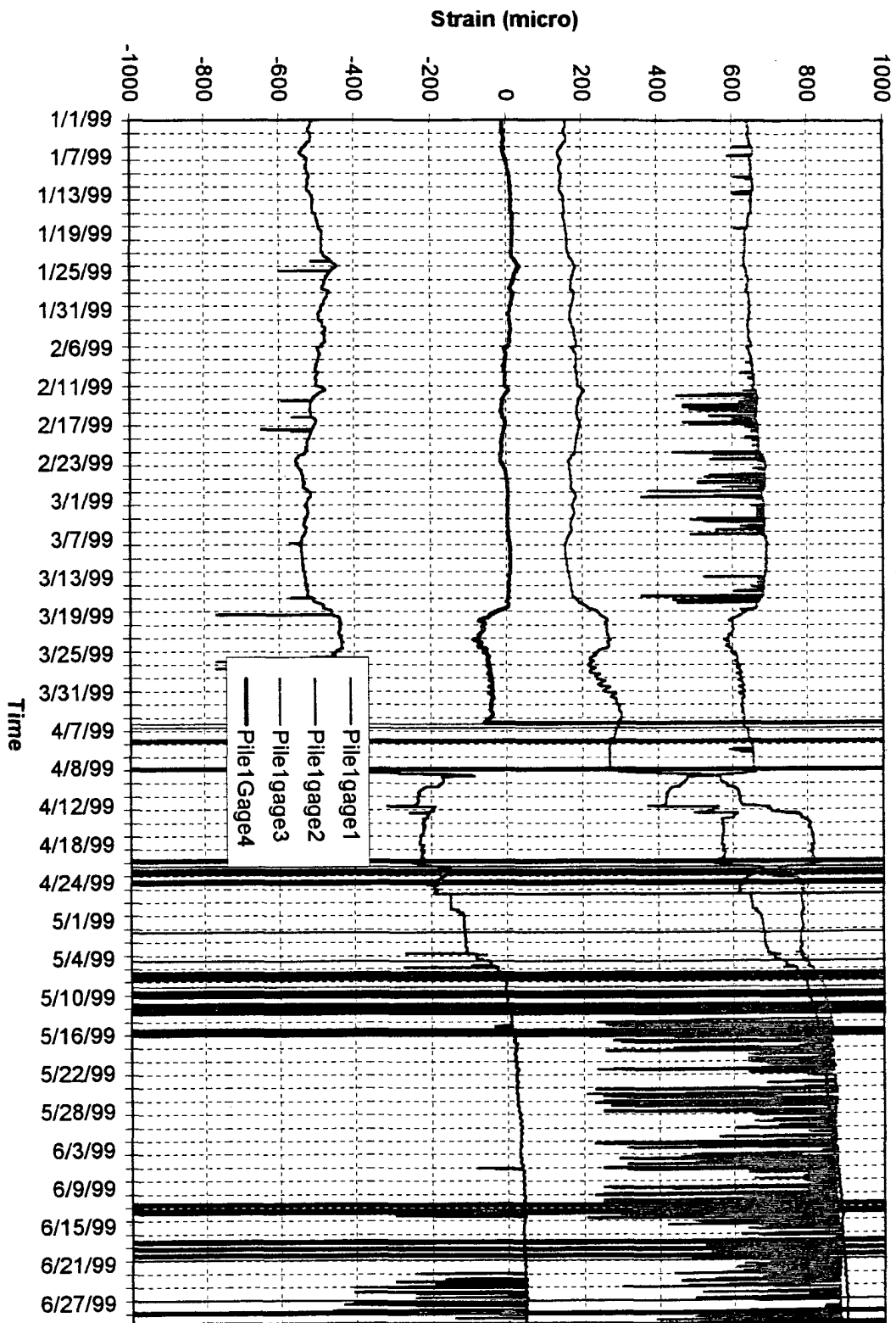


Fig. 4.127: Long-term monitoring of strain in Pile # 1 in the anchor cap structure (1/1/99 ~ 6/30/99)



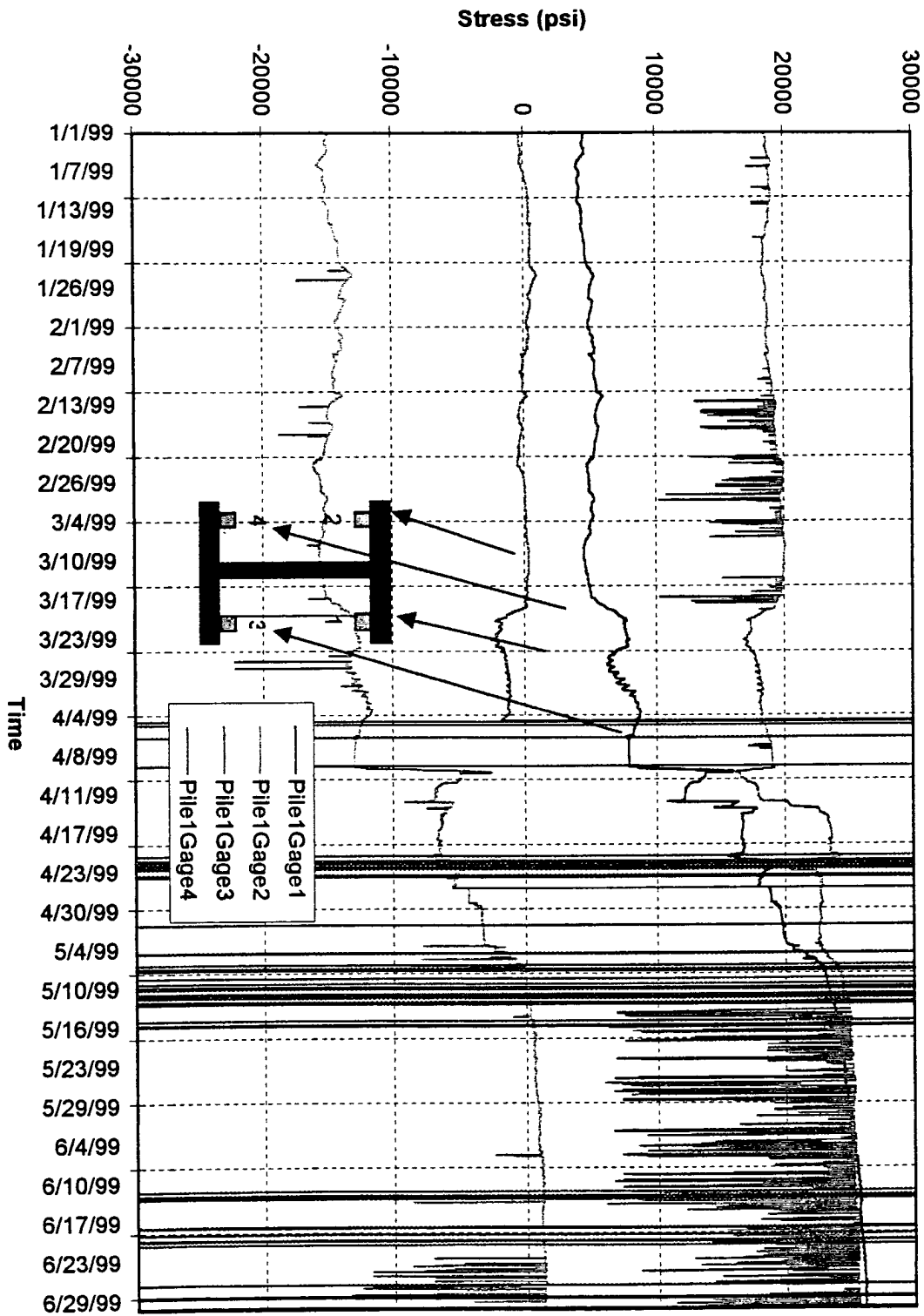


Fig. 4.128: Long-term monitoring of stress in Pile # 1 in the anchor cap structure (1/1/99 ~ 6/30/99)

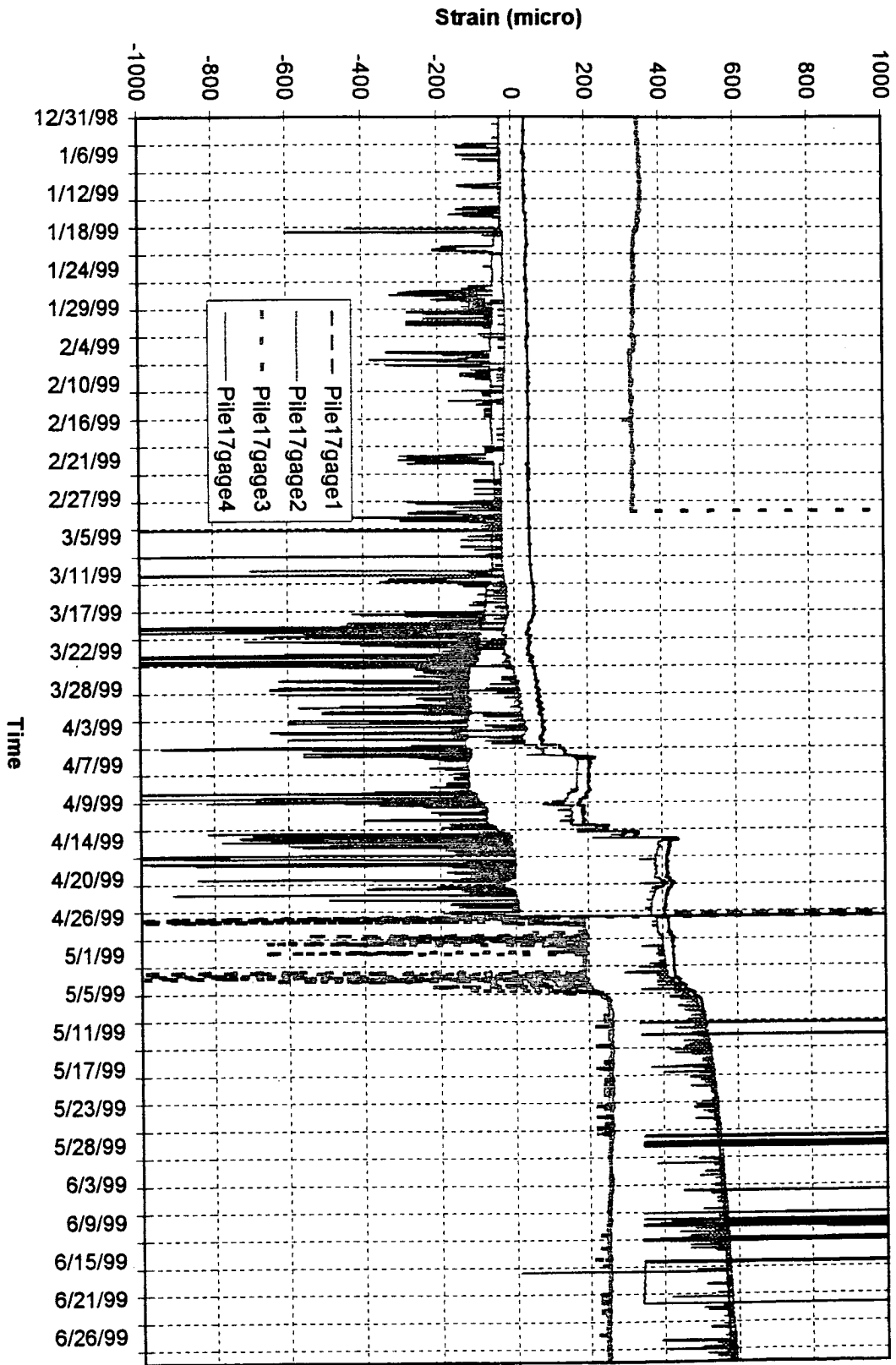


Fig. 4.129: Long-term monitoring of strain in Pile # 17 in the anchor cap structure (1/1/99 ~ 6/30/99)

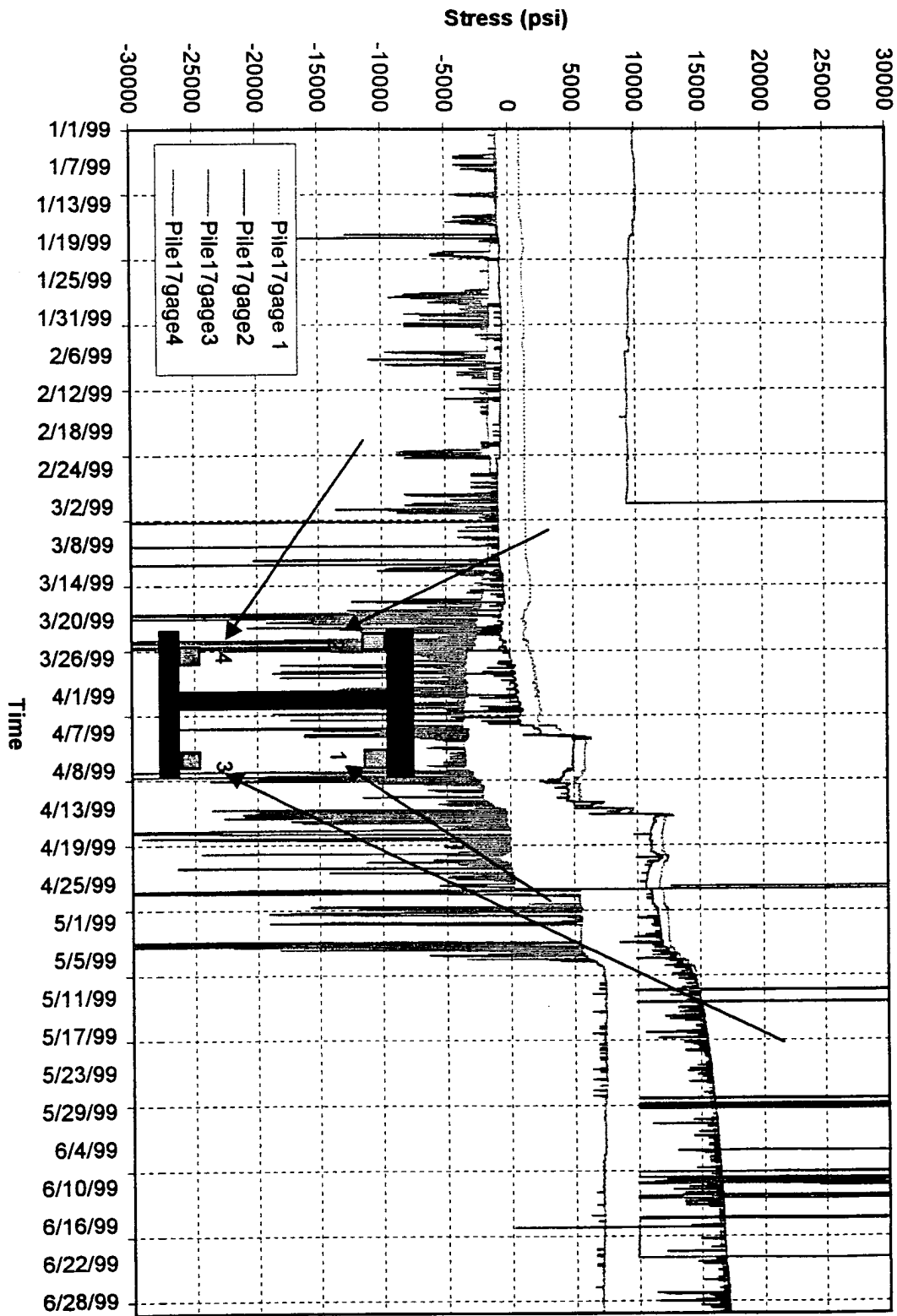


Fig. 4.130: Long-term monitoring of stress in Pile # 17 in the anchor cap structure (1/1/99 ~ 6/30/99)

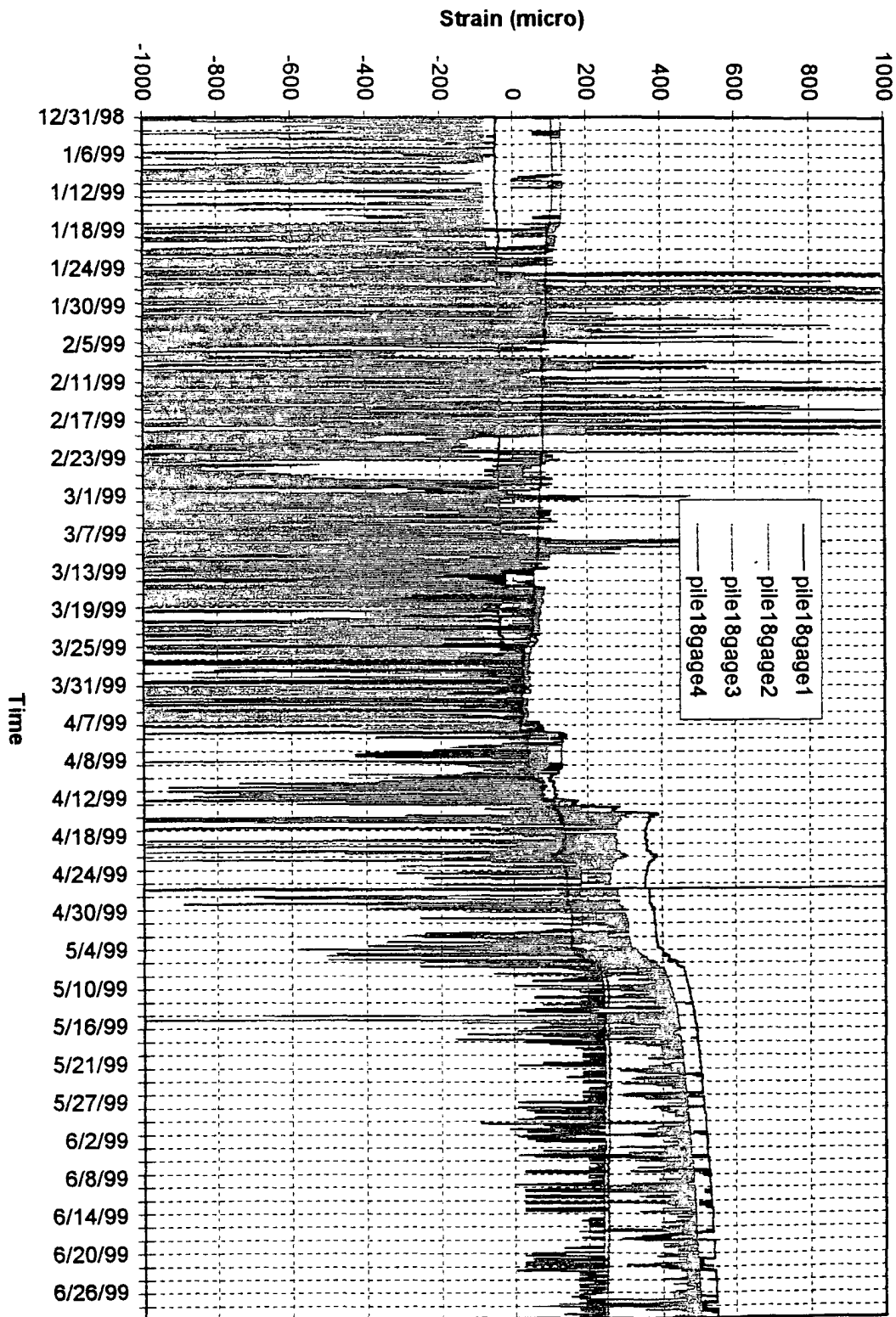


Fig. 4.131: Long-term monitoring of strain in Pile # 18 in the anchor cap structure (1/1/99 ~ 6/30/99)

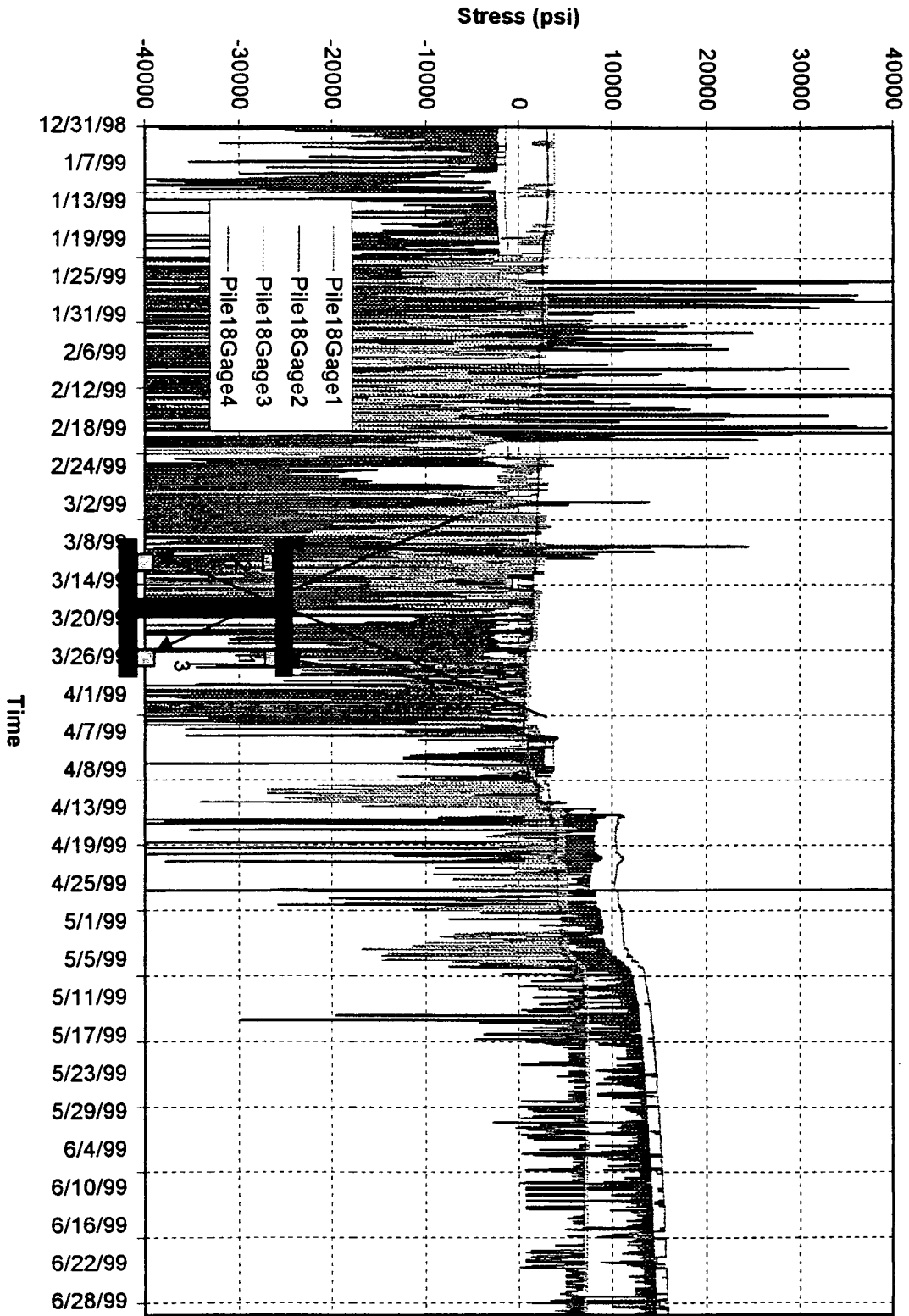


Fig. 4.132: Long-term monitoring of stress in Pile # 18 in the anchor cap structure (1/1/99 ~ 6/30/99)

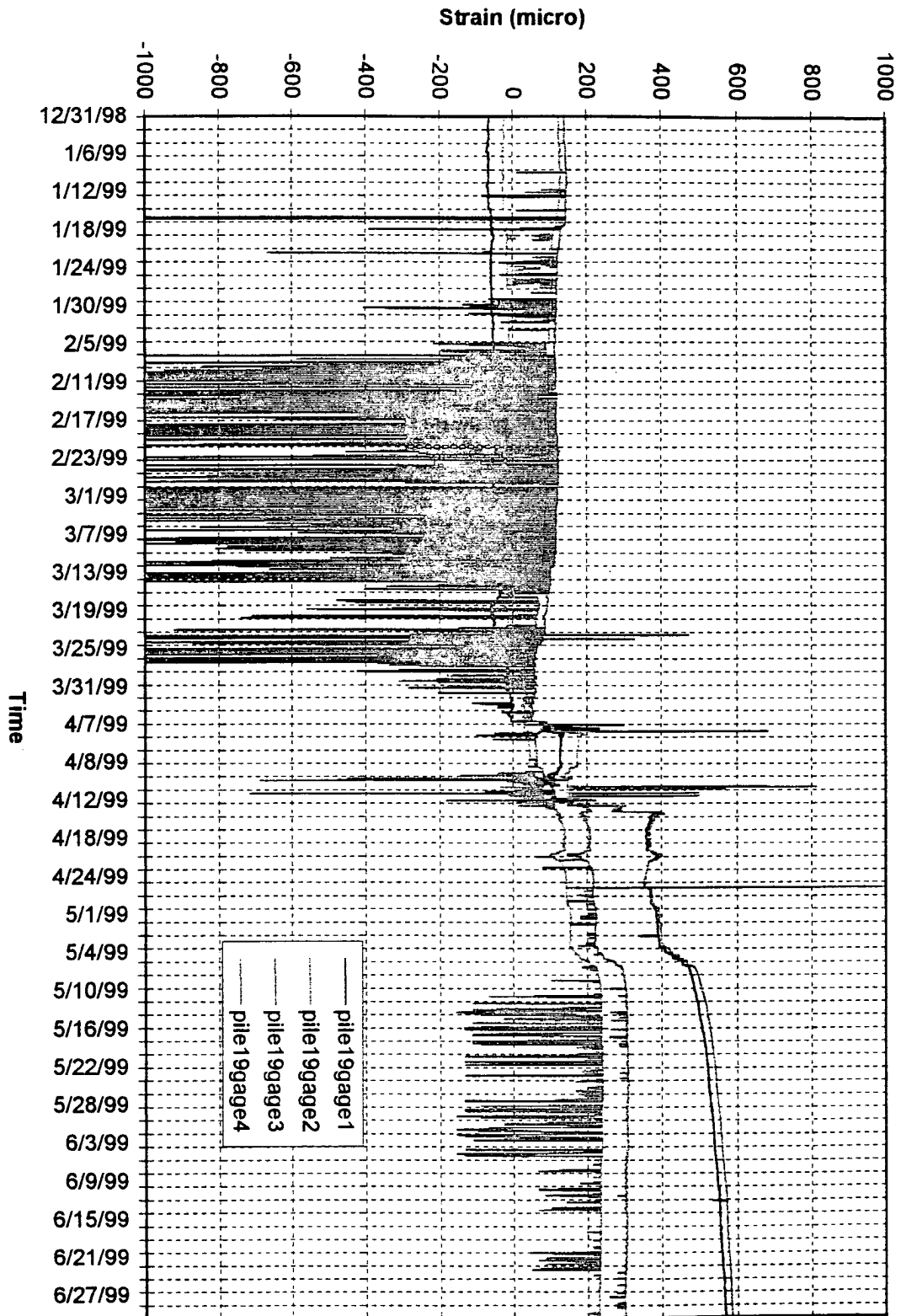


Fig. 4.133: Long-term monitoring of strain in Pile # 19 in the anchor cap structure (1/1/99 ~ 6/30/99)

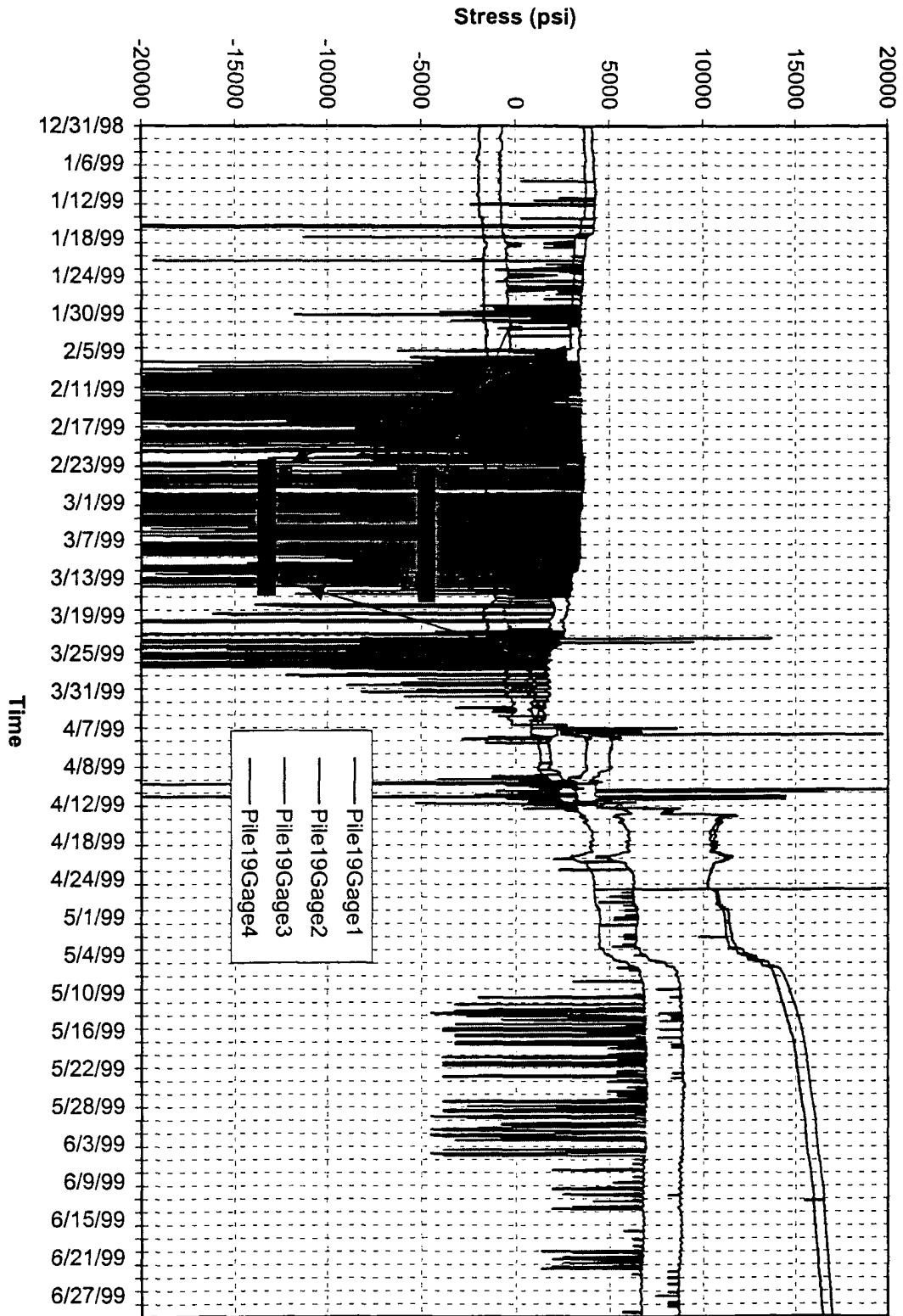


Fig. 4.134: Long-term monitoring of stress in Pile # 19 in the anchor cap structure (1/1/99 ~ 6/30/99)

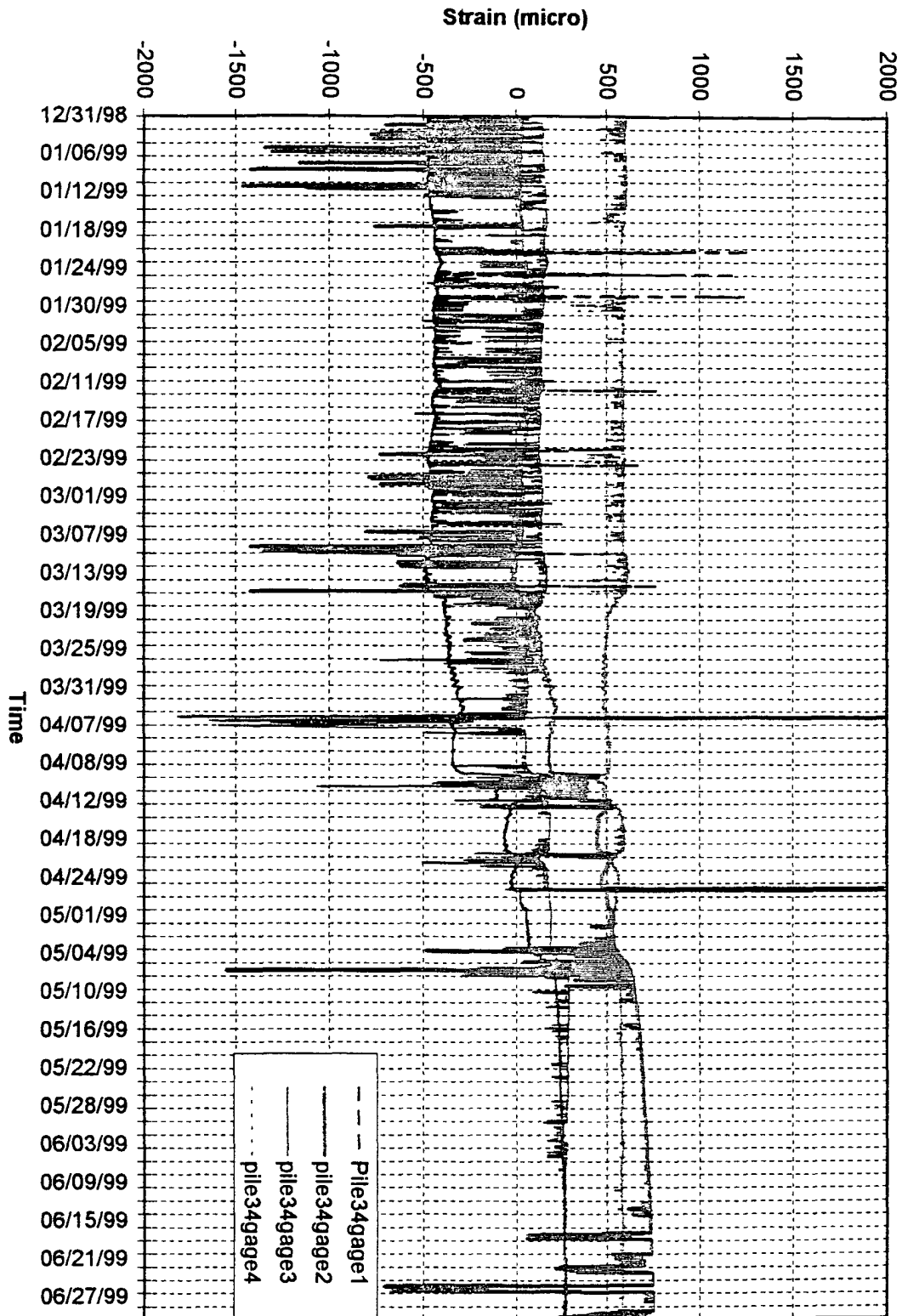


Fig. 4.135: Long-term monitoring of strain in Pile # 34 in the anchor cap structure (1/1/99 ~ 6/30/99)



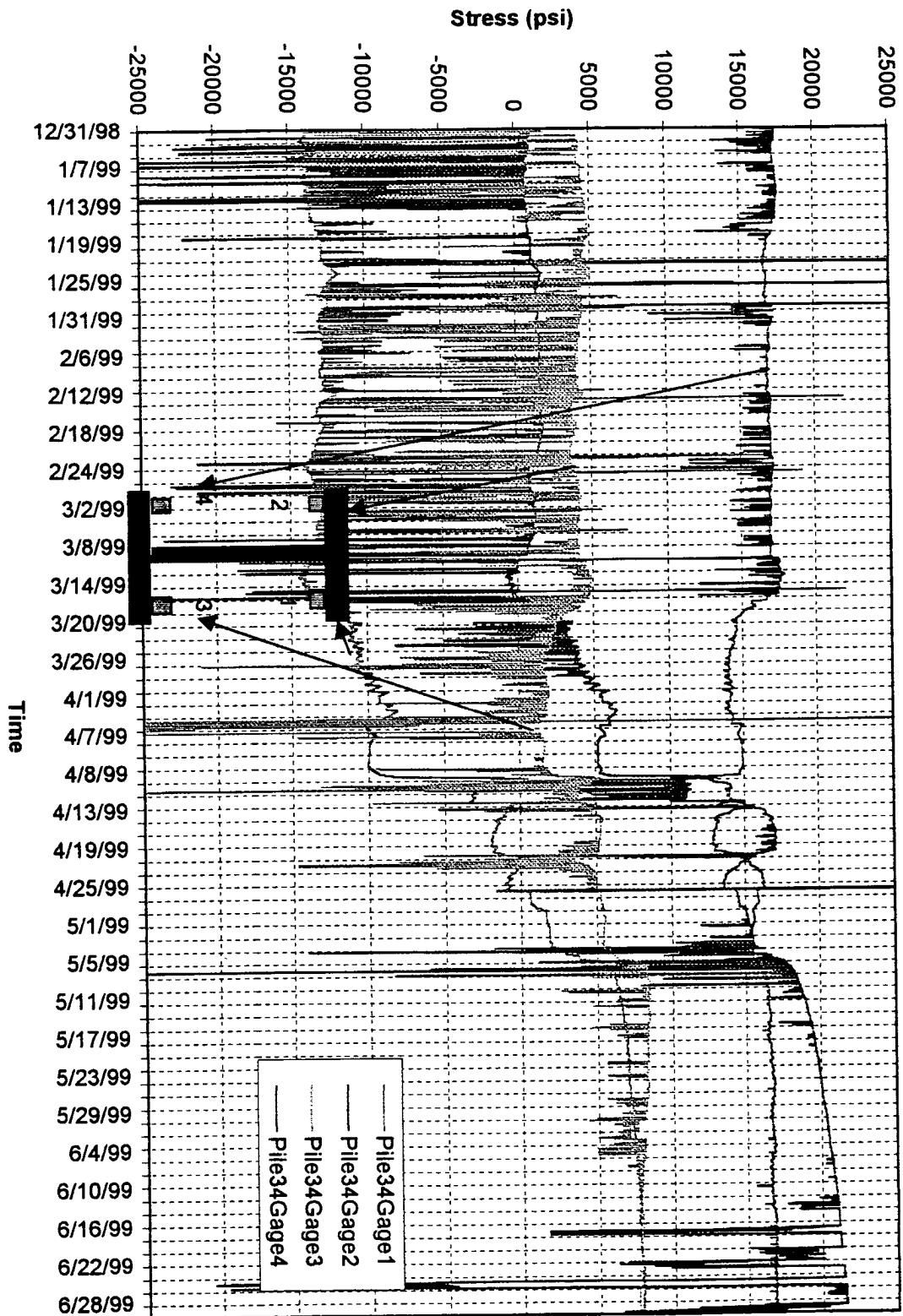


Fig. 4.136: Long-term monitoring of stress in Pile # 34 in the anchor cap structure (1/1/99 ~ 6/30/99)

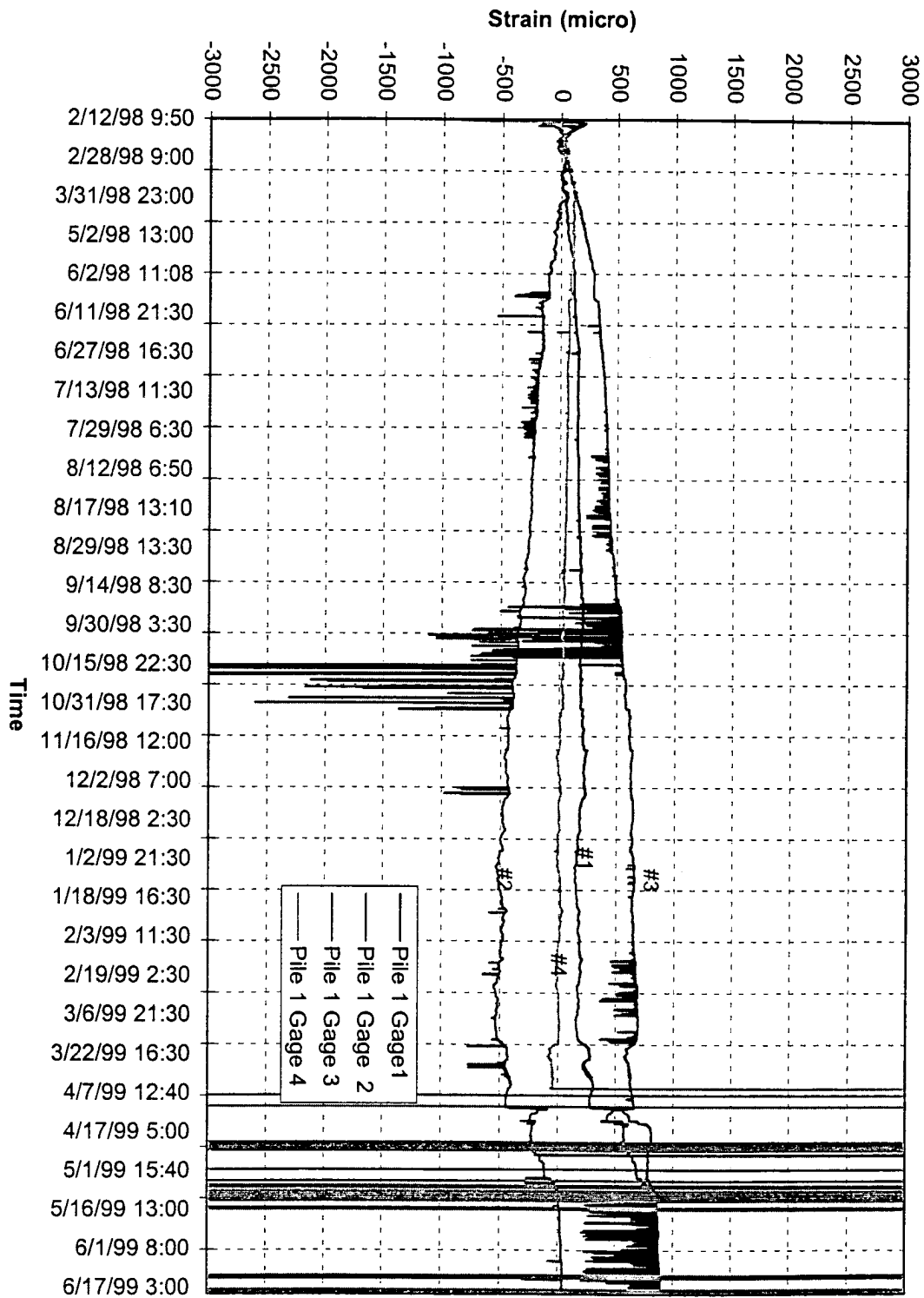


Fig. 4.137: Long-term monitoring of strain in Pile # 1 in the anchor cap structure (2/12/98 ~ 6/30/99)

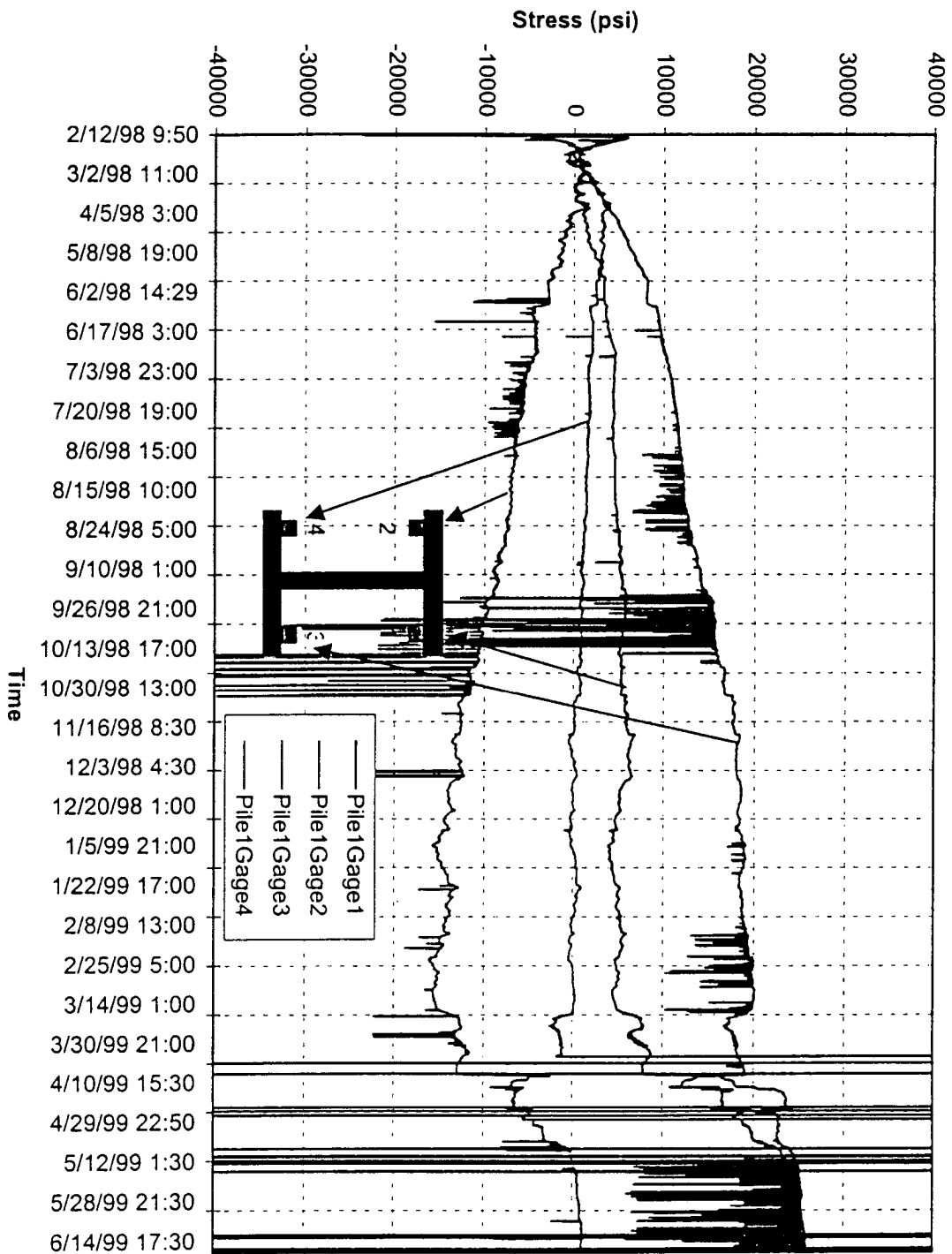


Fig. 4.138: Long-term monitoring of stress in Pile # 1 in the anchor cap structure (2/12/98 ~ 6/30/99)

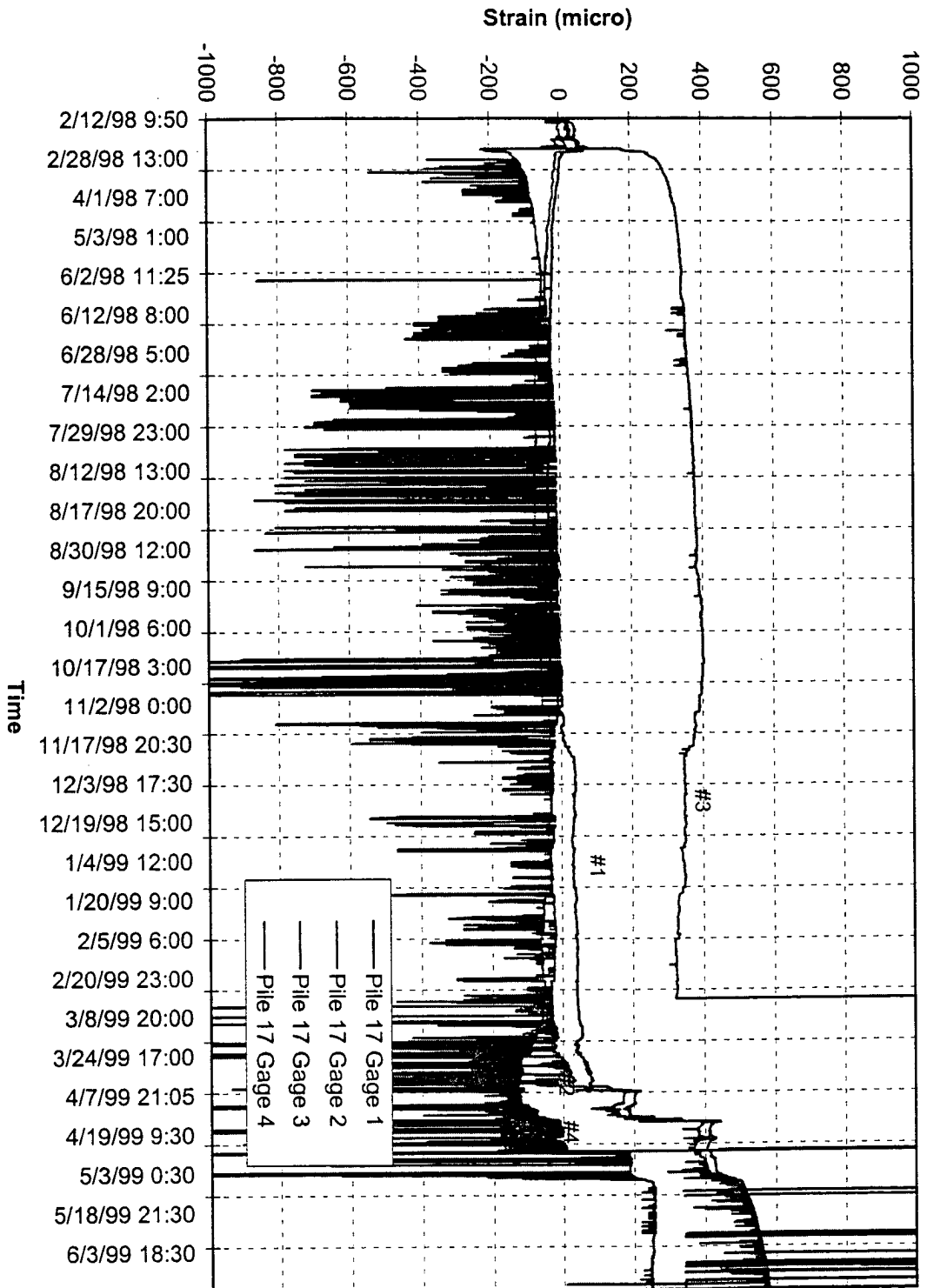


Fig. 4.139: Long-term monitoring of strain in Pile # 17 in the anchor cap structure (2/12/98 ~ 6/30/99)

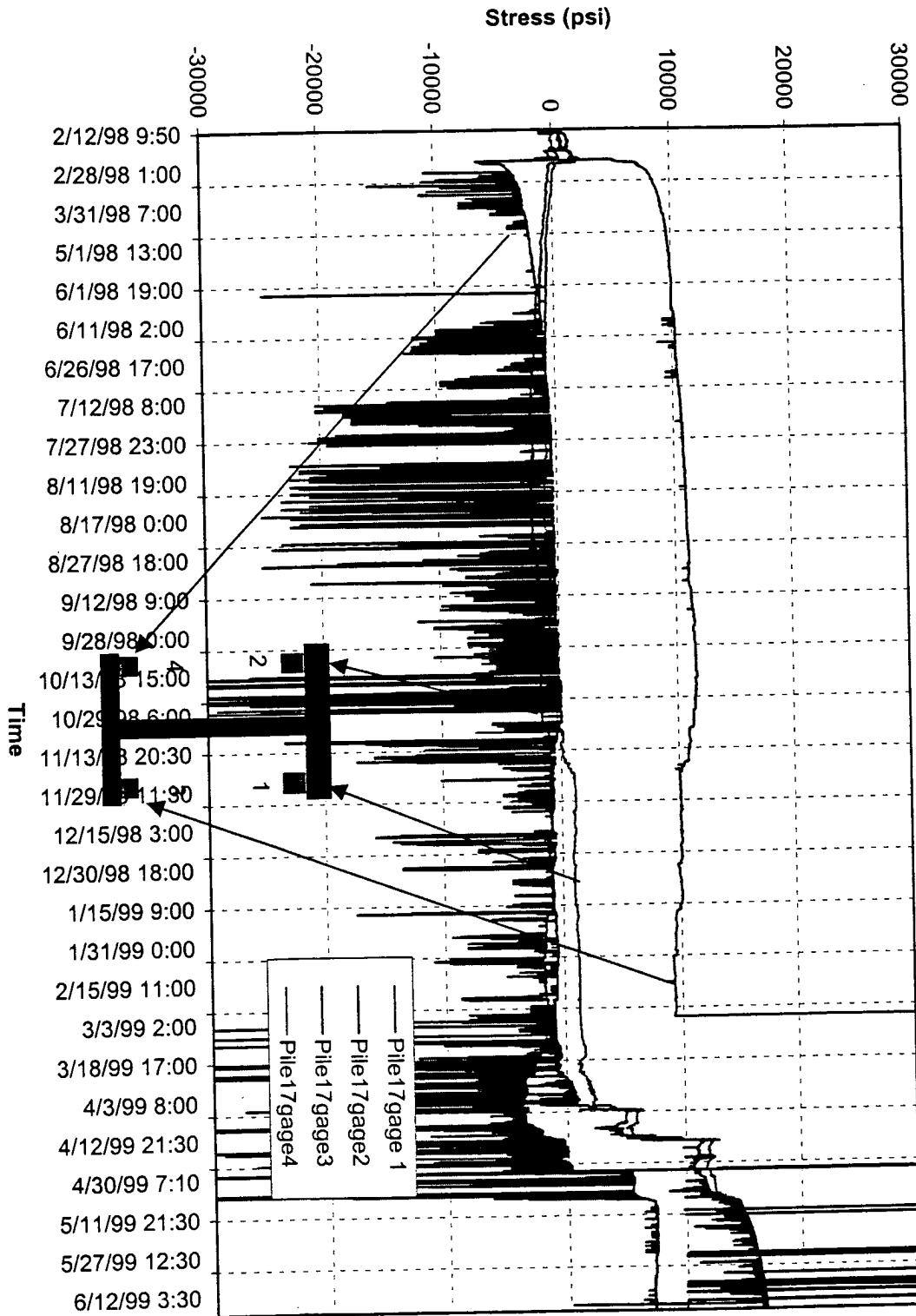


Fig. 4.140: Long-term monitoring of stress in Pile # 17 in the anchor cap structure (2/12/98 ~ 6/30/99)

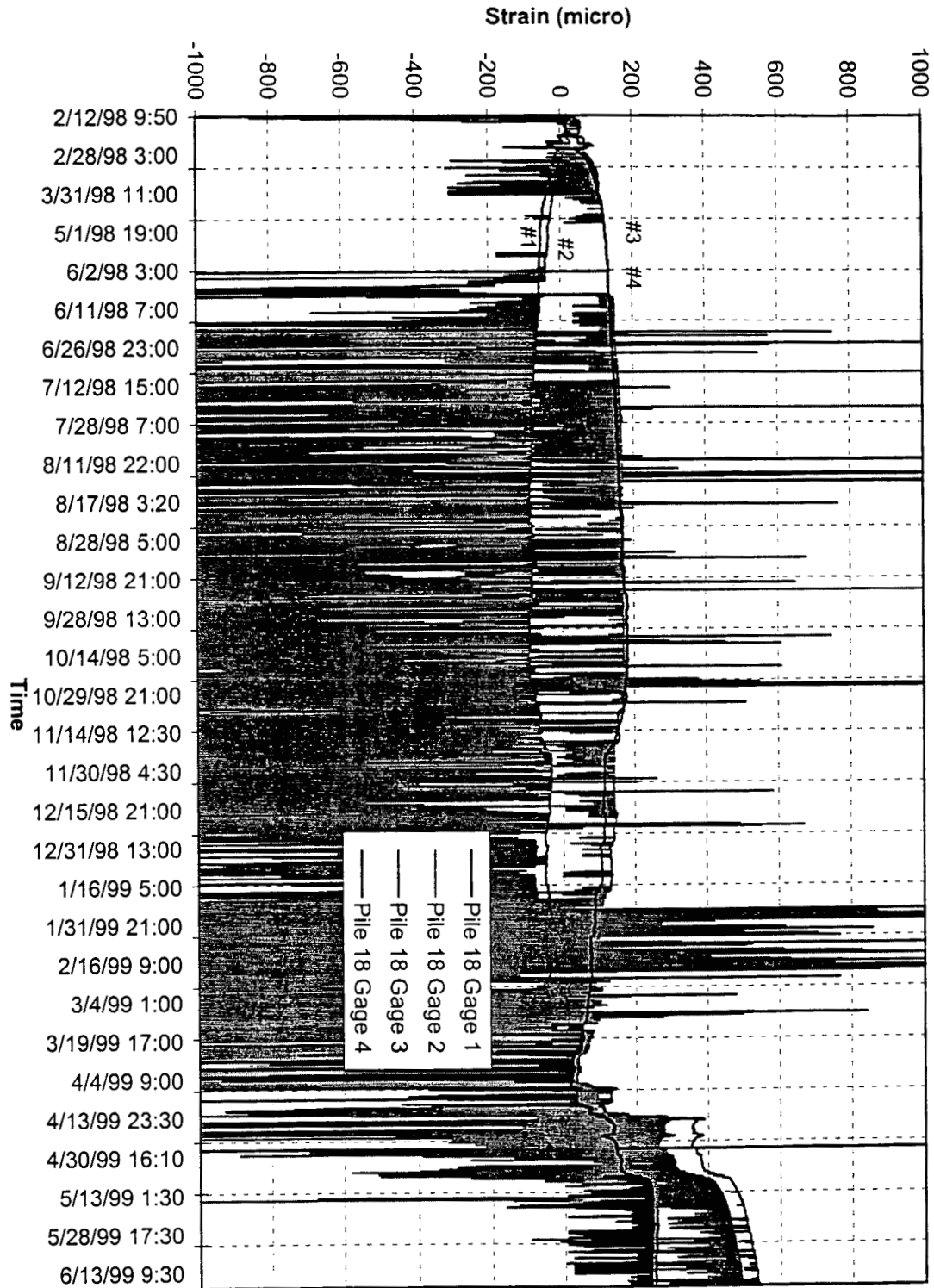


Fig. 4.141: Long-term monitoring of strain in Pile # 18 in the anchor cap structure (2/12/98 ~ 6/30/99)

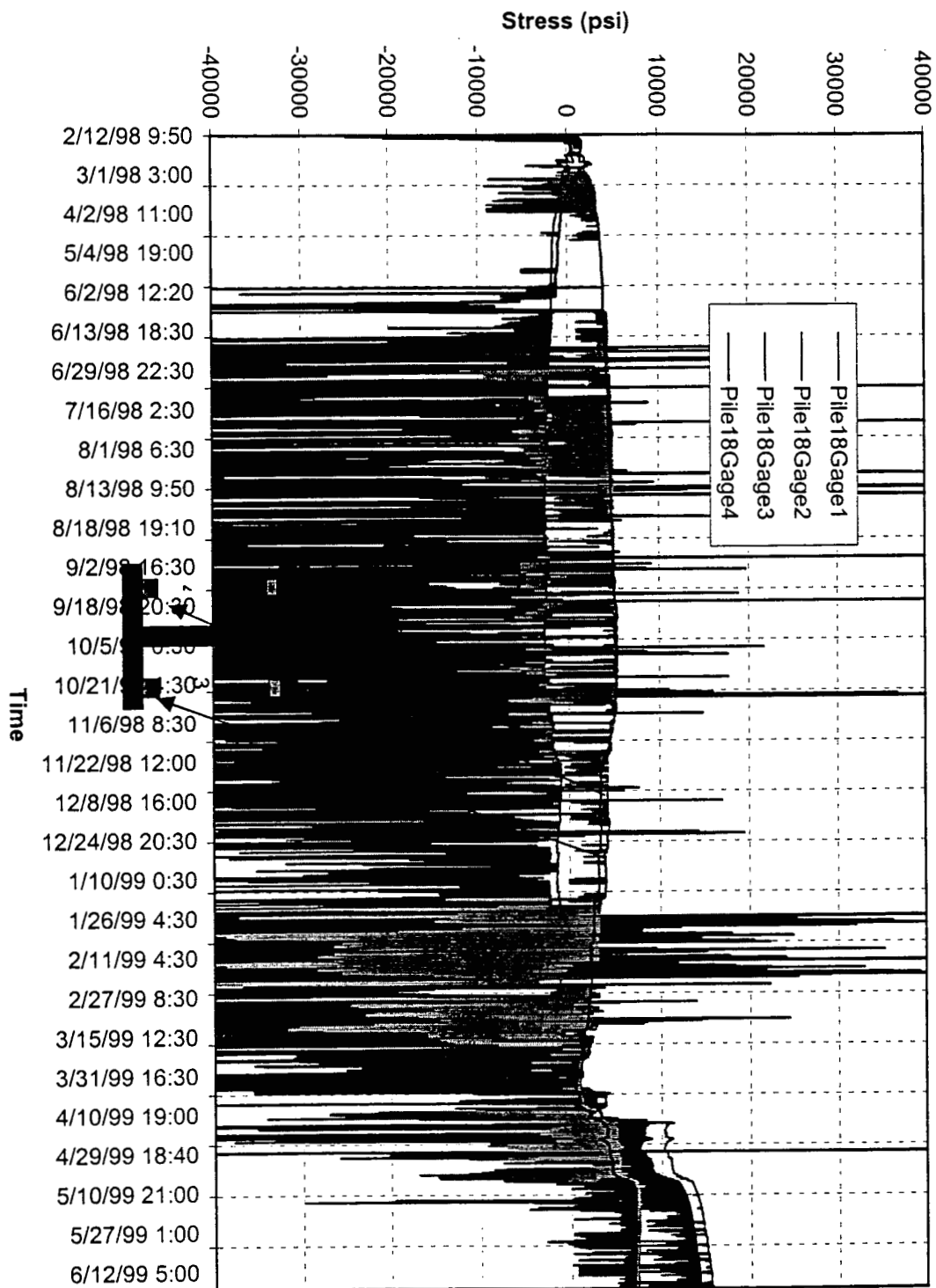


Fig. 4.142: Long-term monitoring of stress in Pile # 18 in the anchor cap structure (2/12/98 ~ 6/30/99)

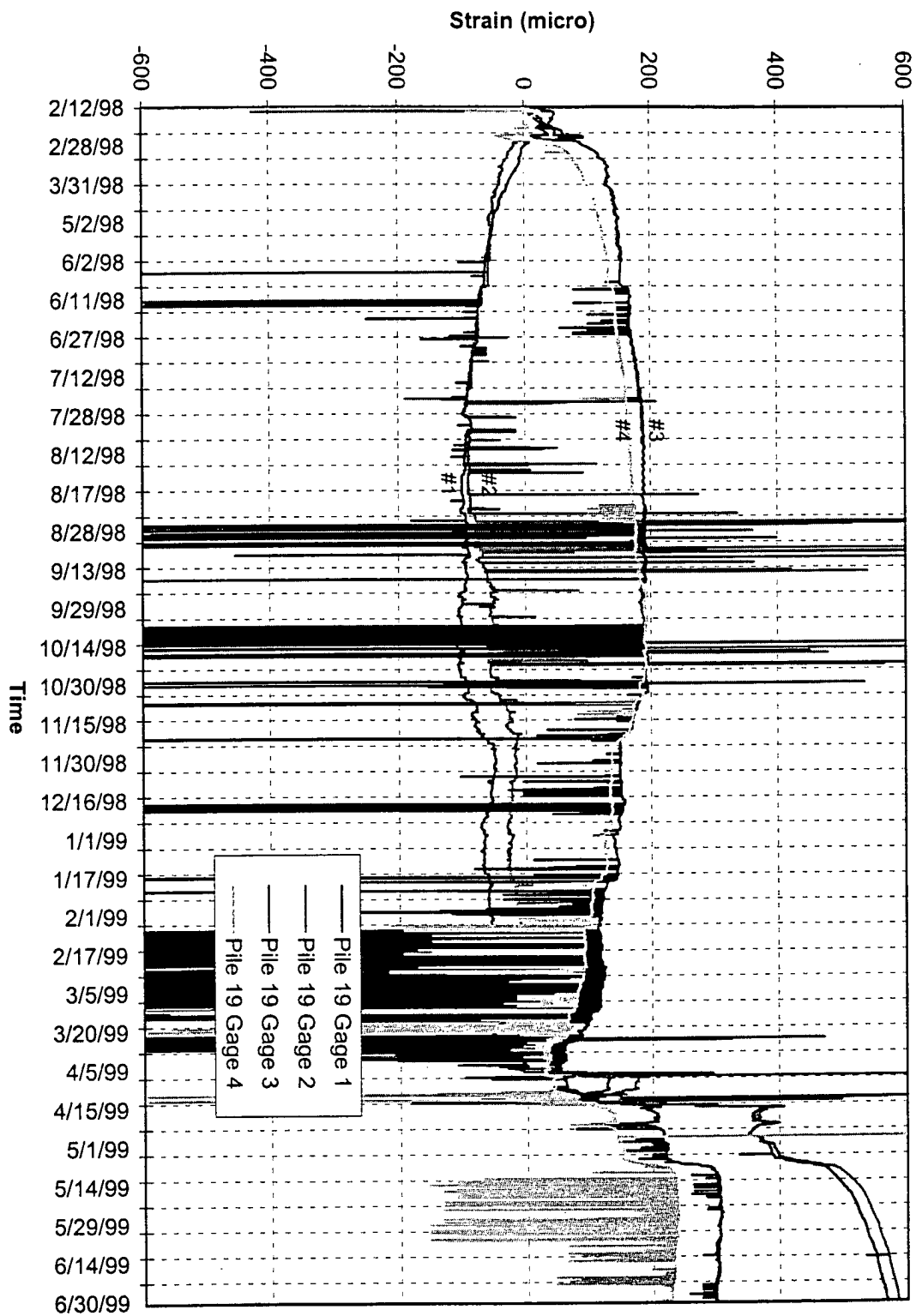


Fig. 4.143: Long-term monitoring of strain in Pile # 19 in the anchor cap structure (2/12/98 ~ 6/30/99)



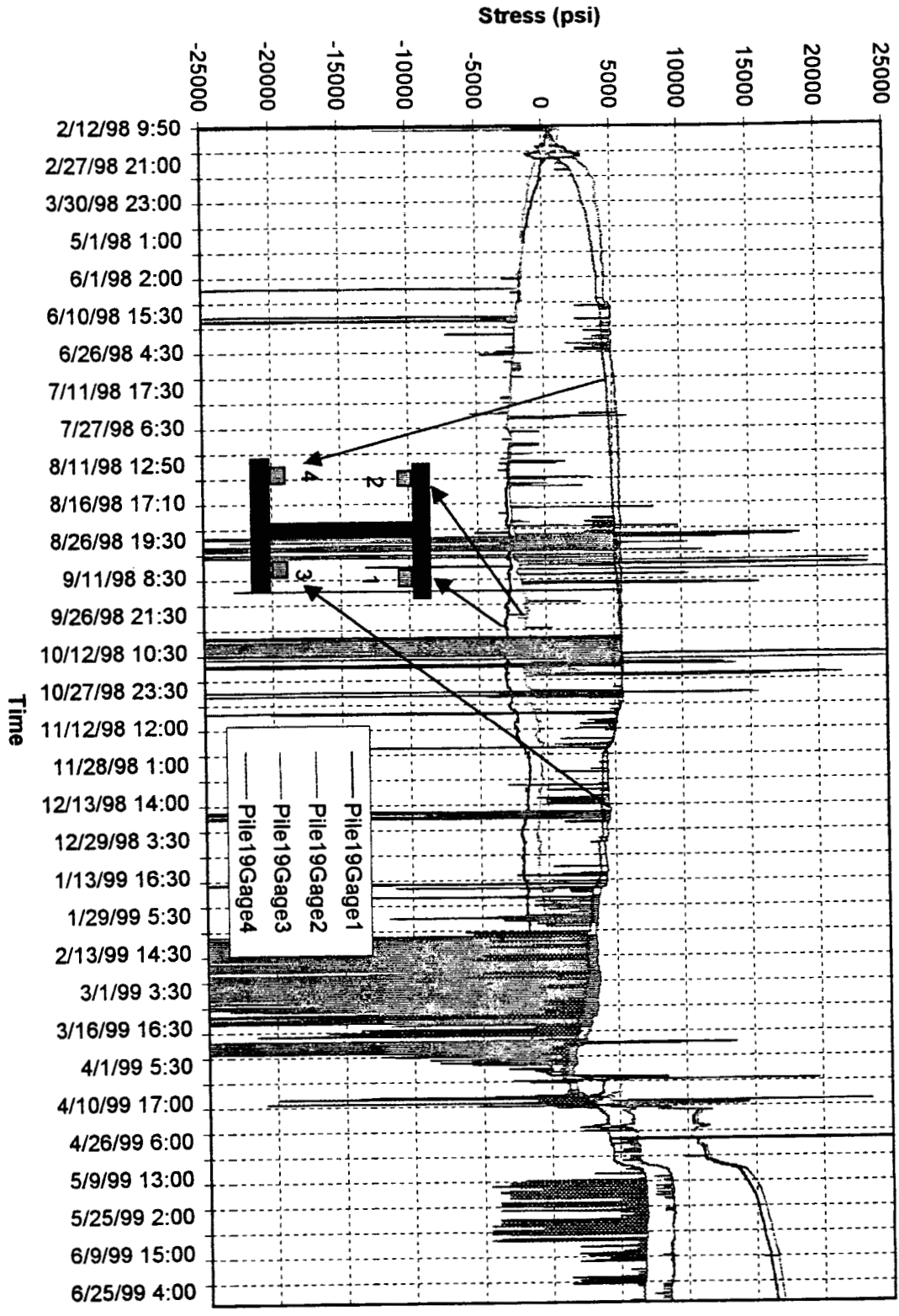


Fig. 4.144: Long-term monitoring of stress in Pile # 19 in the anchor cap structure (2/12/98 ~ 6/30/99)

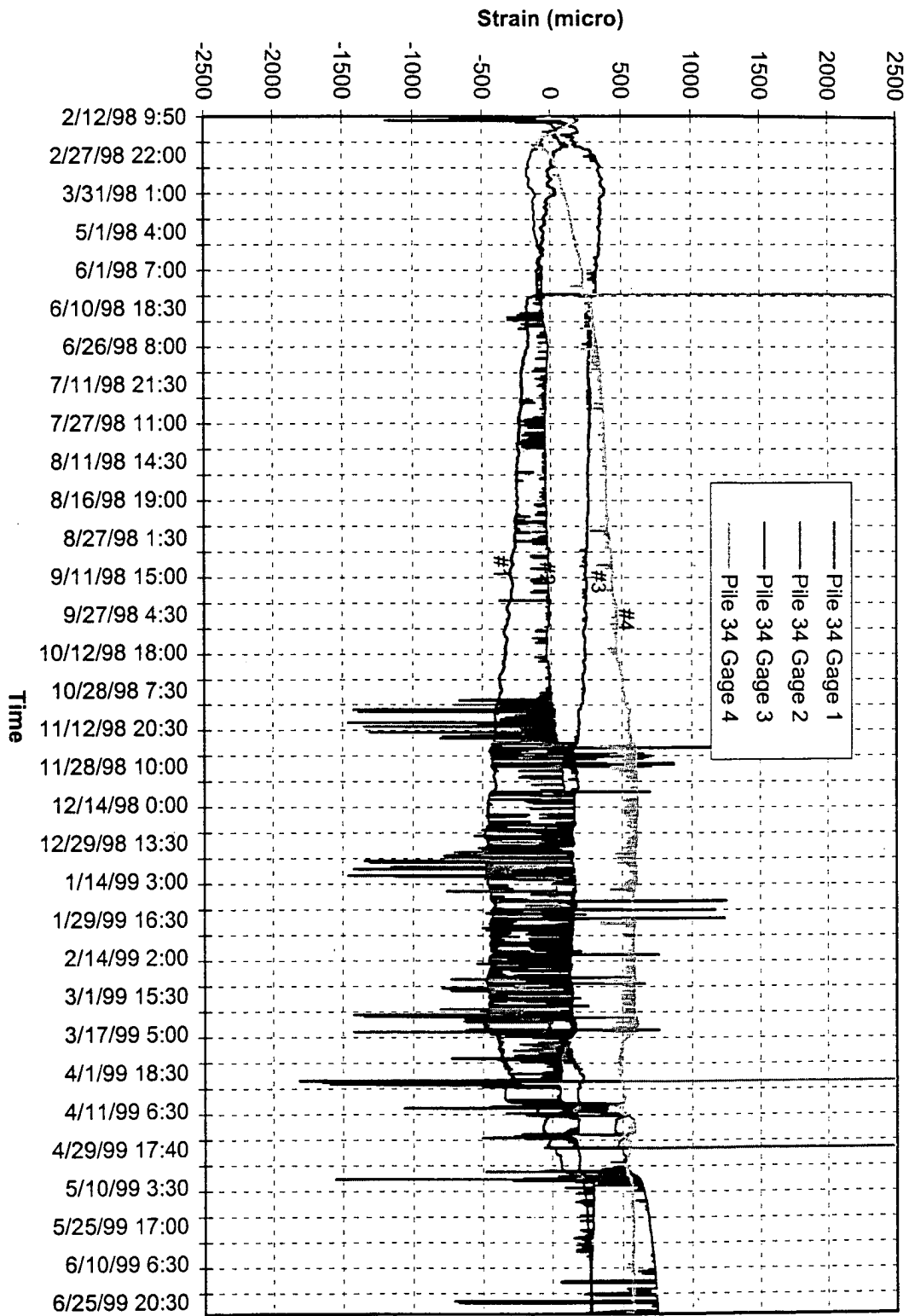


Fig. 4.145: Long-term monitoring of strain in Pile # 34 in the anchor cap structure (2/12/98 ~ 6/30/99)

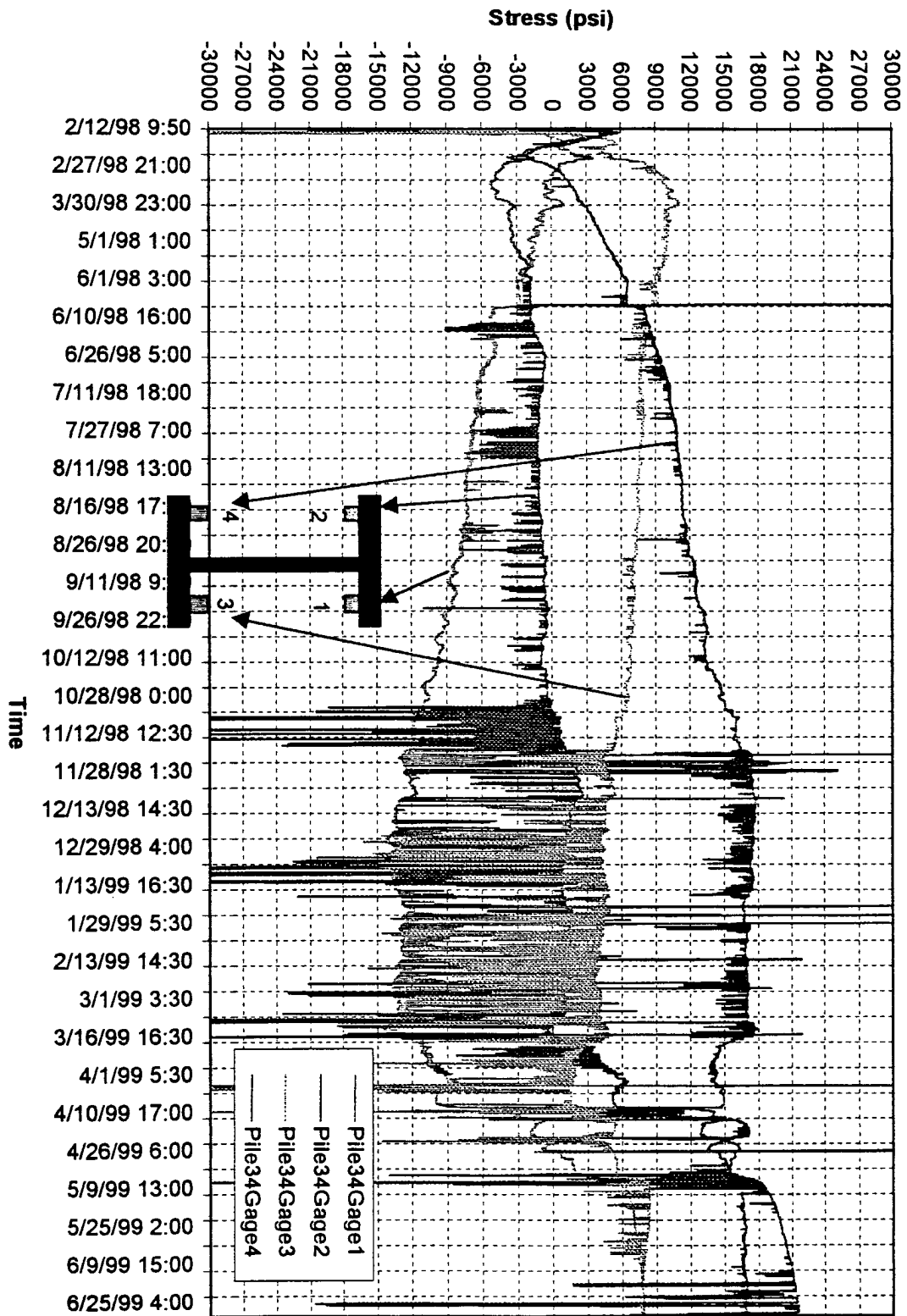


Fig. 4.146: Long-term monitoring of stress in Pile # 34 in the anchor cap structure (2/12/98 ~ 6/30/99)

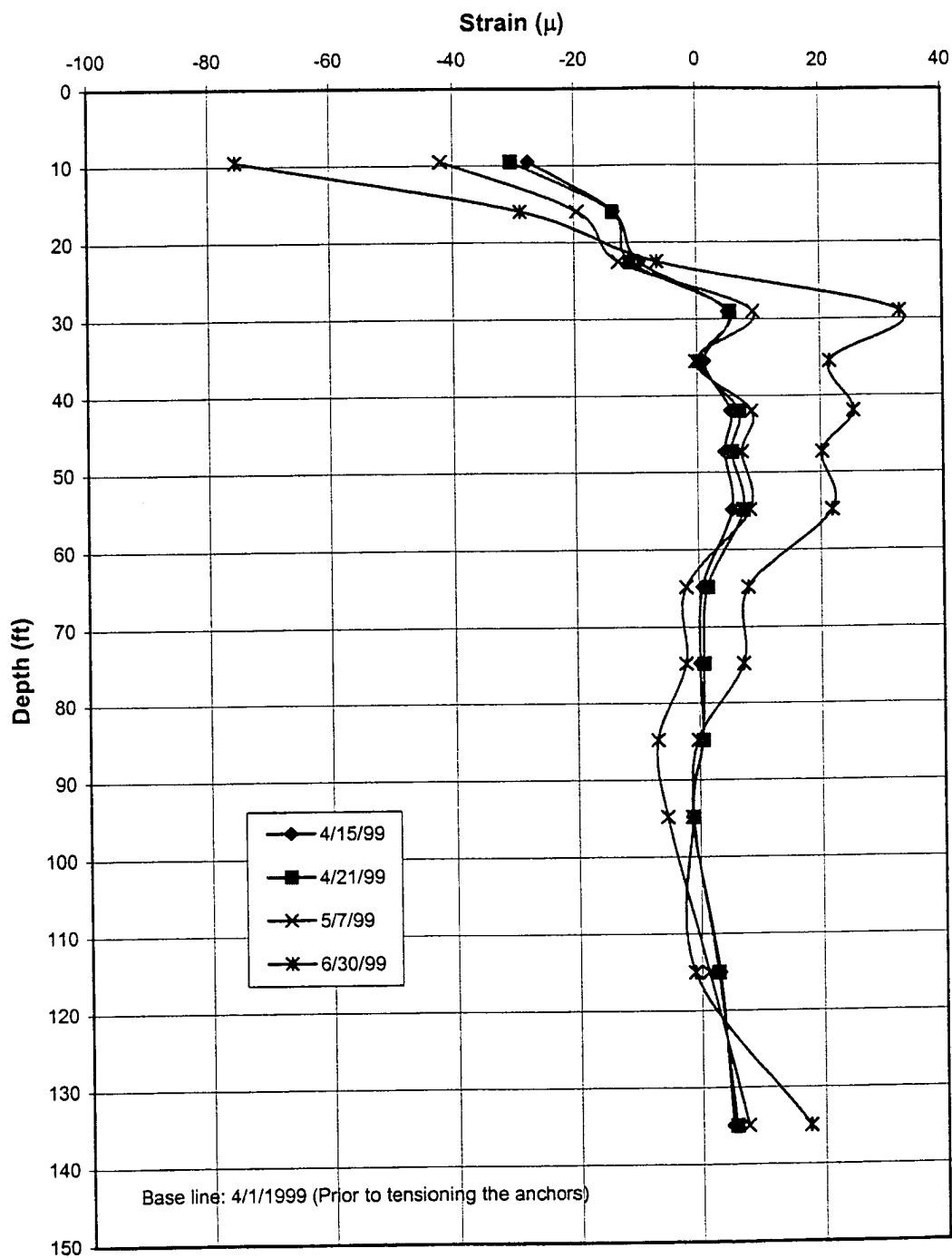


Fig. 4.147: Shaft # 1, South side, strain vs. depth for major events after tensioning rock anchors.

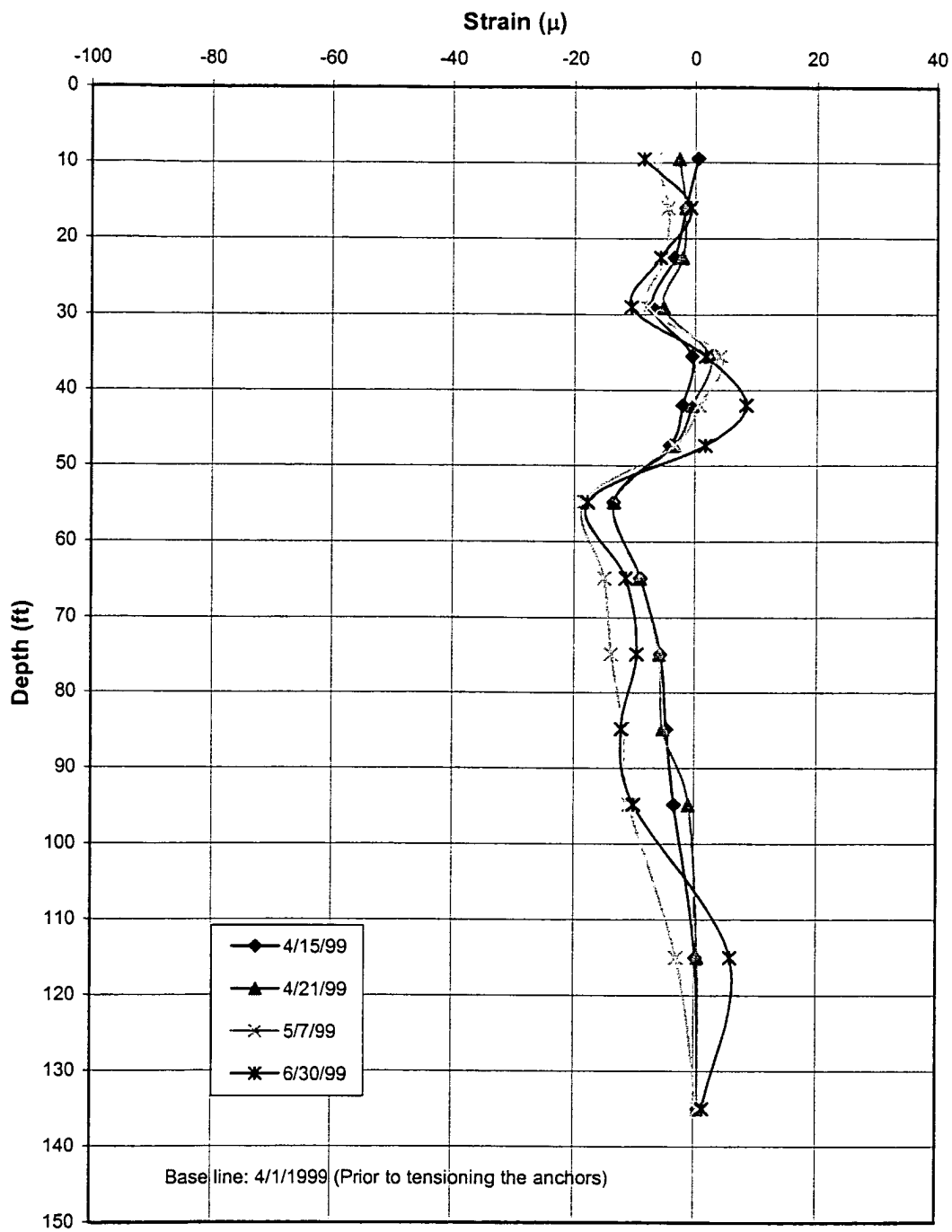


Fig. 4.148: Shaft # 1, North side, strain vs. depth for major events after tensioning rock anchors.

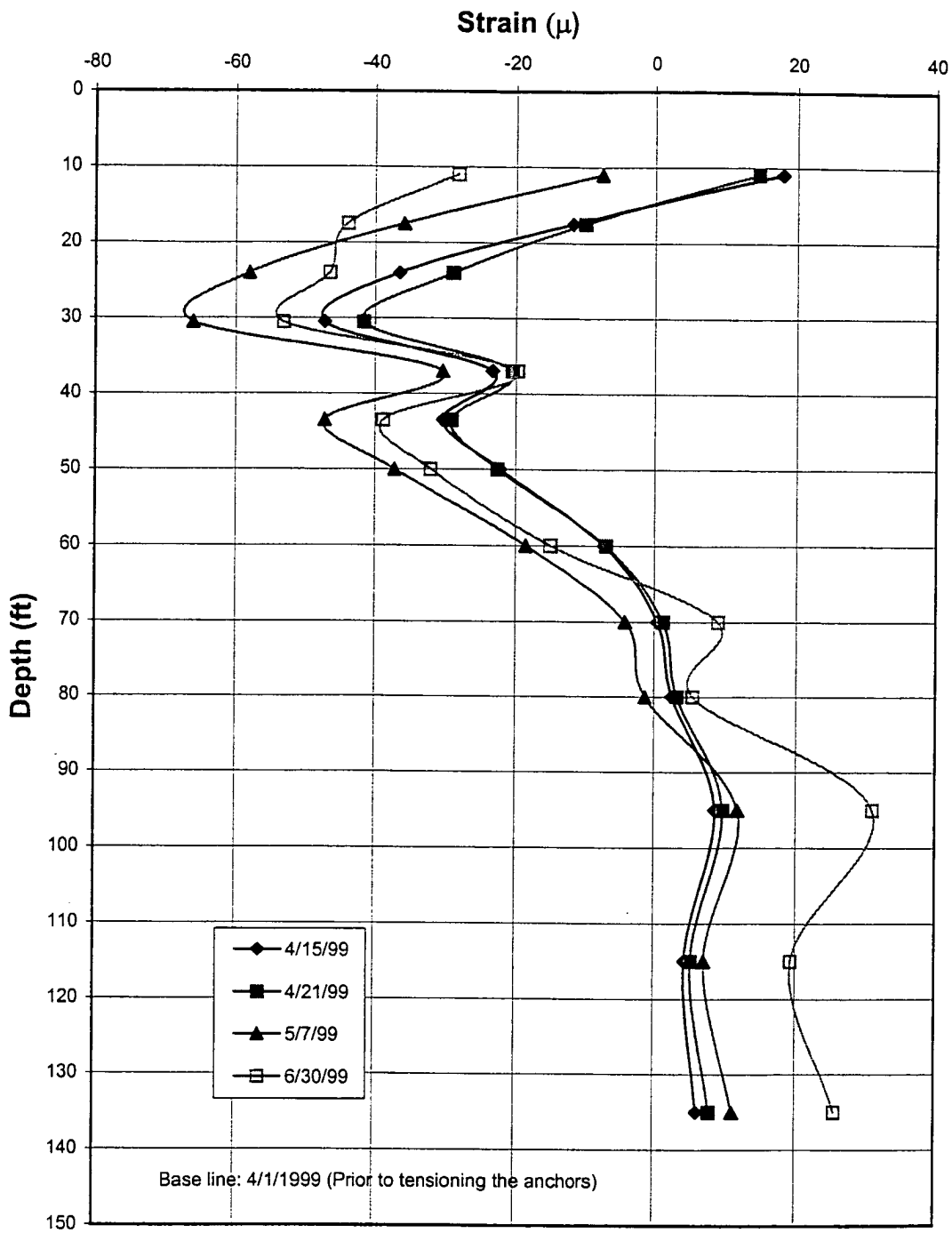


Fig. 4.149: Shaft # 9, Tension side, strain vs. depth for major events after tensioning rock anchors.

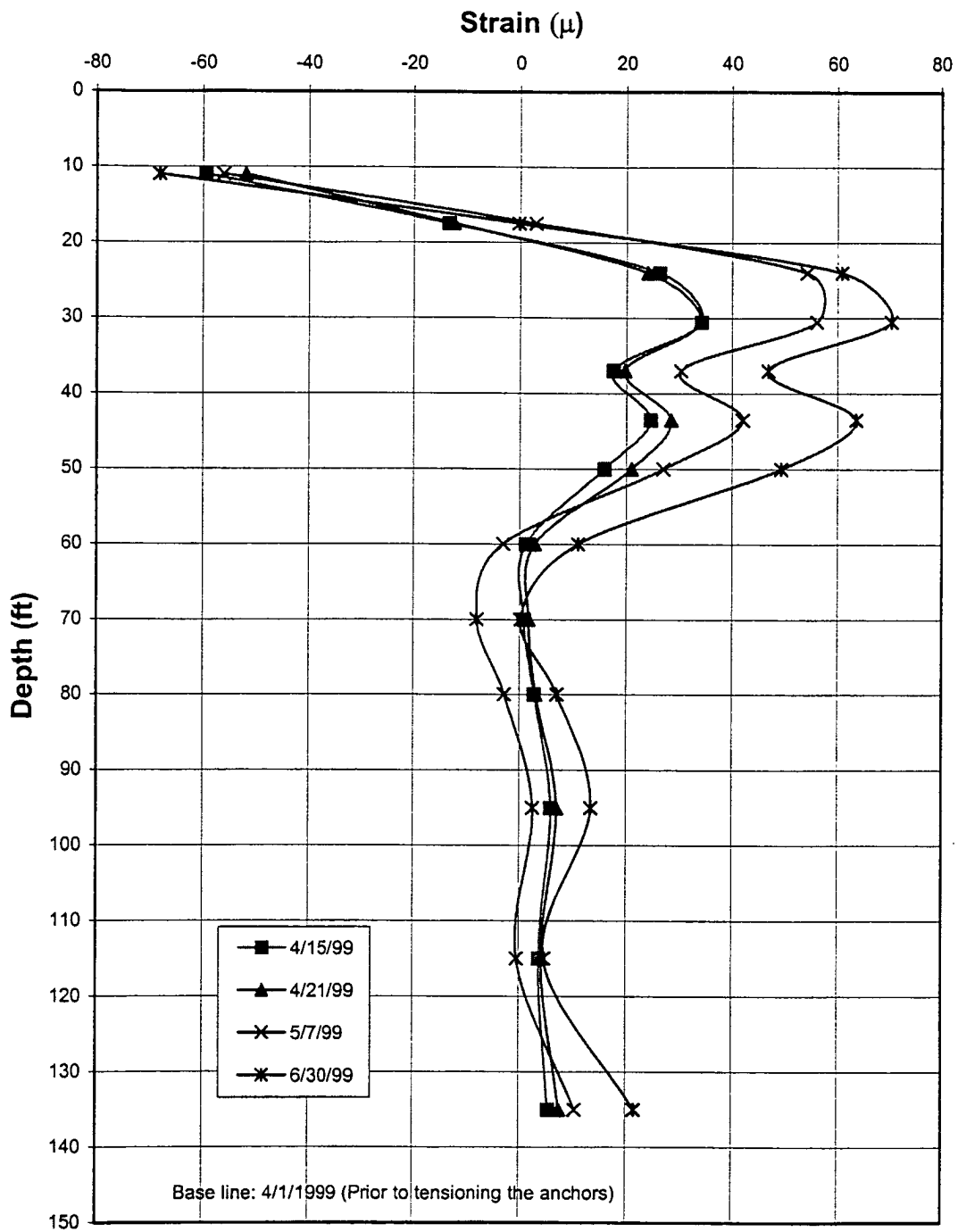


Fig. 4.150: Shaft # 9, Compression side, strain vs. depth for major events after tensioning rock anchors.

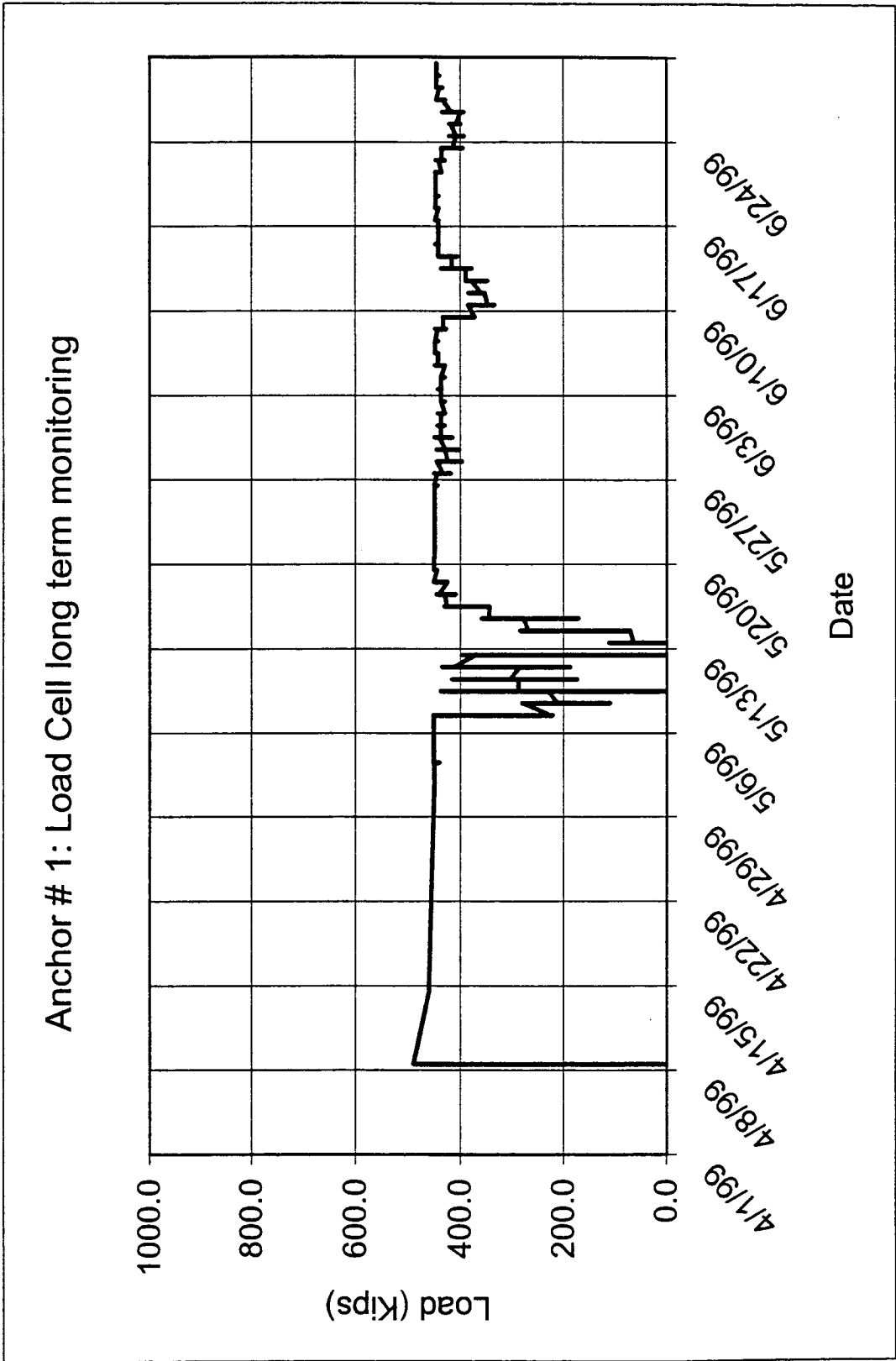


Fig. 4.151: Anchor # 1, long-term monitoring of load from load cell at anchor head.



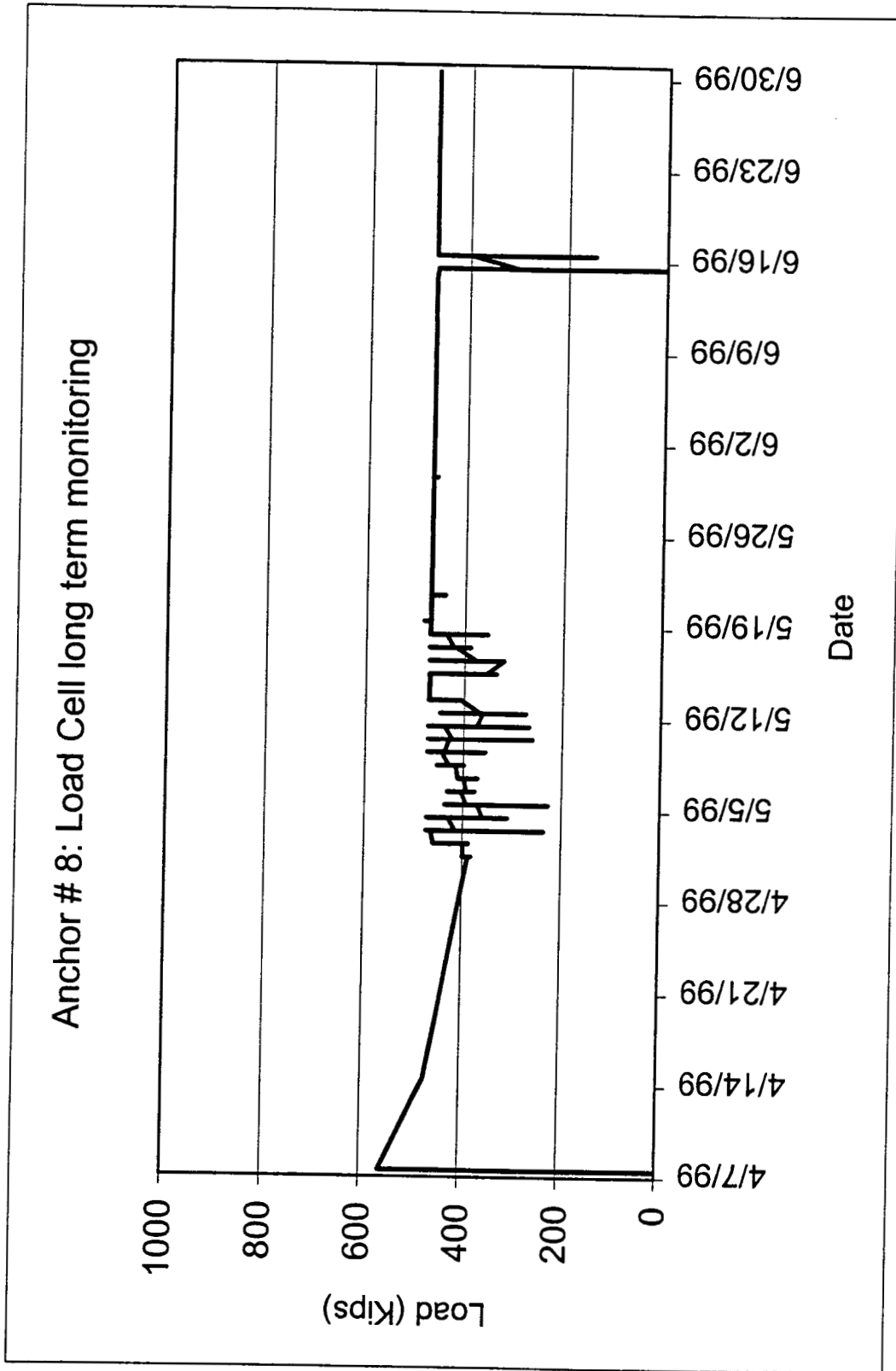


Fig. 4.152: Anchor # 8, long-term monitoring of load from load cell at anchor head.

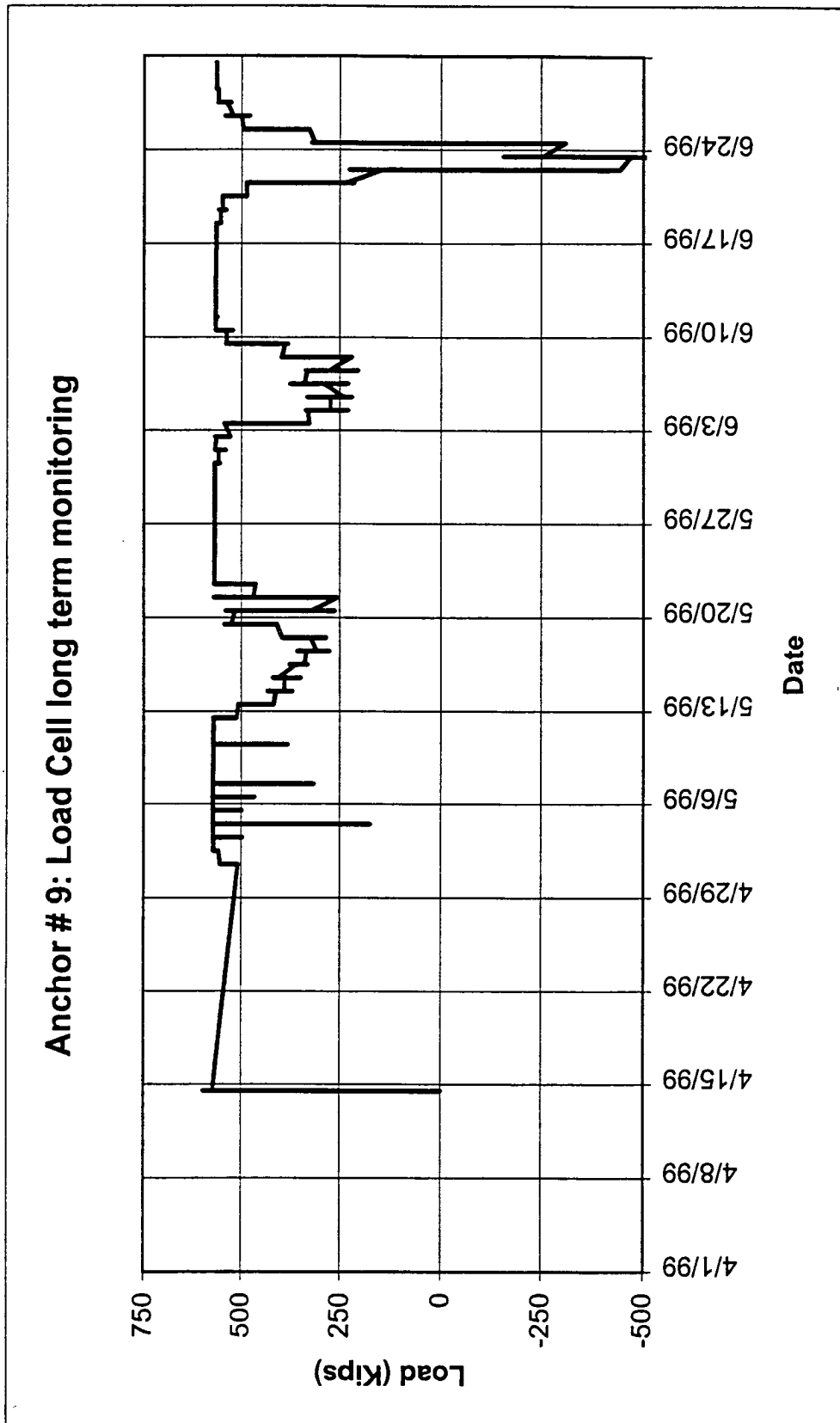


Fig. 4.153: Anchor # 9, long-term monitoring of load from load cell at anchor head.

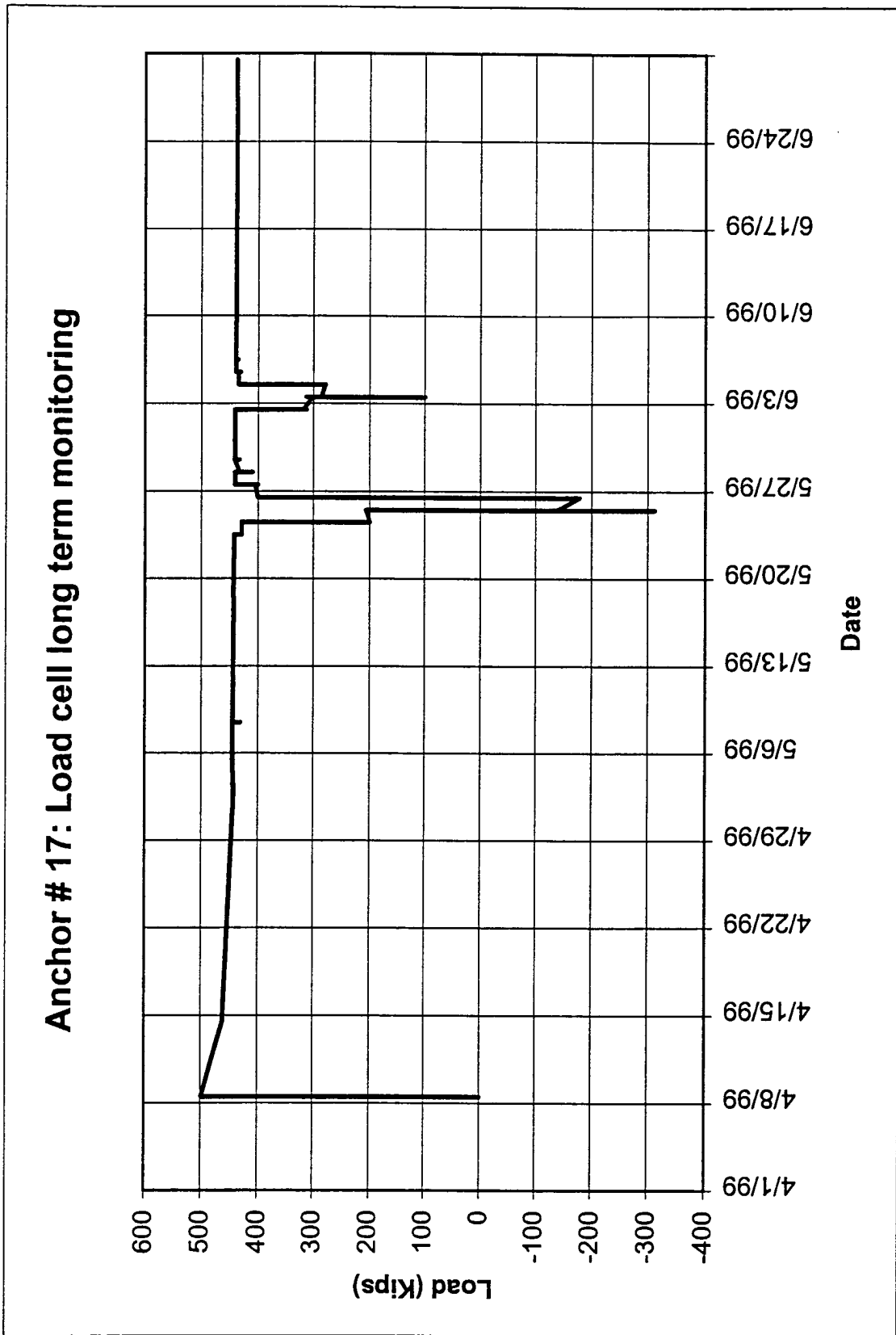


Fig. 4.154: Anchor # 17, long-term monitoring of load from load cell at anchor head.

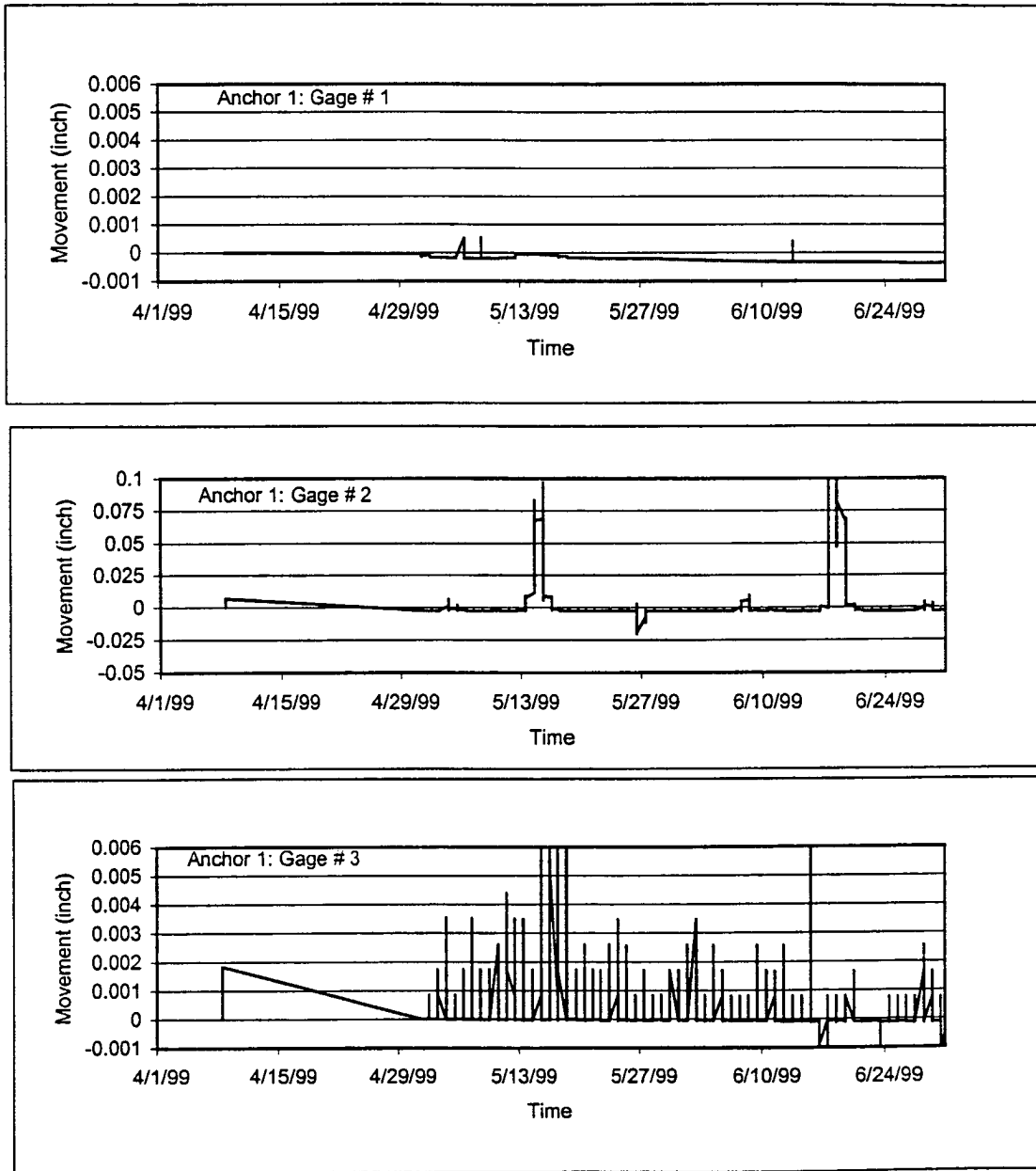


Fig. 4.155: Anchor # 1, movement at each gage location in the bonded length.

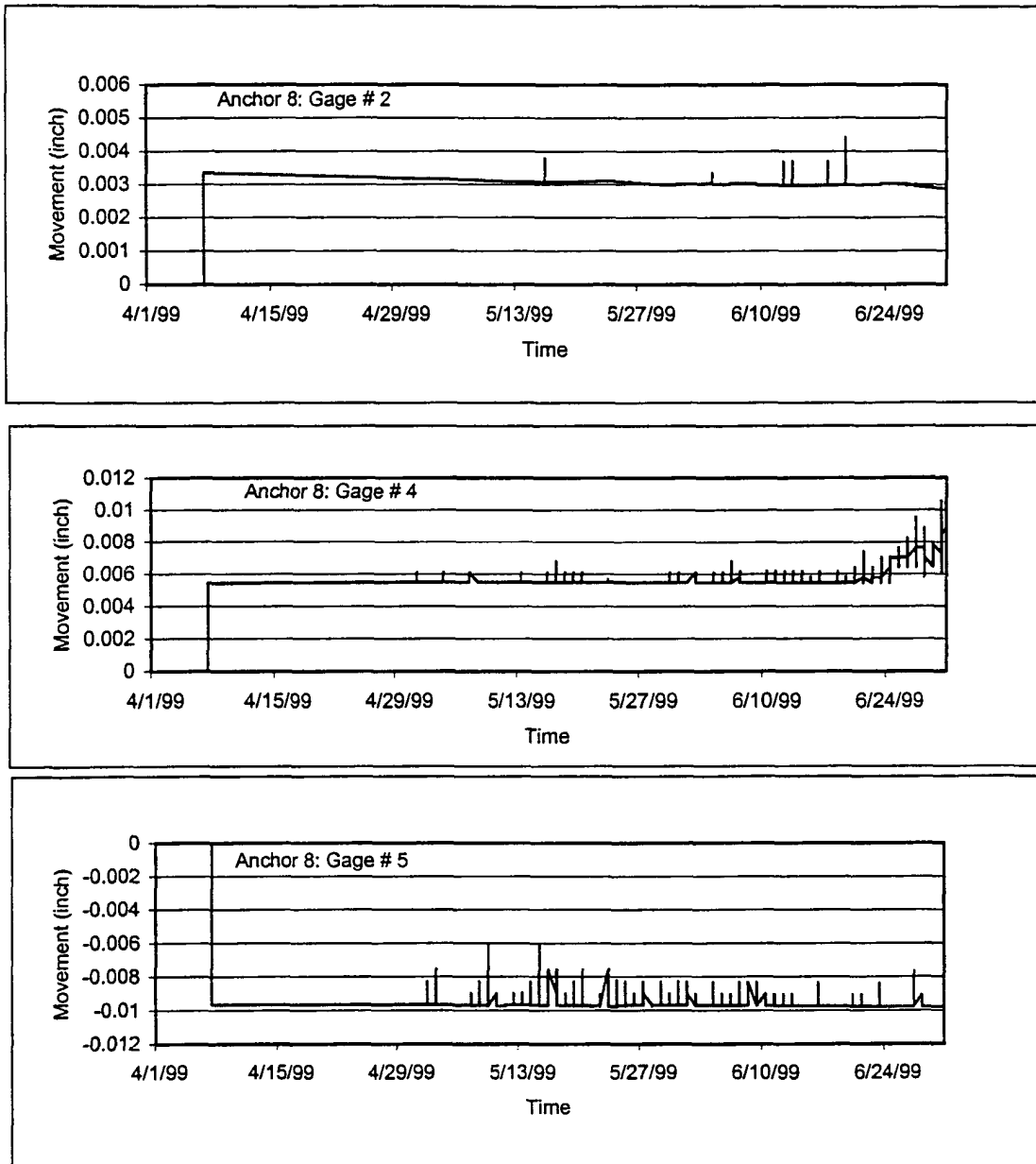


Fig. 4.156: Anchor # 8, movement at each gage location in the bonded length.

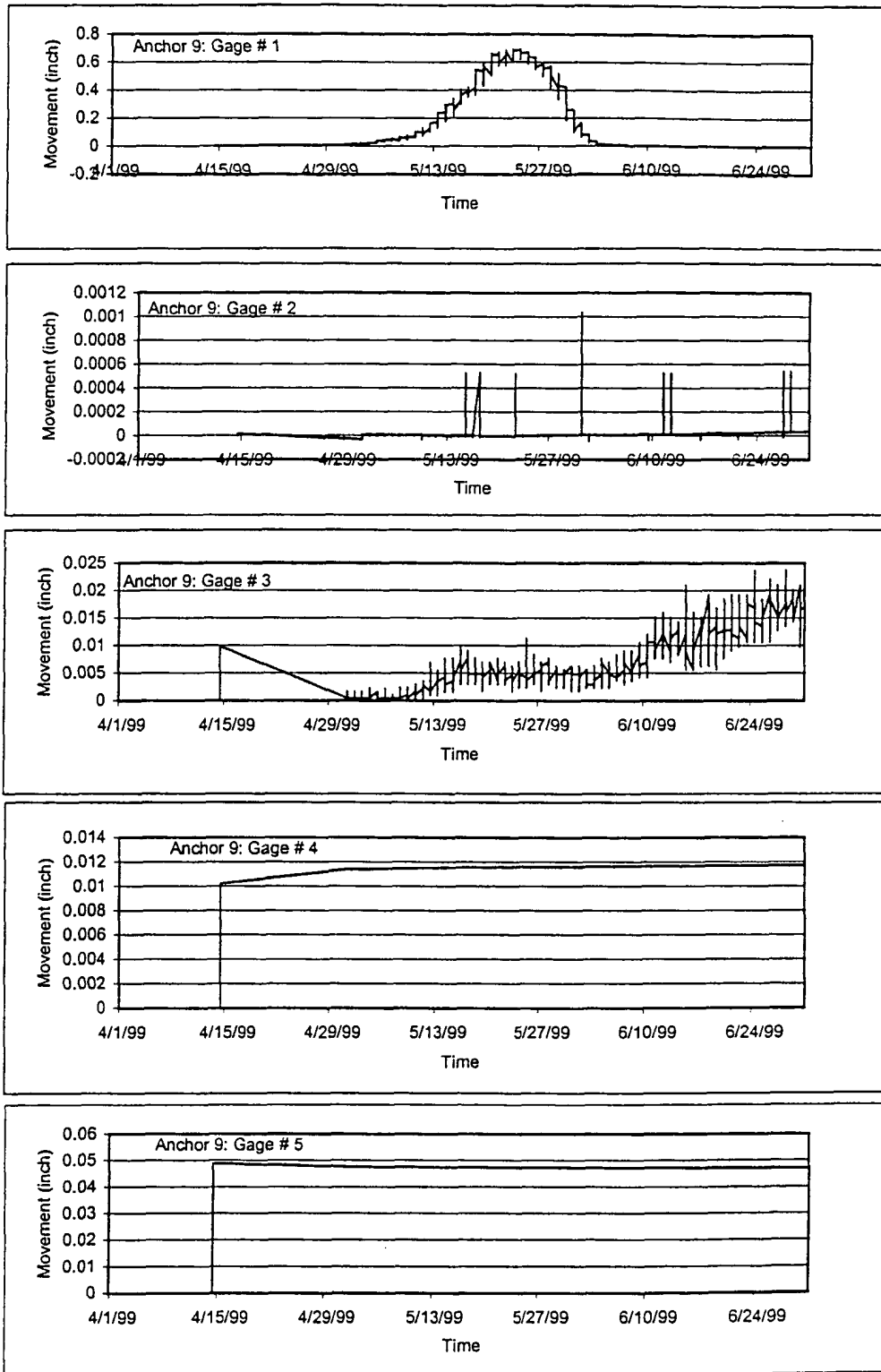


Fig. 4.157: Anchor # 9, movement at each gage location in the bonded length.

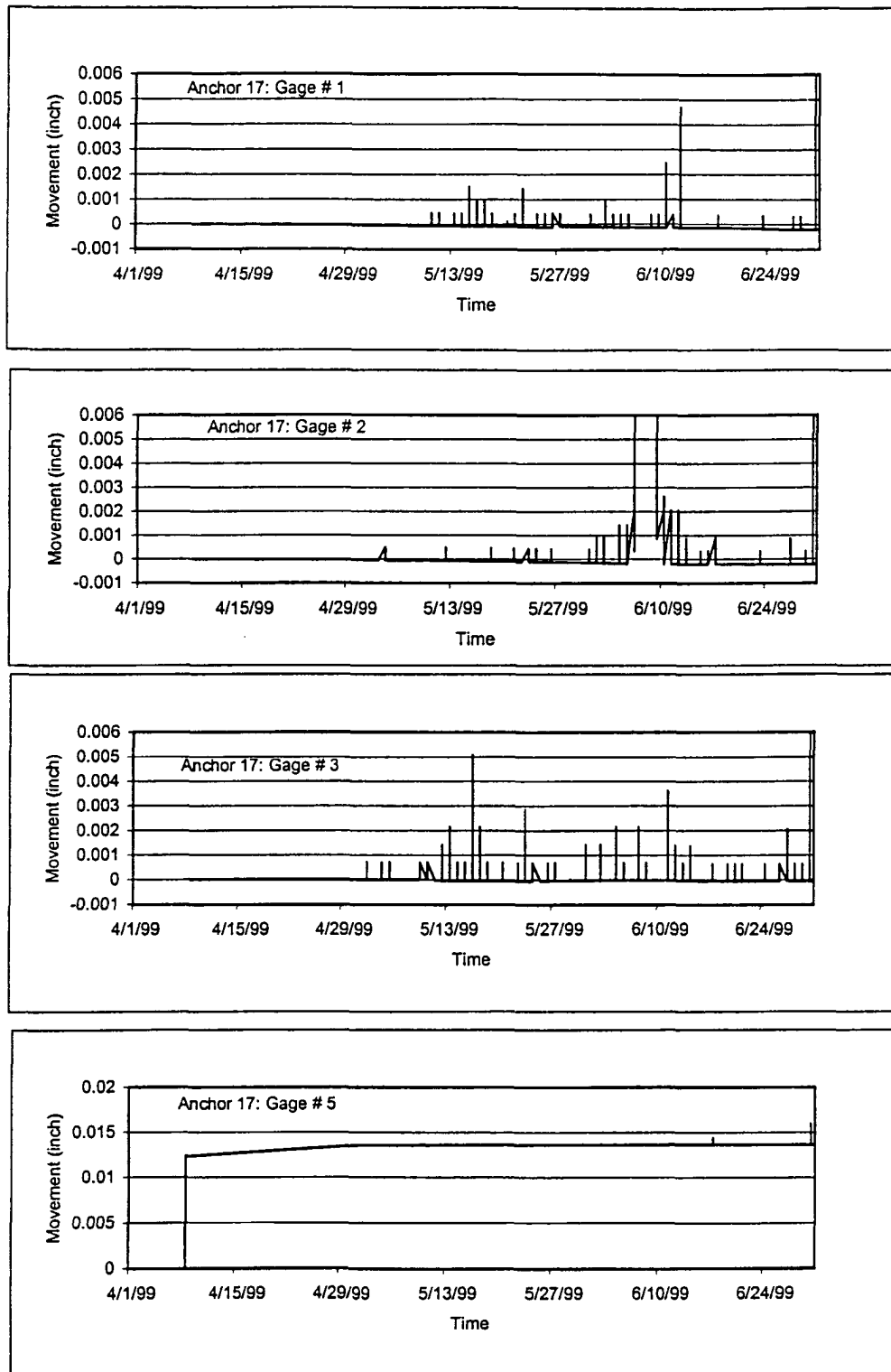


Fig. 4.158: Anchor # 17, movement at each gage location in the bonded length.

### Tiltmeter 878

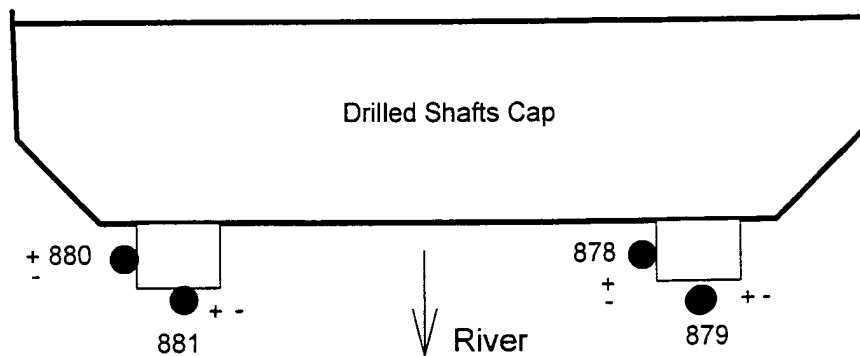
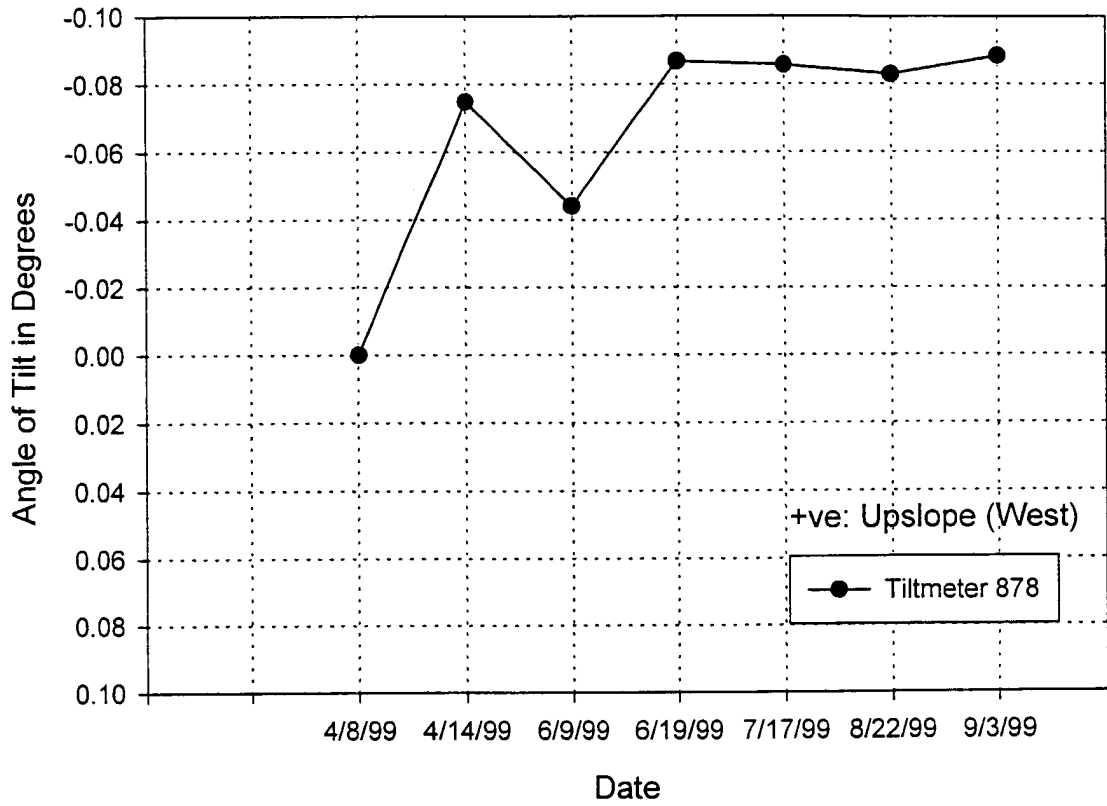


Fig 4.159: Angle of tilt in degrees for tiltmeter 878



### Tiltmeter 879

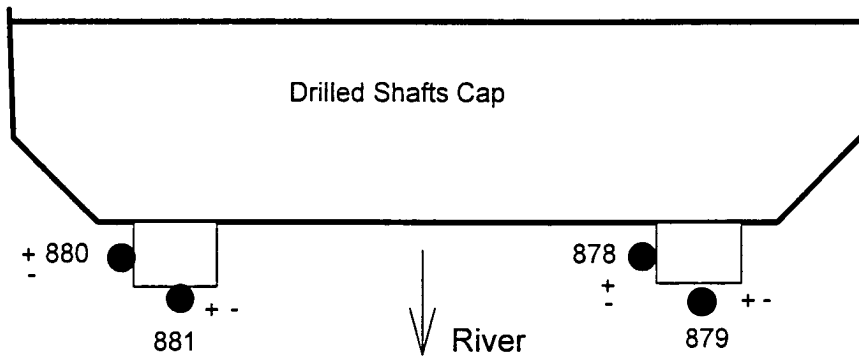
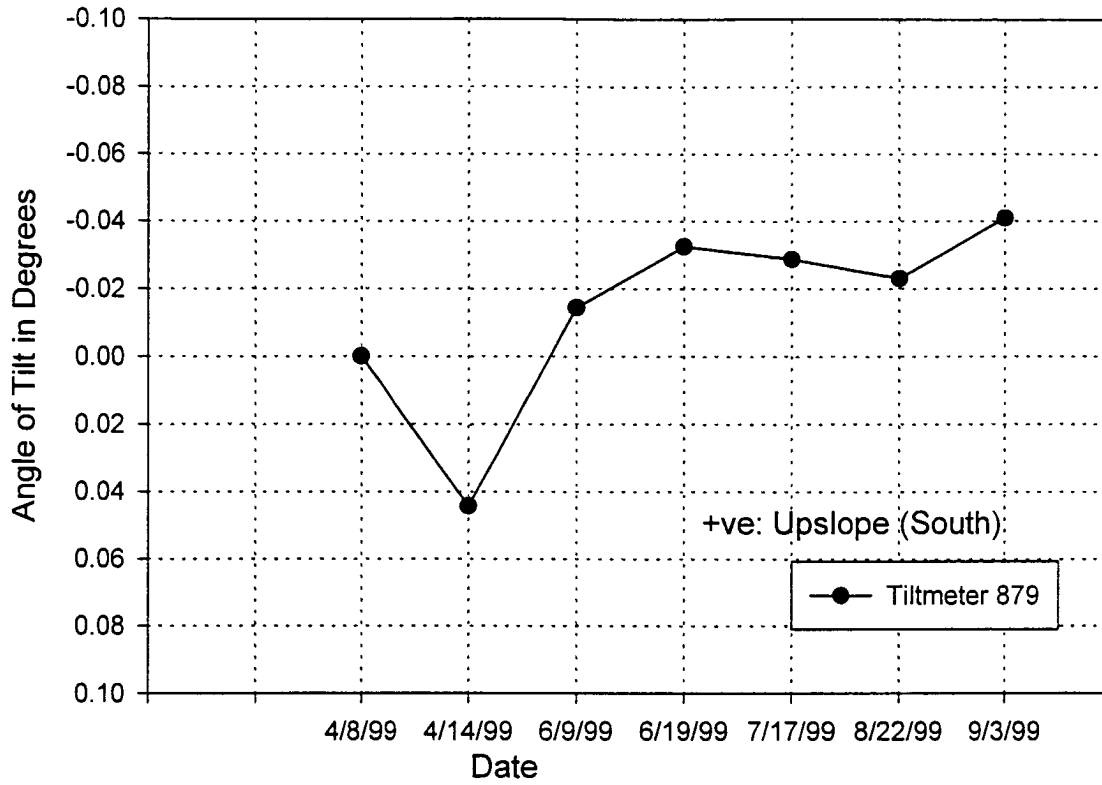


Fig 4.160: Angle of tilt in degrees for tiltmeter 879

### Tiltmeter 880

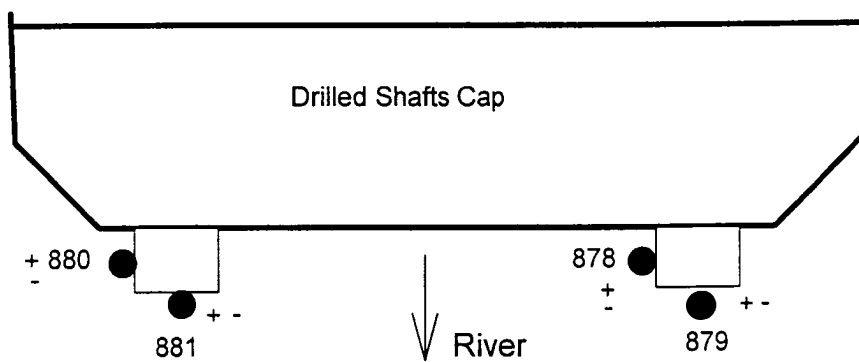
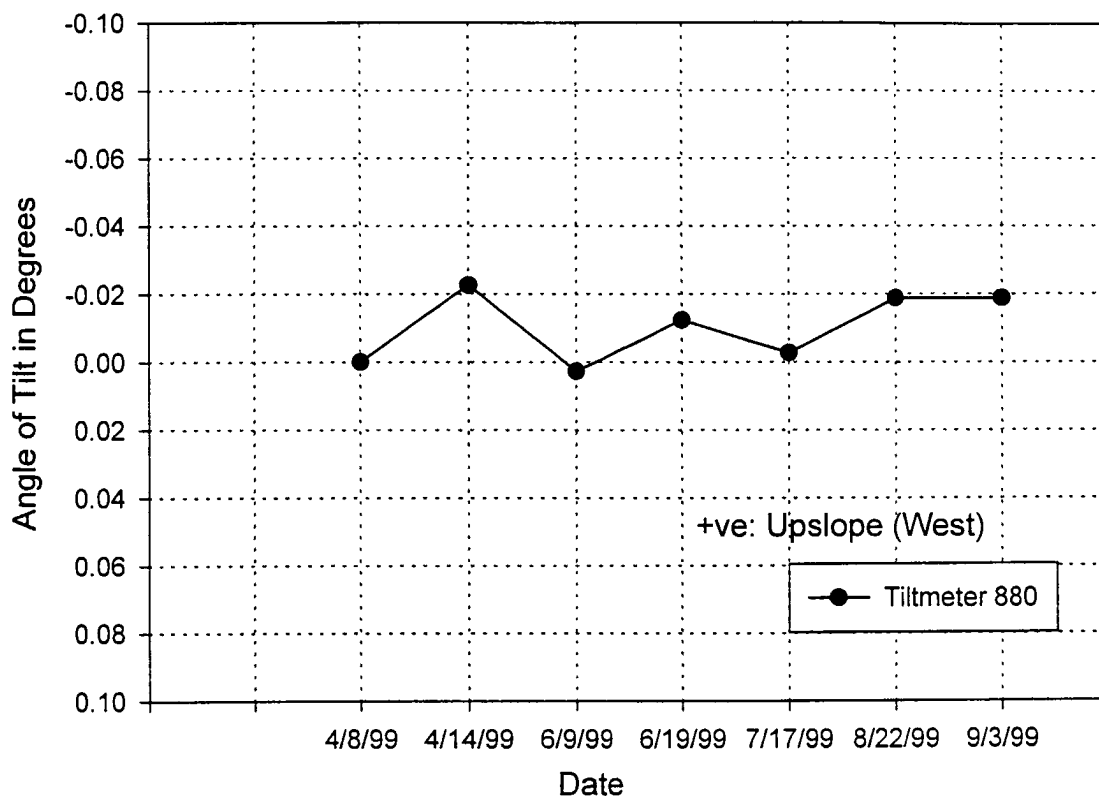


Fig 4.161: Angle of tilt in degrees for tiltmeter 880

### Tiltmeter 881

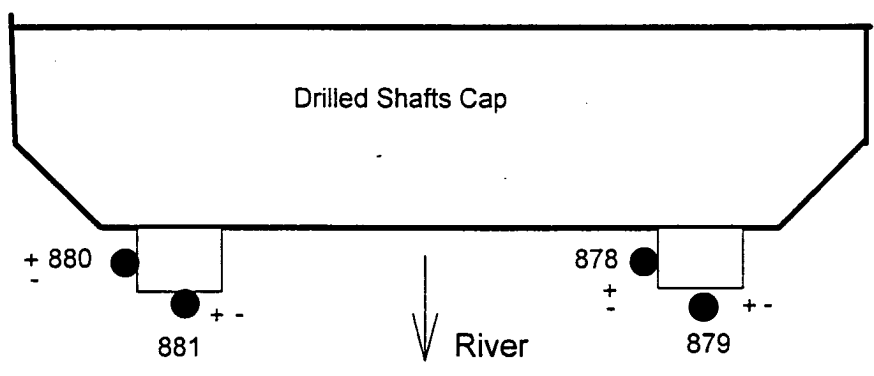
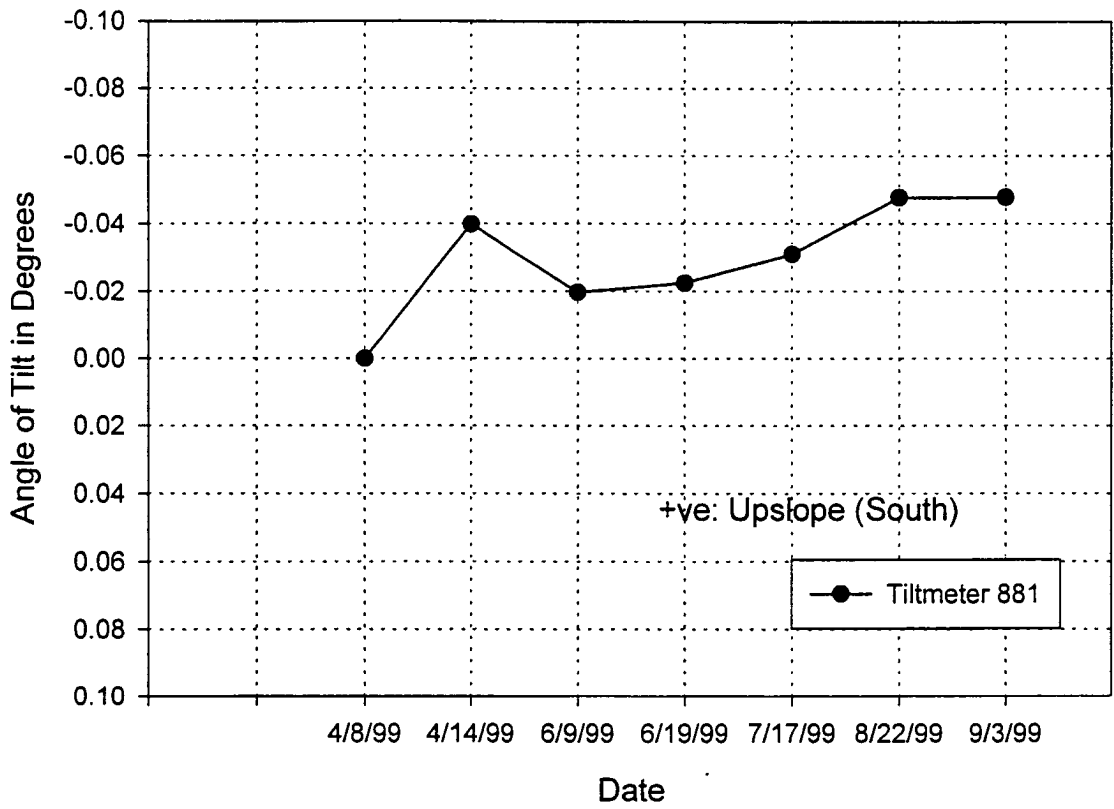
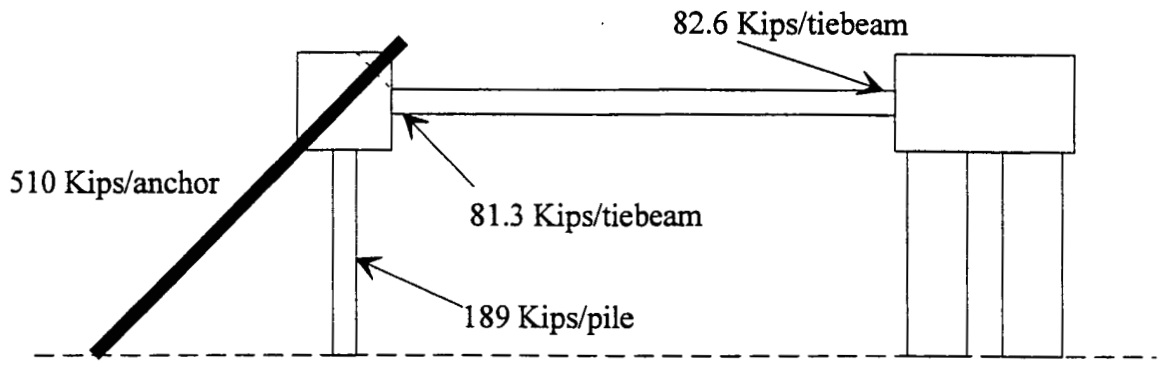
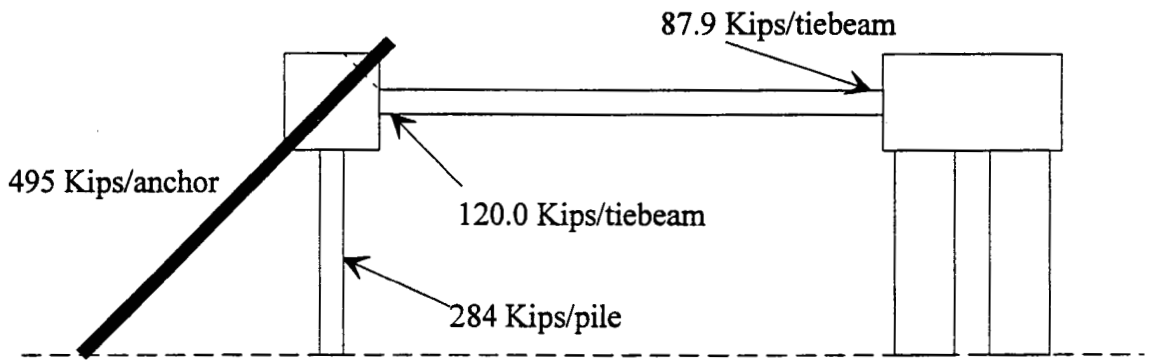


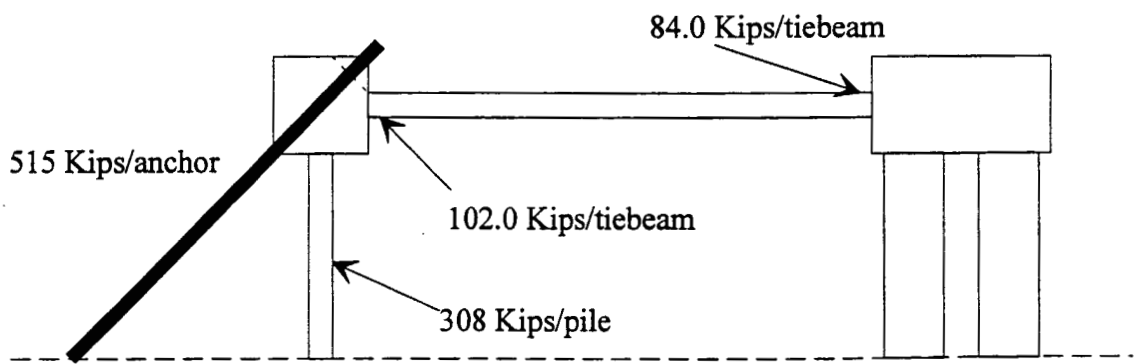
Fig 4.162: Angle of tilt in degrees for tiltmeter 881



Case I: After tensioning all rock anchors on 4/14/1999.



Case II: After complete backfilling of the slope on 5/7/1999.



Case III: At end of monitoring phase I on 6/30/1999.

Fig. 4.163: Force diagrams for the major events after tensioning the rock anchors.

## CHAPTER V

### FINITE ELEMENT ANALYSIS ON REINFORCED SLOPE

#### V.1 INTRODUCTION

The recent advent of computer techniques and finite element analysis methods has provided a powerful analytical tool that can be used for analysis of large-scale complex geotechnical problems. The employment of the finite element method for analysis of the stabilized slope behavior offers the following advantages:

- (a) The versatility of elements makes available the representation of the enormous geometry complexities involved in slope surface, critical slip plane and various existing and stabilization structures.
- (b) The versatility of constitutive models makes it capable of accounting for such complexities as nonlinear material behavior and discontinuities along the weak joint or slip surface.
- (c) The availability of high-speed digital computers makes it practical to incorporate all components of reinforcing structures, such as the stabilizing drilled shafts, prestressed ground anchors, tie-beams, and other slope stabilization structures.
- (d) The repeated computer runs using various soil parameters make it possible to systematically investigate the various aspects of factors controlling the slope stabilization mechanisms.

## V.2 FINITE ELEMENT MODELING OF CUY-90 PROJECT

A two-dimensional finite element program, PLAXIS, is used to simulate the construction of various stabilization structures at the CUY-90 project site. The main features of the slope geometry and the arrangement of the reinforced structures, including the drilled shafts, driven piles and prestressed anchors, make it true that a plane strain condition does prevail. Hence, the two-dimensional finite element model appears to be applicable. For the existing piers supported by pile group, their spatial behaviors are studied separately by a separate three-dimensional finite element (Florida Pier) model to determine an equivalent two-dimensional parameters to be used in the PLAXIS program.

A cross-section of the bridge abutment area is shown in Fig. 5.1. A finite element domain representing the cross-section between Stat. 14+50 and Stat. 20+60 is shown in Fig. 5.2. This domain includes all new stabilization structures and the existing structures (i.e. Pier 1, West End Pier and Pier 1A). The finite element mesh of the domain and the pertinent structures are shown in Fig. 5.3. The mesh consists of a total of 1032 elements and 2291 nodes. The soil layer is represented by five layers shown in Fig. 5.4. The driven steel piles, the drilled shafts and the tie-beams are modeled with beam elements. The ground anchors are modeled with the node-to-node anchor elements while the bond part of the ground anchors is modeled with the geotextile interface elements. In order to fully simulate the behaviors of the two slip planes, which were clearly indicated by the inclinometer readings, the interface elements allowing for the slippage are employed.

### V.3 MATERIAL PROPERTIES

#### V.3.1 Soil

The detailed soil boring information of the project site has been presented in Chapter III. Based on the interpretation of the available SPT N values and the description of the subsurface soil profile, the soil is divided into five layers with the corresponding parameters summarized in Table 5.1. These parameters were used as input in the PLAXIS FEM analysis.

**Table 5.1. Soil Properties**

Layer	Type	$\gamma_{dry}$ (pcf)	$\gamma_{wet}$ (pcf)	E (lb/ft <sup>2</sup> )	$\nu$	c (lb/ft <sup>2</sup> )	$\phi$ (°)
1	Sand	100.0	120.0	3.0e+5	0.25	2.0	38.0
2	Sand	100.0	125.0	1.0e+6	0.25	10.0	34.0
3	Clay	105.0	130.0	1.3e+6	0.33	3740	25.0
4	Clay	110.0	130.0	1.76e+6	0.33	3730	25.0
5	Bed rock	115.0	140.0	2.0e+6	0.20	10000	38.0

#### V.3.2 Stabilization Structures

The slope stabilization structures installed to enhance the slope stability in this project consist of the drilled shafts, driven piles, prestressed ground anchors and tie-beams. Detailed information on the dimensions, properties and layout of those structures can be found in Chapter III. The relevant structure parameters required as input in the PLAXIS are summarized in Table 5.2.

**Table 5.2. Properties of Reinforcement structures**

Component	Type	Spacing (ft)	E (lb/ft <sup>2</sup> )	$\nu$	EA (lb)	EI (lb·ft <sup>2</sup> )
Driven pile	HP14×89	4.4	4.177e+09	0.3	7.571e+08	1.821e+08
Anchor Strand	Φ0.6×16	8	4.177e+09	0.3	1.335e+08	/
Drilled Shaft	Φ72	16	6.251e+08	0.27	1.767e+10	4.578e+10
Tie-Beam	HP8×36	4	4.177e+09	0.3	2.988e+08	2.558e+07

#### **V.4 THREE-DIMENSIONAL EFFECT OF EXISTING PILE SUPPORTED PIER**

There are three types of piers in the finite element domain (i.e. Pier 1, West End Pier and Pier 1A). Since they are the main foundation to support the bridge, and consequently transfer the load induced from the bridge to the deeper soil of the slope, it is important to use representative structure parameters in the FEM simulation. On the other hand, the stiffness of the piers certainly plays an important role in resisting the slope deformation and movement. The dimension and layout of the piles underneath the piers of the CUY-90 project do not meet plane strain condition. Consequently, a separated three-dimensional finite element analysis using the FLPIER program was carried out to study the effects of the existing piers. In FLPIER, each pile is modeled with sixteen beam elements and the cap for pile group is modeled with shell elements accounting for shear deformation. The finite element meshes of the 9 × 9 -pile pier of Pier 1 with cross-section shown in Fig. 5.5 for in situ case and a 9 × 36 -pile pier intentionally designed for simulating plane strain condition are shown in Fig. 5.6 and 5.7, respectively. The pile and soil properties required as input in FLPIER are summarized in Table 5.3 and 5.4.



**Table 5.3. Properties of pile and cap**

	E (ksi)	v	length (in)	diameter (in)	thickness (in)
Pile	3125	0.3	1056	14	/
Cap	3125	0.3	/	/	91.2

**Table 5.4. Properties of soil**

Soil layer	Soil type	Elevation (in)	$\phi$ (degree)	Cu (ksi)	K (kci)	$\epsilon_{50}$	$\gamma$ (kci)	G (ksi)
1	sand	0~91.2	38	/	0.06	/	$5.787 \times 10^{-5}$	2.778
2	sand	91.2~259.2	34	/	0.06	/	$7.234 \times 10^{-5}$	2.778
3	clay	259.2~583.2	/	0.0260	1.00	0.005	$7.523 \times 10^{-5}$	3.394
4	clay	583.2~1687.2	/	0.0259	1.00	0.005	$7.523 \times 10^{-5}$	4.595

The differences between the two models are investigated under the condition that all pile parameters such as diameter, length and stiffness are identical together with the same soil properties. The deflections for the two models subject to lateral loads are plotted in Fig. 5.8 for comparison. As expected, the  $9 \times 9$ -pile pier with less number of piles yields larger movement than the  $9 \times 36$ -pile pier does. The initial slope of the load-deflection curve for the  $9 \times 9$ -pile pier is approximately 7425 kips/in, whereas the slope for the  $9 \times 36$ -pile pier is 43813 kips/in. The factor of these slopes reaches as high as 5.9.

This indicates that the pier's ability to provide lateral load against slope movement might be significantly exaggerated if it is assessed using a two-dimensional model.

In order to find an equivalent two-dimensional model for the three-dimensional effect of the pier, a series of calculations through adjusting the stiffness of the pier have been carried out. A representative  $EI$  is finally obtained as  $60831 \text{ kips}\cdot\text{in}^2$  which is only 3% of the original stiffness. As shown in Fig. 5.9, the deflection behavior of the  $9 \times 36$ -pile pier with the new stiffness is almost identical to that of the  $9 \times 36$ -pile pier. The value of the representative  $EI$  of  $60831 \text{ kips}\cdot\text{in}^2$  is used for representing the pile stiffness of the pier in the two-dimensional finite element analysis of the entire slope system.

The methodology used to simulate the three-dimensional effects of pile-supported pier can be described as follows

- a) A unit of three-dimensional pile group for in situ case shown in Fig. 5.6 was developed for the Florida Pier computer runs to obtain the load vs. deflection behavior.
- b) A special unit of three-dimensional (3-D) pile group, shown in Fig. 5.7, which simulates two-dimensional condition, was developed for the Florida Pier computer runs.
- c) Compare the results obtained from a) and b) for a wide range of load conditions. From these comparison results, the pile properties for two-dimensional case were adjusted so that the load-deflection curves would match the true 3-D case.

## V.5 CALIBRATION STUDY TO DETERMINE SLIP SURFACE PROPERTIES

As indicated by the inclinometer readings, there are two apparent slip surfaces, shown in Fig 5.2, where the shear strength has been fully mobilized and significant slippage approximately 2.5 inches has been observed. It is known that the strength and stiffness of soil along the slip planes would have been weakened due to relative slippage. Therefore, the two sliding surfaces with reduced strength properties need to be incorporated in the finite element model.

The decrease of strength of the slip plane is represented by a strength reduction factor  $R_{inter}$  in PLAXIS. The slip plane properties are calculated from following equations:

$$c_{inter} = R_{inter} c_{soil}$$

$$\tan \varphi_{inter} = R_{inter} \tan \varphi_{soil}$$

where  $c_{inter}$  and  $\varphi_{inter}$  are the cohesion and friction angle of the interface and  $c_{soil}$  and  $\varphi_{soil}$  are the cohesion and friction angle of the adjacent soil. In addition to the Coulomb's strength criterion, the tension cut-off criterion also applies:

$$\sigma_{n,inter} < \sigma_{t,inter} = R_{inter} \sigma_{t,soil}$$

where  $\sigma_{n,inter}$  is normal stress acting on the interface, and  $\sigma_{t,inter}$  and  $\sigma_{t,soil}$  are the tensile strength of the interface and soil, respectively.

In general, the interface used to simulate the slip planes is weaker in strength and stiffness than the adjacent soil layers. Typically, the value of  $R_{inter}$  varies between 0 and 1. For this project, the slip surfaces run through four soil layers, each with different properties. Therefore, different combinations of strength reduction factors associated with

each layer need to be calibrated by matching the FEM predictions with field inclinometer measurements. An extensive amount of efforts has been spent to calibrate the interface slip plane properties. Table 5.5 provides an example of soil properties for the six runs

**Table 5.5. Typical Combinations of Strength Reduction Factors  $R_{inter}$**

	Layer 1	Layer 2	Layer 3	Layer 4
Case 1	0.333	0.333	0.333	0.333
Case 2	0.500	0.500	0.500	0.500
Case 3	0.333	0.333	0.333	0.500
Case 4	0.333	0.333	0.500	0.500
Case 5	0.333	0.333	0.400	0.500
Case 6	0.333	0.340	0.360	0.500

As shown in Fig. 5.10, the deflection profile measured at bore hole B-103 was matched with the calculations in case 6. The slip plane properties with the corresponding reduction factors listed for case 6 were used for the subsequent numerical simulations.

## V.6 SIMULATION OF CONSTRUCTION PROCESSES

It is well known that the final stress and deformation state of the nonlinear problems, encountered in most earth structure constructions similar to the project considered here, is highly path and initial stress dependent. The stabilization structure construction in the CUY-90 project involves sequentially an excavation for driven piles and installation of various stabilization structures. For a realistic evaluation of stress and

deformation in these structures, the construction sequences and initial stress should be simulated as carefully as possible so as to account for the path and initial stress dependency and material nonlinearity introduced by incremental constructions.

For the initial stress, the in situ stress under gravity and superstructure-induced loads are first introduced into the finite element mesh. The calculated stress and deformation at this stage can be considered as the initial state. For the subsequent constructions, the construction sequences are carefully simulated in correspondence with the construction events described in Chapter III. The entire simulation approach involves the following steps in sequence.

- Phase 1. In situ stress under gravity and groundwater pressure.
- Phase 2. Activation of the pier structures, including Pier 1, West End Pier, and Pier 1A.
- Phase 3. Application of the loads from bridge.
- Phase 4. Excavation for pile driving.
- Phase 5. Installation of temporary retaining structures with drilled shafts.
- Phase 6. Installation of driven piles, pile cap, and partial backfilling.
- Phase 7. Excavation of the rest of top soil for drilled shafts and tie-beams.
- Phase 8. Installation of drilled shafts.
- Phase 9. Installation of tie-beams.
- Phase 10. Tensioning of rock anchors.
- Phase 11. Backfill to the final grade.

## V.7 FEM ANALYSIS RESULTS AND DISCUSSION

### V.7.1 Stresses and Deformations in Soil Mass

The execution of computer program PLAXIS requires that the loading path due to construction be strictly followed. For each construction phase, the loading step has to be further divided into several sub-steps, as required by the incremental finite element method to ensure the convergence of nonlinear iteration. Table V.6 summarizes the number of calculation step for all stages.

**Table V.6 Incremental steps for nonlinear calculation**

Phase No.	1	2	3	4	5	6	7	8	9	10	11
Steps	23	3	5	8	3	4	3	2	3	7	6

The computer simulation results for each phase are presented in a variety of plots. These plots include: (a) the total displacement vectors indicating the major direction of soil movement, (b) the total displacement contours, (c) the principal stress directions and magnitude, (d) the mean effective stress contours, (e) the relative shear stress ratio contour, where relative shear stress ratio is defined as the shear stress applied over the shear strength available. These plots are presented in Fig. 5.11 to Fig. 5.65.

### V.7.2 Force in Structure Members

In addition to the stresses and deformations calculated for the soil mass, the computer simulation also generates the resulting forces and moments in the stabilization

structures. The calculated results for each structure at different construction stages are presented below.

#### **V.7.2.1 Temporary Retaining Wall Structure**

The temporary retaining wall system consists of drilled shafts and the lagging system, as detailed in Chapter III. The calculated deflections of the structure at stage 6 are shown in Fig. 5.66.

#### **V.7.2.2 Driven Piles**

At various construction stages, the calculated bending moments, axial forces, and lateral deflections, along the pile length, are shown in Fig. 5.67 to Fig. 5.72, respectively.

#### **V.7.2.3 Drilled Shafts**

At various construction stages, the calculated bending moments, axial forces, and lateral deflections, along the shaft length, are shown in Fig. 5.73 to Fig. 5.84, respectively.

#### **V.7.2.4 Tie-beams**

The calculated bending moments, shear forces, and axial forces, along the tie-beam axis, are shown in Fig. 5.85 to Fig. 5.90, respectively.

#### **V.7.2.5 Ground Anchors**

The calculated axial force along the ground anchor length after the tension of the anchor is shown in Fig. 5.91.

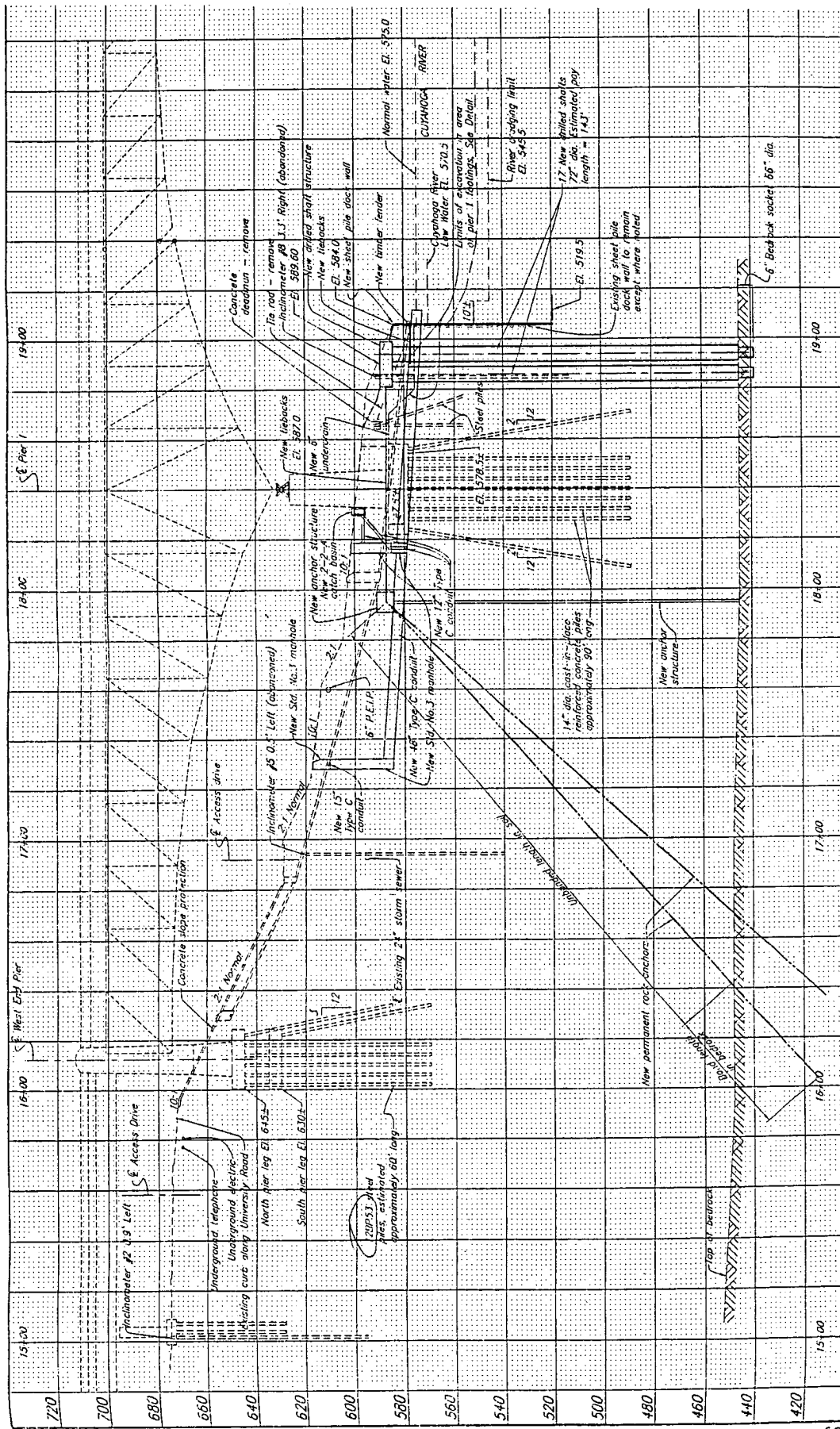


Fig. 5.1: Centerline cross-section of CUY-90 project



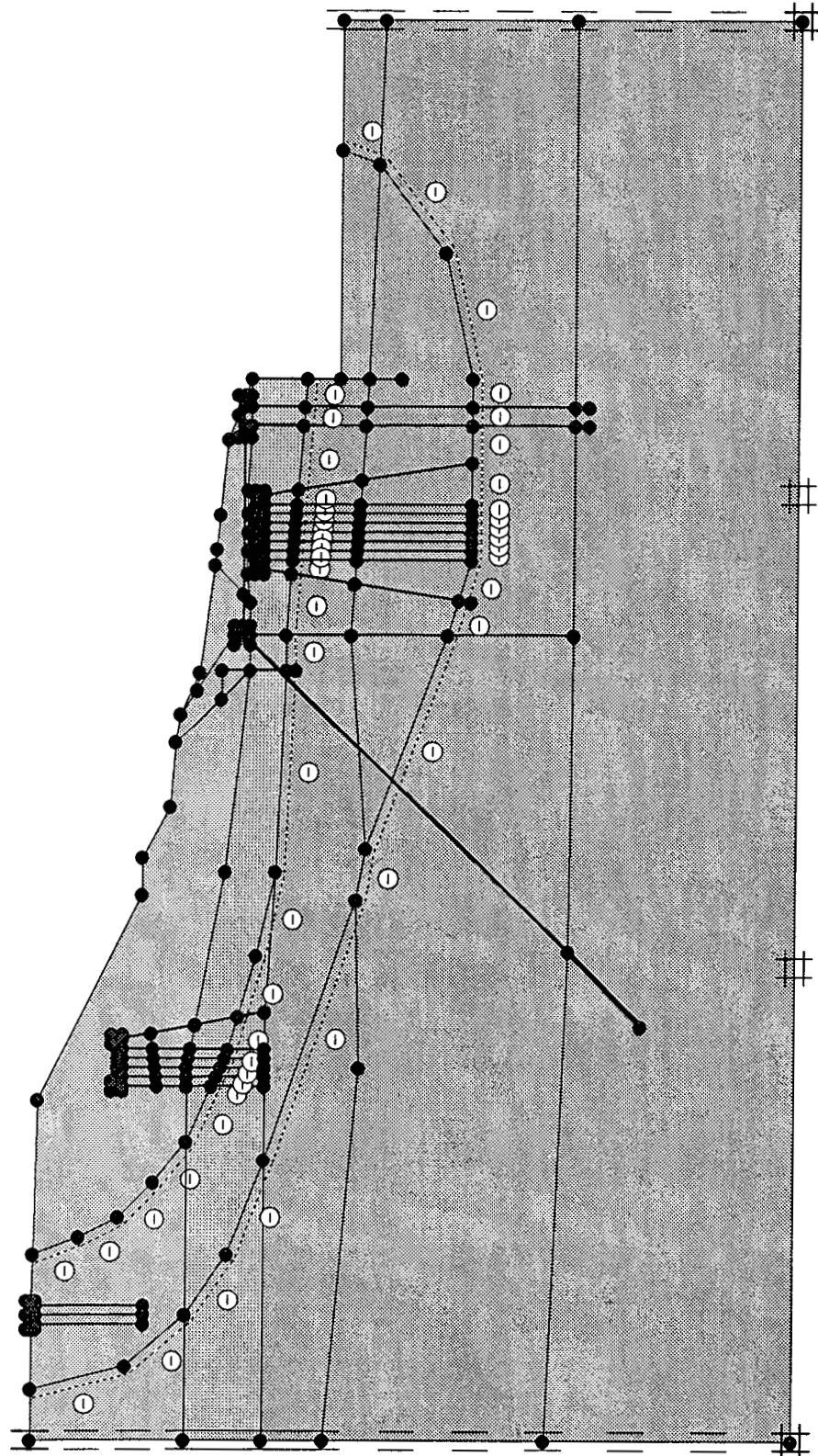


Fig. 5.2: Calculation model

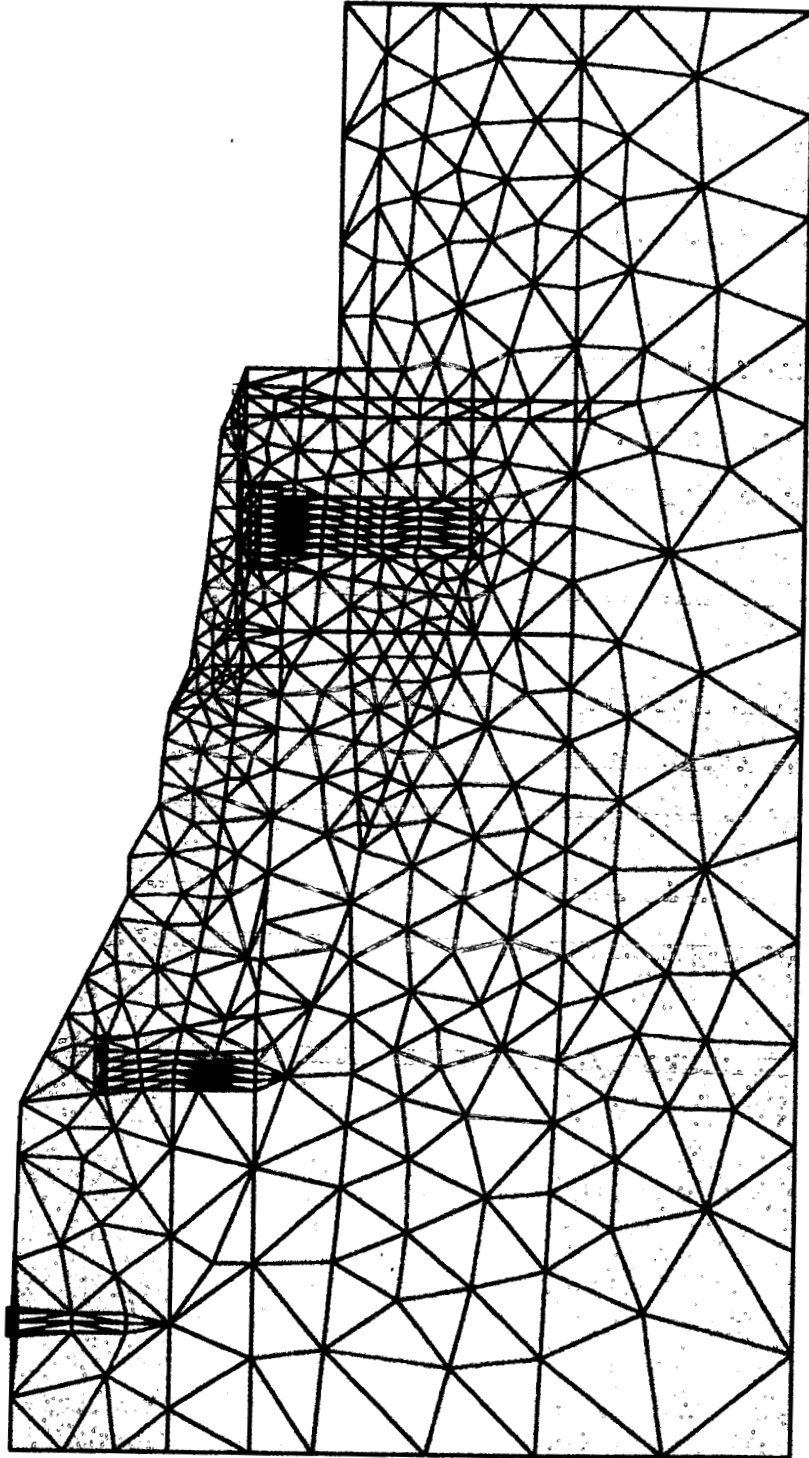


Fig. 5.3: Finite element mesh

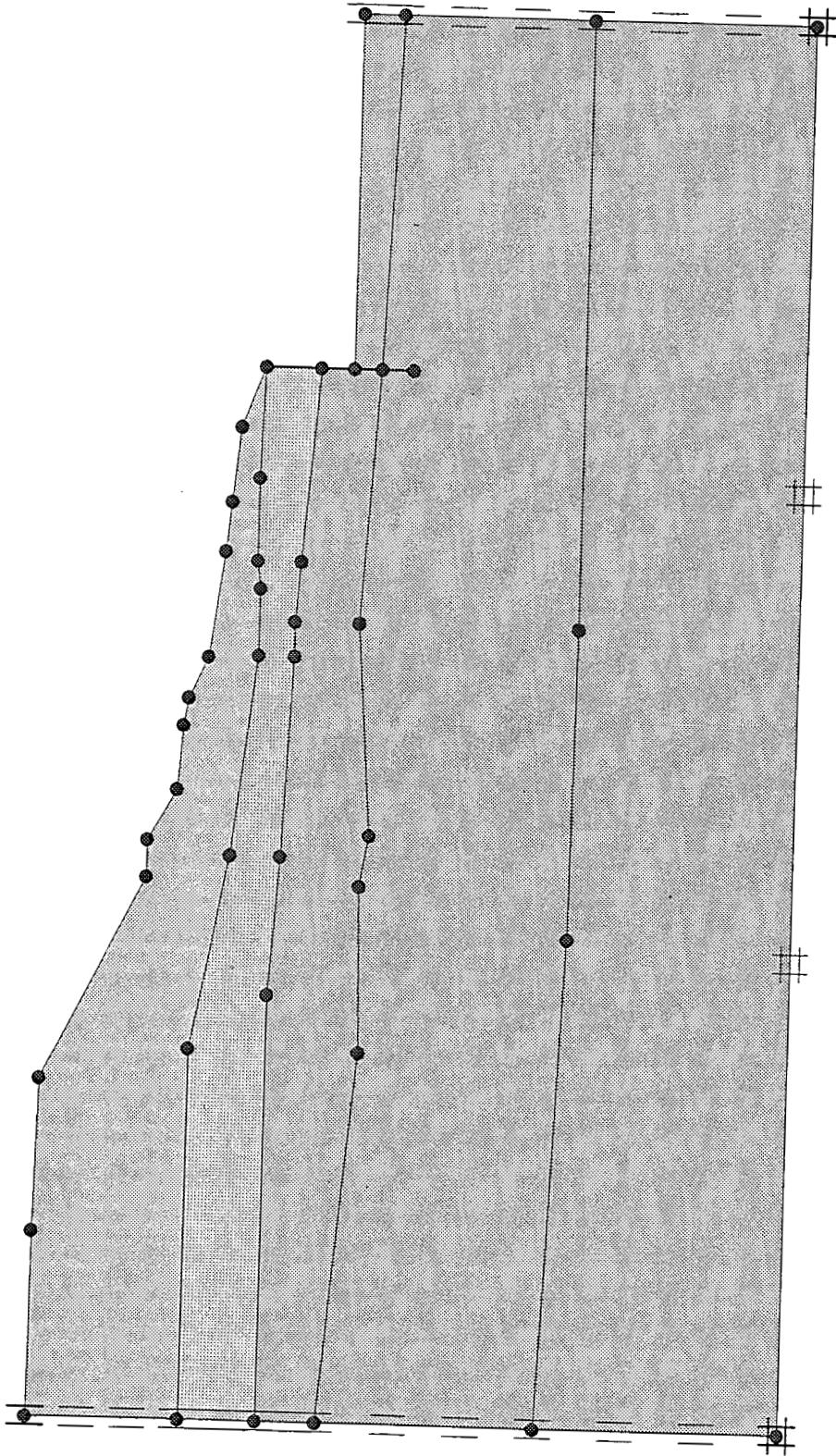


Fig. 5.4: Soil layering information

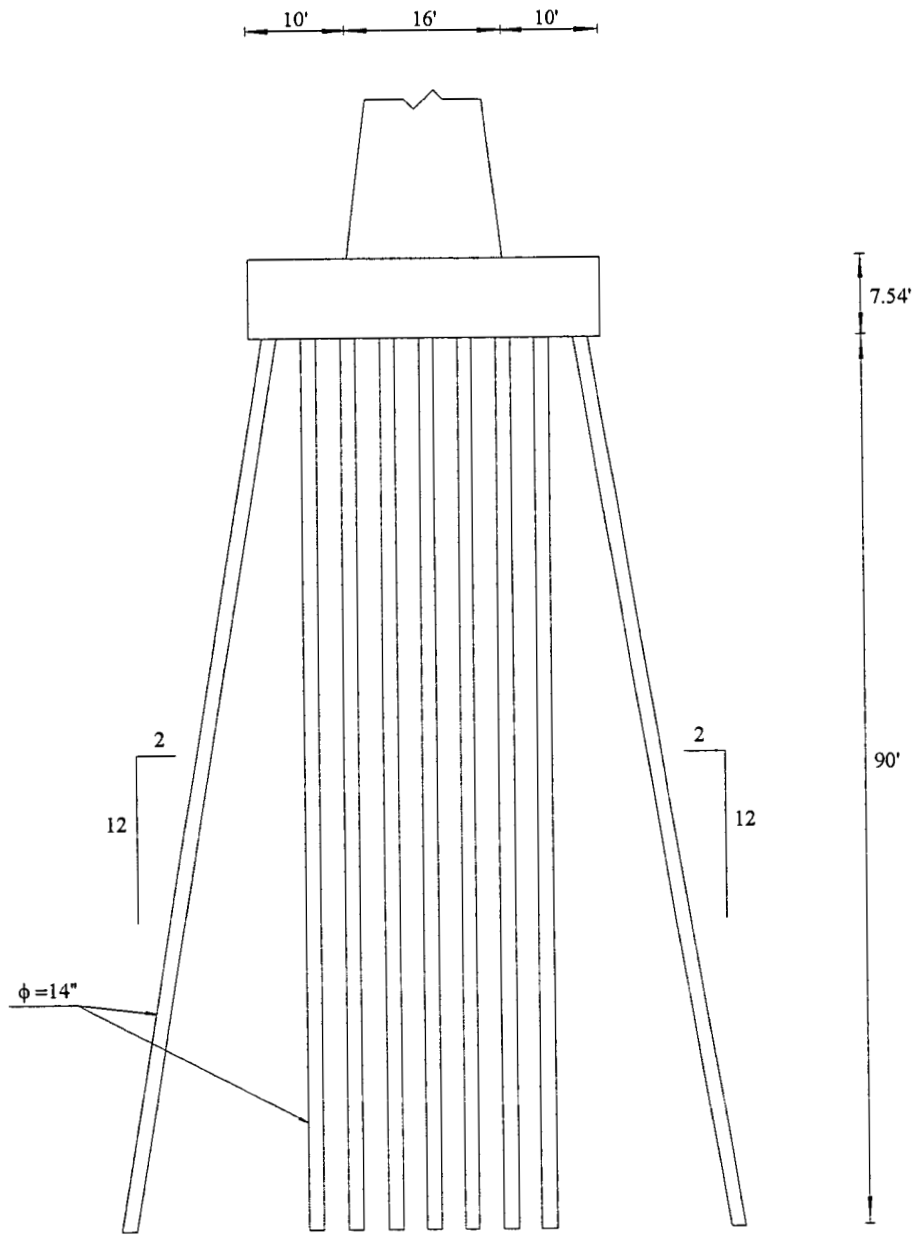


Fig. 5.5: Cross-section of Pier 1 foundation

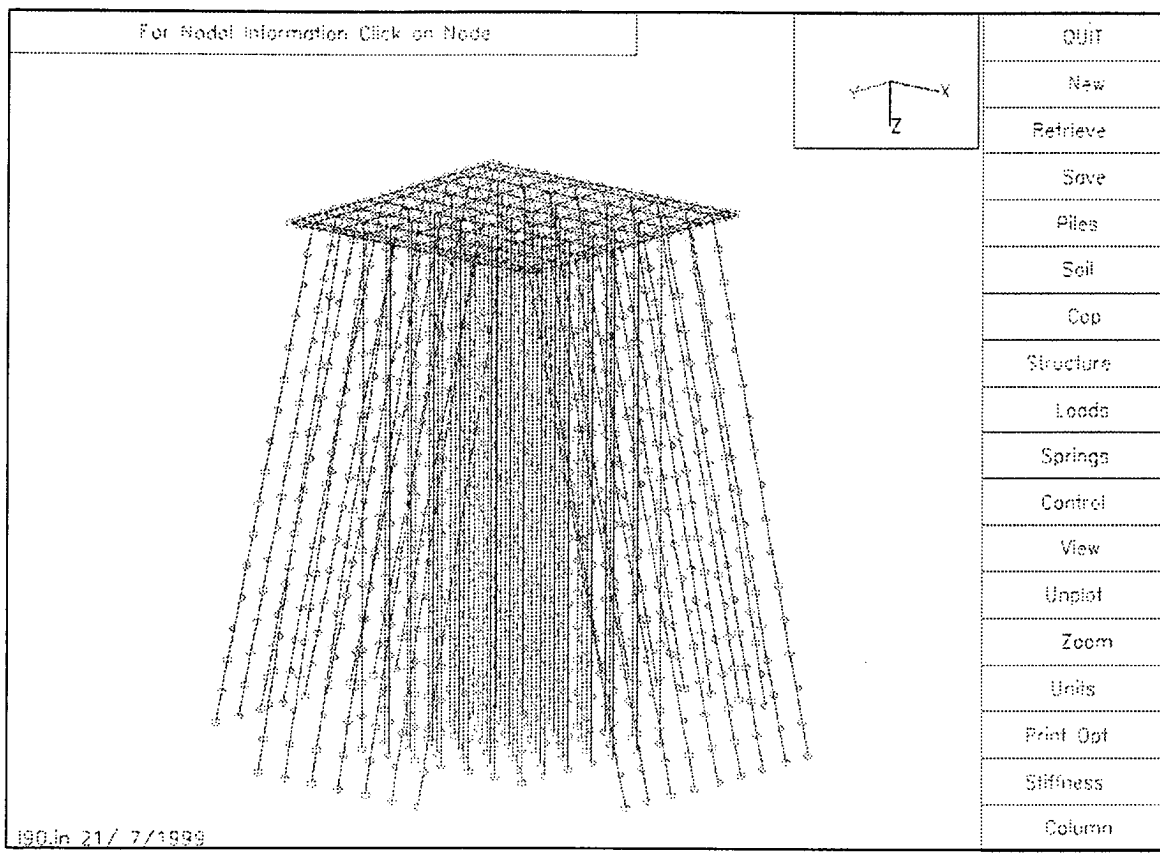


Fig. 5.6: FLPIER finite element mesh of  $9 \times 9$  -pile pier

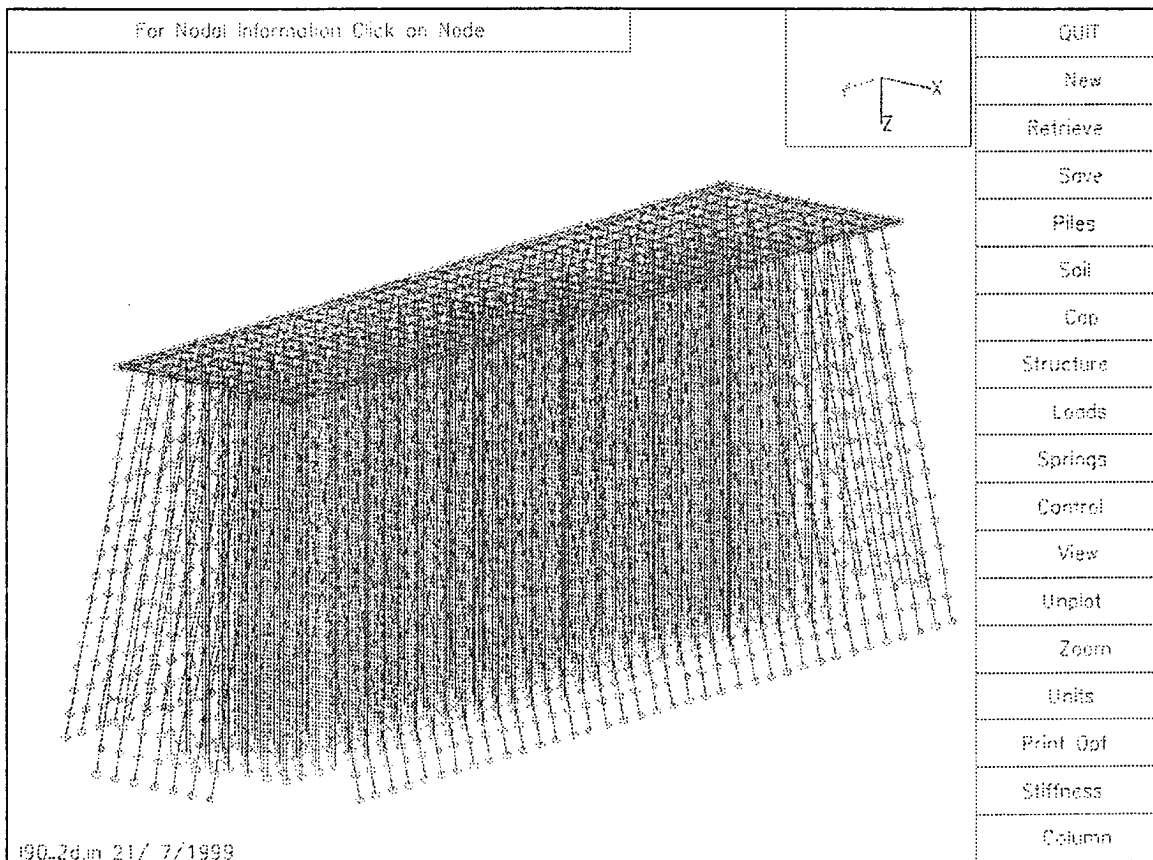


Fig. 5.7: FLPIER finite element mesh of  $9 \times 36$  -pile pier

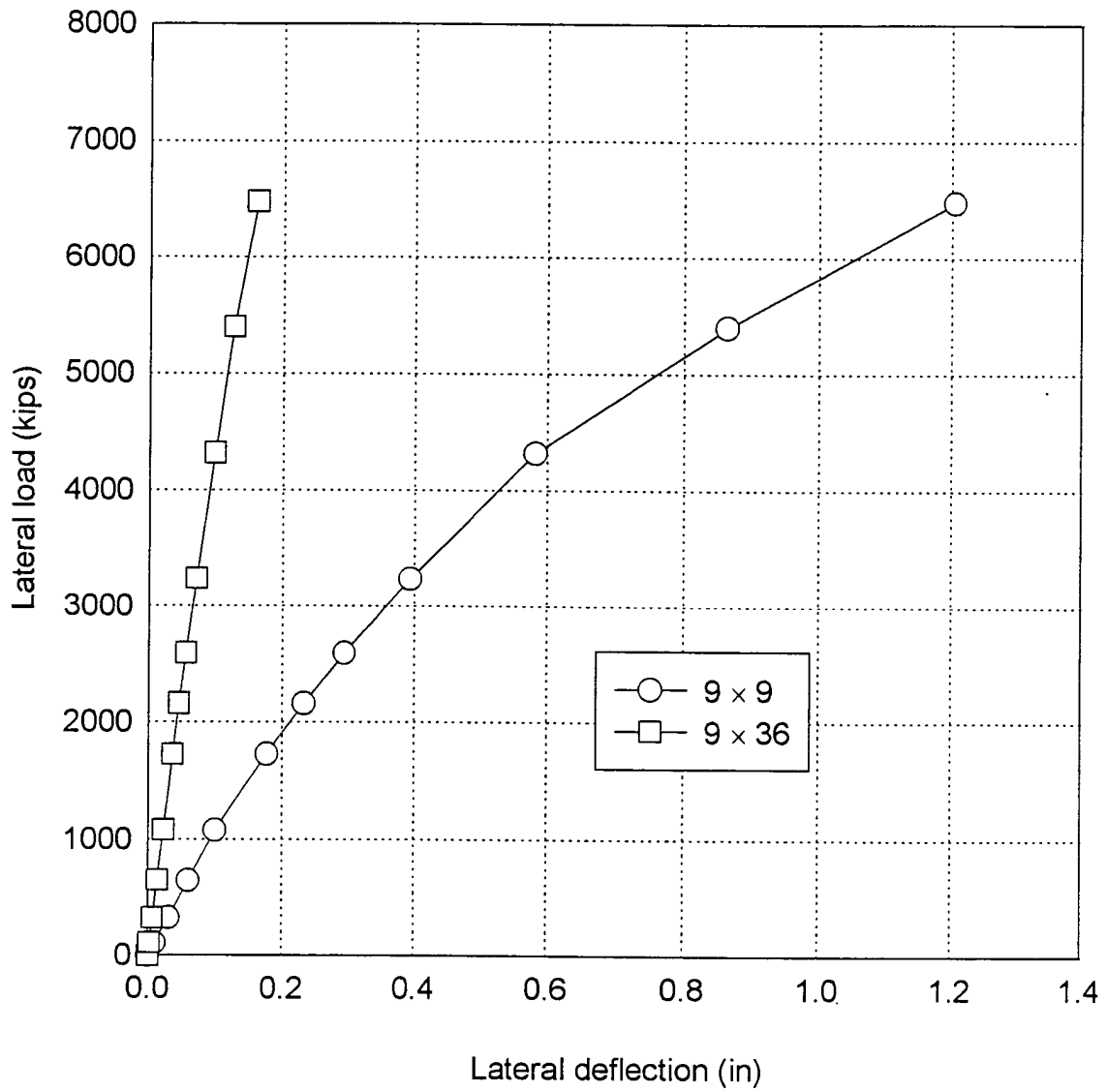


Fig. 5.8: Calculated load vs. deflections of 9 x 9 -pile pier and 9 x 36 -pile pier

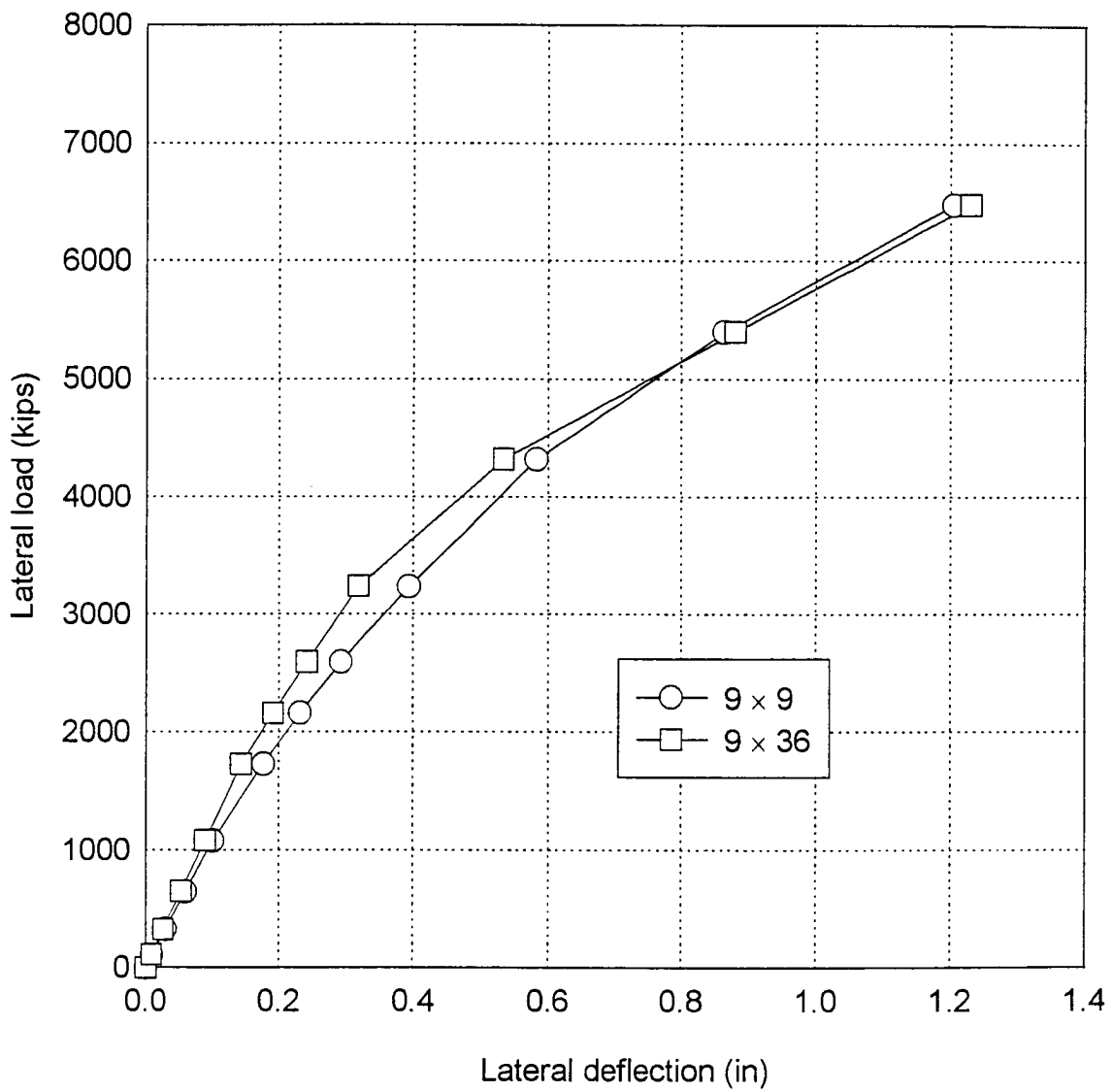


Fig. 5.9: Calculated load vs. deflections of 9 × 9 -pile pier and 9 × 36 -pile pier with modified stiffness



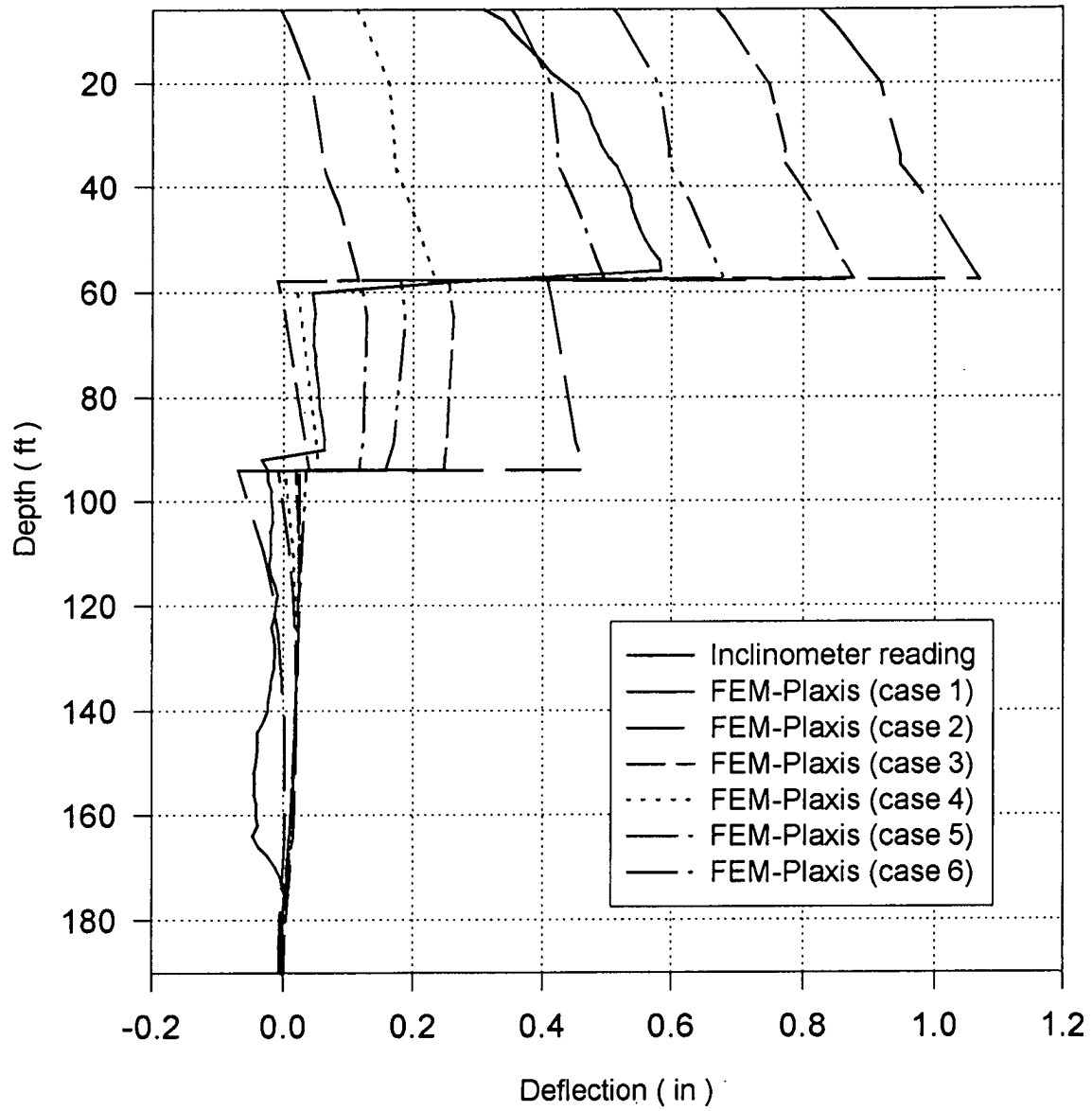


Fig. 5.10: Comparison of soil movement along bore hole ZB103

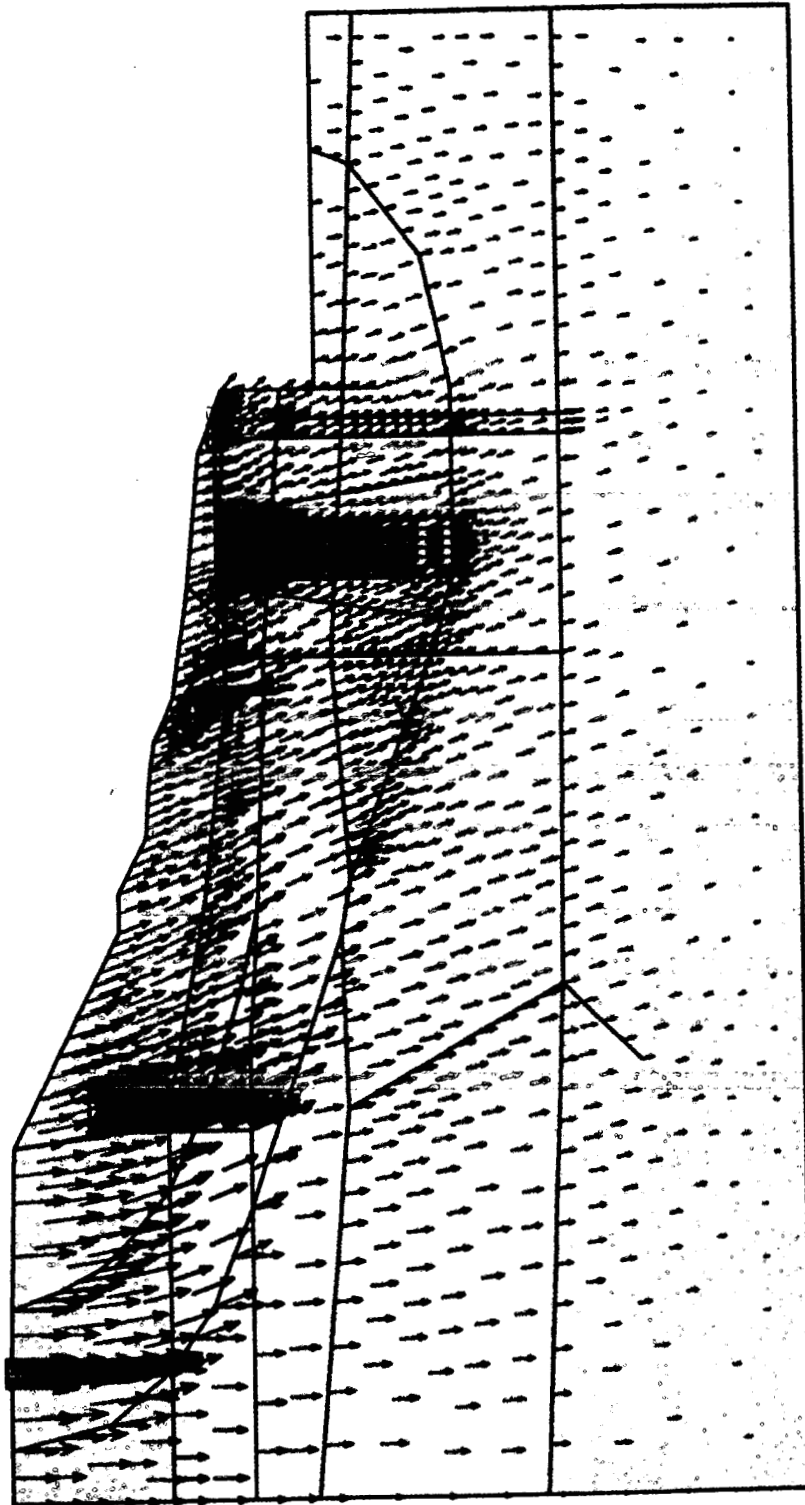


Fig. 5.11: Soil displacement vectors due to phase 1

r

3.600

3.240

2.880

2.520

2.160

1.800

1.440

1.080

0.720

0.360

0.000

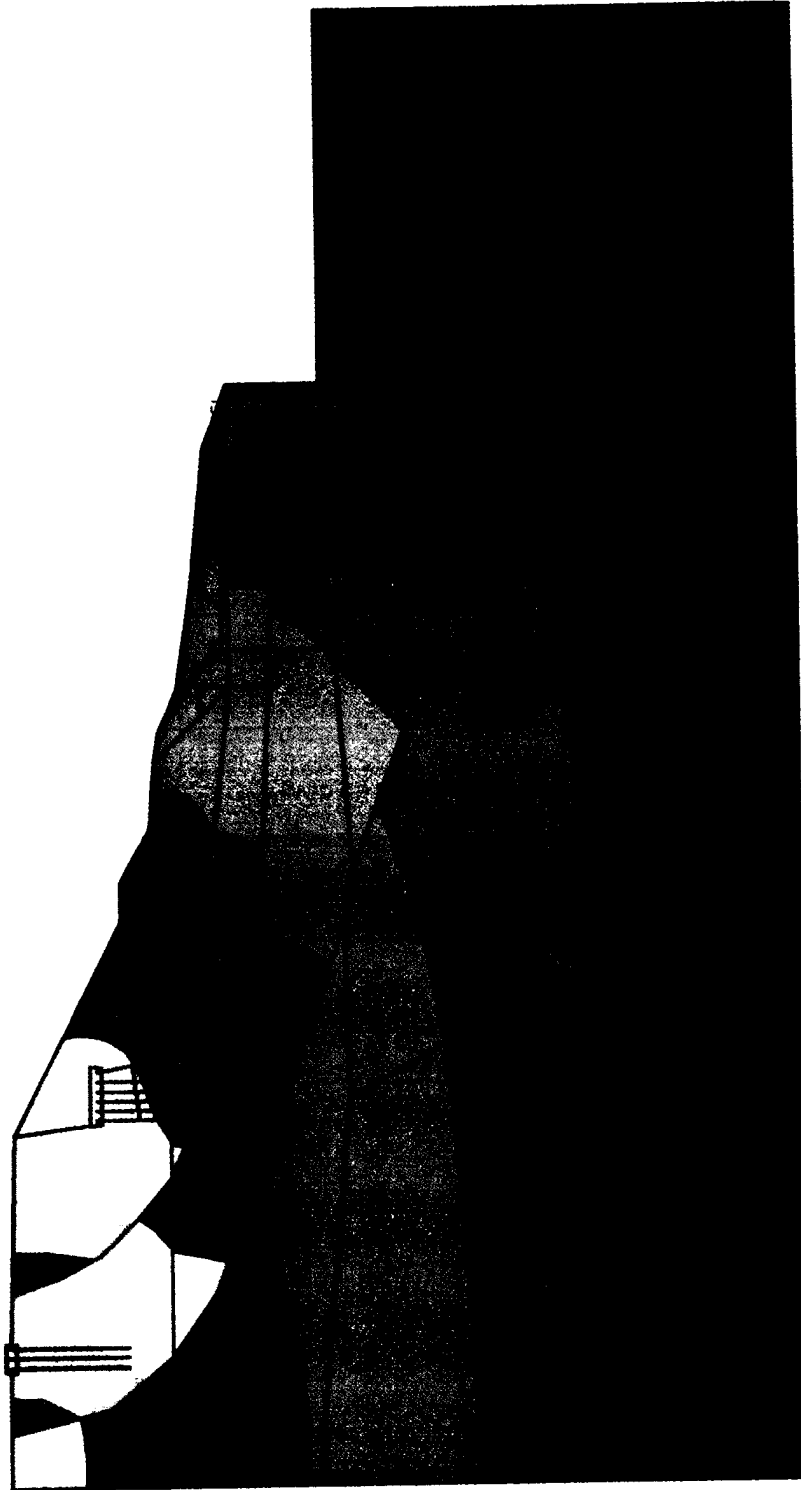


Fig. 5.12: Soil displacement contours due to phase 1

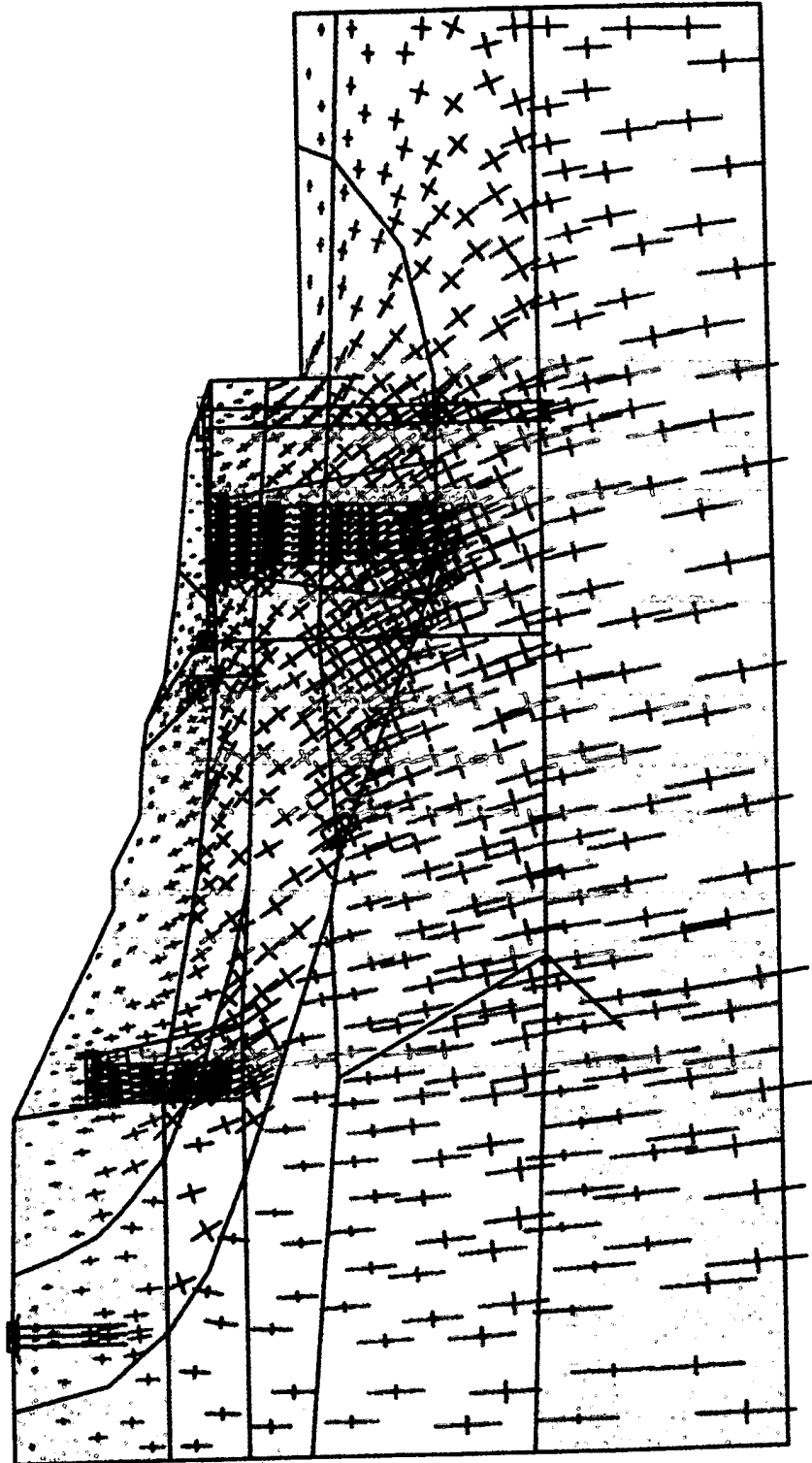


Fig. 5.13: Principal stress direction and magnitude due to phase 1

$\cdot 10^3 \text{ lb/ft}^2$

0.000

-1.100

-2.200

-3.300

-4.400

-5.500

-6.600

-7.700

-8.800

-9.900

-11.000

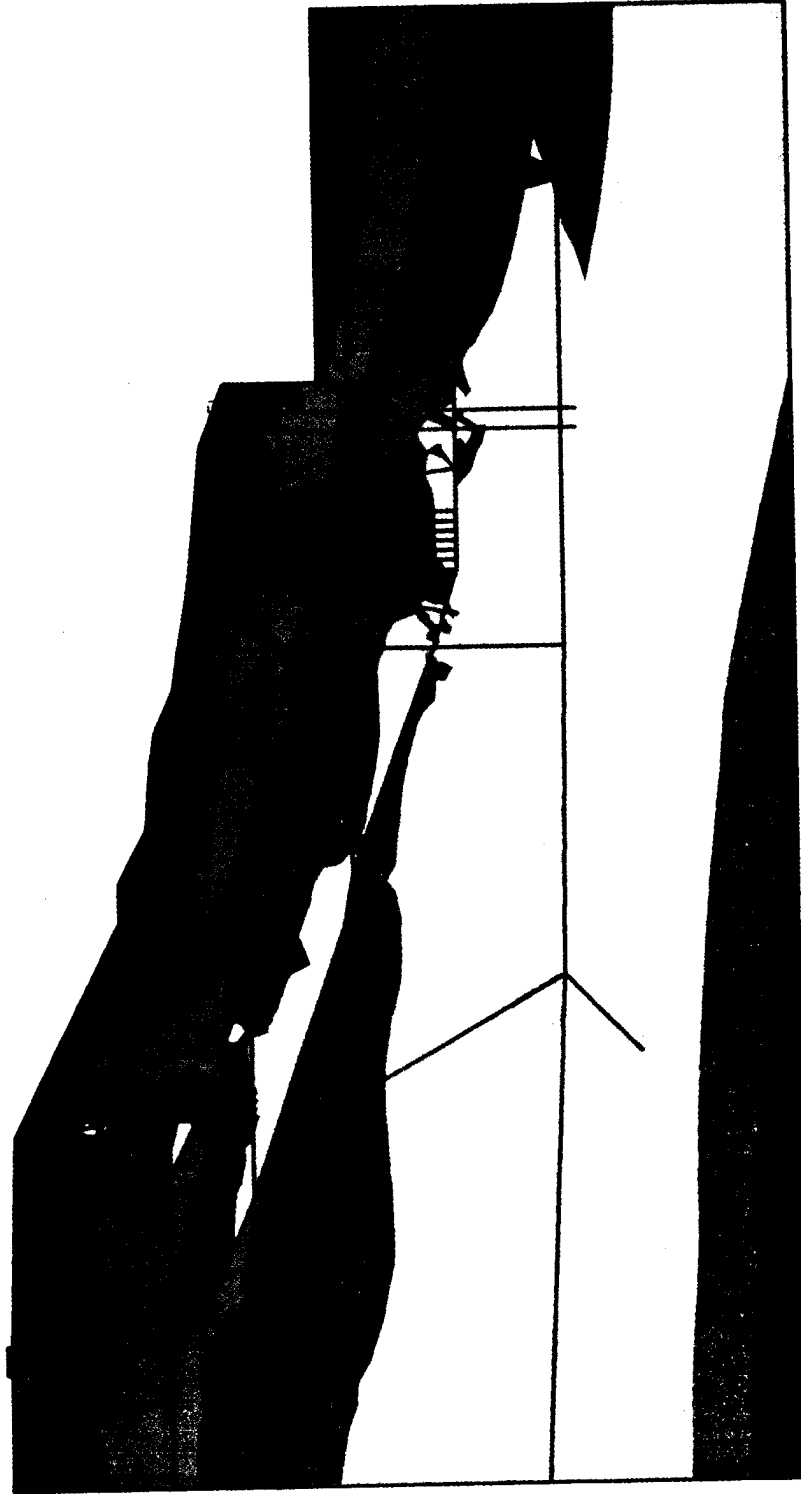


Fig. 5.14: Mean effective stress contours after phase 1

1.000  
0.900  
0.800  
0.700  
0.600  
0.500  
0.400  
0.300  
0.200  
0.100  
0.000

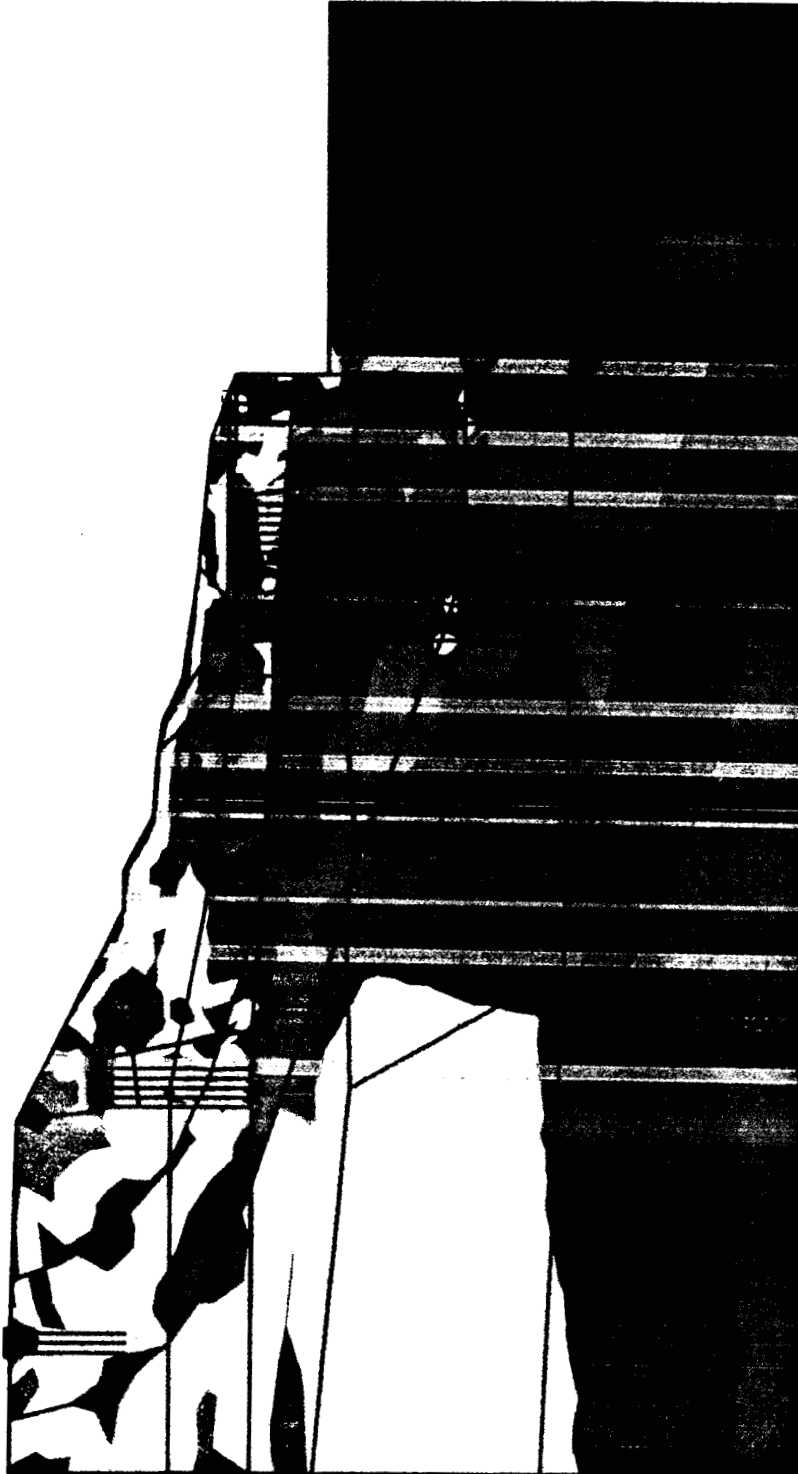


Fig. 5.15: Relative shear stress ratio contours after phase I

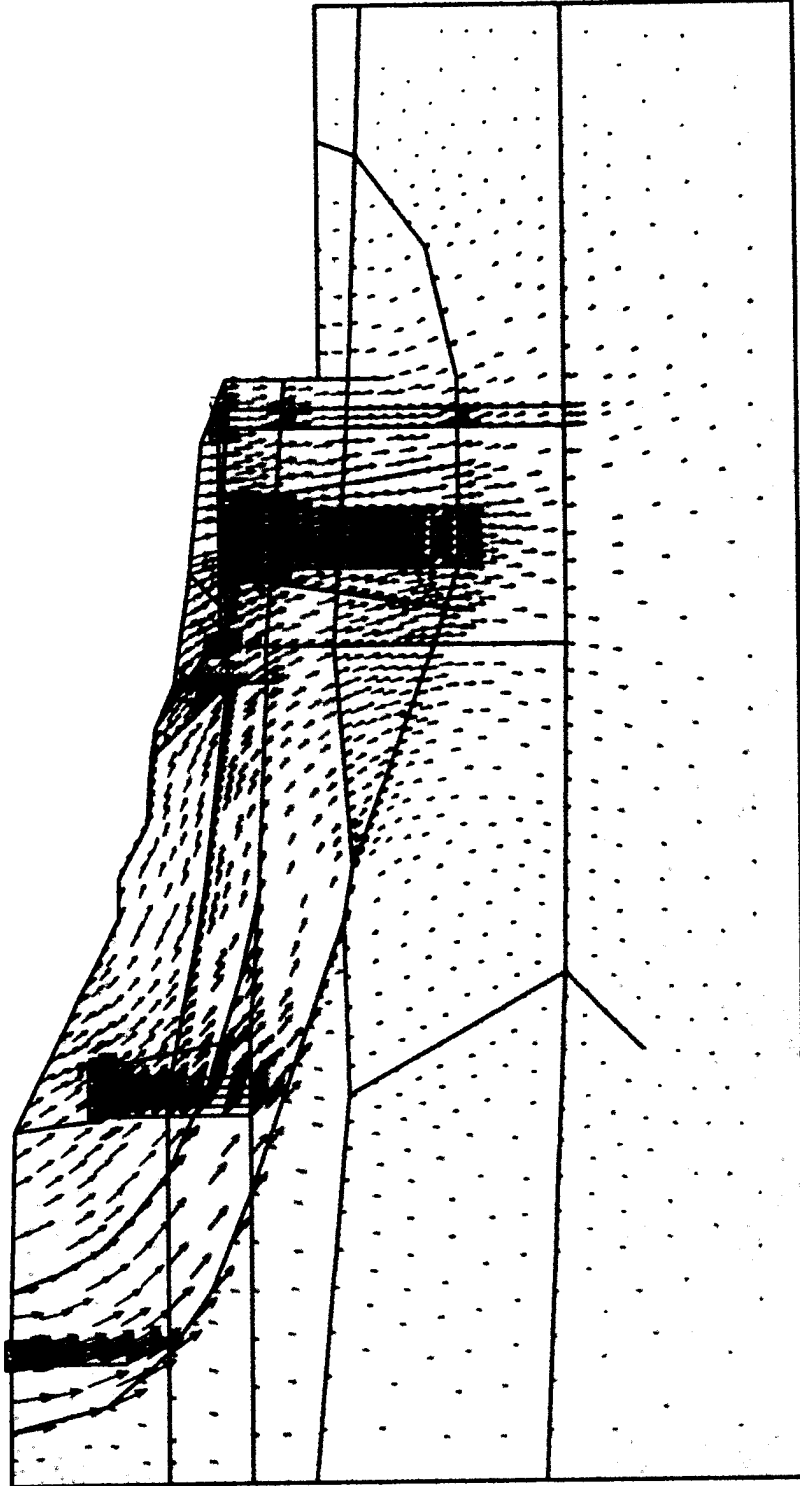


Fig. 5.16: Soil displacement vectors due to phase 2

\*10<sup>-3</sup> ft

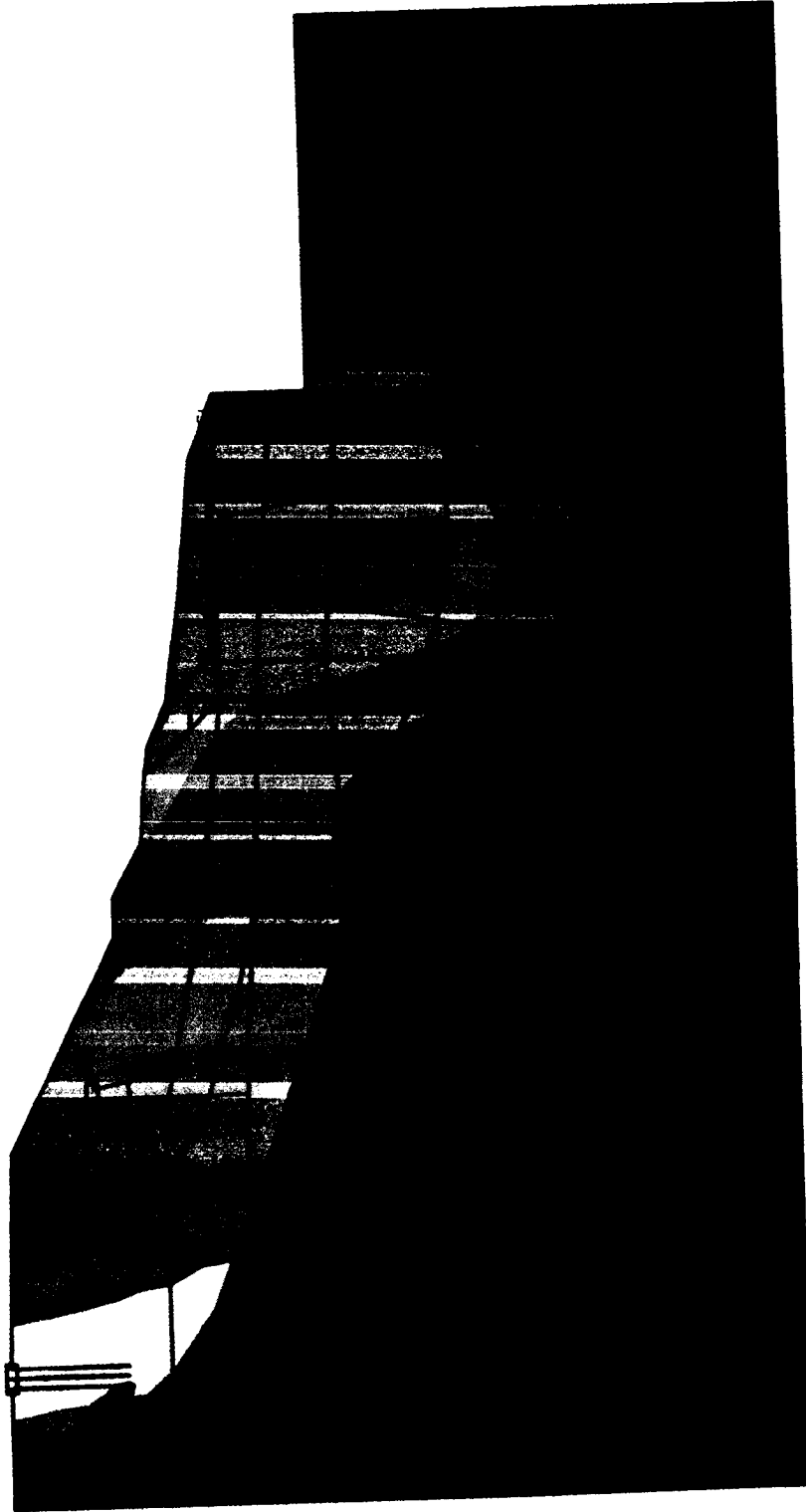
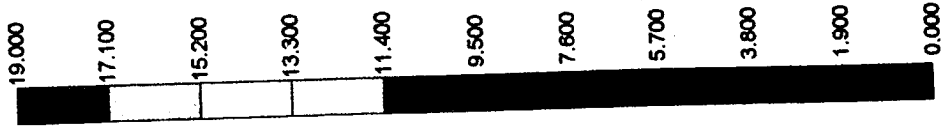


Fig. 5.17: Soil displacement contours due to phase 2



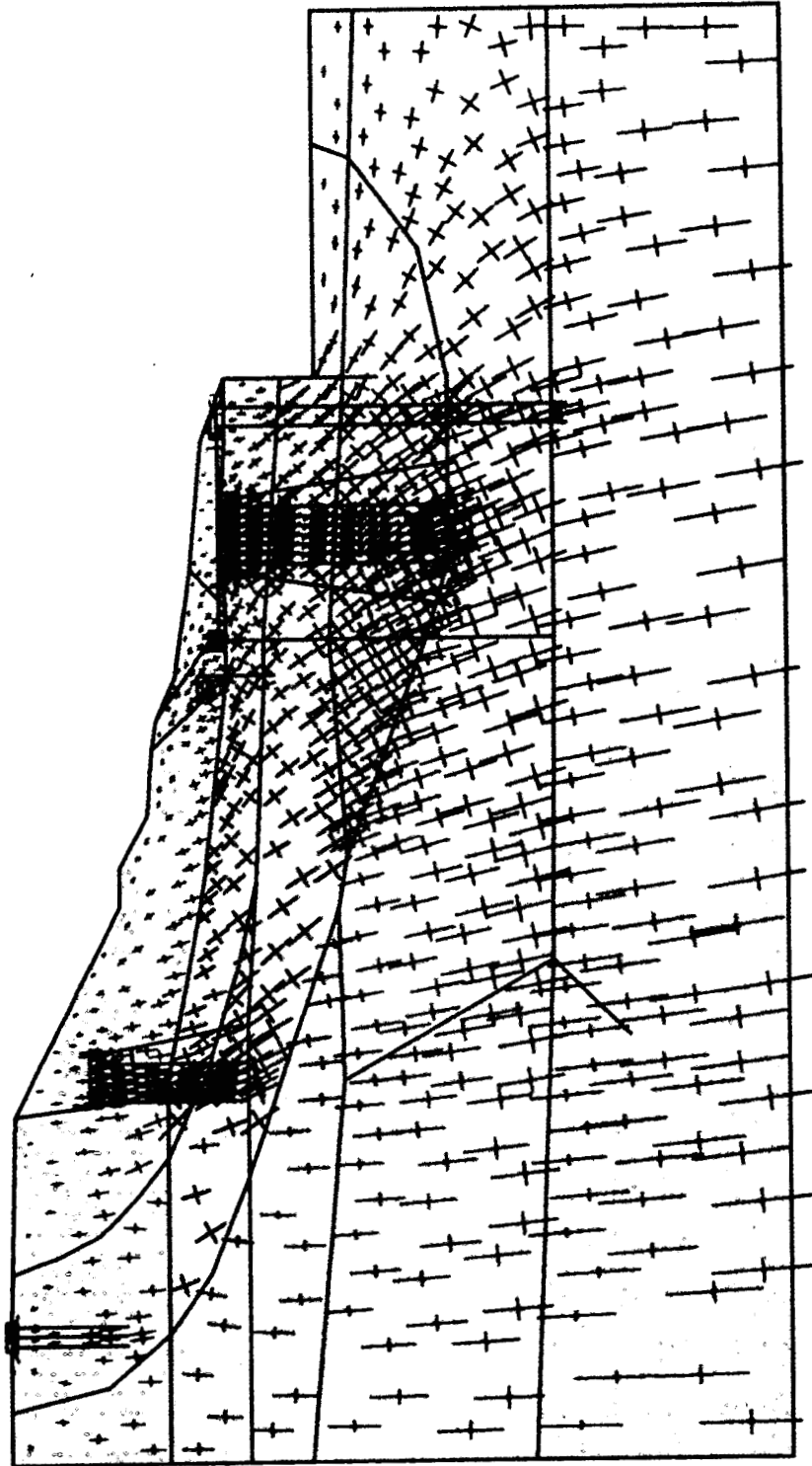


Fig. 5.18: Principal stress direction and magnitude due to phase 2

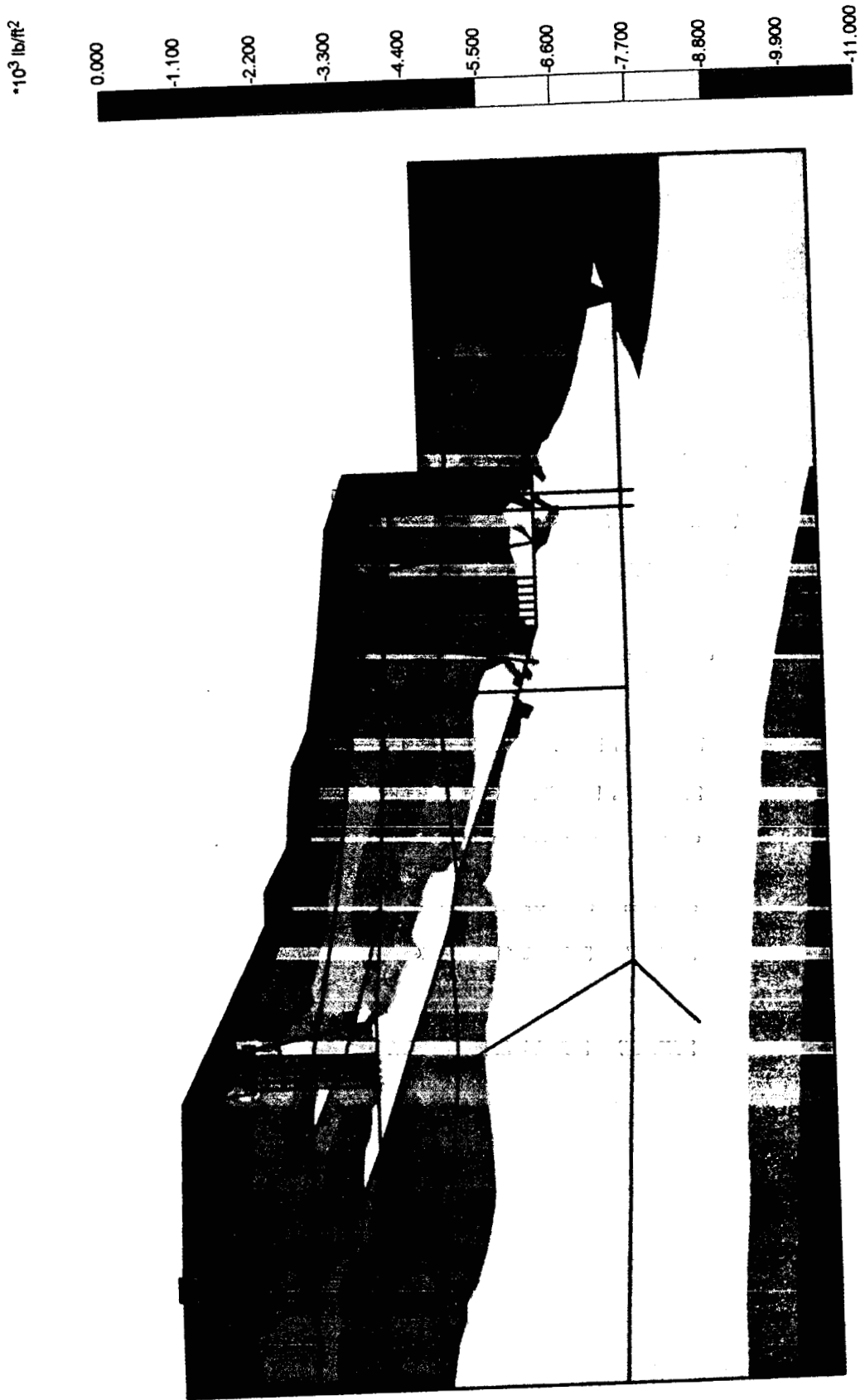


Fig. 5.19: Mean effective stress contours after phase 2

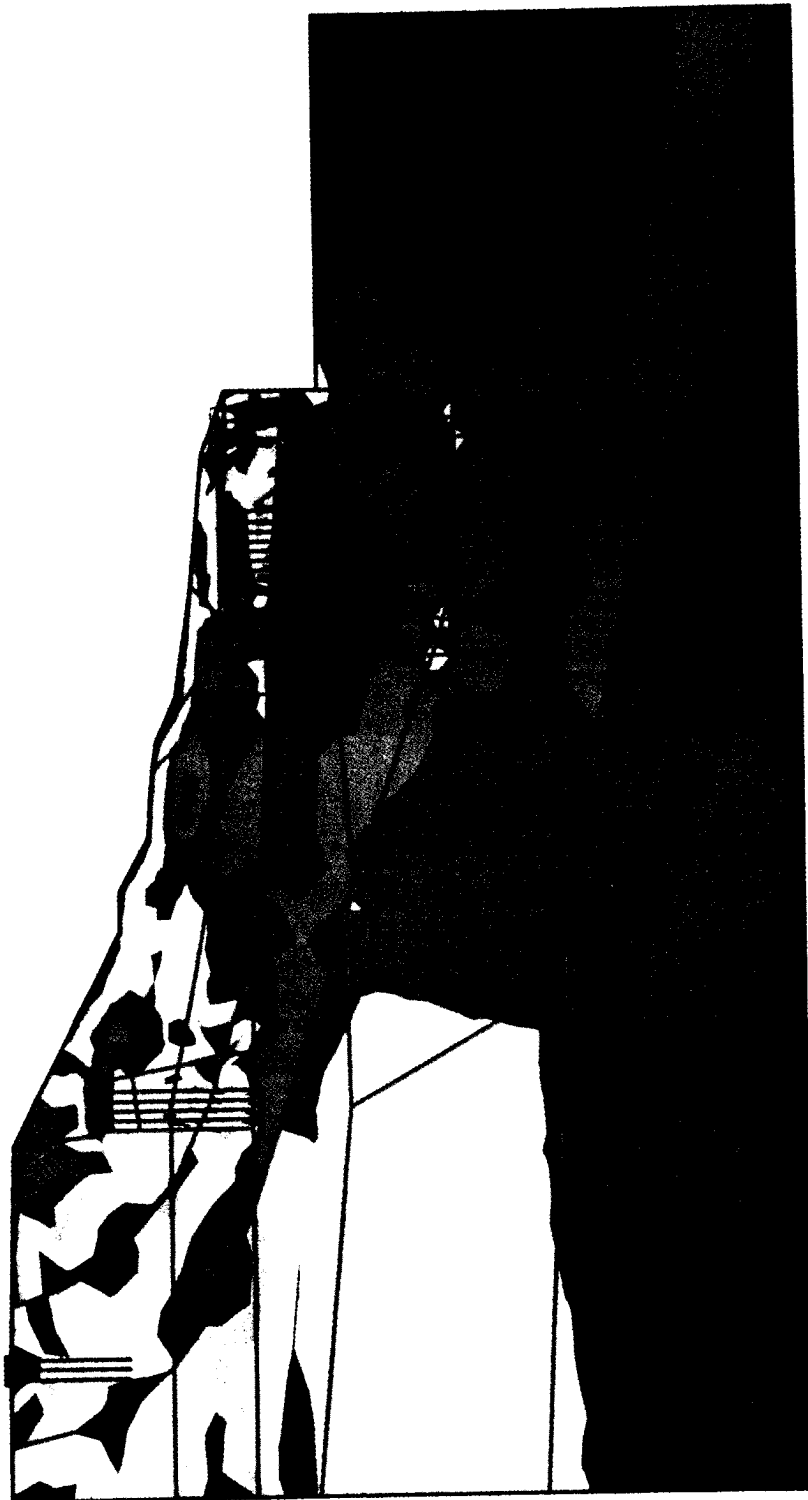
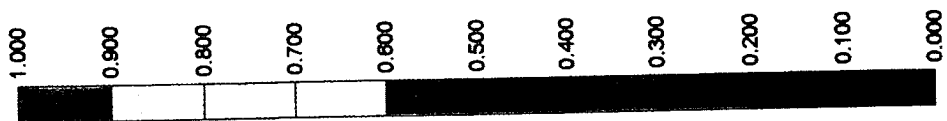


Fig. 5.20: Relative shear stress ratio contours after phase 2

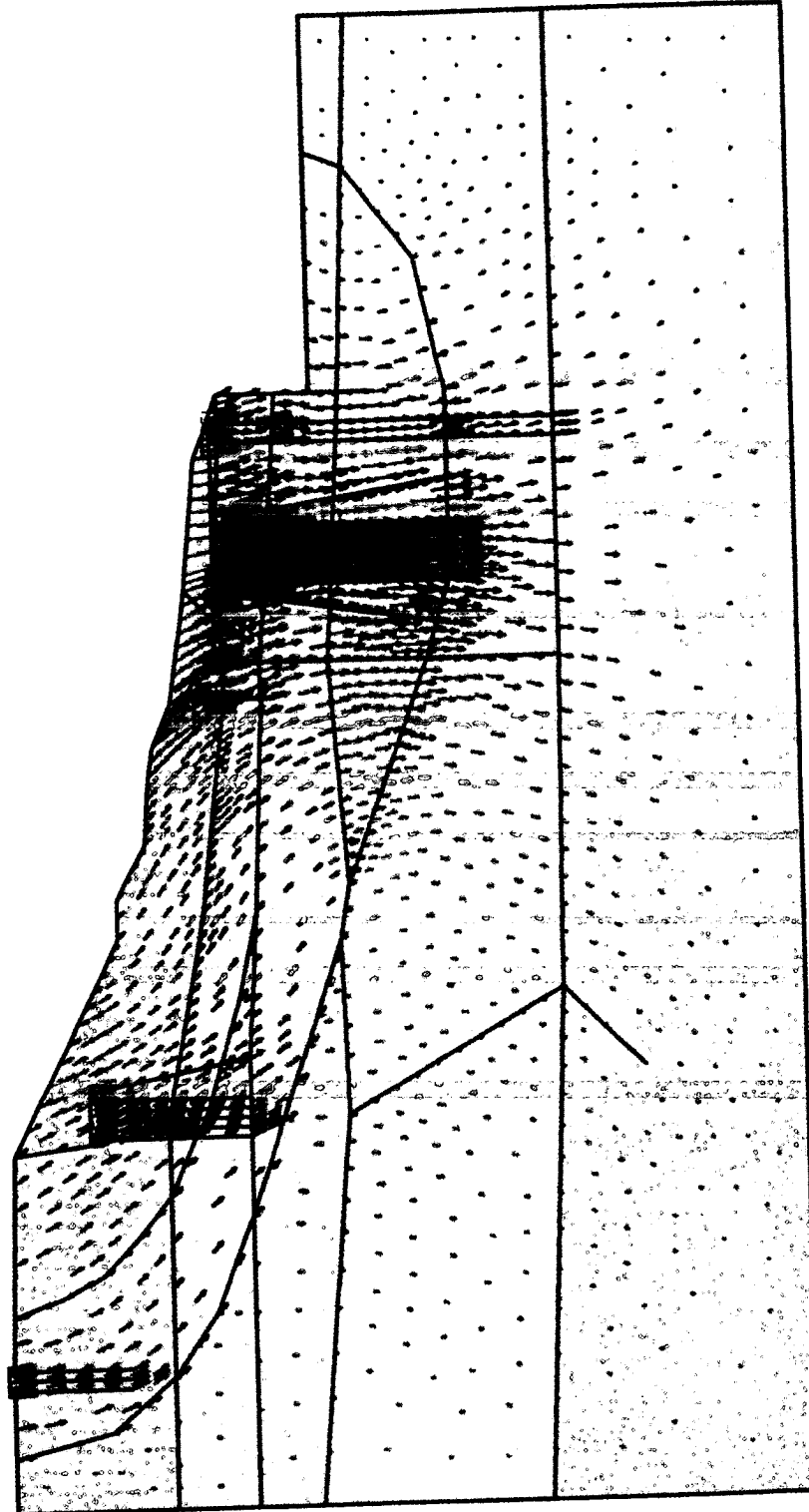


Fig. 5.21: Soil displacement vectors due to phase 3

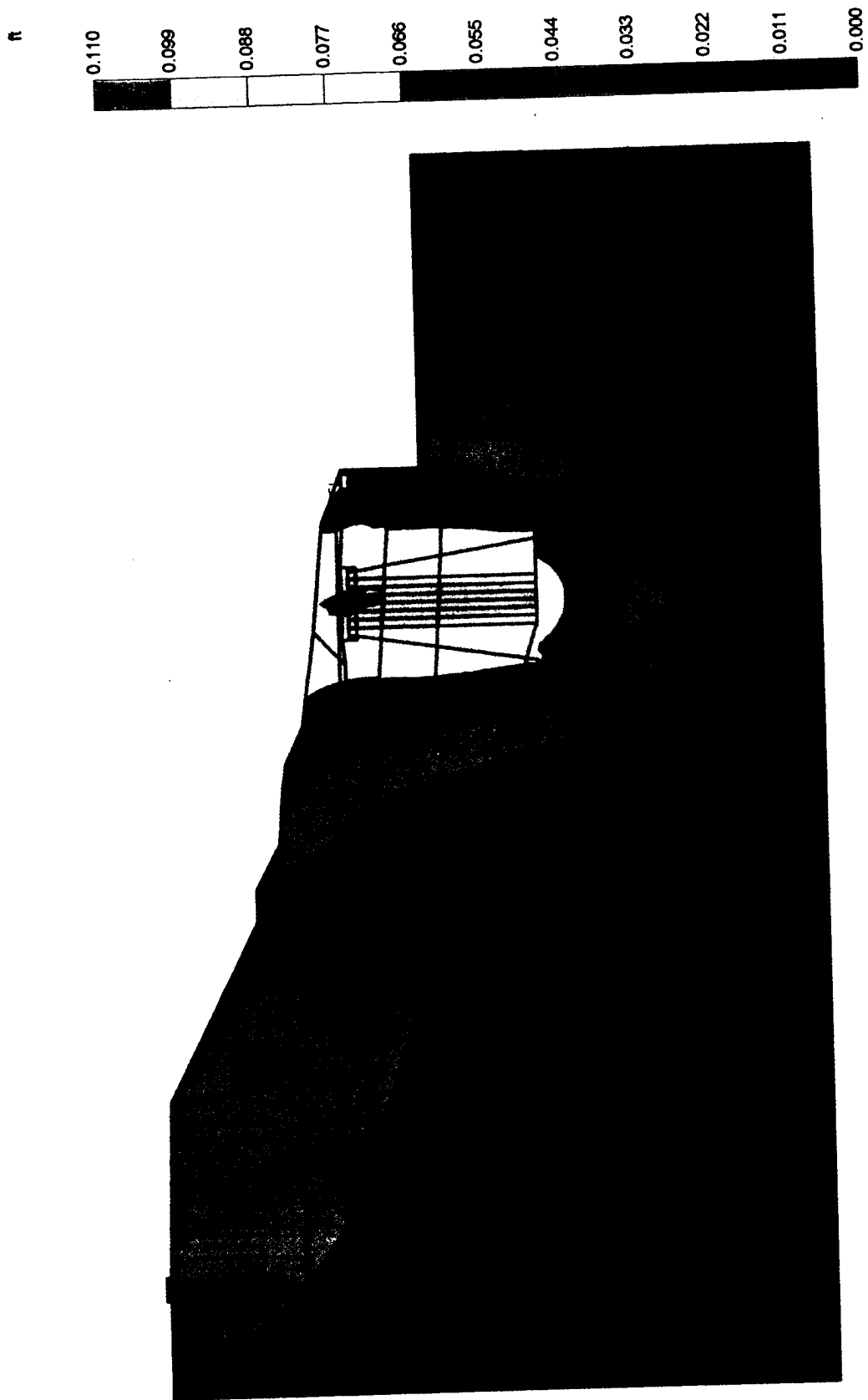


Fig. 5.22: Soil displacement contours due to phase 3

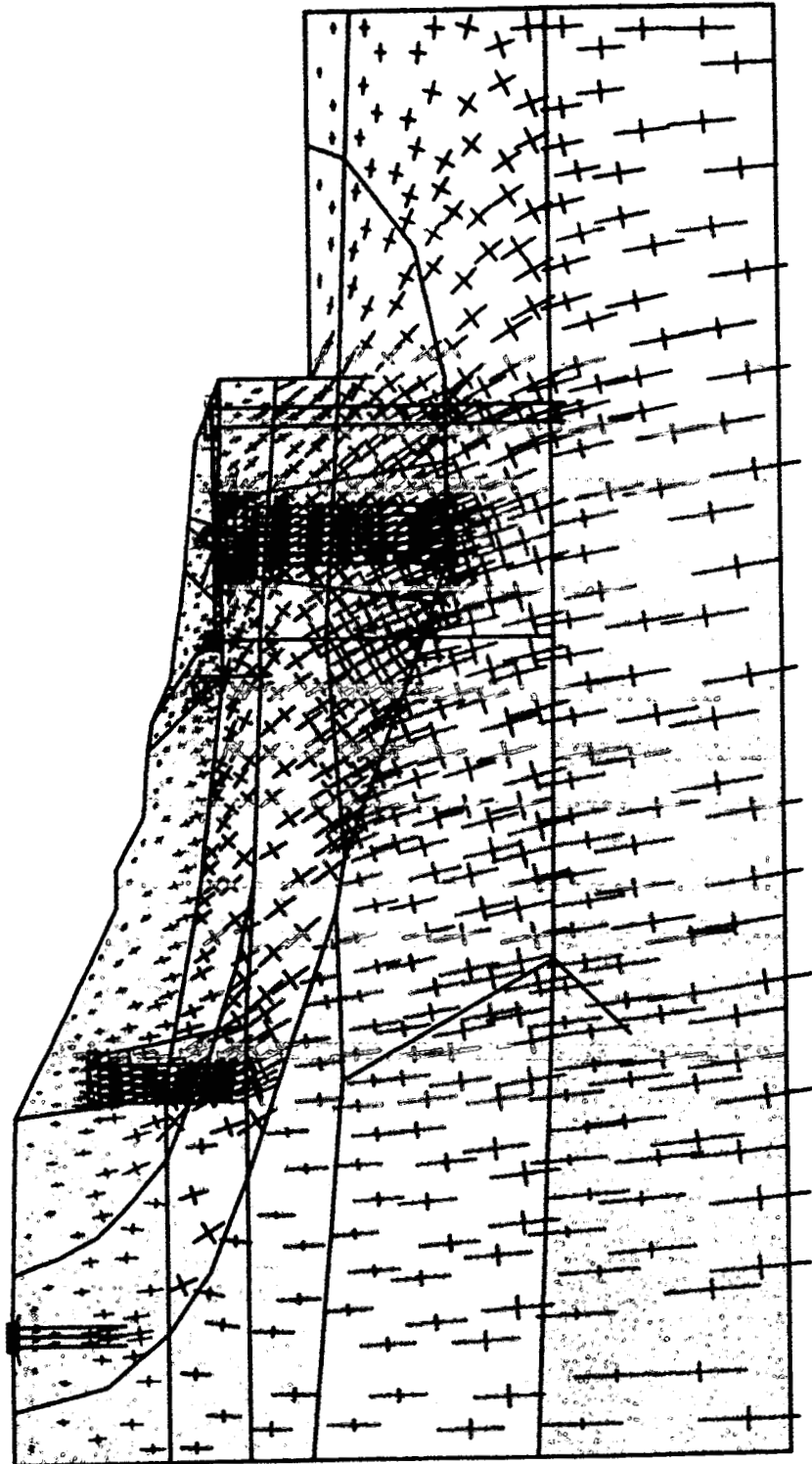


Fig. 5.23: Principal stress direction and magnitude due to phase 3

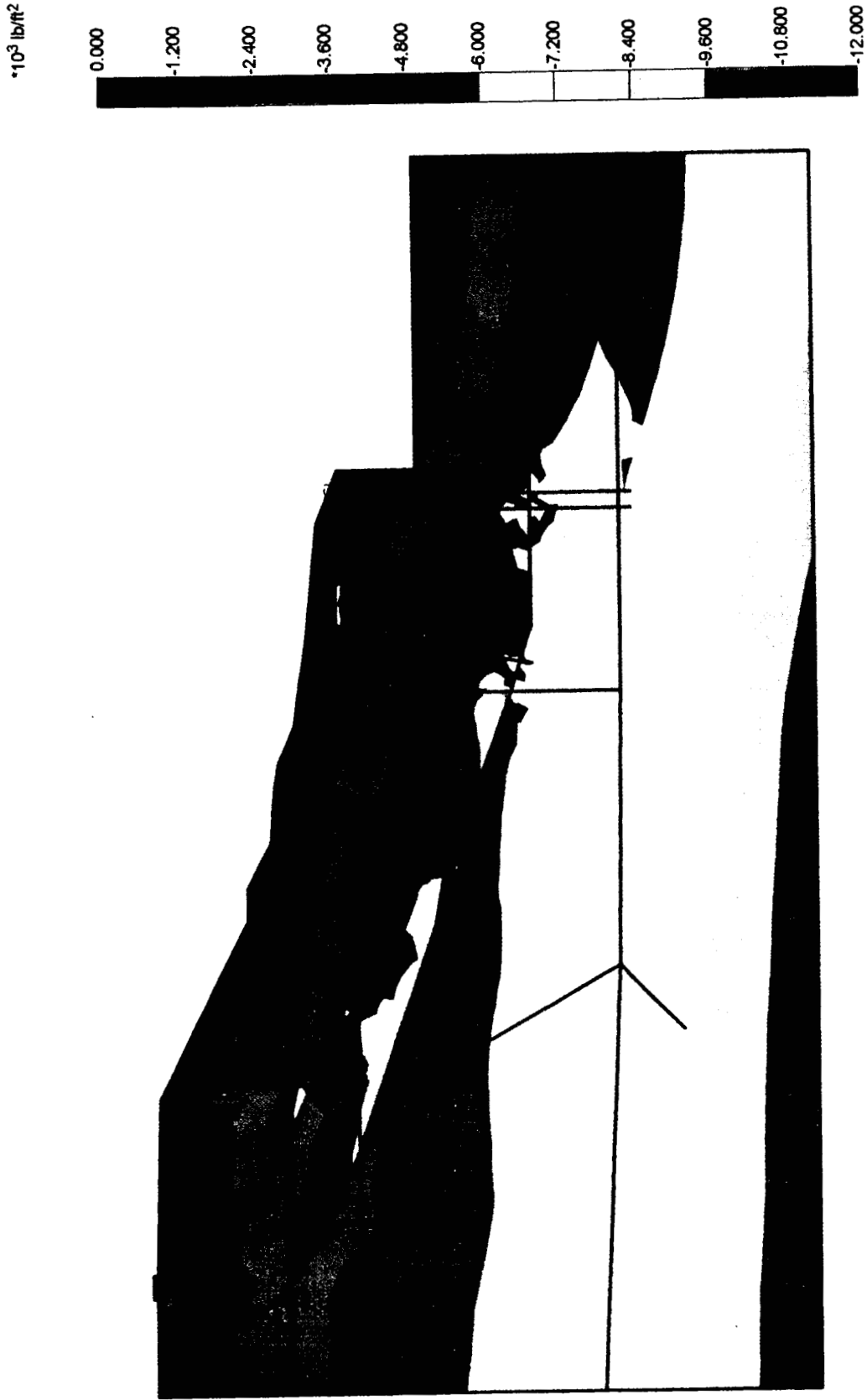


Fig. 5.24: Mean effective stress contours after phase 3

1.000  
0.900  
0.800  
0.700  
0.600  
0.500  
0.400  
0.300  
0.200  
0.100  
0.000

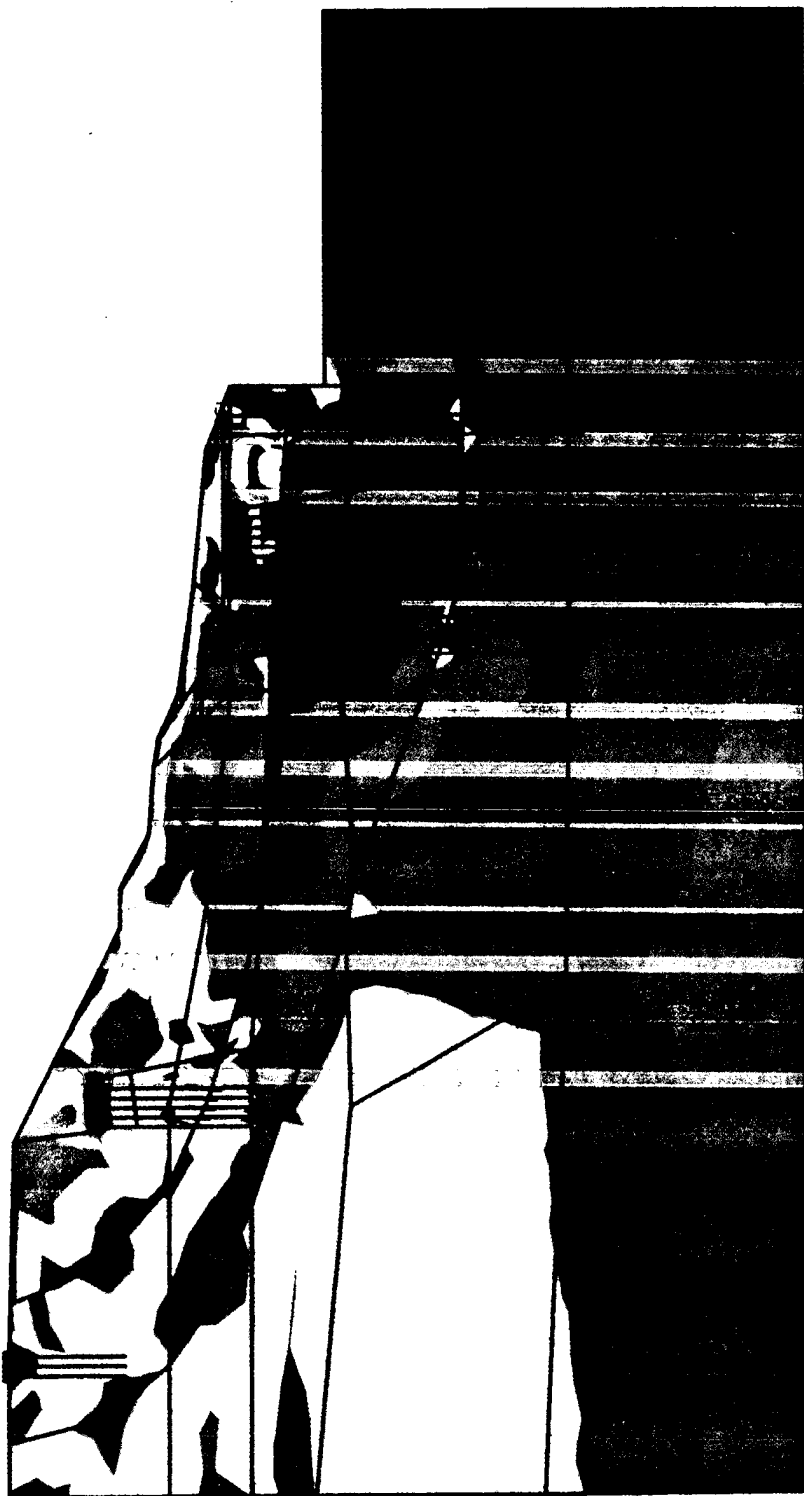


Fig. 5.25: Relative shear stress ratio contours after phase 3



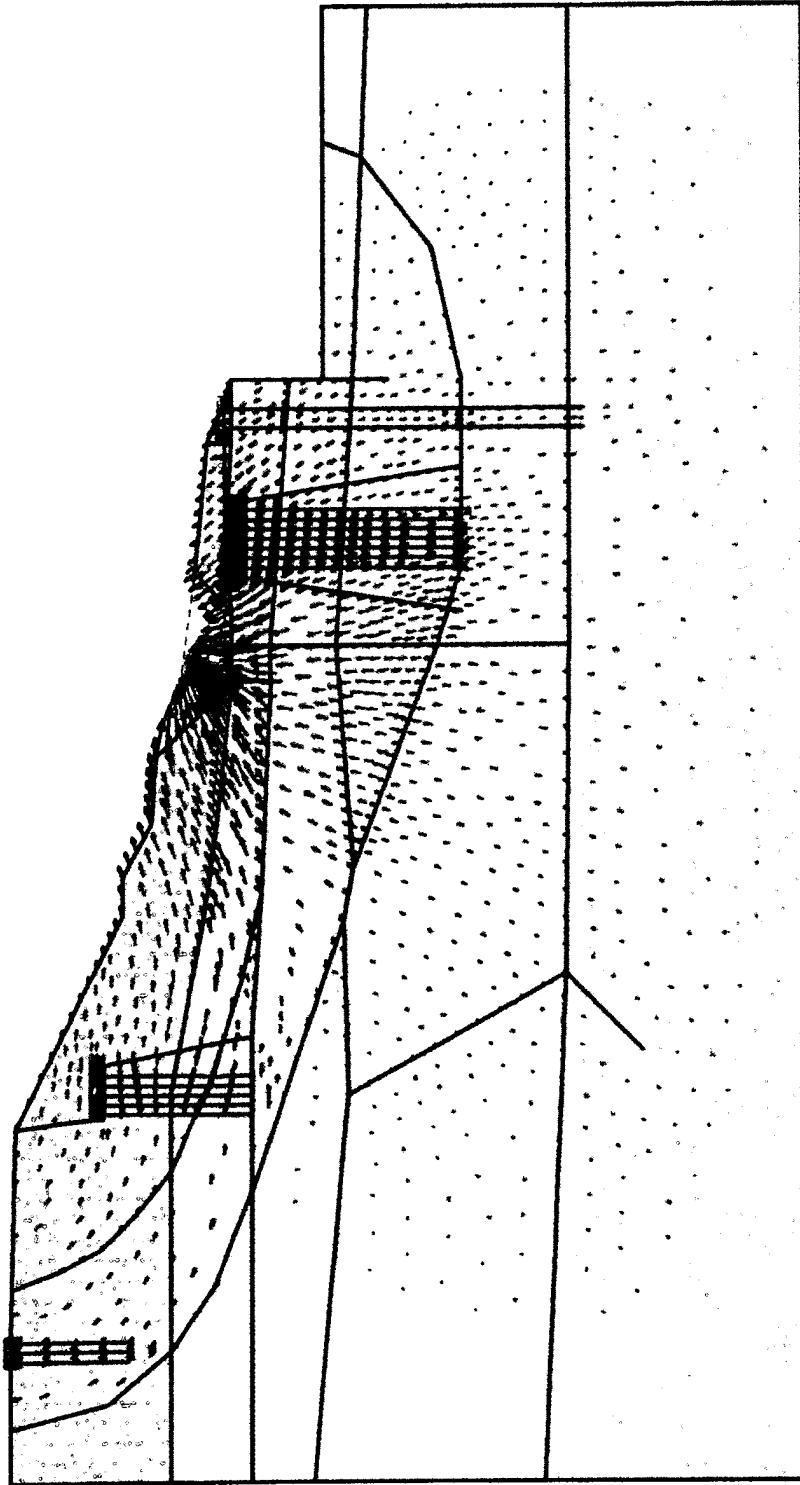


Fig. 5.26: Soil displacement vectors due to phase 4

ft  
0.220  
0.198  
0.176  
0.154  
0.132  
0.110  
0.088  
0.066  
0.044  
0.022  
0.000



Fig. 5.27: Soil displacement contours due to phase 4

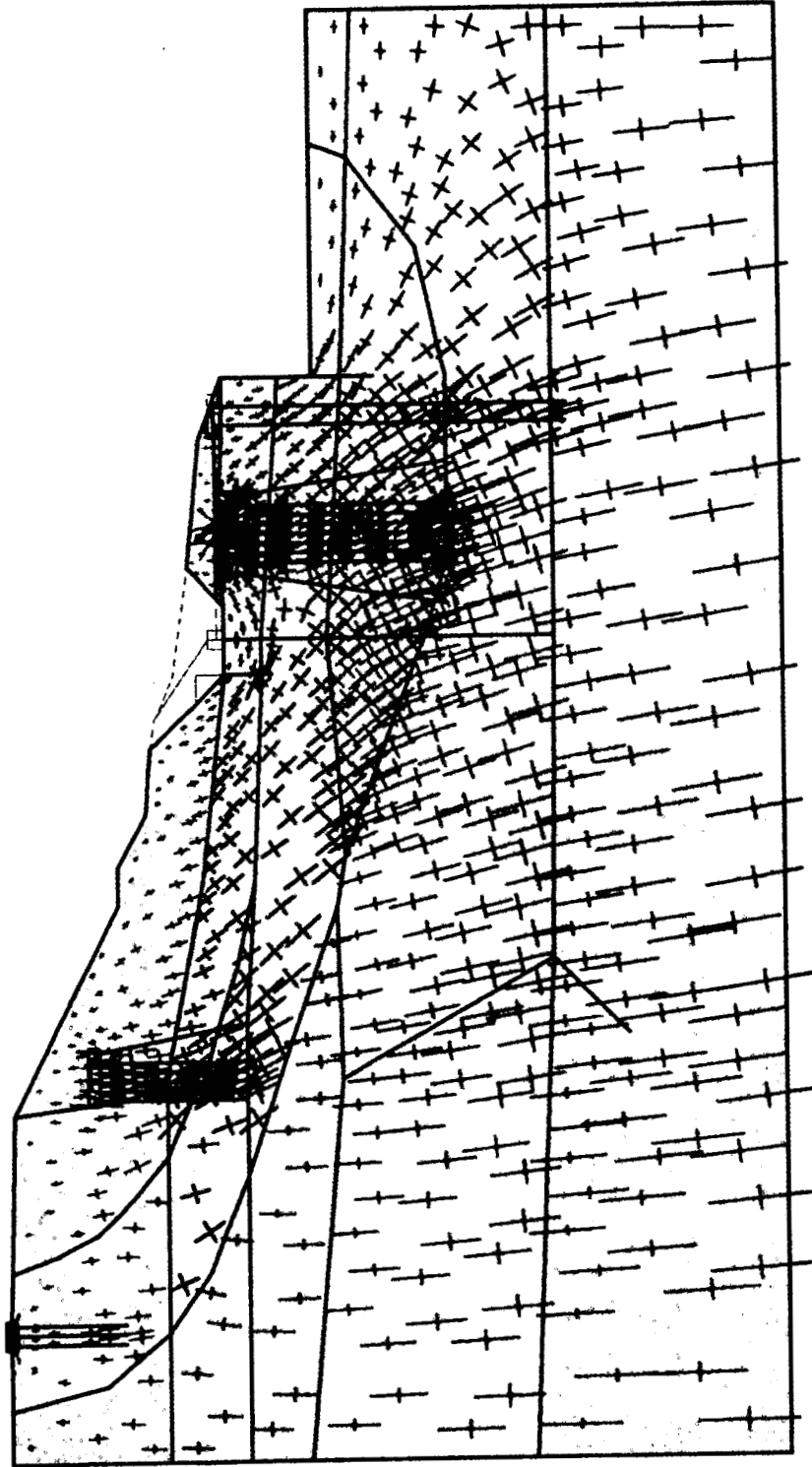


Fig. 5.28: Principal stress direction and magnitude due to phase 4

\*10<sup>3</sup> lb/ft<sup>2</sup>

0.000

-1.100

-2.200

-3.300

-4.400

-5.500

-6.600

-7.700

-8.800

-9.900

-11.000

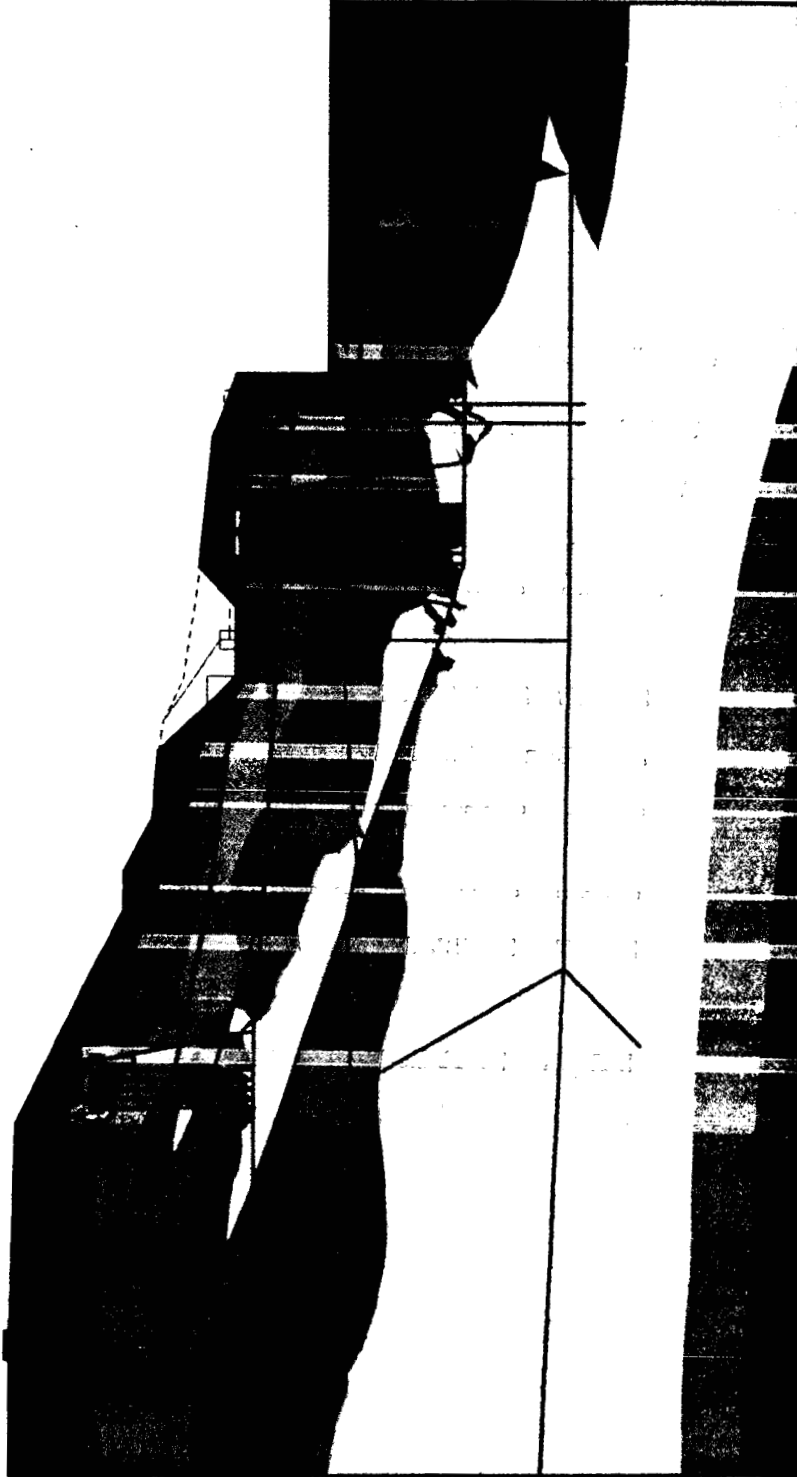


Fig. 5.29: Mean effective stress contours after phase 4

1.000  
0.900  
0.800  
0.700  
0.600  
0.500  
0.400  
0.300  
0.200  
0.100  
0.000

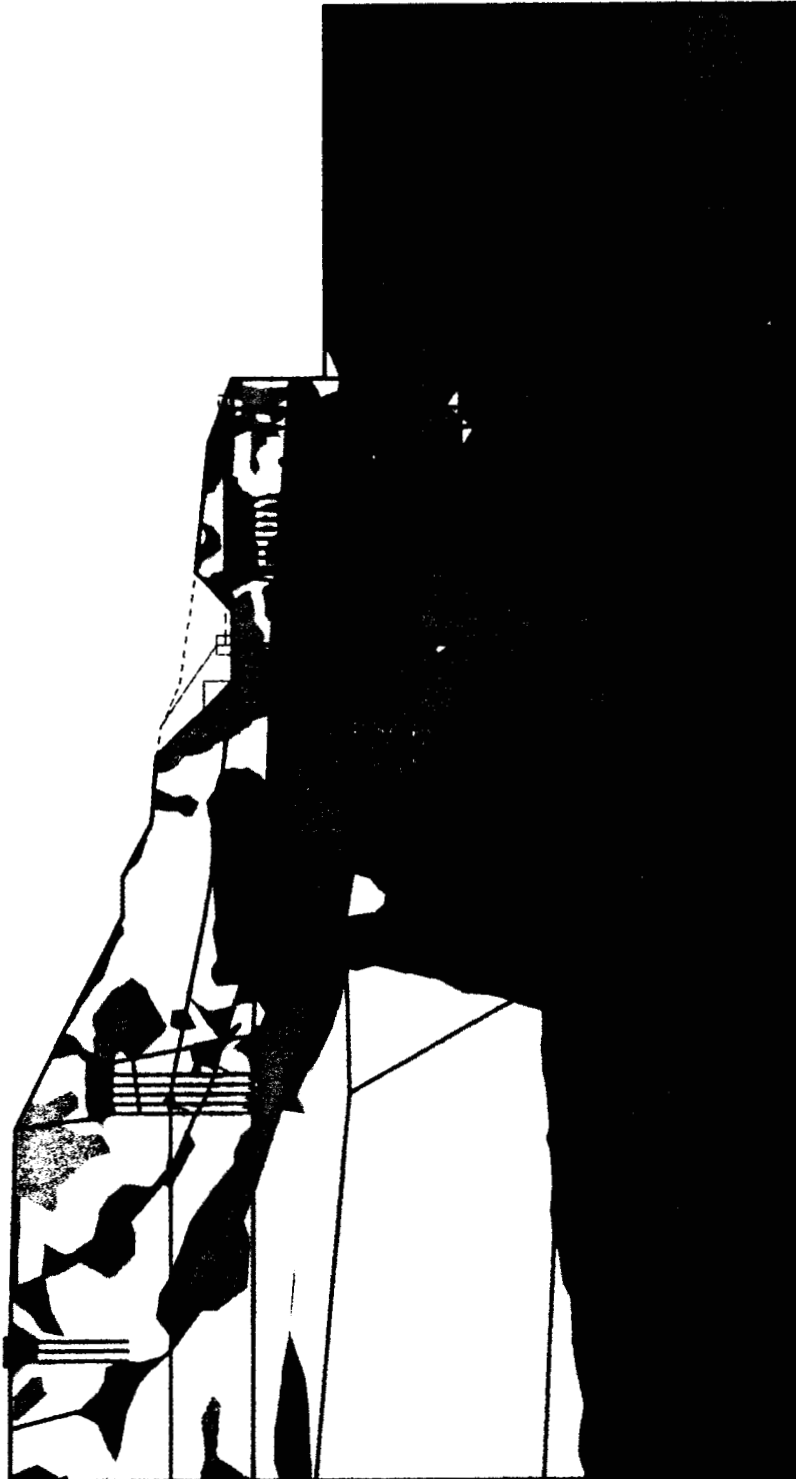


Fig. 5.30: Relative shear stress ratio contours after phase 4

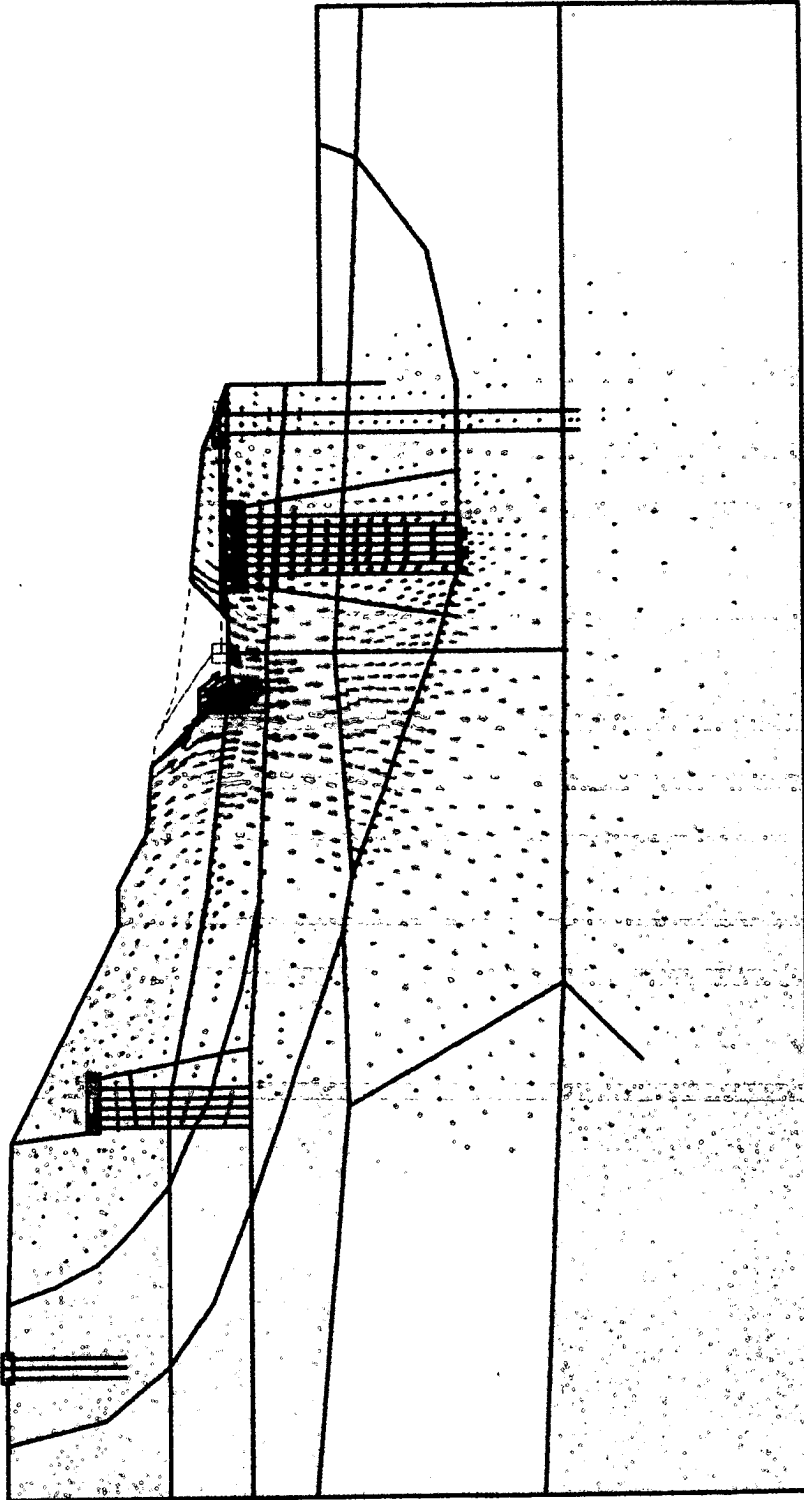


Fig. 5.31: Soil displacement vectors due to phase 5

\*10<sup>-3</sup> ft  
32.000  
28.800  
25.600  
22.400  
19.200  
16.000  
12.800  
9.600  
6.400  
3.200  
0.000

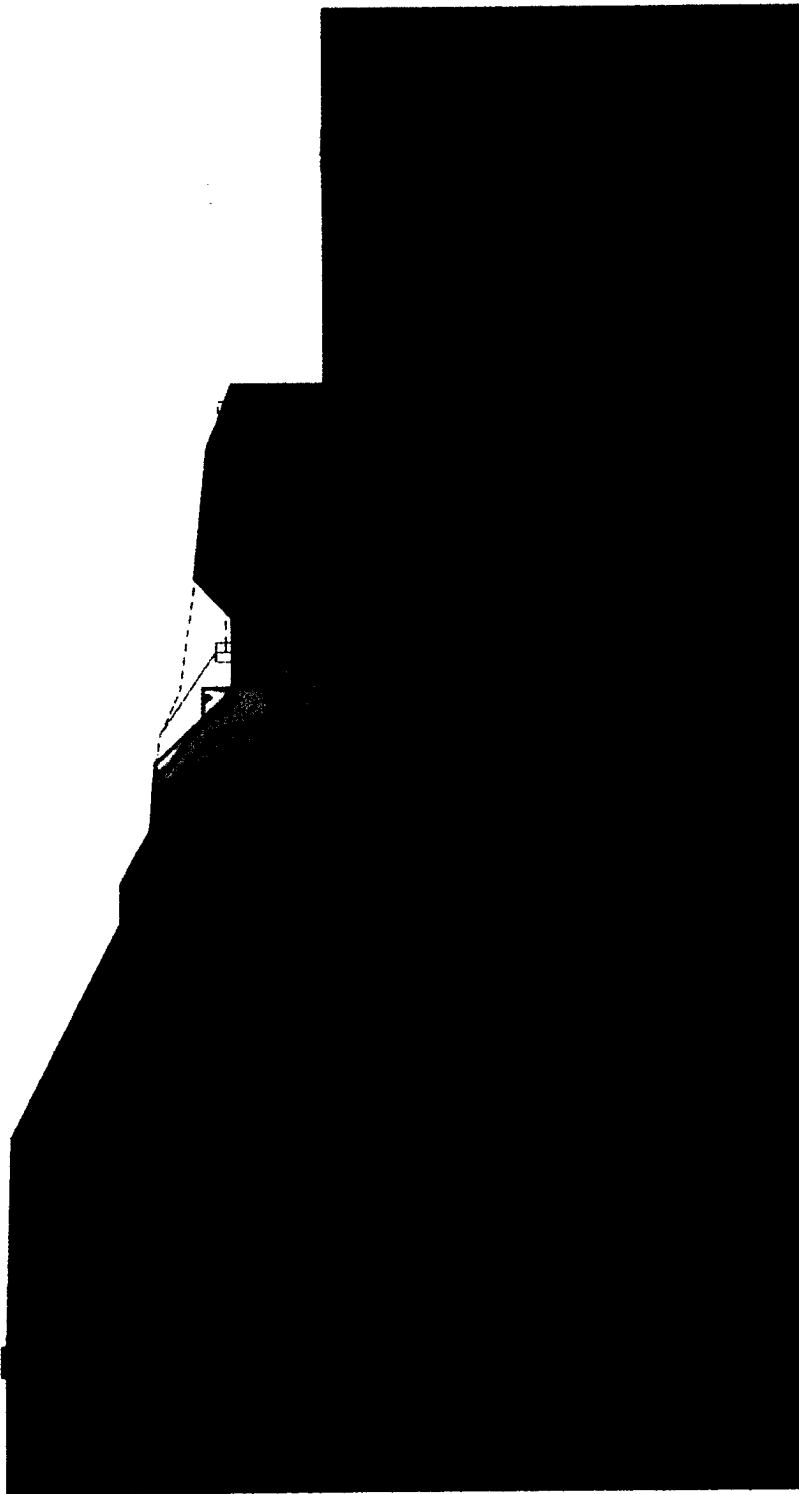


Fig. 5.3.2: Soil displacement contours due to phase 5

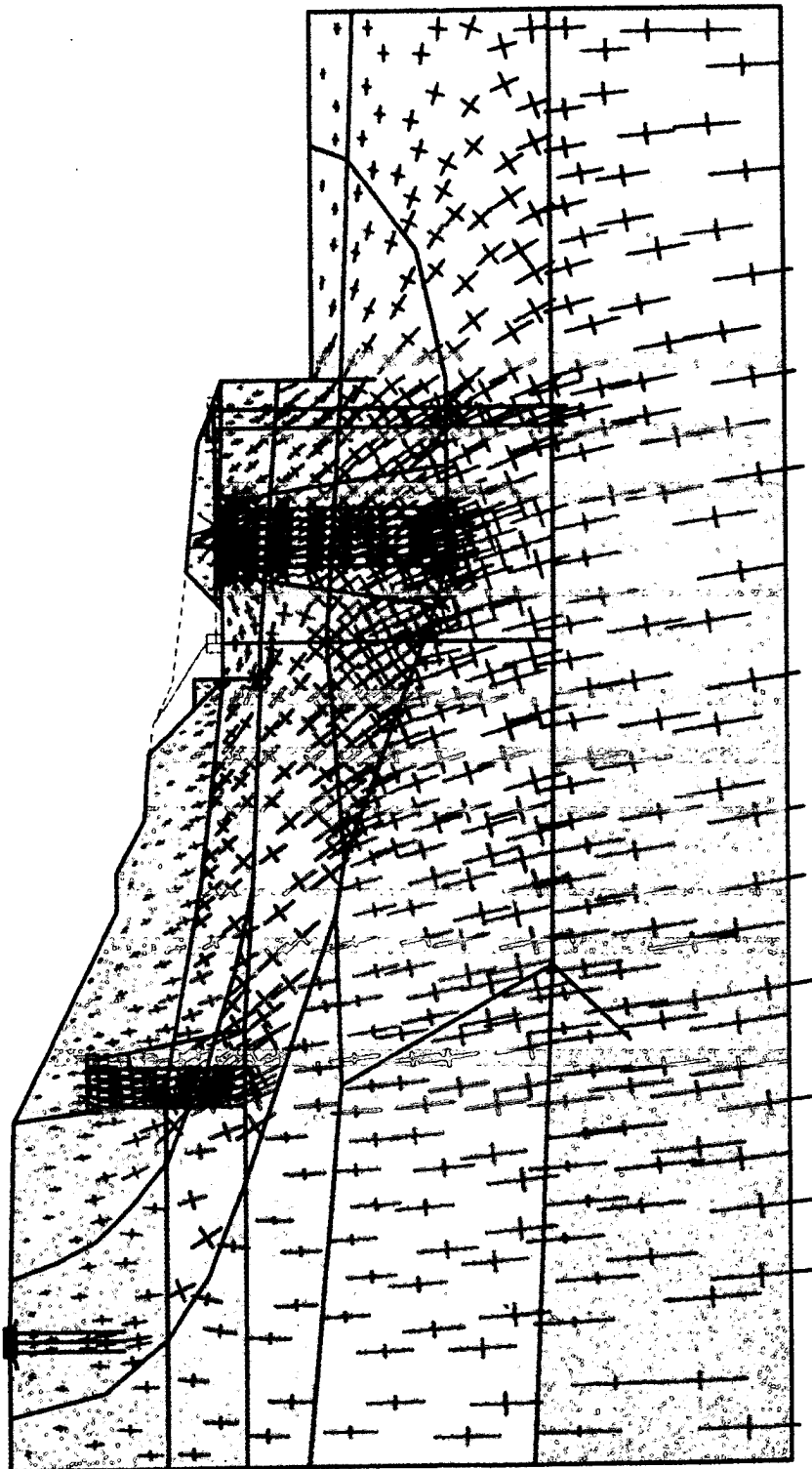


Fig. 5.33: Principal stress direction and magnitude due to phase 5



$\cdot 10^3 \text{ lb/in}^2$   
0.000  
-1.100  
-2.200  
-3.300  
-4.400  
-5.500  
-6.600  
-7.700  
-8.800  
-9.900  
-11.000

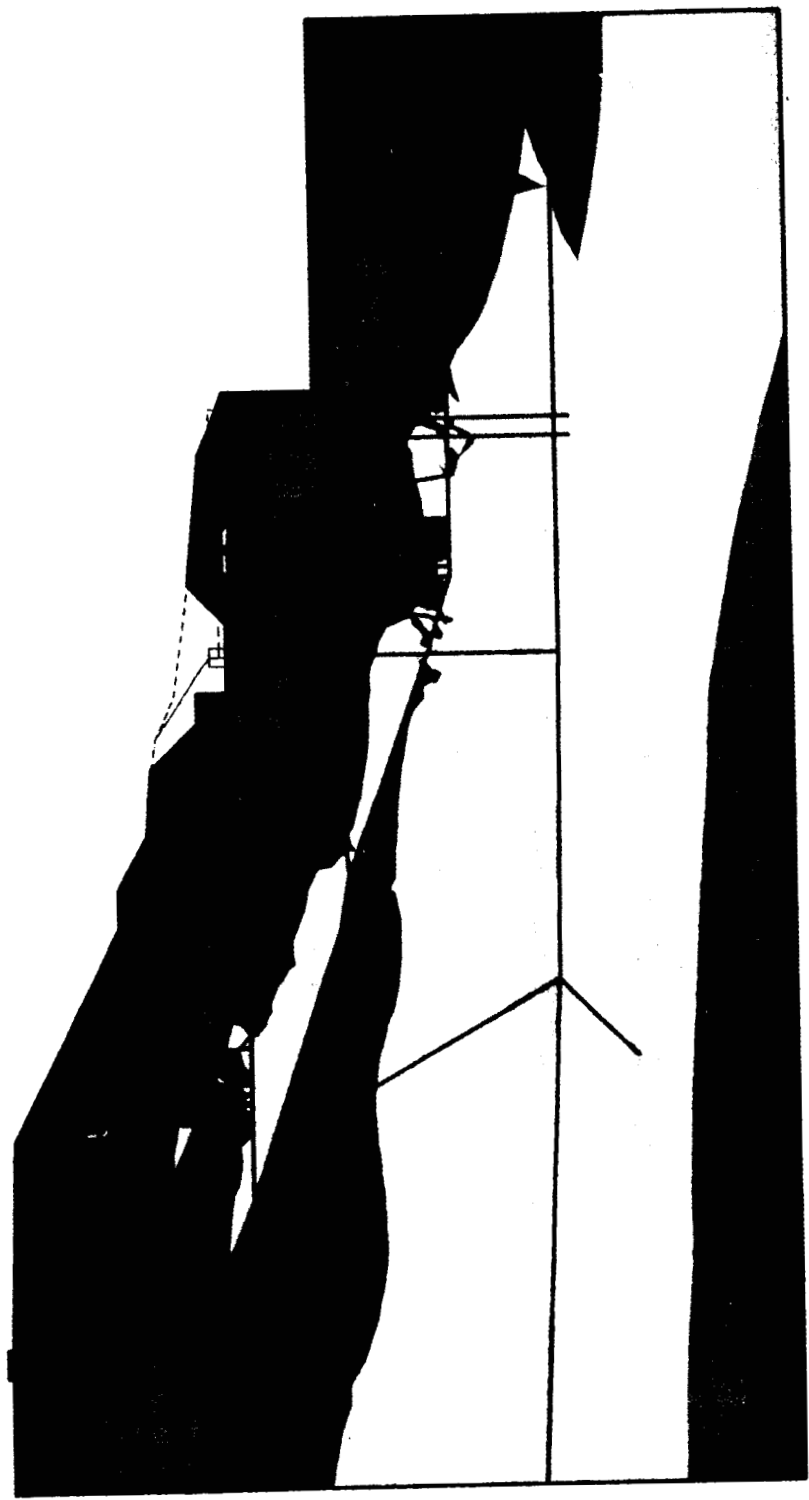


Fig. 5.34: Mean effective stress contours after phase 5

1.000  
0.900  
0.800  
0.700  
0.600  
0.500  
0.400  
0.300  
0.200  
0.100  
0.000

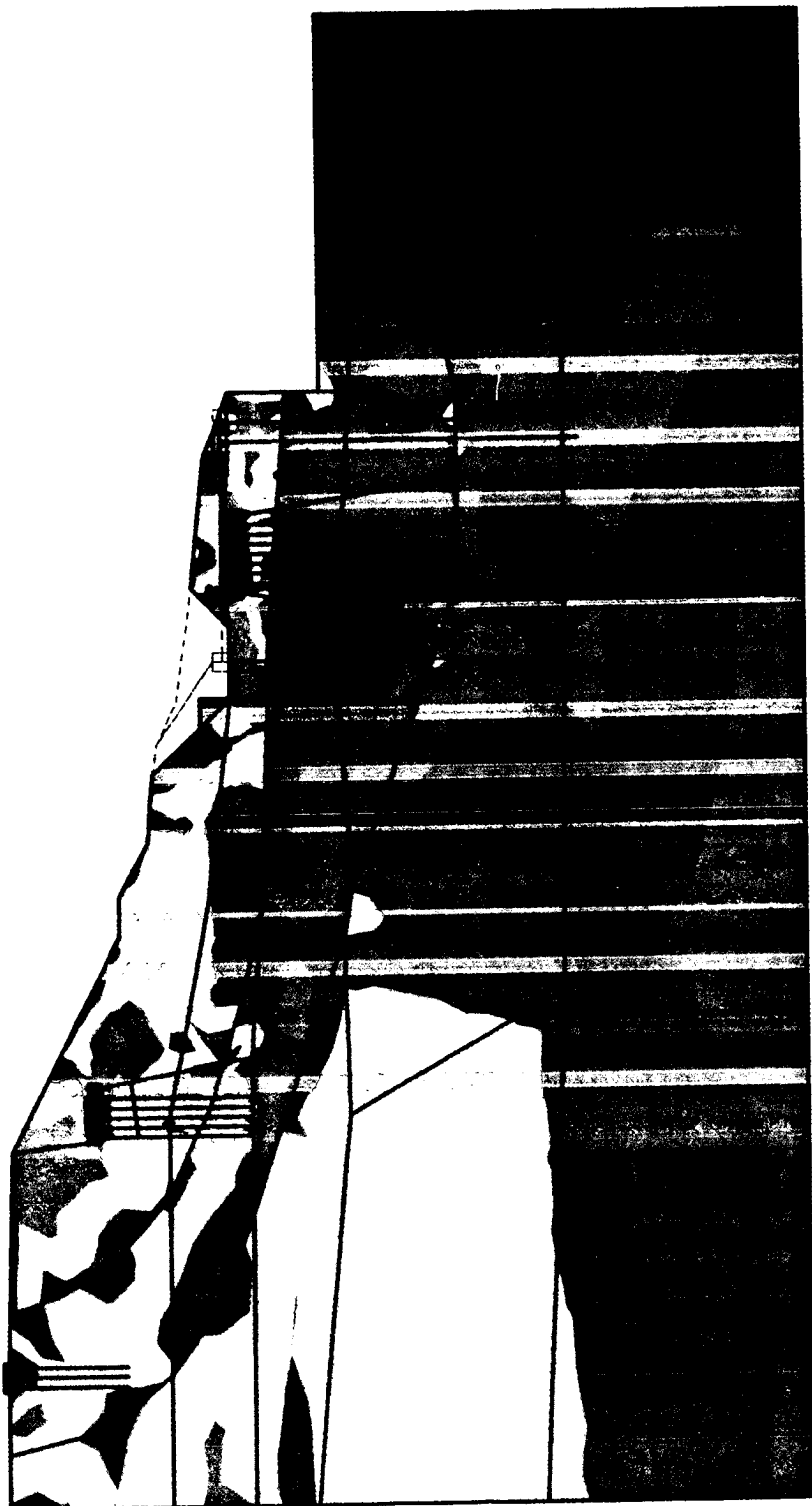


Fig. 5.35: Relative shear stress ratio contours after phase 5

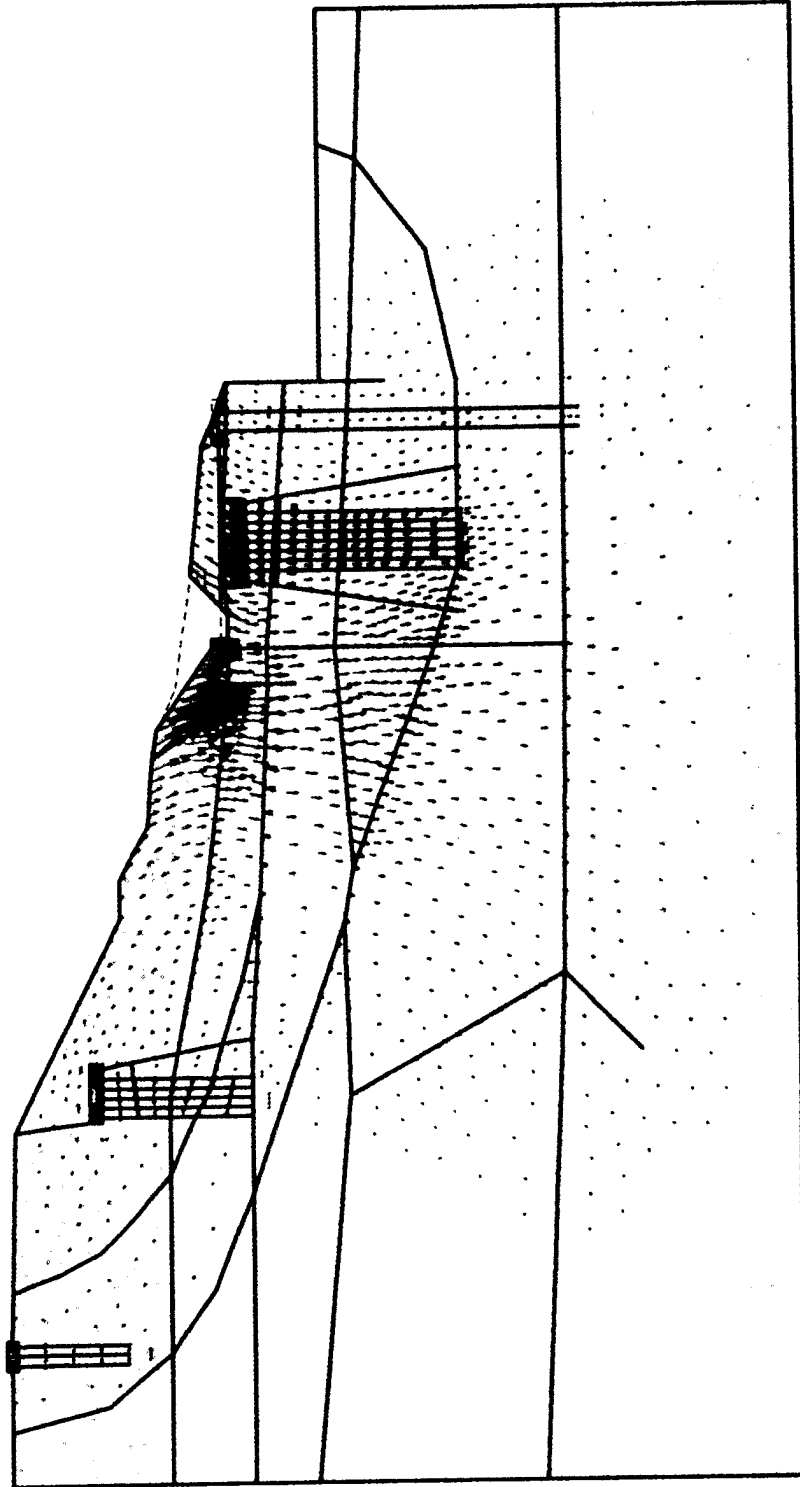


Fig. 5.36: Soil displacement vectors due to phase 6

ft  
0.120  
0.108  
0.096  
0.084  
0.072  
0.060  
0.048  
0.036  
0.024  
0.012  
0.000



Fig. 5.37: Soil displacement contours due to phase 6

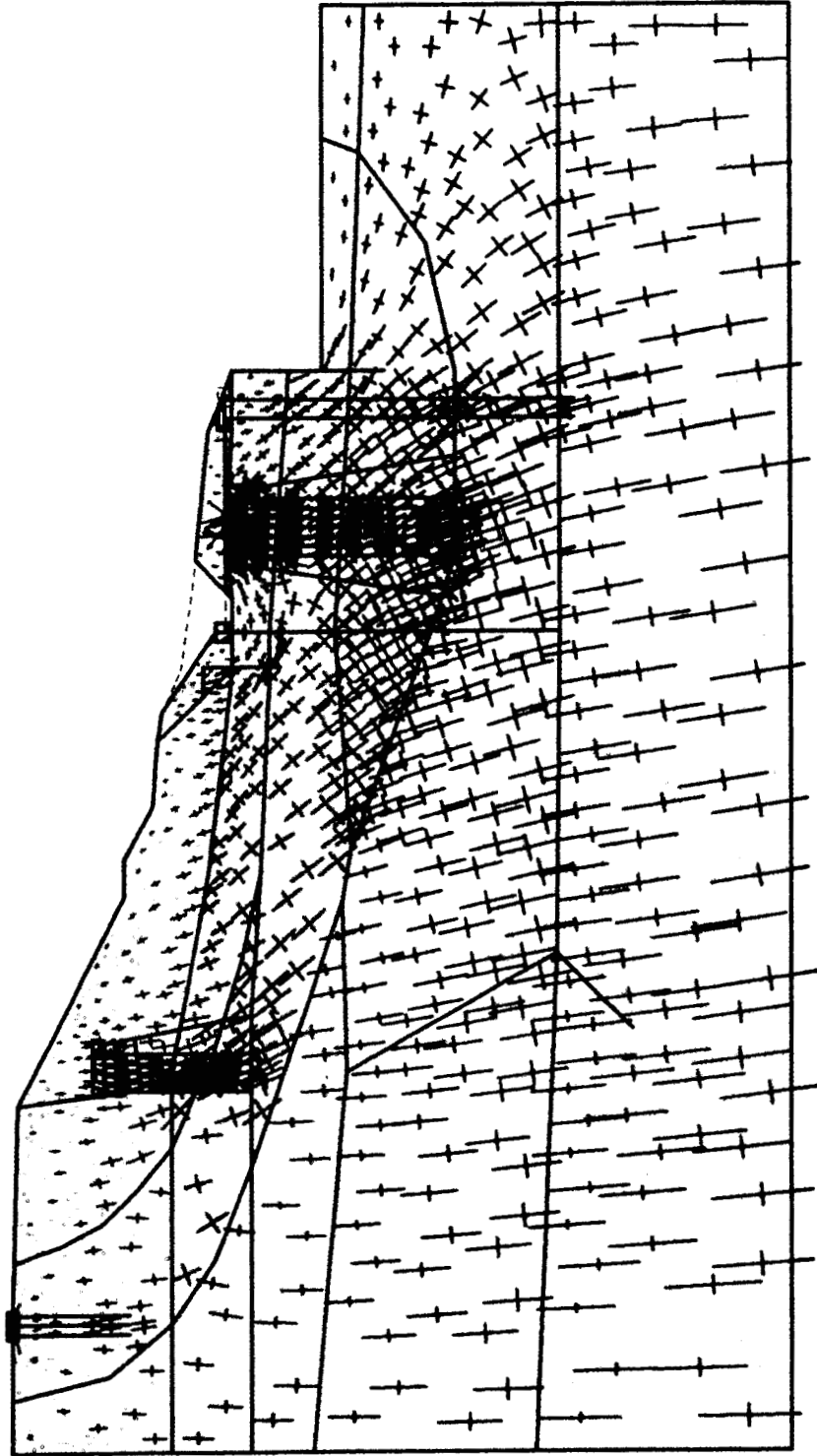


Fig. 5.38: Principal stress direction and magnitude due to phase 6

\*10<sup>3</sup> lb/in<sup>2</sup>  
0.000  
-1.100  
-2.200  
-3.300  
-4.400  
-5.500  
-6.600  
-7.700  
-8.800  
-9.900  
-11.000

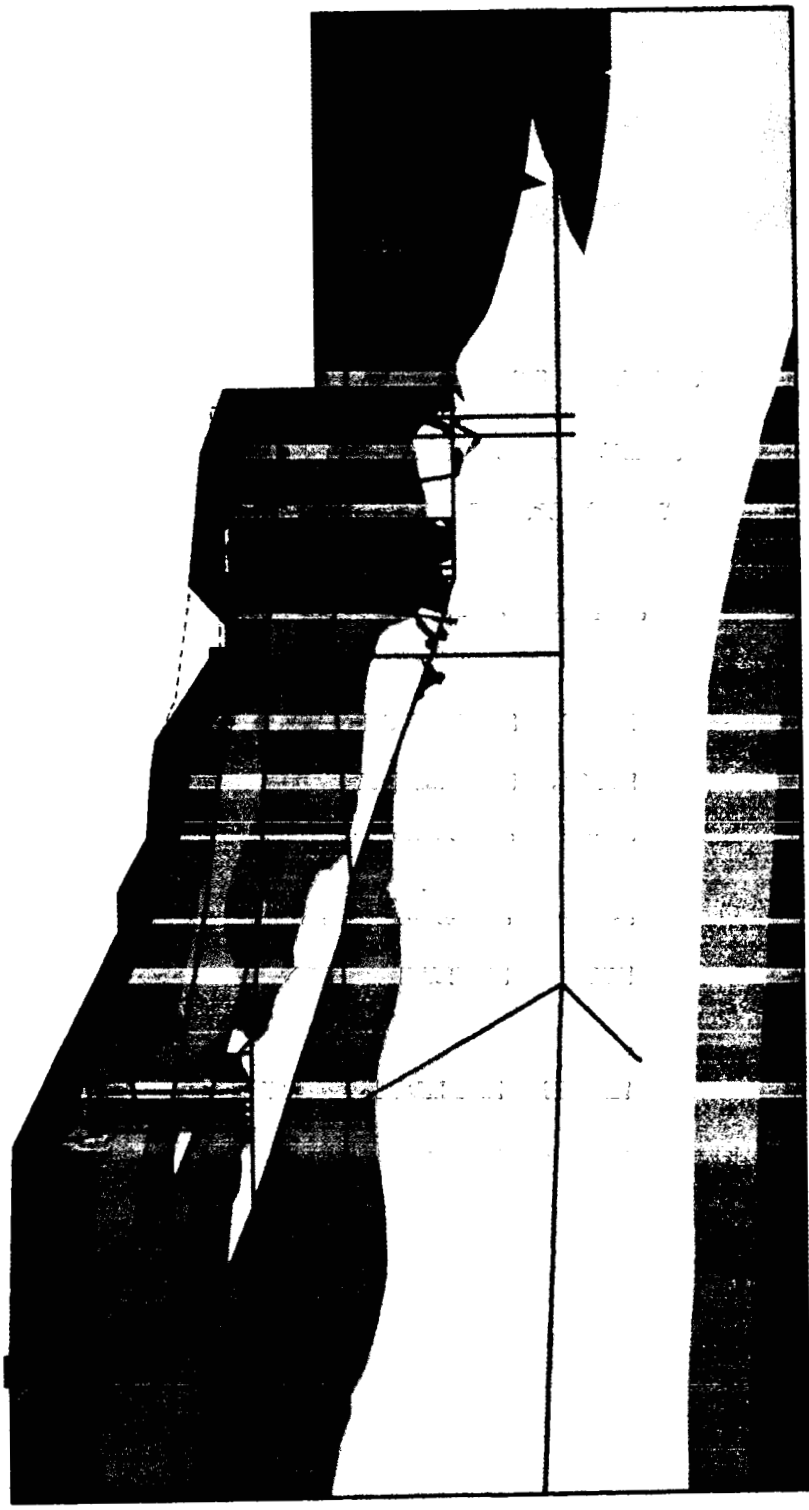


Fig. 5.39: Mean effective stress contours after phase 6

1.000  
0.900  
0.800  
0.700  
0.600  
0.500  
0.400  
0.300  
0.200  
0.100  
0.000

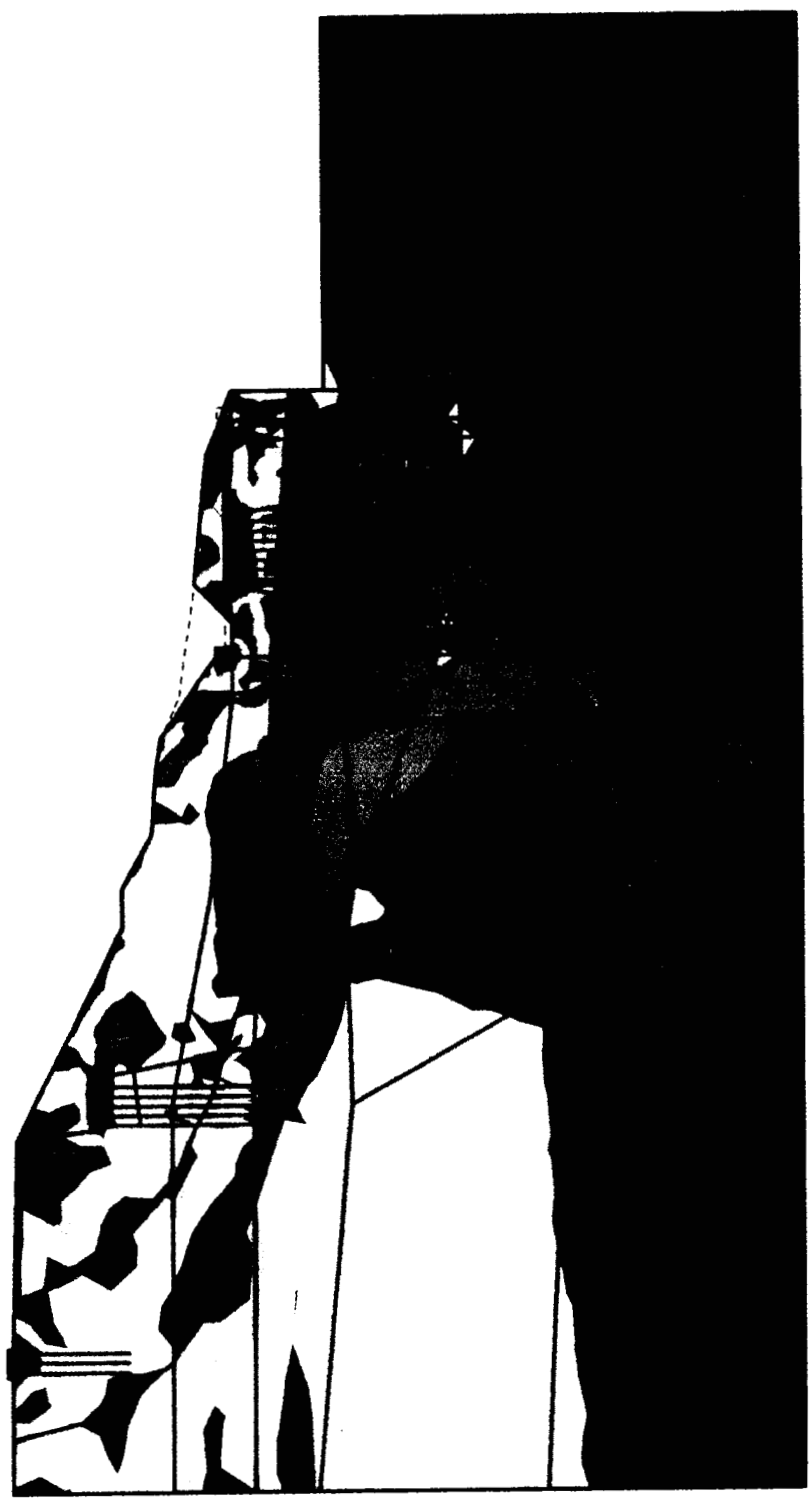


Fig. 5.40: Relative shear stress ratio contours after phase 6

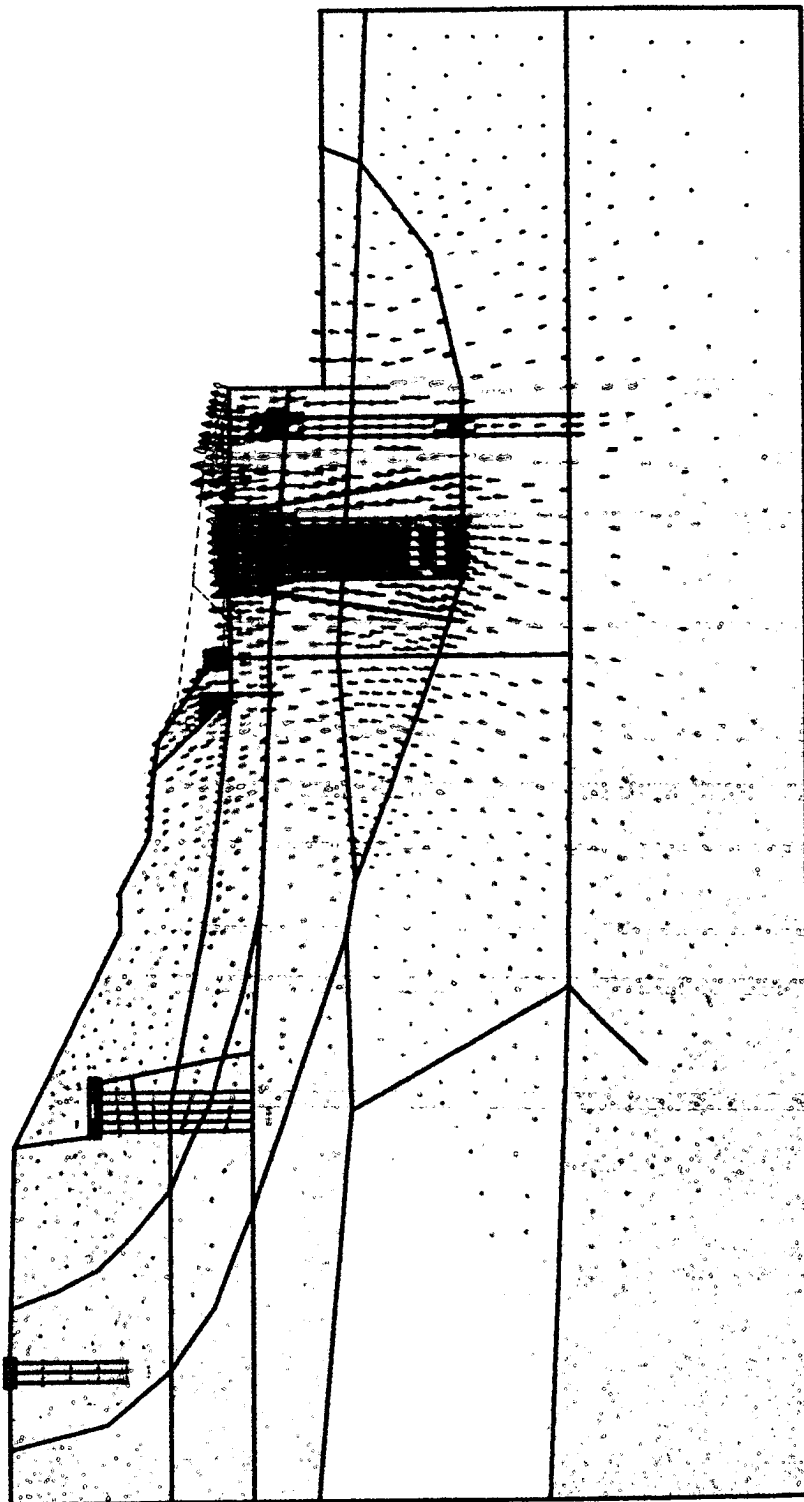


Fig. 5.41: Soil displacement vectors due to phase 7



\*10<sup>-3</sup> ft  
76,000  
68,400  
60,800  
53,200  
45,600  
38,000  
30,400  
22,800  
15,200  
7,600  
0,000

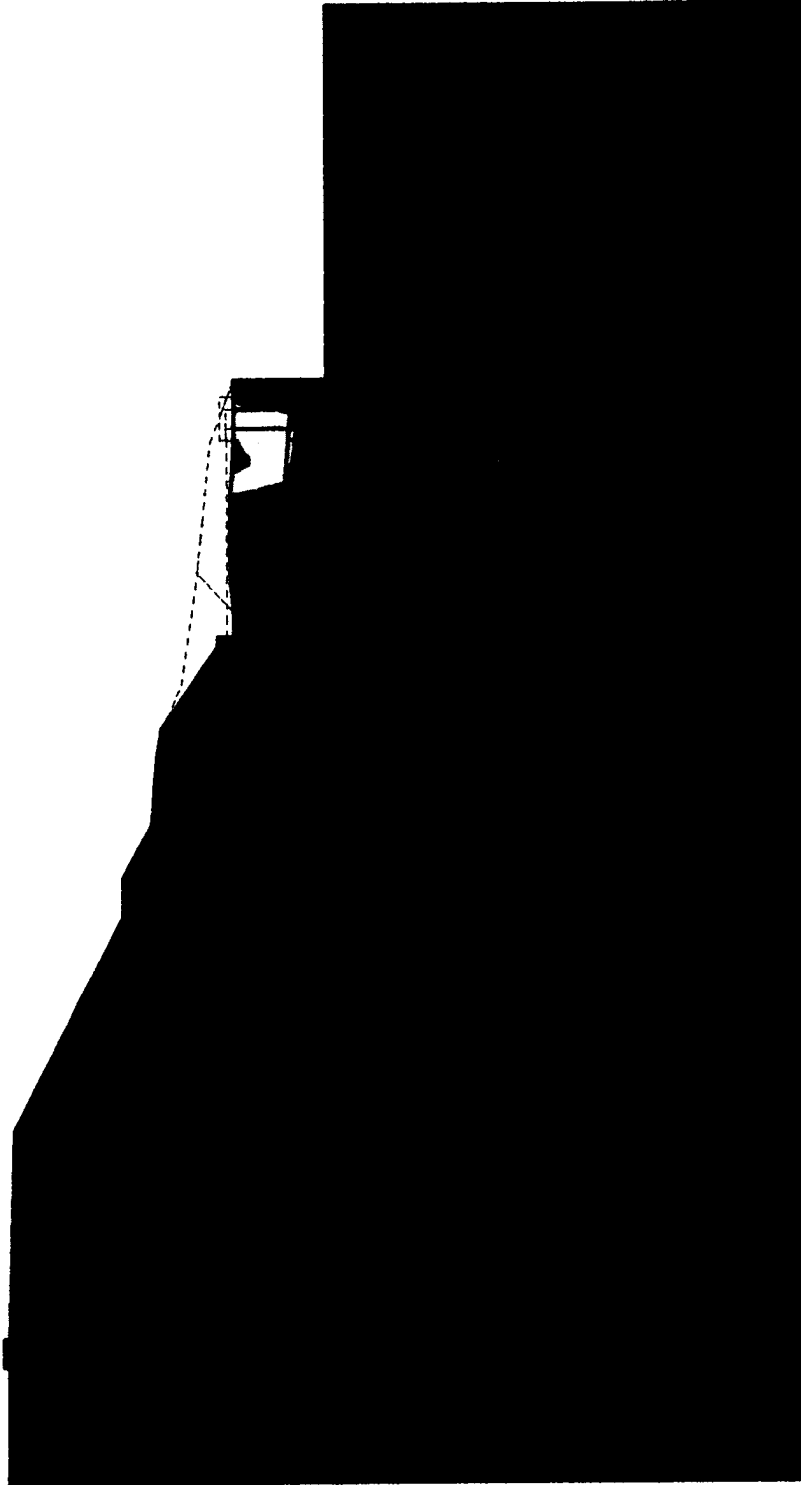


Fig. 5.42: Soil displacement contours due to phase 7

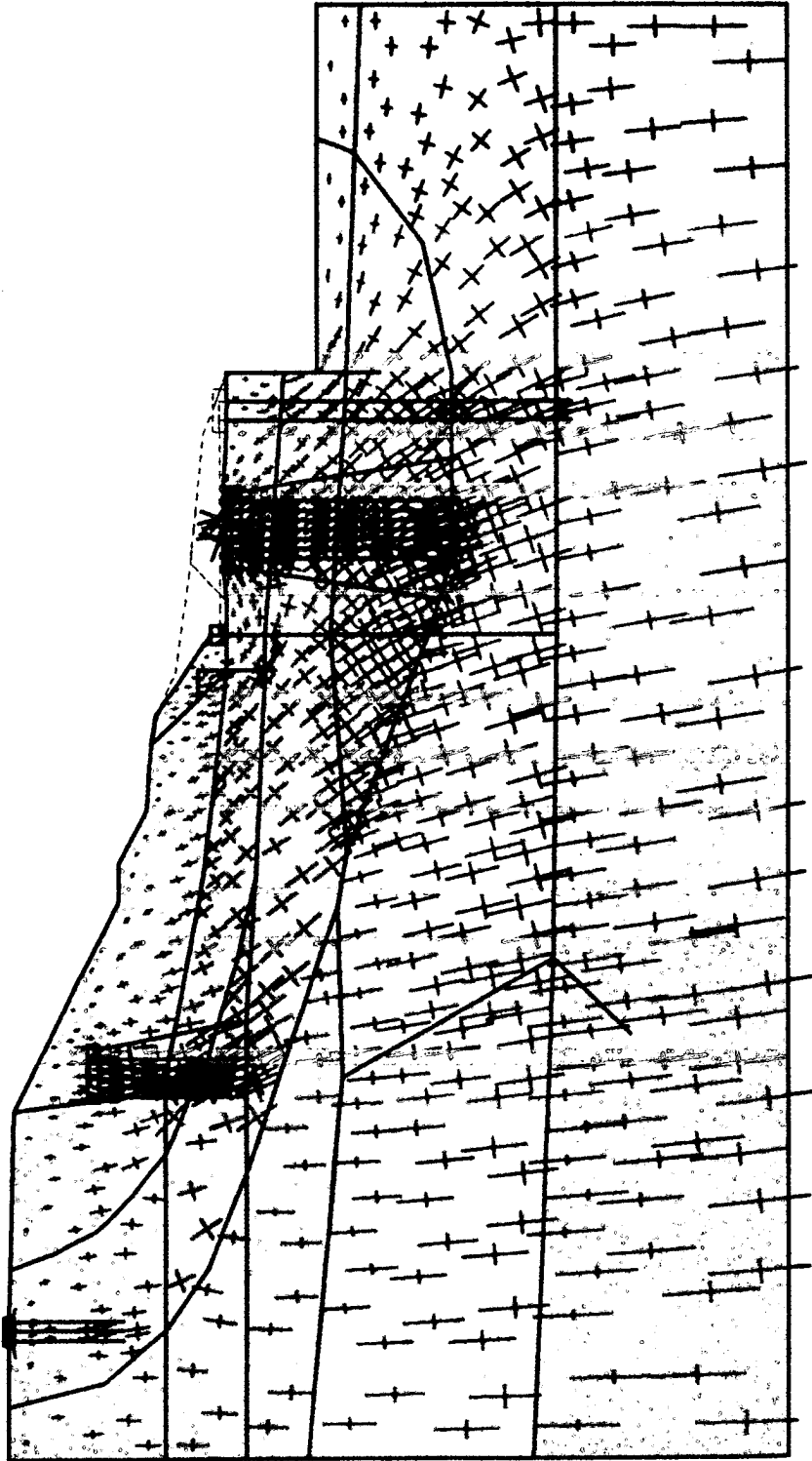


Fig. 5.43: Principal stress direction and magnitude due to phase 7

\*10<sup>3</sup> lb/in<sup>2</sup>  
0.000  
-1.100  
-2.200  
-3.300  
-4.400  
-5.500  
-6.600  
-7.700  
-8.800  
-9.900  
-11.000

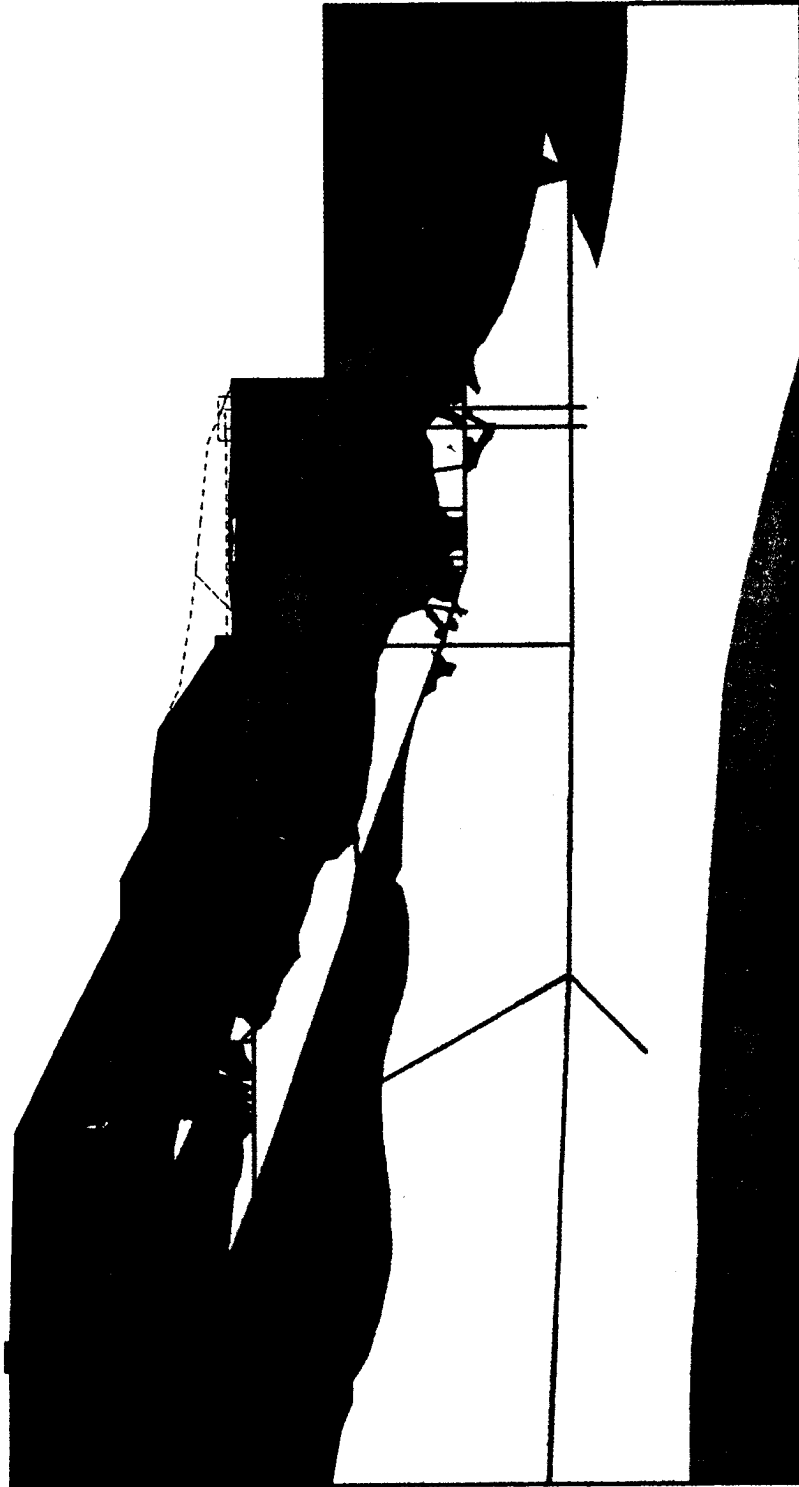


Fig. 5.44: Mean effective stress contours after phase 7

1.000  
0.900  
0.800  
0.700  
0.600  
0.500  
0.400  
0.300  
0.200  
0.100  
0.000



Fig. 5.45: Relative shear stress ratio contours after phase 7

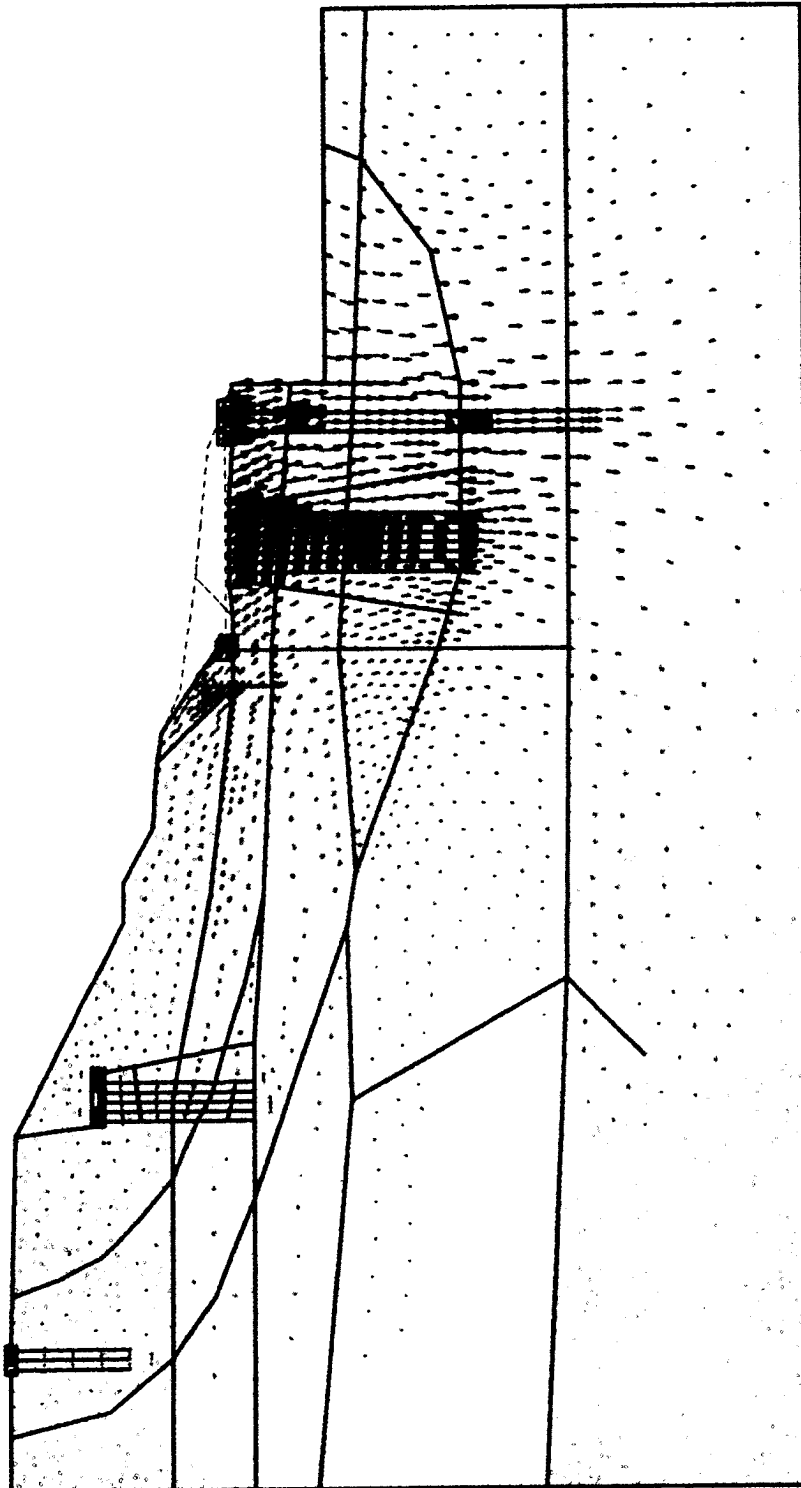


Fig. 5.46: Soil displacement vectors due to phase 8

\*10<sup>-3</sup> ft  
10.000  
9.000  
8.000  
7.000  
6.000  
5.000  
4.000  
3.000  
2.000  
1.000  
0.000

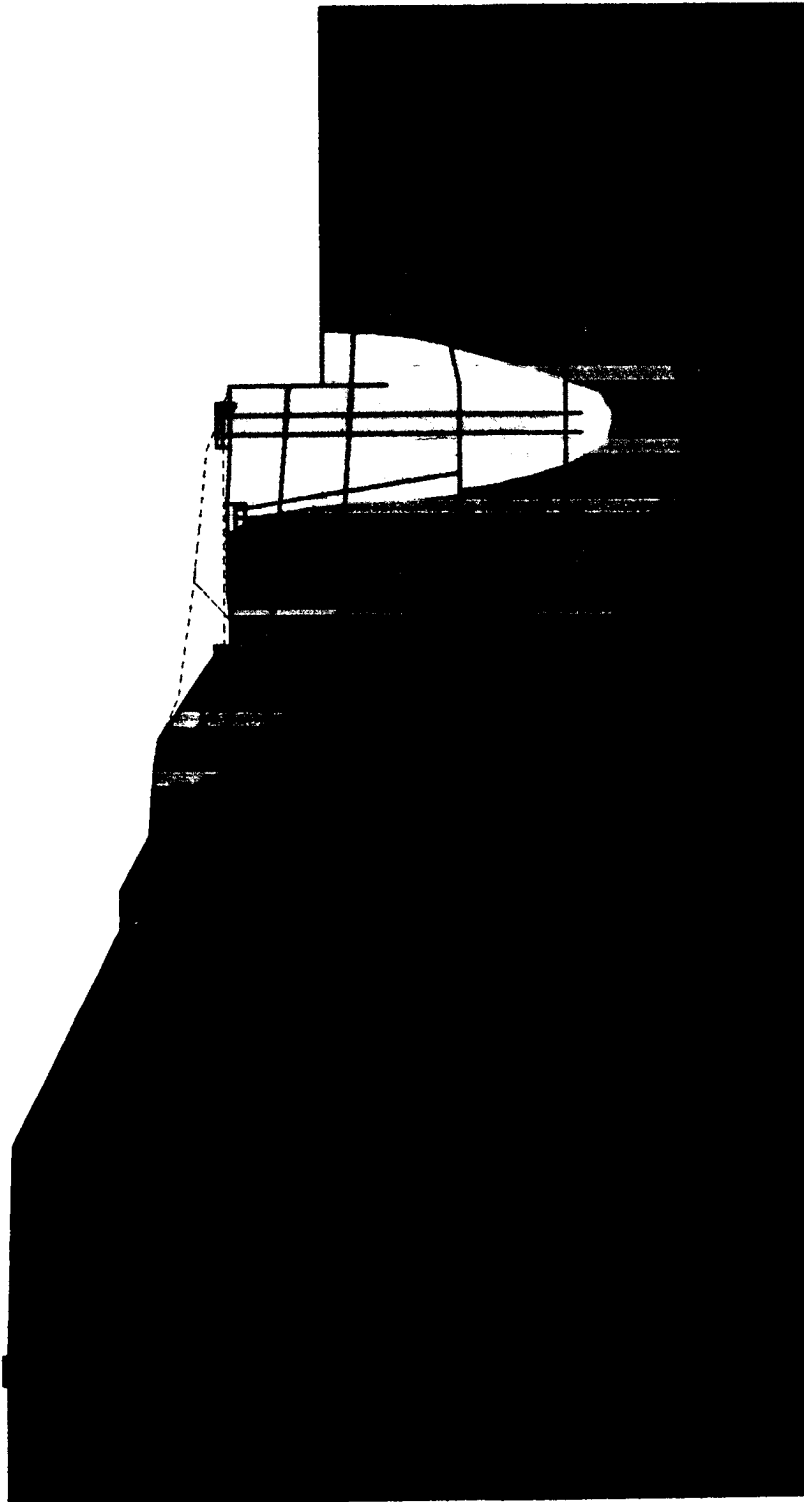


Fig. 5.47: Soil displacement contours due to phase 8

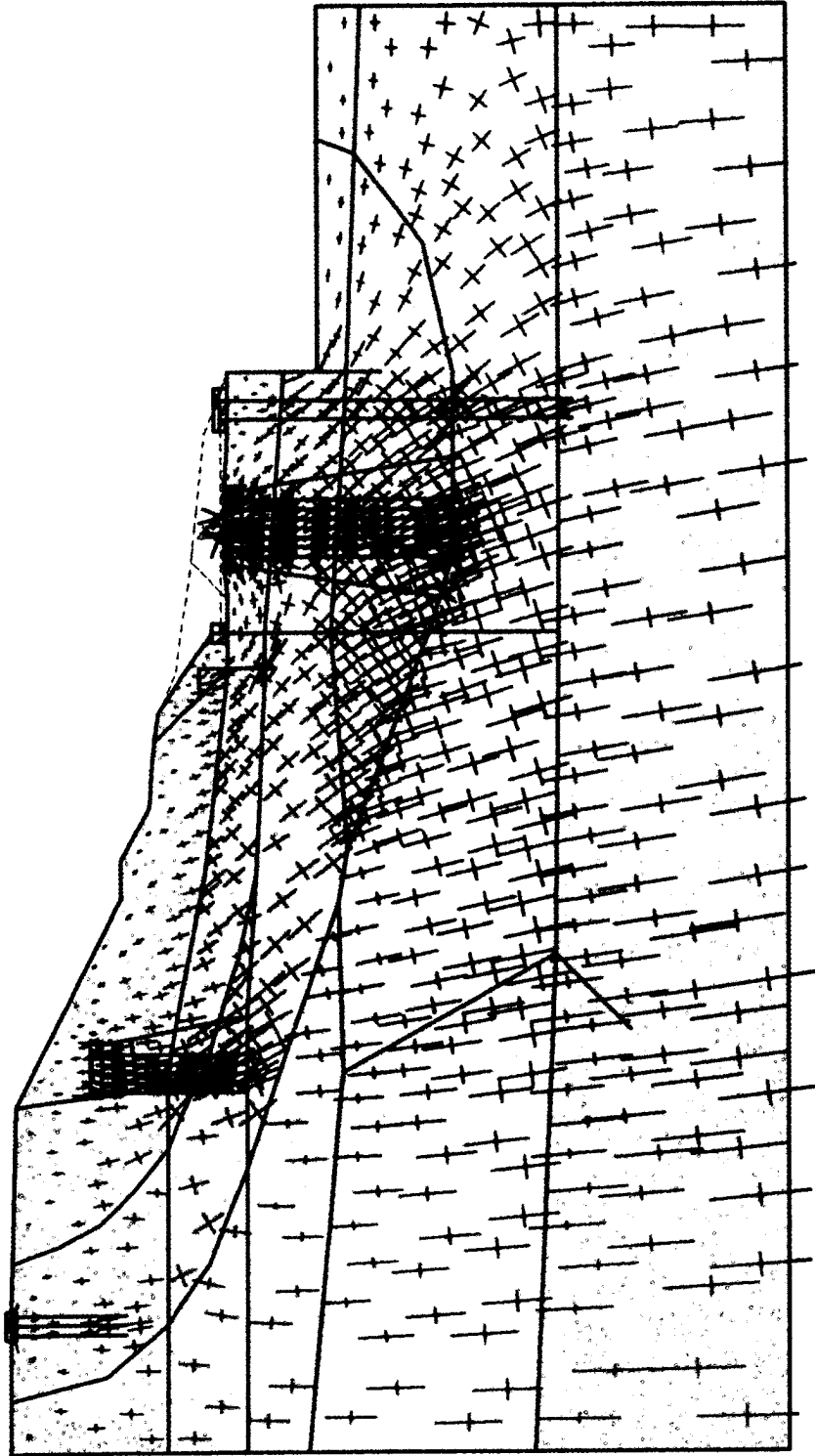


Fig. 5.48: Principal stress direction and magnitude due to phase 8

\*10<sup>3</sup> lb/in<sup>2</sup>  
0.000  
-1.100  
-2.200  
-3.300  
-4.400  
-5.500  
-6.600  
-7.700  
-8.800  
-9.900  
-11.000

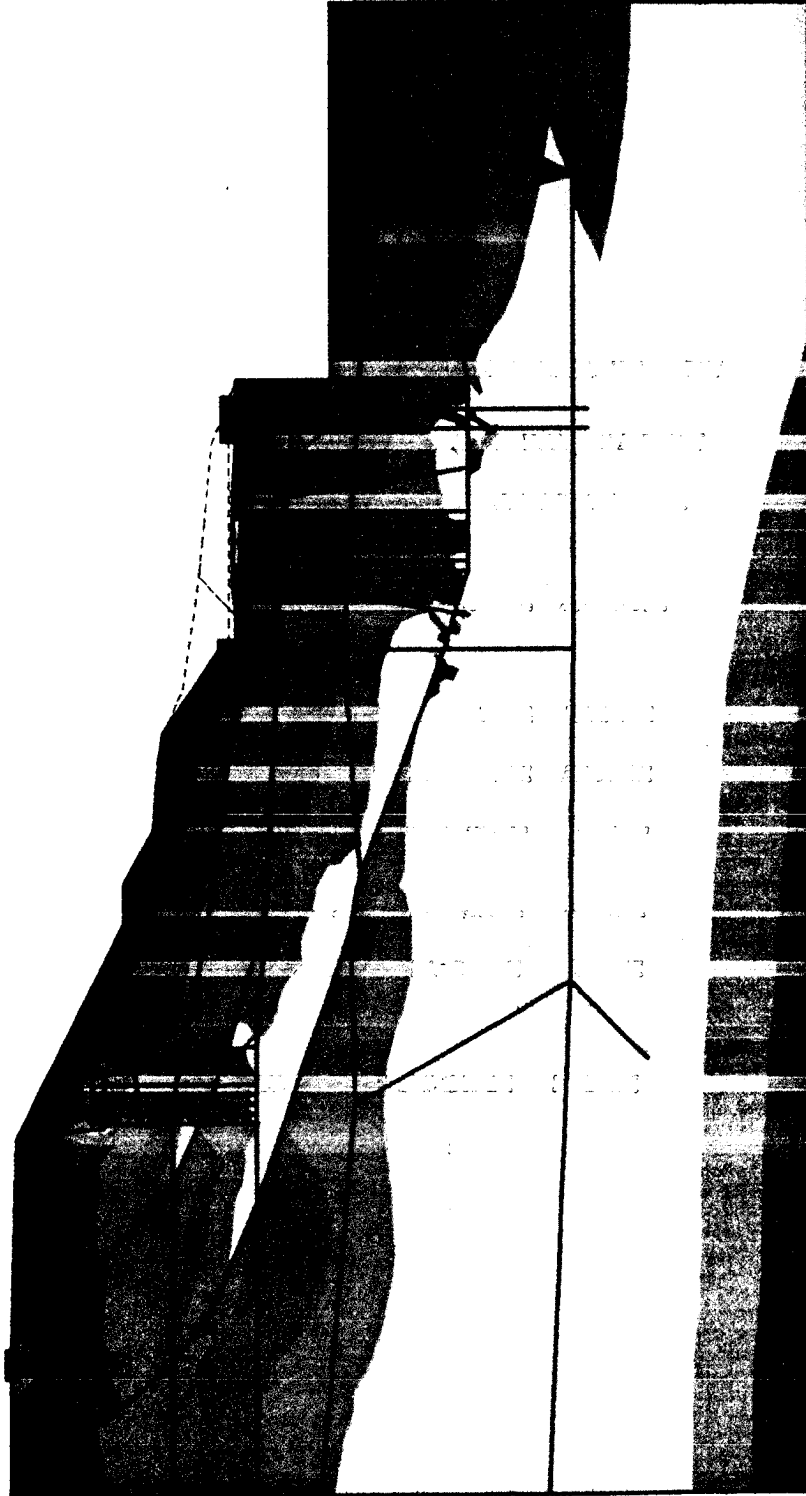


Fig. 5.49: Mean effective stress contours after phase 8



1.000  
0.900  
0.800  
0.700  
0.600  
0.500  
0.400  
0.300  
0.200  
0.100  
0.000

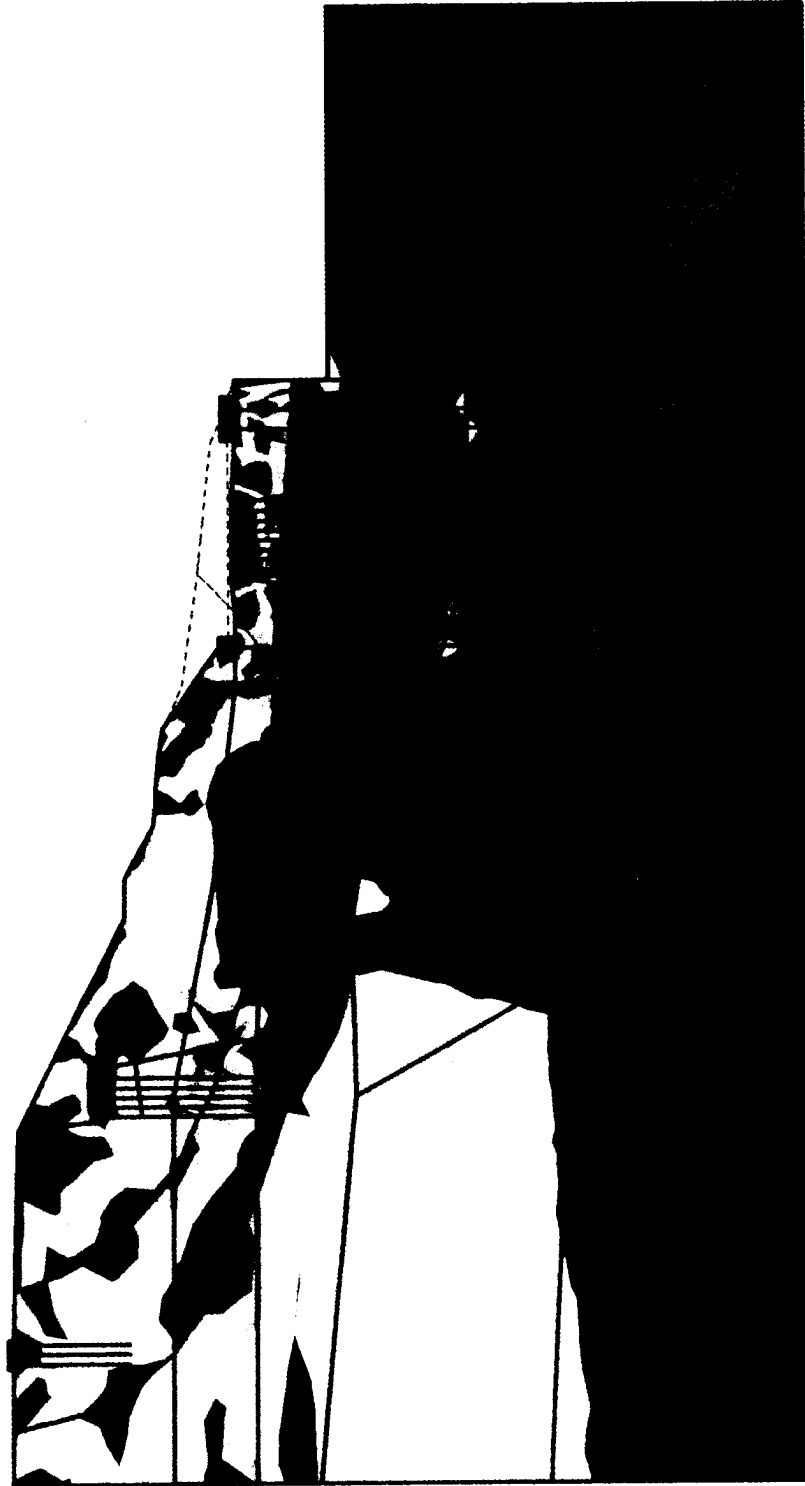


Fig. 5.50: Relative shear stress ratio contours after phase 8

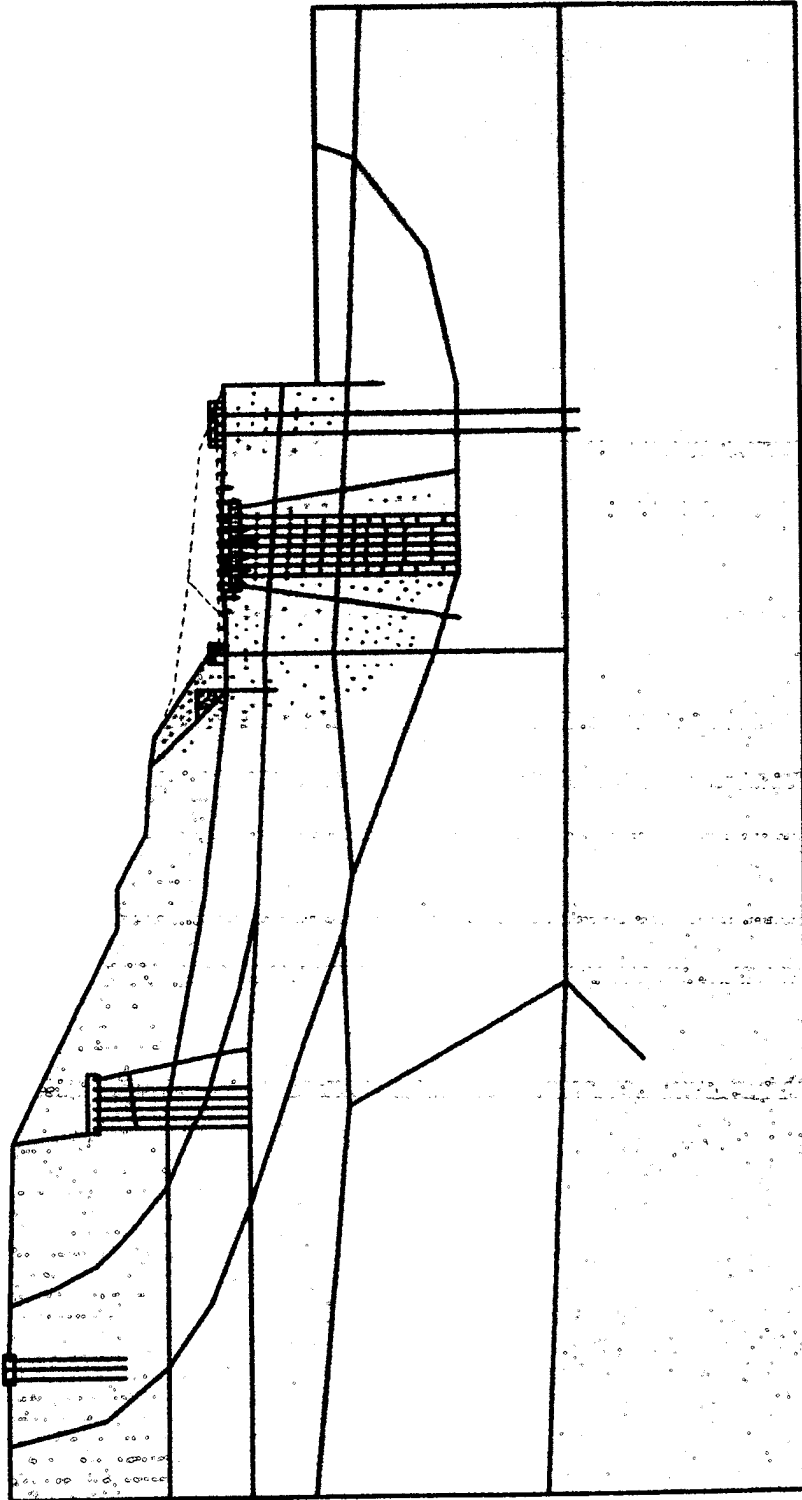


Fig. 5.51: Soil displacement vectors due to phase 9

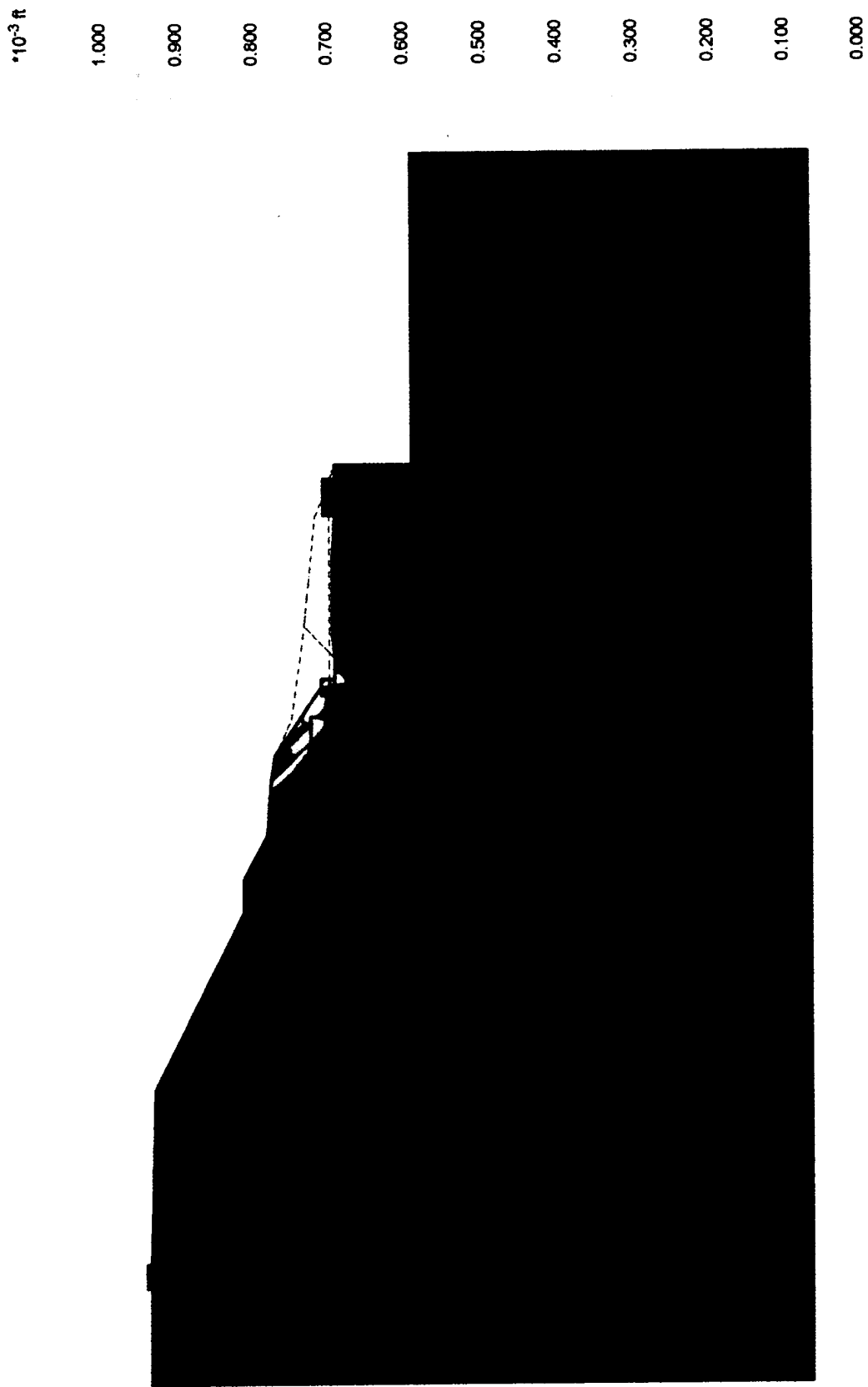


Fig. 5.52: Soil displacement contours due to phase 9

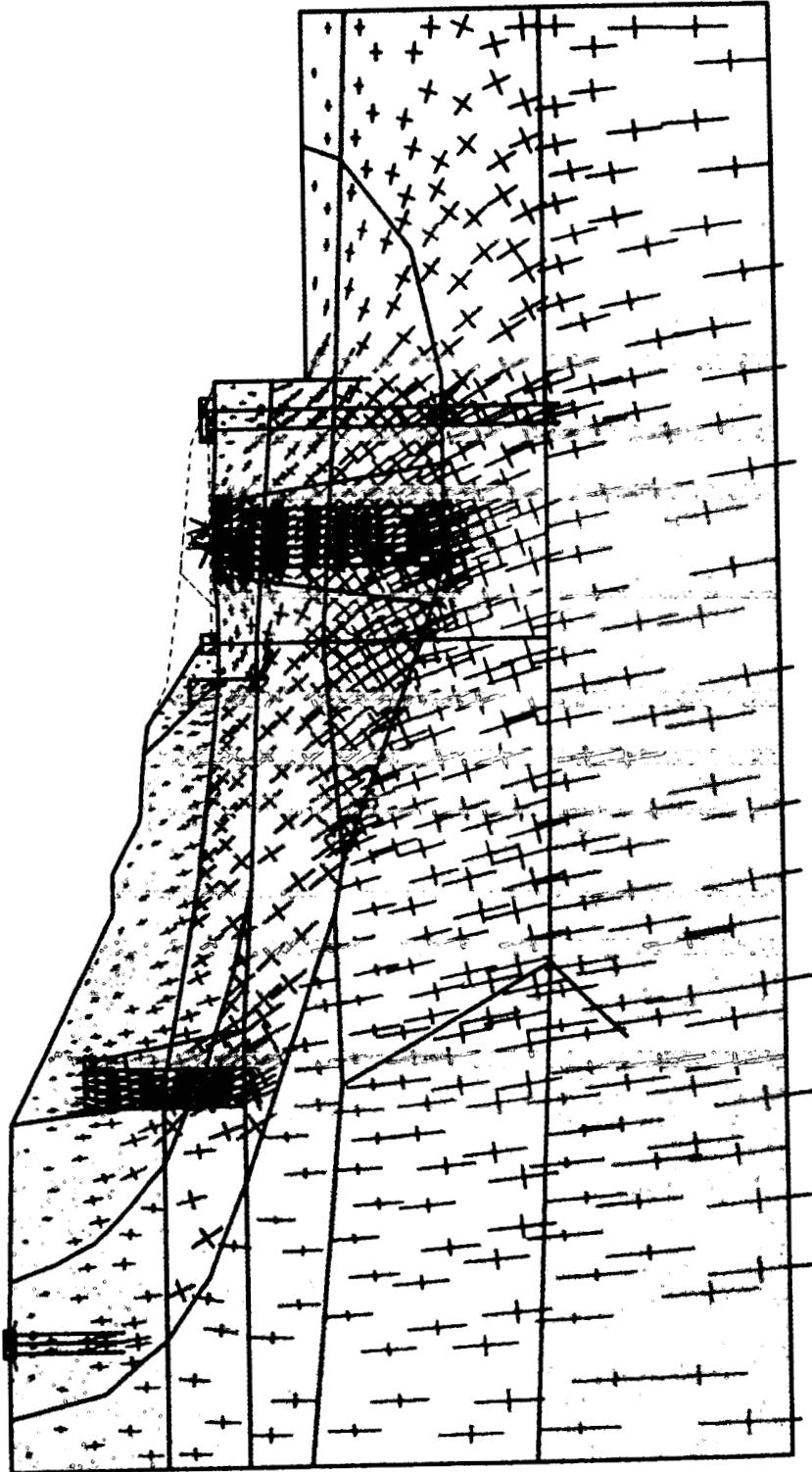


Fig. 5.53: Principal stress direction and magnitude due to phase 9

$\times 10^3 \text{ lb/in}^2$

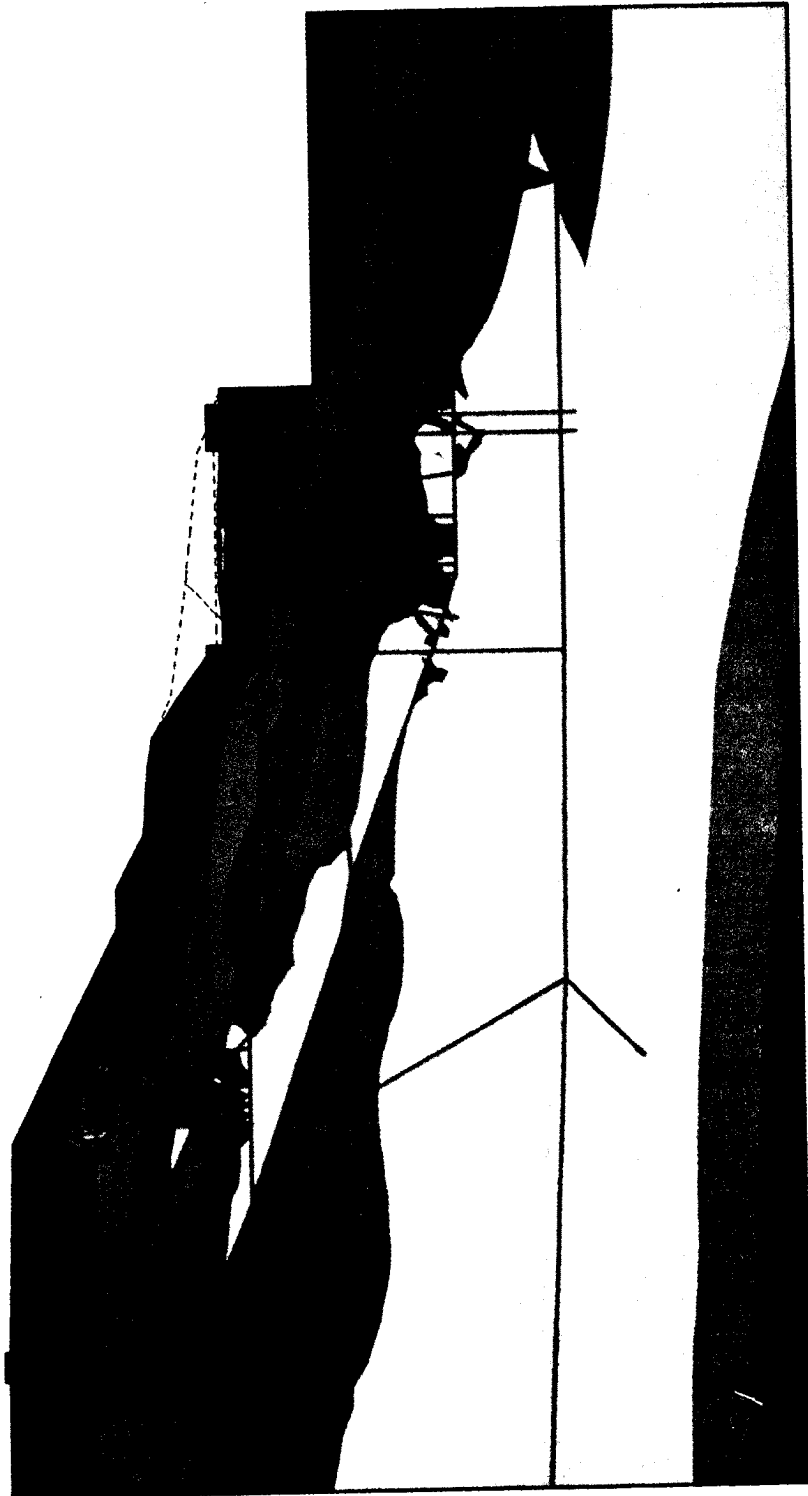
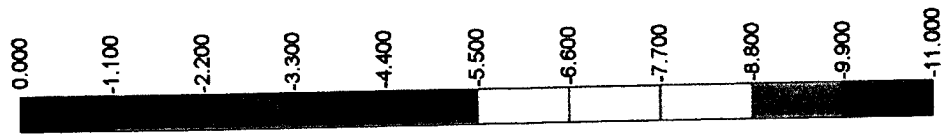


Fig. 5.54: Mean effective stress contours after phase 9

1.000  
0.900  
0.800  
0.700  
0.600  
0.500  
0.400  
0.300  
0.200  
0.100  
0.000

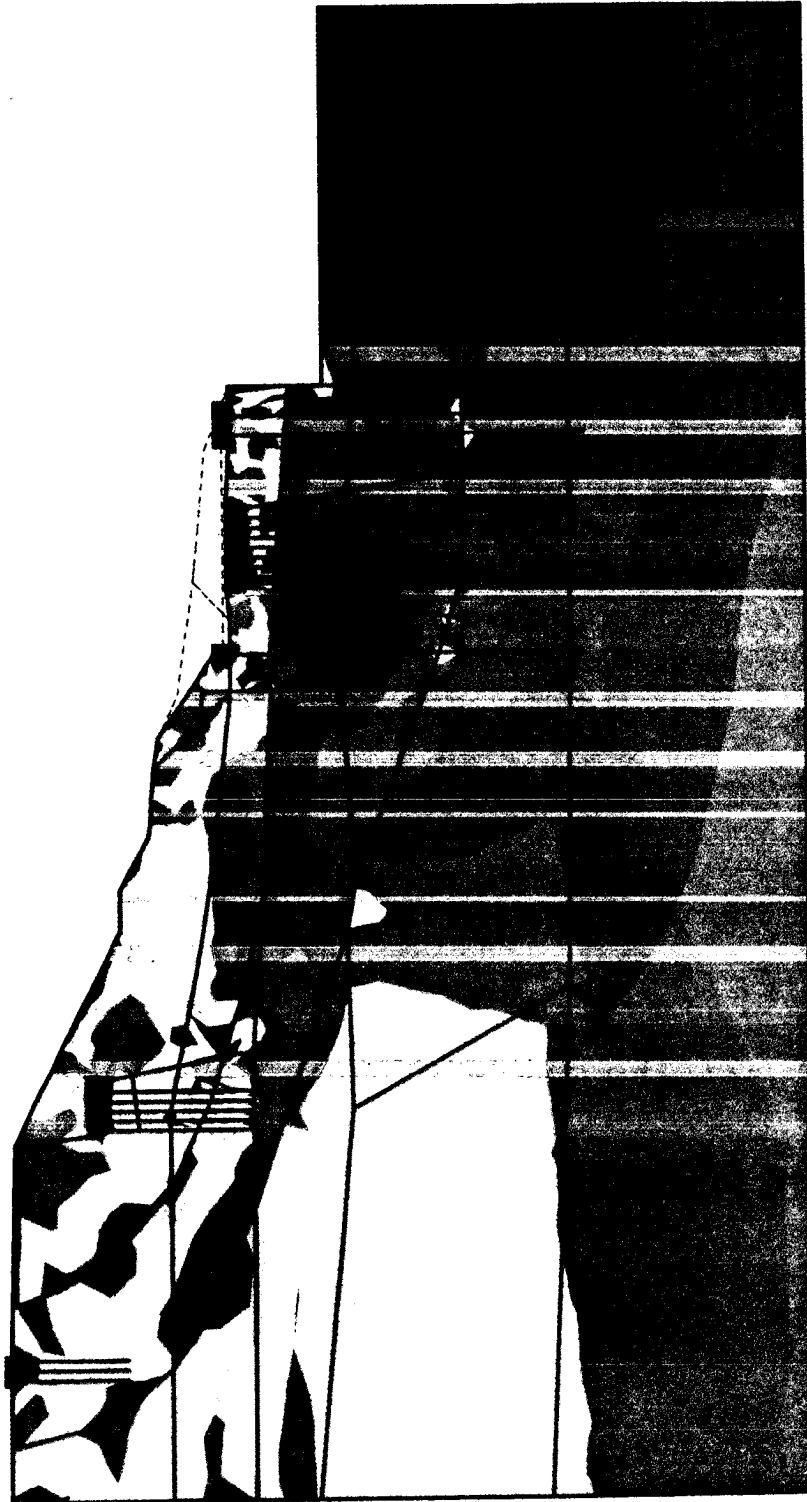


Fig. 5.55: Relative shear stress ratio contours after phase 9

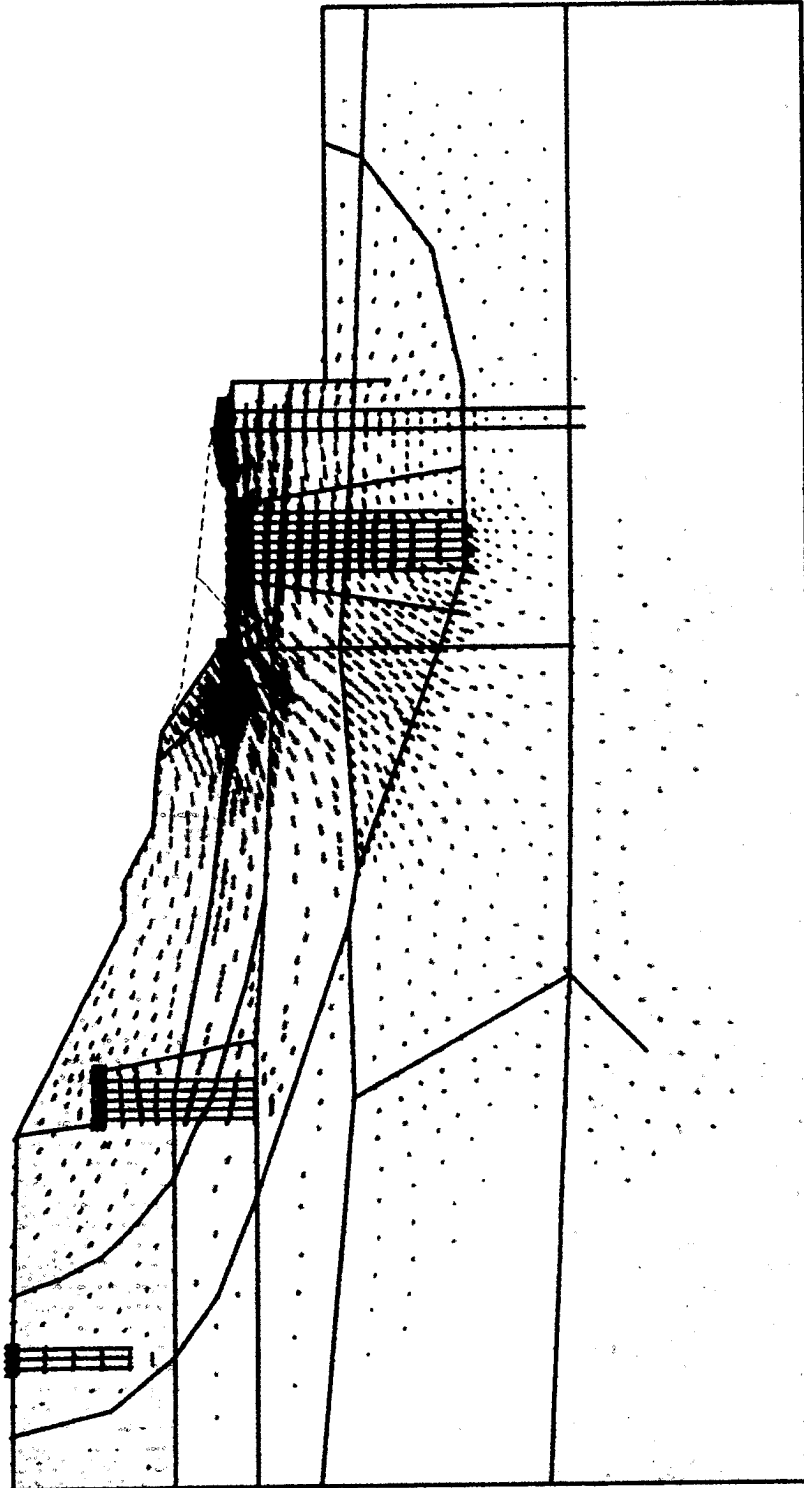


Fig. 5.56: Soil displacement vectors due to phase 10

\*10<sup>-3</sup> ft  
 42,000  
 39,400  
 36,800  
 34,200  
 31,600  
 29,000  
 26,400  
 23,800  
 21,200  
 18,600  
 16,000  
 13,400  
 10,800  
 8,200  
 5,600  
 3,000  
 0,400  
 -2,200  
 -4,800  
 -7,400  
 -10,000

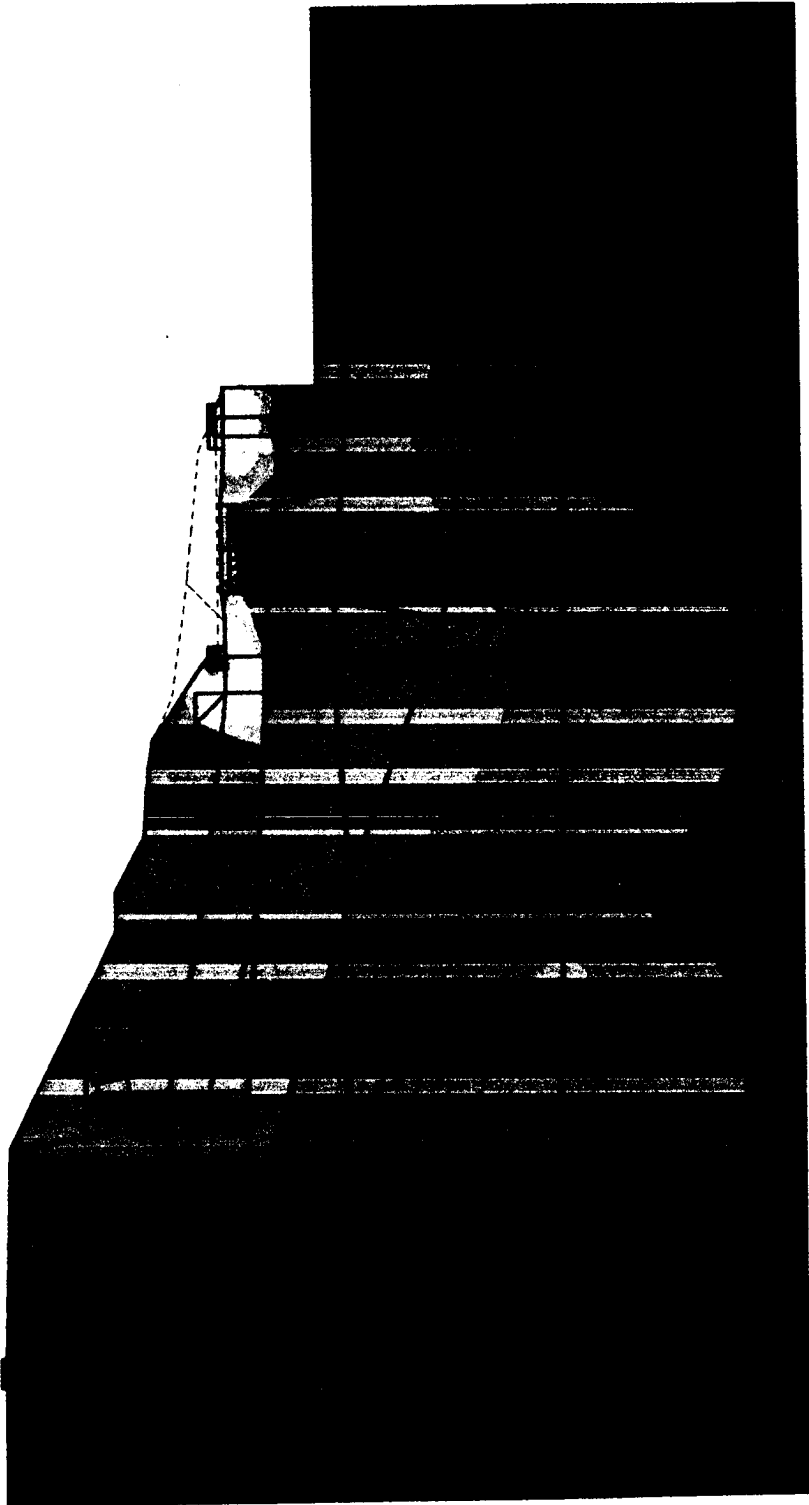


Fig. 5.57: Soil displacement contours due to phase 10



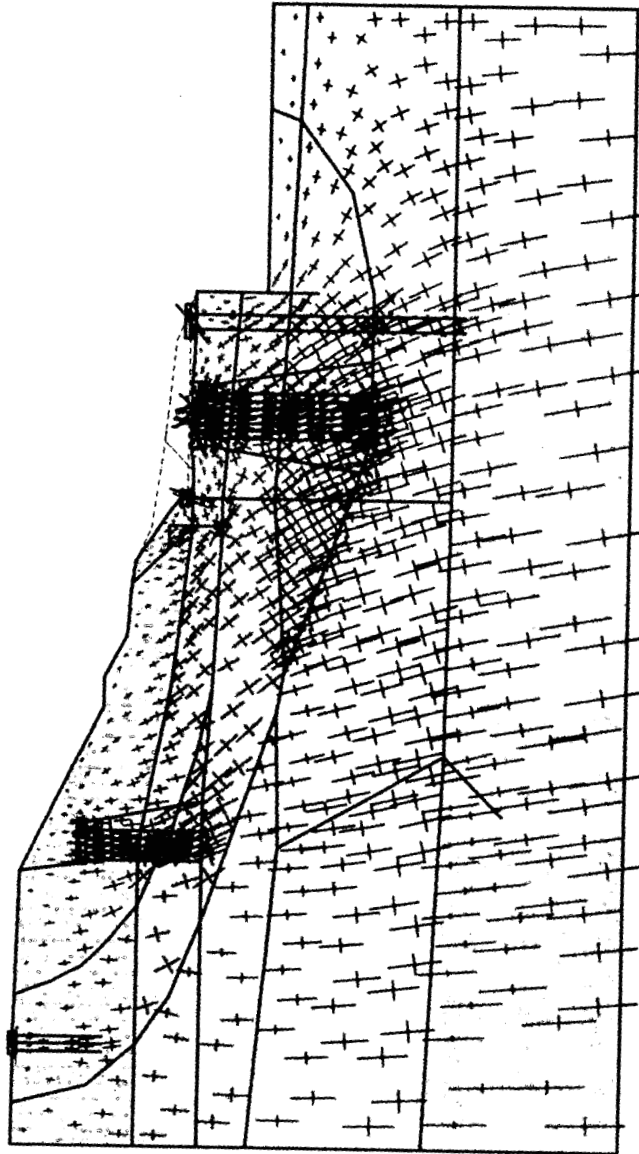


Fig. 5.58: Principal stress direction and magnitude due to phase 10

\*10<sup>3</sup> lb/in<sup>2</sup>  
0.000  
-1.100  
-2.200  
-3.300  
-4.400  
-5.500  
-6.600  
-7.700  
-8.800  
-9.900  
-11.000

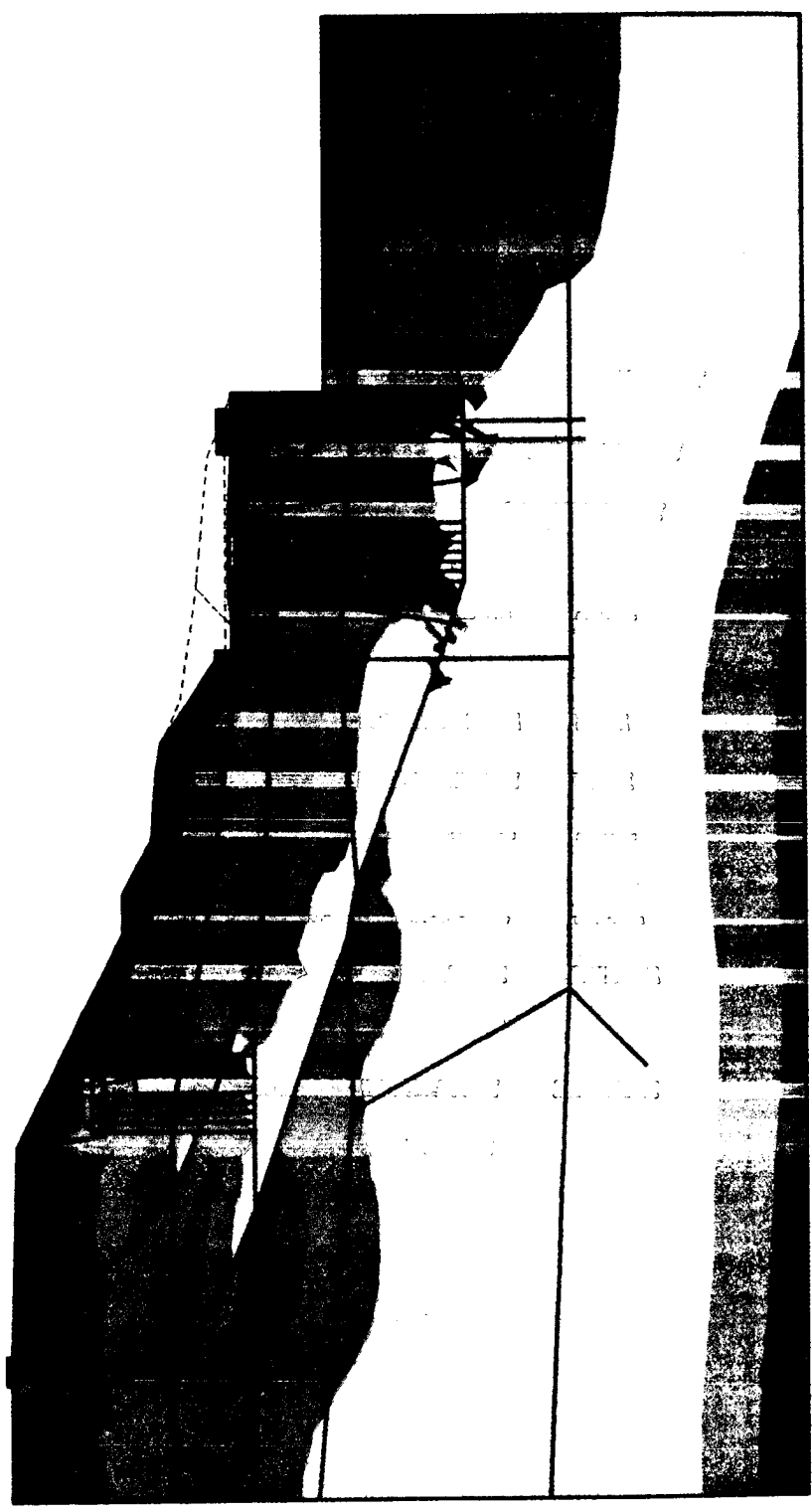


Fig. 5.59: Mean effective stress contours after phase 10

1.000  
0.900  
0.800  
0.700  
0.600  
0.500  
0.400  
0.300  
0.200  
0.100  
0.000

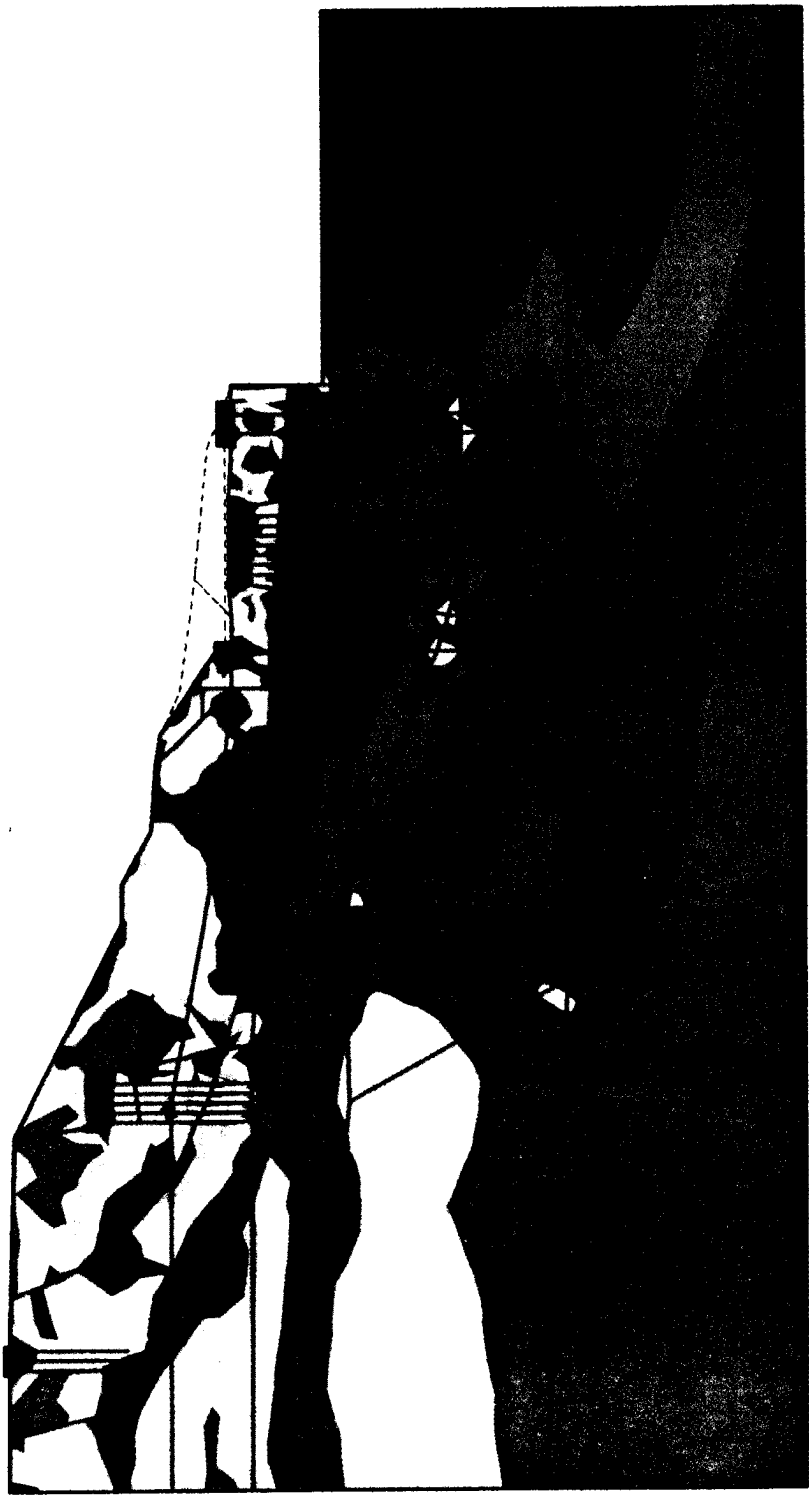


Fig. 5.60: Relative shear stress ratio contours after phase 10

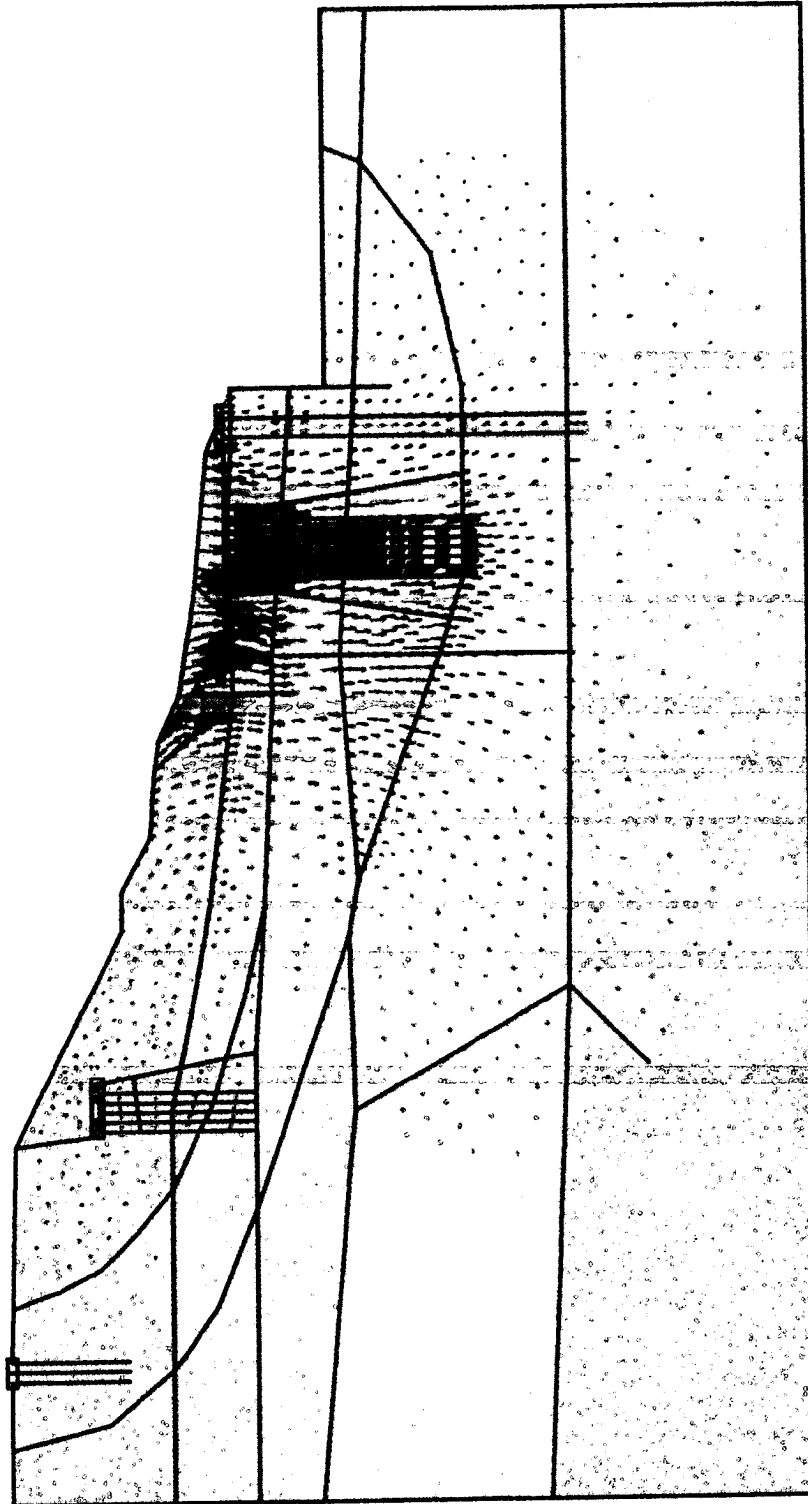


Fig. 5.61: Soil displacement vectors due to phase II

\*10<sup>-3</sup> ft

32.000
28.800
25.600
22.400
19.200
16.000
12.800
9.600
6.400
3.200
0.000



Fig. 5.62: Soil displacement contours due to phase 11

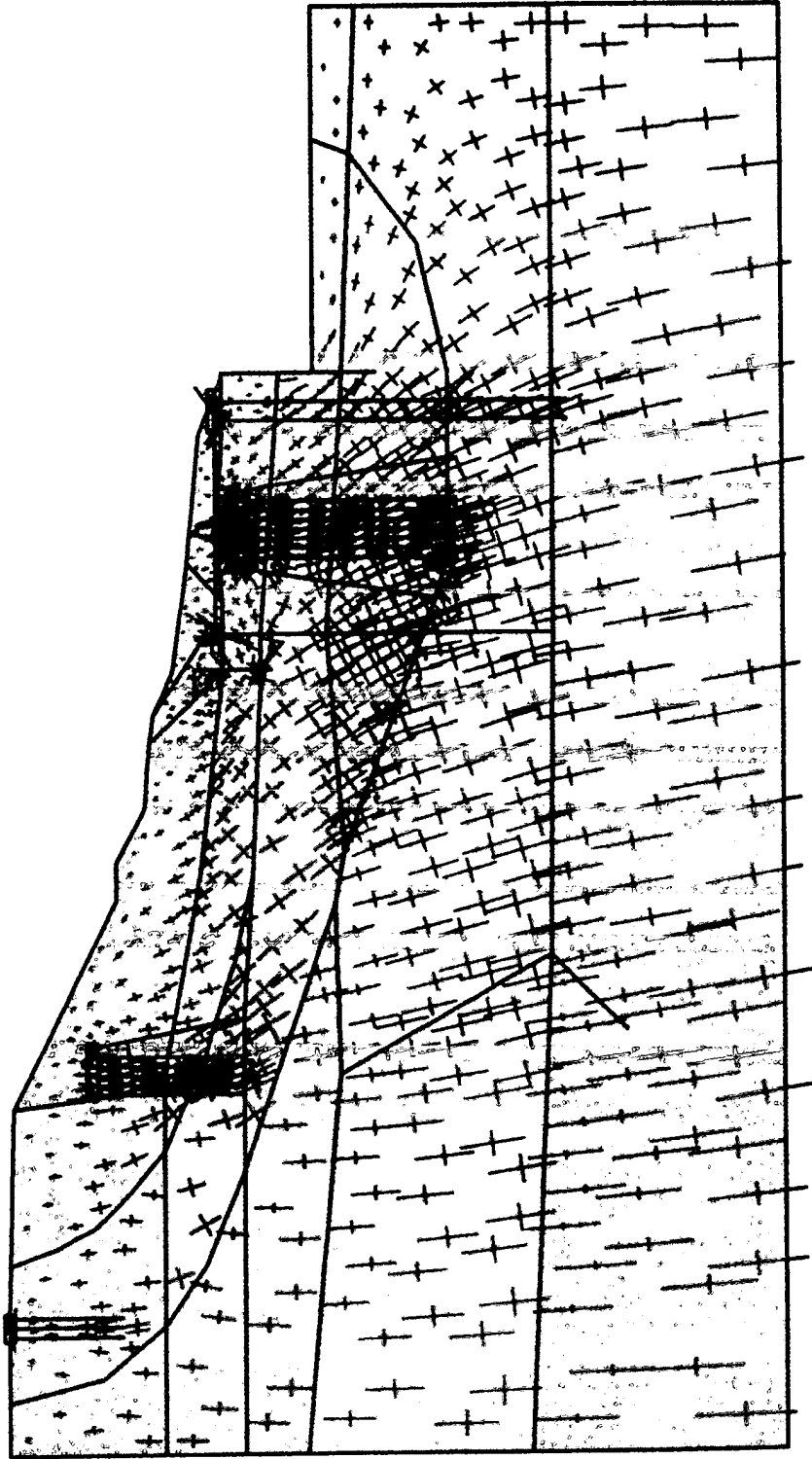


Fig. 5.63: Principal stress direction and magnitude due to phase 11

\*10<sup>3</sup> lb/ft<sup>2</sup>  
0.000  
-1.100  
-2.200  
-3.300  
-4.400  
-5.500  
-6.600  
-7.700  
-8.800  
-9.900  
-11.000

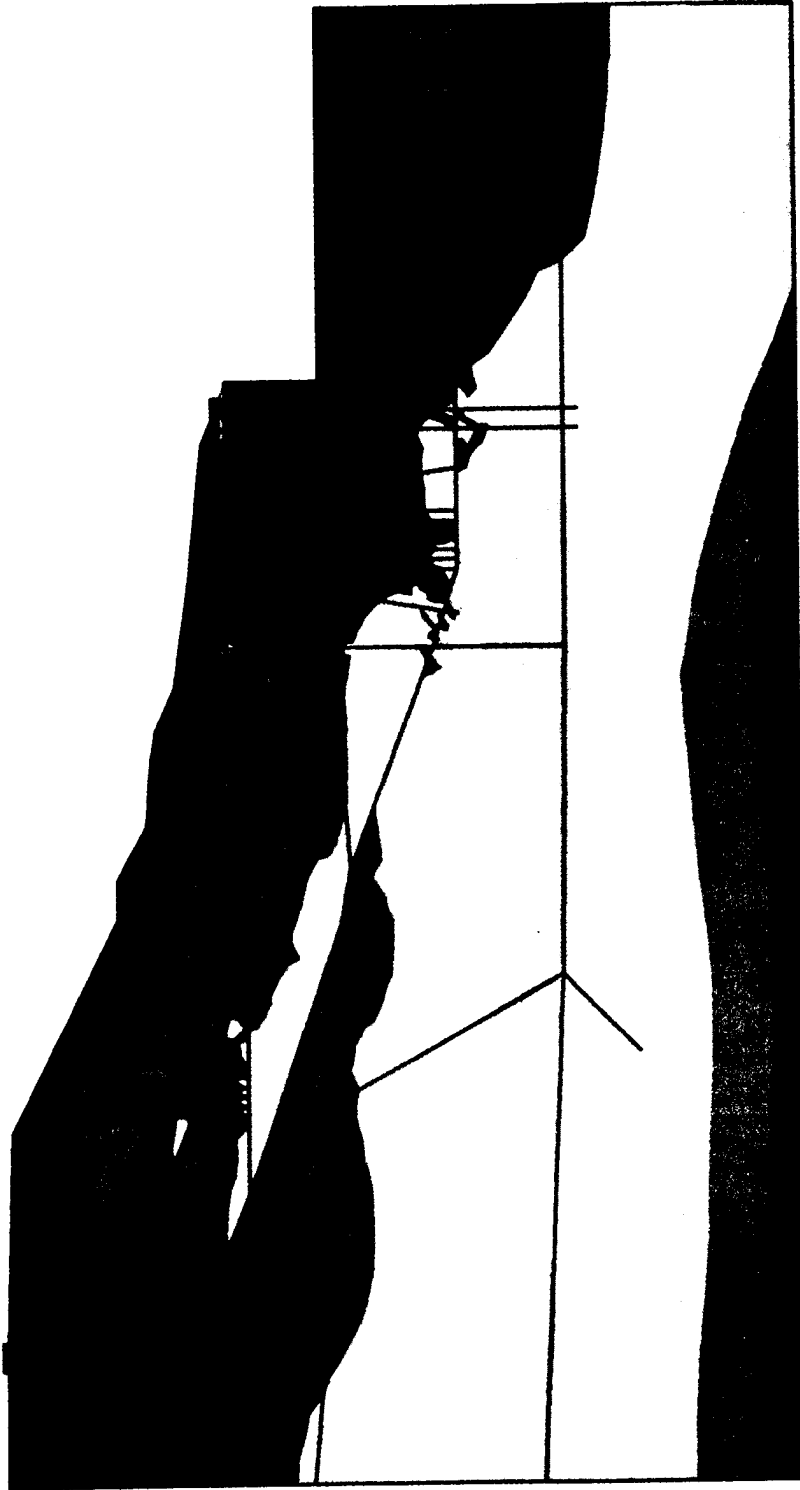


Fig. 5.64: Mean effective stress contours after phase 11

1.000  
0.900  
0.800  
0.700  
0.600  
0.500  
0.400  
0.300  
0.200  
0.100  
0.000



Fig. 5.65: Relative shear stress ratio contours after phase 11



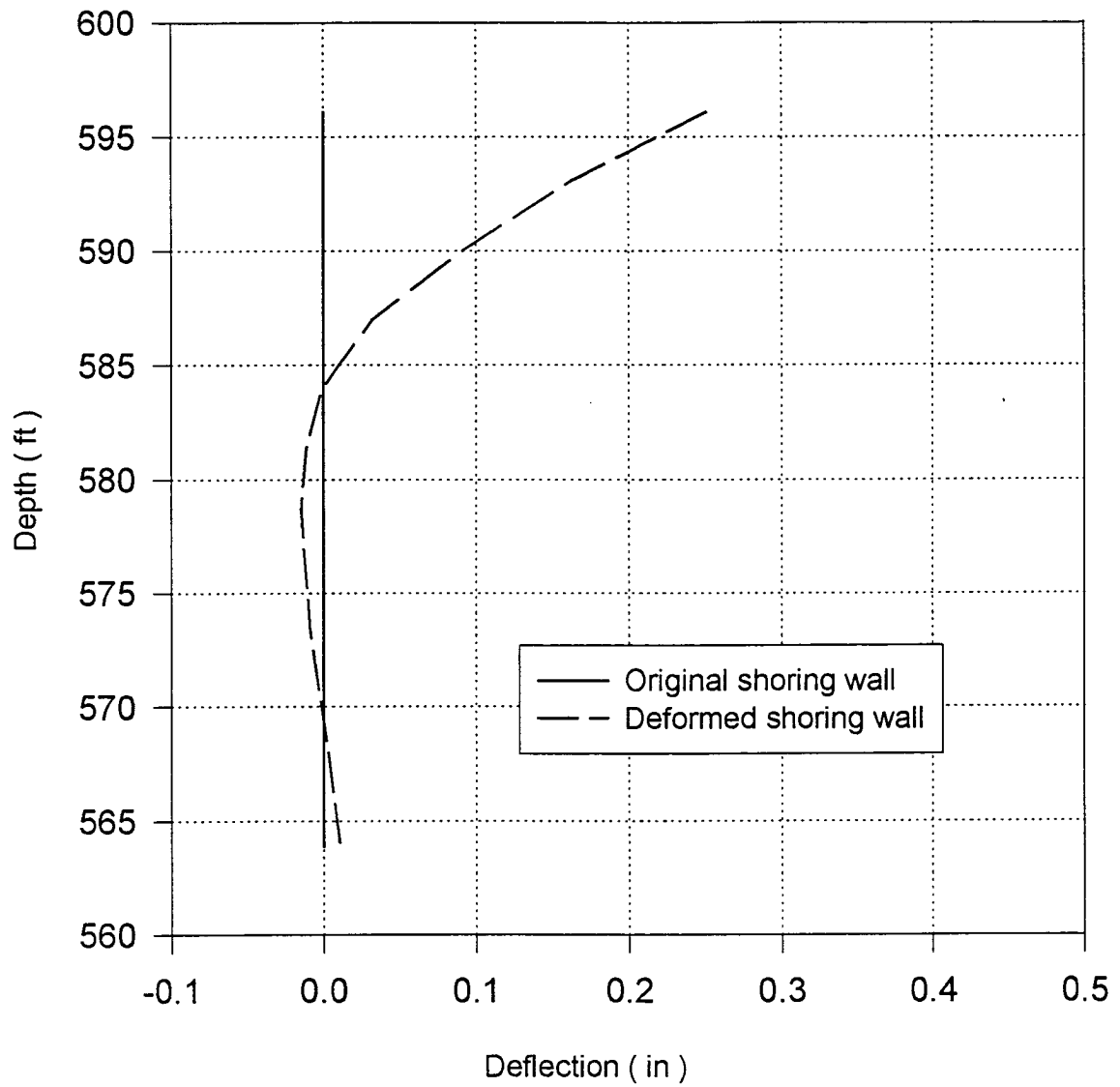


Fig. 5.66: Horizontal deflection of temporary shoring wall due to phase 6

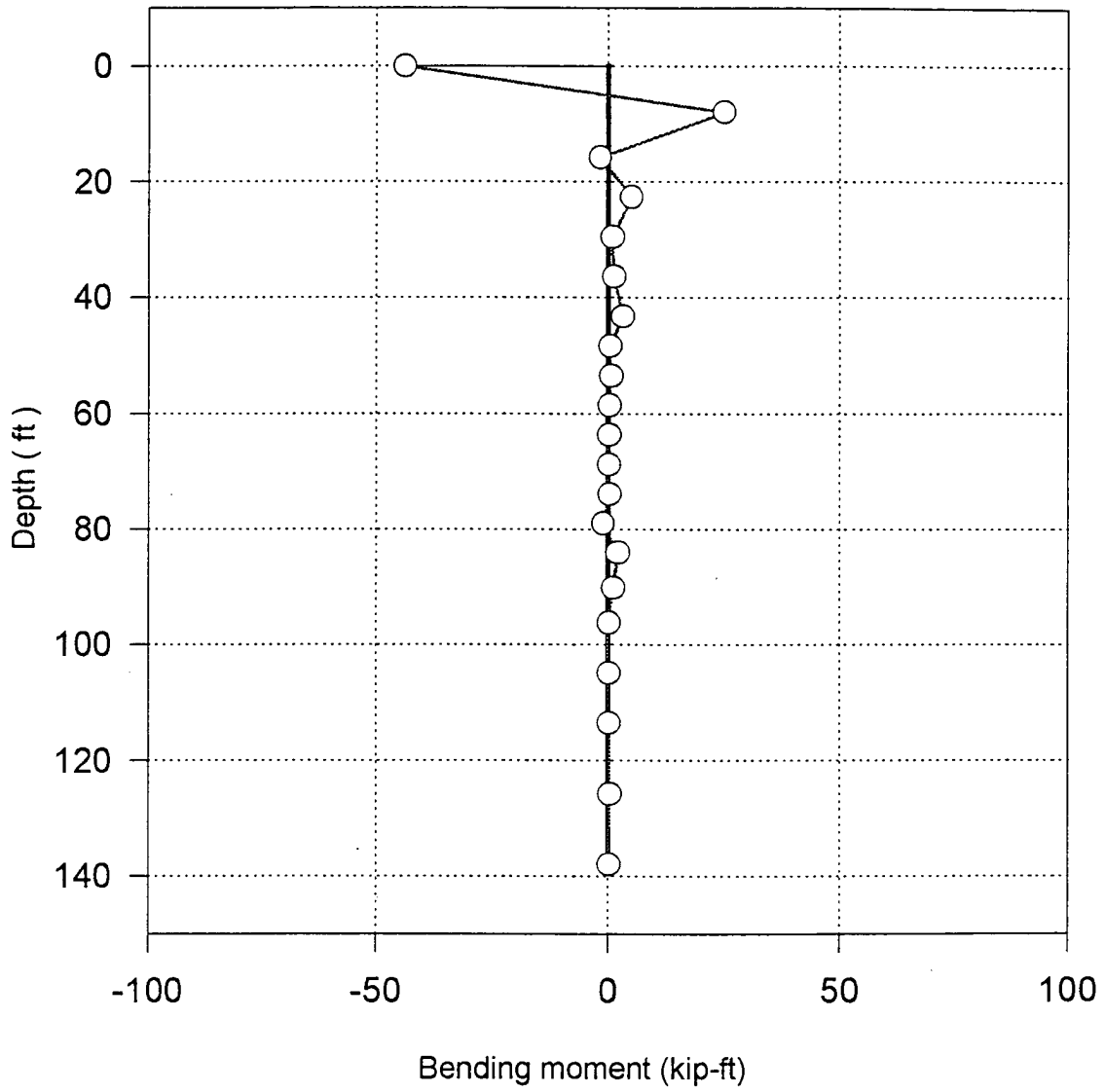


Fig. 5.67: Bending moment along the depth of driven piles due to anchor tension (phase 10)

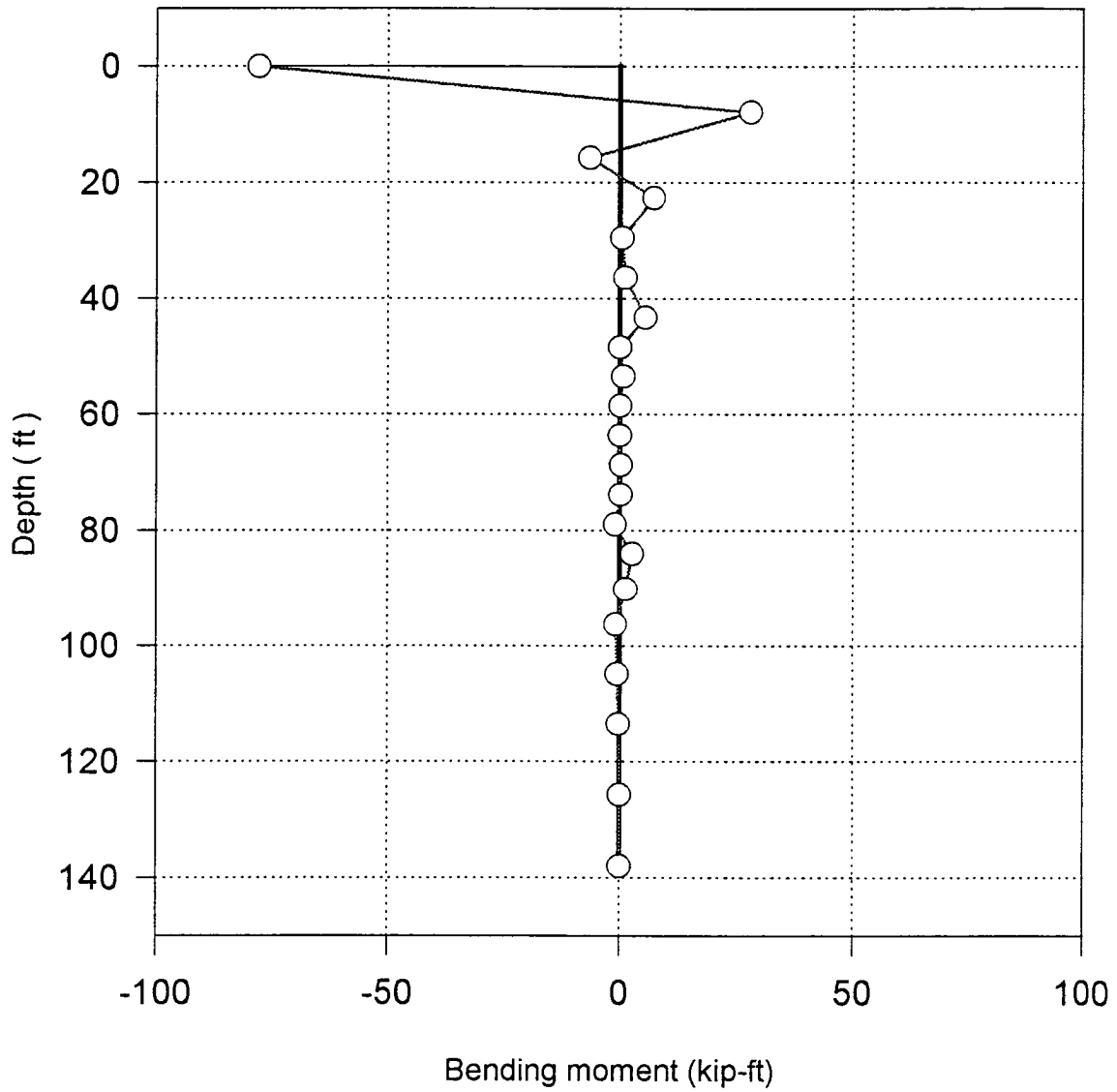


Fig. 5.68: Bending moment along the depth of driven piles due to anchor tension and backfill (phase 11)

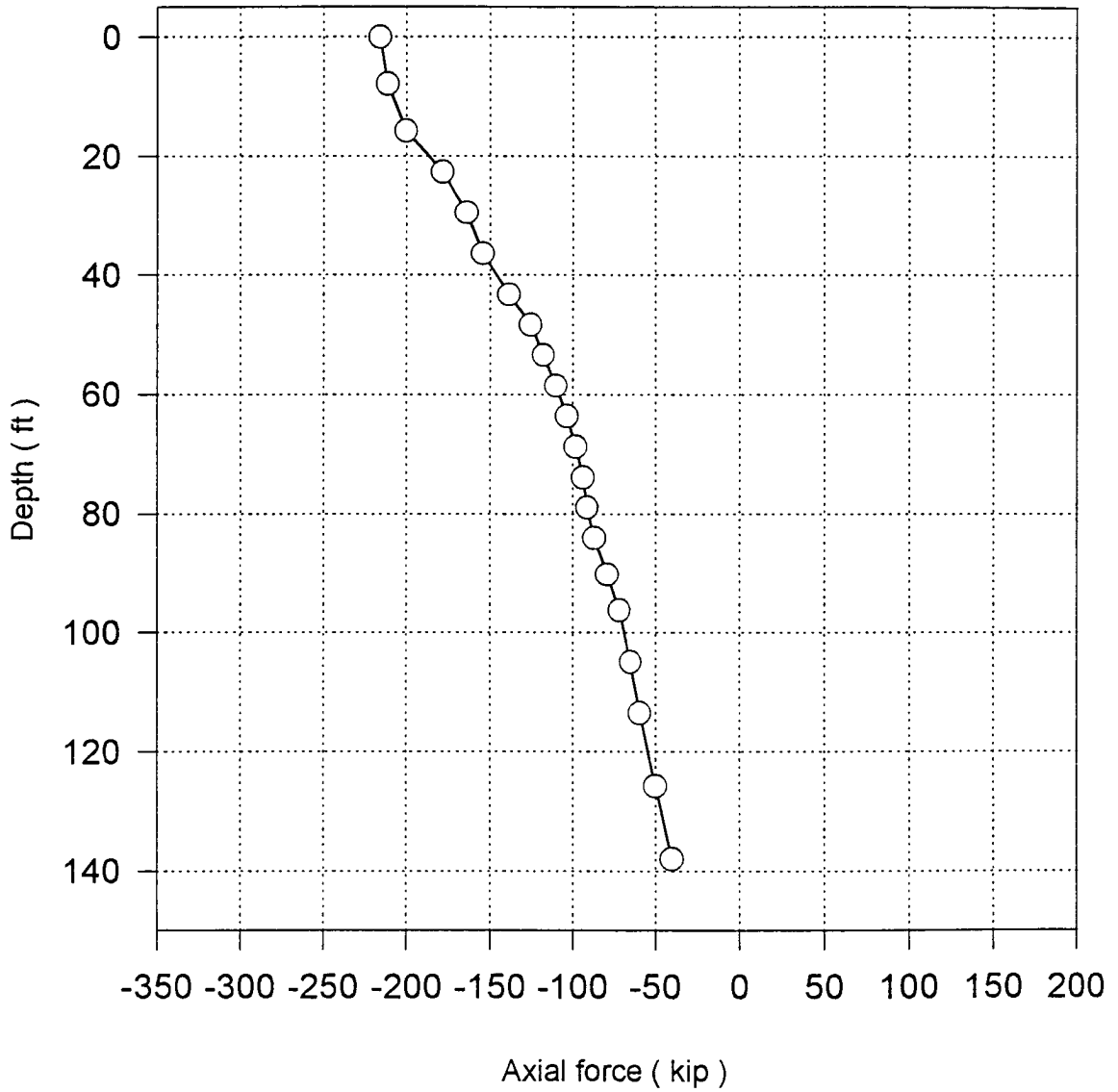


Fig. 5.69: Axial force along the depth of driven piles due to anchor tension (phase 10)

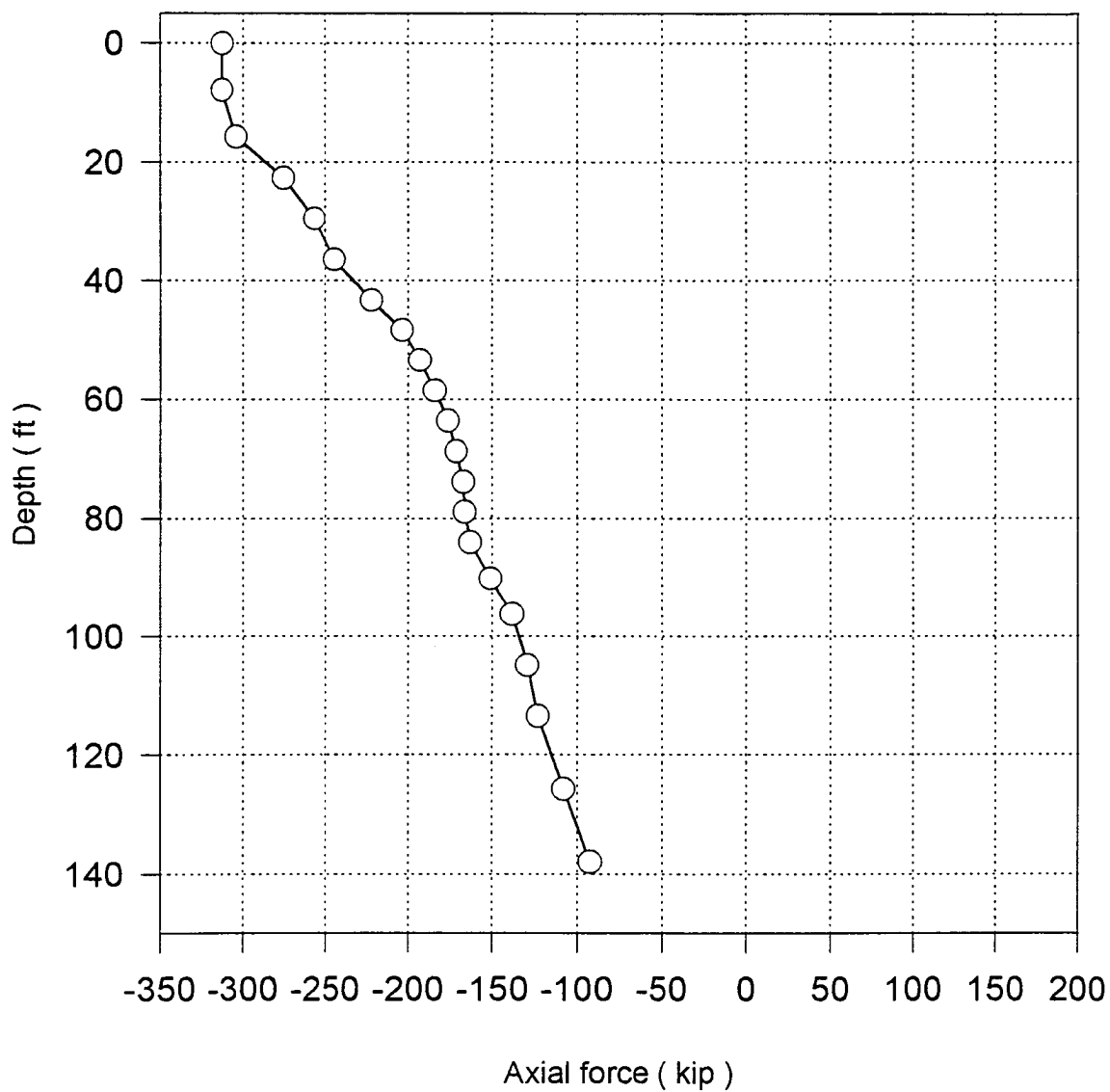


Fig. 5.70: Axial force along the depth of driven piles due to anchor tension and backfill (phase 11)

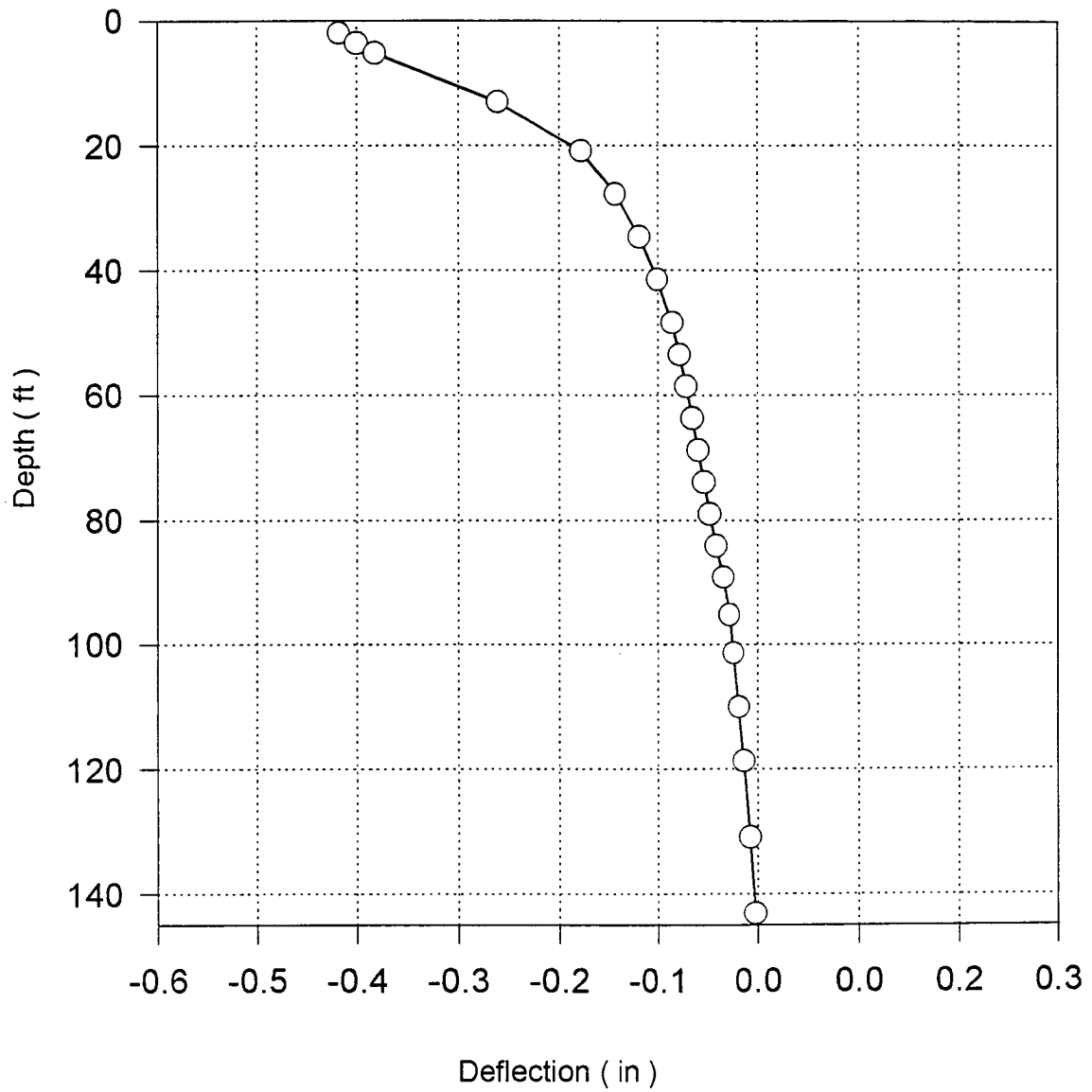


Fig. 5.71: Deflection of driven piles due to anchor tension (phase 10)

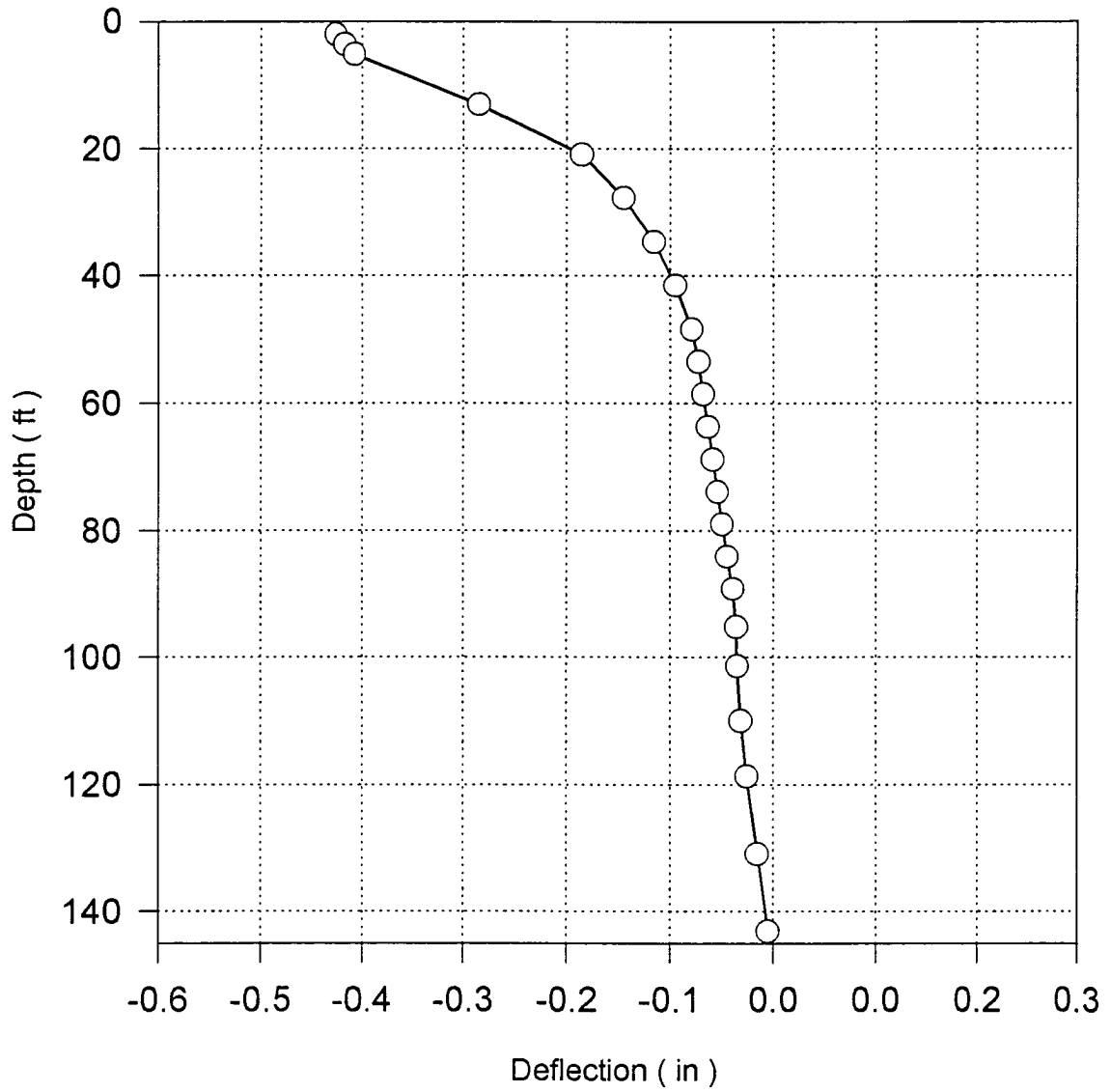


Fig. 5.72: Deflection of driven piles due to tension and backfill (phase 11)

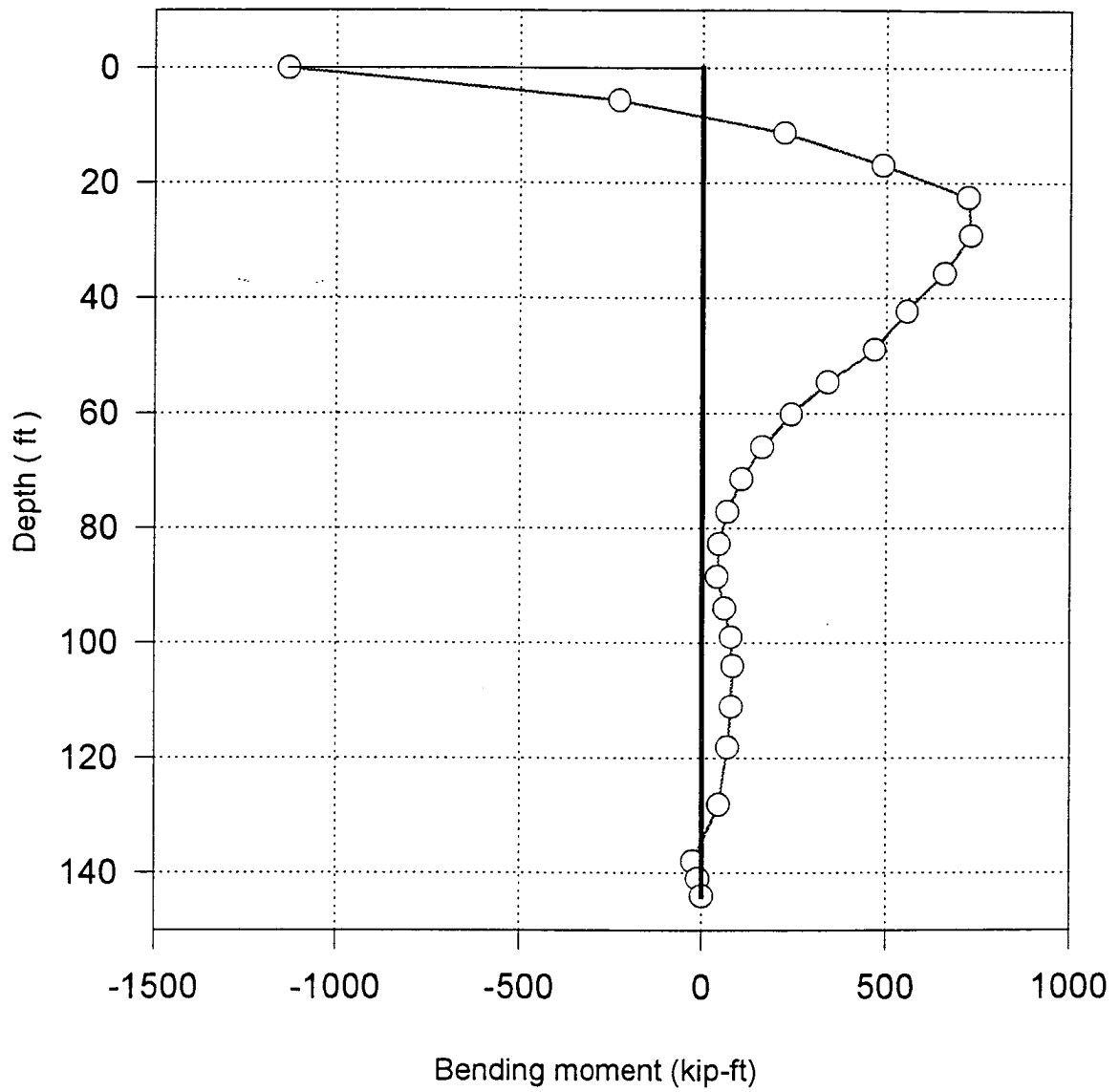


Fig. 5.73: Bending moment along the shaft length for the drilled shaft #9 due to anchor tension (phase 10)



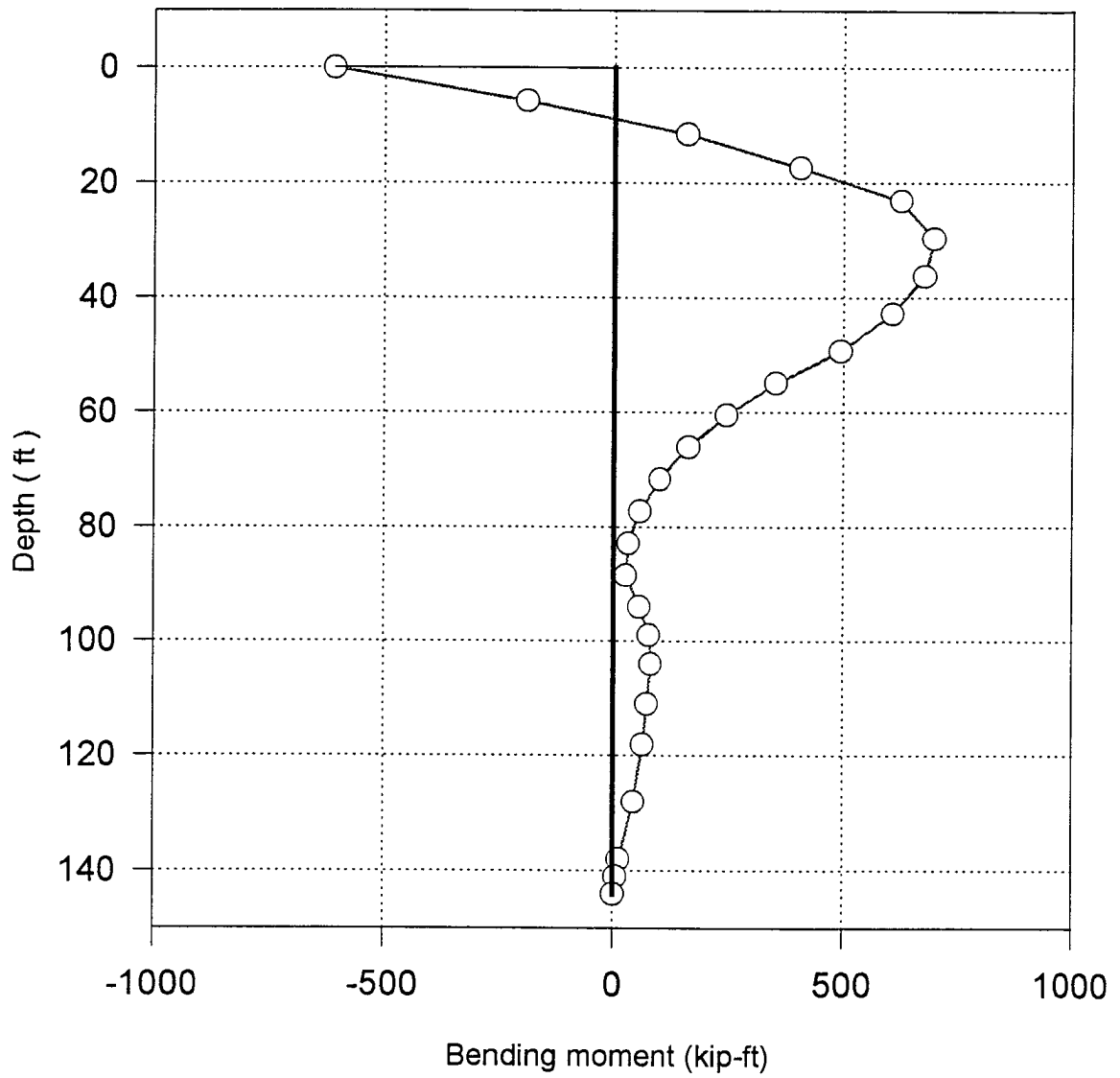


Fig. 5.74: Bending moment along the shaft length for the drilled shaft #10 due to anchor tension (phase 10)

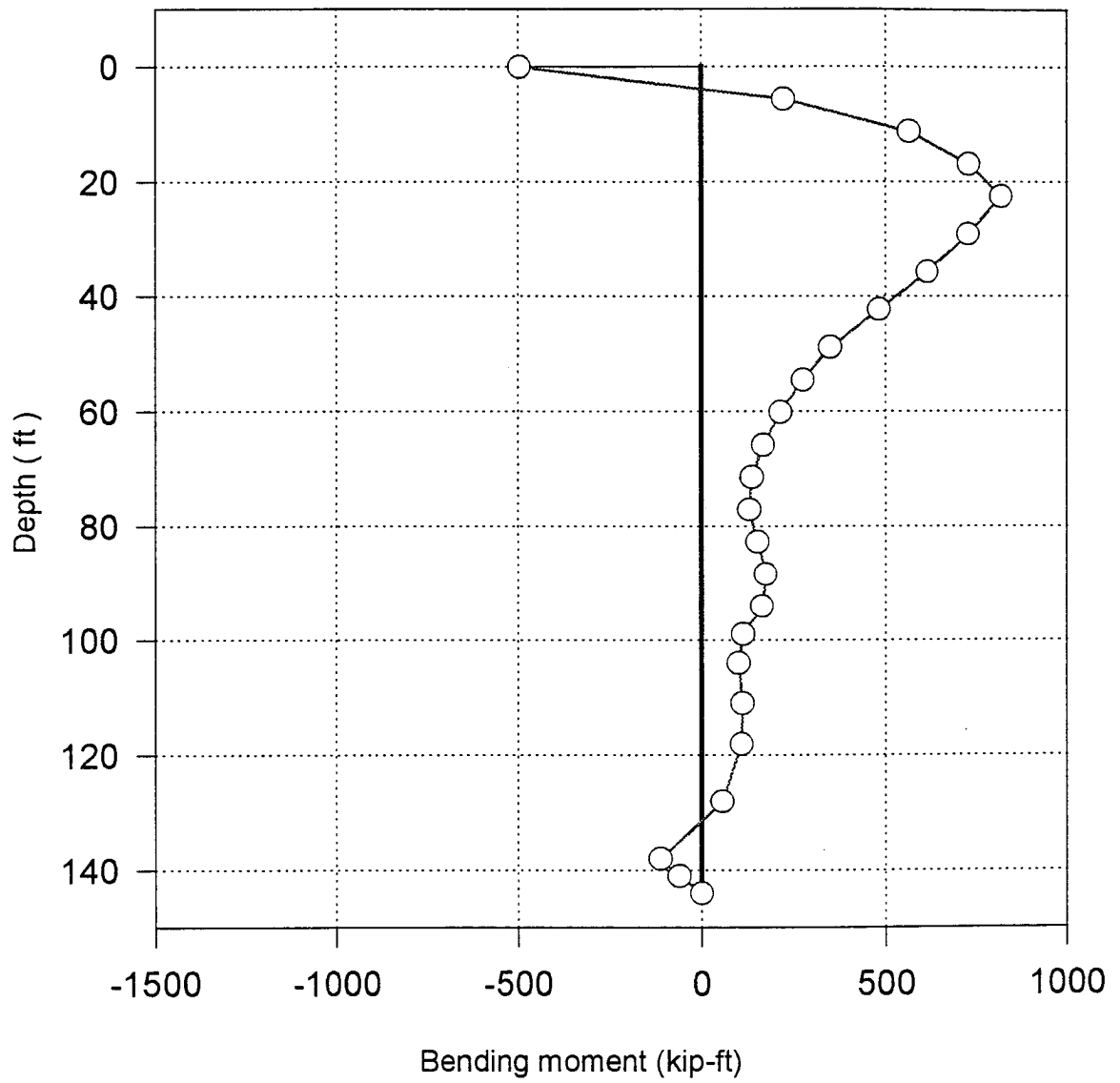


Fig. 5.75: Bending moment along the shaft length for the drilled shaft #9 due to anchor tension and backfill (phase 11)

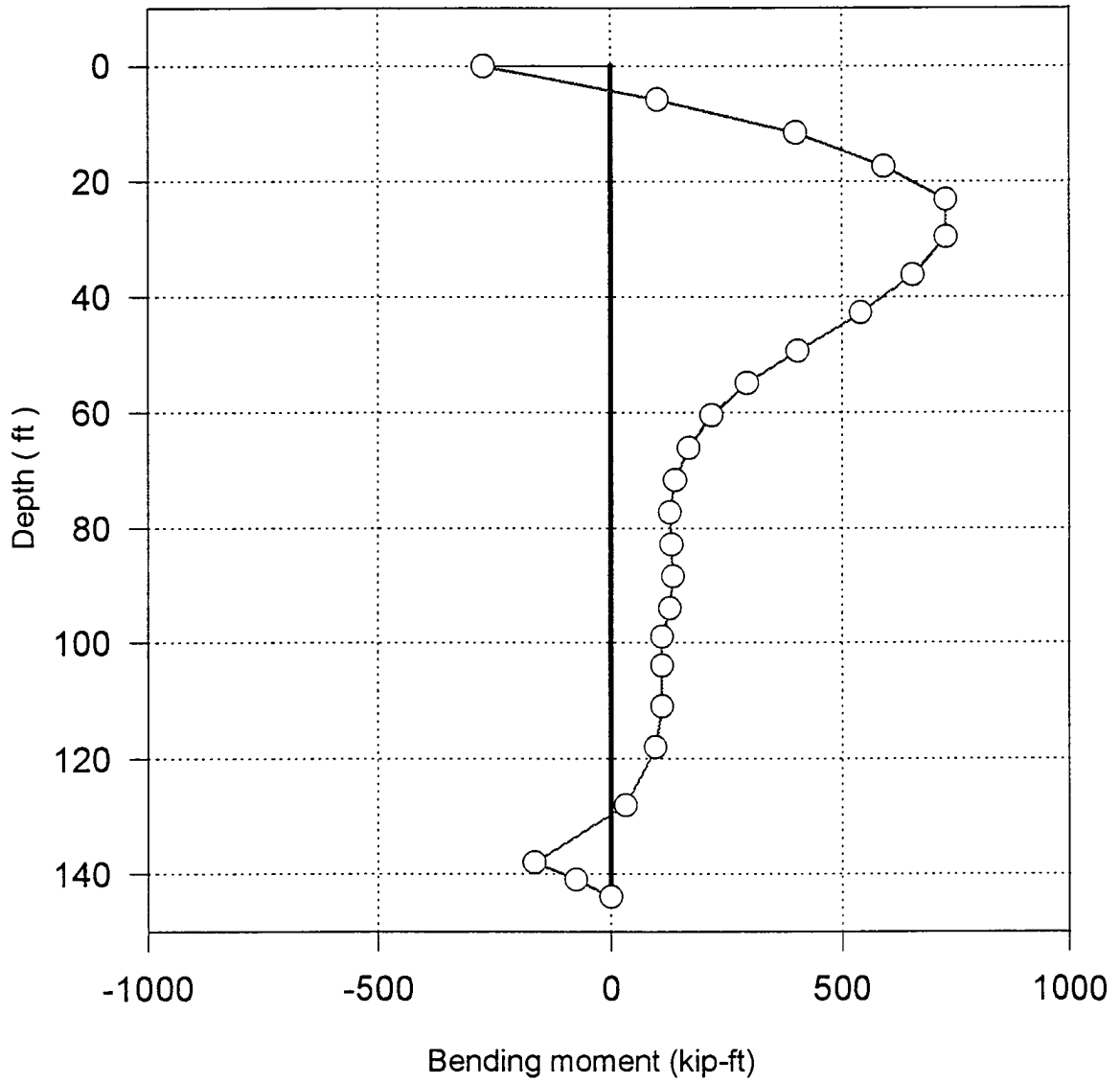


Fig. 5.76: Bending moment along the shaft length for the drilled shaft #10 due to anchor tension and backfill (phase 11)

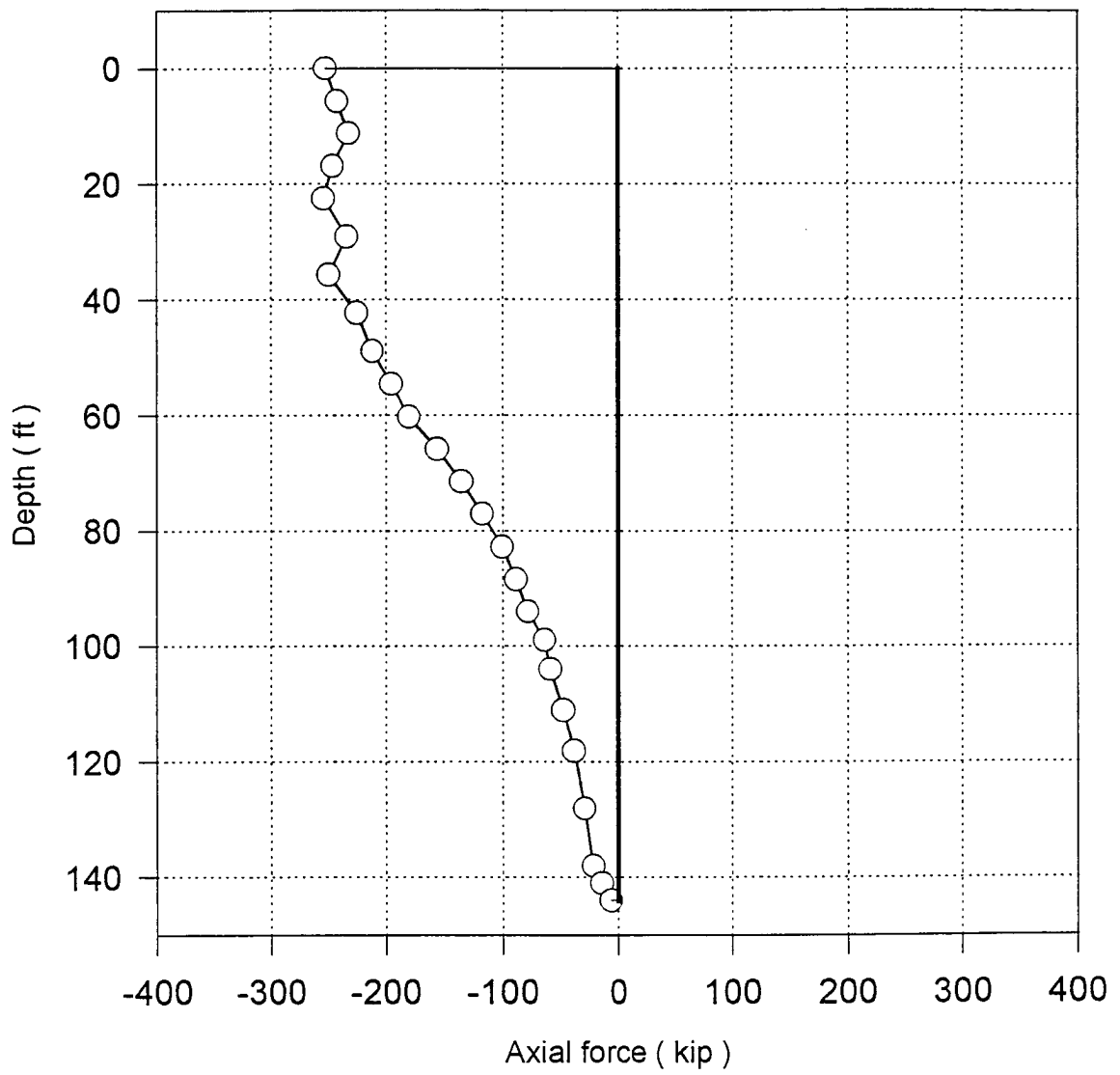


Fig. 5.77: Axial force along the shaft length for the drilled shaft #9 due to anchor tension ( phase 10)

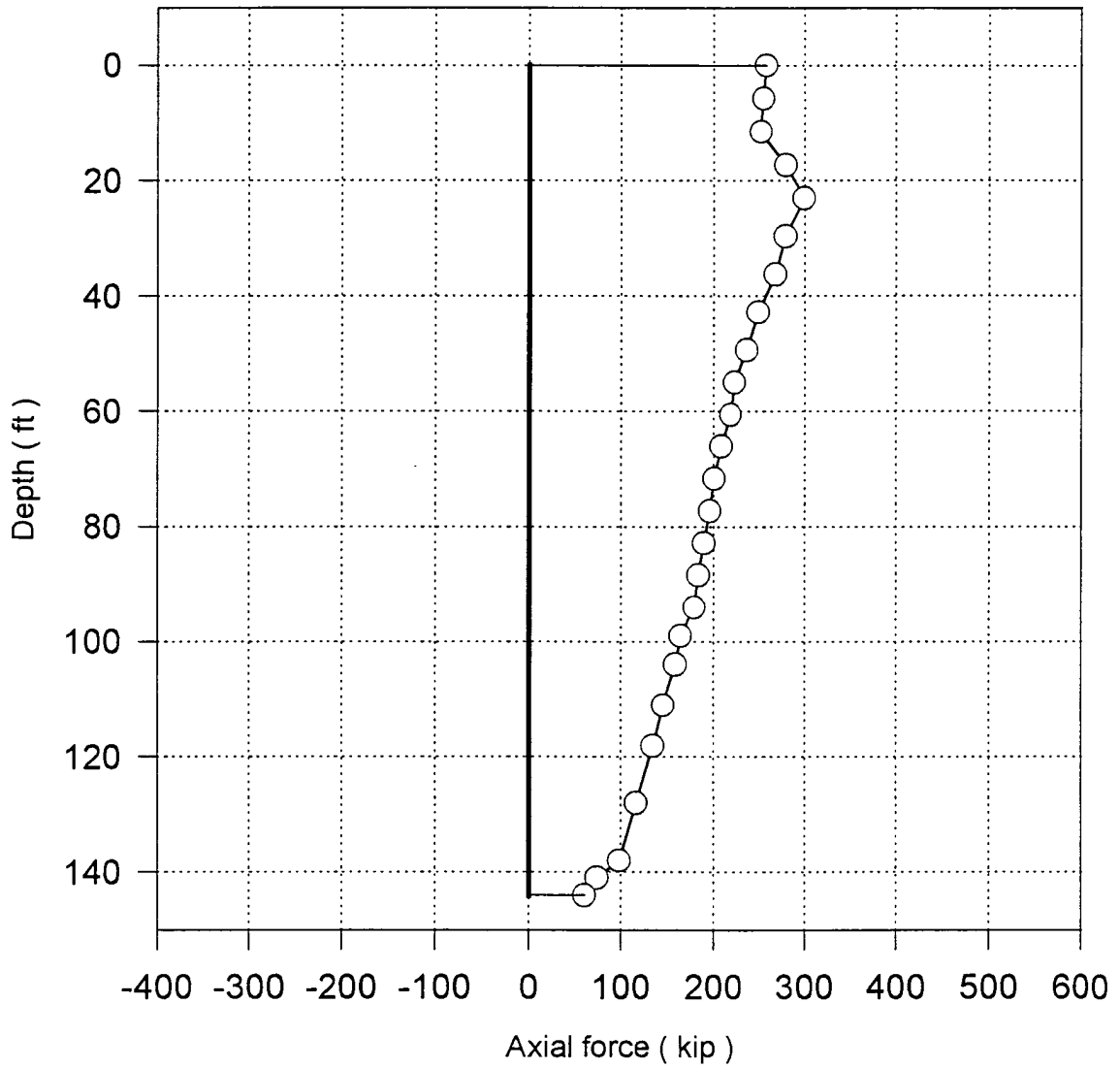


Fig. 5.78: Axial force along the shaft length for the drilled shaft #10 due to anchor tension ( phase 10)

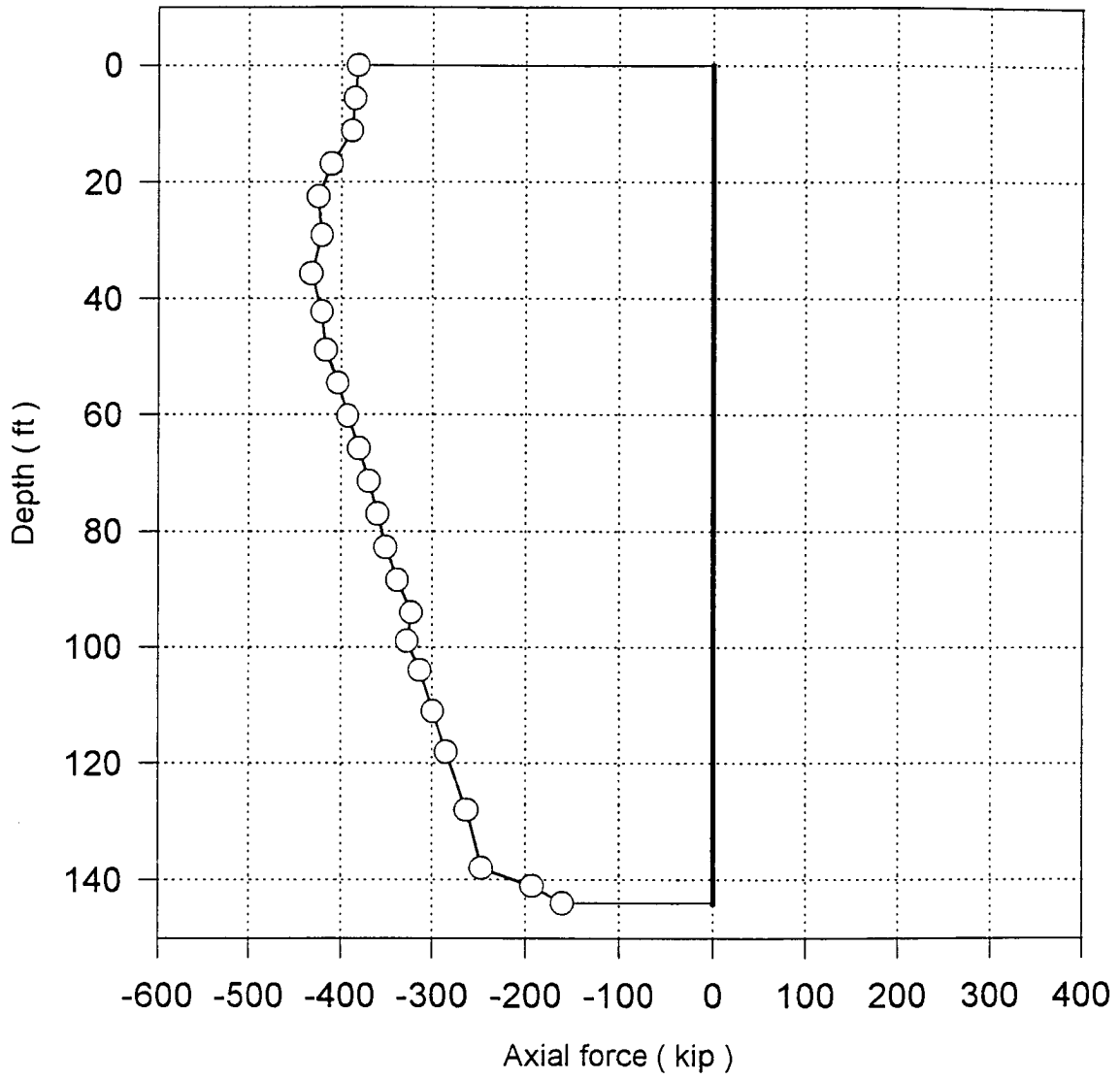


Fig. 5.79: Axial force along the shaft length for the drilled shaft #9 due to anchor tension and backfill ( phase 11)

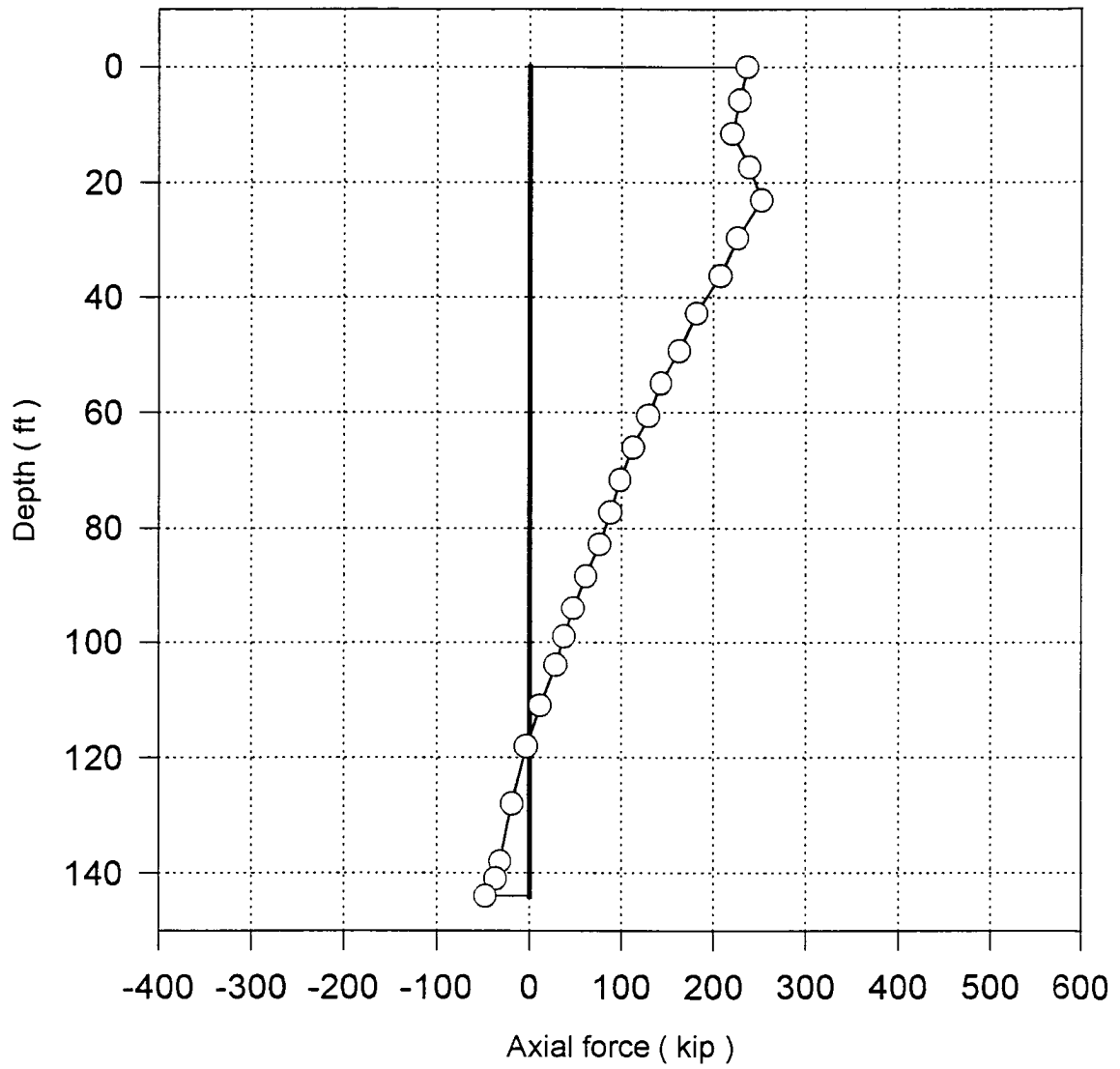


Fig. 5.80: Axial force along the shaft length for the drilled shaft #10 due to anchor tension and backfill ( phase 11)

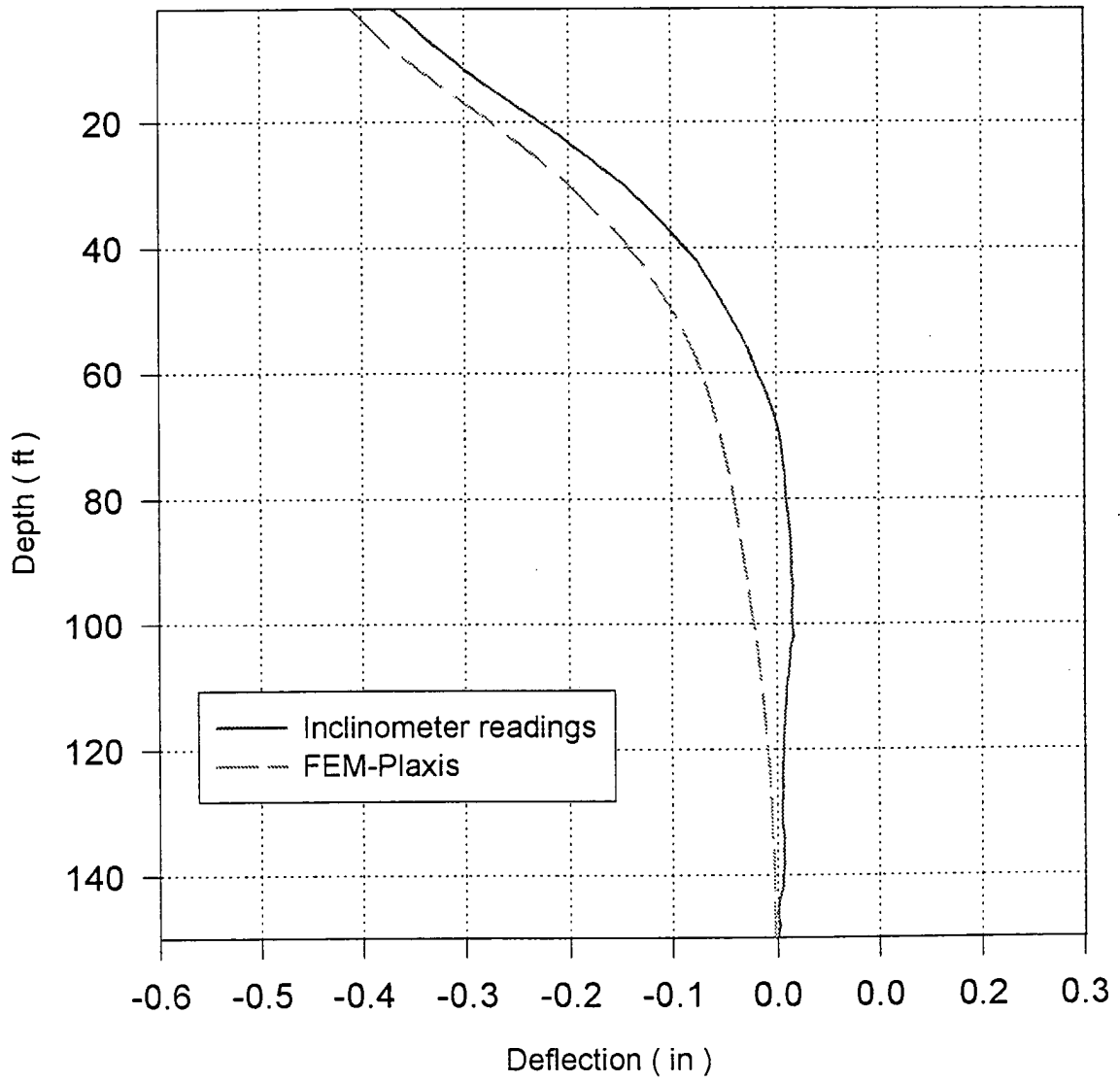


Fig. 5.81: Deflection of drilled shaft #9 due to anchor tension (phase 10)



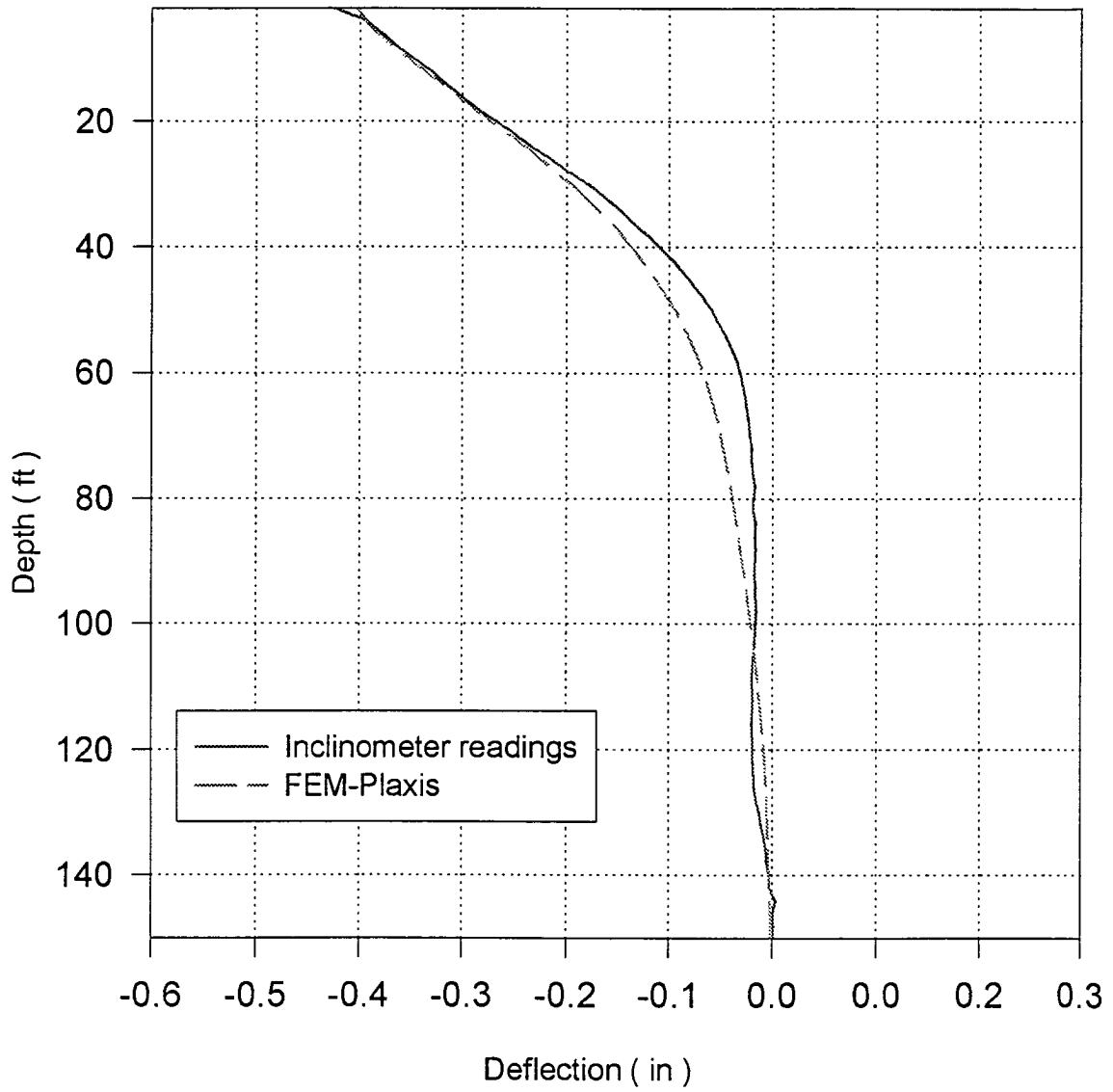


Fig. 5.82: Deflection of drilled shaft #10 due to anchor tension (phase 10)

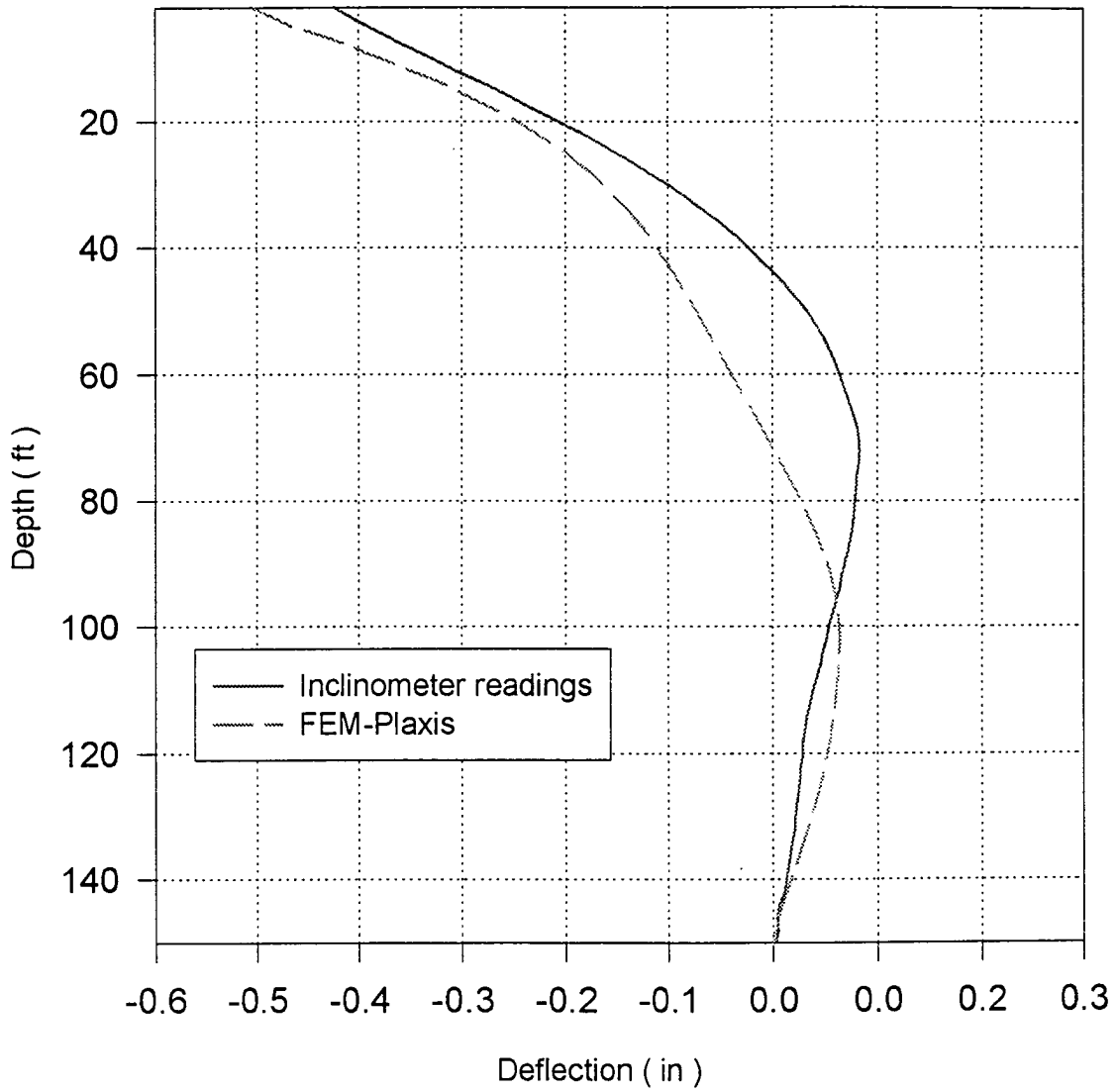


Fig. 5.83: Deflection of drilled shaft #9 due to anchor tension and backfill (phase 11)

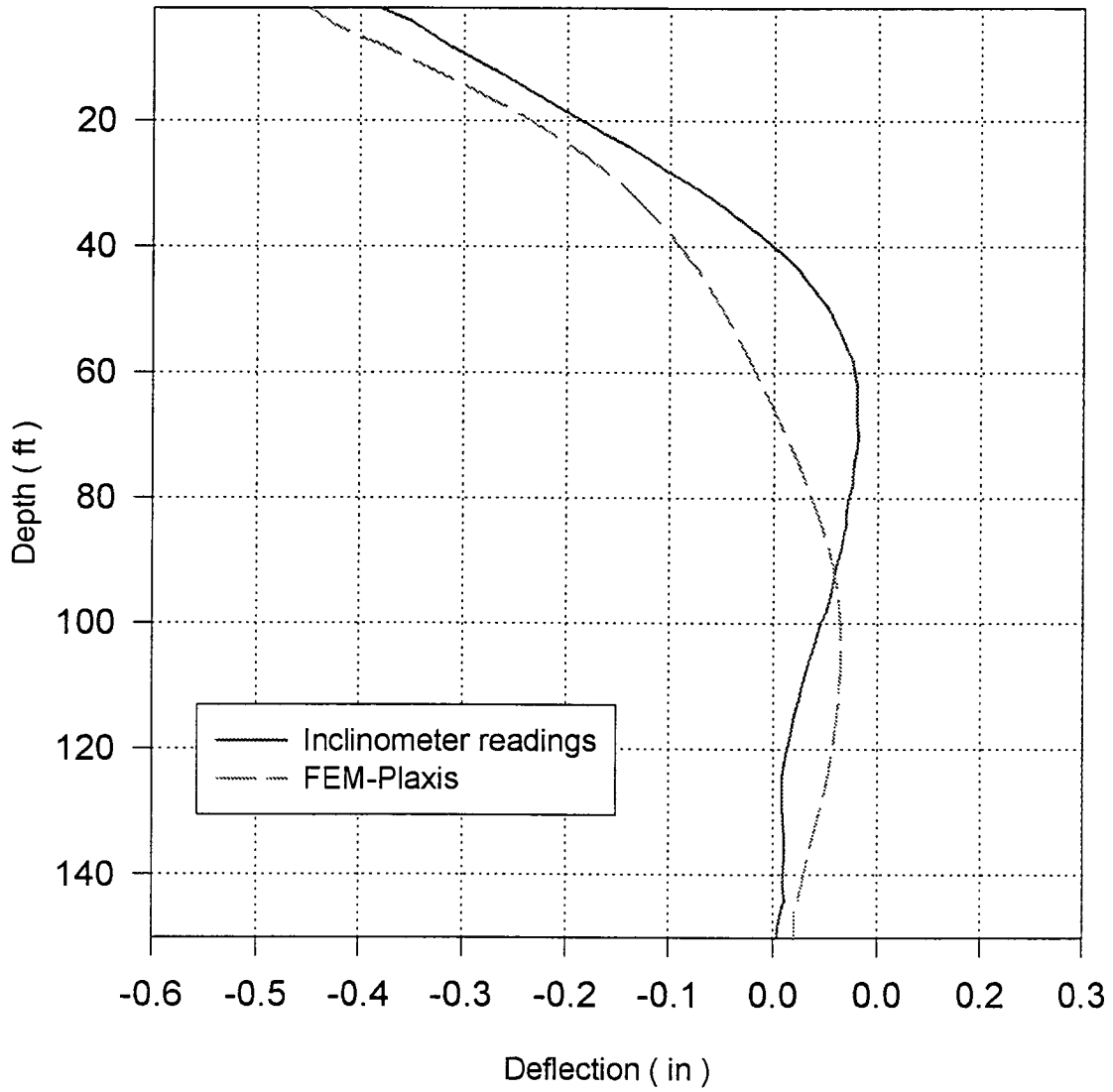


Fig. 5.84: Deflection of drilled shaft #10 due to anchor tension and backfill (phase 11)

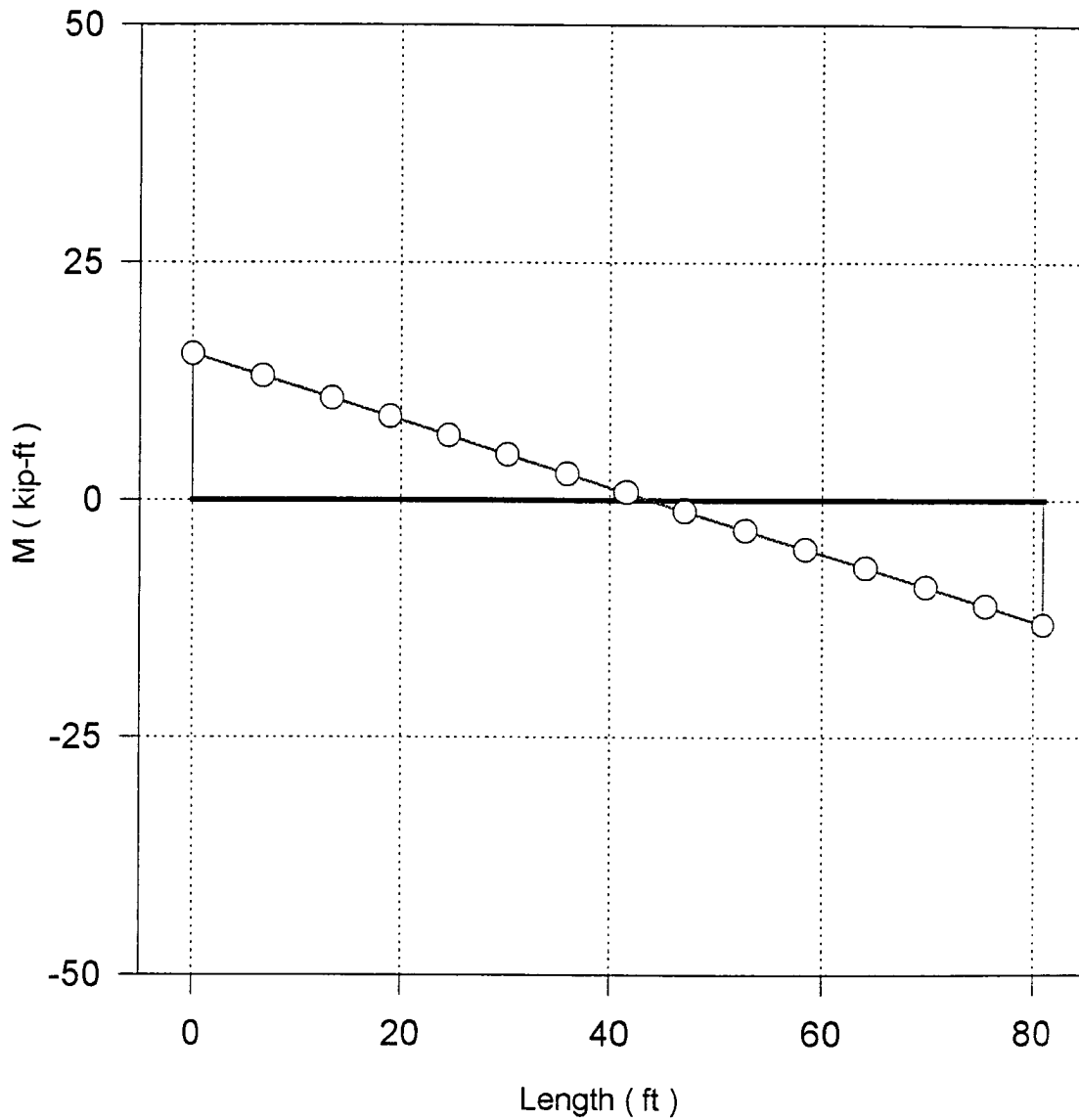


Fig. 5.85: Bending moment along the beam axis for the tie-beam due to anchor tension (phase 10)

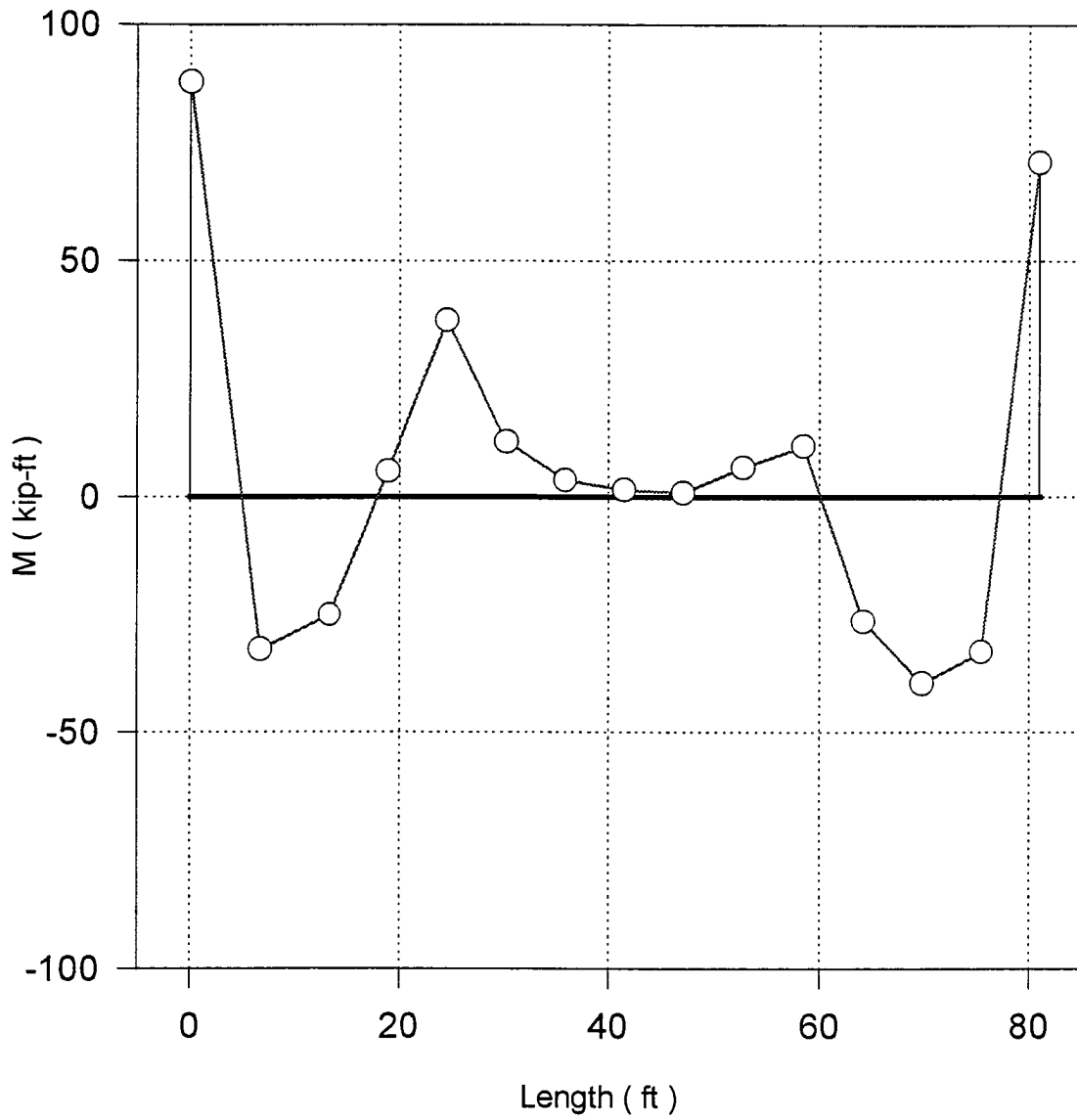


Fig. 5.86: Bending moment along the beam axis for the tie-beam due to anchor tension and backfill (phase 11)

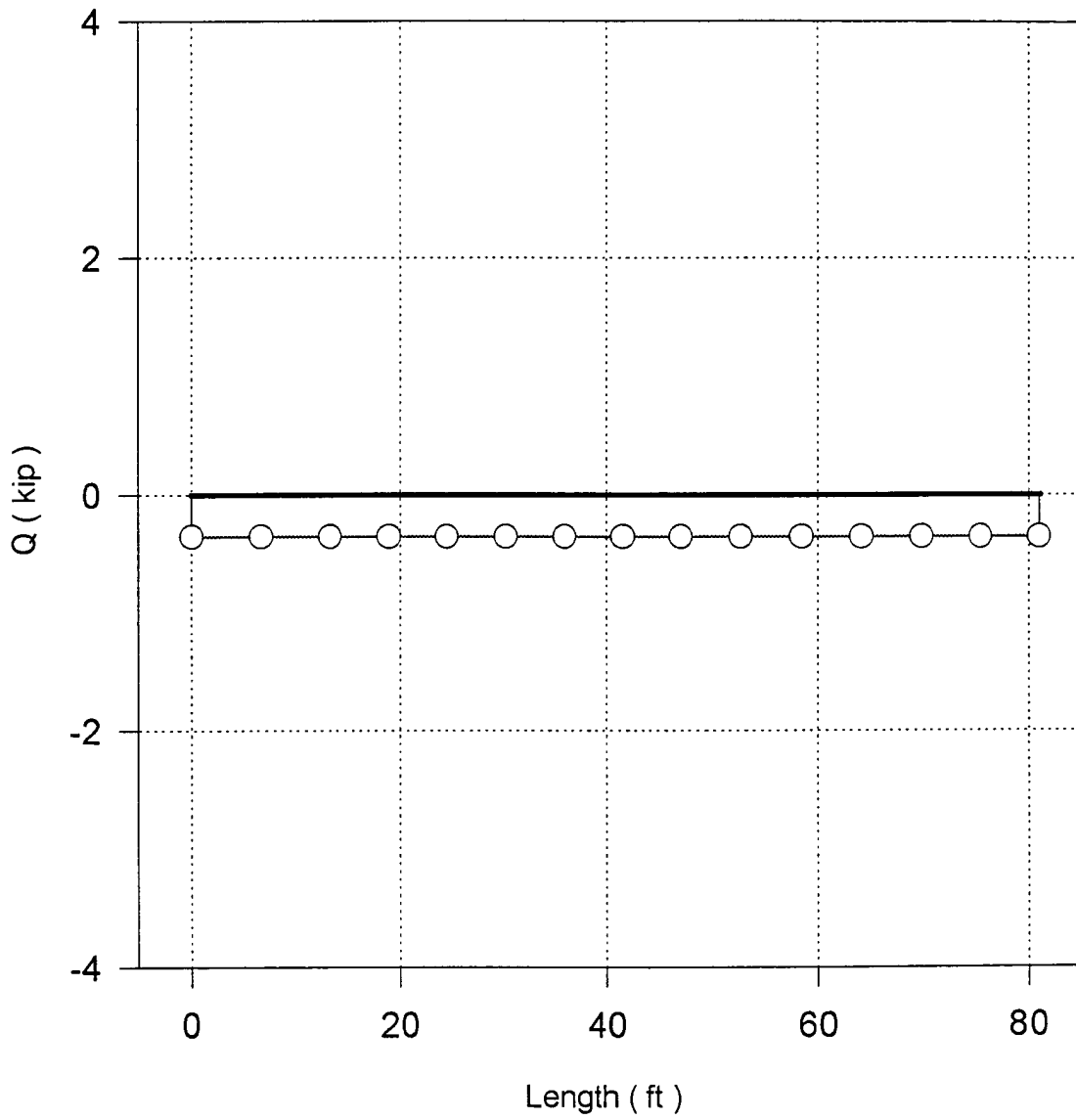


Fig. 5.87: Shear force distribution for the tie-beam due to anchor tension (phase 10)

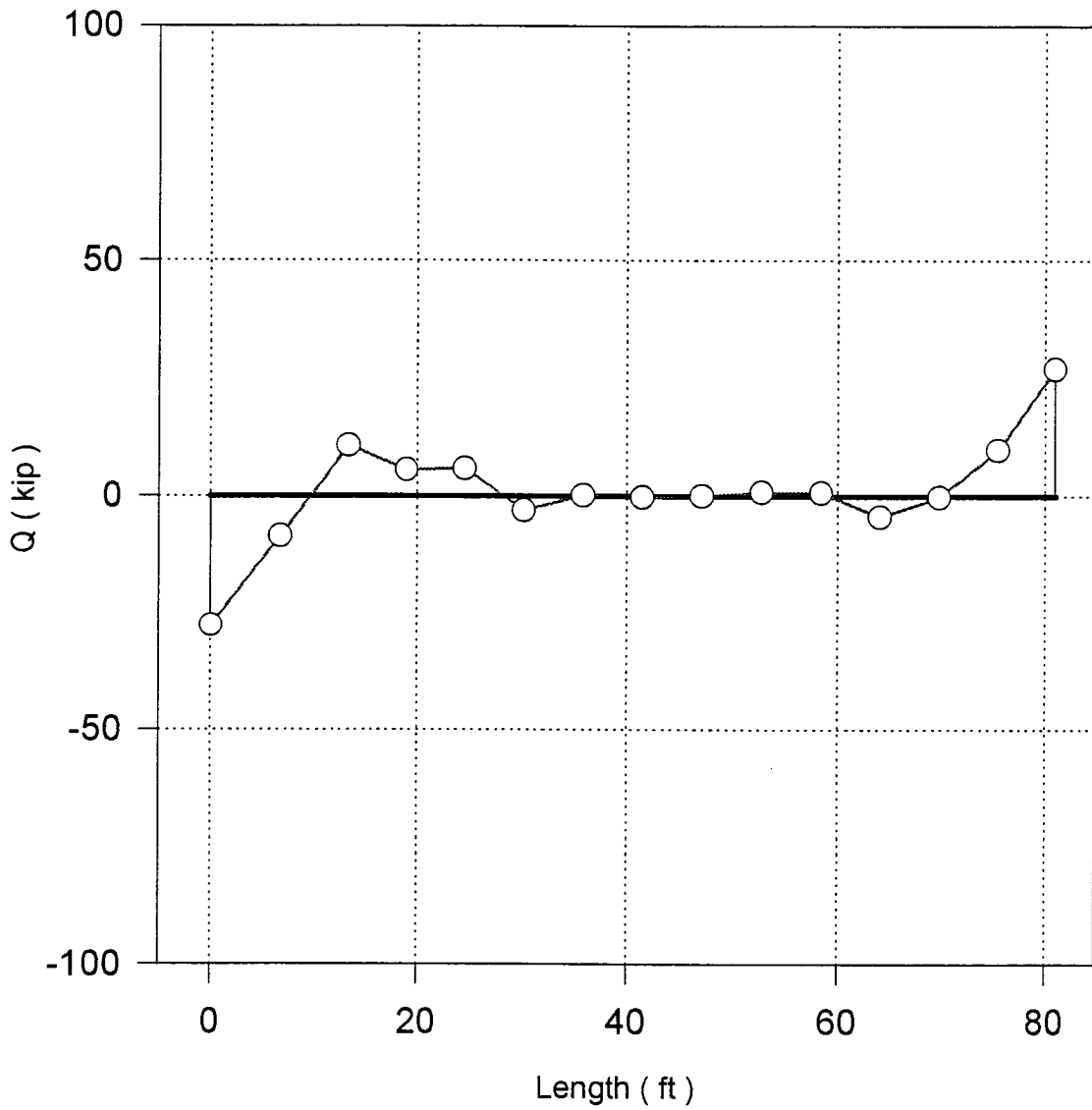


Fig. 5.88: Shear force distribution for the tie-beam due to anchor tension and backfill (phase 11)

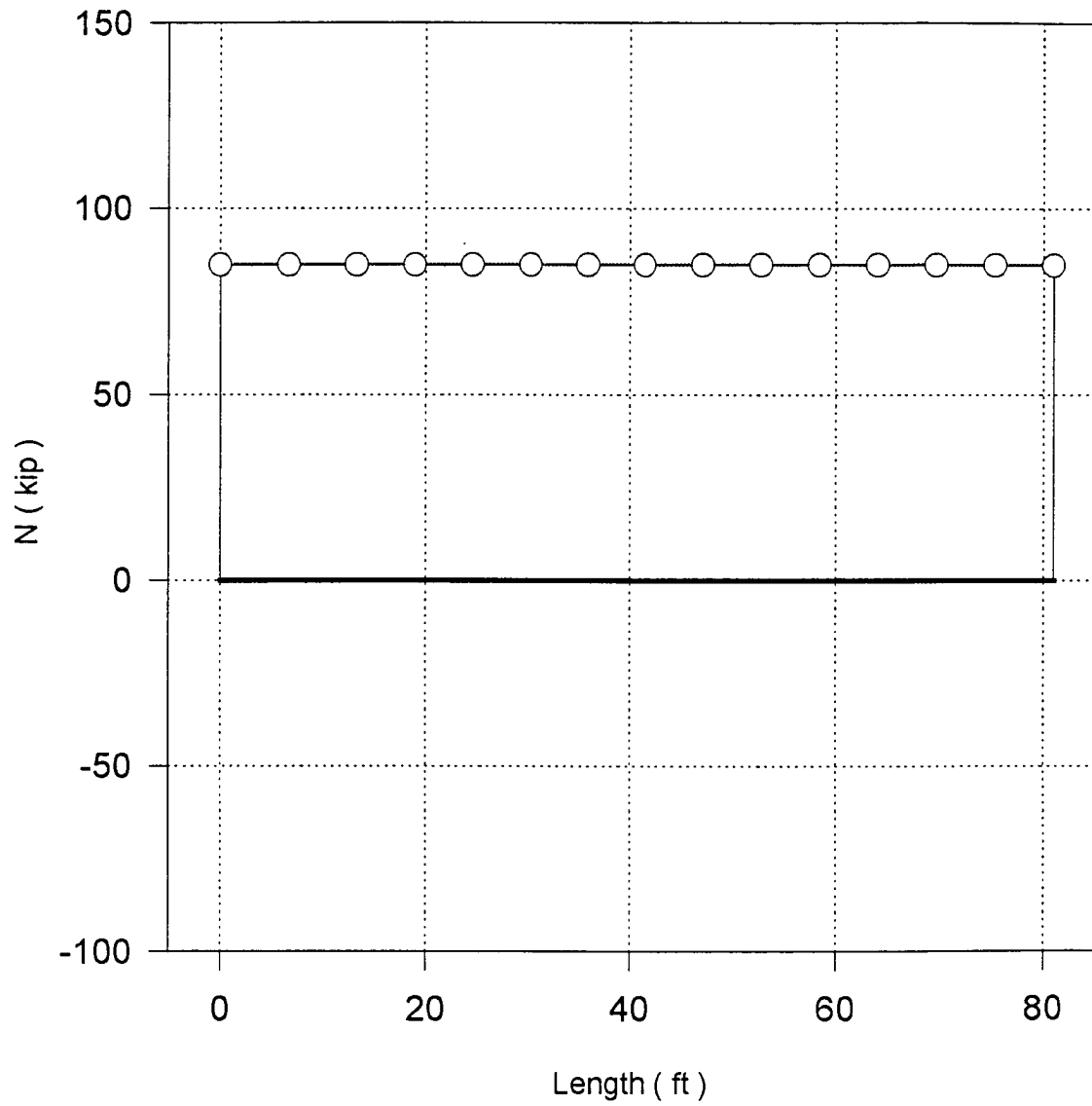


Fig. 5.89: Axial force distribution for the tie-beam due to anchor tension (phase 10)



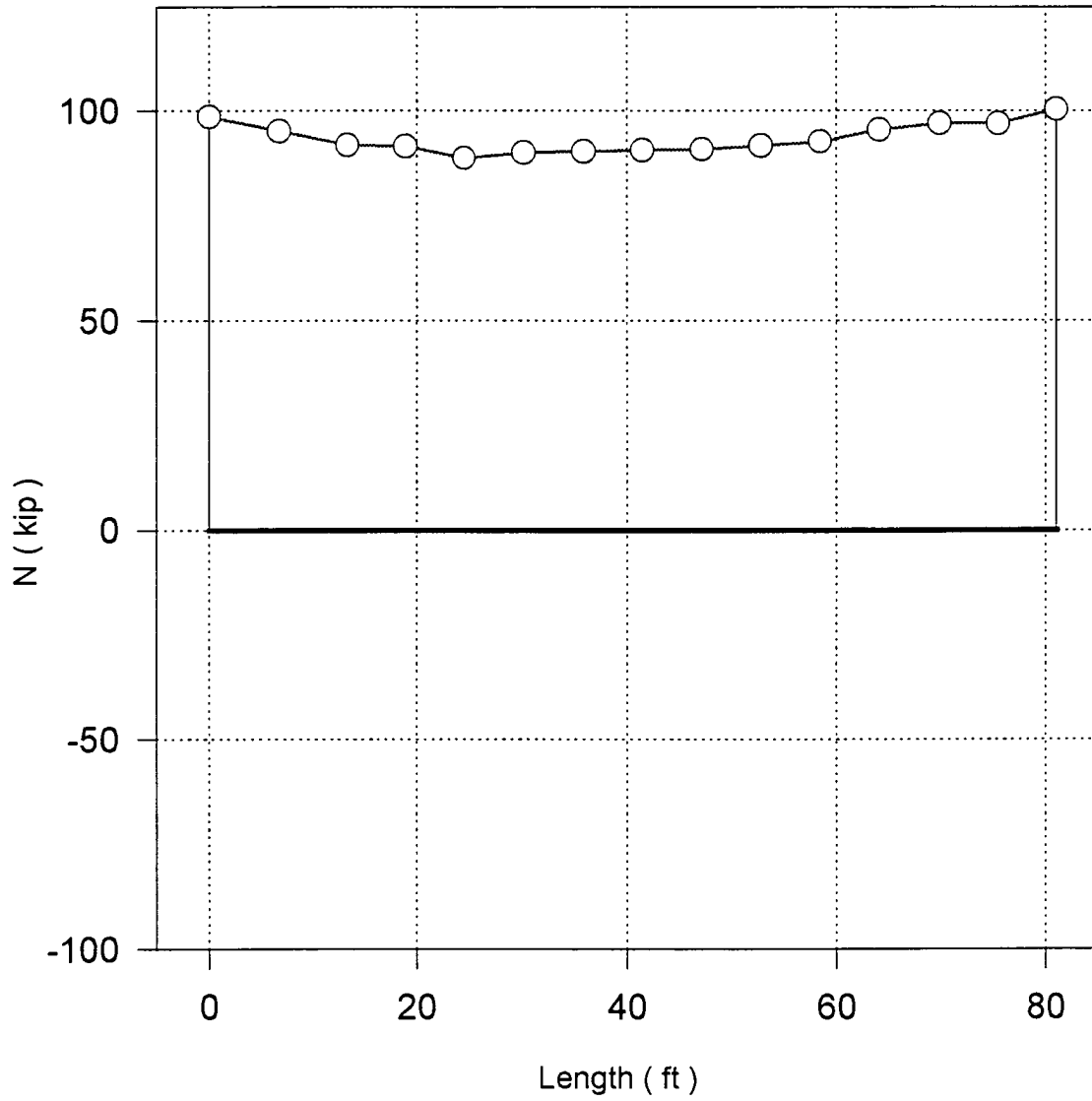


Fig. 5.90: Axial force distribution for the tie-beam due to anchor tension and backfill (phase 11)

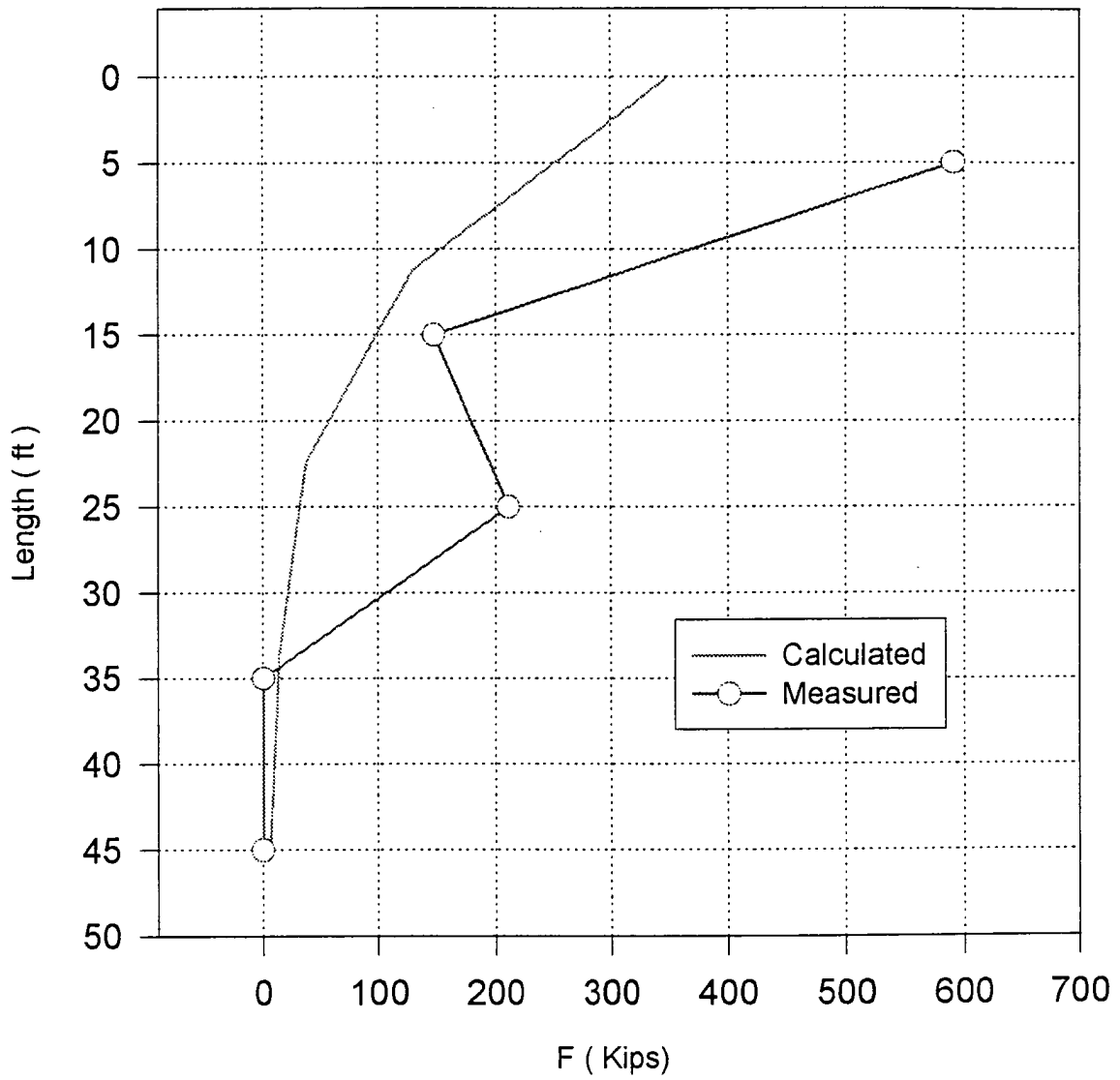


Fig. 5.91: Axial force distribution along the bond length of ground anchor after tension (phase 10)

## CHAPTER VI

### BACK CALCULATION OF P-Y CURVES USING INCLINOMETER DATA

#### VI.1 INTRODUCTION

The load-displacement relationship for an unconstrained, laterally loaded drilled shaft is a highly nonlinear problem. The most common method of analysis for the laterally loaded drilled shafts is the p-y curve method. The p-y curves provide simple and reasonable approach to capture the essential aspects of soil-shaft interaction behavior, including the nonlinear soil resistance as well as variable soil and drilled shaft properties.

The existing p-y curves for design are largely based upon interpretation and empirical evaluation of relatively few, well-instrumented lateral load tests. Clearly, these analytical expressions include a considerable degree of empiricism. Furthermore, there could be inherent uncertainties in extending these empirical p-y criteria to sites of different soil conditions.

The use of existing p-y criteria is no guarantee of the accuracy of the analysis results. The reason is that these p-y criteria were derived only from a limited number of load tests on fully instrumented drilled shafts at various sites with different soil types: cohesionless soil, stiff clay and soft clay. The principle of soil mechanics was used to a large extent to generalize the equations of the p-y curves. However, some significant shortcomings of existing p-y curves still exist:

- 1) The nonlinearity of reinforced concrete shaft under bending (flexural) stresses was not accounted for in the original data deduction.
- 2) Generalization of p-y curves for soils other than those at the test sites results in the requirements of certain soil parameters, such as  $\epsilon_{50}$ , undrained shear strength  $S_u$ , and friction angle  $\phi$ , among others. Sometimes it may be difficult to determine these parameters accurately.
- 3) It has been observed that the construction details can affect the p-y curves, in addition to soil properties, dimension and stiffness of the drilled shafts. In addition, time duration of hole opening before casting concrete, the use of slurry in drilling, and the method of drilling will also affect the in-situ soil stress and soil properties to a large extent, and thus affecting the p-y curves. These construction effects on the p-y curves can not be accounted for by the existing p-y criteria.

Therefore, full-scale load tests are usually needed in order to obtain more accurate p-y curves. In carrying out lateral load tests, full instrumentation such as the incorporation of strain gages along the entire length of the drilled shaft may be too expensive to be done routinely. However, inclinometer data could be obtained within a reasonable cost. As demonstrated by Brown, et al. (1994), the inclinometer data obtained during lateral load tests can be used to derive the site-specific p-y curves.

## **VL2 BACK CALCULATION OF P-Y CURVES FROM INCLINOMETER DATA**

### **VI.2.1 General Principle**

The method outlined below is a means of deriving p-y curves from the measured deflections by making a “best-fit” to the data using a pre-selected analytical functions for the p-y relationship and using a least squares technique. The variation of the shape of the p-y curves and the variations of p-y curves with depth are defined using several variables, which are the subject of the fitting process. For the simple case of using existing analytical p-y curves to fit for a specific site, these variables can simply be taken as the input soil strength and stiffness parameters (e.g.,  $S_u$ ,  $\epsilon_{50}$  for clay,  $\phi$ ,  $k$  for sand). When used to develop or evaluate more general form of analytical p-y curves, other empirical parameters could be used as the unknown for the fitting purpose. The former case may be most useful for evaluating test data at a specific site so that alternative boundary conditions, pile or shaft lengths, etc. could be evaluated. The latter case may be more useful to the development of more reliable analytical p-y curves for a particular type of soils. In either case, the “best-fit” technique would be the same; however, the actual variables to be determined would be different. In the method and case study outlined below, soil strength and stiffness parameters are used as unknowns.

### **VI.2.2 Governing Equation for Soil-Shaft Interaction**

The differential equation to be solved is derived on the assumption that the shaft is a linearly elastic beam and that the soil reaction may be represented as a line load

$$EI \frac{d^4 y}{dx^4} + P_x \frac{d^2 y}{dx^2} - p = 0 \quad \text{VI-1}$$

in which  $P_x$  = axial load applied on drilled shaft;  $y$  = lateral deflection of the drilled shaft at point  $x$  along the shaft length;  $p$  = soil reaction per unit length; and  $EI$  is the flexural rigidity of the drilled shaft.

### VI.2.3 Definition of the Problem

Suppose a drilled shaft is divided into  $i-1$  intervals, so that there are  $i$  nodes along the length. Additionally, the shaft deflections are determined at each of  $j$  sets of boundary conditions (for a load test, the values of shaft head shear use the boundary conditions). Thus, there are a total of  $i \times j = m$  nodes for which the deflection measurements are obtained. The horizontal deflections,  $y$ , are represented as

$$\mathbf{y}(\mathbf{u}) = \begin{Bmatrix} y_1(\mathbf{u}) \\ y_2(\mathbf{u}) \\ \vdots \\ y_m(\mathbf{u}) \end{Bmatrix} \quad \text{VI-2}$$

where

$$\mathbf{u} = \begin{Bmatrix} u_1 \\ u_2 \\ \vdots \\ u_n \end{Bmatrix} \quad \text{VI-3}$$

and

$\mathbf{u}$  = soil parameters affecting the analytical  $p$ - $y$  curves

$n$  = number of soil parameters used to define analytical  $p$ - $y$  curves and their distribution with depth.

The measured deflections during load test are represented as

$$\mathbf{b} = \begin{Bmatrix} b_1 \\ b_2 \\ \vdots \\ b_m \end{Bmatrix} \quad \text{VI-4}$$

The purpose of back-calculation is to determine a set of unknown soil parameters,  $\mathbf{u}$ , by using the measured deflections. Since  $m \gg n$ , there is not an exact solution for  $\mathbf{u}$ . The best estimate of the soil parameters,  $\mathbf{u}$ , is by using a least squares “inversion” technique; that is, the best estimate of the soil parameters,  $\mathbf{u}$ , is found by minimizing

$$Y(\mathbf{u}) = [\mathbf{y}(\mathbf{u}) - \mathbf{b}]^T [\mathbf{y}(\mathbf{u}) - \mathbf{b}] \quad \text{VI-5}$$

#### VI.2.4 Method of solution

Using the Taylor series expansion technique and selecting the first term only, the following equation can be obtained

$$\mathbf{y}(\mathbf{u} + \Delta\mathbf{u}) - \mathbf{y}(\mathbf{u}) = \mathbf{J} \Delta\mathbf{u} \quad \text{VI-6}$$

where  $\mathbf{J}$  is the Jacobian matrix describing the effect of changes in  $\mathbf{u}$  on  $\mathbf{y}$ . The above equation can be re-written as

$$\mathbf{J} \Delta\mathbf{u}_k = \Delta\mathbf{y}_k \quad \text{VI-7}$$

where

$$\Delta\mathbf{y}_k = \mathbf{y}(\mathbf{u} + \Delta\mathbf{u}) - \mathbf{y}(\mathbf{u}) = \mathbf{b} - \mathbf{y}(\mathbf{u}) \quad \text{VI-8}$$

Equation (VI-7) is considered as a linear least squares problem, for which the computed changes in the unknowns,  $\Delta \mathbf{u}_k$ , can be solved. The solution involves an iterative process in which the difference at point  $\mathbf{u}_k$  is used to estimate the next point,  $\mathbf{u}_{k+1}$ . The singular value decomposition (SVD) technique is used to solve Eq. VI-7. In order to obtain a stable converged solution, a damping coefficient which reduces the changes in the unknowns during iteration is applied.

### VI.3 APPLICATIONS TO LOAD TEST RESULTS

Back calculation of P-Y curves for drilled shaft #1 at CUY-90-15.24 Project was preformed. Fig. 6.1 is a schematic diagram depicting the shaft geometry, soil strata at the site. Ten locations where the p-y curves were to be the output from the back calculation include the following: 4 in., 92 in., 100 in., 405 in., 711 in., 1016 in., 1024 in., 1616 in., 1624 in., 1712 in. below the ground surface. The stiff clay p-y criterion for stiff clay developed by Reese et al. (1975) was selected to determine the back calculated soil resistance from the test results. A total of nine sets of inclinometer data corresponding to the lateral load from 50 kips to 800 kips were used to back calculate p-y curves. The initial iteration parameters for each soil layer are summarized below.

Soil layer #1:  $S_u = 7.5$  psi,  $\gamma = 0.07$  pci,  $\epsilon_{50} = 0.01$

Soil layer #2:  $S_u = 9.5$  psi,  $\gamma = 0.07$  pci,  $\epsilon_{50} = 0.005$

Soil layer #3:  $S_u = 30$  psi,  $\gamma = 0.072$  pci,  $\epsilon_{50} = 0.005$

Soil layer #4:  $S_u = 250$  psi,  $\gamma = 0.08$  pci,  $\epsilon_{50} = 0.005$



The knowledge of site soil conditions is important in determining the initial parameters. It should be pointed out that the back calculated soil strength values from this analysis do not represent the actual strengths; rather, the parameter values are only used for producing p-y curves. The comparison of the back calculated p-y curves together with the p-y curves derived from SPT correlations are shown in Fig. 6.2 ~ Fig. 6.5 for the depths at 92 in., 405 in., 711 in., and 1024 in., respectively.

The back calculated p-y curves were then used in the COM624P program to predict the drilled shaft displacement under various lateral loads. The measured and the predicted deflections corresponding to 100 kips, 300 kips, 500 kips, 600 kips, 680 kips are shown in Fig. 6.6 ~ Fig. 6.10, respectively. Furthermore, presented in Fig. 6.11 is the measured and predicted load vs. displacement at the head of the drilled shaft. The predicted displacements by the back calculated p-y curves using the inclinometer data are much closer to the measured displacements when compared to the predictions based on the SPT correlations.

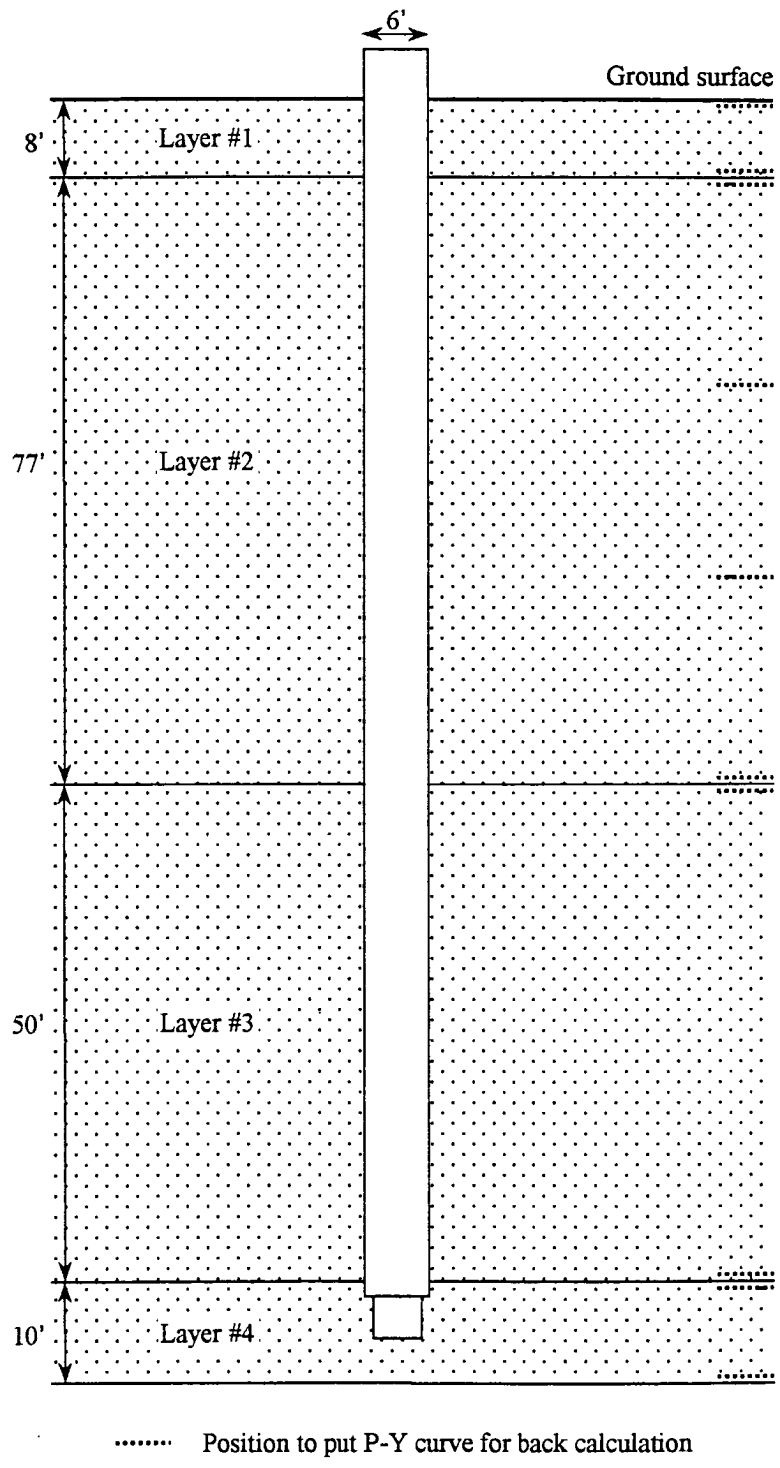


Fig. 6.1: The shaft geometry showing p-y curve positions  
(Shaft #1 at CUY-90-15.24 Project)

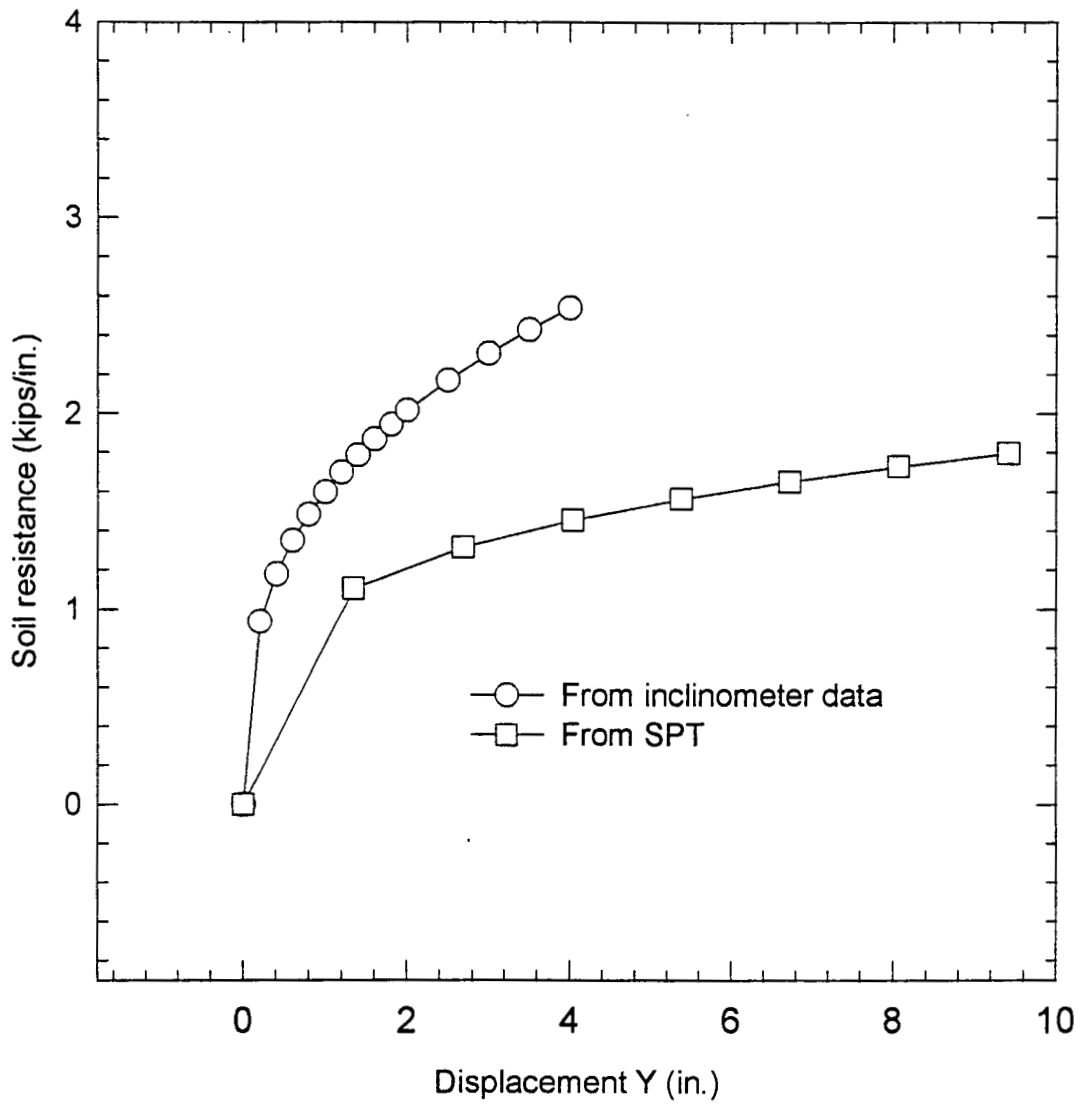


Fig. 6.2: P-Y curves derived from different methods (Shaft #1, depth = 92 in.)

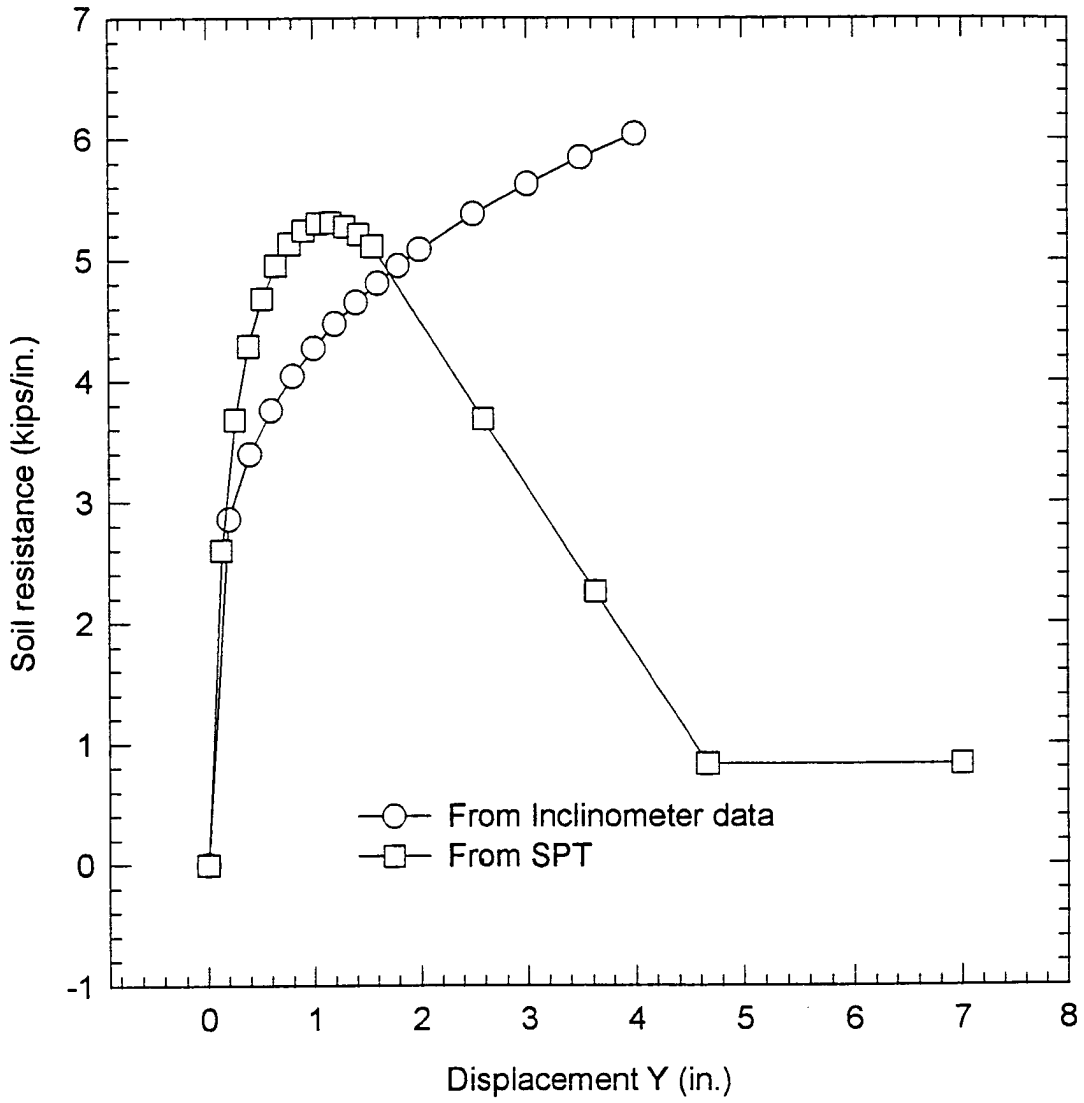


Fig. 6.3: P-Y curves derived from different methods (Shaft #1, depth = 405 in.)

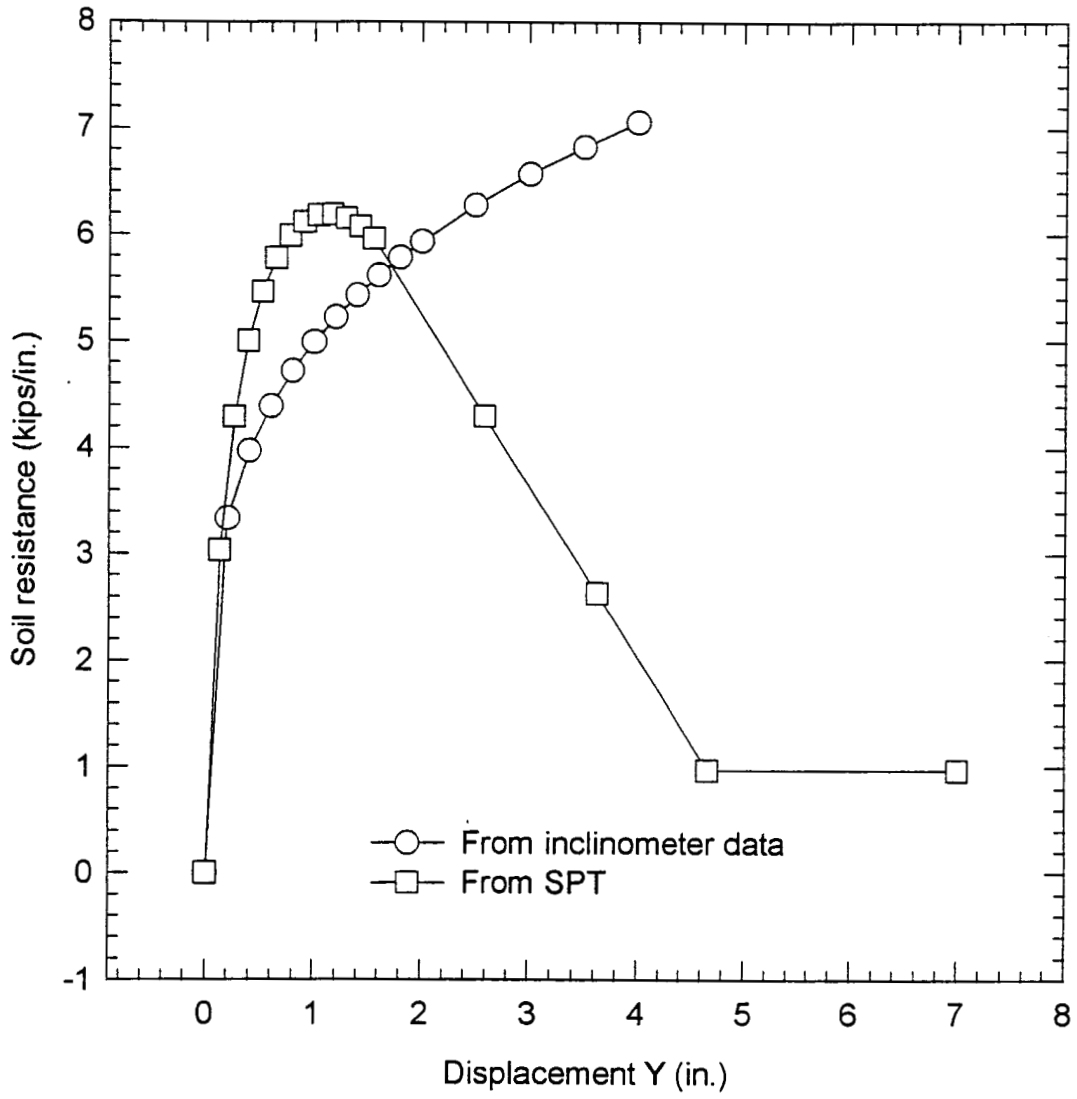


Fig. 6.4: P-Y curves derived from different methods (Shaft #1, depth = 711 in.)

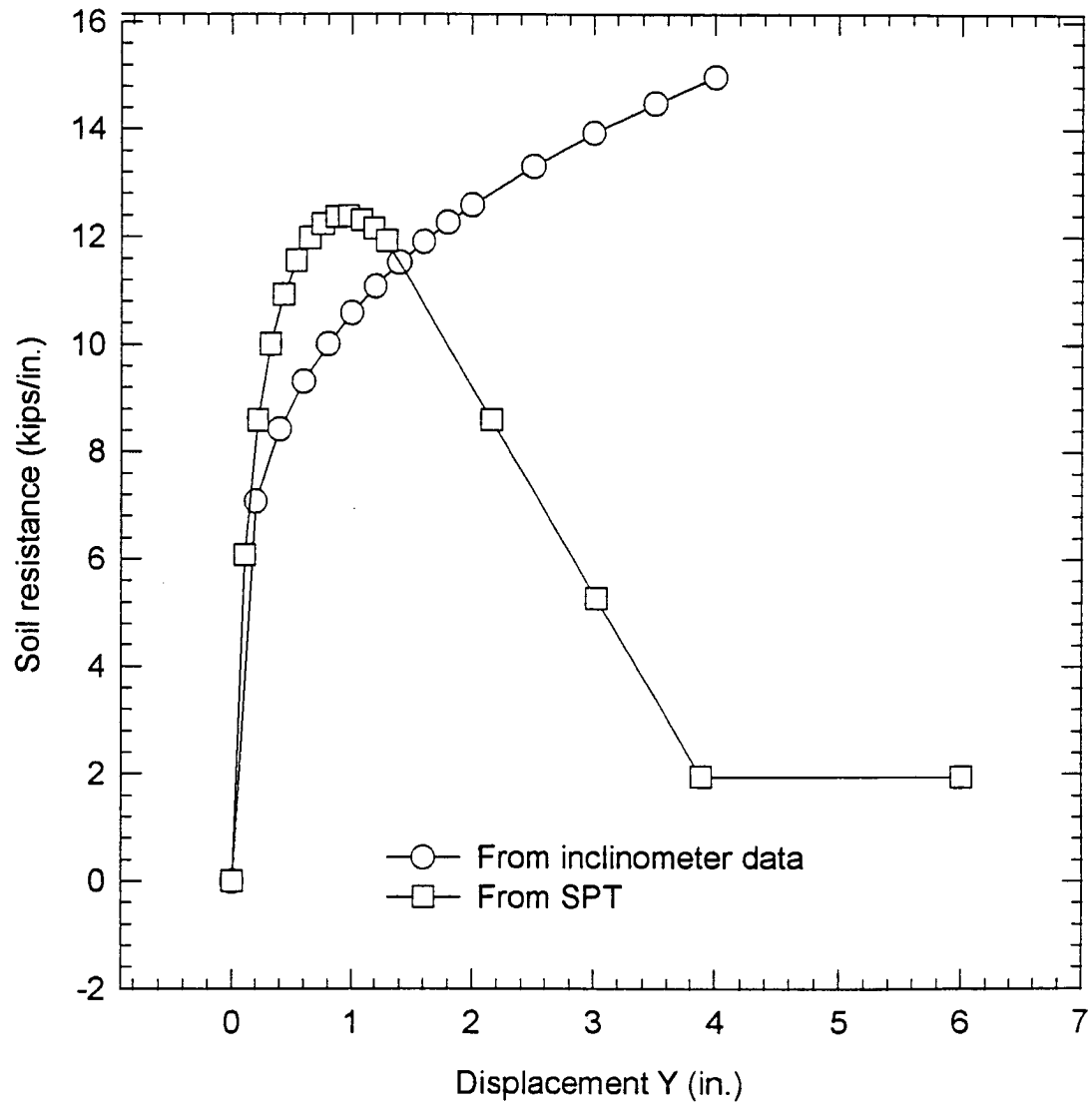


Fig. 6.5: P-Y curves derived from different methods (Shaft #1, depth = 1024 in.)

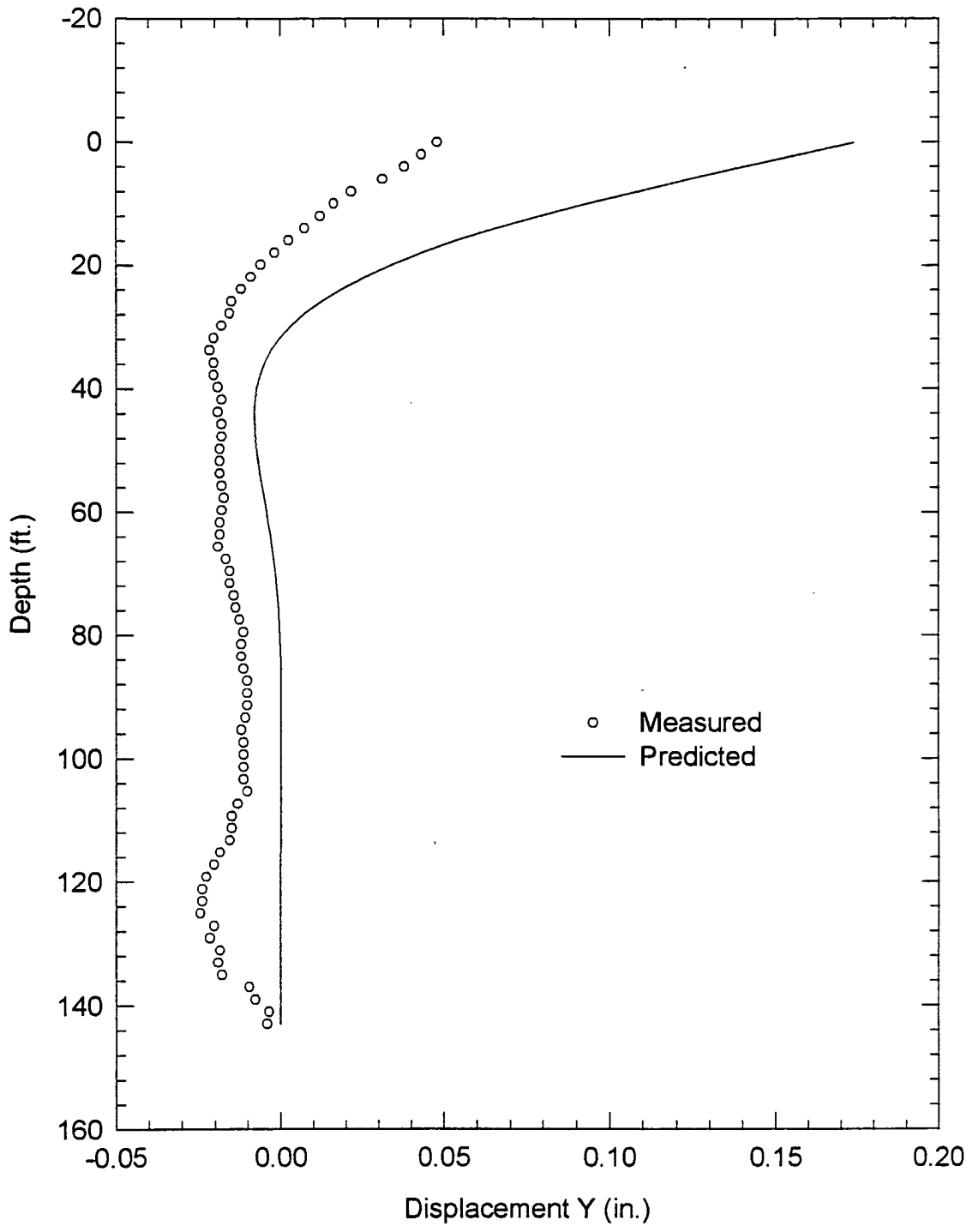


Fig. 6.6: Comparison of deflections (Shaft #1, 100 kips)

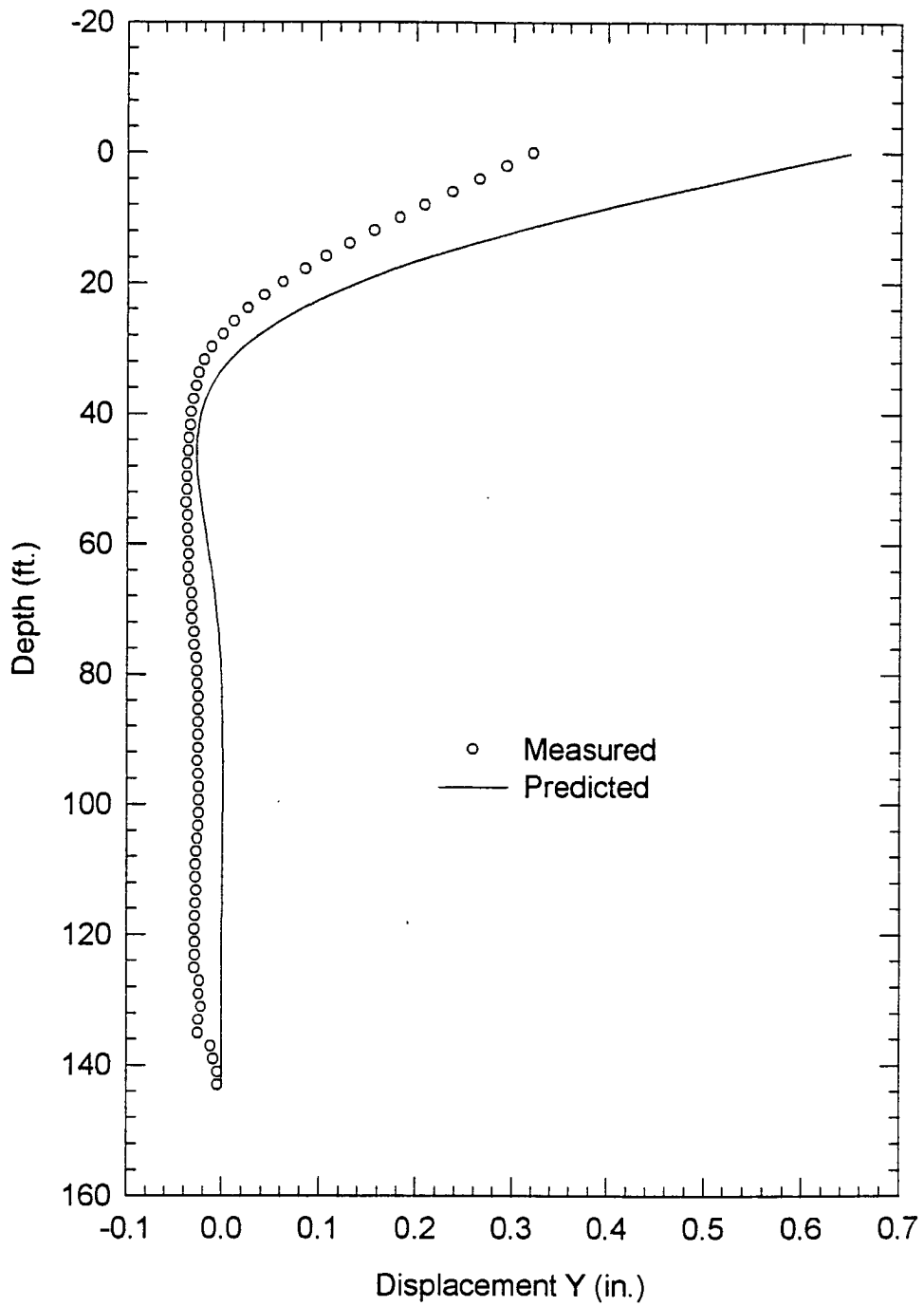


Fig. 6.7: Comparison of deflections (Shaft #1, 300 kips)



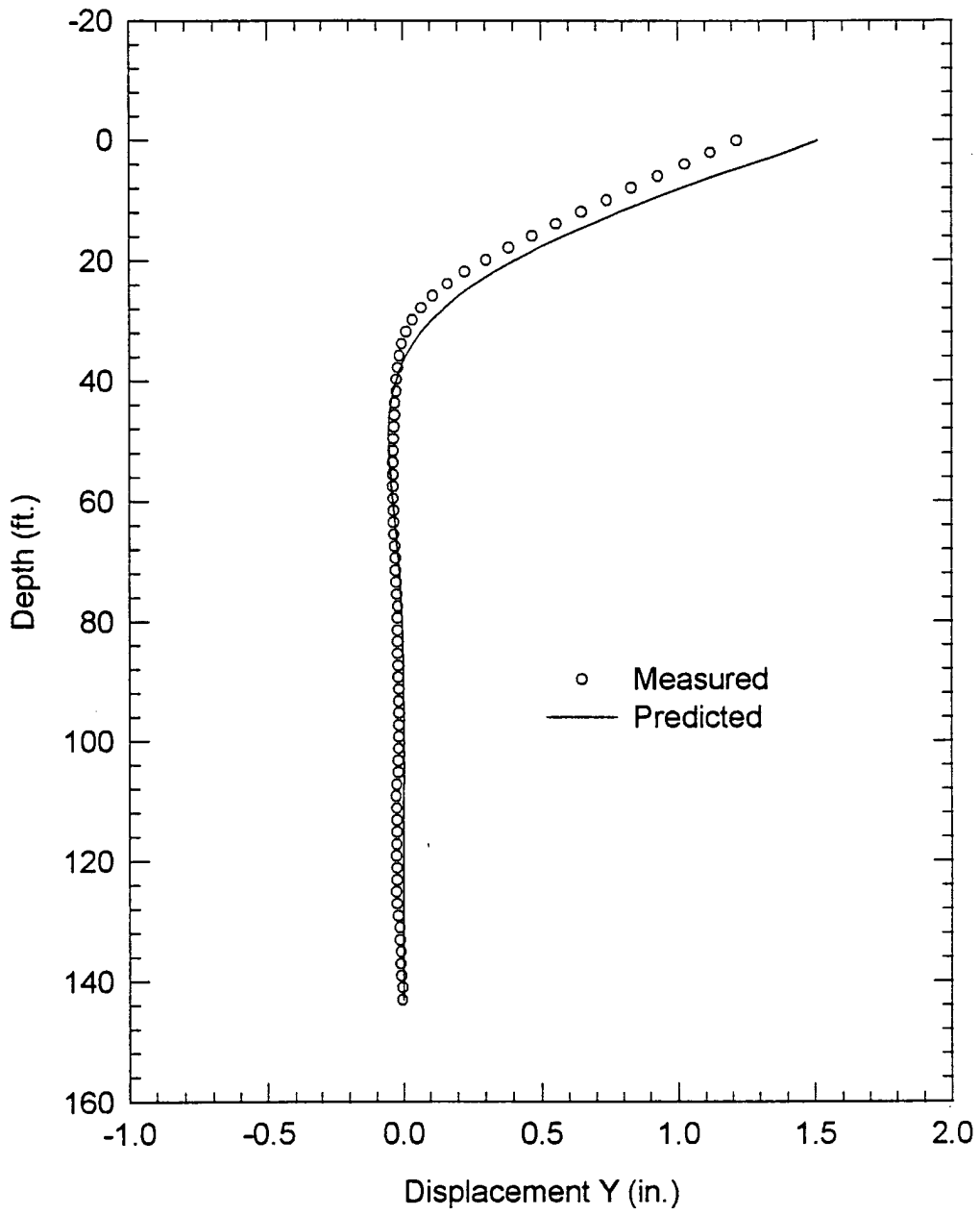


Fig. 6.8: Comparison of deflections (Shaft #1, 500 kips)

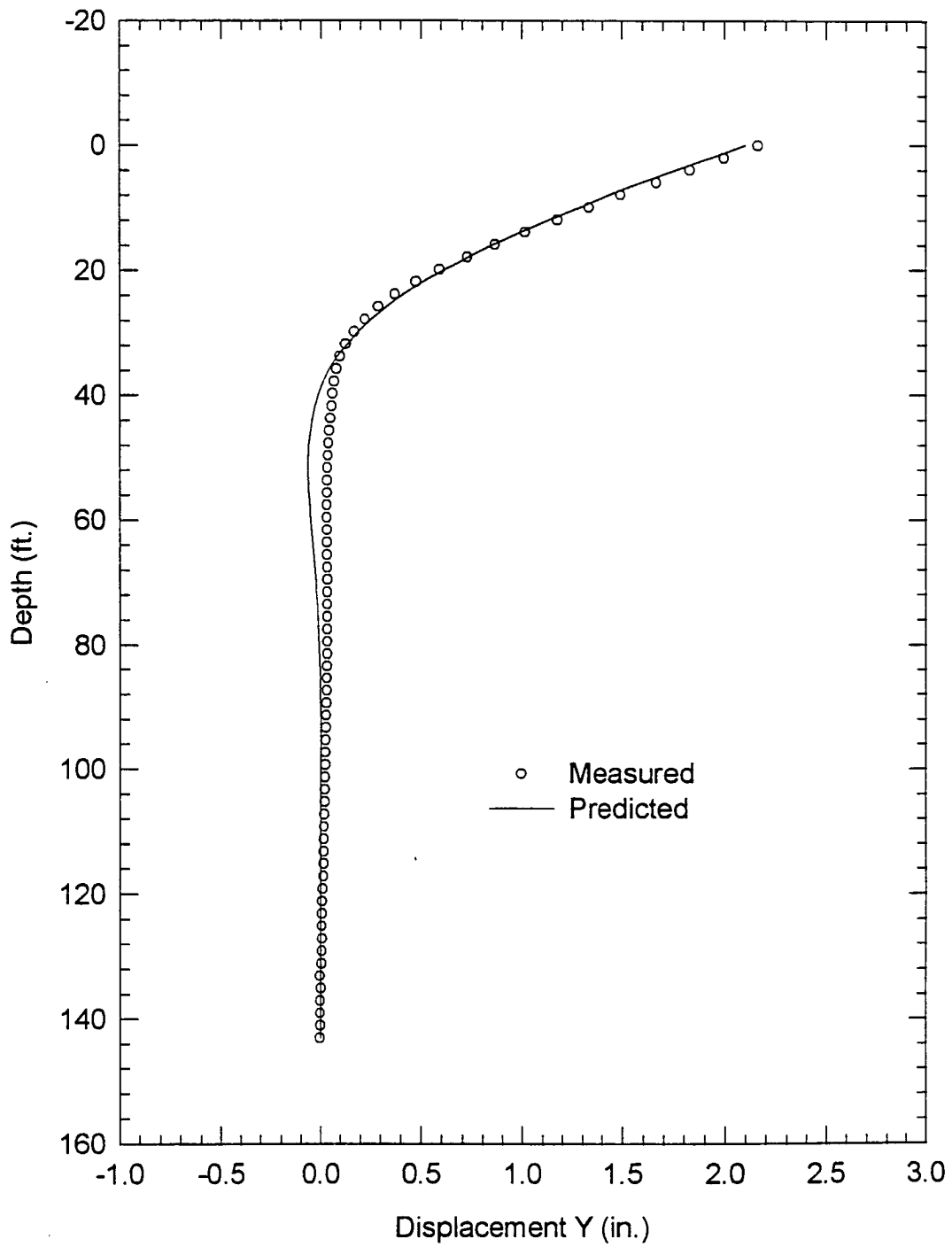


Fig. 6.9: Comparison of deflections (Shaft #1, 600 kips)

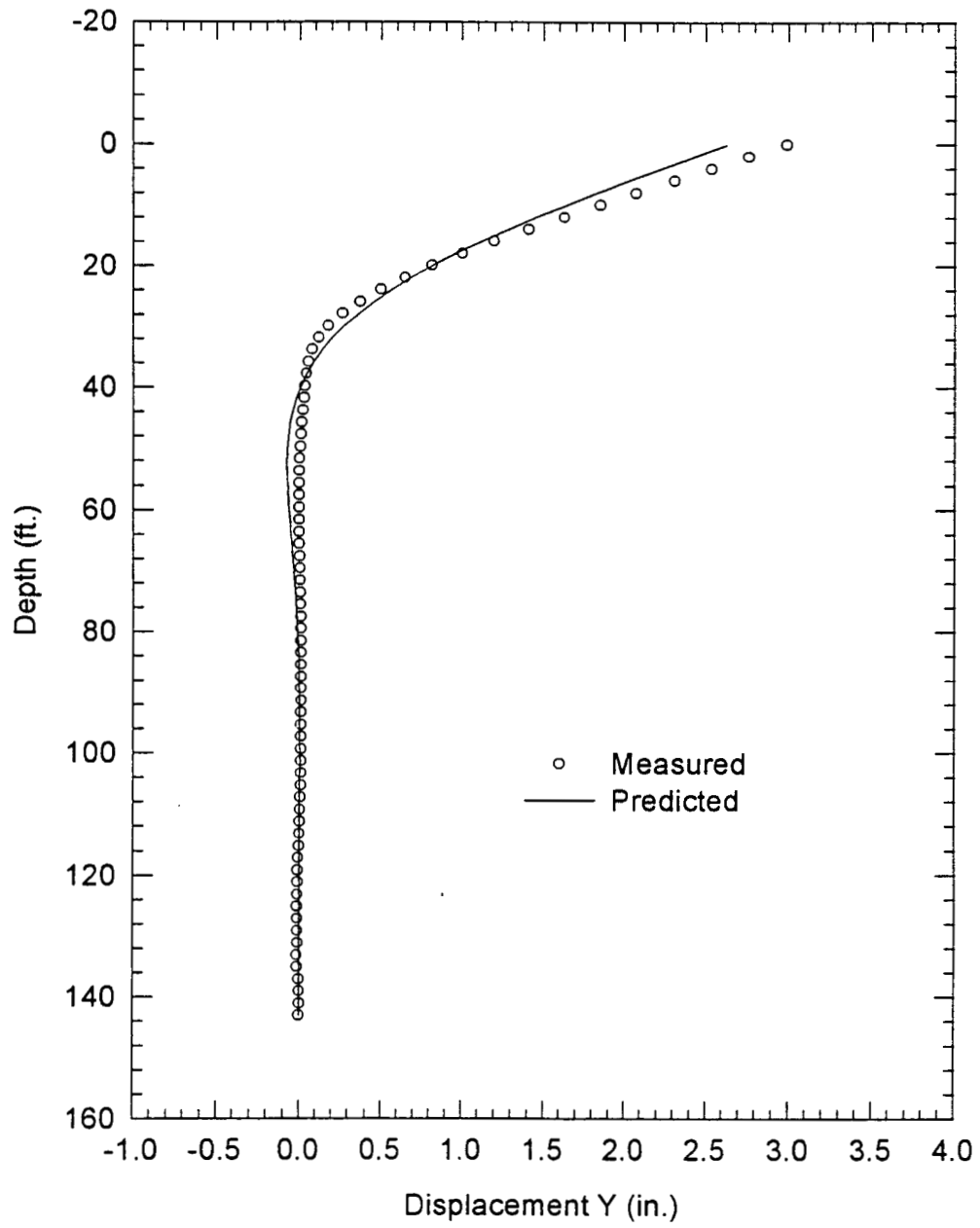


Fig. 6.10: Comparison of deflections (Shaft #1, 680 kips)

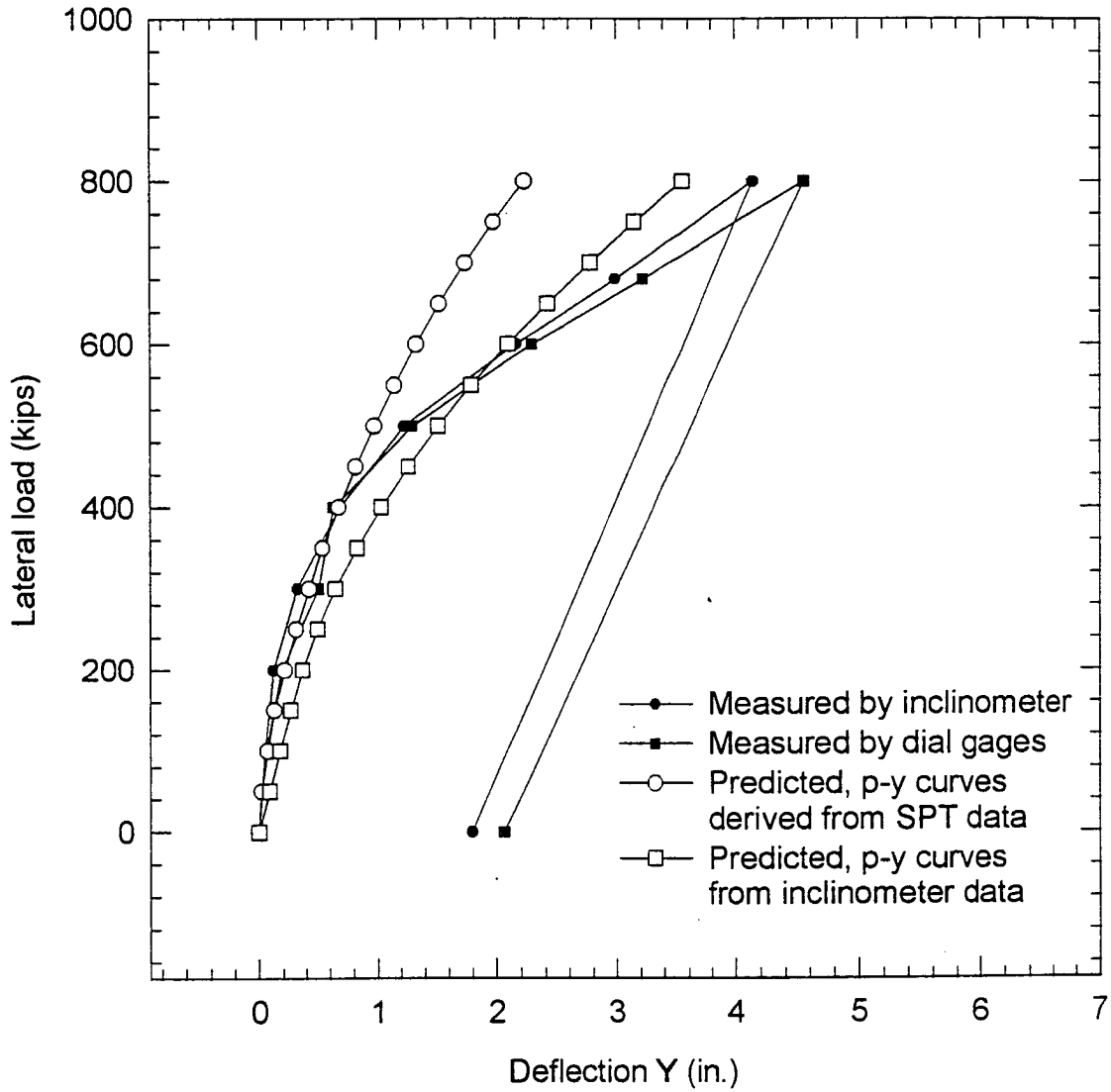


Fig. 6.11: Comparison of pile head movement (Shaft #1)

## CHAPTER VII

### OBSERVATIONS OF FIELD PERFORMANCE

In this chapter, attention is geared toward a detailed analysis of the field measured data, supplemented by the FEM numerical simulation results, to gain a better insight on the general behavior of the stabilized slope during construction as well as during initial stage of service. The response of the slope at various stages of the slope stabilization project will be examined in detail. In addition, lessons learned from the instrumentation/monitoring project will be summarized.

#### VII.1 STAGE I: EXISTING STRESS FIELD PRIOR TO CONSTRUCTION

One of the dominant features of the existing slope is the presence of two distinct slip surfaces, as revealed by the extensive inclinometer readings over a long period of time. Fig. 7.1 shows the representative slope movement measured for B-103, between May 15, 1996 and October 9, 1997. The shallow slip surface, about 60 ft. below the ground surface, had experienced about 0.7 inch relative movement; whereas, the deep slip plane, about 90 ft. below the ground surface, had experienced about 0.2 inch of relative movement. The approximate locations of these two distinct slip surfaces are shown in Fig. 7.2.

The slope stability analysis, based on the soil strength parameters summarized in Fig. 7.3, has shown a F.S. = 1.1 for the shallow slip surface and a F.S. = 1.25 for the deep slip surface.

The finite element simulation results have been shown previously in Chapter 5. The stress ratio, defined as the strength available divided by the shear stress applied, at the slip surface is plotted in Fig. 7.4 and Fig. 7.5 for the shallow and deep slip surface, respectively. As can be seen from these two plots, the shear strength has been fully mobilized along the upper portion of the slip surface. This clearly indicates the slope is experiencing marginal resistance against continued slope movement.

## **VII.2 STAGE II: EXCAVATION TO PILE CAP ELEVATION (9/23/97) AND BEGINNING OF PILE DRIVING (10/3/97)**

Excavation for pile driving has created a change of stress regime in the slope. As shown in Fig. 7.6 and Fig. 7.7, the stress ratio at the two slip surfaces has changed to a state where larger portion of the slip surfaces has experienced full strength mobilization. More importantly, the excavation has induced rotational movement shown in a plot of the deformation field in Fig. 7.8. There have been observations about tension cracks near the edge of the excavation and surficial movement near west-end pier.

The calculated soil movement profile at B103 is compared with the measured in Fig. 7.9. It is noted that the soil properties at the slip surfaces were calibrated so that the calculated and the measured soil movement would match. Once this calibration is done, the soil properties remain unchanged for the analysis of subsequent construction stages.

Among the possible reasons for the intensified slope movement, the following are deemed to be the main cause.

- a. Change of slope geometry has caused the increased applied shear stresses along the pre-existing slip surfaces, thus further reducing the overall F.S. for the two slip surfaces.
- b. Vibrations induced by pile driving has added additional inertia force, which increases the driving force, thus a reduced global F.S. for the two slip surfaces.
- c. The addition of aggregate piles near the upper portion of the slope may have added additional driving force, causing a reduction of overall F.S. of the slope.

Because of the heightened slope movement, pile driving activity was temporarily halt and a temporary earth retaining structure consisting of drilled shafts with steel plate laggings was designed and installed.

The remedial retaining structure has resulted in stress changes in the region near the excavated slope. As shown in Fig. 7.10, the stress ratio for the two major slip surfaces has not shown significant improvement. In any event, construction was proceeded.

### **VII.3 STAGE III. COMPLETE PILE DRIVING (1/19/98), COMPLETE PILE CAP (2/11/98), BACKFILL PORTION OF THE SLOPE (2/23/98), AND EXCAVATION FOR DRILLED SHAFTS AND TIE BEAMS.**

During this construction stage, the inclinometer reading from B-103 showed continued slope movement. Fig. 7.11 represents the measured slope movement between 1/20/98 and 6/30/98. In addition, the deflection of the temporary retaining structure was calculated from the FEM simulation and is shown in Fig. 7.12. Due to continuing slope movement, the construction of drilled shafts was moved ahead of the schedule.

#### **VII.4 STAGE IV. DRILLED SHAFTS CONSTRUCTION (8/14/98 – 12/10/98)**

The construction of drilled shafts involves the use of polymer slurry. Although there has been incidences of the holes filled with running sand, by and large the polymer slurry has served very well in stabilizing the opening of the hole. Installation of sister bar strain gages and inclinometer casing was a success. Fig. 7.13 shows a general view of the construction site during drilled shaft construction. Fig. 7.14 shows the pouring of the polymer slurry into the opening. Fig. 7.15 shows the inclinometer casing in the drilled shafts.

The slope movement during the drilled shafts construction is shown in Fig. 7.16. Because of the hole opening and running sands into the openings, the slope continued to show movements. However, when approaching the completion date, the slope movement has apparently slowed down. It appears that installation of drilled shafts has provided needed resistance against further slope movement.

#### **VII.5 STAGE V. LATERAL LOAD TESTS OF DRILLED SHAFTS #1 AND #3 (1/13/99)**

A lateral load test was carried out in January 1999. Detailed discussion of this test is presented in chapter 4.



**VII.6 STAGE VI. INSTALLATION OF ROCK ANCHORS (12/12/98 – 2/18/99),  
INSTALLATION OF TIEBEAMS (3/1/99 – 3/25/99), TENSIONING OF  
ROCK ANCHORS (4/7/99 – 4/14/99), AND GROUTING OF THE  
CORRUGATED TUBES (4/20/99)**

Tensioning of rock anchors has introduced a significant amount of stresses in the installed structures members, including driven piles, tiebeams, and drilled shafts. The FEM calculated deflection for the driven piles is shown in Fig. 7.17. The measured and calculated bending moments are shown in Fig. 7.18. For drilled shafts, the comparisons between the FEM calculated bending moment and calculated and measured deflection are shown in Fig. 7.19 and Fig. 7.20, respectively. For the tiebeams, a comparison between the measured and calculated stresses is summarized in Table 7.1.

Table 7.1: Comparisons between calculated and measured results for tiebeams after completion of anchor tensioning

Location	Structure cap end		Shaft cap end	
	FEM	Measured	FEM	Measured
Axial force( kip)	84.858	84.924	84.858	89.216
Shear force(kip)	-0.351	/	-0.351	/
Bending moment(kip-ft)	15.393	12.803	-13.043	-12.083

Overall, the match between the calculated and the measured is astonishingly good. The power of the FEM computer simulation has been clearly demonstrated in this case.

The soil movement at the B-303 inclinometer location are shown in Fig. 7.21. The rate of slope movement at the two slip surfaces has been arrested. The stress ratio for the two slip surfaces are shown in Fig. 7.22 and 7.23.

## VII.7 STAGE VII. FINAL STAGE OF BACKFILLING TO FINAL GRADE

(4/23/99 – 5/7/99)

Subsequent to the final grading at the site, a comparison was made between the measured and the calculated stresses and deformations of the stabilization structures. Presented in Fig. 7.24 and Fig. 7.25 are the deflection and bending moment of the driven piles.

Similarly, the deflection and bending moment for drilled shafts are compared in Fig. 7.26 and Fig. 7.27, respectively. The stresses in the tiebeams are compared in Table 7.2. Comparison was also made between the measured and calculated axial force in the bond zone of rock anchors. The location of the strain gages in the bond zone is shown in Fig. 7.28 and the axial force distribution is shown in Fig. 7.29.

Table 7.2: Comparison between calculated and measured results for tiebeam after backfill

Location	Structure cap end		Shaft cap end	
	FEM	Measured	FEM	Measured
Axial force (Kips)	97.971	103.921	99.016	95.323
Shear force (Kips)	-21.576	/	20.673	/
Bending moment (K-ft.)	32.324	28.030	6.412	3.570

The stress ratio at the two slip surfaces is shown in Fig. 7.30 and Fig. 7.31 for the shallow and deep surfaces, respectively. There appears to be some improvement of stress ratios after anchor tensioning on both slip surfaces.

A plot of movement at slip surface during the construction period (8/24/98 – 6/30/98) is shown in Fig. 7.32. A schematic diagram showing the forces in the structure at the end of construction is presented in Fig. 7.33.

A comparison is made between the measured stresses and the ultimate capacity of each structure. The comparisons are summarized in Table 7.3. It appears that the structure have been adequately sized to carry the loads and stresses.

Table 7.3: Comparison between measured and ultimate capacity of each structure

Sub-Structure component		Measured	Ultimate
Stress Ratio at slip plane		0.3~0.95	1.0
Tie beams	Axial force (kips)	102	287
	Shear force (kips)	21.6	44.3
	Bending moment (k-ft)	28	82.1
Drilled shaft	top deflection (inches)	0.4	1.6 @ 500 Kips*
Pile	End bearing (kips)	322	890
	Bending moment (k-ft)	47	306
Rock anchor	Axial load	567	750
	Creep movement at design load (inch)	0.01	0.08**

\* From lateral load test on shafts #1 and #3

\*\* 0.08 inches per logarithmic cycle of time.

## VII.8 LESSONS LEARNED FROM THE PROJECT

The following statements can be made based on the experiences and findings from the project:

- Construction can induce slope instability. Construction involving excavation in a slope needs engineer's supervision.
- Redundancy in geotechnical structures for slope stabilization is needed to provide multiple defense mechanisms.
- Instrumentation/monitoring provides factual data and important insights to assist project engineers to make critical decisions during construction (can save both time and money).
- Instrumentation/monitoring provides quality assurance of completed structures.
- Long-term monitoring can ensure long-term safety and assist in bridge maintenance decisions.

On the basis of the experiences learned from the project, it is apparent that instrumentation and monitoring can be a very effective approach for the following situations.

- Design/Build Projects
- Contractor can modify design as construction proceeds based on the monitoring data (Cost savings can be passed on to both owner and contractor)
- Critical/Complex structures
- Instrumentation/monitoring cost can be fully recovered from savings of construction cost.

- Projects involving innovative/new designs, unknown/uncertain soil properties, lack of existing design/analysis methodology.
- 1 ~ 2% construction cost for instrumentation could result in 20 ~ 30% of savings in construction cost, yet let engineers sleep soundly at night.

## VII.9 TELLTALE SIGNS FOR LONG-TERM MONITORING

A continuation of monitoring of the behavior of the foundation structures can serve at least two purposes: (i) to ascertain the safety of the slope over a long period of time, and (ii) to gather valuable data for better understanding of the slope stabilization mechanisms involved. To provide a meaningful benchmark or reference point for assessing the state of safety of the slope, the FEM simulation was carried out for a case with increased unit weight of the soil mass. This is to induce additional driving force along the slip surfaces, and to determine the response of the foundation structures. Fig. 7.34 shows the horizontal displacement contours after an increase of soil unit weight above the two slip surfaces by 20 percent. The horizontal displacement vs. depth at Borehole B-303 location is also shown in Fig. 7.34. It is apparent that the two slip surfaces move additional slippage due to this artificial overload in the computer simulation. Of interest are the calculated stresses in the foundation structures, as they would reveal the telltale signs to watch during the long-term monitoring. Table 7.4 provides a summary of the stresses in each foundation structure before and after the 20% increase in unit weight of the soil. These numerical values provide a reference for assessing the condition of the slope over time.

Table 7.4: Stresses in each foundation structure before and after the 20% increase in unit weight of the soil.

Sub-Structure Component		Before	After	Change (%)
Rock Anchor	Axial force (kips)	542	559	3
Tie-beam	Axial force (kips)	98	85	-13
	Shear force (kips)	22	23	3
	Bending moment (kips-ft)	32	34	7
Driven Pile	Axial force (kips)	313	324	4
	Bending moment (kips-ft)	47	49	5
Drilled Shaft	Bending moment (kips-ft)	817	866	6

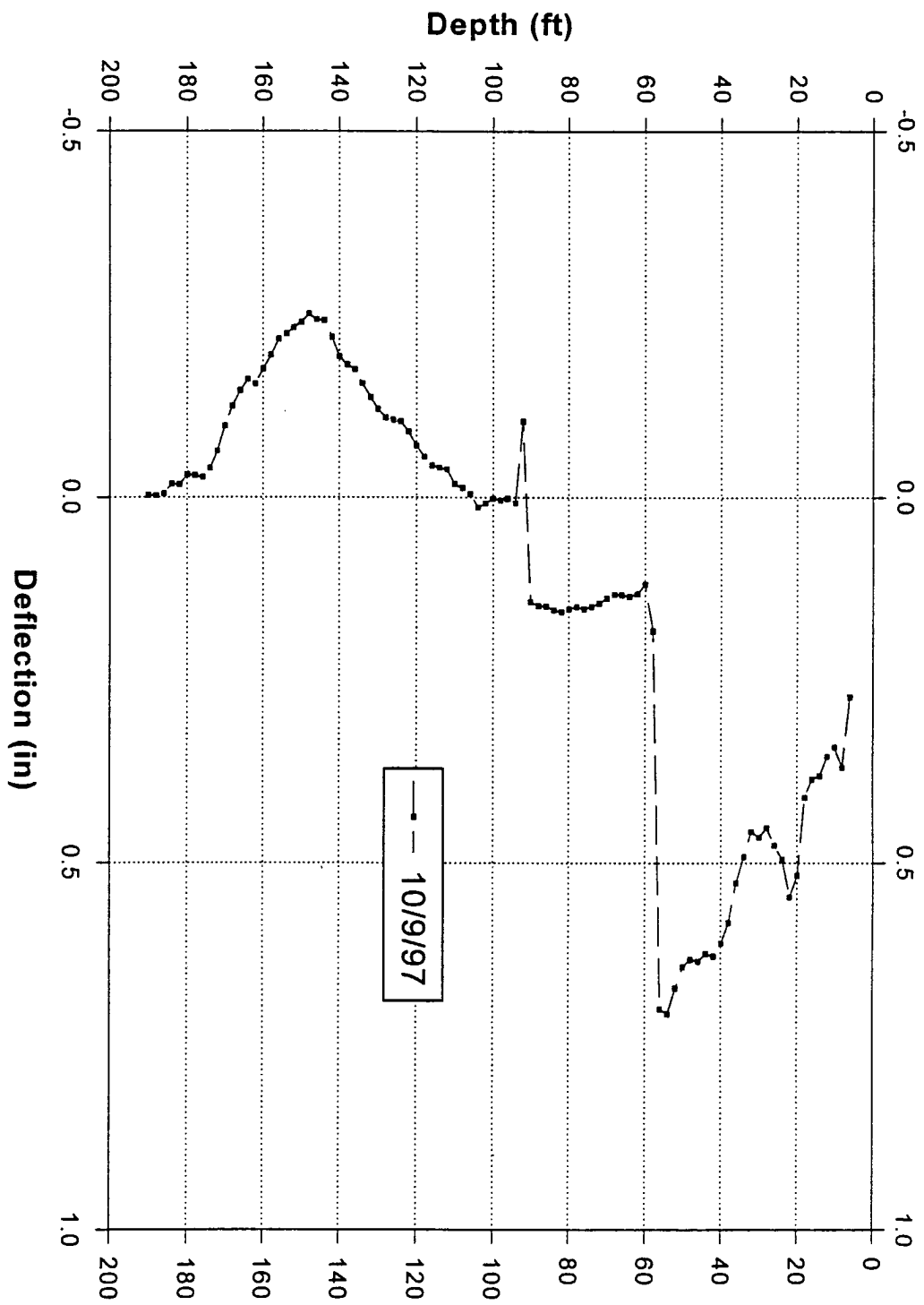


Fig. 7.1: Monitoring of deflection since 5/15/96 for B-103 inclinometer, A-Direction

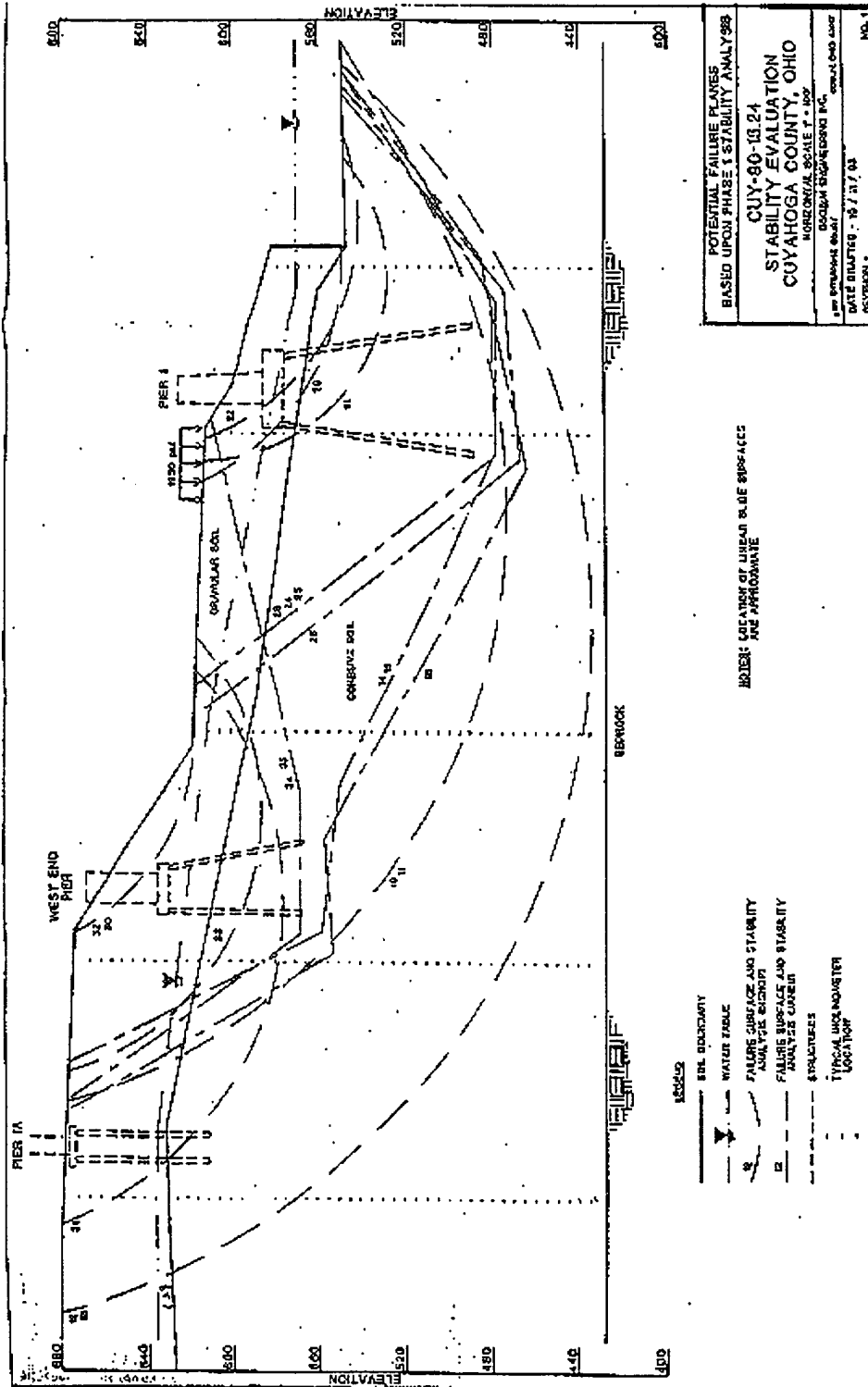


Fig. 7.2: Stability Evaluation and slip surfaces.



**CUY-90-15.24 Project**  
**Analysis of lateral capacity of drilled shafts**  
**Soil Properties used in the Analysis based on SPT**

Depth (ft)	Soil Layer	Soil Properties
0	1	Su = 7.5 psi, E50 = 0.007, K = 300 pci, U.W. = 120 pcf
7	2	Su = 6.94psi, E50 = 0.007, K = 300 pci, U.W. = 120 pcf
14	3	Su = 9.5 psi, E50 = 0.007, K = 400 pci, U.W. = 120 pcf
35	4	Su = 12 psi, E50 = 0.006, K = 500 pci, U.W. = 125 pcf
47	5	Su = 14. psi, E50 = 0.006, K = 600 pci, U.W. = 125 pcf
91	6	Su = 28. psi, E50 = 0.005, K = 1000 pci, U.W. = 125 pcf
107	7	Su = 45. psi, E50 = 0.005, K = 1000 pci, U.W. = 130 pcf
113	8	Su = 37. psi, E50 = 0.005, K = 1000 pci, U.W. = 130 pcf
141	9	Su = 250. psi, E50 = 0.004, K = 1200 pci, U.W. = 140 pcf

Fig. 7.3: Soil properties model

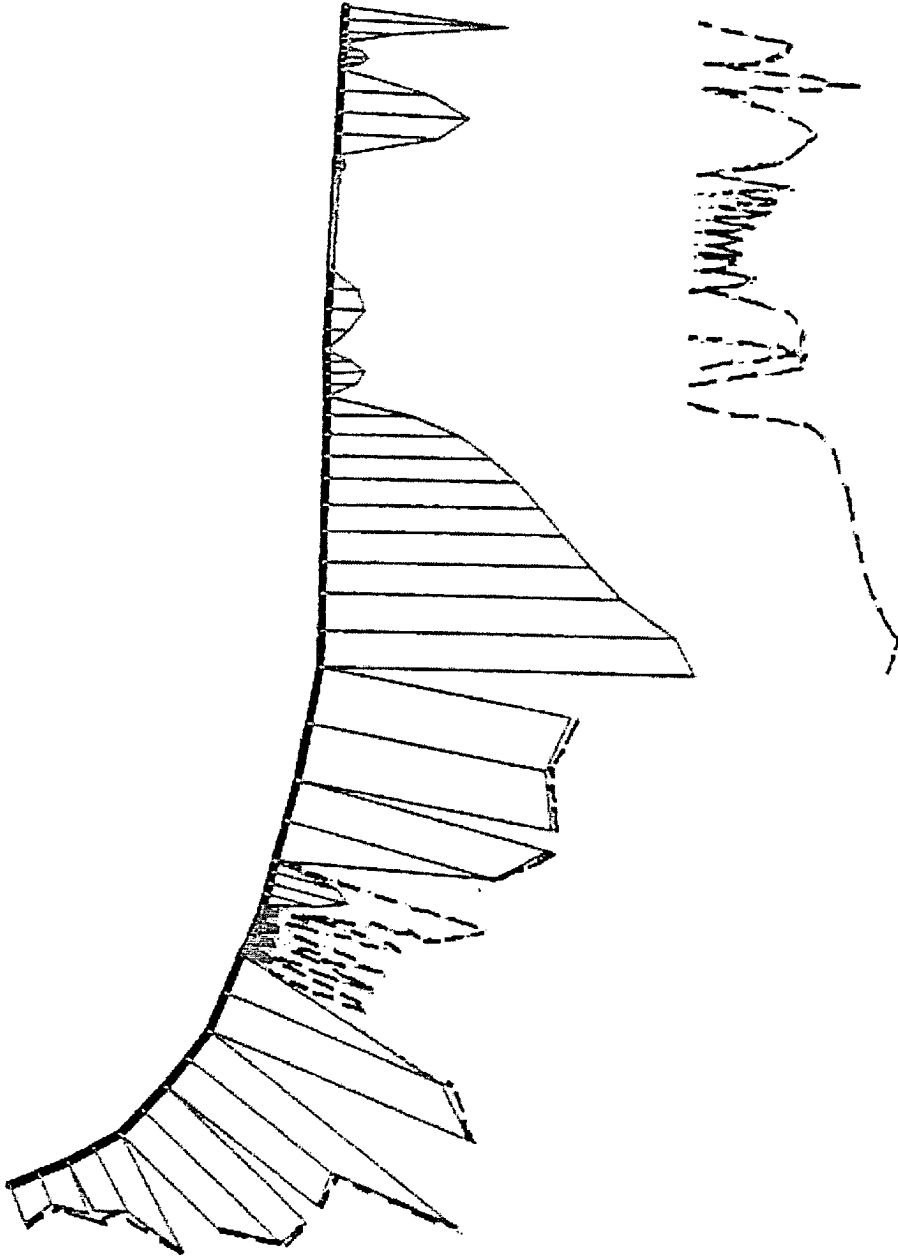


Fig. 7.4: Stress ratio at shallow slip plane prior to construction (Stage I).

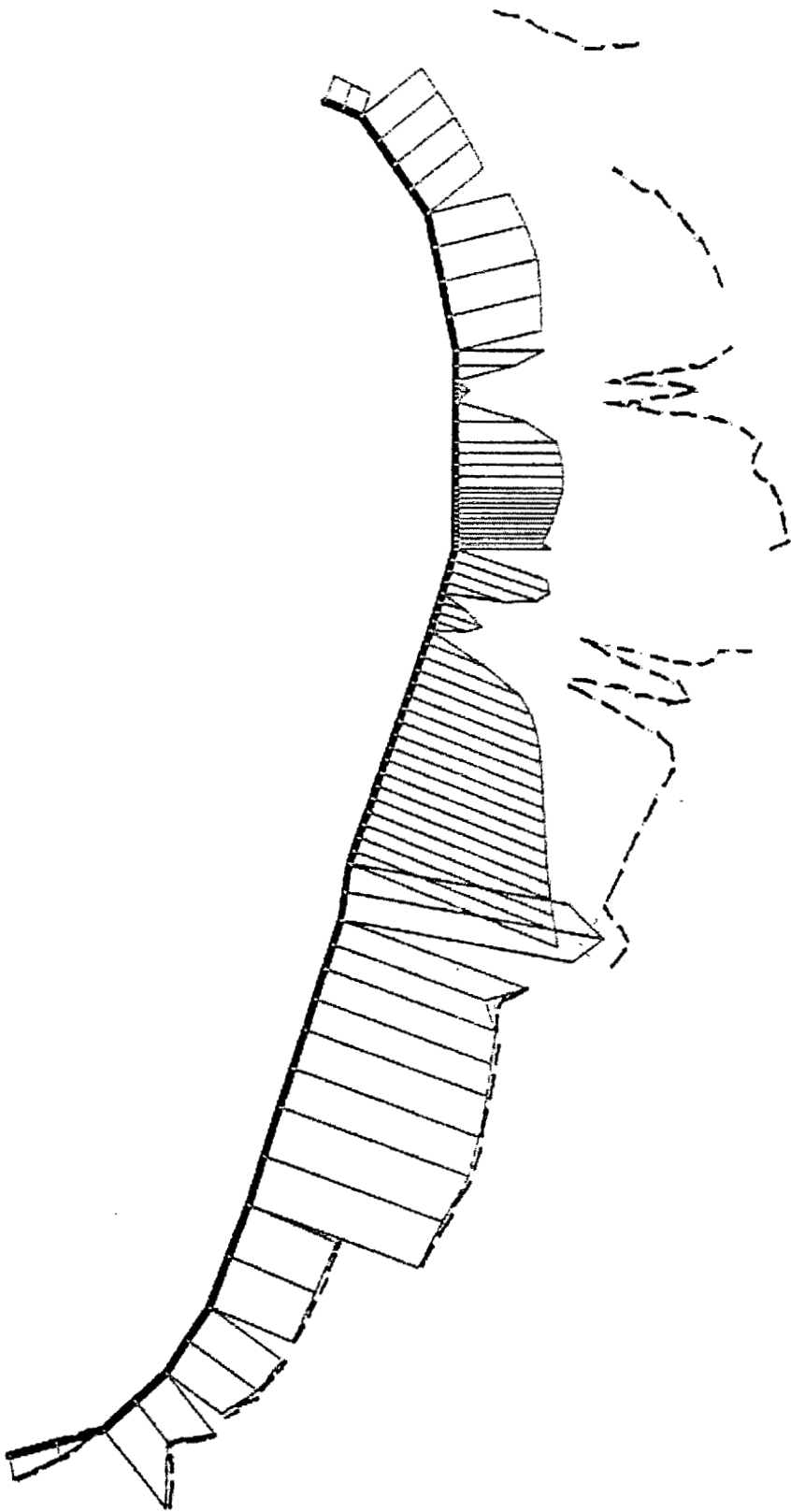


Fig. 7.5: Stress ratio at deep slip plane prior to construction (Stage I).

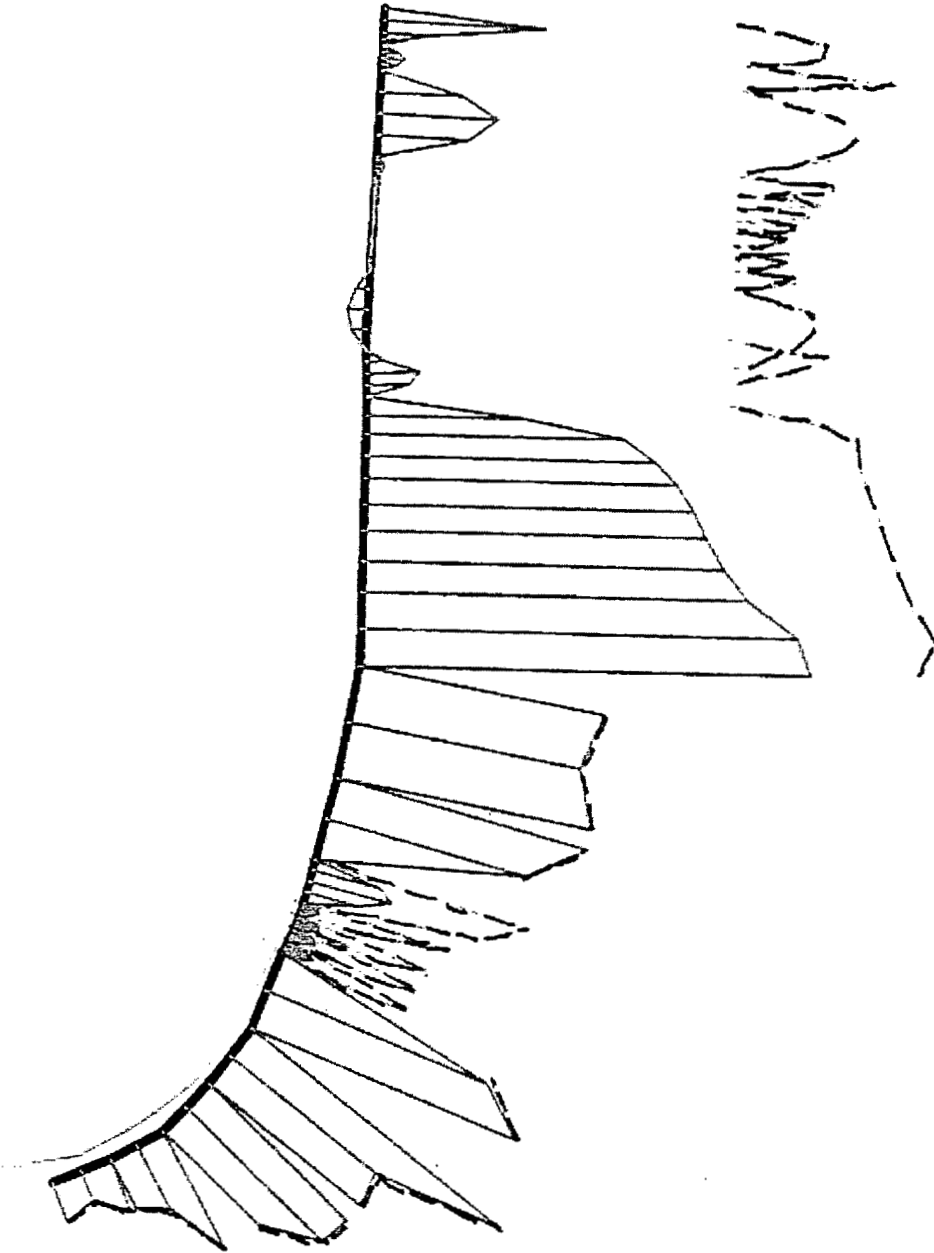


Fig. 7.6: Stress ratio at shallow slip plane after excavation to pile cap elevation (Stage II).

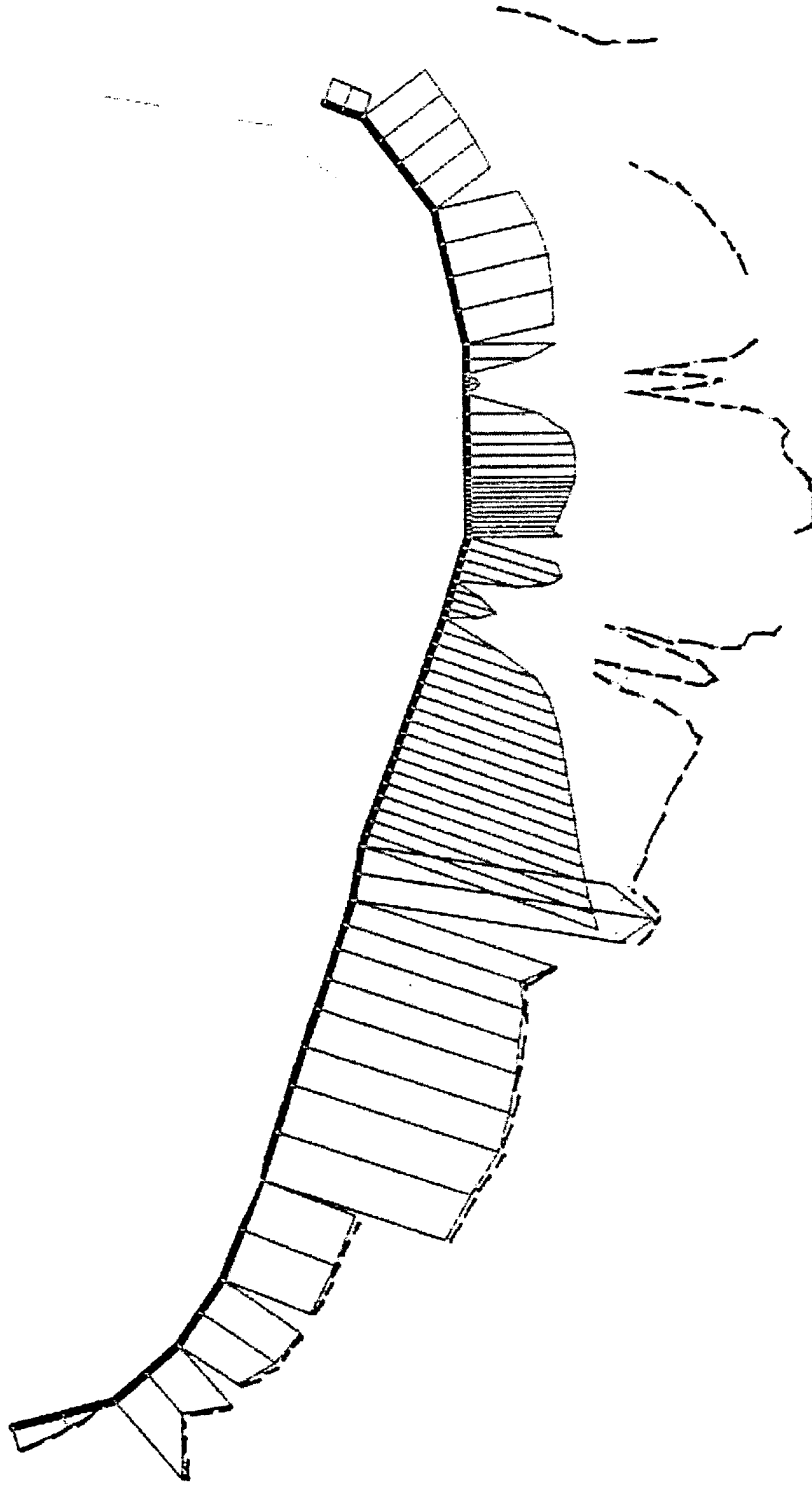


Fig. 7.7: Stress ratio at deep slip plane after excavation to pile cap elevation (Stage II).

0.220

0.198

0.176

0.154

0.132

0.110

0.088

0.066

0.044

0.022

0.000

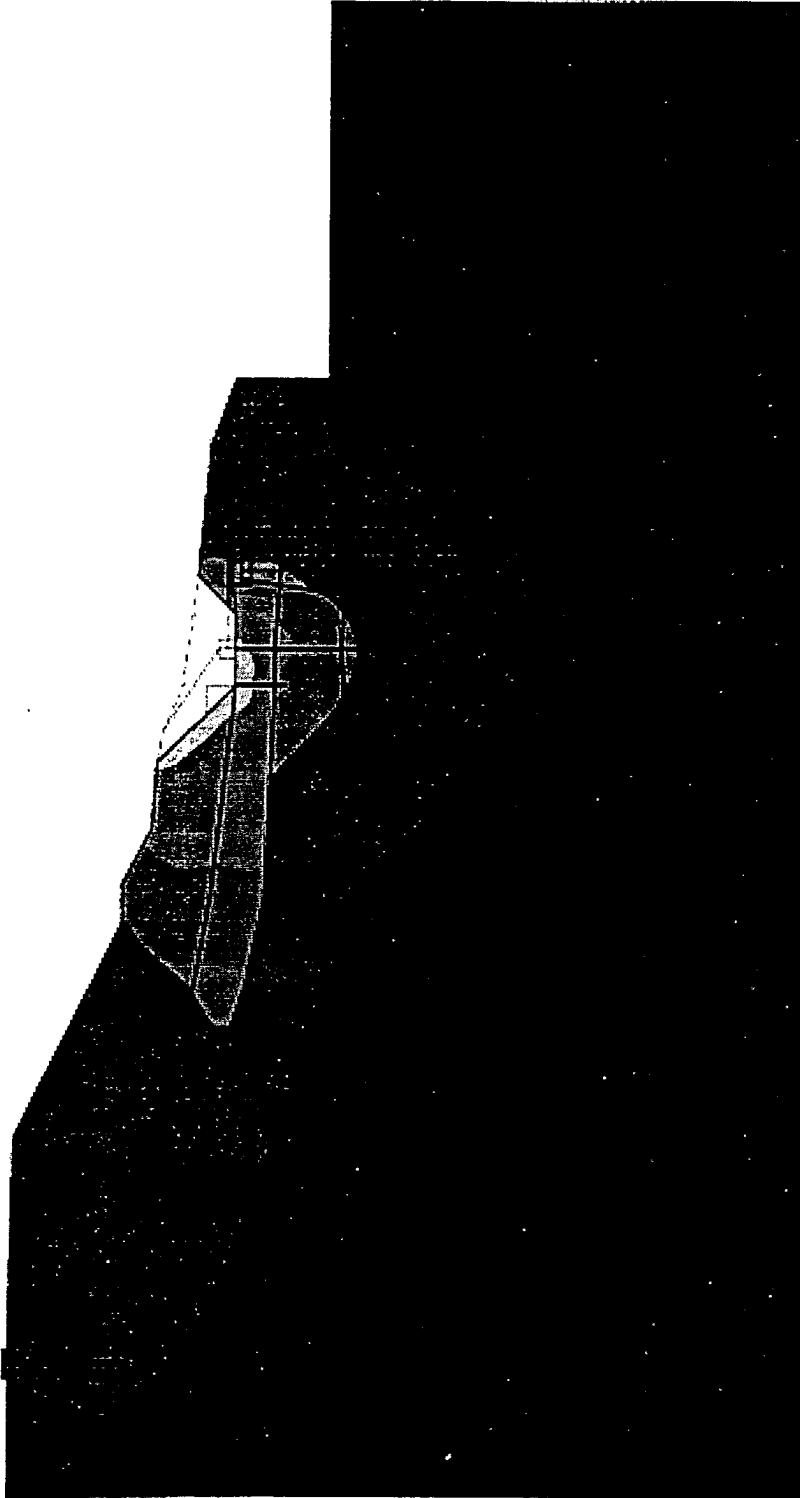


Fig. 7.8: Deformation field due to excavation.

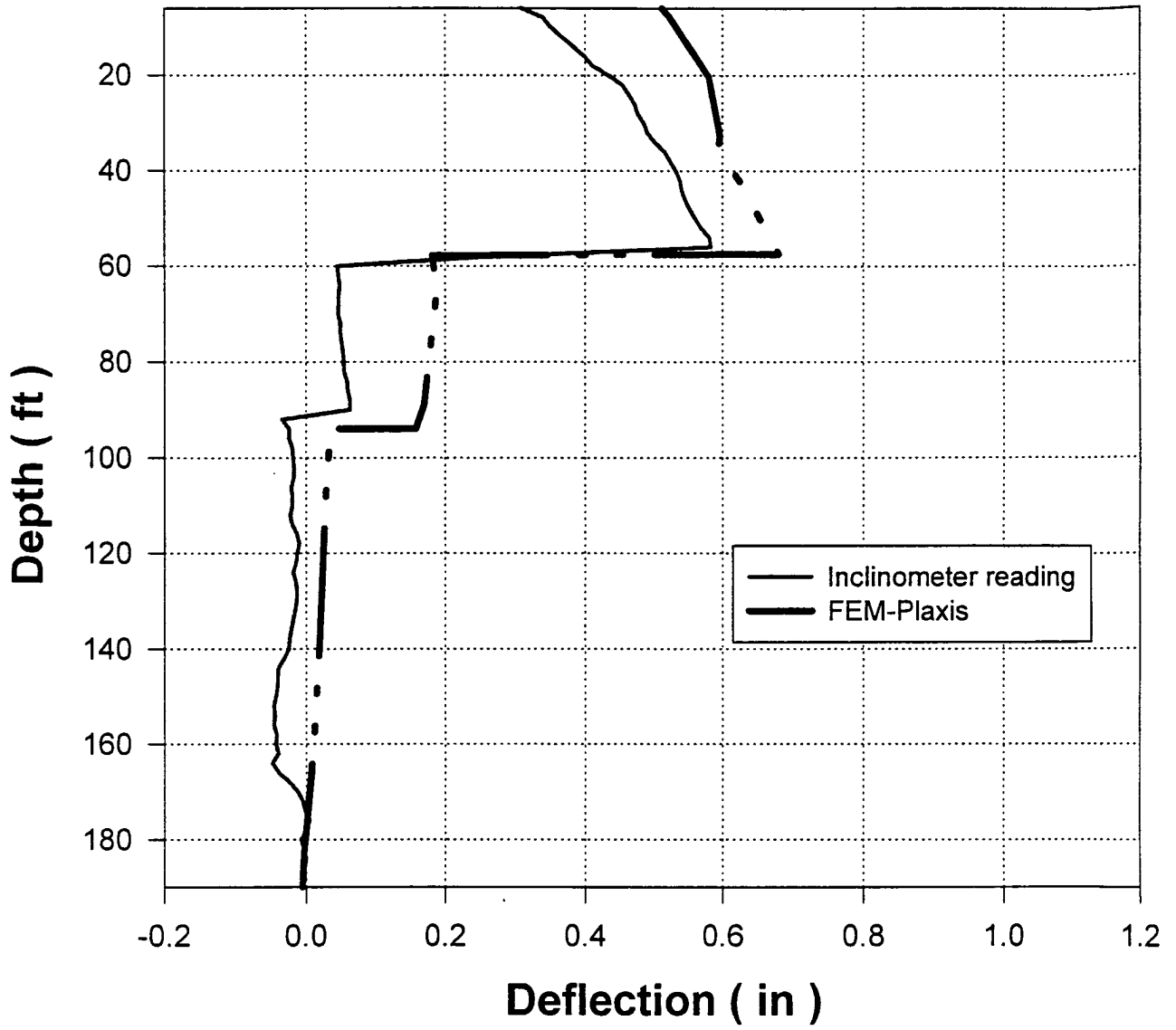


Fig. 7.9: Deflection vs. depth (Stage II).

1.000  
0.900  
0.800  
0.700  
0.600  
0.500  
0.400  
0.300  
0.200  
0.100  
0.000

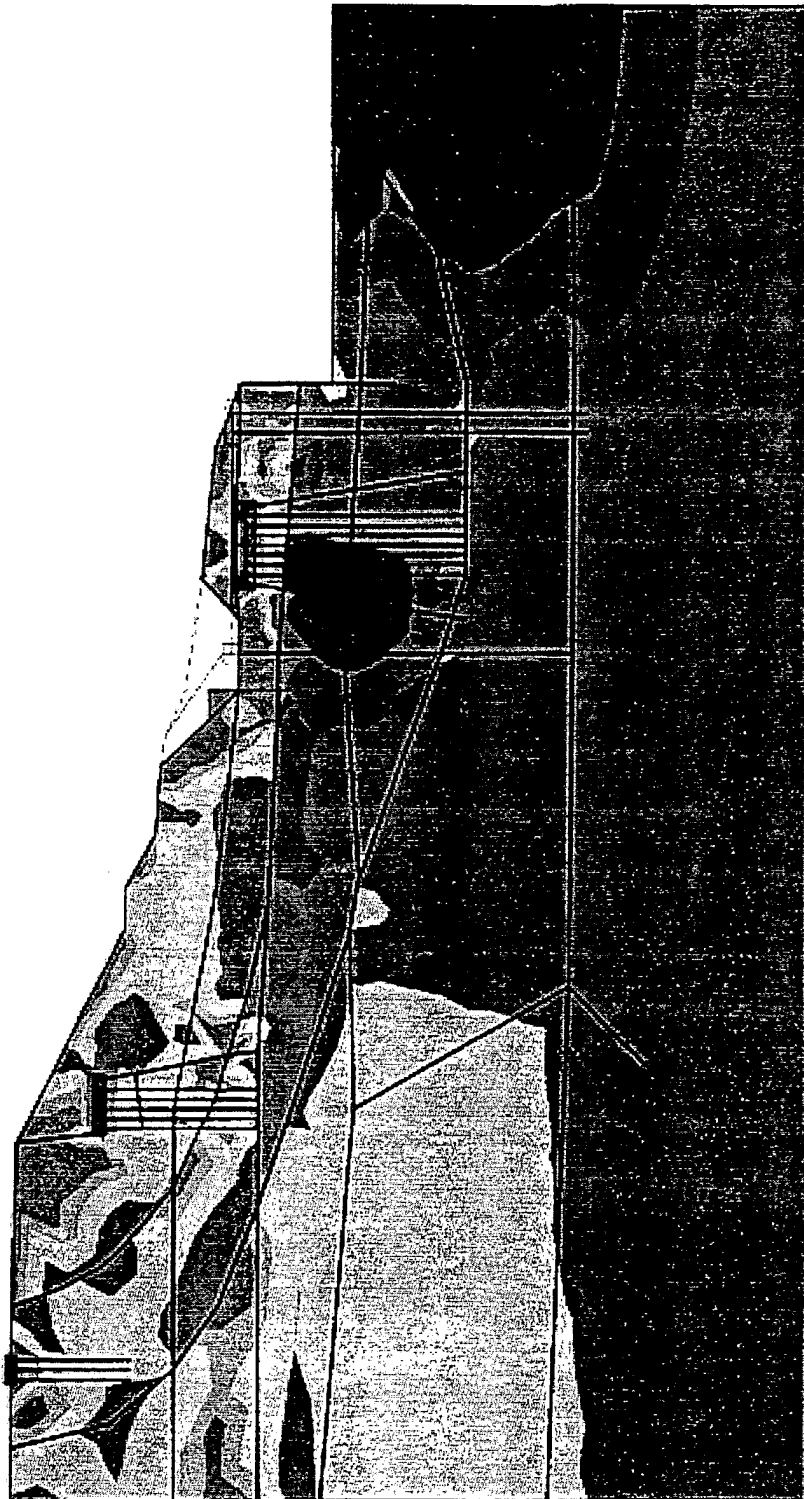


Fig. 7.10: Stress ratio contour (Stage II).



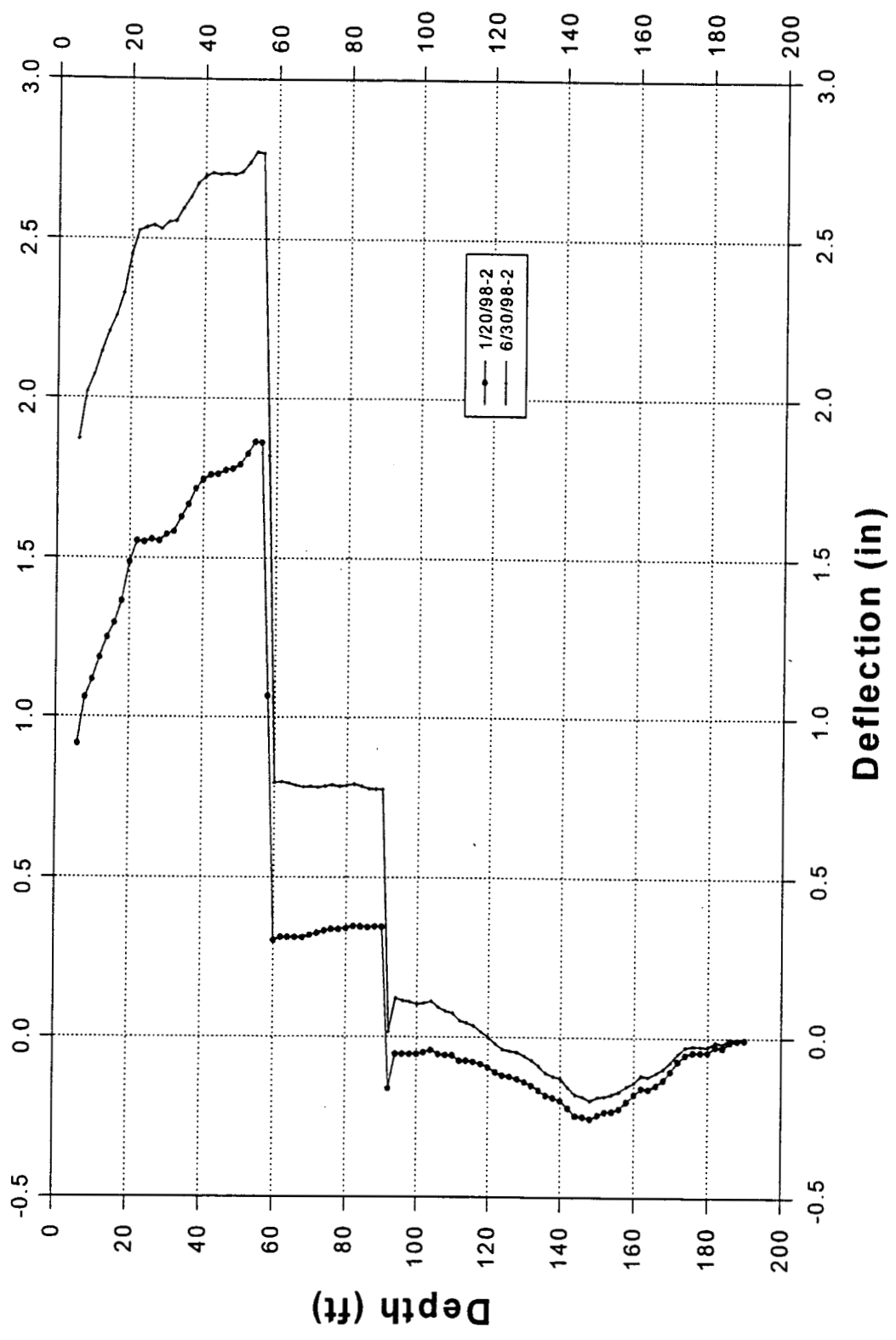


Fig. 7.11: Inclinometer reading after pile driving is completed till before start of shaft construction (Stage III).

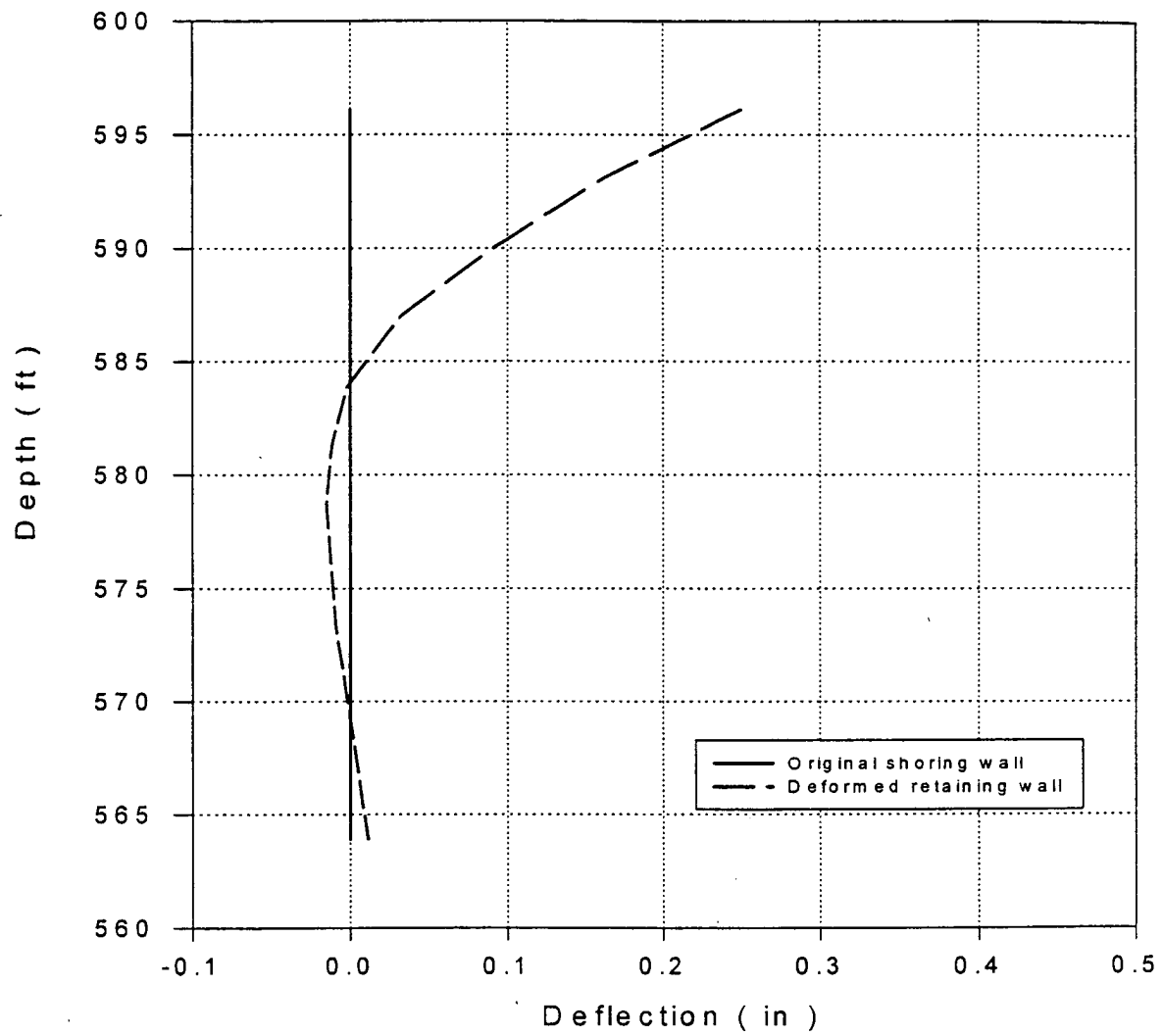


Fig. 7.12: Horizontal deflection of temporary retaining structure from FEM (Stage III).

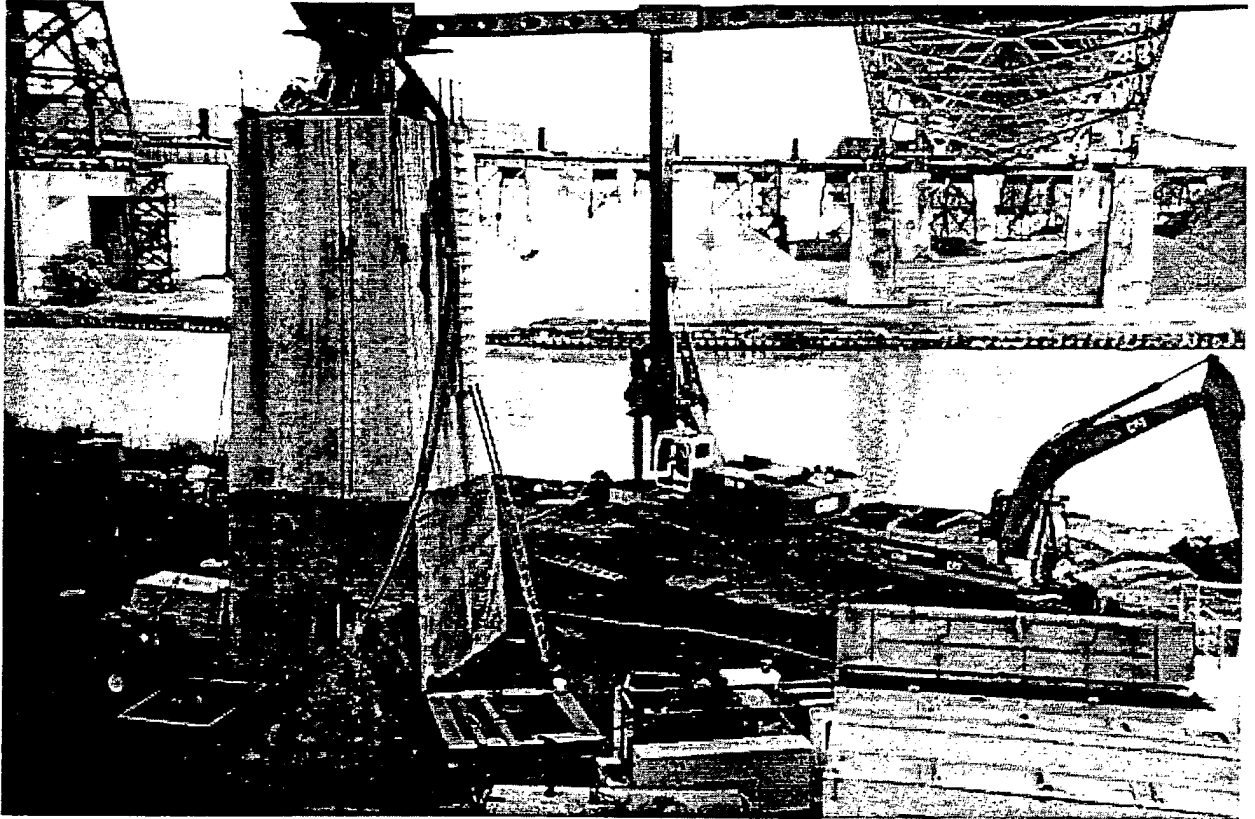


Fig. 7.13: Slurry tanks and shafts drilling.



Fig. 7.14: Use of polymer slurry.



Fig. 7.15: Inclinator casing in drilled shafts.

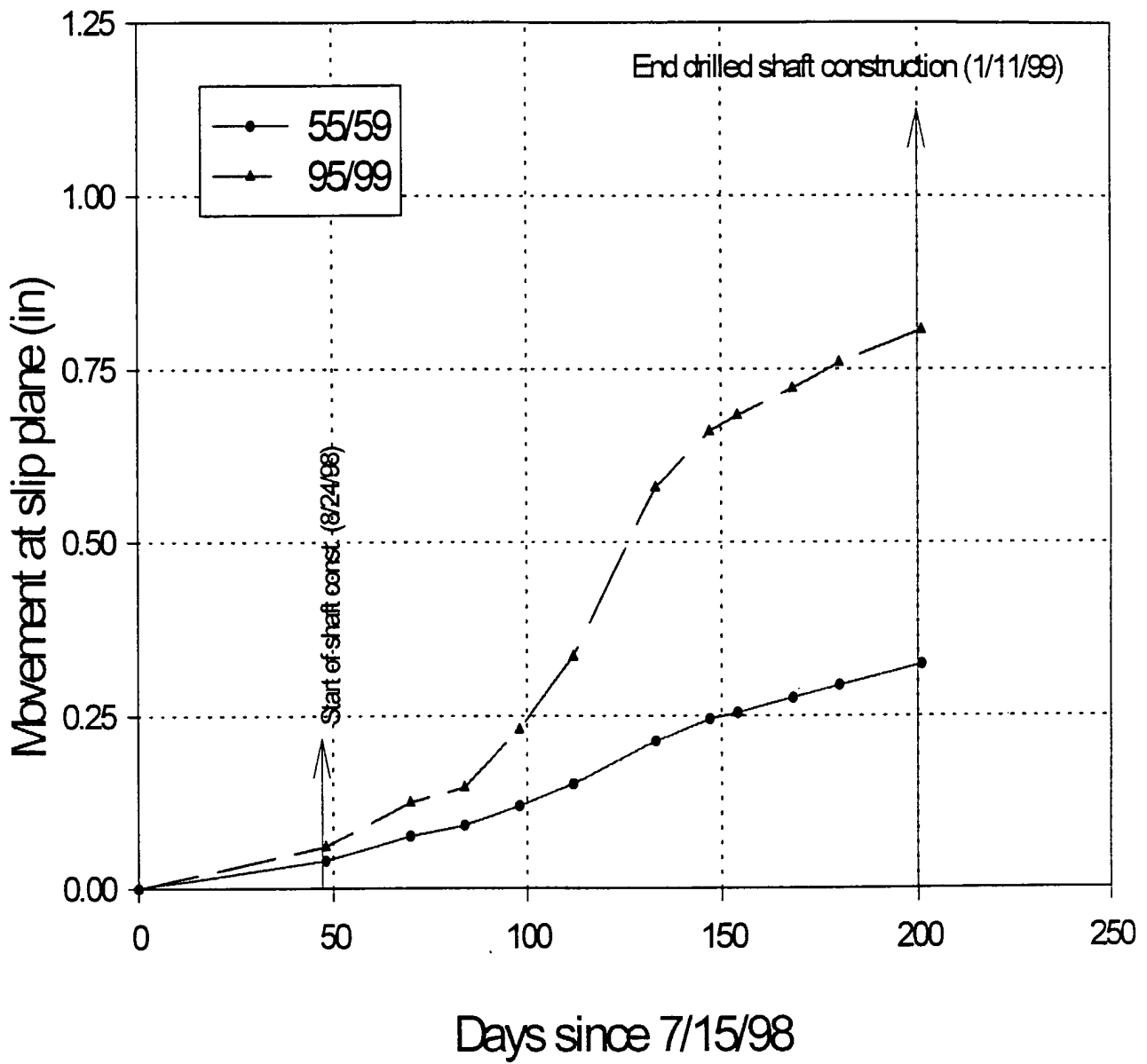


Fig. 7.16: Slope movement after completion of shaft installation, inclinometer B-303 (Stage IV).

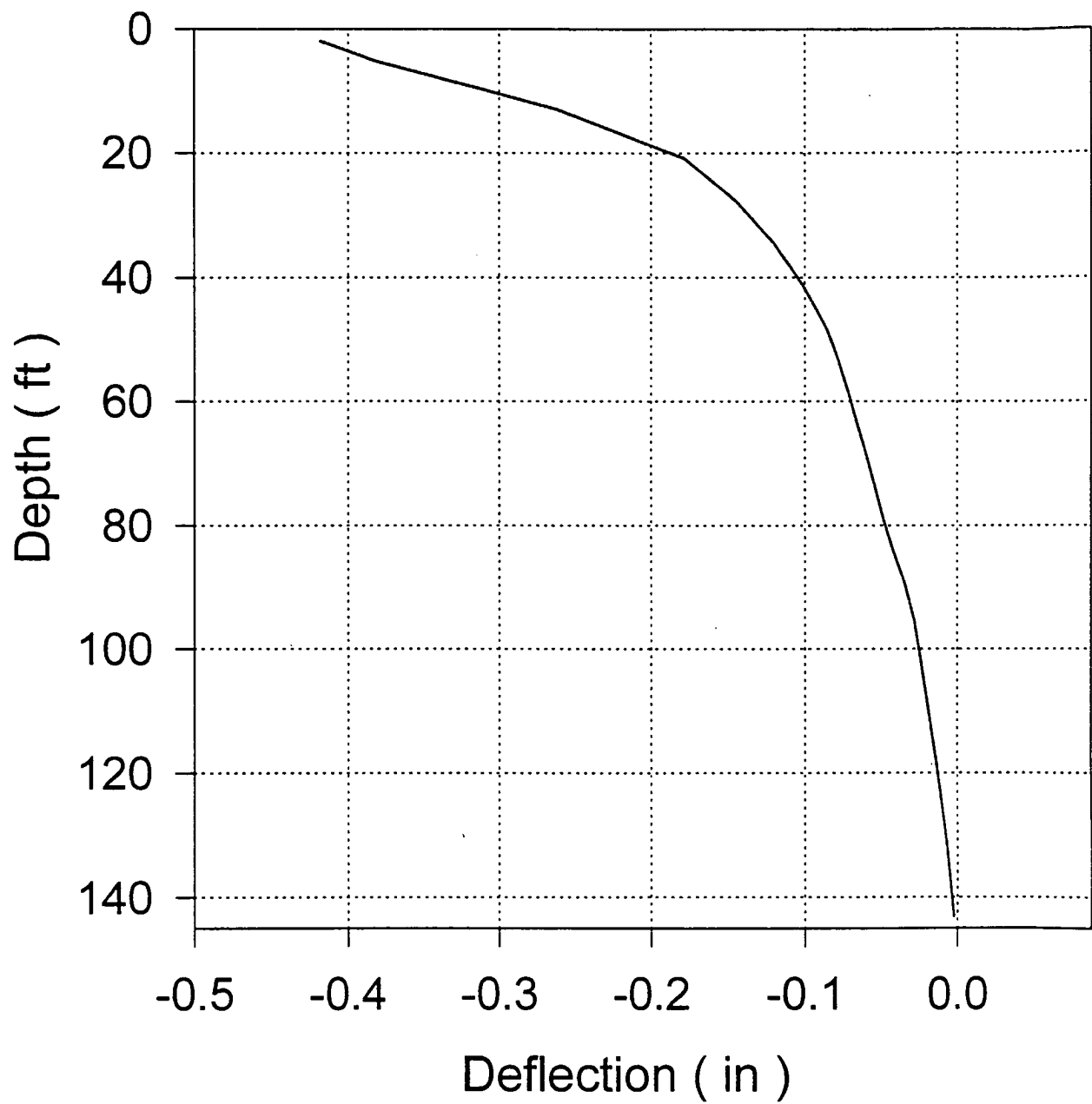


Fig. 7.17: Calculated pile deflection after anchor tensioning (Stage VI).

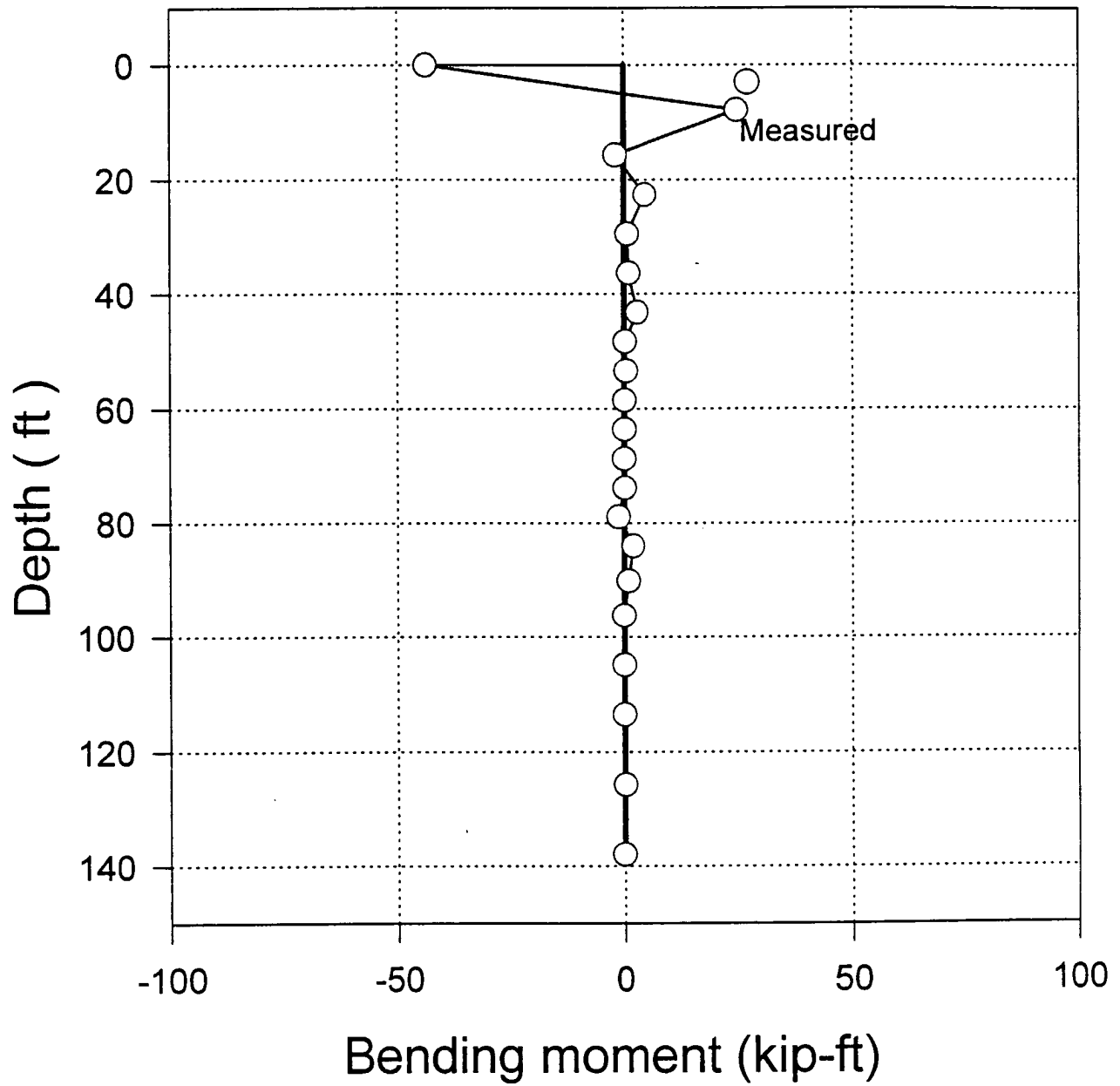


Fig. 7.18: Calculated pile bending moment after anchor tensioning (Stage VI).



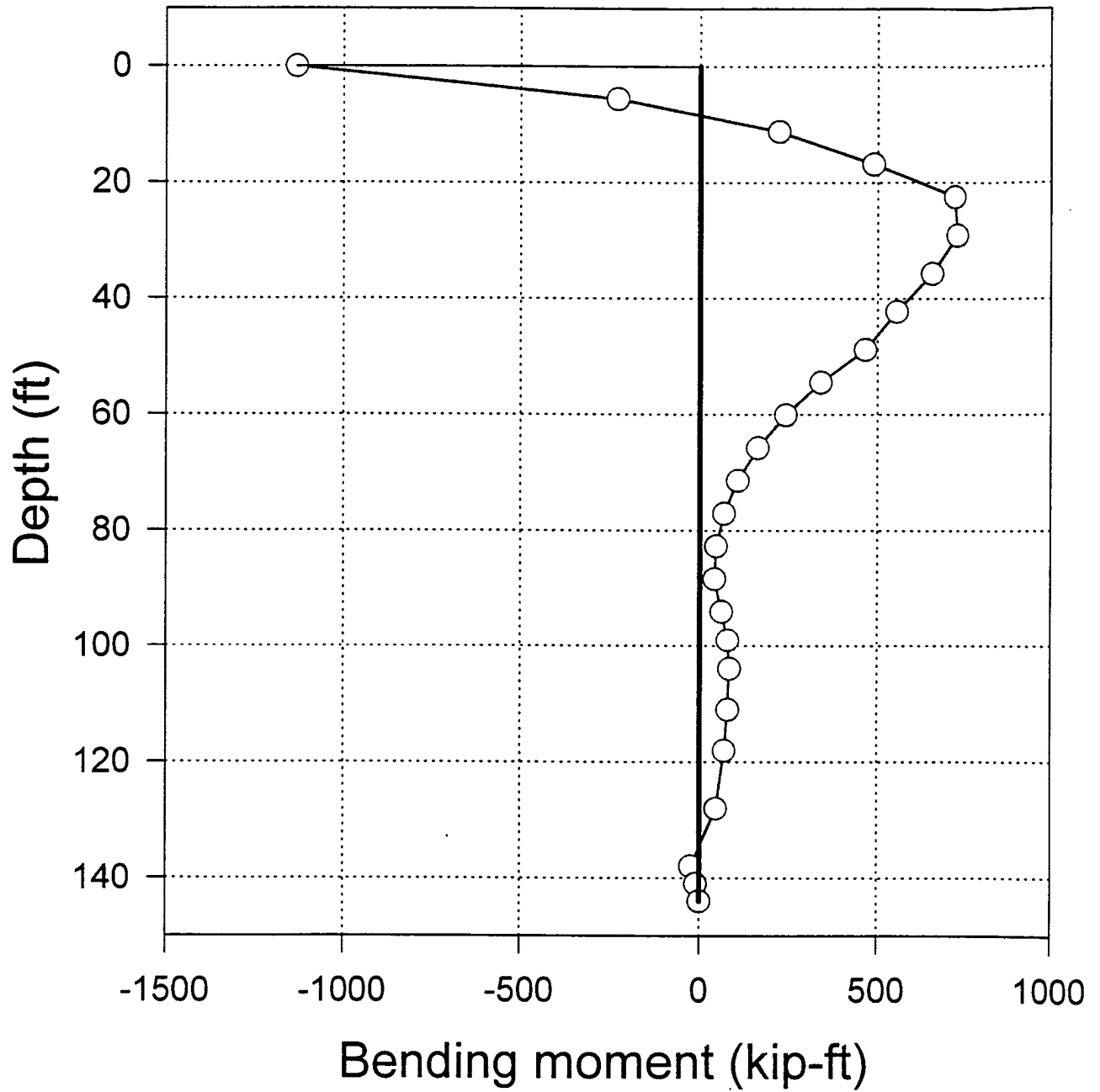


Fig. 7.19: Bending moment calculated by FEM in shafts after anchor tensioning (Case VI).

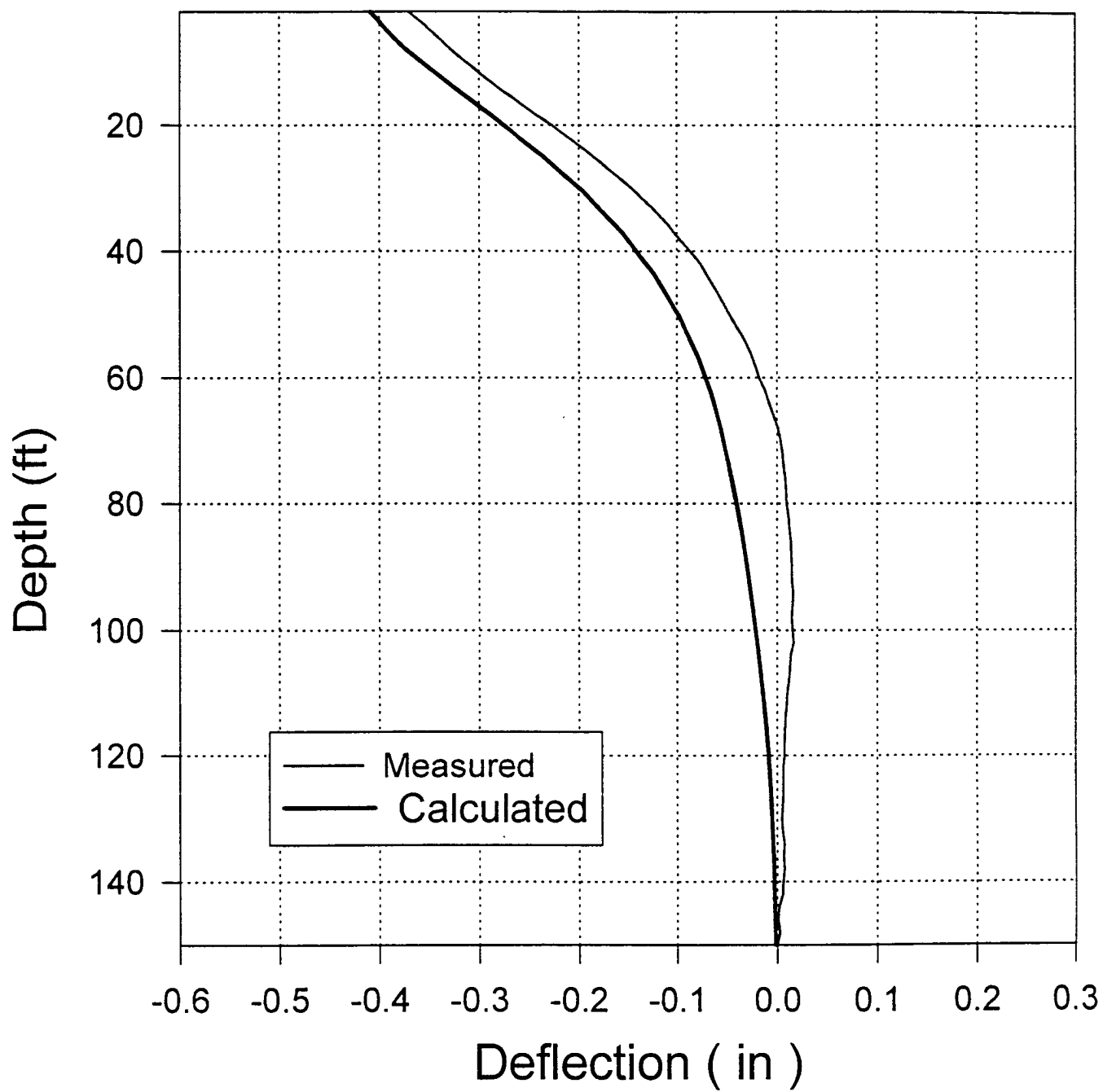


Fig. 7.20: Deflection of shafts calculated by FEM vs. measured after anchor tensioning (Stage VI).

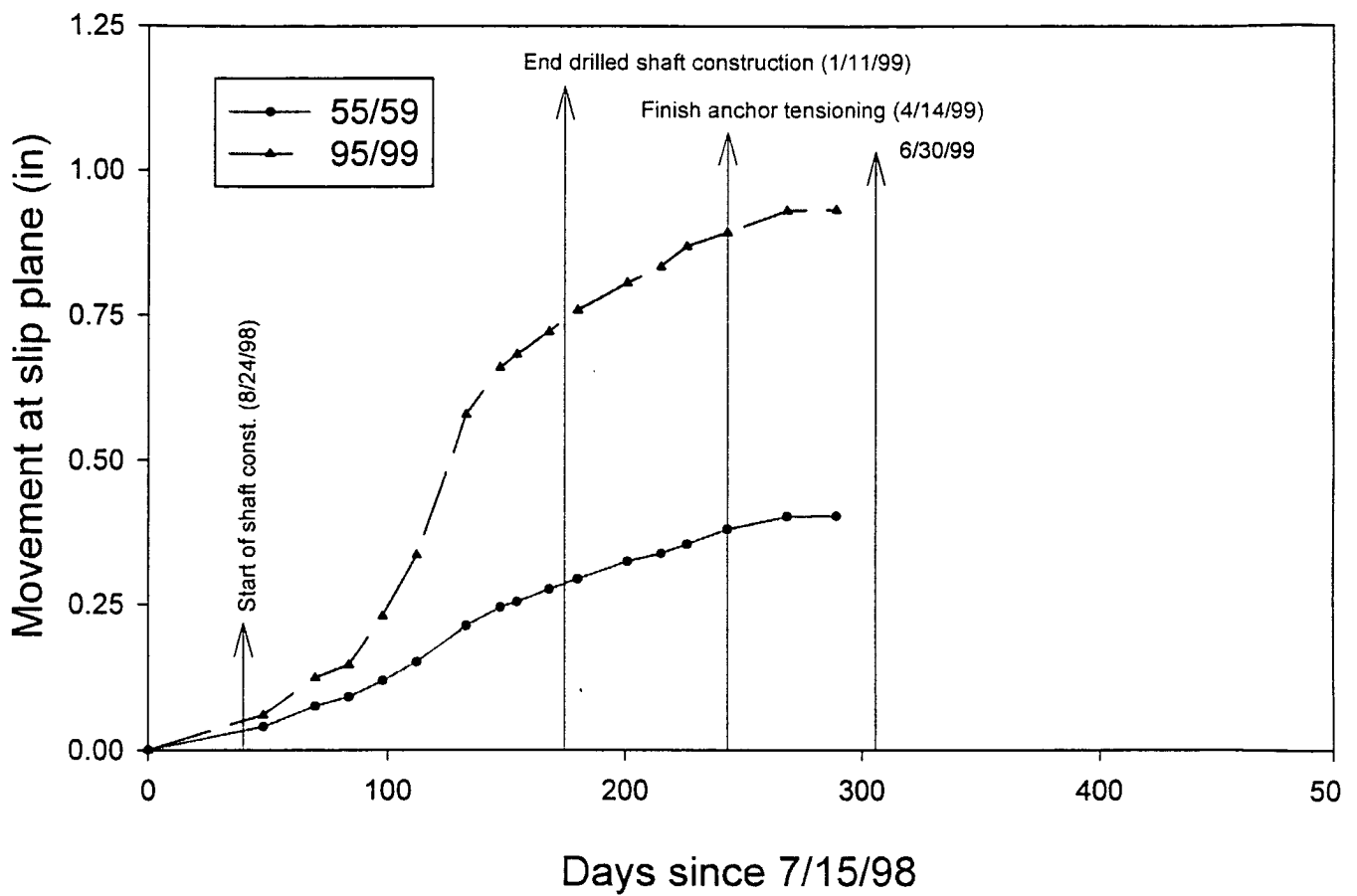


Fig. 7.21: Soil movement at B-303 after finishing anchors tensioning (Stage VI).



Fig. 7.22: Stress ratio at shallow slip plane after anchor tensioning (Stage VI).

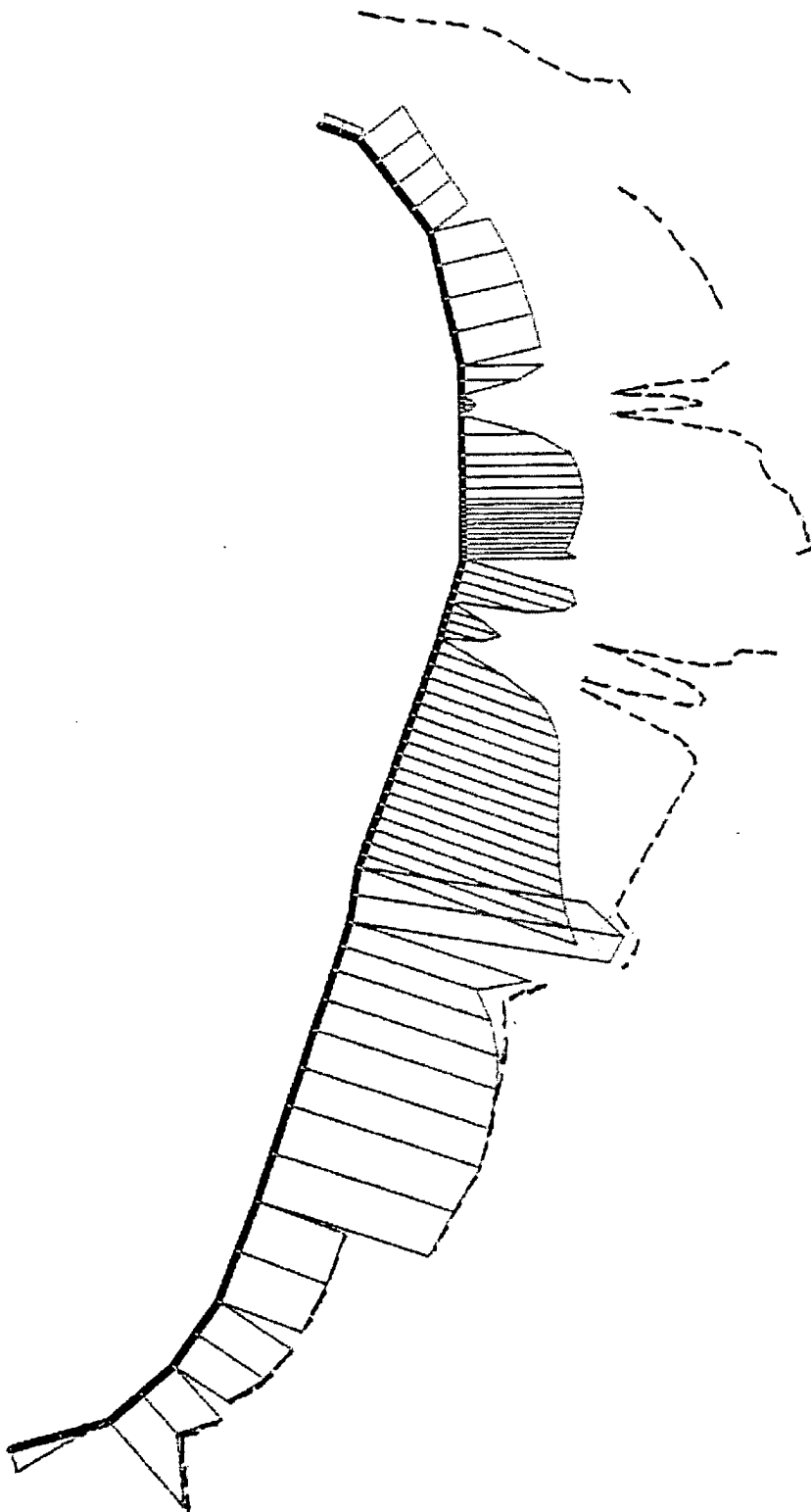


Fig. 7.23: Stress ratio at deep slip plane after anchor tensioning (Stage VI).

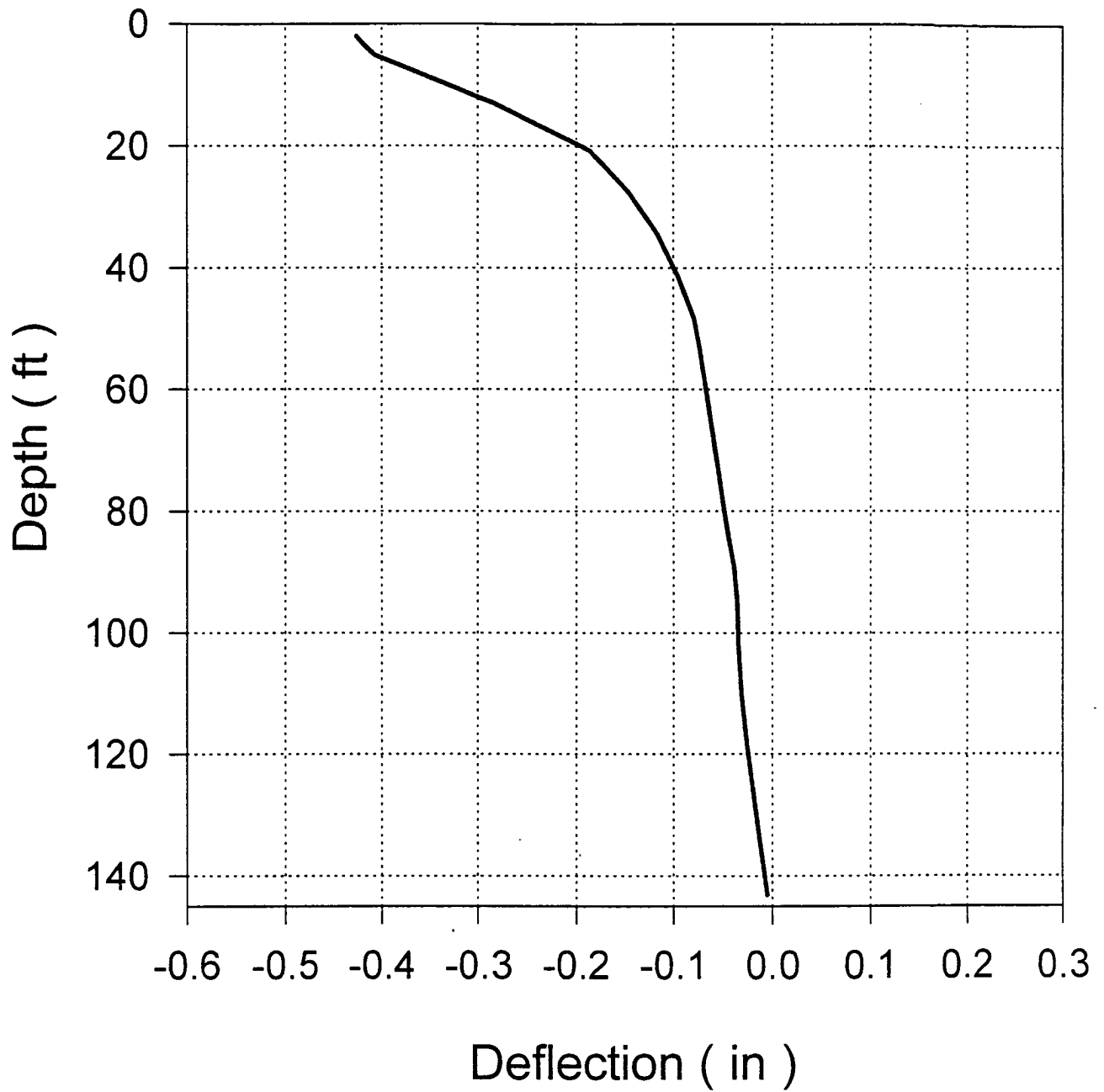


Fig. 7.24: Deflection of driven piles after backfilling to final grade (Stage VII).

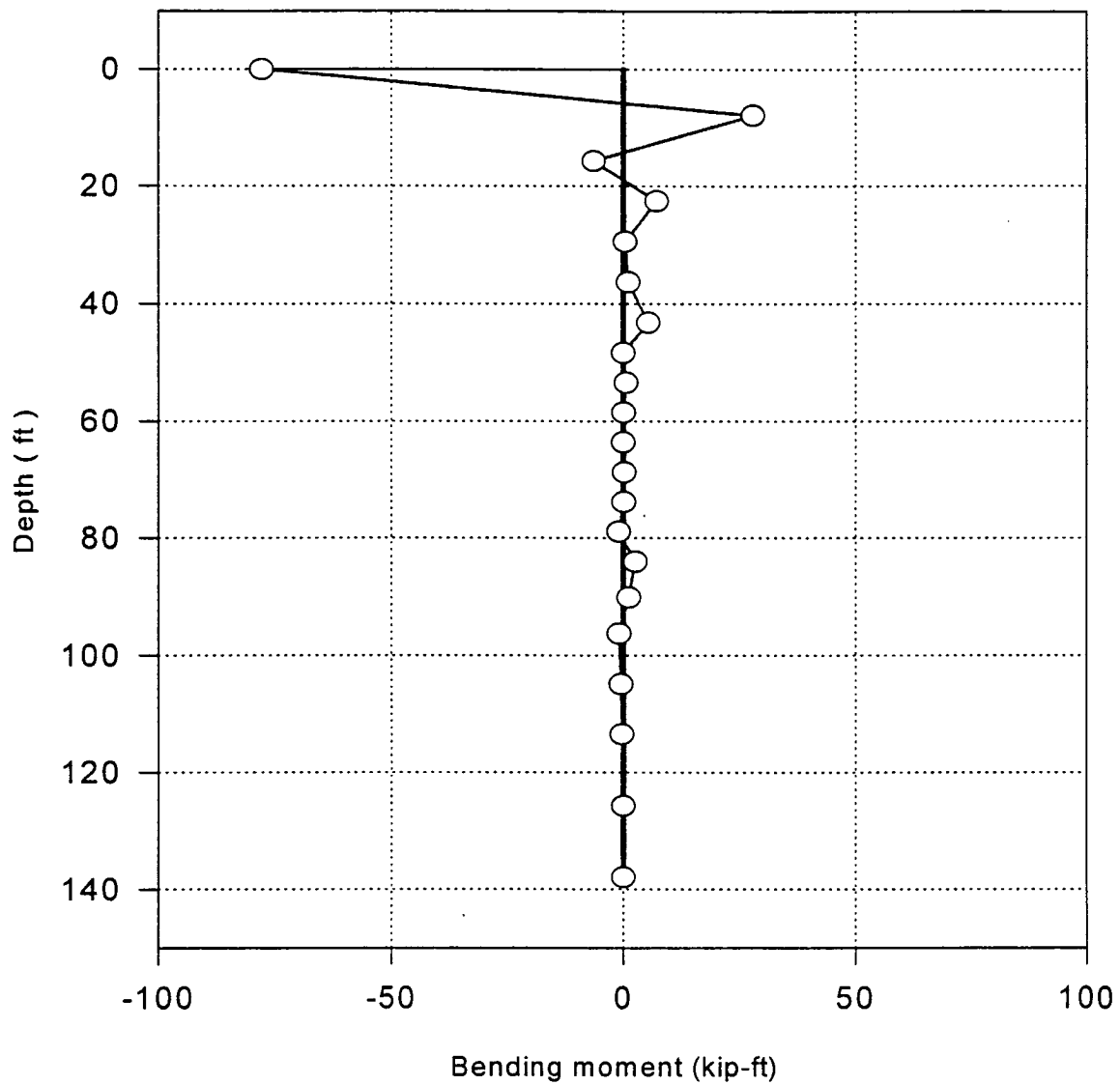


Fig. 7.25: Driven piles bending moment after backfilling the slope (Stage VII).

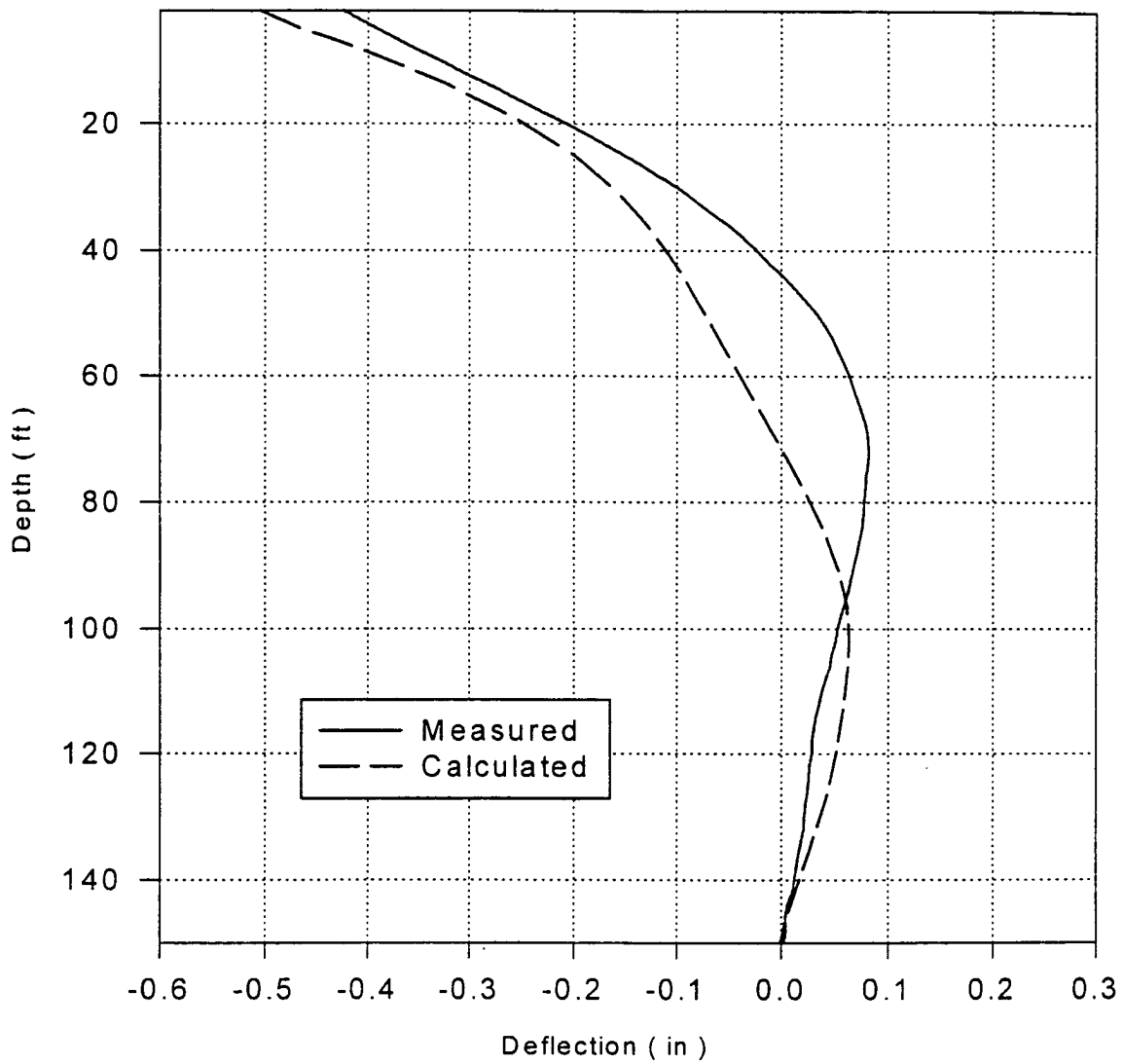


Fig. 7.26: Drilled shaft deflection after backfilling the slope (Stage VII).



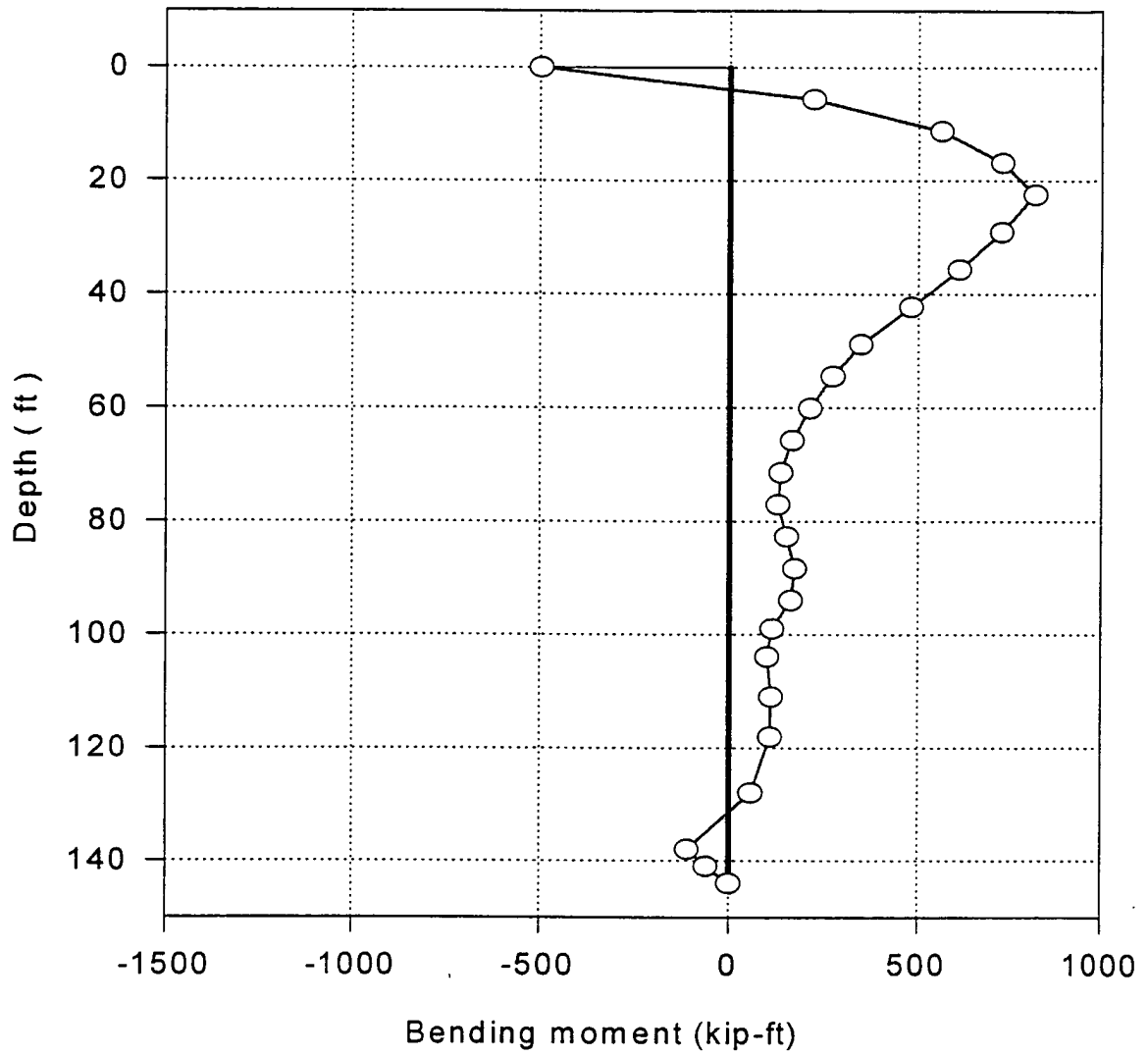


Fig. 7.27: Drilled shaft #9 bending moment after backfilling the slope (Stage VII).

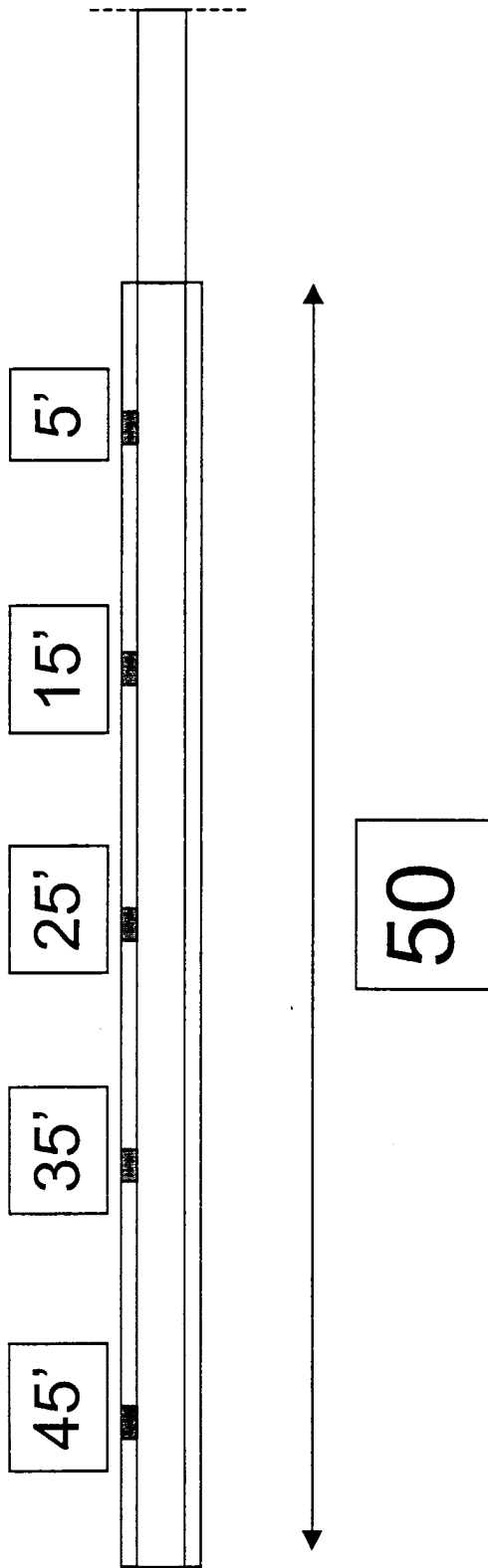


Fig. 7.28: Schematic of gage locations on the rock anchor.

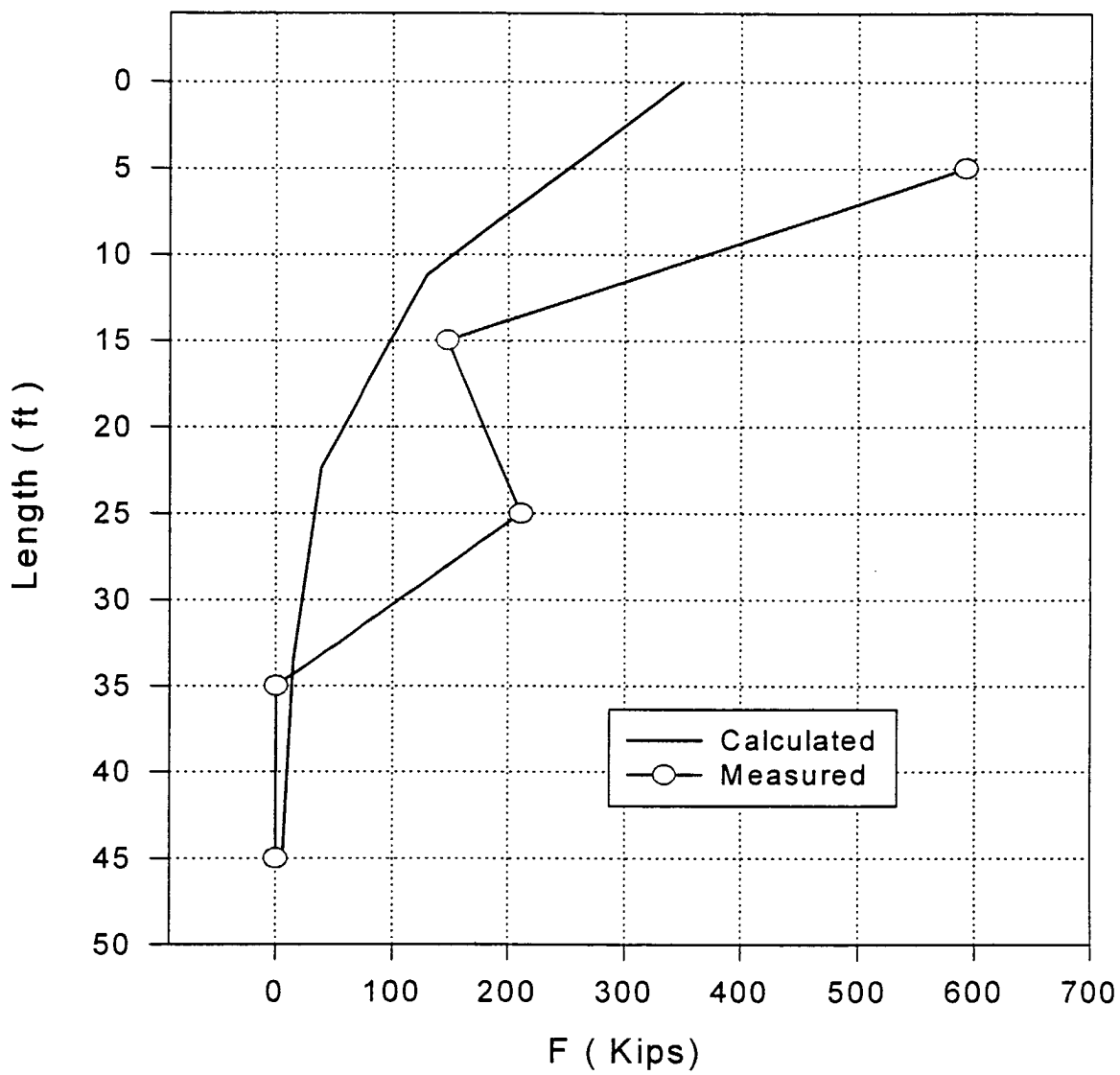


Fig. 7.29: Comparison between measured and calculated axial force along bond length of the anchor.

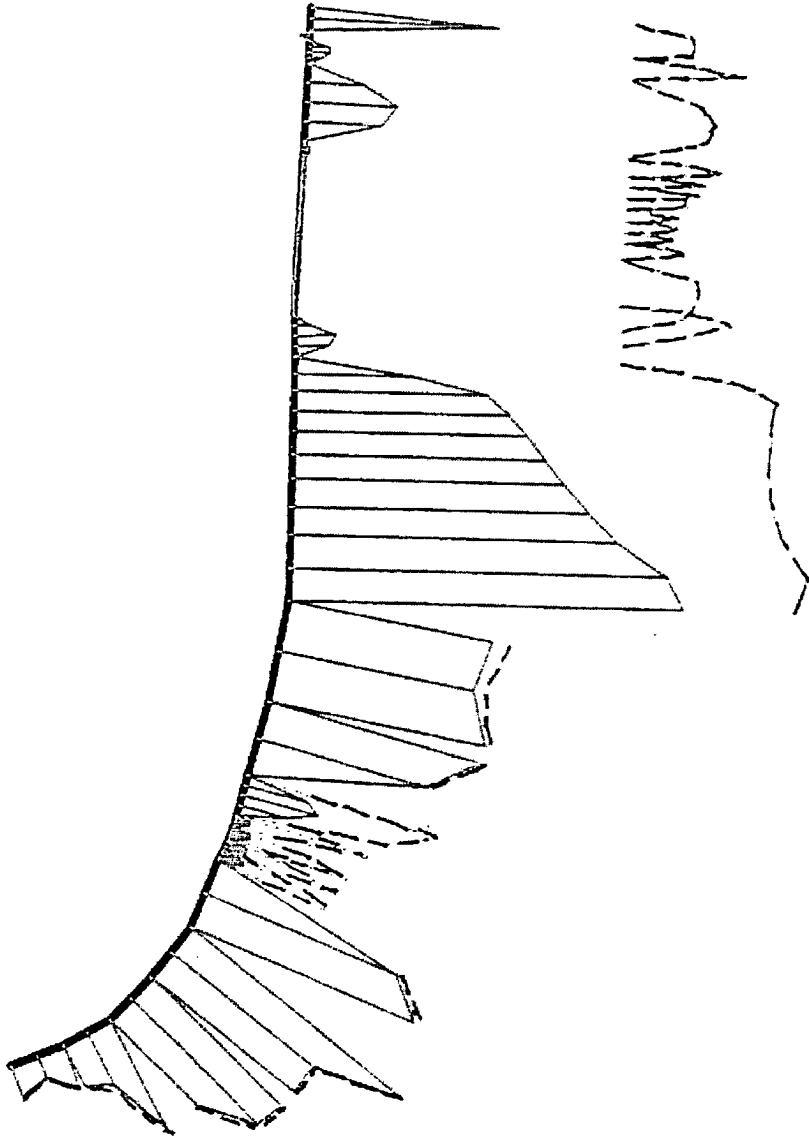


Fig. 7.30: Stress ratio at shallow slip plane (Stage VII).

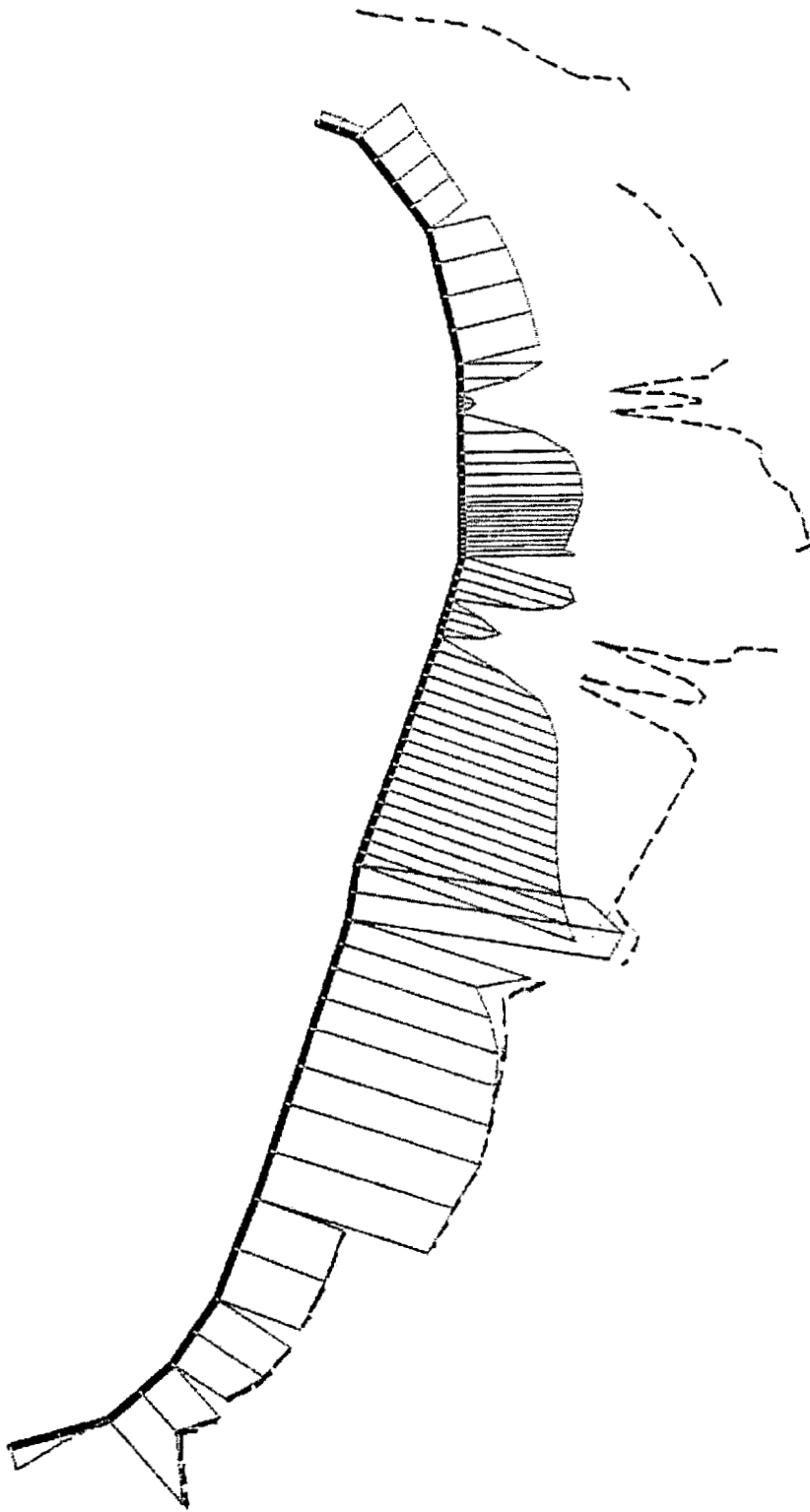


Fig. 7.31: Stress ratio at deep slip plane (Stage VII).

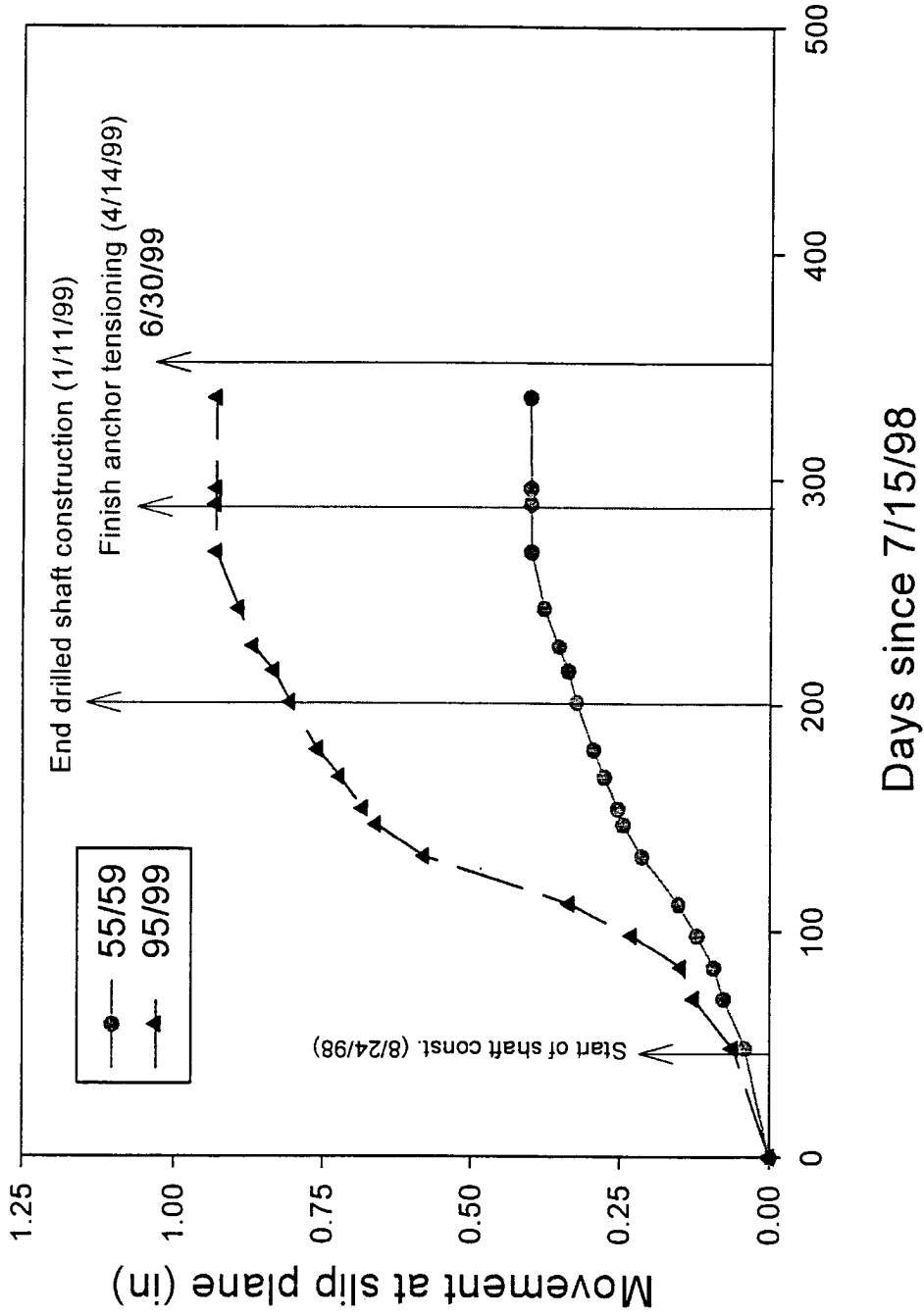


Fig. 7.32: Soil movement at B-303 at the end of monitoring phase I.

**End of monitoring phase I on 6/30/1999.**

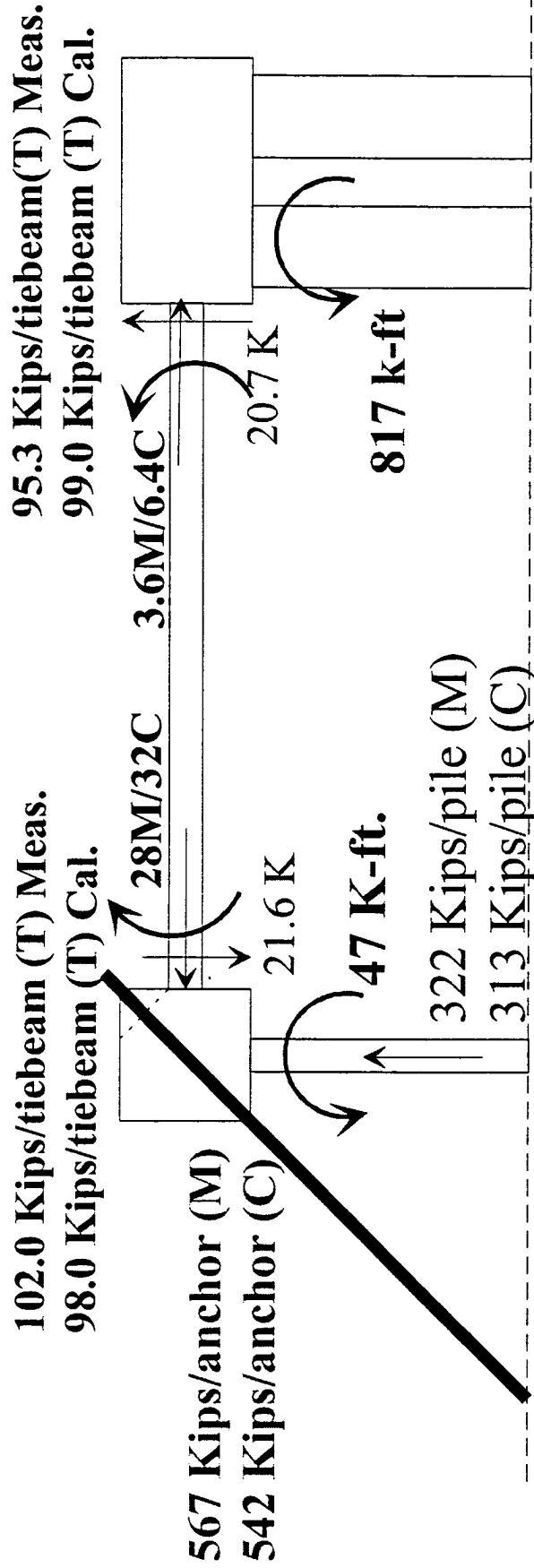


Fig. 7.33: Force diagram at the end of monitoring phase I on 6/30/1999.

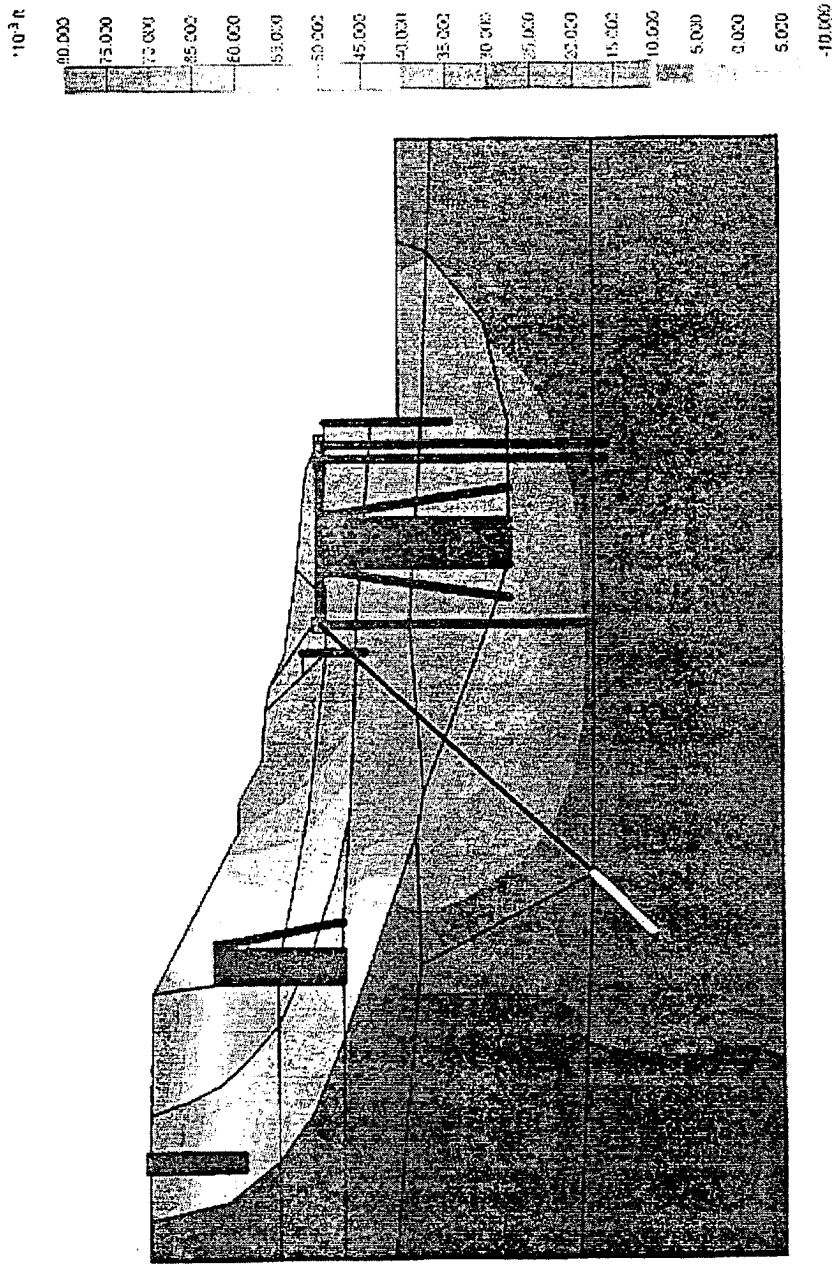
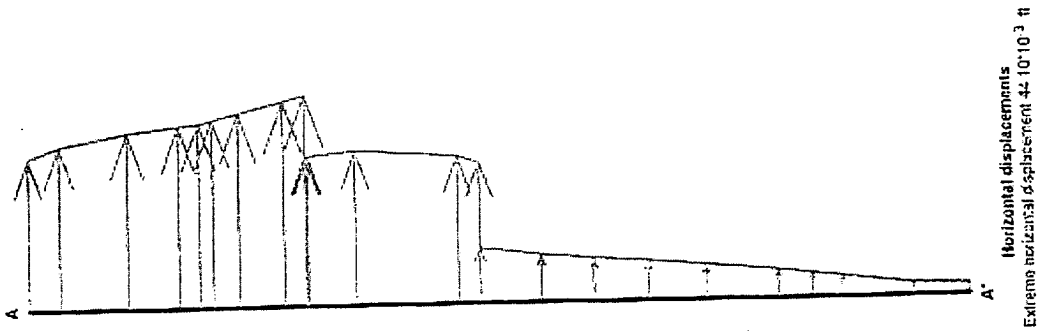


Fig. 7.34: Displacement and displacement contour due to overload.



## CHAPTER VIII

### SUMMARY AND CONCLUSIONS

#### VIII.1 Summary of Tasks Accomplished

During the course of the project, the following tasks have been successfully accomplished.

- a. A series of stability analysis have been performed for the existing slope condition to assess the strength parameters of the soil, in particular, the strength parameters of the slip surfaces. Pertinent soil properties have been summarized previously in Table 2.1.
- b. As part of the planning process, the instrumentation plan of various types of sensors has been developed and incorporated in the final design plan.
- c. All instrumentation sensors have been individually calibrated and checked prior to field deployment.
- d. All planned sensors have been successfully installed during construction according to the design plans. The locations of these sensors have been clearly identified and summarized in chapter 3. Altogether, these have been seven inclinometers installed in the drilled shafts #1, #3, #8, two in #9, #10, and #17. In addition, 5 tie-beams, each with a total of 8 strain gages, have been instrumented. The driven pile # 1, # 17, # 18, # 19, and # 34 have been each instrumented with 4 strain gages. Finally, the rock anchors # 1, # 8, # 9, and # 17 have been fully instrumented to include 5 strand gages in the bond zone and a load cell at the head of the instrumented rock anchors. To date, all gages have been functioning well, providing meaningful data for further analysis.

- e. Real-time monitoring of all sensors has been successfully carried out using the Geokon's datalogger system. Monitoring of the foundation behavior was commenced immediately after the sensors had been connected to the data acquisition system.
- f. As part of the study, a FEM program PLAXIS was employed to perform a numerical simulation. The FEM simulation process involved the calibration of soil properties to match the initial inclinometer reading from B-103 during initial site excavation. After this initial calibration, the soil parameters were fixed for the subsequent computer simulation of the subsequent construction stages. Since the soil behavior is highly nonlinear and stress-path dependent, the numerical simulation was carefully staged to mimic the actual construction stages in the field. However, the FEM did not possess the capability of capturing the time-dependent behavior of the soil, the soil creep was therefore not included in the analysis. The overall quality of the numerical simulation appeared to be very good, when the computed soil deformation and stresses in the foundation were compared favorably with the measured data. The close matching between the computed and measured behavior of the slope during the entire construction period lends credibility to the detailed information provided by the computer analysis.
- g. After the installation of the drilled shafts, a lateral load test on drilled shafts # 1 and # 3 was successfully conducted. The lateral load test was carried out to the extent when the full stroke of the hydraulic jack (10 inch) had been reached. Detailed measurements of the lateral load tests included the measured strains and deflections along the length of the shafts at each applied load. A class A prediction of the drilled shaft behavior has been done using the COM624 computer program with the p-y

curves derived from the correlations with the SPT N values. The predictions based on the SPT correlations appeared to be quite conservative, under predicting the drilled shafts deflection significantly. After the load test, a back calculation algorithm was used to back calculate the p-y curves from the "best-fit" technique outlined in chapter 6. The back calculated p-y curves, when used in the COM624 program, seemed to provide very good match with the actual measured shaft response at various load levels. It is noted that the drilled shafts at the project site are extremely long with heavy reinforcement. The normal p-y curves criteria may not be applicable to the shafts involved. Thus, the back calculation technique clearly demonstrated its potential uses in other projects involving the design and analysis of laterally loaded drilled shafts.

- h. Each rock anchor at the project site was proof tested in accordance with the Post Tensioning Institute (PTI) specifications except the instrumented ones. Instrumented anchors # 1, # 8, and # 17 were performance tested. Instrumented anchor # 9 was creep tested. Detailed test results of this rock anchor has been discussed in chapter IV. The test results indicated that the anchor met the creep criteria set forth in the PTI specifications. Furthermore, the strain gage readings during testing and after anchor lock-off showed that the bond length was adequate, as the gages located at the end of the bond zone registered zero load transfer.
- i. The measured data, together with detailed FEM simulation results, have provided a powerful and insightful picture of the behavior of the slope and the foundation structures. Of particular interest is the nature and amount of the stresses developed in the foundation structures. The numerical values of pertinent stresses in each

foundation have been compared with the ultimate load-carrying capacity of the structure. These comparisons were presented in detail in chapter 7. Based on these comparisons, it is re-assured that all the foundation structures would have adequate capacity to carry existing or potential future loads. It is worth mentioning that the primary stress contributors to the foundation structures appeared to come from the anchor tension force.

- j. The global stability of the slope with the constructed foundation structures has been assessed from two vantage points: The measured slope movement and the calculated stress ratios at the slip surfaces. The slope movement has slowed down significantly since the completion of anchor tensioning. Similarly, the stress ratio has been improved once the anchor tension force was activated.
- k. The FEM simulation was carried out for a hypothetical case in which the unit weight of the soil above the slip surfaces had been artificially increased by 20 percent. The purpose of the artificial overloading in the FEM simulation was to facilitate additional slippage along the slip surface. The calculated numerical values of additional stresses in the foundation structures have been summarized in Table 7.4, which can be used as a benchmark or reference for long-term monitoring. That is, some warning telltale signs could be spotted during long-term monitoring, allowing engineers to take cautionary measures in a timely fashion.

## VIII.2 Conclusions

Based on the experiences gained from field instrumentation and monitoring results, coupled with the detailed FEM simulation analysis results, the following conclusions can be made.

- a. Construction itself can cause significant slope instability, particularly when activities such as excavation at the toe of the slope, pile driving, and boring holes for cast-in-place shafts. Therefore, it is imperative that engineers pay attention to these construction activities during remediation of a slope stability problem.
- b. The design of drilled shafts for stabilizing the slope was based on the assumption that active earth pressure could have developed and fully thrust upon the shafts. This may be a very conservative approach, as it ignores the arching developed behind the drilled shafts. It also appears that if rock anchors are used at the site, the tensioning force would reduce the amount of earth thrust acting on the drilled shafts as well. Therefore, it maybe concluded that if a slope stabilization scheme involves the use of a combination of drilled shafts and rock anchors, then the amount of earth thrust acting on the drilled shafts could be smaller than the anticipated from the active earth pressure theory. Moreover, the stresses measured in the drilled shafts seemed to be derived primarily from the anchor tensioning force.
- c. The design of geotechnical structures usually involves uncertainties about soil profile, soil properties, and mechanisms of the soil-structure interaction; therefore, it is prudent to incorporate the concept of structure redundancy. This project shows a sensible way of ensuring multiple defensive structures, while fulfilling

the design criteria set forth by the owner. Specifically, the use of the rock anchors was deemed necessary to minimize the amount of structural deflection of the drilled shafts due to earth thrust. However, the added benefit from the use of rock anchors is that the reduction of the amount of earth thrust applied to the shafts. As a result, much improved global stability and much higher safety margin was realized for the slope and each foundation element, respectively.

- d. Instrumentation and monitoring of geotechnical structures in the project has provided very useful factual data and important insights on the behavior of the slope, thus assisting the project engineers to make time-sensitive, critical decisions during construction. The benefits of making informed decisions in a major construction project can be enormous, including, but not limited to, avoidance of change orders, construction delays, additional engineering design work.
- e. This project clearly demonstrated that instrumentation and monitoring can serve the purpose of construction quality assurance as well. If the construction of foundation structures involved defects, such as broken H-piles, necking in the drilled shafts, the inclinometer reading would certainly reveal anomaly. Also, the inclinometer reading served the function of ensuring slope stabilization, as the relative slip movement at the two critical slip surfaces had been stopped.
- f. The technology of vibrating-wire based strain gages has been shown to provide long-term, reliable strain measurements in a very difficult construction site. The planning, hands-on experiences, dedication of engineers, cooperation from

contractors, and efficient data reduction software all played important role to ensure the success of the field instrumentation/monitoring project.

- g. A combined technique involving field instrumentation/monitoring and FEM simulation provides a powerful tool for design verification. This is particularly important for projects involving innovative/new designs, unknown/uncertain soil properties, and lack of existing design/analysis methodology.
- h. The deployment of instrumentation sensors during the construction (birth) of the foundation structure can be used throughout its life for diagnostics of any maintenance needs.





## CHAPTER IX

### REFERENCES

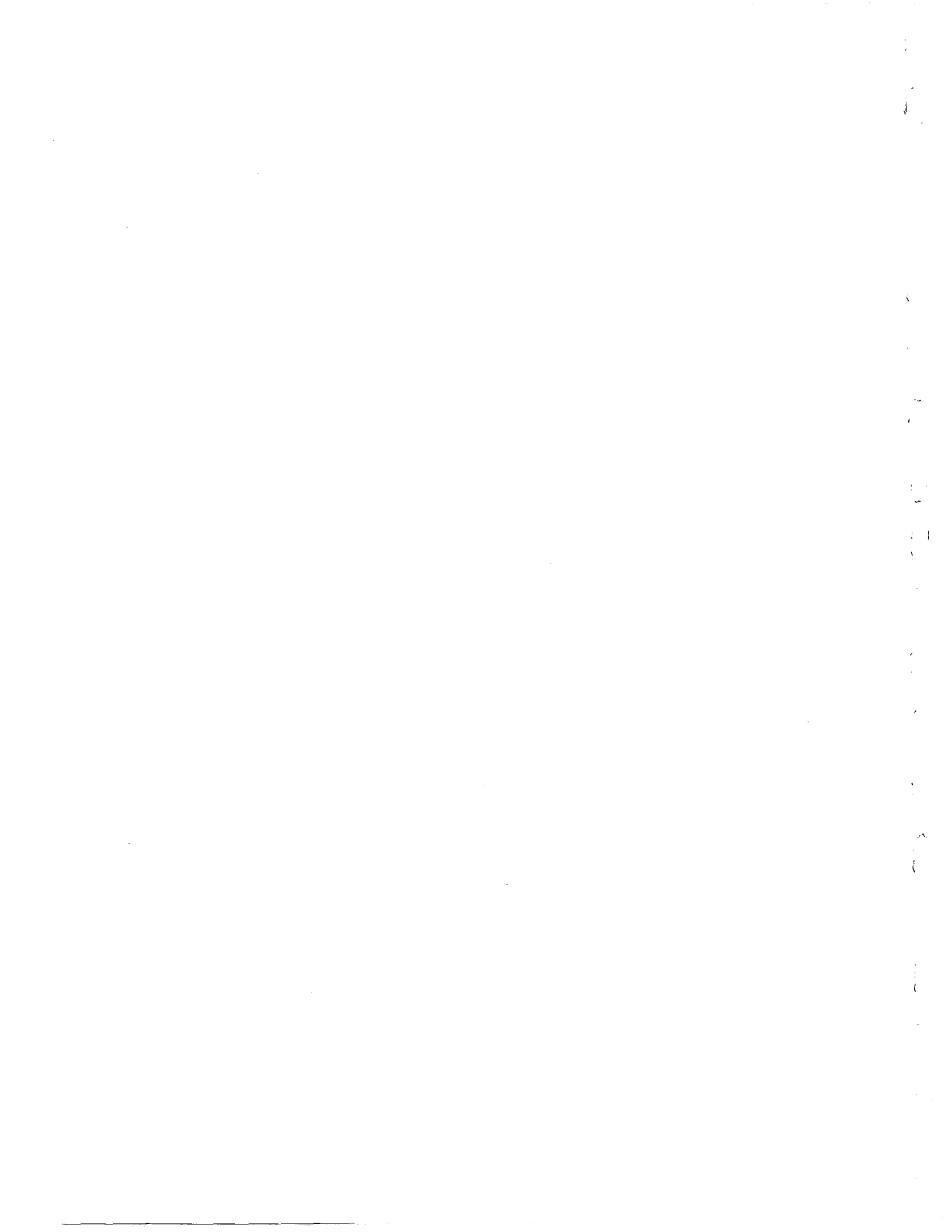
1. Brown, D.A., Shie, C.F. (1990), "Three - Dimensional Finite Element Model of Laterally Loaded Piles", Computers and Geomechanics, Elsevier Publishers Ltd., England, pp. 59-79.
2. Brown, D.A., Shie, C.F. (1989), "P-y curves for laterally loaded piles derived from three-dimensional finite element model", Numerical Models in Geomechanics, Ed. S. Pietruszczak & G. N. Pande, Elsevier Appl. Sci. Publishers, pp. 683-690.
3. Brown, D.A., Hidden, S.A., and Zhang, S. (1994), "Determination of P-Y curves using inclinometer data", ASTM.
4. Dunnycliff, J. (1988). "Geotechnical Instrumentation for Monitoring Field Performance", Wiley.
5. Hanna, T. H. (1982), "Foundation in tension: Ground anchors", Tran tech publication and McGraw-M book company.
6. McVay, M., Hays, C., Hoit, M. (1996a), "User's Manual for FLORIDA PIER, Version 5.1", Department of Civil Engineering, University of Florida, Gainesville, Florida.
7. Plaxis, B. V., (1998), "PLAXIS – Finite Element Code for Soil and Rock Analysis", Ver. 7, Netherlands.
8. Post-Tensioning Institute (1996), " Recommendations for Prestressed Rock and Soil Anchors", Third Edition.

9. Poulos, H.G. and Davis, E.H. (1980), "Pile Foundation Analysis and Design", John Wiley and Sons.
10. Prakash, S. and Sharma, H.D. (1990). "Pile Foundation in Engineering Practice", John Wiley & Sons, Inc.
11. Reese, L.C. (1984). "Handbook on Design of Piles and Drilled Shafts Under Lateral Load", FHWA-IP-84-11, 386 pp.
12. Reese, L.C. and Wang, T. (1994). "Analysis of Piles Under Lateral Loading With Nonlinear Flexural Rigidity", Proceedings, International Conference on Design and Construction of Deep Foundations, Vol. II, pp. 842-856.
13. Reese L. C., Wang, S. T. and Fouse, J. L. (1992). "Use of drilled shafts in stabilizing a slope", Proc. of a specialty conference on stability and performance of slopes and embankments, Berkeley.
14. Reese, L. C. (1977), "Laterally Loaded Piles: Program Documentation", JGED, ASCE, Vol. 103, No.GT4, April, pp. 286-305.
15. Richland Engineering Limited (1996), "Preliminary Design Report, CUY-90-15.24 Central Viaduct, PID No. 12374, Stabilize Pier 1 and Relocate Span 1", January.
16. Schnabel, H. Jr. (1982), "Tiebacks in foundation engineering and construction", McGraw-Hill book company, New York.
17. Terzaghi, K. (1954), "Theoretical Soil Mechanics", Wiley, New York.
18. Wang, S. and Reese, L.C. (1993). "COM624P- Laterally Loaded Pile Analysis Program for the Microcomputer, Version 2.0", Report No.FHWA-SA-91-002, U.S. Department of Transportation, Federal Highway Administration, Washington, DC.

APPENDICES



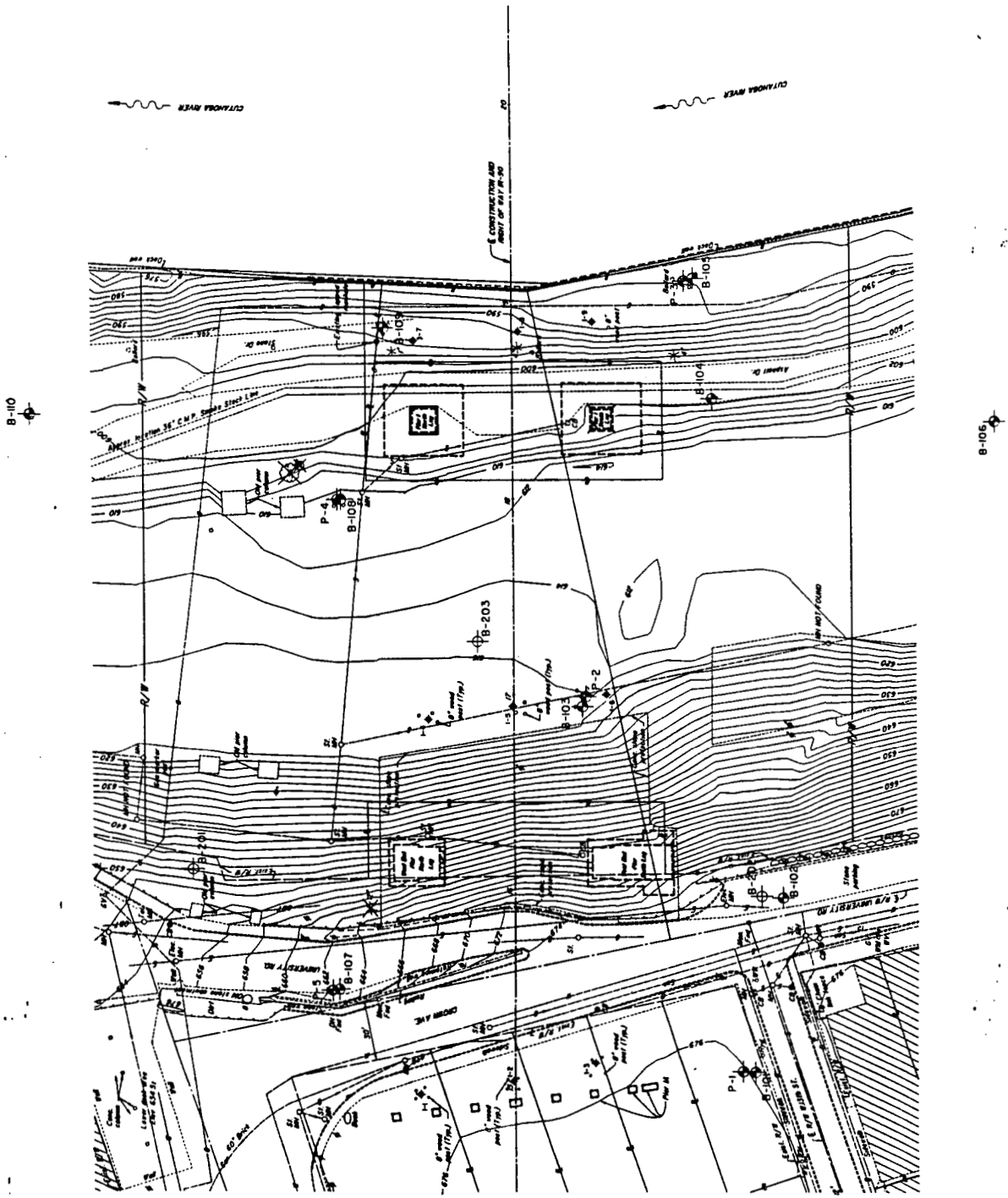
Appendix A: Detailed information about the soil borings for inclinometers and piezometers installed by BBC&M, Inc. in 1994.











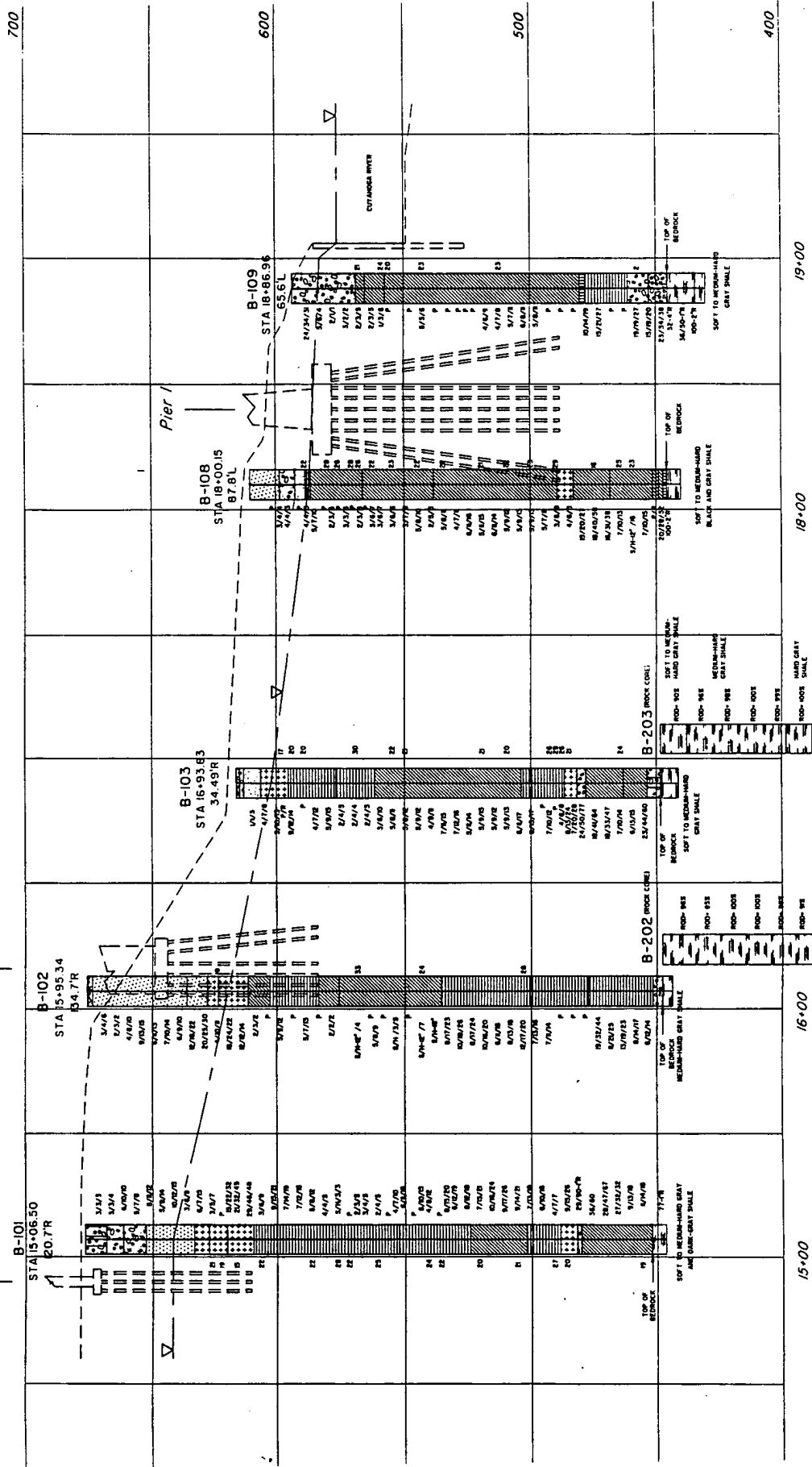
**LEGEND**

- B-1 SLOPE INDICATOR INSTALLED BY  
MCCAN ENGINEERING, INC. (1994)
- P-1 PERIMETER INSTALLED BY  
MCCAN ENGINEERING, INC. (1994)
- B-10 SLOPE INDICATOR INSTALLED BY  
COOT ENGINEERING
- B-201 BORING LOCATION DRILLED IN 1994

SCALE



Pier IA West End Pier

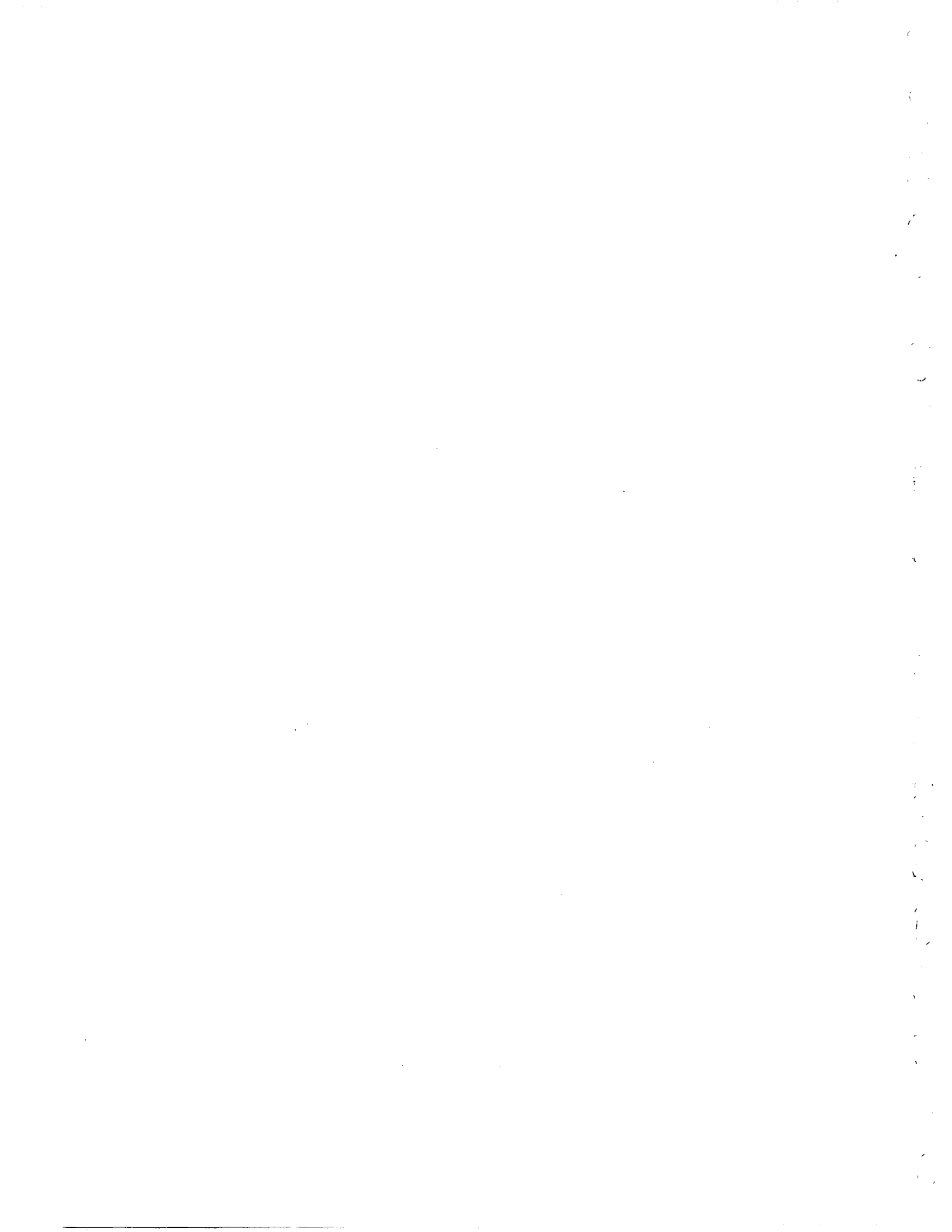










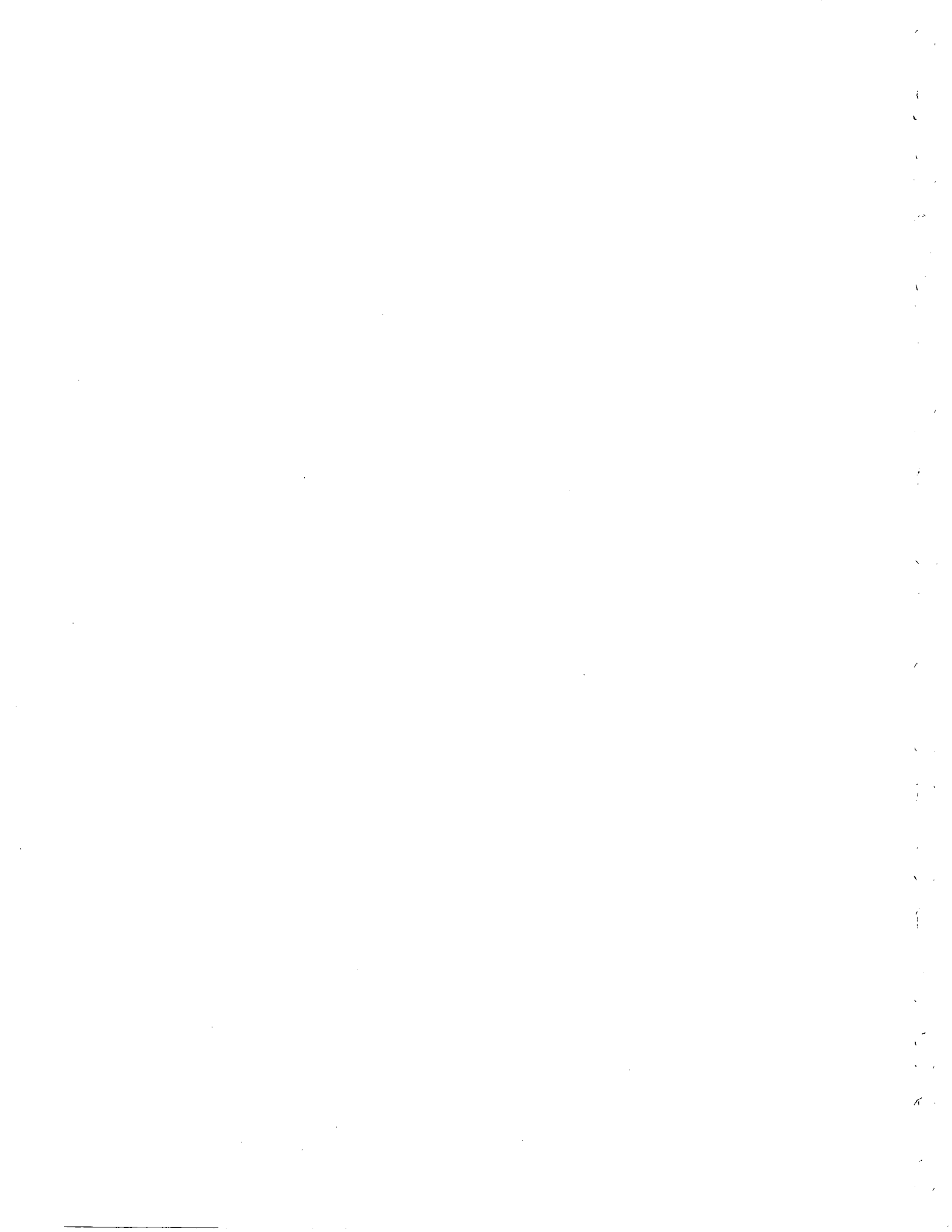


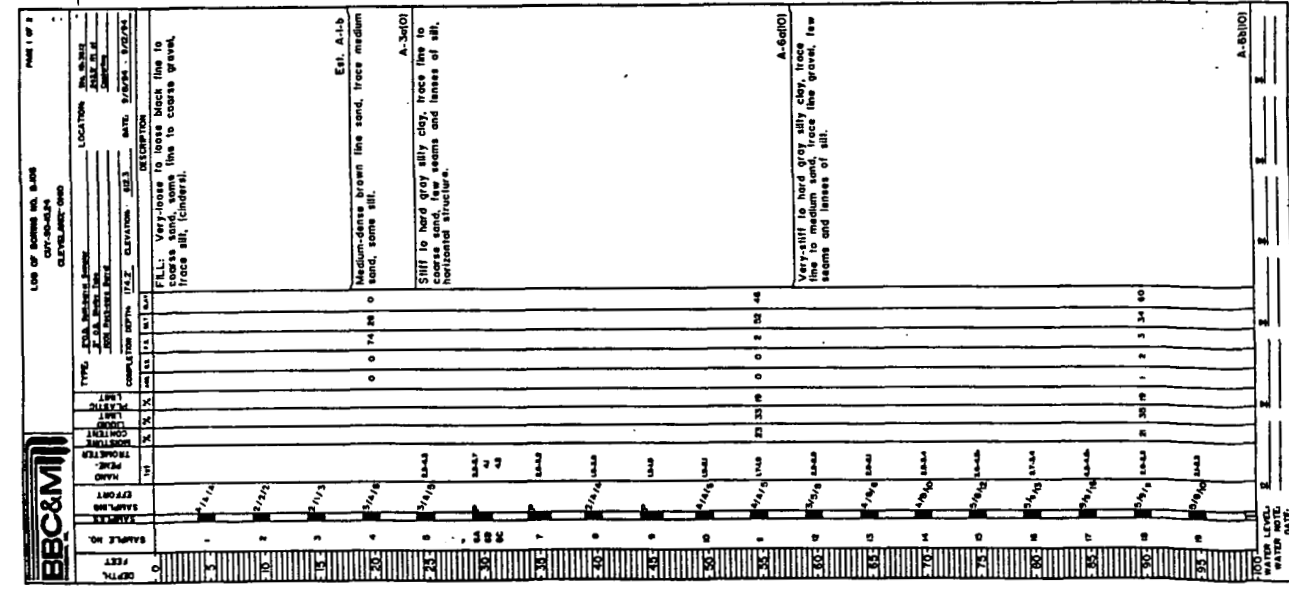
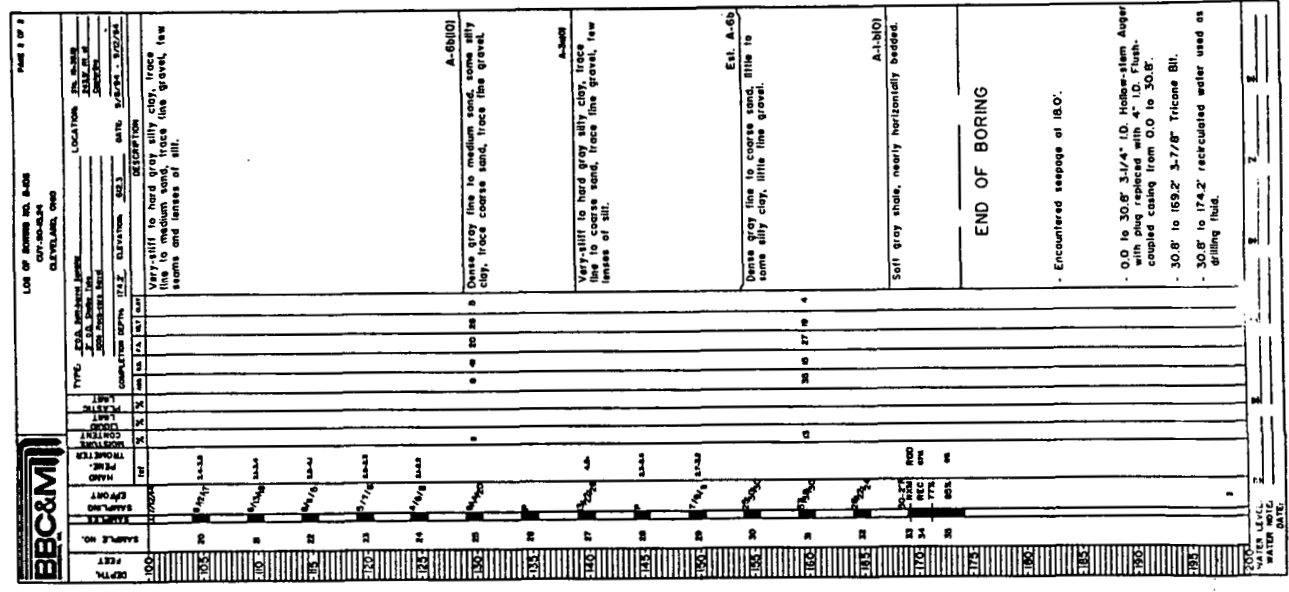
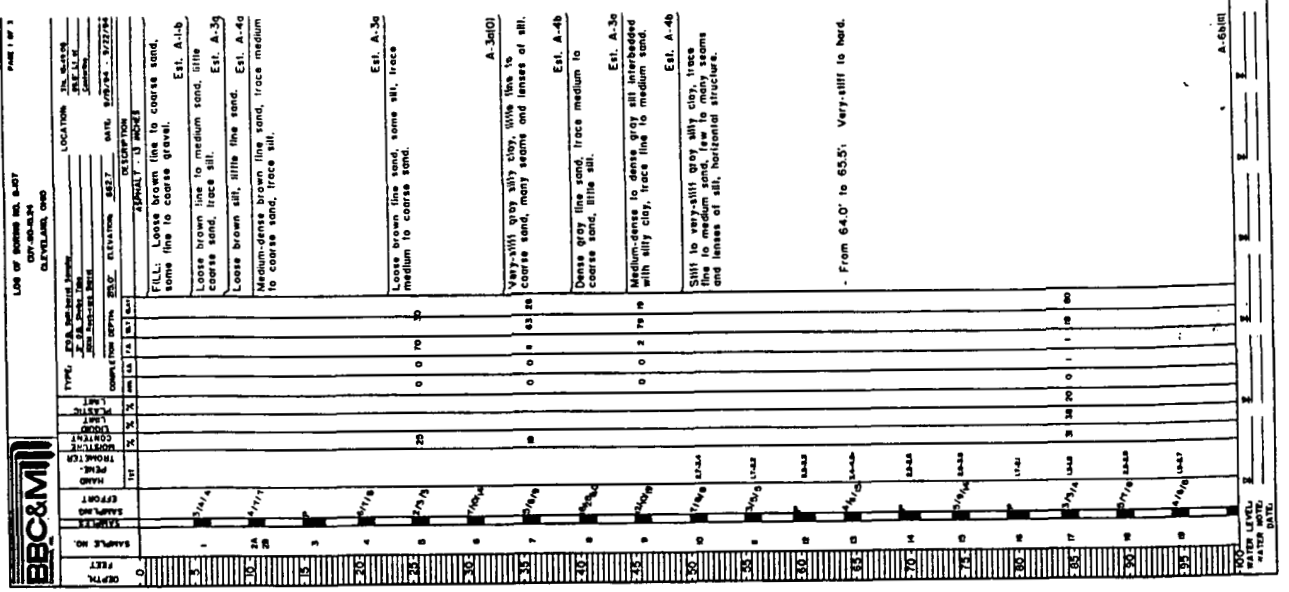










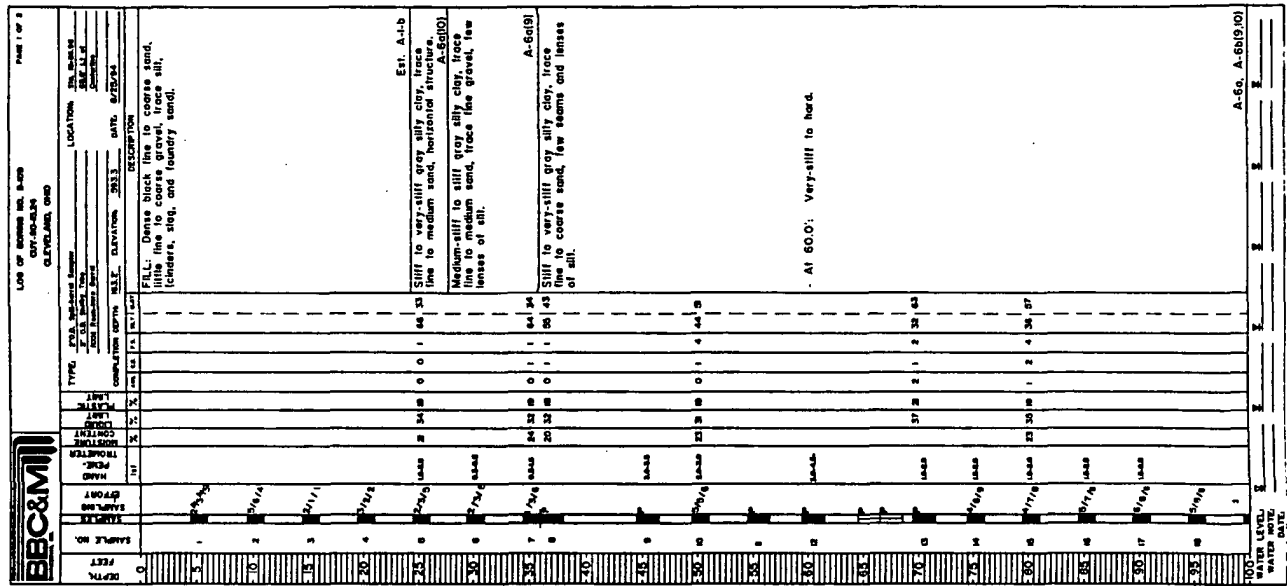
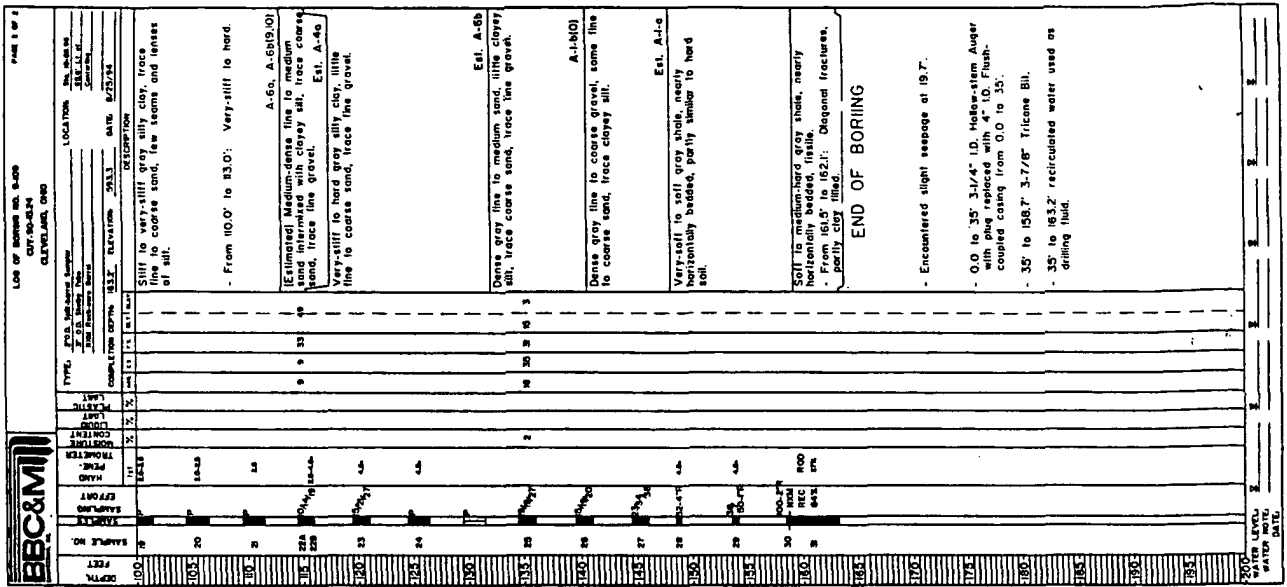














LOG OF BORING NO. 6-4  
CITY-BOULEVARD  
CLEVELAND, OHIO

PAGE 1 OF 3

DEPTH FEET	SAMPLE NO.	STARTING EFFORT	HEAD EFFORT	TRAILER EFFORT	TYPE OF SOIL	COMPLETION DEPTH FEET	ELEVATION FEET	DATE BORING RUN	LOCATION IN BLOCK	DESCRIPTION
0										
1	1	3 1/2	1 1/2			0	100	6/27/51 - 9/2/51	CITY-BOULEVARD	FILL. Loose brown and black fine to coarse gravel, some to "and" fine to coarse sand, trace to little clayey silt, (clayey and shaly).
10	2	2 1/2	1 1/2			0	90			Est. A-1-b Very-fine brown and grey silt, "and" fine sand, trace medium to coarse sand.
15	3	2 1/2	1 1/2			0	85			Est. A-1-b Medium-stiff to stiff grey silty clay, trace fine to medium sand, few lenses of silt.
20	4	2 1/2	1 1/2			0	80			Est. A-1-b Stiff to very-stiff grey silty clay, trace fine to medium sand, many lenses of silt and fine sand.
25	5	2 1/2	1 1/2			0	75			Est. A-1-b Stiff to very-stiff grey silty clay, trace fine to medium sand, many lenses of silt and fine sand.
30	6	2 1/2	1 1/2			0	70			Est. A-1-b Stiff to very-stiff grey silty clay, trace fine to medium sand, many lenses of silt and fine sand.
35	7	2 1/2	1 1/2			0	65			Est. A-1-b Stiff to very-stiff grey silty clay, trace fine to medium sand, many lenses of silt and fine sand.
40	8	2 1/2	1 1/2			0	60			Est. A-1-b Stiff to very-stiff grey silty clay, trace fine to medium sand, many lenses of silt and fine sand.
45	9	2 1/2	1 1/2			0	55			Est. A-1-b Stiff to very-stiff grey silty clay, trace fine to medium sand, many lenses of silt and fine sand.
50	10	2 1/2	1 1/2			0	50			Est. A-1-b Stiff to very-stiff grey silty clay, trace fine to medium sand, many lenses of silt and fine sand.
55	11	2 1/2	1 1/2			0	45			Est. A-1-b Stiff to very-stiff grey silty clay, trace fine to medium sand, many lenses of silt and fine sand.
60	12	2 1/2	1 1/2			0	40			Est. A-1-b Stiff to very-stiff grey silty clay, trace fine to medium sand, many lenses of silt and fine sand.
65	13	2 1/2	1 1/2			0	35			Est. A-1-b Stiff to very-stiff grey silty clay, trace fine to medium sand, many lenses of silt and fine sand.
70	14	2 1/2	1 1/2			0	30			Est. A-1-b Stiff to very-stiff grey silty clay, trace fine to medium sand, many lenses of silt and fine sand.
75	15	2 1/2	1 1/2			0	25			Est. A-1-b Stiff to very-stiff grey silty clay, trace fine to medium sand, many lenses of silt and fine sand.
80	16	2 1/2	1 1/2			0	20			Est. A-1-b Stiff to very-stiff grey silty clay, trace fine to medium sand, many lenses of silt and fine sand.
85	17	2 1/2	1 1/2			0	15			Est. A-1-b Stiff to very-stiff grey silty clay, trace fine to medium sand, many lenses of silt and fine sand.
90	18	2 1/2	1 1/2			0	10			Est. A-1-b Stiff to very-stiff grey silty clay, trace fine to medium sand, many lenses of silt and fine sand.
95	19	2 1/2	1 1/2			0	5			Est. A-1-b Stiff to very-stiff grey silty clay, trace fine to medium sand, many lenses of silt and fine sand.
100							0			Est. A-1-b Stiff to very-stiff grey silty clay, trace fine to medium sand, many lenses of silt and fine sand.

LOG OF BORING NO. 6-4  
CITY-BOULEVARD  
CLEVELAND, OHIO

PAGE 2 OF 3

DEPTH FEET	SAMPLE NO.	STARTING EFFORT	HEAD EFFORT	TRAILER EFFORT	TYPE OF SOIL	COMPLETION DEPTH FEET	ELEVATION FEET	DATE BORING RUN	LOCATION IN BLOCK	DESCRIPTION
100	20	2 1/2	1 1/2			0	0			Est. A-6-a Stiff to very-stiff grey silty clay, trace fine to coarse sand, trace fine gravel.
105	21	2 1/2	1 1/2			0	5			Est. A-6-a Stiff to very-stiff grey silty clay, trace fine to coarse sand, trace fine gravel.
110	22	2 1/2	1 1/2			0	10			Est. A-6-a Stiff to very-stiff grey silty clay, trace fine to coarse sand, trace fine gravel.
115	23	2 1/2	1 1/2			0	15			Est. A-6-a Stiff to very-stiff grey silty clay, trace fine to coarse sand, trace fine gravel.
120	24	2 1/2	1 1/2			0	20			Est. A-6-a Stiff to very-stiff grey silty clay, trace fine to coarse sand, trace fine gravel.
125	25	2 1/2	1 1/2			0	25			Est. A-6-a Stiff to very-stiff grey silty clay, trace fine to coarse sand, trace fine gravel.
130	26	2 1/2	1 1/2			0	30			Est. A-6-a Stiff to very-stiff grey silty clay, trace fine to coarse sand, trace fine gravel.
135	27	2 1/2	1 1/2			0	35			Est. A-6-a Stiff to very-stiff grey silty clay, trace fine to coarse sand, trace fine gravel.
140	28	2 1/2	1 1/2			0	40			Est. A-6-a Stiff to very-stiff grey silty clay, trace fine to coarse sand, trace fine gravel.
145	29	2 1/2	1 1/2			0	45			Est. A-6-a Stiff to very-stiff grey silty clay, trace fine to coarse sand, trace fine gravel.
150	30	2 1/2	1 1/2			0	50			Est. A-6-a Stiff to very-stiff grey silty clay, trace fine to coarse sand, trace fine gravel.
155	31	2 1/2	1 1/2			0	55			Est. A-6-a Stiff to very-stiff grey silty clay, trace fine to coarse sand, trace fine gravel.
160	32	2 1/2	1 1/2			0	60			Est. A-6-a Stiff to very-stiff grey silty clay, trace fine to coarse sand, trace fine gravel.
165	33	2 1/2	1 1/2			0	65			Est. A-6-a Stiff to very-stiff grey silty clay, trace fine to coarse sand, trace fine gravel.
170	34	2 1/2	1 1/2			0	70			Est. A-6-a Stiff to very-stiff grey silty clay, trace fine to coarse sand, trace fine gravel.
175	35	2 1/2	1 1/2			0	75			Est. A-6-a Stiff to very-stiff grey silty clay, trace fine to coarse sand, trace fine gravel.
180	36	2 1/2	1 1/2			0	80			Est. A-6-a Stiff to very-stiff grey silty clay, trace fine to coarse sand, trace fine gravel.
185	37	2 1/2	1 1/2			0	85			Est. A-6-a Stiff to very-stiff grey silty clay, trace fine to coarse sand, trace fine gravel.
190	38	2 1/2	1 1/2			0	90			Est. A-6-a Stiff to very-stiff grey silty clay, trace fine to coarse sand, trace fine gravel.
195	39	2 1/2	1 1/2			0	95			Est. A-6-a Stiff to very-stiff grey silty clay, trace fine to coarse sand, trace fine gravel.
200	40	2 1/2	1 1/2			0	100			Est. A-6-a Stiff to very-stiff grey silty clay, trace fine to coarse sand, trace fine gravel.

LOG OF BORING NO. 7-4  
CITY-BOULEVARD  
CLEVELAND, OHIO

PAGE 1 OF 3

DEPTH FEET	SAMPLE NO.	STARTING EFFORT	HEAD EFFORT	TRAILER EFFORT	TYPE OF SOIL	COMPLETION DEPTH FEET	ELEVATION FEET	DATE BORING RUN	LOCATION IN BLOCK	DESCRIPTION
0										
1	1	3 1/2	1 1/2			0	100	6/27/51 - 9/2/51	CITY-BOULEVARD	FILL. Loose brown and black fine to coarse gravel, some to "and" fine to coarse sand, trace to little clayey silt, (clayey and shaly).
10	2	2 1/2	1 1/2			0	90			Est. A-2-a Medium-dense brown fine to medium sand, trace to little silt, trace coarse to coarse gravel, contains occasional thin seams of silt or clayey silt.
20	3	2 1/2	1 1/2			0	80			Est. A-1-b Medium-dense brown fine to coarse sand, trace to coarse gravel, trace silt.
30	4	2 1/2	1 1/2			0	70			Est. A-1-b Medium-dense to dense brown fine to medium sand, trace to little silt, trace coarse to coarse gravel, contains occasional thin seams of silt, fine sand, and silty clay.
40	5	2 1/2	1 1/2			0	60			Est. A-1-b Dense grey silt, little fine sand, trace clay.
50	6	2 1/2	1 1/2			0	50			Est. A-4-b Medium-dense grey silt interbedded with silty clay, trace fine to medium sand.
60	7	2 1/2	1 1/2			0	40			Est. A-4-b Dense grey silt, little to "and" fine sand, trace to "and" silt.
70	8	2 1/2	1 1/2			0	30			Est. A-4-b Medium-silty grey silty clay interbedded with silt, trace fine to medium sand.
80	9	2 1/2	1 1/2			0	20			Est. A-6-d Stiff to hard grey silty clay, trace fine sand, few thin seams of clayey silt and silt.
90	10	2 1/2	1 1/2			0	10			Est. A-6-d Medium-silty grey silty clay interbedded with silt, trace fine to medium sand.
100							0			Est. A-6-d Stiff to hard grey silty clay, trace fine sand, few thin seams of clayey silt and silt.







LOG OF BORING NO. P-3  
CITY-COLUMBIAN  
CLEVELAND, OHIO

DATE: 6/22/63

LOCATION: 2140 W. 13th St.  
CITY-COLUMBIAN  
CLEVELAND, OHIO

TYPE: J.A. Mohr, Inc.  
J.A. Mohr, Inc.  
J.A. Mohr, Inc.

COMPLETION DEPTH: 102.0' ELEVATION: 585.3' DATE: 6/22/63

DESCRIPTION: FILL: Loose dark-brown line to coarse sand some to "one" line to coarse gravel (chairs and logs).

EST. A-2.4  
Stiff gray silty clay, trace fine sand, few very-fine silt seams.

- At 24.0': Encountered cobbles.

Est. A-7-6(3)  
Stiff to very-stiff gray silty clay, trace fine to coarse sand, few to many seams and lenses of silt.

Stiff to very-stiff gray silty clay, trace fine to coarse sand, trace fine gravel, few lenses of silt.

A-6(9)  
Stiff to very-stiff gray silty clay, trace fine to coarse sand, trace fine gravel, few lenses of silt.

Sample (6): Stiff to very-stiff silty clay, trace fine to coarse sand, few seams of silt.

A-6a, A-6b(1)  
Medium-stiff to stiff gray silty clay, trace fine to coarse sand, few seams of silt.

A-6b(2)  
Medium-stiff to stiff gray silty clay, trace fine to coarse sand, few seams of silt.

DEPTH FEET	SAMPLE NO.	LABORATORY	WATER LEVEL	WATER NOTE	DATE
0					
1	2143				
2	2144				
3	2145				
4	2146				
5	2147				
6	2148				
7	2149				
8	2150				
9	2151				
10	2152				
11	2153				
12	2154				
13	2155				
14	2156				
15	2157				
16	2158				
17	2159				
18	2160				
19	2161				
20	2162				
21	2163				
22	2164				
23	2165				
24	2166				
25	2167				
26	2168				
27	2169				
28	2170				
29	2171				
30	2172				
31	2173				
32	2174				
33	2175				
34	2176				
35	2177				
36	2178				
37	2179				
38	2180				
39	2181				
40	2182				
41	2183				
42	2184				
43	2185				
44	2186				
45	2187				
46	2188				
47	2189				
48	2190				
49	2191				
50	2192				
51	2193				
52	2194				
53	2195				
54	2196				
55	2197				
56	2198				
57	2199				
58	2200				
59	2201				
60	2202				
61	2203				
62	2204				
63	2205				
64	2206				
65	2207				
66	2208				
67	2209				
68	2210				
69	2211				
70	2212				
71	2213				
72	2214				
73	2215				
74	2216				
75	2217				
76	2218				
77	2219				
78	2220				
79	2221				
80	2222				
81	2223				
82	2224				
83	2225				
84	2226				
85	2227				
86	2228				
87	2229				
88	2230				
89	2231				
90	2232				
91	2233				
92	2234				
93	2235				
94	2236				
95	2237				
96	2238				
97	2239				
98	2240				
99	2241				
100	2242				

LOG OF BORING NO. P-3  
CITY-COLUMBIAN  
CLEVELAND, OHIO

DATE: 6/22/63

LOCATION: 2140 W. 13th St.  
CITY-COLUMBIAN  
CLEVELAND, OHIO

TYPE: J.A. Mohr, Inc.  
J.A. Mohr, Inc.  
J.A. Mohr, Inc.

COMPLETION DEPTH: 102.0' ELEVATION: 585.3' DATE: 6/22/63

DESCRIPTION: Medium-stiff to stiff gray silty clay, trace fine to coarse sand, few seams of silt.

A-6b(2)  
Medium-dense gray silt, trace clay.

A-6b(1)  
Stiff to very-stiff gray silty clay, trace fine to coarse sand, few seams and lenses of silt.

Sample 23: Stiff to very-stiff silty clay, trace fine to coarse sand, few seams and lenses of silt.

Est. A-3a  
Medium-dense gray line to coarse sand, trace silt, trace fine to coarse gravel.

Very-stiff gray silty clay, some line to coarse sand, trace fine gravel. Est. A-6b

END OF BORING

- Encountered slight seepage at 13.0'.  
- Encountered water at 17.0'.  
- O.G. to 27.5'; 3-1/4" I.D. Miller-stem Auger equipped with 4" U.S. Fish. coupled casing from 0.0 to 30'.  
- 27.5' to 140' 3-7/8" Tricone Bit.  
- 30.2' to 149.5' recirculated water used as drilling fluid.

DEPTH FEET	SAMPLE NO.	LABORATORY	WATER LEVEL	WATER NOTE	DATE
0					
1	2243				
2	2244				
3	2245				
4	2246				
5	2247				
6	2248				
7	2249				
8	2250				
9	2251				
10	2252				
11	2253				
12	2254				
13	2255				
14	2256				
15	2257				
16	2258				
17	2259				
18	2260				
19	2261				
20	2262				
21	2263				
22	2264				
23	2265				
24	2266				
25	2267				
26	2268				
27	2269				
28	2270				
29	2271				
30	2272				
31	2273				
32	2274				
33	2275				
34	2276				
35	2277				
36	2278				
37	2279				
38	2280				
39	2281				
40	2282				
41	2283				
42	2284				
43	2285				
44	2286				
45	2287				
46	2288				
47	2289				
48	2290				
49	2291				
50	2292				
51	2293				
52	2294				
53	2295				
54	2296				
55	2297				
56	2298				
57	2299				
58	2300				
59	2301				
60	2302				
61	2303				
62	2304				
63	2305				
64	2306				
65	2307				
66	2308				
67	2309				
68	2310				
69	2311				
70	2312				
71	2313				
72	2314				
73	2315				
74	2316				
75	2317				
76	2318				
77	2319				
78	2320				
79	2321				
80	2322				
81	2323				
82	2324				
83	2325				
84	2326				
85	2327				
86	2328				
87	2329				
88	2330				
89	2331				
90	2332				
91	2333				
92	2334				
93	2335				
94	2336				
95	2337				
96	2338				
97	2339				
98	2340				
99	2341				
100	2342				

LOG OF BORING NO. P-4  
CITY-COLUMBIAN  
CLEVELAND, OHIO

DATE: 6/22/63

LOCATION: 2140 W. 13th St.  
CITY-COLUMBIAN  
CLEVELAND, OHIO

TYPE: J.A. Mohr, Inc.  
J.A. Mohr, Inc.  
J.A. Mohr, Inc.

COMPLETION DEPTH: 102.0' ELEVATION: 585.3' DATE: 6/22/63

DESCRIPTION: Loose to medium-dense black chert, trace fine to coarse gravel, trace silt, trace fine to medium sand, trace brick or tile fragments.

- From 10.0' to 10.9': Boulder. Est. A-3a

POSSIBLE FILL: Medium-dense brown line to coarse sand, little line to coarse gravel, contains few thin lenses of clayey silt, trace silt.

- From 21.0' to 22.0': Interbedded with brown silty clay. A-3a(1)

Stiff to very-stiff gray silty clay, trace fine to coarse sand, trace silt, trace fine to medium sand. A-6(9)

Medium-stiff to stiff gray silty clay, trace fine to coarse sand, few lenses of silt and fine sand.

Sample 9: Medium-stiff silty clay. A-6b(1)

Stiff to very-stiff gray silty clay, trace fine to coarse sand, trace fine gravel, few seams and lenses of silt.

- From 69.0' to 75.0': With horizontal fracture. A-6b(1)

- From 72.5' to 74.0': Medium-stiff to stiff. A-6b(1)

Stiff to very-stiff gray silty clay, trace to little line to coarse sand, trace fine gravel, few lenses of silt.

DEPTH FEET	SAMPLE NO.	LABORATORY	WATER LEVEL	WATER NOTE	DATE
0					
1	2343				
2	2344				
3	2345				
4	2346				
5	2347				
6	2348				
7	2349				
8	2350				
9	2351				
10	2352				
11	2353				
12	2354				
13	2355				
14	2356				
15	2357				
16	2358				
17	2359				
18	2360				
19	2361				
20	2362				
21	2363				
22	2364				
23	2365				
24	2366				
25	2367				
26	2368				
27	2369				
28	2370				
29	2371				
30	2372				
31	2373				
32	2374				
33	2375				
34	2376				
35	2377				
36	2378				
37	2379				
38	2380				
39	2381				
40	2382				
41	2383				
42	2384				
43	2385				
44	2386				
45	2387				
46	2388				
47	2389				
48	2390				
49	2391				
50	2392				
51	2393				
52	2394				
53	2395				
54	2396				
55	2397				
56	2398				
57	2399				
58	2400				
59	2401				
60	2402				
61	2403				
62	2404				
63	2405				
64	2406				
65	2407				
66	2408				
67	2409				
68	2410				
69	2411				
70	2412				
71	2413				
72	2414				
73	2415				
74	2416				
75	2417				
76	2418				
77	2419				
78	2420				
79	2421				
80	2422				
81	2423				
82	2424				
83	2425				
84	2426				









LOG OF BORING NO. B-203  
CITY OF CLEVELAND  
CLEVELAND, OHIO

TYPE: 3 1/2" Compression Log  
DATE: 5/21/52  
COMPLETION DEPTH: 333' ELEVATION: 333.7'

LOCATION: CLEVELAND, OHIO  
DATE: 5/21/52

DEPTH (FEET)	SAMPLE NO.	LABORATORY	EFFORT	HARD POINT	REMARKS
300					
301					
302					
303					
304					
305					
306					
307					
308					
309					
310					
311					
312					
313					
314					
315					
316					
317					
318					
319					
320					
321					
322					
323					
324					
325					
326					
327					
328					
329					
330					
331					
332					
333					

Soil is medium-hard dark-gray shale, nearly horizontally bedded with low to slightly irregularly bedded siliceous seams. - Ultimate Unclassified Compression Strength  $Q_u = 4425 \text{ psi}$  @ Strain 1.25%.

Medium-hard dark-gray shale, nearly horizontally bedded with low to slightly irregularly bedded siliceous seams. - Ultimate Unclassified Compression Strength  $Q_u = 4425 \text{ psi}$  @ Strain 1.25%.

Water Level: \_\_\_\_\_ Date: \_\_\_\_\_  
Water Note: \_\_\_\_\_ Date: \_\_\_\_\_

LOG OF BORING NO. B-202  
CITY OF CLEVELAND  
CLEVELAND, OHIO

TYPE: 3 1/2" Compression Log  
DATE: 5/21/52  
COMPLETION DEPTH: 300' ELEVATION: 317.7'

LOCATION: CLEVELAND, OHIO  
DATE: 5/21/52

DEPTH (FEET)	SAMPLE NO.	LABORATORY	EFFORT	HARD POINT	REMARKS
300					
301					
302					
303					
304					
305					
306					
307					
308					
309					
310					
311					
312					
313					
314					
315					
316					
317					
318					
319					
320					
321					
322					
323					
324					
325					
326					
327					
328					
329					
330					
331					
332					
333					

Medium-hard to hard dark-gray shale, nearly horizontally bedded with low to medium siliceous seams. - Ultimate Unclassified Compression Strength  $Q_u = 6800 \text{ psi}$  @ Strain 1.80%.

From 291.7' to 292.6': Lost section.

Water Level: \_\_\_\_\_ Date: \_\_\_\_\_  
Water Note: \_\_\_\_\_ Date: \_\_\_\_\_

LOG OF BORING NO. B-201  
CITY OF CLEVELAND  
CLEVELAND, OHIO

TYPE: 3 1/2" Compression Log  
DATE: 5/21/52  
COMPLETION DEPTH: 333' ELEVATION: 333.7'

LOCATION: CLEVELAND, OHIO  
DATE: 5/21/52

DEPTH (FEET)	SAMPLE NO.	LABORATORY	EFFORT	HARD POINT	REMARKS
300					
301					
302					
303					
304					
305					
306					
307					
308					
309					
310					
311					
312					
313					
314					
315					
316					
317					
318					
319					
320					
321					
322					
323					
324					
325					
326					
327					
328					
329					
330					
331					
332					
333					

Soil is medium-hard dark-gray shale, nearly horizontally bedded with low horizontal to slightly irregularly bedded siliceous and brownish siliceous seams.

Medium-hard dark-gray shale, nearly horizontally bedded with low horizontal to slightly irregularly bedded siliceous and brownish siliceous seams.

- Ultimate Unclassified Compression Strength  $Q_u = 2665 \text{ psi}$  @ Strain 1.5%.

From 216.5' to 219.4': Fractured.  
From 231' to 233.4': Trace pyrite seams.

Water Level: \_\_\_\_\_ Date: \_\_\_\_\_  
Water Note: \_\_\_\_\_ Date: \_\_\_\_\_













STATE OF OHIO  
Department of Transportation  
Division of Geotechnical Engineering  
Soils Testing Laboratory

PROJECT: 6072  
DATE: 1/27/00  
SHEET: 15 OF 15

BORING NO. 6072-01  
DEPTH: 100 FT  
DATE COMPLETED: 5/17/00

DEPTH (FT)	DEPTH (M)	SOIL TYPE	DESCRIPTION	WATER CONTENT (%)	LIQUID LIMIT (%)	PLASTICITY INDEX	UNSATURATED SWELLING (%)	LABORATORY TESTS
0	0	0	UNDURABLE SAND AND GRAVEL					
1	0.30	62000	BROWN SAND					
2	0.61	62000	BROWN SAND					
3	0.91	62000	BROWN SAND					
4	1.22	62000	BROWN SAND					
5	1.52	62000	BROWN SAND					
6	1.83	62000	BROWN SAND					
7	2.13	62000	BROWN SAND					
8	2.44	62000	BROWN SAND					
9	2.74	62000	BROWN SAND					
10	3.05	62000	BROWN SAND					
11	3.35	62000	BROWN SAND					
12	3.66	62000	BROWN SAND					
13	3.96	62000	BROWN SAND					
14	4.27	62000	BROWN SAND					
15	4.57	62000	BROWN SAND					
16	4.88	62000	BROWN SAND					
17	5.18	62000	BROWN SAND					
18	5.49	62000	BROWN SAND					
19	5.79	62000	BROWN SAND					
20	6.10	62000	BROWN SAND					
21	6.40	62000	BROWN SAND					
22	6.71	62000	BROWN SAND					
23	7.01	62000	BROWN SAND					
24	7.32	62000	BROWN SAND					
25	7.62	62000	BROWN SAND					
26	7.93	62000	BROWN SAND					
27	8.23	62000	BROWN SAND					
28	8.54	62000	BROWN SAND					
29	8.84	62000	BROWN SAND					
30	9.15	62000	BROWN SAND					
31	9.45	62000	BROWN SAND					
32	9.76	62000	BROWN SAND					
33	10.06	62000	BROWN SAND					
34	10.37	62000	BROWN SAND					
35	10.67	62000	BROWN SAND					
36	10.98	62000	BROWN SAND					
37	11.28	62000	BROWN SAND					
38	11.59	62000	BROWN SAND					
39	11.89	62000	BROWN SAND					
40	12.20	62000	BROWN SAND					
41	12.50	62000	BROWN SAND					
42	12.81	62000	BROWN SAND					
43	13.11	62000	BROWN SAND					
44	13.42	62000	BROWN SAND					
45	13.72	62000	BROWN SAND					
46	14.03	62000	BROWN SAND					
47	14.33	62000	BROWN SAND					
48	14.64	62000	BROWN SAND					
49	14.94	62000	BROWN SAND					
50	15.25	62000	BROWN SAND					
51	15.55	62000	BROWN SAND					
52	15.86	62000	BROWN SAND					
53	16.16	62000	BROWN SAND					
54	16.47	62000	BROWN SAND					
55	16.77	62000	BROWN SAND					
56	17.08	62000	BROWN SAND					
57	17.38	62000	BROWN SAND					
58	17.69	62000	BROWN SAND					
59	17.99	62000	BROWN SAND					
60	18.30	62000	BROWN SAND					
61	18.60	62000	BROWN SAND					
62	18.91	62000	BROWN SAND					
63	19.21	62000	BROWN SAND					
64	19.52	62000	BROWN SAND					
65	19.82	62000	BROWN SAND					
66	20.13	62000	BROWN SAND					
67	20.43	62000	BROWN SAND					
68	20.74	62000	BROWN SAND					
69	21.04	62000	BROWN SAND					
70	21.35	62000	BROWN SAND					
71	21.65	62000	BROWN SAND					
72	21.96	62000	BROWN SAND					
73	22.26	62000	BROWN SAND					
74	22.57	62000	BROWN SAND					
75	22.87	62000	BROWN SAND					
76	23.18	62000	BROWN SAND					
77	23.48	62000	BROWN SAND					
78	23.79	62000	BROWN SAND					
79	24.09	62000	BROWN SAND					
80	24.40	62000	BROWN SAND					
81	24.70	62000	BROWN SAND					
82	25.01	62000	BROWN SAND					
83	25.31	62000	BROWN SAND					
84	25.62	62000	BROWN SAND					
85	25.92	62000	BROWN SAND					
86	26.23	62000	BROWN SAND					
87	26.53	62000	BROWN SAND					
88	26.84	62000	BROWN SAND					
89	27.14	62000	BROWN SAND					
90	27.45	62000	BROWN SAND					
91	27.75	62000	BROWN SAND					
92	28.06	62000	BROWN SAND					
93	28.36	62000	BROWN SAND					
94	28.67	62000	BROWN SAND					
95	28.97	62000	BROWN SAND					
96	29.28	62000	BROWN SAND					
97	29.58	62000	BROWN SAND					
98	29.89	62000	BROWN SAND					
99	30.19	62000	BROWN SAND					
100	30.50	62000	BROWN SAND					

STATE OF OHIO  
Department of Transportation  
Division of Geotechnical Engineering  
Soils Testing Laboratory

PROJECT: 6072  
DATE: 1/27/00  
SHEET: 15 OF 15

BORING NO. 6072-02  
DEPTH: 100 FT  
DATE COMPLETED: 5/17/00

DEPTH (FT)	DEPTH (M)	SOIL TYPE	DESCRIPTION	WATER CONTENT (%)	LIQUID LIMIT (%)	PLASTICITY INDEX	UNSATURATED SWELLING (%)	LABORATORY TESTS
0	0	0	UNDURABLE SAND AND GRAVEL					
1	0.30	62000	GRAY SILTY SAND					
2	0.61	62000	GRAY SILTY SAND					
3	0.91	62000	GRAY SILTY SAND					
4	1.22	62000	GRAY SILTY SAND					
5	1.52	62000	GRAY SILTY SAND					
6	1.83	62000	GRAY SILTY SAND					
7	2.13	62000	GRAY SILTY SAND					
8	2.44	62000	GRAY SILTY SAND					
9	2.74	62000	GRAY SILTY SAND					
10	3.05	62000	GRAY SILTY SAND					
11	3.35	62000	GRAY SILTY SAND					
12	3.66	62000	GRAY SILTY SAND					
13	3.96	62000	GRAY SILTY SAND					
14	4.27	62000	GRAY SILTY SAND					
15	4.57	62000	GRAY SILTY SAND					
16	4.88	62000	GRAY SILTY SAND					
17	5.18	62000	GRAY SILTY SAND					
18	5.49	62000	GRAY SILTY SAND					
19	5.79	62000	GRAY SILTY SAND					
20	6.10	62000	GRAY SILTY SAND					
21	6.40	62000	GRAY SILTY SAND					
22	6.71	62000	GRAY SILTY SAND					
23	7.01	62000	GRAY SILTY SAND					
24	7.32	62000	GRAY SILTY SAND					
25	7.62	62000	GRAY SILTY SAND					
26	7.93	62000	GRAY SILTY SAND					
27	8.23	62000	GRAY SILTY SAND					
28	8.54	62000	GRAY SILTY SAND					
29	8.84	62000	GRAY SILTY SAND					
30	9.15	62000	GRAY SILTY SAND					
31	9.45	62000	GRAY SILTY SAND					
32	9.76	62000	GRAY SILTY SAND					
33	10.06	62000	GRAY SILTY SAND					
34	10.37	62000	GRAY SILTY SAND					
35	10.67	62000	GRAY SILTY SAND					
36	10.98	62000	GRAY SILTY SAND					
37	11.28	62000	GRAY SILTY SAND					
38	11.59	62000	GRAY SILTY SAND					
39	11.89	62000	GRAY SILTY SAND					
40	12.20	62000	GRAY SILTY SAND					
41	12.50	62000	GRAY SILTY SAND					
42	12.81	62000	GRAY SILTY SAND					
43	13.11	62000	GRAY SILTY SAND					
44	13.42	62000	GRAY SILTY SAND					
45	13.72	62000	GRAY SILTY SAND					
46	14.03	62000	GRAY SILTY SAND					
47	14.33	62000	GRAY SILTY SAND					
48	14.64	62000	GRAY SILTY SAND					
49	14.94	62000	GRAY SILTY SAND					
50	15.25	62000	GRAY SILTY SAND					
51	15.55	62000	GRAY SILTY SAND					
52	15.86	62000	GRAY SILTY SAND					
53	16.16	62000	GRAY SILTY SAND					
54	16.47	62000	GRAY SILTY SAND					
55	16.77	62000	GRAY SILTY SAND					
56	17.08	62000	GRAY SILTY SAND					
57	17.38	62000	GRAY SILTY SAND					
58	17.69	62000	GRAY SILTY SAND					
59	17.99	62000	GRAY SILTY SAND					
60	18.30	62000	GRAY SILTY SAND					
61	18.60	62000	GRAY SILTY SAND					
62	18.91	62000	GRAY SILTY SAND					
63	19.21	62000	GRAY SILTY SAND					
64	19.52	62000	GRAY SILTY SAND					
65	19.82	62000	GRAY SILTY SAND					
66	20.13	62000	GRAY SILTY SAND					
67	20.43	62000	GRAY SILTY SAND					
68	20.74	62000	GRAY SILTY SAND					
69	21.04	62000	GRAY SILTY SAND					
70	21.35	62000	GRAY SILTY SAND					
71	21.65	62000	GRAY SILTY SAND					
72	21.96	62000	GRAY SILTY SAND					
73	22.26	62000	GRAY SILTY SAND					
74	22.57	62000	GRAY SILTY SAND					
75	22.87	62000	GRAY SILTY SAND					
76	23.18	62000	GRAY SILTY SAND					
77	23.48	62000	GRAY SILTY SAND					
78	23.79	62000	GRAY SILTY SAND					
79	24.09	62000	GRAY SILTY SAND					
80	24.40	62000	GRAY SILTY SAND					
81	24.70	62000	GRAY SILTY SAND					
82	25.01	62000	GRAY SILTY SAND					
83	25.31	62000	GRAY SILTY SAND					
84	25.62	62000	GRAY SILTY SAND					
85	25.92	62000	GRAY SILTY SAND					
86	26.23	62000	GRAY SILTY SAND					
87	26.53	62000	GRAY SILTY SAND					
88	26.84	62000	GRAY SILTY SAND					
89	27.14	62000	GRAY SILTY SAND					
90	27.45	62000	GRAY SILTY SAND					
91	27.75	62000	GRAY SILTY SAND					
92	28.06	62000	GRAY SILTY SAND					
93	28.36	62000	GRAY SILTY SAND					
94	28.67	62000	GRAY SILTY SAND					
95	28.97	62000	GRAY SILTY SAND					
96	29.28	62000	GRAY SILTY SAND					
97	29.58	62000	GRAY SILTY SAND					



State of Ohio  
Department of Transportation  
Division of Inspection  
Testing Laboratory

Project Identification: 00220000

Date Started: 5/12/00 Sample Type: 53 No. of Borings: 10  
Date Completed: 5/12/00 Completion: On No. of Test Units: 10

Boring No. 10

Depth (Feet)	Soil Description	Soil Class	Soil Color	Soil Moisture (%)	Soil Density (pcf)	Soil Unit Weight (pcf)	Soil Specific Gravity	Soil Void Ratio	Soil Liquid Limit (%)	Soil Plastic Limit (%)	Soil Shrinkage (%)	Soil Swell (%)	Soil Compaction (%)	Soil Proctor (20%)	Soil Proctor (95%)	Soil Proctor (100%)
0.0																
0.5	GRAY CLAYEY SILT	GM/GC														
1.0																
1.5																
2.0																
2.5																
3.0																
3.5																
4.0																
4.5																
5.0																
5.5																
6.0																
6.5																
7.0																
7.5																
8.0																
8.5																
9.0																
9.5																
10.0																
10.5																
11.0																
11.5																
12.0																
12.5																
13.0																
13.5																
14.0																
14.5																
15.0																
15.5																
16.0																
16.5																
17.0																
17.5																
18.0																
18.5																
19.0																
19.5																
20.0																
20.5																
21.0																
21.5																
22.0																
22.5																
23.0																
23.5																
24.0																
24.5																
25.0																
25.5																
26.0																
26.5																
27.0																
27.5																
28.0																
28.5																
29.0																
29.5																
30.0																
30.5																
31.0																
31.5																
32.0																
32.5																
33.0																
33.5																
34.0																
34.5																
35.0																
35.5																
36.0																
36.5																
37.0																
37.5																
38.0																
38.5																
39.0																
39.5																
40.0																
40.5																
41.0																
41.5																
42.0																
42.5																
43.0																
43.5																
44.0																
44.5																
45.0																
45.5																
46.0																
46.5																
47.0																
47.5																
48.0																
48.5																
49.0																
49.5																
50.0																
50.5																
51.0																
51.5																
52.0																
52.5																
53.0																
53.5																
54.0																
54.5																
55.0																
55.5																
56.0																
56.5																
57.0																
57.5																
58.0																
58.5																
59.0																
59.5																
60.0																
60.5																
61.0																
61.5																
62.0																
62.5																
63.0																
63.5																
64.0																
64.5																
65.0																
65.5																
66.0																
66.5																
67.0																
67.5																
68.0																
68.5																
69.0																
69.5																
70.0																
70.5																
71.0																
71.5																
72.0																
72.5																
73.0																
73.5																
74.0																
74.5																
75.0																
75.5																
76.0																
76.5																
77.0																







PAGE 3 OF 3

State of Ohio  
Department of Transportation  
Division of Laboratory Testing

Date Started: 5/27/20    Station: 53    On: 1.5" Water Elev. 482    Project Identification: 07740004  
 Date Completed: 5/27/20    Comp. Length: 0    On: 1.5" Water Elev. 482    Project Identification: 07740004

Boring No. 35    Station & Offset    Section Elev. 200.0    Project Identification: 07740004

DEPTH (Feet)	DEPTH (Meters)	DESCRIPTION	NO. OF SAMPLES	TESTS PERFORMED	TEST RESULTS
100.0	30.5				
99.5	30.0				
99.0	29.5				
98.5	29.0				
98.0	28.5				
97.5	28.0				
97.0	27.5				
96.5	27.0				
96.0	26.5				
95.5	26.0				
95.0	25.5				
94.5	25.0				
94.0	24.5				
93.5	24.0				
93.0	23.5				
92.5	23.0				
92.0	22.5				
91.5	22.0				
91.0	21.5				
90.5	21.0				
90.0	20.5				
89.5	20.0				
89.0	19.5				
88.5	19.0				
88.0	18.5				
87.5	18.0				
87.0	17.5				
86.5	17.0				
86.0	16.5				
85.5	16.0				
85.0	15.5				
84.5	15.0				
84.0	14.5				
83.5	14.0				
83.0	13.5				
82.5	13.0				
82.0	12.5				
81.5	12.0				
81.0	11.5				
80.5	11.0				
80.0	10.5				
79.5	10.0				
79.0	9.5				
78.5	9.0				
78.0	8.5				
77.5	8.0				
77.0	7.5				
76.5	7.0				
76.0	6.5				
75.5	6.0				
75.0	5.5				
74.5	5.0				
74.0	4.5				
73.5	4.0				
73.0	3.5				
72.5	3.0				
72.0	2.5				
71.5	2.0				
71.0	1.5				
70.5	1.0				
70.0	0.5				
69.5	0.0				
69.0	-0.5				
68.5	-1.0				
68.0	-1.5				
67.5	-2.0				
67.0	-2.5				
66.5	-3.0				
66.0	-3.5				
65.5	-4.0				
65.0	-4.5				
64.5	-5.0				
64.0	-5.5				
63.5	-6.0				
63.0	-6.5				
62.5	-7.0				
62.0	-7.5				
61.5	-8.0				
61.0	-8.5				
60.5	-9.0				
60.0	-9.5				
59.5	-10.0				
59.0	-10.5				
58.5	-11.0				
58.0	-11.5				
57.5	-12.0				
57.0	-12.5				
56.5	-13.0				
56.0	-13.5				
55.5	-14.0				
55.0	-14.5				
54.5	-15.0				
54.0	-15.5				
53.5	-16.0				
53.0	-16.5				
52.5	-17.0				
52.0	-17.5				
51.5	-18.0				
51.0	-18.5				
50.5	-19.0				
50.0	-19.5				
49.5	-20.0				
49.0	-20.5				
48.5	-21.0				
48.0	-21.5				
47.5	-22.0				
47.0	-22.5				
46.5	-23.0				
46.0	-23.5				
45.5	-24.0				
45.0	-24.5				
44.5	-25.0				
44.0	-25.5				
43.5	-26.0				
43.0	-26.5				
42.5	-27.0				
42.0	-27.5				
41.5	-28.0				
41.0	-28.5				
40.5	-29.0				
40.0	-29.5				
39.5	-30.0				
39.0	-30.5				
38.5	-31.0				
38.0	-31.5				
37.5	-32.0				
37.0	-32.5				
36.5	-33.0				
36.0	-33.5				
35.5	-34.0				
35.0	-34.5				
34.5	-35.0				
34.0	-35.5				
33.5	-36.0				
33.0	-36.5				
32.5	-37.0				
32.0	-37.5				
31.5	-38.0				
31.0	-38.5				
30.5	-39.0				
30.0	-39.5				
29.5	-40.0				
29.0	-40.5				
28.5	-41.0				
28.0	-41.5				
27.5	-42.0				
27.0	-42.5				
26.5	-43.0				
26.0	-43.5				
25.5	-44.0				
25.0	-44.5				
24.5	-45.0				
24.0	-45.5				
23.5	-46.0				
23.0	-46.5				
22.5	-47.0				
22.0	-47.5				
21.5	-48.0				
21.0	-48.5				
20.5	-49.0				
20.0	-49.5				
19.5	-50.0				
19.0	-50.5				
18.5	-51.0				
18.0	-51.5				
17.5	-52.0				
17.0	-52.5				
16.5	-53.0				
16.0	-53.5				
15.5	-54.0				
15.0	-54.5				
14.5	-55.0				
14.0	-55.5				
13.5	-56.0				
13.0	-56.5				
12.5	-57.0				
12.0	-57.5				
11.5	-58.0				
11.0	-58.5				
10.5	-59.0				
10.0	-59.5				
9.5	-60.0				
9.0	-60.5				
8.5	-61.0				
8.0	-61.5				
7.5	-62.0				
7.0	-62.5				
6.5	-63.0				
6.0	-63.5				
5.5	-64.0				
5.0	-64.5				
4.5	-65.0				
4.0	-65.5				
3.5	-66.0				
3.0	-66.5				
2.5	-67.0				
2.0	-67.5				
1.5	-68.0				
1.0	-68.5				
0.5	-69.0				
0.0	-69.5				
-0.5	-70.0				
-1.0	-70.5				
-1.5	-71.0				
-2.0	-71.5				
-2.5	-72.0				
-3.0	-72.5				
-3.5	-73.0				
-4.0	-73.5				
-4.5	-74.0				
-5.0	-74.5				
-5.5	-75.0				
-6.0	-75.5				
-6.5	-76.0				
-7.0	-76.5				
-7.5	-77.0				
-8.0	-77.5				
-8.5	-78.0				
-9.0	-78.5				
-9.5	-79.0				
-10.0	-79.5				
-10.5	-80.0				
-11.0	-80.5				
-11.5	-81.0				
-12.0	-81.5				
-12.5	-82.0				
-13.0	-82.5				
-13.5	-83.0				
-14.0	-83.5				
-14.5	-84.0				
-15.0	-84.5				
-15.5	-85.0				
-16.0	-85.5				
-16.5	-86.0				
-17.0	-86.5				
-17.5	-87.0				
-18.0	-87.5				
-18.5	-88.0				
-19.0	-88.5				
-19.5	-89.0				
-20.0	-89.5				
-20.5	-90.0				
-21.0	-90.5				
-21.5	-91.0				
-22.0	-91.5				
-22.5	-92.0				
-23.0	-92.5				
-23.5	-93.0				
-24.0	-93.5				
-24.5	-94.0				
-25.0	-94.5				
-25.5	-95.0				
-26.0	-95.5				
-26.5	-96.0				
-27.0	-96.5				
-27.5	-97.0				
-28.0	-97.5				
-28.5	-98.0				
-29.0	-98.5				
-29.5	-99.0				
-30.0	-99.5				
-30.5	-100.0				

NOTE: SLOPE INDICATOR PIPE INSTALLED AT 130.0'

NOTE: BORING LOGS PROVIDED BY ODOT.

PAGE 1 OF 3

State of Ohio  
Department of Transportation  
Division of Laboratory Testing

Date Started: 5/27/20    Station: 53    On: 1.5" Water Elev. 482    Project Identification: 07740004  
 Date Completed: 5/27/20    Comp. Length: 0    On: 1.5" Water Elev. 482    Project Identification: 07740004

Boring No. 35    Station & Offset    Section Elev. 200.0    Project Identification: 07740004

DEPTH (Feet)	DEPTH (Meters)	DESCRIPTION	NO. OF SAMPLES	TESTS PERFORMED	TEST RESULTS
100.0	30.5				
99.5	30.0				
99.0	29.5				
98.5	29.0				
98.0	28.5				
97.5	28.0				
97.0	27.5				
96.5	27.0				
96.0	26.5				
95.5	26.0				
95.0	25.5				
94.5	25.0				
94.0	24.5				
93.5	24.0				
93.0	23.5				
92.5	23.0				
92.0	22.5				
91.5	22.0				
91.0	21.5				
90.5	21.0				
90.0	20.5				
89.5	20.0				
89.0	19.5				
88.5	19.0				
88.0	18.5				
87.5	18.0				
87.0	17.5				
86.5	17.0				
86.0	16.5				
85.5	16.0				
85.0	15.5				
84.5	15.0				
84.0	14.5				
83.5	14.0				
83.0	13.5				
82.5	13.0				
82.0	12.5				
81.5	12.0				
81.0	11.5				
80.5	11.0				
80.0					





State of Ohio  
Department of Transportation  
Division of Highway  
Testing Laboratory

Date Started: 6/25/72  
Date Completed: 6/25/72  
Contract: 67-2-12

Section/Type: SS  
Dist: 1.3/2  
Water Elev: 587.2

Project Identification: 07-10000

Sheet No.: 10  
Sheet of: 10

Surface Elev: 577

Boring No.: 10  
Boring Description: 10

Depth (ft)	Soil Description	Moisture (%)	Specific Gravity	Unit Weight (pcf)	Penetration (lb/in)	Notes
0	CHUCKS, SAND AND STONE FRAGMENTS (DRILLER'S DESCRIPTION)	-	-	-	-	
2	GRAY SILT WITH WOOD FRAGMENTS	0	0.10	12	100	
3	GRAY SILT	0	0.10	12	100	
4	GRAY SILT	0	0.10	12	100	
5	GRAY SILT	0	0.10	12	100	
6	GRAY SILT	0	0.10	12	100	
7	GRAY SILT	0	0.10	12	100	
8	GRAY SILT	0	0.10	12	100	
9	GRAY SILT	0	0.10	12	100	
10	GRAY SILT	0	0.10	12	100	
11	GRAY SILT	0	0.10	12	100	
12	GRAY SILT	0	0.10	12	100	
13	GRAY SILT	0	0.10	12	100	
14	GRAY SILT	0	0.10	12	100	
15	GRAY SILT	0	0.10	12	100	
16	GRAY SILT	0	0.10	12	100	
17	GRAY SILT	0	0.10	12	100	
18	GRAY SILT	0	0.10	12	100	
19	GRAY SILT	0	0.10	12	100	
20	GRAY SILT	0	0.10	12	100	
21	GRAY SILT	0	0.10	12	100	
22	GRAY SILT	0	0.10	12	100	
23	GRAY SILT	0	0.10	12	100	
24	GRAY SILT	0	0.10	12	100	
25	GRAY SILT	0	0.10	12	100	
26	GRAY SILT	0	0.10	12	100	
27	GRAY SILT	0	0.10	12	100	
28	GRAY SILT	0	0.10	12	100	
29	GRAY SILT	0	0.10	12	100	
30	GRAY SILT	0	0.10	12	100	
31	GRAY SILT	0	0.10	12	100	
32	GRAY SILT	0	0.10	12	100	
33	GRAY SILT	0	0.10	12	100	
34	GRAY SILT	0	0.10	12	100	
35	GRAY SILT	0	0.10	12	100	
36	GRAY SILT	0	0.10	12	100	
37	GRAY SILT	0	0.10	12	100	
38	GRAY SILT	0	0.10	12	100	
39	GRAY SILT	0	0.10	12	100	
40	GRAY SILT	0	0.10	12	100	
41	GRAY SILT	0	0.10	12	100	
42	GRAY SILT	0	0.10	12	100	
43	GRAY SILT	0	0.10	12	100	
44	GRAY SILT	0	0.10	12	100	
45	GRAY SILT	0	0.10	12	100	
46	GRAY SILT	0	0.10	12	100	
47	GRAY SILT	0	0.10	12	100	
48	GRAY SILT	0	0.10	12	100	
49	GRAY SILT	0	0.10	12	100	
50	GRAY SILT	0	0.10	12	100	
51	GRAY SILT	0	0.10	12	100	
52	GRAY SILT	0	0.10	12	100	
53	GRAY SILT	0	0.10	12	100	
54	GRAY SILT	0	0.10	12	100	
55	GRAY SILT	0	0.10	12	100	
56	GRAY SILT	0	0.10	12	100	
57	GRAY SILT	0	0.10	12	100	
58	GRAY SILT	0	0.10	12	100	
59	GRAY SILT	0	0.10	12	100	
60	GRAY SILT	0	0.10	12	100	
61	GRAY SILT	0	0.10	12	100	
62	GRAY SILT	0	0.10	12	100	
63	GRAY SILT	0	0.10	12	100	
64	GRAY SILT	0	0.10	12	100	
65	GRAY SILT	0	0.10	12	100	
66	GRAY SILT	0	0.10	12	100	
67	GRAY SILT	0	0.10	12	100	
68	GRAY SILT	0	0.10	12	100	
69	GRAY SILT	0	0.10	12	100	
70	GRAY SILT	0	0.10	12	100	
71	GRAY SILT	0	0.10	12	100	
72	GRAY SILT	0	0.10	12	100	
73	GRAY SILT	0	0.10	12	100	
74	GRAY SILT	0	0.10	12	100	
75	GRAY SILT	0	0.10	12	100	
76	GRAY SILT	0	0.10	12	100	
77	GRAY SILT	0	0.10	12	100	
78	GRAY SILT	0	0.10	12	100	
79	GRAY SILT	0	0.10	12	100	
80	GRAY SILT	0	0.10	12	100	
81	GRAY SILT	0	0.10	12	100	
82	GRAY SILT	0	0.10	12	100	
83	GRAY SILT	0	0.10	12	100	
84	GRAY SILT	0	0.10	12	100	
85	GRAY SILT	0	0.10	12	100	
86	GRAY SILT	0	0.10	12	100	
87	GRAY SILT	0	0.10	12	100	
88	GRAY SILT	0	0.10	12	100	
89	GRAY SILT	0	0.10	12	100	
90	GRAY SILT	0	0.10	12	100	
91	GRAY SILT	0	0.10	12	100	
92	GRAY SILT	0	0.10	12	100	
93	GRAY SILT	0	0.10	12	100	
94	GRAY SILT	0	0.10	12	100	
95	GRAY SILT	0	0.10	12	100	
96	GRAY SILT	0	0.10	12	100	
97	GRAY SILT	0	0.10	12	100	
98	GRAY SILT	0	0.10	12	100	
99	GRAY SILT	0	0.10	12	100	
100	GRAY SILT AND CLAY	0	0.10	12	100	

State of Ohio  
Department of Transportation  
Division of Highway  
Testing Laboratory

Date Started: 6/25/72  
Date Completed: 6/25/72  
Contract: 67-2-12

Section/Type: SS  
Dist: 1.3/2  
Water Elev: 587.2

Project Identification: 07-10000

Sheet No.: 11  
Sheet of: 10

Surface Elev: 577

Boring No.: 11  
Boring Description: 11

Depth (ft)	Soil Description	Moisture (%)	Specific Gravity	Unit Weight (pcf)	Penetration (lb/in)	Notes
0	GRAY SILT	0	0.10	12	100	
1	GRAY SILT	0	0.10	12	100	
2	GRAY SILT	0	0.10	12	100	
3	GRAY SILT	0	0.10	12	100	
4	GRAY SILT	0	0.10	12	100	
5	GRAY SILT	0	0.10	12	100	
6	GRAY SILT	0	0.10	12	100	
7	GRAY SILT	0	0.10	12	100	
8	GRAY SILT	0	0.10	12	100	
9	GRAY SILT	0	0.10	12	100	
10	GRAY SILT	0	0.10	12	100	
11	GRAY SILT	0	0.10	12	100	
12	GRAY SILT	0	0.10	12	100	
13	GRAY SILT	0	0.10	12	100	
14	GRAY SILT	0	0.10	12	100	
15	GRAY SILT	0	0.10	12	100	
16	GRAY SILT	0	0.10	12	100	
17	GRAY SILT	0	0.10	12	100	
18	GRAY SILT	0	0.10	12	100	
19	GRAY SILT	0	0.10	12	100	
20	GRAY SILT	0	0.10	12	100	
21	GRAY SILT	0	0.10	12	100	
22	GRAY SILT	0	0.10	12	100	
23	GRAY SILT	0	0.10	12	100	
24	GRAY SILT	0	0.10	12	100	
25	GRAY SILT	0	0.10	12	100	
26	GRAY SILT	0	0.10	12	100	
27	GRAY SILT	0	0.10	12	100	
28	GRAY SILT	0	0.10	12	100	
29	GRAY SILT	0	0.10	12	100	
30	GRAY SILT	0	0.10	12	100	
31	GRAY SILT	0	0.10	12	100	
32	GRAY SILT	0	0.10	12	100	
33	GRAY SILT	0	0.10	12	100	
34	GRAY SILT	0	0.10	12	100	
35	GRAY SILT	0	0.10	12	100	
36	GRAY SILT	0	0.10	12	100	
37	GRAY SILT	0	0.10	12	100	
38	GRAY SILT	0	0.10	12	100	
39	GRAY SILT	0	0.10	12	100	
40	GRAY SILT	0	0.10	12	100	
41	GRAY SILT	0	0.10	12	100	
42	GRAY SILT	0	0.10	12	100	
43	GRAY SILT	0	0.10	12	100	
44	GRAY SILT	0	0.10	12	100	
45	GRAY SILT	0	0.10	12	100	
46	GRAY SILT	0	0.10	12	100	
47	GRAY SILT	0	0.10	12	100	
48	GRAY SILT	0	0.10	12	100	
49	GRAY SILT	0	0.10	12	100	
50	GRAY SILT	0	0.10	12	100	
51	GRAY SILT	0	0.10	12	100	
52	GRAY SILT	0	0.10	12	100	
53	GRAY SILT	0	0.10	12	100	
54	GRAY SILT	0	0.10	12	100	
55	GRAY SILT	0	0.10	12	100	
56	GRAY SILT	0	0.10	12	100	
57	GRAY SILT	0	0.10	12	100	
58	GRAY SILT	0	0.10	12	100	
59	GRAY SILT	0	0.10	12	100	
60	GRAY SILT	0	0.10	12	100	
61	GRAY SILT	0	0.10	12	100	
62	GRAY SILT	0	0.10	12	100	
63	GRAY SILT	0	0.10	12	100	
64	GRAY SILT	0	0.10	12	100	
65	GRAY SILT	0	0.10	12	100	
66	GRAY SILT	0	0.10	12	100	
67	GRAY SILT	0	0.10	12	100	
68	GRAY SILT	0	0.10	12	100	
69	GRAY SILT	0	0.10	12	100	
70	GRAY SILT	0	0.10	12	100	
71	GRAY SILT	0	0.10	12	100	
72	GRAY SILT	0	0.10	12	100	
73	GRAY SILT	0	0.10	12	100	
74	GRAY SILT	0	0.10	12	100	
75	GRAY SILT	0	0.10	12	100	
76	GRAY SILT	0	0.10	12	100	
77	GRAY SILT	0	0.10	12	100	
78	GRAY SILT	0	0.10	12	100	
79	GRAY SILT	0	0.10	12	100	
80	GRAY SILT	0	0.10	12	100	
81	GRAY SILT	0	0.10	12	100	
82	GRAY SILT	0	0.10	12	100	
83	GRAY SILT	0	0.10	12	100	
84	GRAY SILT	0	0.10	12	100	
85	GRAY SILT	0	0.10	12	100	
86	GRAY SILT	0	0.10	12	100	
87	GRAY SILT	0	0.10	12	100	
88	GRAY SILT	0	0.10	12	100	
89	GRAY SILT	0	0.10	12	100	
90	GRAY SILT	0	0.10	12	100	
91	GRAY SILT	0	0.10	12	100	
92	GRAY SILT	0	0.10	12	100	
93	GRAY SILT	0	0.10	12	100	
94	GRAY SILT	0	0.10	12	100	
95	GRAY SILT	0	0.10	12	100	
96	GRAY SILT	0	0.10	12	100	
97	GRAY SILT	0	0.10	12	100	
98	GRAY SILT	0	0.10	12	100	
99	GRAY SILT	0	0.10	12	100	
100	GRAY SILT AND CLAY	0	0.10	12	100	

NOTE: BORING LOGS PROVIDED BY ODOT.



**Appendix B: Sequence of installation and detailed inspection of the drilled shafts.**



**INSPECTION RECORD FOR DRILLED S S**

Project Number 457-97	Drilling Contractor  Agra Foundations	Type and Model of Drilling Machinery CMV TH18-50 Crawler Hydraulic Piling Rig	Bid Price Above Bedrock (\$/ft) 713			
Bridge Number CUY-90-15.24		Max. Continuous Torque (ft-lbs) 132,752 @ 7.4 RPM	Bid Price in Bedrock Socket (\$/ft) 1620			
Structure File Number 1809393	Project Engineer Kirk M. Gegick, PE	CROWD (max. Cont. Downward Force (lbs) 44,805 (Which is Equal To The Extraction Force)	Type of Slurry Used KB Technologies' "Slurry Pro"			
			Type of Bedrock Soft to Medium Hard Shale			
DRILLED SHAFT NUMBER		1	3	5	7	
DATE & TIME OF DRILLING	STARTED	DATE	9/9/98	11/9/98	10/30/98	10/19/98
		TIME	9:00 AM	9:30 AM	1:30 PM	3:00 PM
	FINISHED	DATE	10/13/98	11/12/98	11/4/98	10/22/98
		TIME	5:00 PM	9:00 AM	11:00 AM	1:30 PM
APPROXIMATE ELEVATION OF TOP OF OVERBURDEN		586.00	586.00	586.00	586.00	
LENGTH OF DRILLED SHAFTS ABOVE THE BEDROCK SOCKET	THROUGH AIR (FT)	N/A	N/A	N/A	N/A	
	THROUGH OVERBURDEN (FT)	140.00	141.50	143.00	142.50	
	PAY LENGTH (FT)	140.00	141.50	143.00	142.50	
OBSTRUCTIONS ENCOUNTERED	NUMBER	1	2	2	2	
	SIZE (IN)	See Below	See Below	See Below	See Below	
	TIME OF REMOVAL (HR)	See Below	See Below	See Below	See Below	
LENGTH OF DRILLED SHAFTS IN BEDROCK SOCKET	ELEV. TOP OF BEDROCK SOCKET	446.00	444.50	443.00	443.50	
	ELEV. BOTTOM OF BEDROCK	439.00	438.50	437.00	437.50	
	LENGTH OF BEDROCK SOCKET	7	6	6	6	
STEEL CASING	CASING THICKNESS (IN)	5/8	5/8	5/8	5/8	
	CASING LEFT IN PLACE (FT)	0	0	0	0	
REINFORCING STEEL	VERTICAL	BAR SIZE-NUMBER	#11	#11	#11	#11
		NUMBER OF REBAR	24	24	24	24
	SPIRAL	BAR SIZE-NUMBER	#4	#4	#4	#4
		PITCH (IN)	4.5	4.5	4.5	4.5
CONCRETE	SLUMP (IN)	7-9	7-9	7-9	7-9	
	CYLINDER STRENGTH (PSI)	4390/5190	6700/6580	6290/6360	5906/5900	
	AIR TEMPERATURE	64/46	48/34	52/46	65/45	
	DATE PLACED	10/15/98	11/13/98	11/6/98	10/27/98	
	QUANTITY (CY)	205	189	202	187	
TOLERANCES	LATERAL DEVIATION	N-S (FT)	0.50-N	0.02-N	0.42-N	0.24-N
		E-W (FT)	0.50-W	0.30-E	0.24-W	0.60-W
PLAN SHAFT DIAMETER ABOVE/BELOW BEDROCK SOCKET (IN)		72/66	72/66	72/66	72/66	
ACTUAL DIAMETER ABOVE/BELOW BEDROCK SOCKET (IN)		72/72	72/72	72/72	72/72	
PROJECT ENGINEER'S COMMENTS: See Obstruction Table Below						
Drilled Shaft #	Date	Time	Type			Depth
1	9/9 - 10/8	3 pm - 5:30pm	H-Pile			48'
3	11/9	9:30am - 3 pm	Timber			12'
3	11/9 - 11/11	4 pm - 4:30 pm	H-Pile			54'
5	10/30 - 11/2	4 pm - 9 am	Timber			16'
5	11/2	9 am - 4 pm	H-Pile			54'
7	10/19 - 10/20	4 pm - 11 am	Timber			17'
7	10/20 - 10/21	11 am - 11:30 am	H-Pile x2			42'



**INSPECTION RECORD FOR D D S**

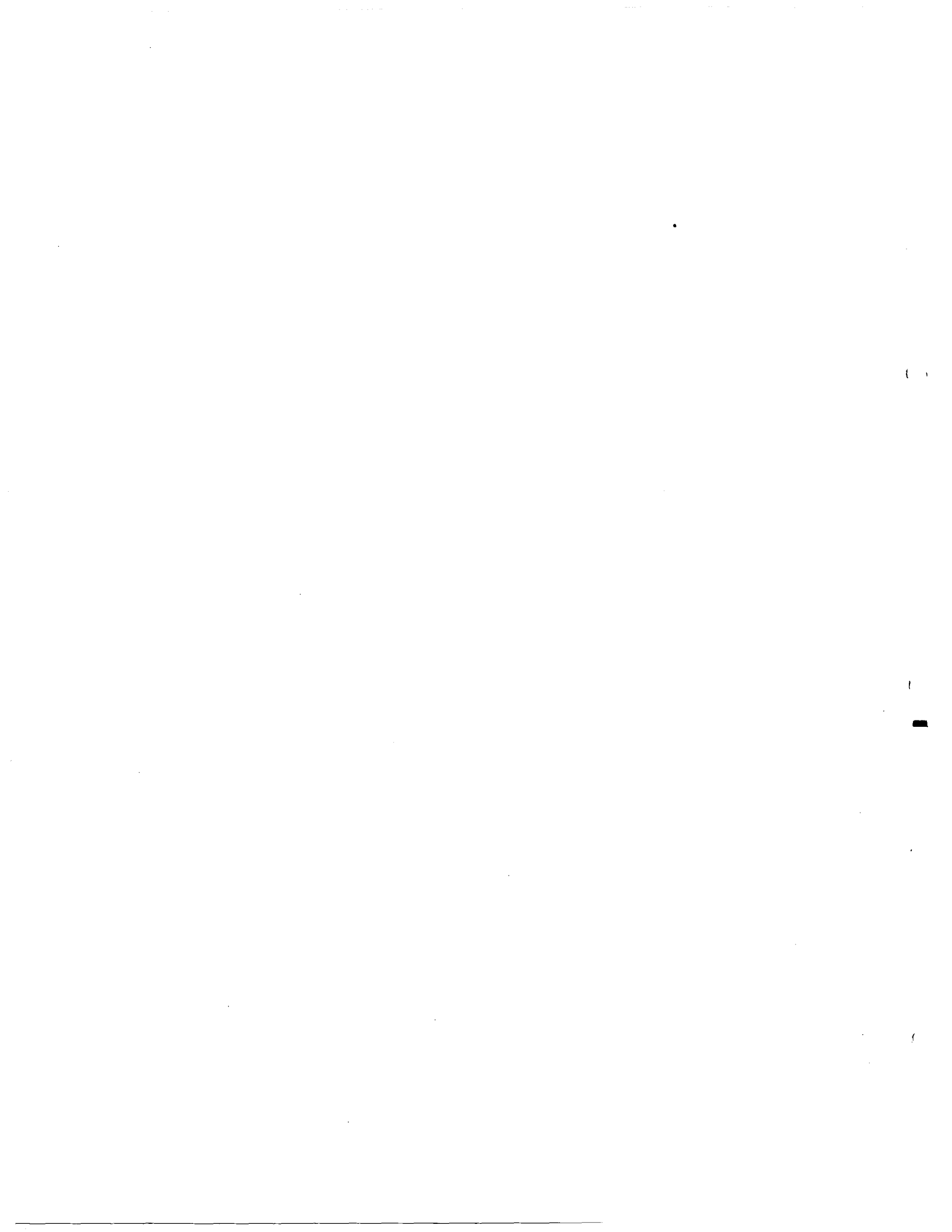
Project Number 457-97	Drilling Contractor  Agra Foundations	Type and Model of Drilling Machinery CMV TH18-50 Crawler Hydraulic Piling Rig	Bid Price Above Bedrock (\$/ft) 713			
Bridge Number CUY-90-15.24		Max. Continuous Torque (ft-lbs) 132,752 @ 7.4 RPM	Bid Price in Bedrock Socket (\$/ft) 1620			
Structure File Number 1809393	Project Engineer Kirk M. Gegick, PE	CROWD (max. Cont. Downward Force (lbs)) 44,805 (Which is Equal To The Extraction Force)	Type of Slurry Used KB Technologies' "Slurry Pro"			
			Type of Bedrock Soft to Medium Hard Shale			
DRILLED SHAFT NUMBER		9	11	13	15	
DATE & TIME OF DRILLING	STARTED	DATE	10/30/98	9/23/98	11/4/98	10/22/98
		TIME	3:30 PM	8:30 AM	11:00 AM	1:30 PM
	FINISHED	DATE	11/19/98	9/30/98	11/6/98	10/30/98
		TIME	5:30 PM	3:30 PM	11:30 AM	1:30 PM
APPROXIMATE ELEVATION OF TOP OF OVERBURDEN		586.00	586.00	586.00	586.00	
LENGTH OF DRILLED SHAFTS ABOVE THE BEDROCK SOCKET	THROUGH AIR (FT)		N/A	N/A	N/A	N/A
	THROUGH OVERBURDEN (FT)		143.00	140.50	144.00	144.50
	PAY LENGTH (FT)		143.00	140.50	144.00	144.50
OBSTRUCTIONS ENCOUNTERED	NUMBER		1	3	0	4
	SIZE (IN)		See Below	See Below	N/A	See Below
	TIME OF REMOVAL (HR)		See Below	See Below	N/A	See Below
LENGTH OF DRILLED SHAFTS IN BEDROCK SOCKET	ELEV., TOP OF BEDROCK SOCKET		443.00	442.50	442.00	441.50
	ELEV., BOTTOM OF BEDROCK		437.00	436.50	436.00	435.50
	LENGTH OF BEDROCK SOCKET		6	9	6	6
STEEL CASING	CASING THICKNESS (IN)		5/8	5/8	5/8	5/8
	CASING LEFT IN PLACE (FT)		0	0	0	0
REINFORCING STEEL	VERTICAL	BAR SIZE-NUMBER	#11	#11	#11	#11
		NUMBER OF REBAR	24	24	24	24
	SPIRAL	BAR SIZE-NUMBER	#4	#4	#4	#4
		PITCH (IN)	4.5	4.5	4.5	4.5
CONCRETE	SLUMP (IN)		7-9	7-9	7-9	7-9
	CYLINDER STRENGTH (PSI)		6790/6960	6530/6620	4970/4780	7880/7730
	AIR TEMPERATURE		50/36	72/45	51/45	47/36
	DATE PLACED		11/23/98	10/2/98	11/10/98	11/3/98
	QUANTITY (CY)		214	196	198	200
TOLERANCES	LATERAL DEVIATION	N-S (FT)	0.29-N	0.83-N	0.03-N	0.52-N
		E-W (FT)	0.65-W	0.17-W	0.07-E	0.25-W
PLAN SHAFT DIAMETER ABOVE/BELOW BEDROCK SOCKET (IN)		72/66	72/66	72/66	72/66	
ACTUAL DIAMETER ABOVE/BELOW BEDROCK SOCKET (IN)		72/72	72/72	72/72	72/72	
PROJECT ENGINEER'S COMMENTS: See Obstruction Table Below.						
Drilled Shaft #	Date	Time	Type			Depth
9	11/2 - 11/19	4 pm - 5:30pm	H-Pile			48'
11	9/23	8:30am - 1:30pm	Timber			18'
11	9/23 - 9/24	5 pm - 2 pm	H-Pile (Stub) #1			50'
11	9/24 - 9/25	5 pm - 10 am	H-Pile (Stub) #2			55'
15	10/22	2 pm - 4 pm	Timber			18'
15	10/22 - 10/27	4 pm - 5pm	H-Pile #1			52'
15	10/27 - 10/28	5 pm - 2 pm	H-Pile #2			60'
15	10/28 - 10/29	2 pm - 5 pm	H-Pile #3			69'





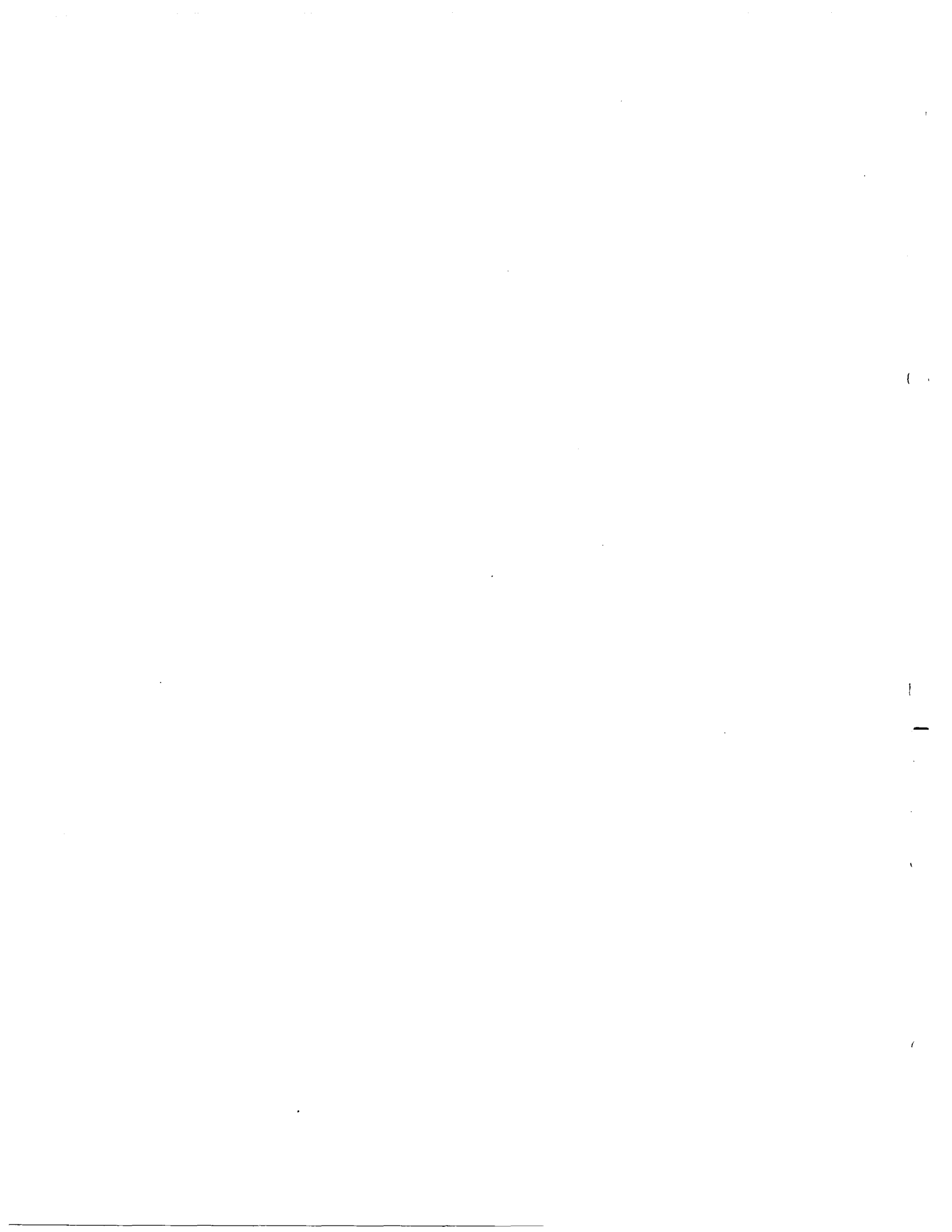
**INSPECTION RECORD FOR D D S**

Project Number 457-97	Drilling Contractor  Agra Foundations	Type and Model of Drilling Machinery CMV TH18-50 Crawler Hydraulic Piling Rig	Bid Price Above Bedrock (\$/ft) 713	
Bridge Number CUY-90-15.24		Max. Continuous Torque (ft-lbs) 132,752 @ 7.4 RPM	Bid Price in Bedrock Socket (\$/ft) 1620	
Structure File Number 1809393	Project Engineer Kirk M. Gegick, PE	CROWD (max. Cont. Downward Force (lbs) 44,805 (Which is Equal To The Extraction Force)	Type of Slurry Used KB Technologies' "Slurry Pro"	
			Type of Bedrock Soft to Medium Hard Shale	
DRILLED SHAFT NUMBER		17		
DATE & TIME OF DRILLING	STARTED	DATE	11/20/98	
		TIME	7:00 am	
	FINISHED	DATE	11/23/98	
		TIME	5:30 pm	
APPROXIMATE ELEVATION OF TOP OF OVERBURDEN		586.00		
LENGTH OF DRILLED SHAFTS ABOVE THE BEDROCK SOCKET	THROUGH AIR (FT)	N/A		
	THROUGH OVERBURDEN (FT)	145.00		
	PAY LENGTH (FT)	145.00		
OBSTRUCTIONS ENCOUNTERED	NUMBER	2		
	SIZE (IN)	See Below		
	TIME OF REMOVAL (HR)	See Below		
LENGTH OF DRILLED SHAFTS IN BEDROCK SOCKET	ELEV., TOP OF BEDROCK SOCKET	441.00		
	ELEV., BOTTOM OF BEDROCK	435.00		
	LENGTH OF BEDROCK SOCKET	6		
STEEL CASING	CASING THICKNESS (IN)	5/8		
	CASING LEFT IN PLACE (FT)	0		
REINFORCING STEEL	VERTICAL	BAR SIZE-NUMBER	#11	
		NUMBER OF REBAR	24	
	SPIRAL	BAR SIZE-NUMBER	#4	
		PITCH (IN)	4.5	
CONCRETE	SLUMP (IN)	7-9		
	CYLINDER STRENGTH (PSI)	5760/5790		
	AIR TEMPERATURE	54/40		
	DATE PLACED	11/25/98		
	QUANTITY (CY)	186		
TOLERANCES	LATERAL DEVIATION	N-S (FT)	0.7-N	
		E-W (FT)	0.42-E	
PLAN SHAFT DIAMETER ABOVE/BELOW BEDROCK SOCKET (IN)		72/66		
ACTUAL DIAMETER ABOVE/BELOW BEDROCK SOCKET (IN)		72/72		
PROJECT ENGINEER'S COMMENTS: See Obstruction Table Below.				
Drilled Shaft #	Date	Time	Type	Depth
17	11/20	8 am - 1 pm	Timber	6'
17	11/20 - 11/21	1:30 pm - 9:30 am	H-Pile	48'



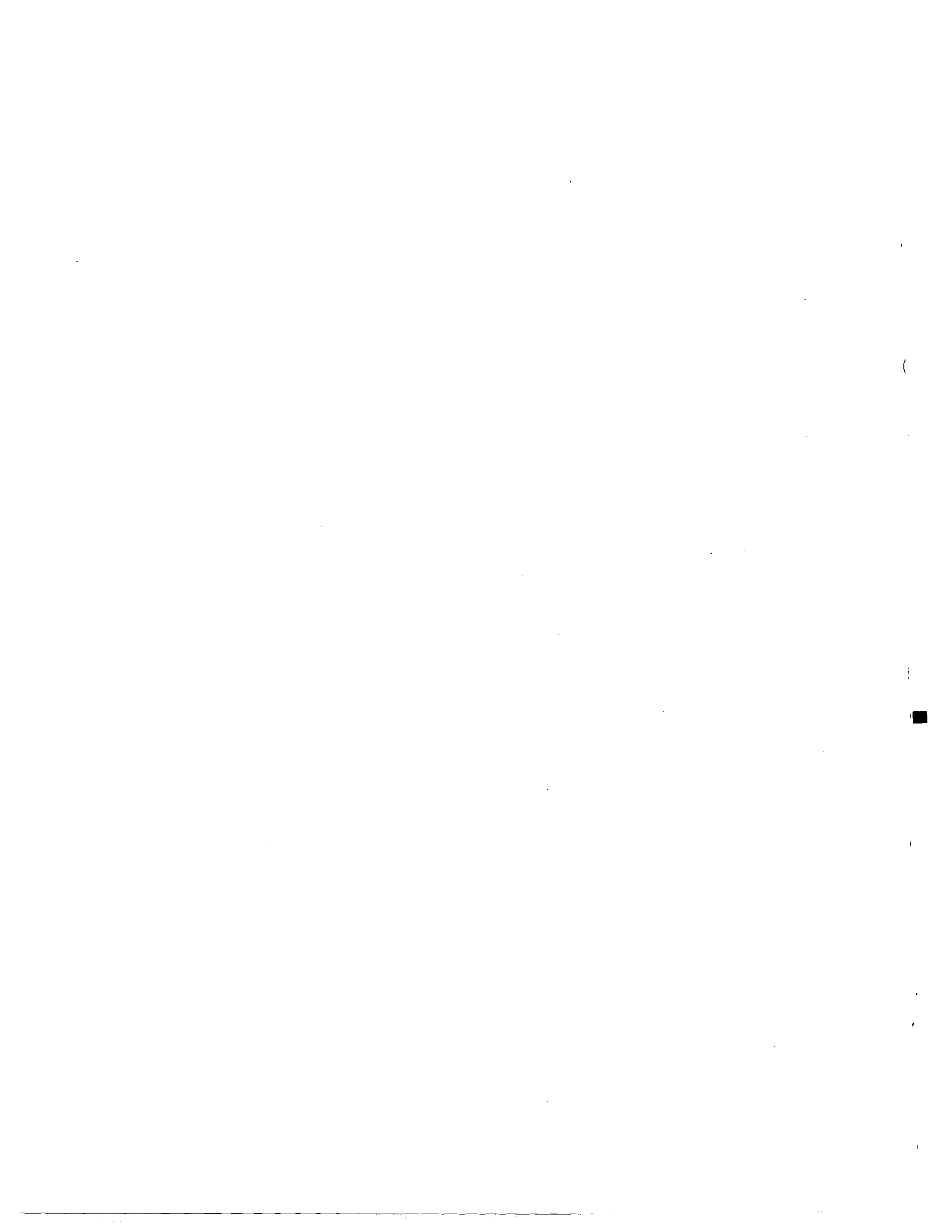
**INSPECTION RECORD FOR D D S S**

Project Number 457-97	Drilling Contractor  Agra Foundations	Type and Model of Drilling Machinery CMV TH18-50 Crawler Hydraulic Piling Rig	Bid Price Above Bedrock (\$/ft) 713			
Bridge Number CUY-90-15.24		Max. Continuous Torque (ft-lbs) 132,752 @ 7.4 RPM	Bid Price in Bedrock Socket (\$/ft) 1620			
Structure File Number 1809393	Project Engineer Kirk M. Gegick, PE	CROWD (max. Cont. Downward Force (lbs)) 44,805 (Which is Equal To The Extraction Force)	Type of Slurry Used KB Technologies' "Slurry Pro"			
			Type of Bedrock Soft to Medium Hard Shale			
DRILLED SHAFT NUMBER		2	4	6	8	
DATE & TIME OF DRILLING	STARTED	DATE	8/20/98	8/3/98	9/17/98	8/24/98
		TIME	10:00 AM	11:30 AM	1:30 PM	12:00 PM
	FINISHED	DATE	8/27/98	8/13/98	9/22/98	9/8/98
		TIME	10:30 AM	9:00 AM	6:30 PM	5:30 PM
APPROXIMATE ELEVATION OF TOP OF OVERBURDEN		586.00	586.00	586.00	586.00	
LENGTH OF DRILLED SHAFTS ABOVE THE BEDROCK SOCKET	THROUGH AIR (FT)	N/A	N/A	N/A	N/A	
	THROUGH OVERBURDEN (FT)	133.80	141.75	142.25	142.75	
	PAY LENGTH (FT)	133.80	141.75	142.25	142.75	
OBSTRUCTIONS ENCOUNTERED	NUMBER	2	0	1	2	
	SIZE (IN)	See Below	N/A	See Below	See Below	
	TIME OF REMOVAL (HR)	See Below	N/A	See Below	See Below	
LENGTH OF DRILLED SHAFTS IN BEDROCK SOCKET	ELEV., TOP OF BEDROCK SOCKET	452.20	444.25	443.75	443.25	
	ELEV., BOTTOM OF BEDROCK	443.00	438.25	437.75	437.25	
	LENGTH OF BEDROCK SOCKET	9.2	6	6	6	
STEEL CASING	CASING THICKNESS (IN)	5/8	5/8	5/8	5/8	
	CASING LEFT IN PLACE (FT)	0	0	0	0	
REINFORCING STEEL	VERTICAL	BAR SIZE-NUMBER	#11	#11	#11	#11
		NUMBER OF REBAR	24	24	24	24
	SPIRAL	BAR SIZE-NUMBER	#4	#4	#4	#4
		PITCH (IN)	4.5	4.5	4.5	4.5
CONCRETE	SLUMP (IN)	7-9	7-9	7-9	7-9	
	CYLINDER STRENGTH (PSI)	5060/5110	5740/5950	5090/5300	4210/4070	
	AIR TEMPERATURE	84/66	80/67	69/45	65/50	
	DATE PLACED	8/28/98	8/19/98	9/24/98	9/10/98	
	QUANTITY (CY)	180	202	185	180	
TOLERANCES	LATERAL DEVIATION	N-S (FT)	0.28-N	0.05-N	1.16-N	1.24-N
		E-W (FT)	0.01-E	0.28-E	0.31-W	0.21-E
PLAN SHAFT DIAMETER ABOVE/BELOW BEDROCK SOCKET (IN)		72/66	72/66	72/66	72/66	
ACTUAL DIAMETER ABOVE/BELOW BEDROCK SOCKET (IN)		72/72	72/72	72/72	72/72	
PROJECT ENGINEER'S COMMENTS: See Obstruction Table Below.						
Drilled Shaft #	Date	Time	Type			Depth
2	8/21 - 8/24	1 pm - 9am	H-Pile (Stub)			75'
2	8/24 - 8/25	11am - 1pm	Methane			117'
6	9/18 - 9/21	1:30pm - 3:30pm	H-Pile (Stub)			74'
8	8/24	1pm - 3pm	Timber			15'
8	8/24 - 9/3	4pm - 3pm	H-Pile (Stub)			65'

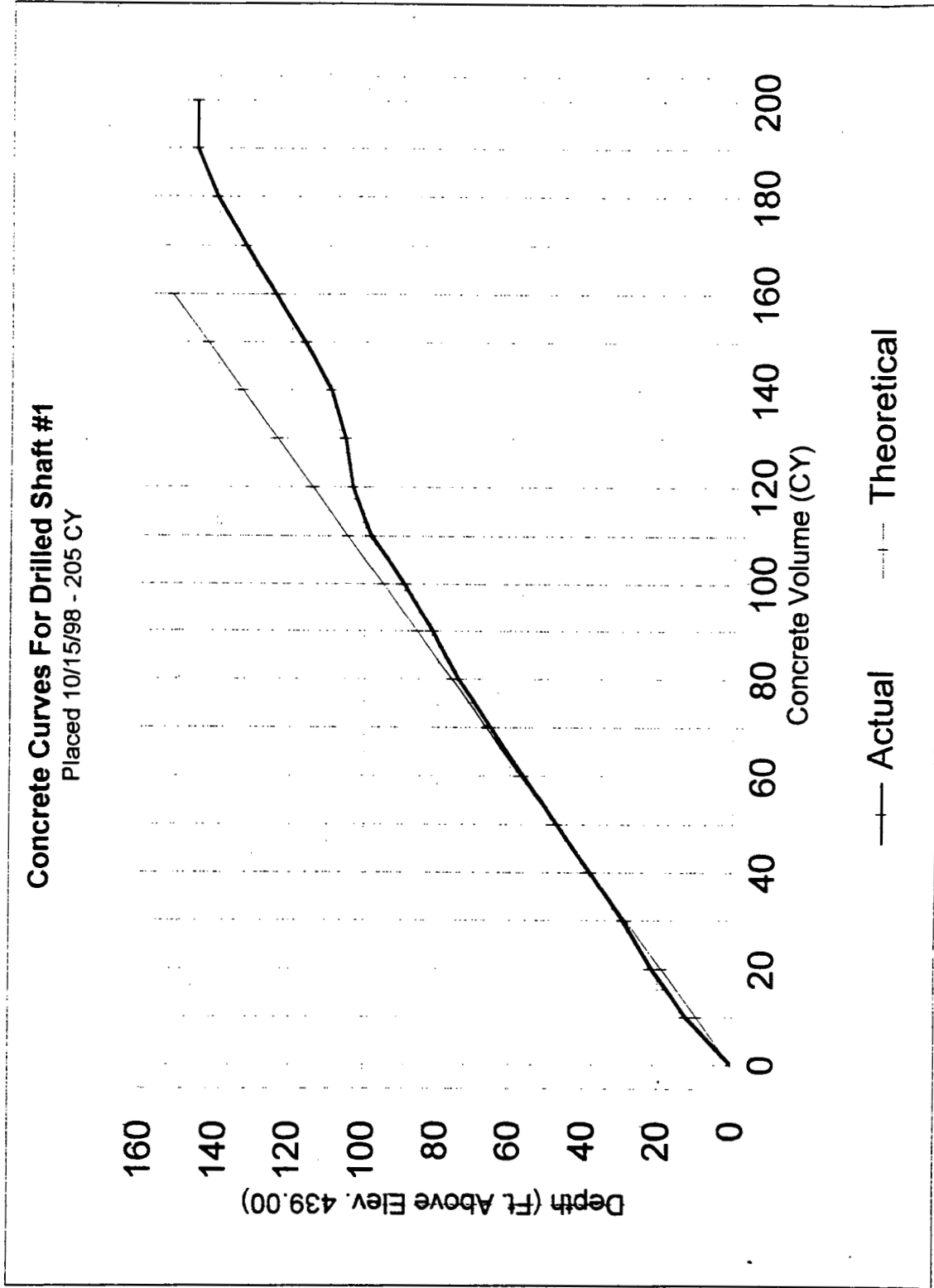


**INSPECTION RECORD FOR D D S S**

Project Number 457-97	Drilling Contractor  Agra Foundations	Type and Model of Drilling Machinery CMV TH18-S0 Crawler Hydraulic Piling Rig	Bid Price Above Bedrock (\$/ft) 713			
Bridge Number CUY-90-15.24		Max. Continuous Torque (ft-lbs) 132,752 @ 7.4 RPM	Bid Price in Bedrock Socket (\$/ft) 1620			
Structure File Number 1809393	Project Engineer Kirk M. Gegick, PE	CROWD (max. Cont. Downward Force (lbs)) 44,805 (Which is Equal To The Extraction Force)	Type of Slurry Used KB Technologies' "Slurry Pro"			
			Type of Bedrock Soft to Medium Hard Shale			
DRILLED SHAFT NUMBER		10	12	14	16	
DATE & TIME OF DRILLING	STARTED	DATE	8/13/98	8/27/98	10/9/98	11/12/98
		TIME	10:00 am	2:00 pm	3:00 pm	2:00 pm
	FINISHED	DATE	8/20/98	9/2/98	10/19/98	11/18/98
		TIME	9:00 am	5:30 pm	3:00 pm	5:30 pm
APPROXIMATE ELEVATION OF TOP OF OVERBURDEN		586.00	586.00	586.00	586.00	
LENGTH OF DRILLED SHAFTS ABOVE THE BEDROCK SOCKET	THROUGH AIR (FT)		N/A	N/A	N/A	N/A
	THROUGH OVERBURDEN (FT)		143.25	143.75	144.25	144.75
	PAY LENGTH (FT)		143.25	143.75	144.25	144.75
OBSTRUCTIONS ENCOUNTERED	NUMBER		0	0	2	2
	SIZE (IN)		N/A	N/A	See below	See below
	TIME OF REMOVAL (HR)		N/A	N/A	See below	See below
LENGTH OF DRILLED SHAFTS IN BEDROCK SOCKET	ELEV., TOP OF BEDROCK SOCKET		442.75	442.25	441.75	441.25
	ELEV., BOTTOM OF BEDROCK		436.75	436.25	435.75	435.25
	LENGTH OF BEDROCK SOCKET		6	6	6	6
STEEL CASING	CASING THICKNESS (IN)		5/8	5/8	5/8	5/8
	CASING LEFT IN PLACE (FT)		0	0	0	0
REINFORCING STEEL	VERTICAL	BAR SIZE-NUMBER	#11	#11	#11	#11
		NUMBER OF REBAR	24	24	24	24
	SPIRAL	BAR SIZE-NUMBER	#4	#4	#4	#4
		PITCH (IN)	4.5	4.5	4.5	4.5
CONCRETE	SLUMP (IN)		7-9	7-9	7-9	7-9
	CYLINDER STRENGTH (PSI)		6260/6590	5560/5780	6250/6190	4740/4730
	AIR TEMPERATURE		82/62	76/53	48/36	58/42
	DATE PLACED		8/21/98	9/4/98	10/21/98	11/18/98
	QUANTITY (CY)		195	186	180	190
TOLERANCES	LATERAL DEVIATION	N-S (FT)	0.07-S	0.99-S	0.60-N	0.47-N
		E-W (FT)	0.01-W	0.25-W	0.02-E	0.26-W
PLAN SHAFT DIAMETER ABOVE/BELOW BEDROCK SOCKET (IN)		72/66	72/66	72/66	72/66	
ACTUAL DIAMETER ABOVE/BELOW BEDROCK SOCKET (IN)		72/72	72/72	72/72	72/72	
PROJECT ENGINEER'S COMMENTS: See Obstruction Table Below.						
Drilled Shaft #	Date	Time	Type			Depth
14	10/9 - 10/12	4 pm - 9 am	Timber			19'
14	10/12 - 10/16	5 pm - 12 pm	H-Pile			34'
16	11/13	8 am - 4 pm	H-Pile #1			35'
16	11/13 - 11/14	4 pm - 3 pm	H-Pile #2			45'



ODOT PROJECT 457-97

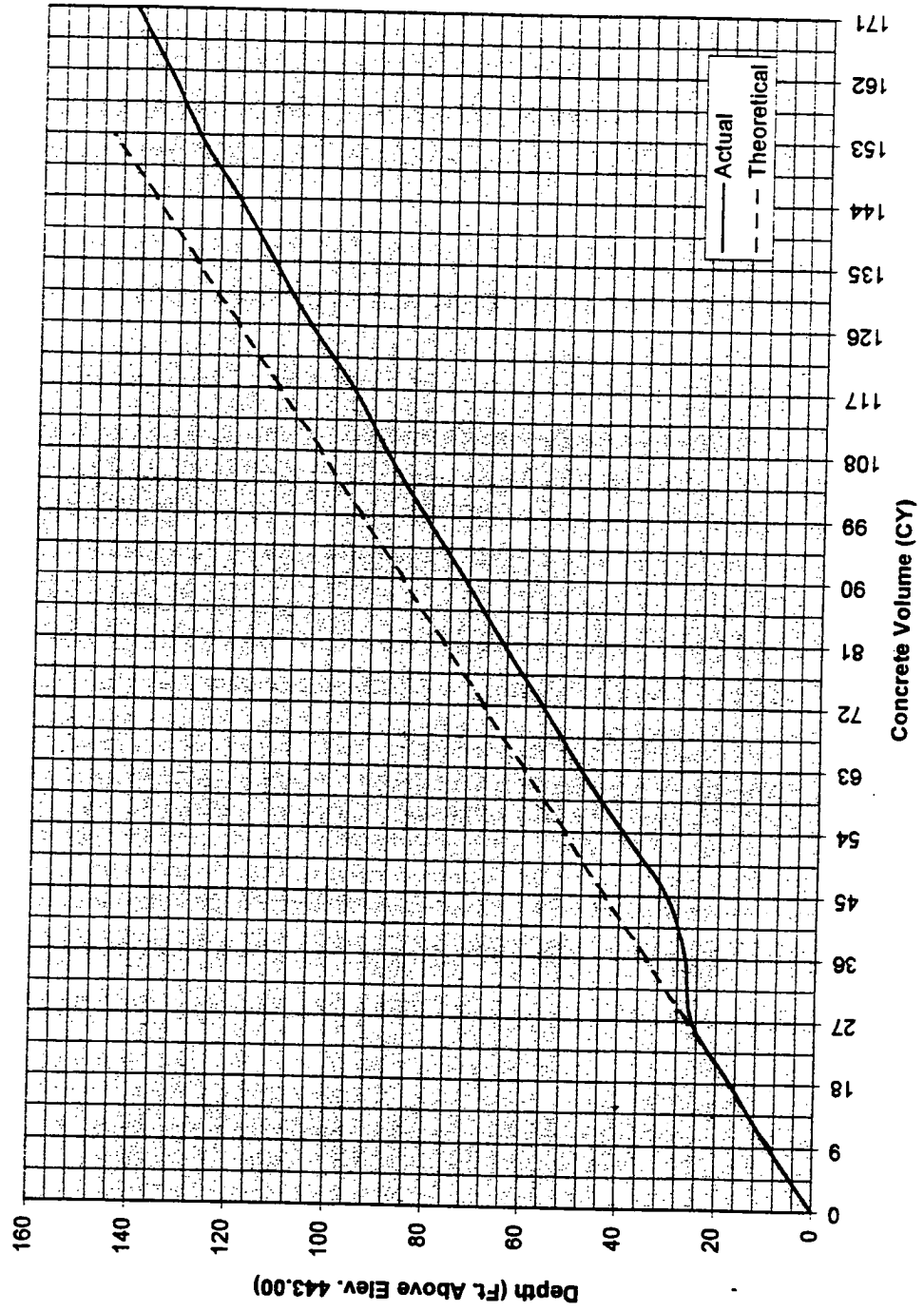


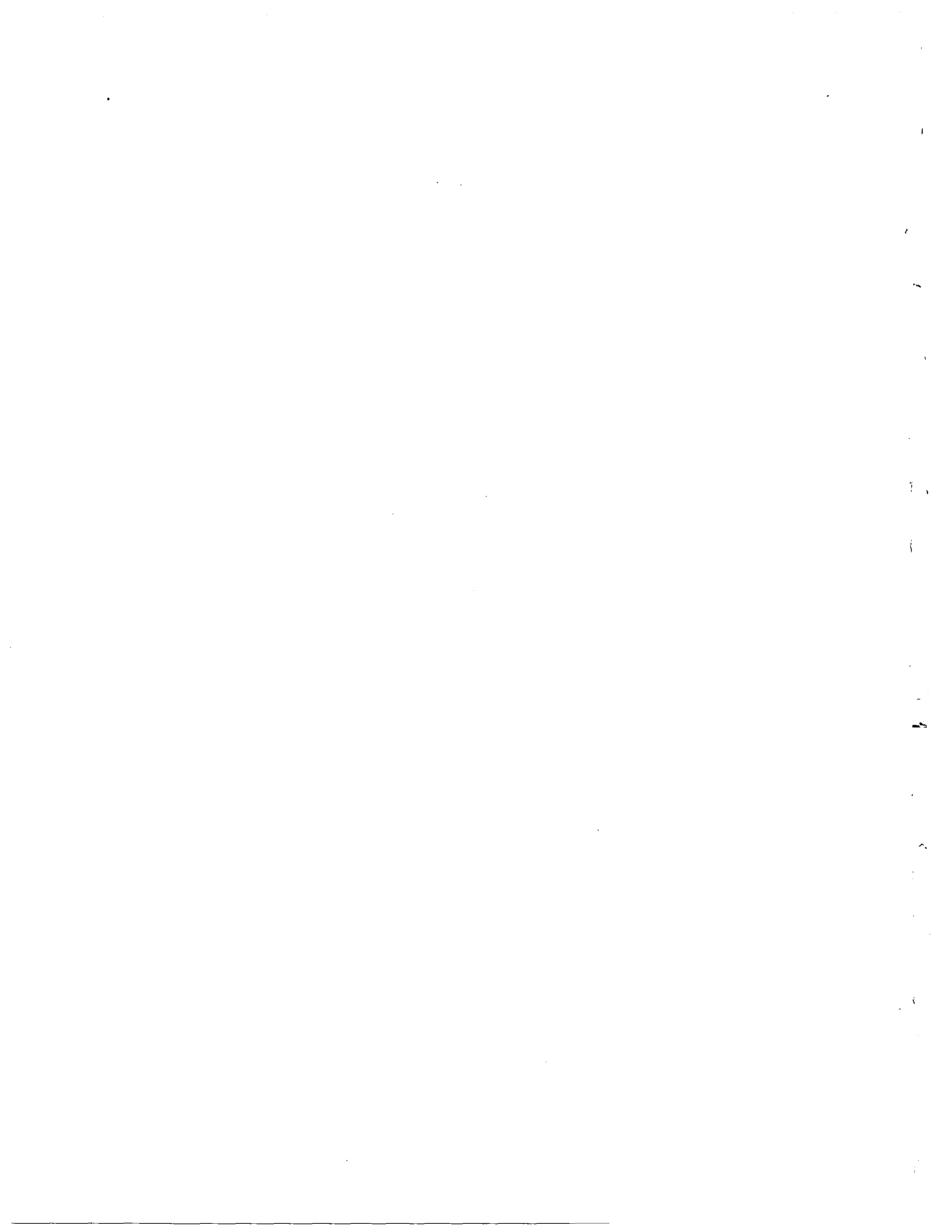




ODOT PROJECT 457-97

Concrete Curves For Drilled Shaft #2

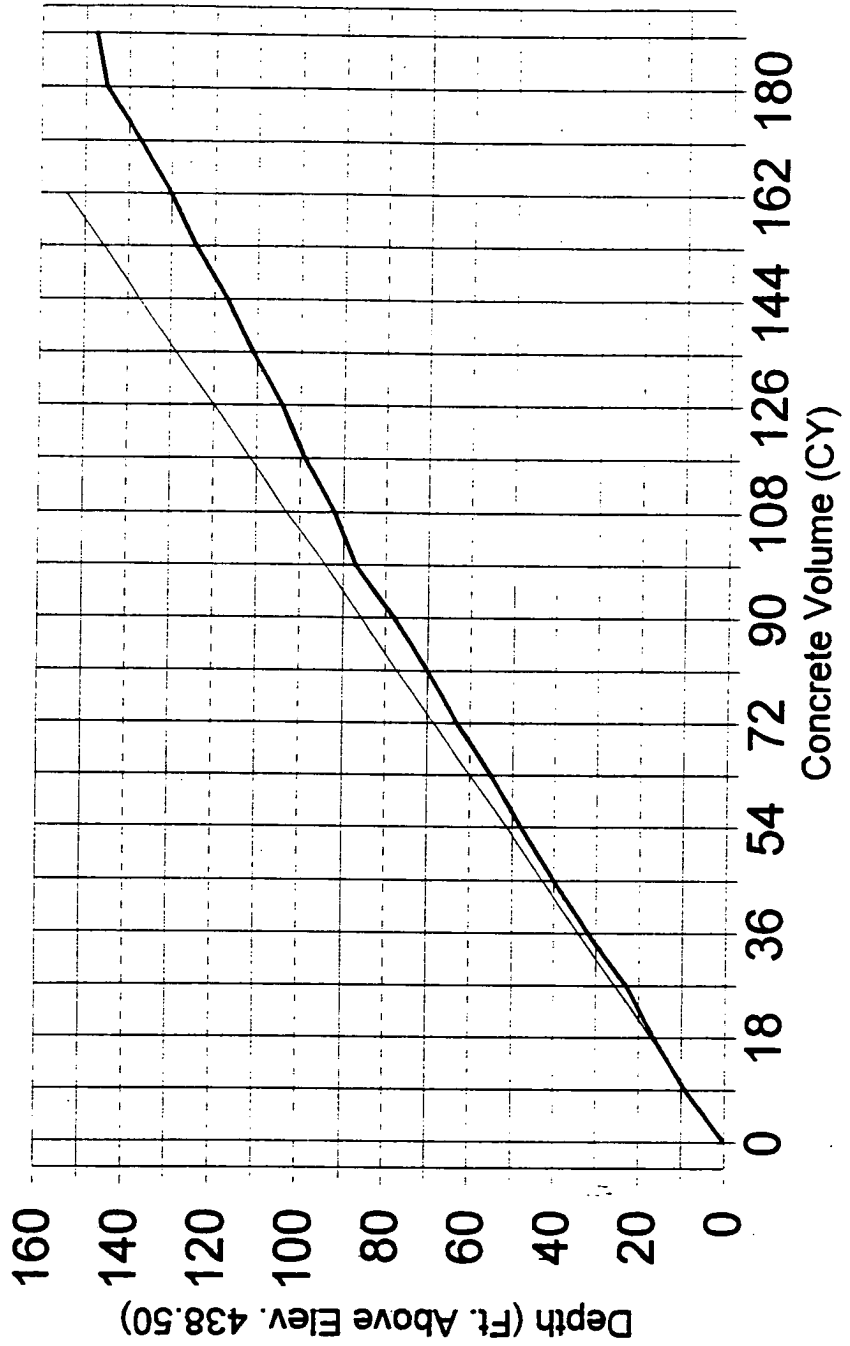




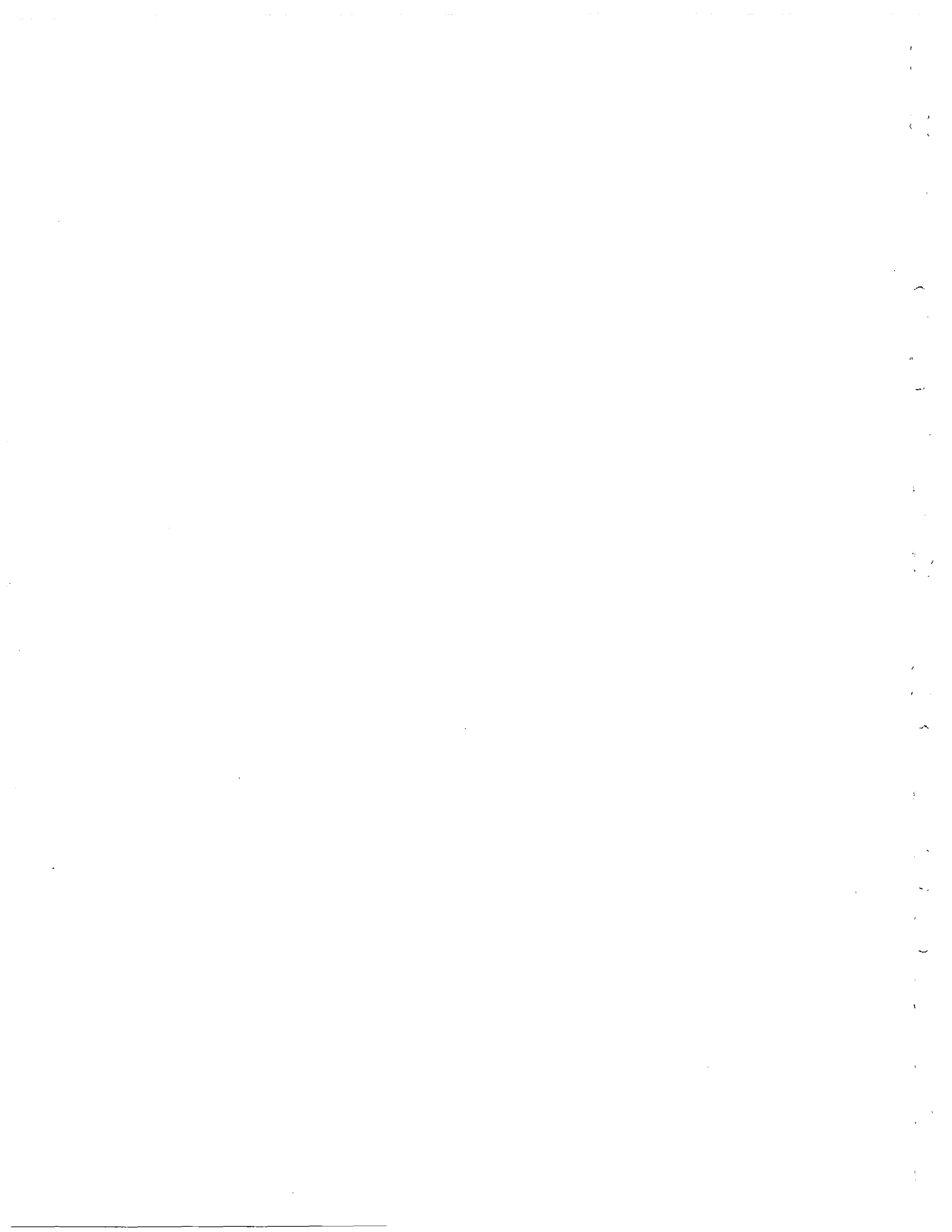
ODOT PROJECT 457-97

### Concrete Curves For Drilled Shaft #3

Placed 11/13/98 - 189 CY

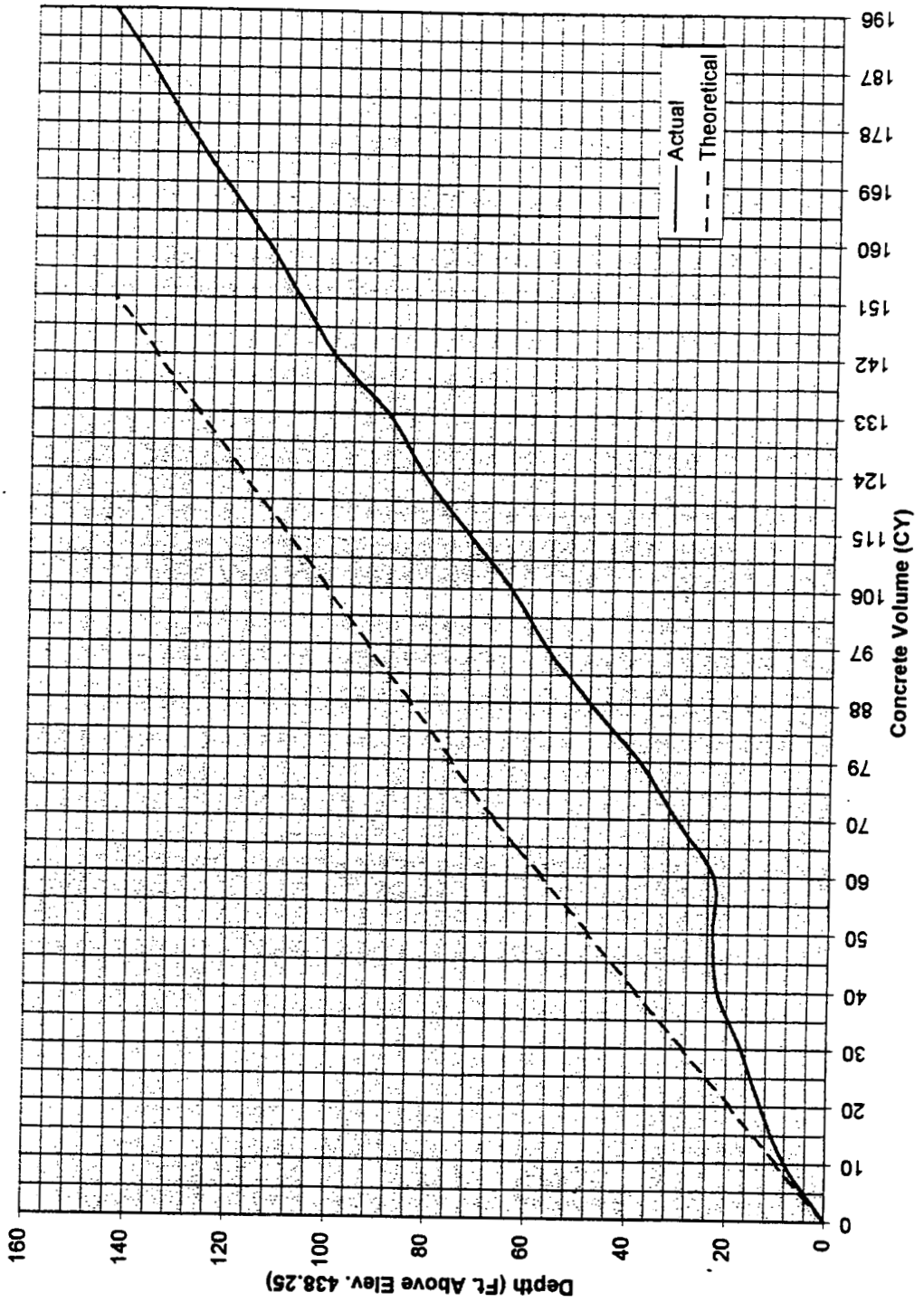


— Actual      - - - Theoretical



ODOT PROJECT 457-97

Concrete Curves For Drilled Shaft #4

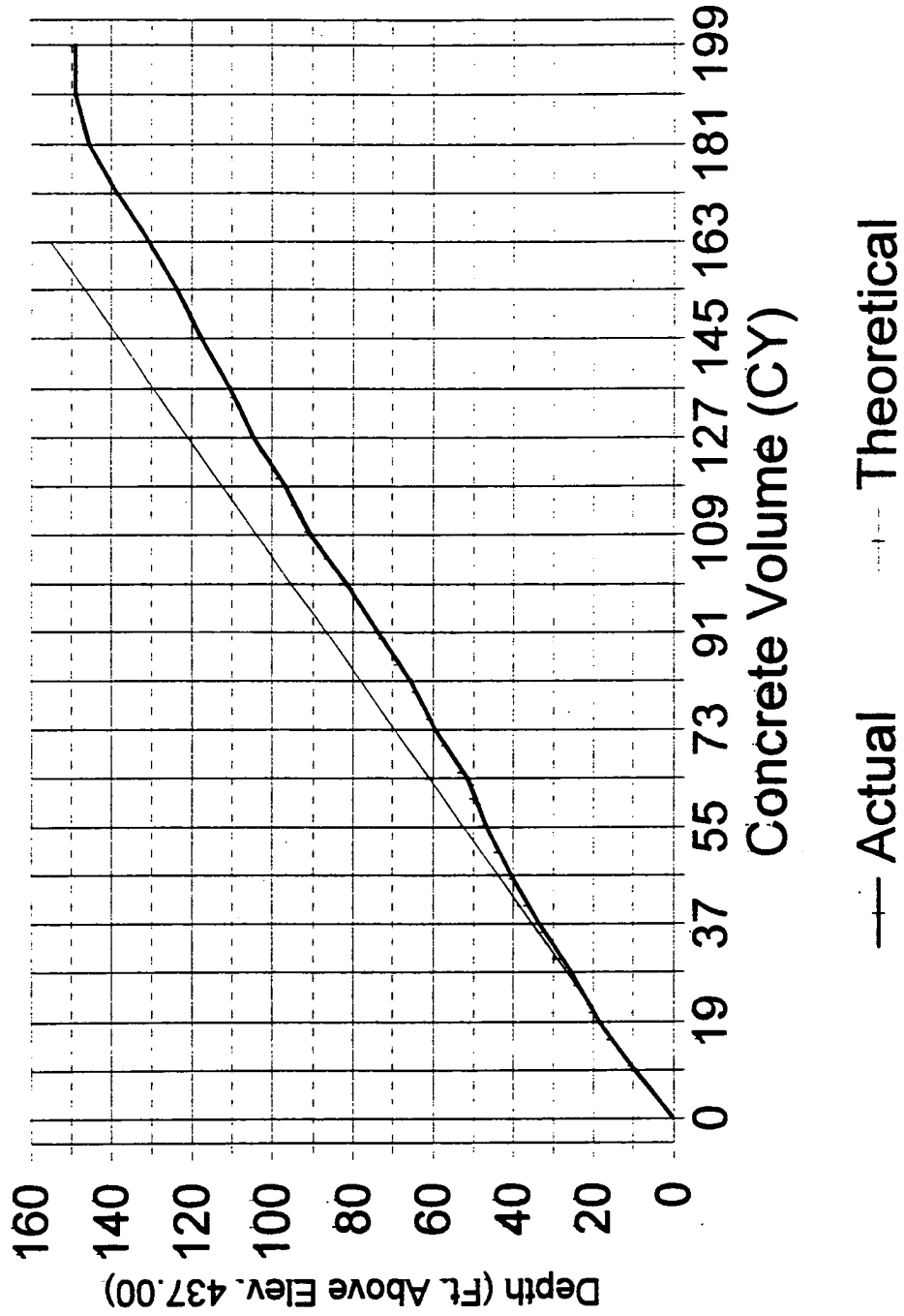


1  
2  
3  
4  
5  
6  
7  
8  
9  
10  
11  
12  
13  
14  
15  
16  
17  
18  
19  
20  
21  
22  
23  
24  
25  
26  
27  
28  
29  
30  
31  
32  
33  
34  
35  
36  
37  
38  
39  
40  
41  
42  
43  
44  
45  
46  
47  
48  
49  
50  
51  
52  
53  
54  
55  
56  
57  
58  
59  
60  
61  
62  
63  
64  
65  
66  
67  
68  
69  
70  
71  
72  
73  
74  
75  
76  
77  
78  
79  
80  
81  
82  
83  
84  
85  
86  
87  
88  
89  
90  
91  
92  
93  
94  
95  
96  
97  
98  
99  
100

ODOT PROJECT 457-97

### Concrete Curves For Drilled Shaft #5

Placed 11/6/98 - 202 CY

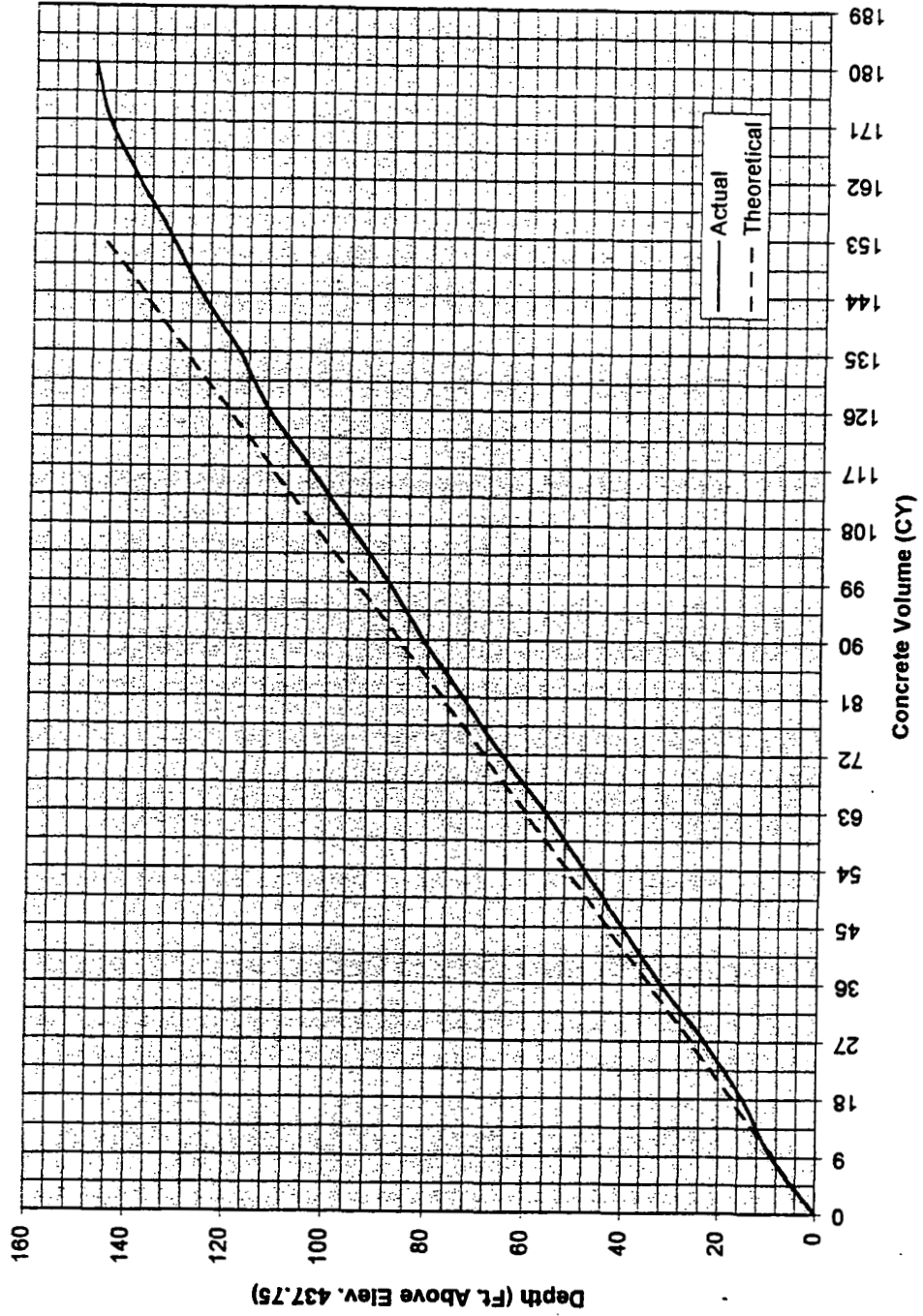


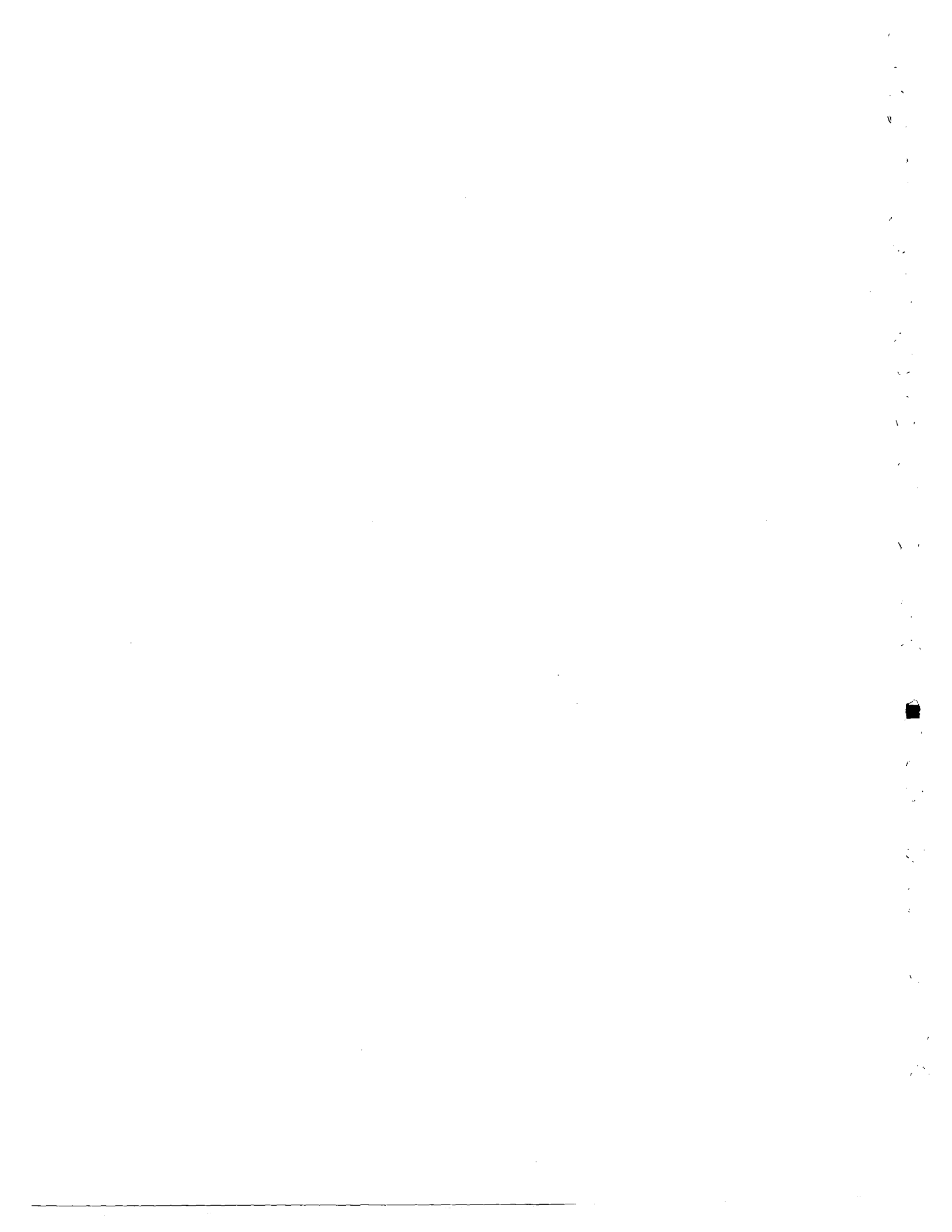




ODOT PROJECT 457-97

Concrete Curves For Drilled Shaft #6

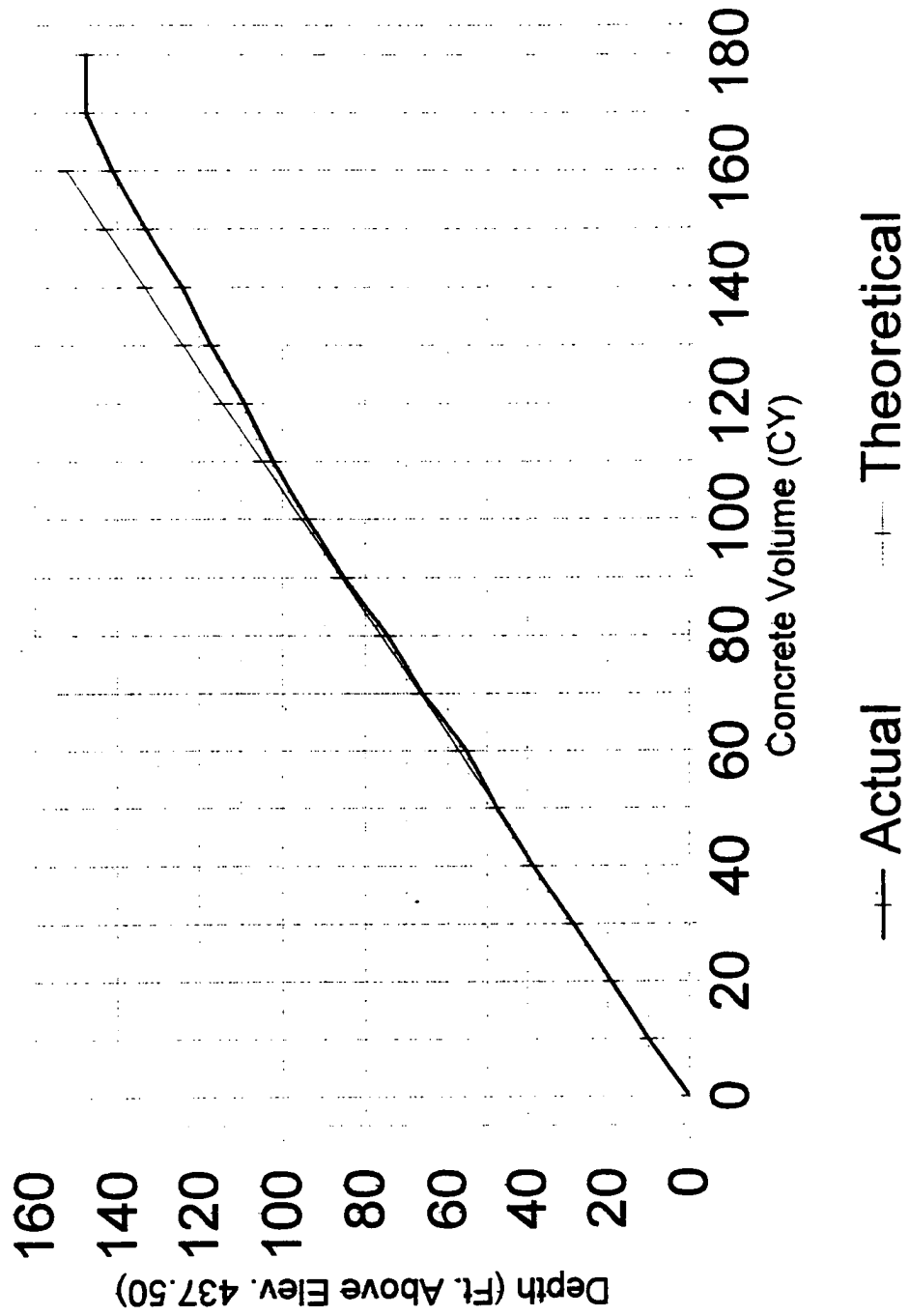




ODOT PROJECT 457-97

### Concrete Curves For Drilled Shaft #7

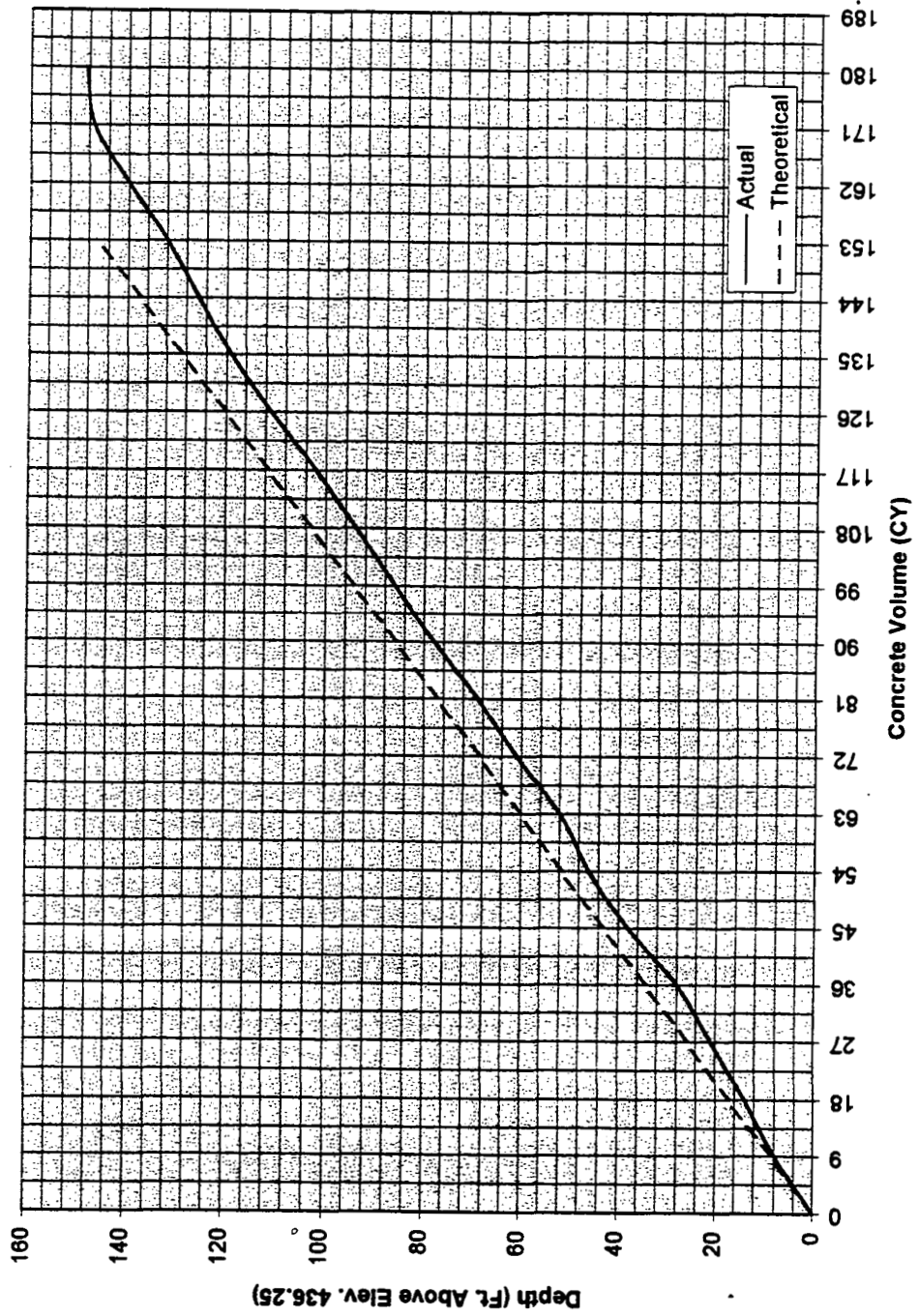
Placed 10/27/98 - 187 CY

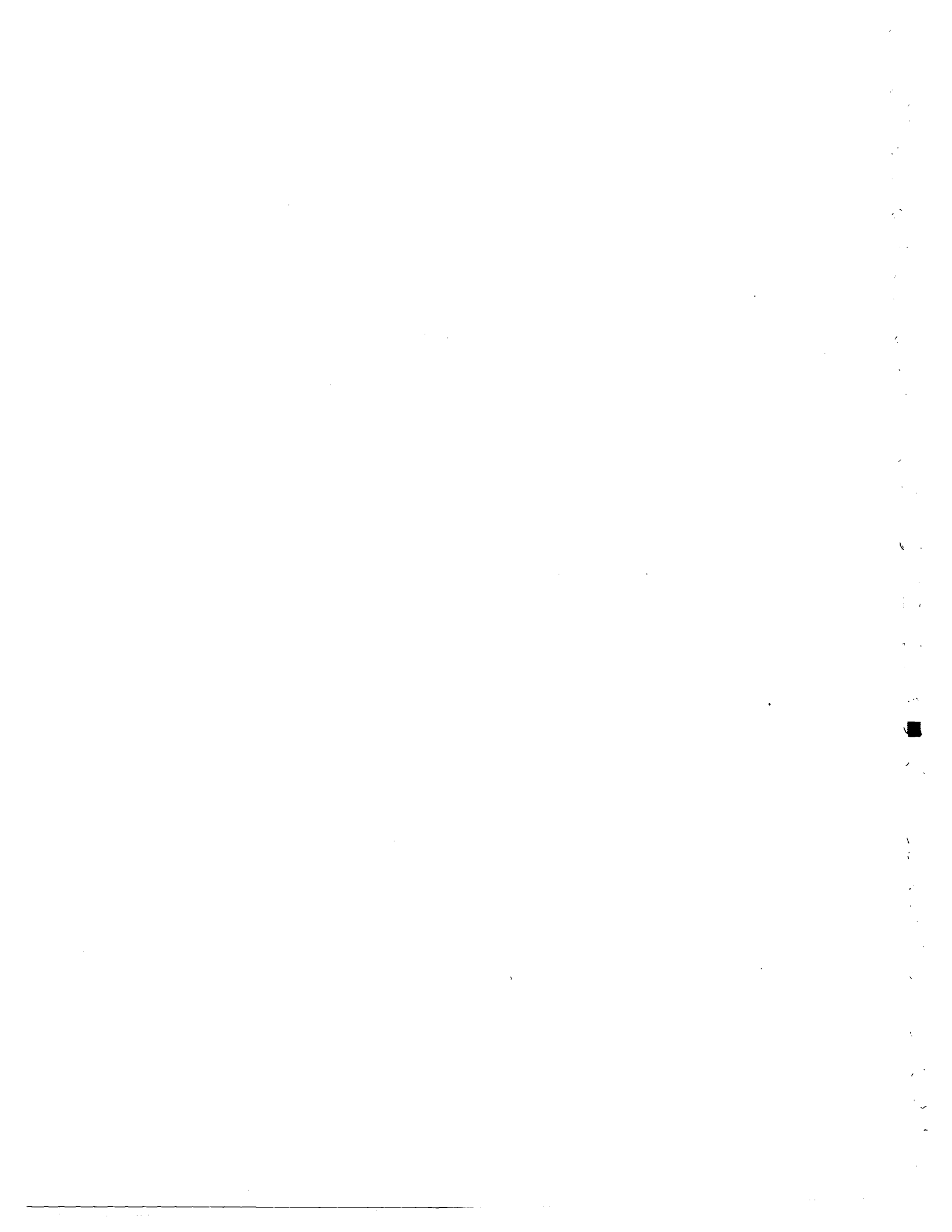




ODOT PROJECT 457-97

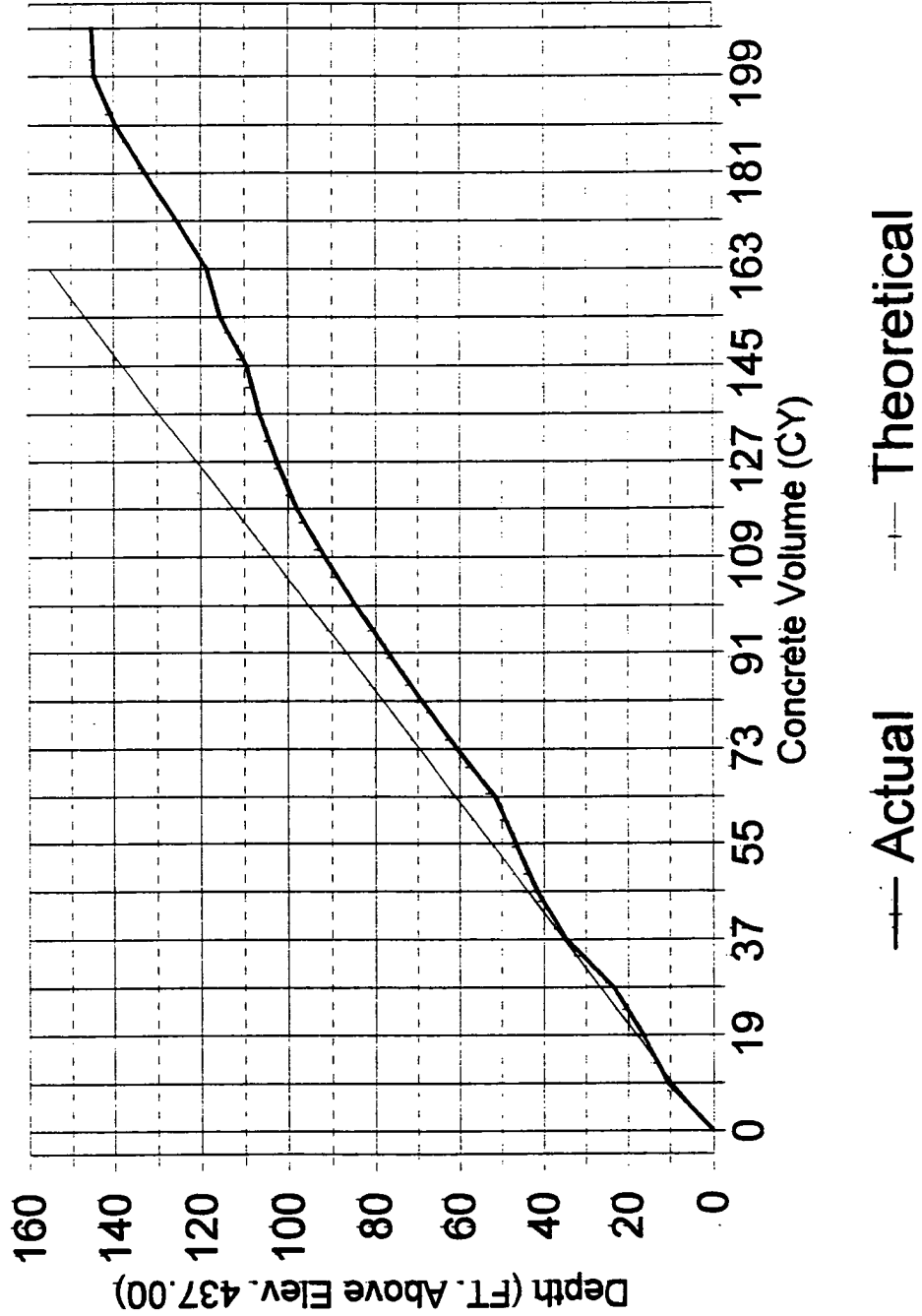
Concrete Curves For Drilled Shaft #8





ODOT PROJECT 457-97

**Concrete Curves For Drilled Shaft #9**  
Placed 11/23/98 - 214 CY

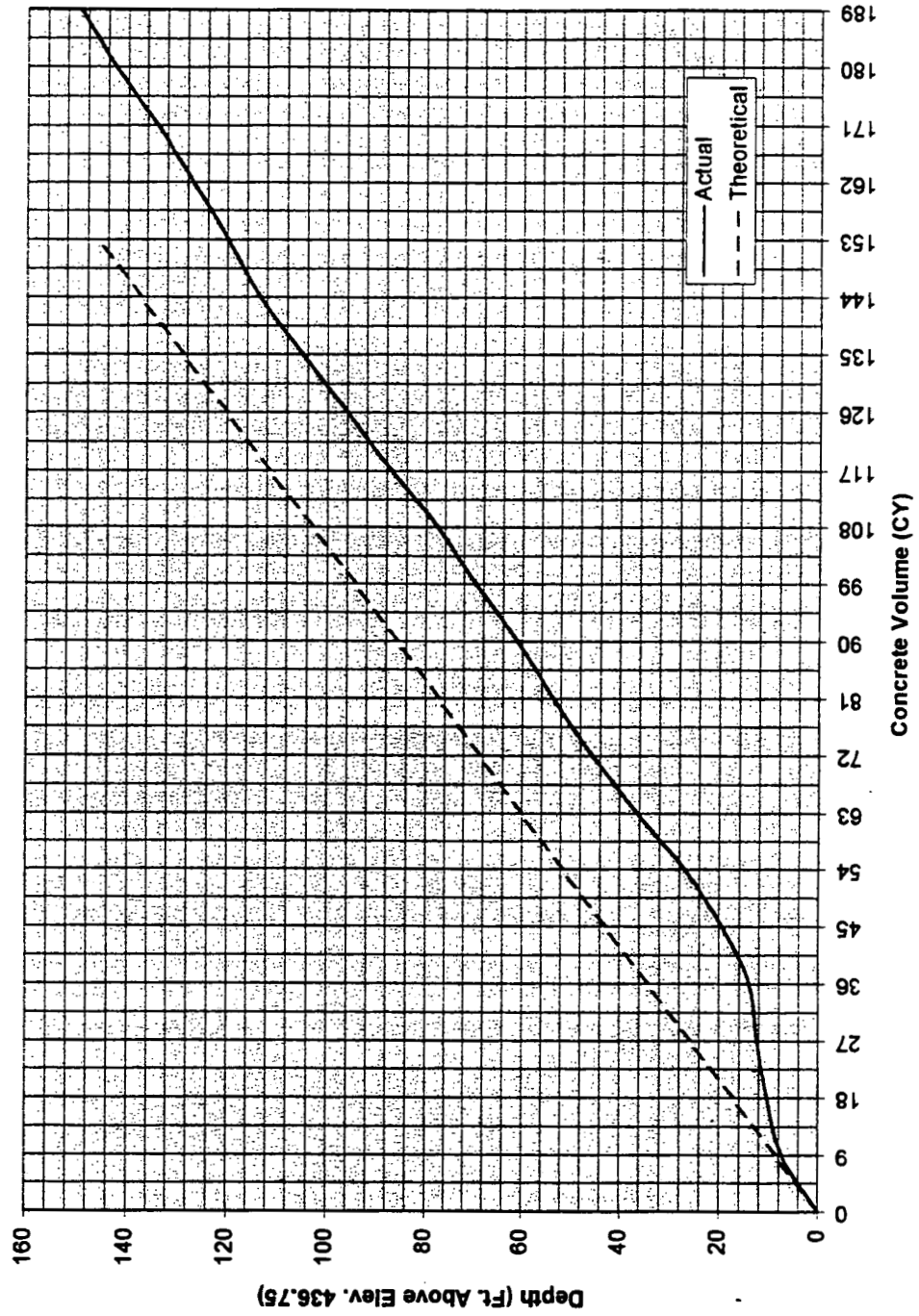


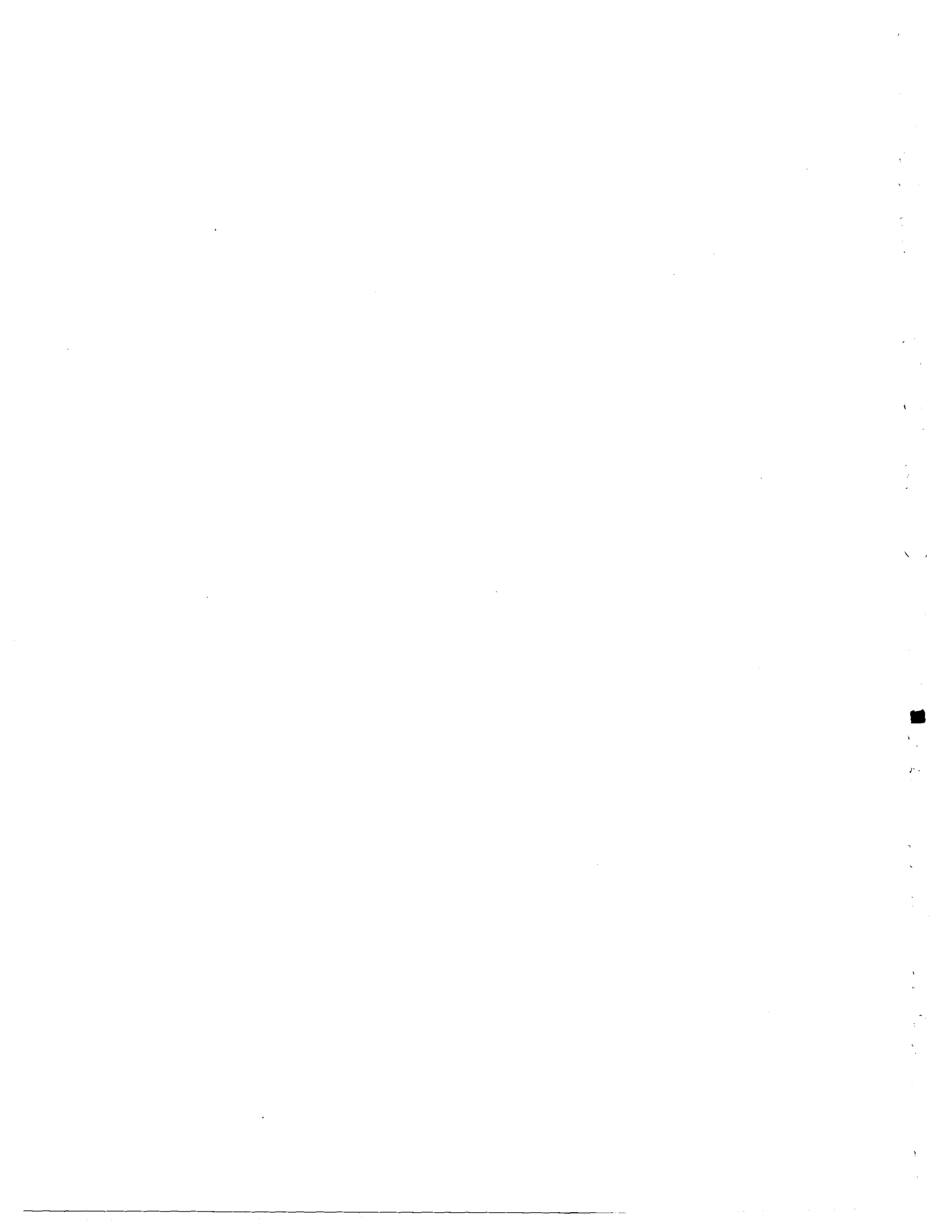




ODOT PROJECT 457-97

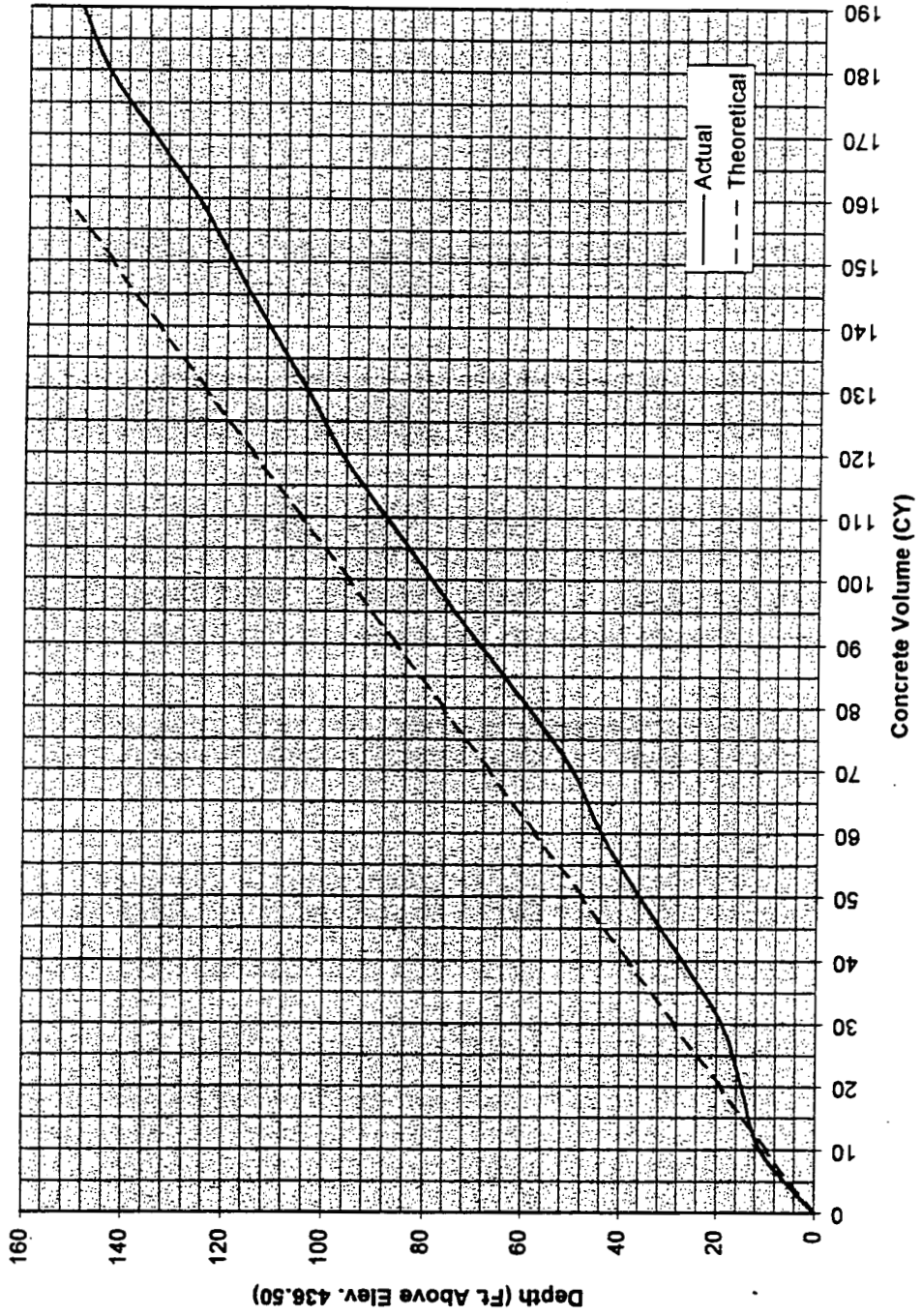
Concrete Curves For Drilled Shaft #10





ODOT PROJECT 457-97

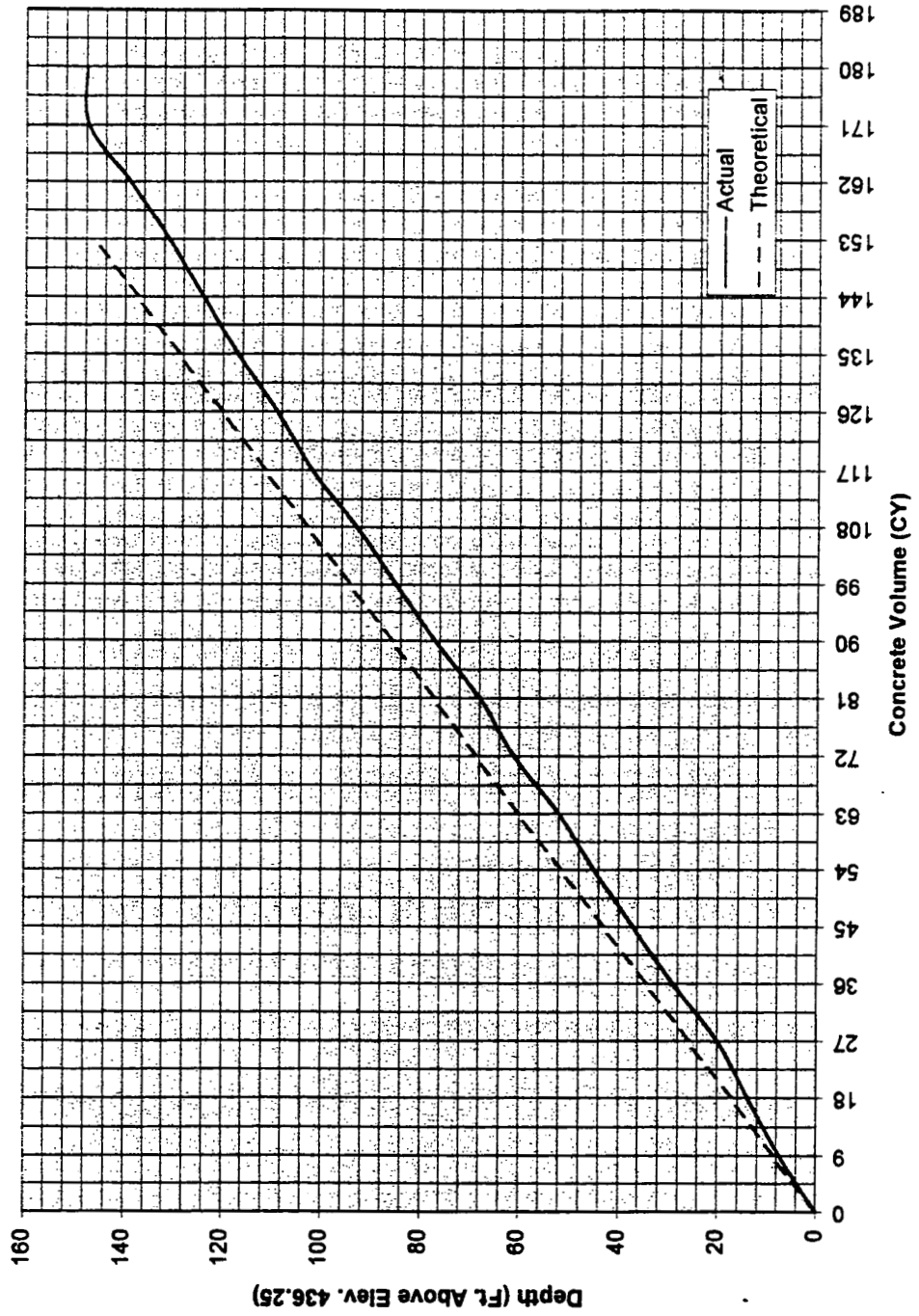
Concrete Curves For Drilled Shaft #11



1  
2  
3  
4  
5  
6  
7  
8  
9  
10  
11  
12  
13  
14  
15  
16  
17  
18  
19  
20  
21  
22  
23  
24  
25  
26  
27  
28  
29  
30  
31  
32  
33  
34  
35  
36  
37  
38  
39  
40  
41  
42  
43  
44  
45  
46  
47  
48  
49  
50  
51  
52  
53  
54  
55  
56  
57  
58  
59  
60  
61  
62  
63  
64  
65  
66  
67  
68  
69  
70  
71  
72  
73  
74  
75  
76  
77  
78  
79  
80  
81  
82  
83  
84  
85  
86  
87  
88  
89  
90  
91  
92  
93  
94  
95  
96  
97  
98  
99  
100

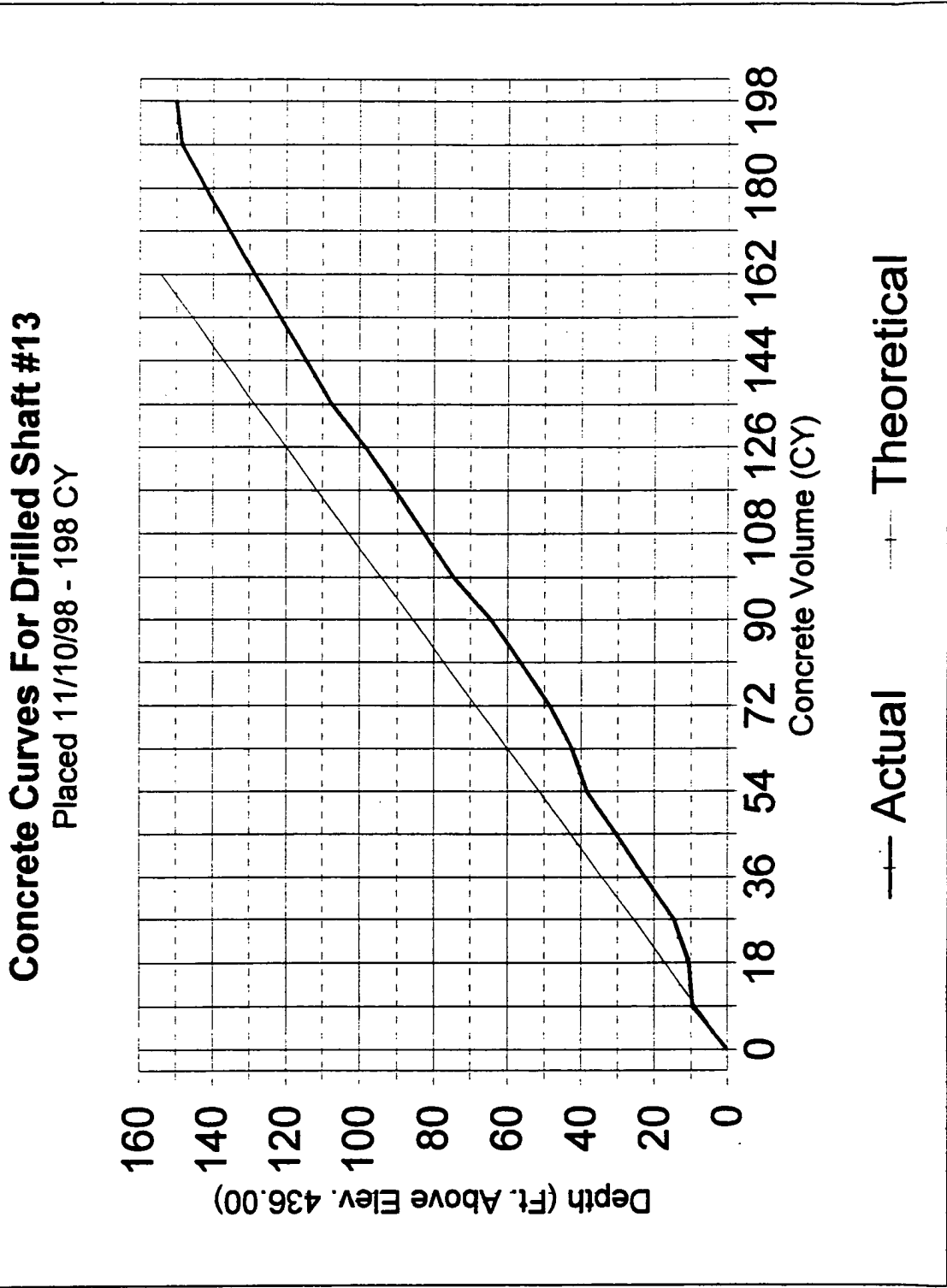
ODOT PROJECT 457-97

Concrete Curves For Drilled Shaft #12





ODOT PROJECT 457-97



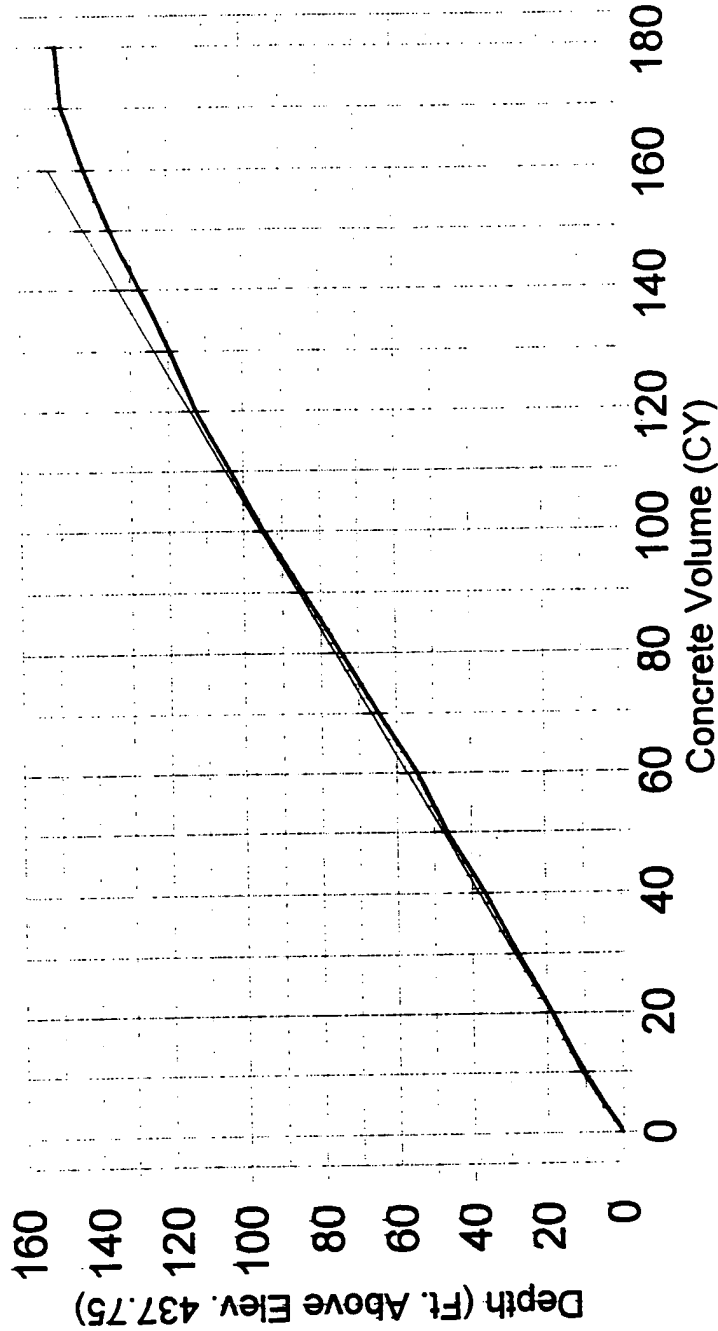




ODOT PROJECT 457-97

### Concrete Curves For Drilled Shaft #14

Placed 10/21/98 - 180 CY



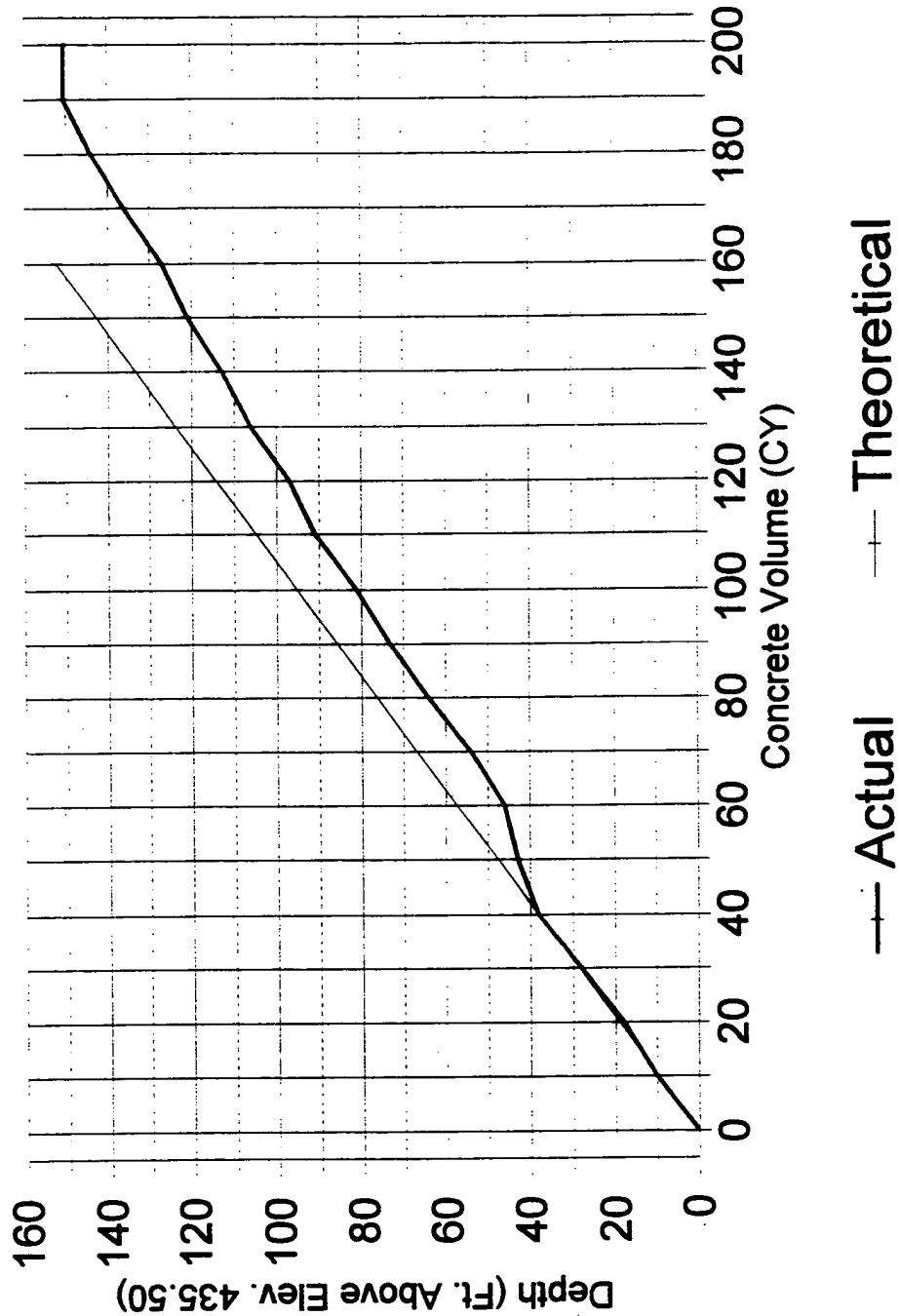
— Actual      - - - Theoretical



ODOT PROJECT 457-97

### Concrete Curves For Drilled Shaft #15

Placed 11/3/98 - 200 CY

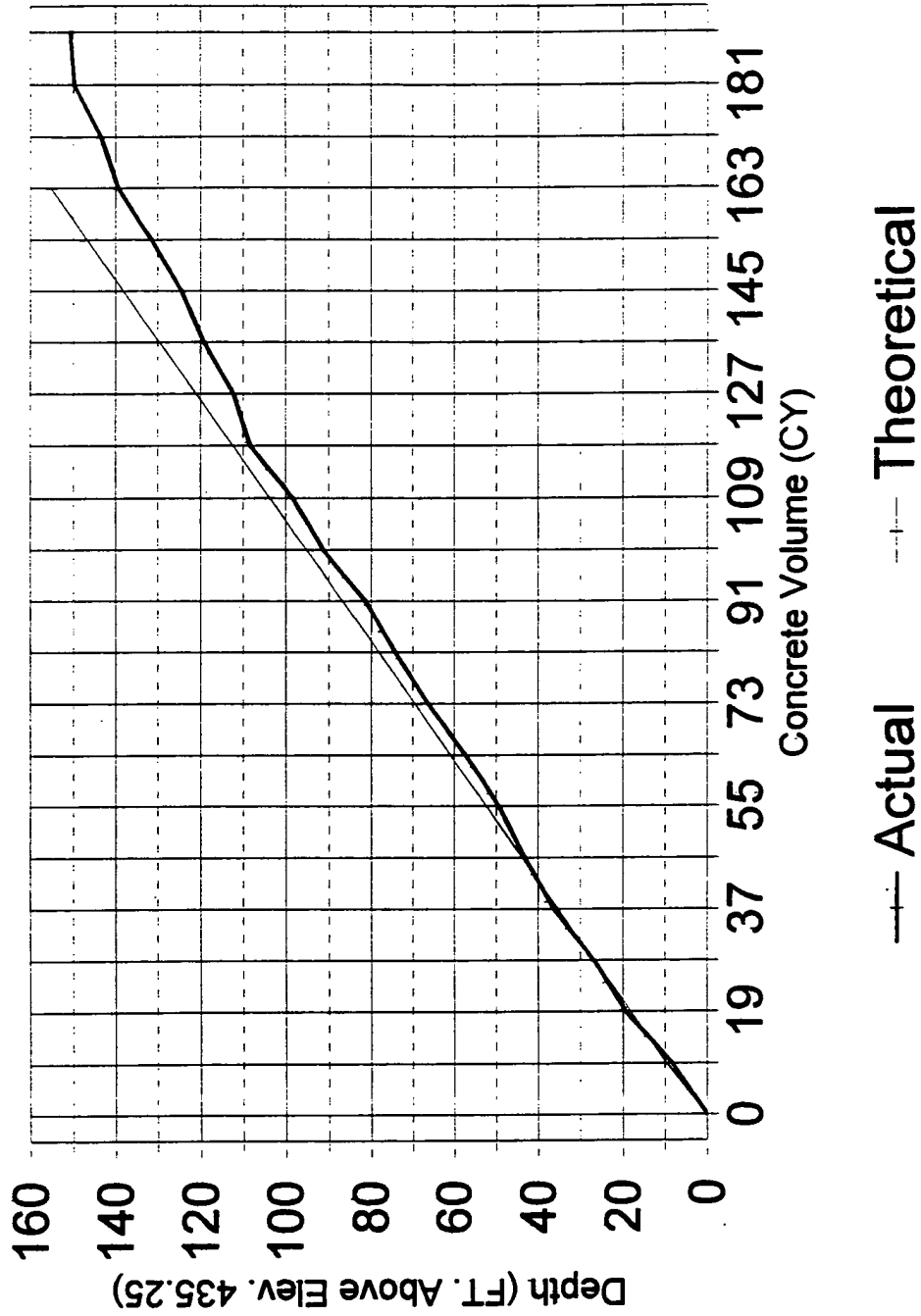




ODOT PROJECT 457-97

### Concrete Curves For Drilled Shaft #16

Placed 11/18/98 - 190 CY

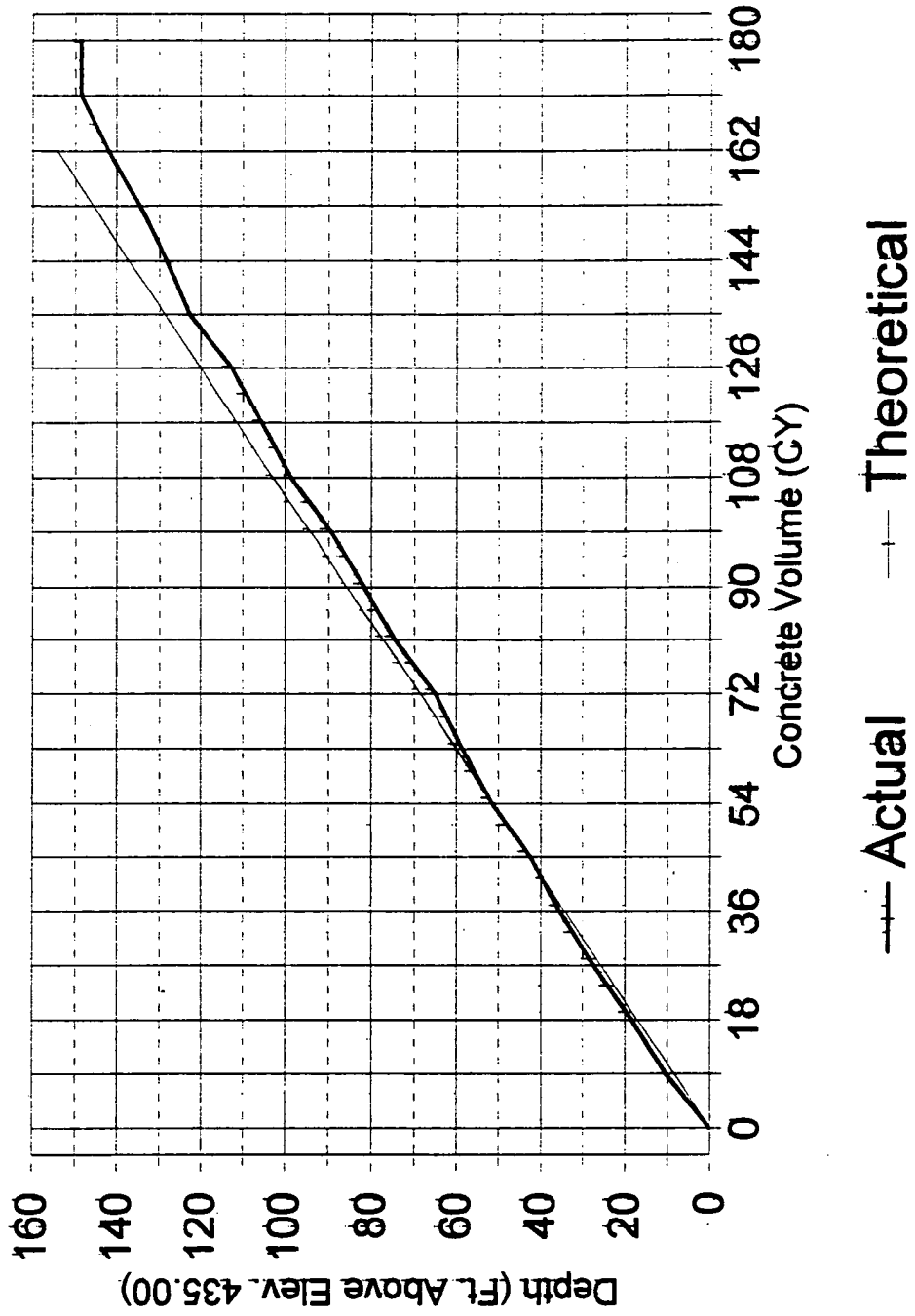




ODOT PROJECT 457-97

### Concrete Curves For Drilled Shaft #17

Placed 11/25/98 - 186 CY







Appendix C: Dynamic test results of Pile # 18.



Project Name : I90  
Pile Name: PN18

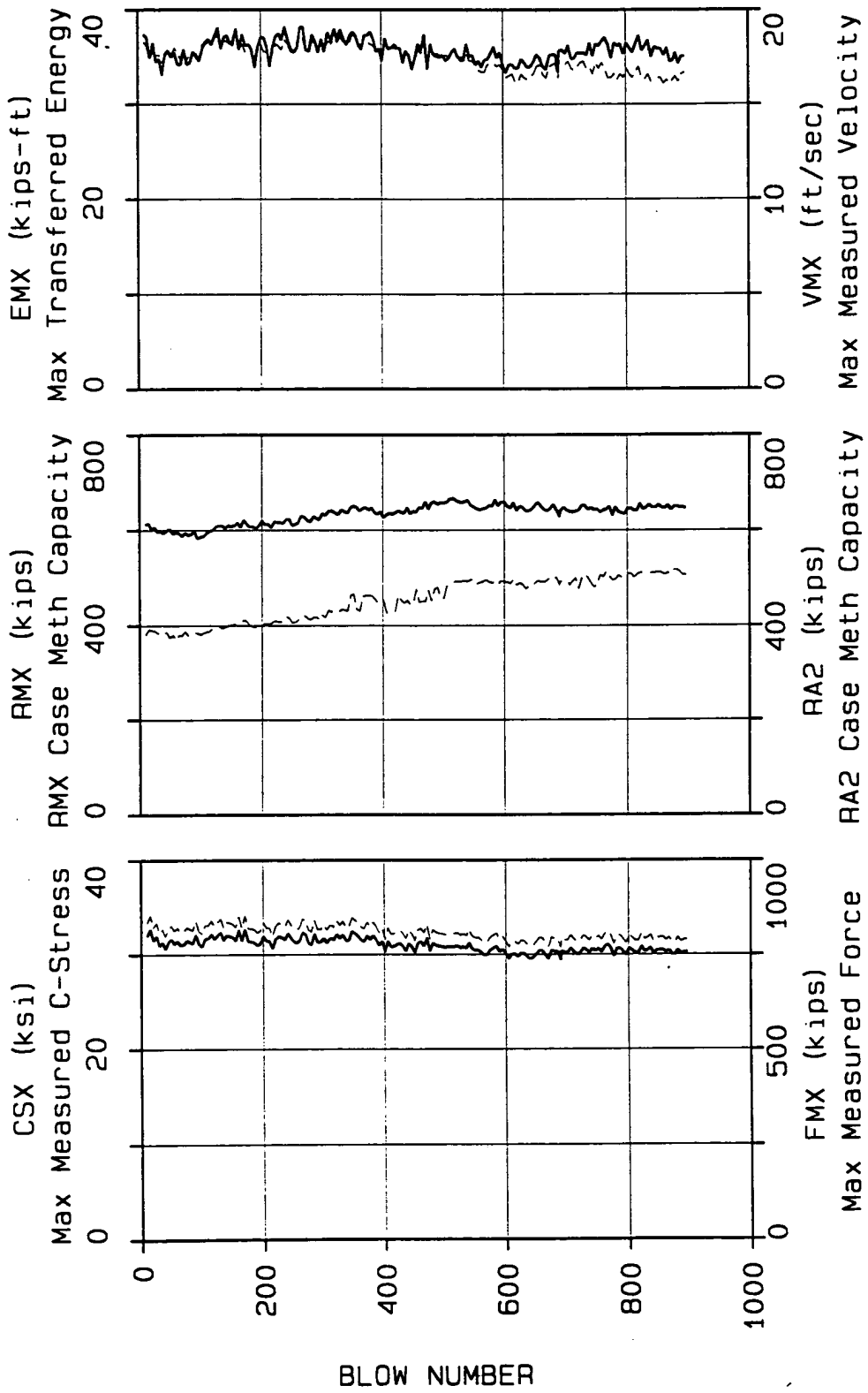
Penetration (ft)	Blow per ft	Penetration (ft)	Blow per ft	Penetration (ft)	Blow per ft
1-10	7	82	24	111	42
11-20	13	88	22	112	46
21-30	68	84	25	113	52
31-35	121	85	23	114	55
36-45	---	86	27	115	53
46-50	63	87	24	116	100
51-55	70	88	26	117	70
56-60	75	89	25	118	53
61	16	90	26	119	63
62	14	91	23	120	58
63	18	92	18	121	65
64	21	99	20	122	58
65	21	94	20	123	60
66	20	95	28	124	55
67	23	96	26	125	55
68	21	97	27	126	56
69	20	98	32	127	51
70	21	99	33	128	54
71	22	100	30	129	55
72	23	101	32	130	55
77	21	102	31	131	73
74	20	103	36	132	72
75	22	104	33	133	82
76	21	105	35	134	94
77	22	106	38	135	98
78	22	107	36	136	120
79	25	108	34	137	152
80	22	109	35	138	182
81	23	110	38	139	22 (0.08ft)



16-Dec-97

OHIO DEPT. OF TRANS.

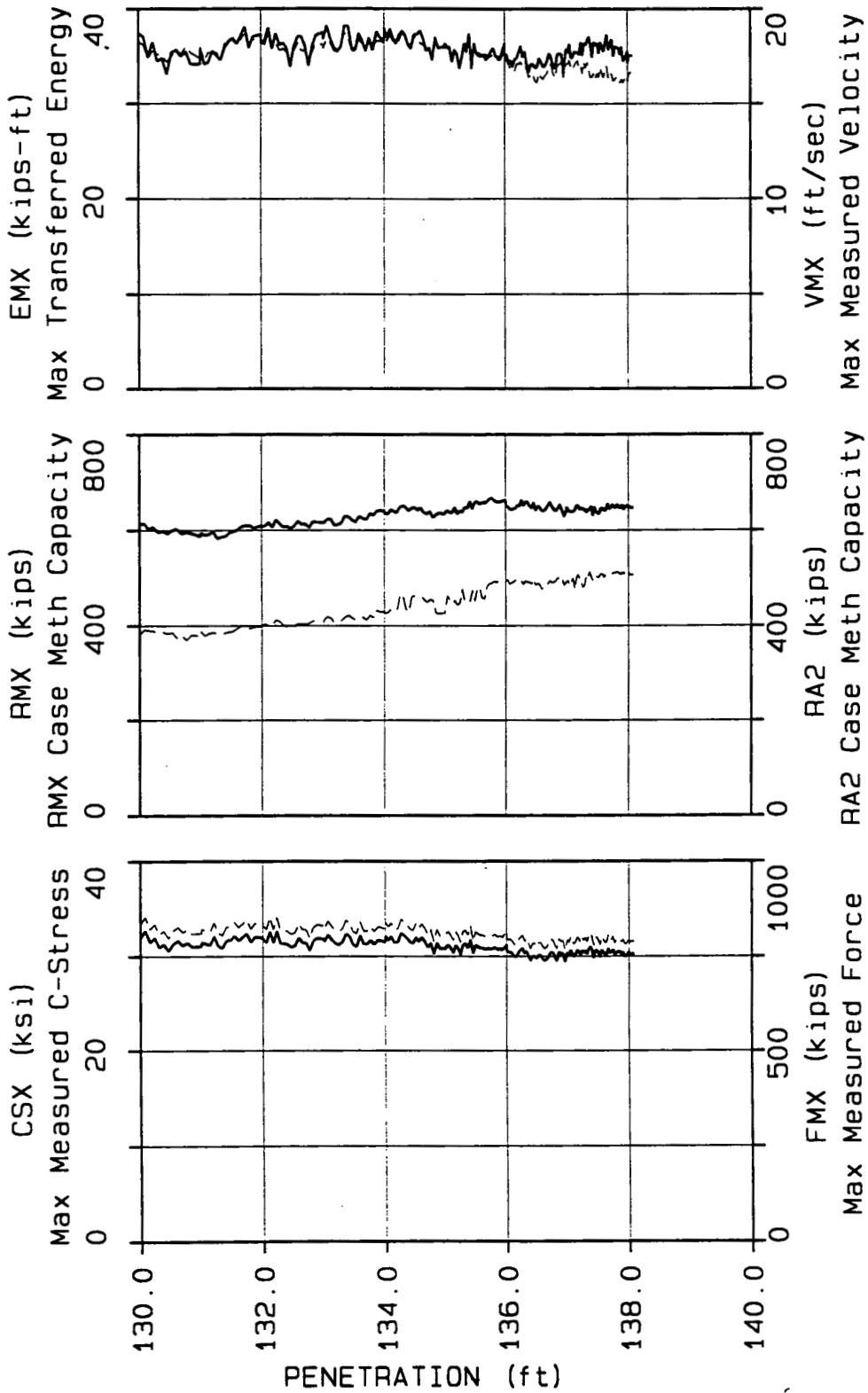
I90, PN18, ICE- 80-S: OED





OHIO DEPT. OF TRANS. 16-Dec-97

I90, PN18, ICE- 80-S: OED







Proj: I90  
 File: PN18  
 Desc: ICE- 80-S:.OED

FileName = PN18.Q00  
 BL# 5 to 895 16-Dec-97

Pg1

CSX: Max Measured C-Stress  
 FMX: Max Measured Force  
 RMX: RMX Case Meth Capacity  
 RA2: RA2 Case Meth Capacity  
 EMX: Max Transferred Energy  
 VMX: Max Measured Velocity

BL#	depth ft	CSX ksi	FMX kips	RMX kips	RA2 kips	EMX kips-ft	VMX ft/sec	BLC bl/ft
5	130.00	31.99	835	609	385	36.5	17.8	0
10		31.99	835	612	381	37.4	18.3	65
15		32.72	854	615	392	37.1	18.1	65
20		31.49	822	602	390	34.9	17.4	65
25		31.99	835	607	389	36.5	17.8	65
30		30.95	808	596	384	34.5	17.6	65
35		31.30	817	599	387	34.8	17.6	65
40		30.57	798	593	383	33.1	17.2	65
45		31.34	818	600	386	35.4	17.5	65
50		31.68	827	603	374	35.7	17.9	65
55		31.14	813	593	380	35.0	17.6	65
60		31.45	821	596	370	35.5	18.0	65
65		30.99	809	594	380	34.2	17.7	65
70	131.00	31.07	811	587	379	34.2	17.4	65
75		31.49	822	595	388	35.8	18.0	75
80		31.34	818	590	379	34.2	17.3	75
85		31.18	814	592	384	34.4	17.7	75
90		32.14	839	598	386	35.6	17.7	75
95		31.11	812	583	384	35.1	17.7	75
100		30.84	805	586	381	34.6	17.4	75
105		31.68	827	588	385	35.9	18.2	75
110		31.72	828	595	387	36.6	18.2	75
115		32.18	840	598	389	36.9	18.3	75
120		31.64	826	601	395	36.3	18.2	75
125		32.03	836	608	399	37.2	18.4	75
130		32.41	846	610	399	38.1	18.7	75
135		31.49	822	610	394	35.9	18.1	75
140		32.06	837	604	397	37.1	18.4	75
145	132.00	31.95	834	610	399	37.3	18.3	75
150		31.83	831	608	401	36.4	18.3	85
155		31.45	821	610	403	36.6	18.1	85
160		32.64	852	616	400	38.0	18.7	85
165		31.45	821	606	402	35.8	17.9	85
170		32.68	853	622	412	37.4	18.2	85
175		31.37	819	614	409	36.2	17.8	85
180		31.37	819	607	401	36.4	17.9	85
185		31.26	816	608	398	35.8	17.7	85
190		30.95	808	603	397	33.9	17.5	85
195		31.14	813	610	401	36.1	17.8	85
200		31.99	835	620	404	37.1	18.2	85
205		31.45	821	612	404	37.1	17.8	85
210		31.41	820	613	403	36.1	17.8	85
215		30.61	799	605	405	34.0	17.2	85
220		31.64	826	618	410	36.1	17.7	85
225		31.95	834	617	409	37.2	18.2	85
230	133.00	31.80	830	616	407	37.5	18.1	85
235		31.57	824	615	411	36.8	17.9	86



Proj: I90  
 File: PN18  
 Desc: ICE- 80-S:. OED

FileName = PN18.Q00  
 BL# 5 to 895 16-Dec-97

Pg2

BL#	depth ft	CSX ksi	FMX kips	RMX kips	RA2 kips	EMX kips-ft	VMX ft/sec	BLC bl/ft
240		32.29	843	623	419	38.2	18.4	86
245		31.76	829	624	416	36.9	18.2	86
250		31.37	819	610	406	35.9	17.8	86
255		31.22	815	612	407	35.5	17.7	86
260		31.53	823	615	411	36.0	18.1	86
265		32.37	845	630	418	38.2	18.7	86
270		32.14	839	628	422	38.2	18.5	86
275		31.22	815	621	416	35.8	17.8	86
280		31.03	810	617	412	35.6	17.7	86
285		32.22	841	629	417	37.4	18.4	86
290		31.30	817	625	418	36.6	18.1	86
295		31.30	817	622	412	35.5	17.9	86
300		31.72	828	635	422	36.9	18.3	86
305		31.22	815	631	417	35.6	17.9	86
310		31.72	828	640	432	37.6	18.3	86
315		31.64	826	641	429	36.9	18.3	86
316	134.00	31.49	822	640	429	36.7	18.2	86
321		32.18	840	636	426	38.0	18.5	100
326		31.72	828	633	427	36.9	18.3	100
331		32.10	838	643	434	37.9	18.6	100
336		31.45	821	639	433	36.9	18.3	100
341		31.49	822	636	431	36.3	18.2	100
346		32.49	848	648	463	37.2	18.3	100
351		32.22	841	651	466	37.7	18.7	100
356		31.95	834	648	435	37.3	18.6	100
361		31.53	823	640	430	36.3	18.3	100
366		31.34	818	646	461	35.8	18.1	100
371		32.03	836	648	463	37.3	18.6	100
376		31.57	824	642	462	37.3	18.3	100
381		32.03	836	647	463	37.7	18.2	100
386		31.57	824	637	456	36.9	18.1	100
391		30.95	808	634	449	35.6	17.9	100
396		31.41	820	639	455	35.9	17.9	100
401		30.22	789	626	453	34.6	17.5	100
406		31.45	821	632	427	37.0	18.3	100
411		30.80	804	636	425	35.9	17.9	100
416	135.00	30.84	805	633	427	36.0	18.0	100
421		31.07	811	637	431	36.1	18.2	124
426		31.22	815	641	463	35.9	18.1	124
431		30.84	805	637	453	36.0	17.9	124
436		30.34	792	636	447	34.4	17.5	124
441		31.18	814	648	453	35.6	17.9	124
446		30.84	805	634	444	35.2	17.6	124
451		30.15	787	640	447	33.7	17.1	124
456		31.22	815	638	476	34.9	17.3	124
461		31.37	819	648	449	36.4	17.9	124
466		30.91	807	646	451	35.7	17.7	124
471		31.80	830	660	451	37.4	18.2	124
476		30.30	791	644	474	33.7	17.3	124
481		31.22	815	658	452	36.4	17.9	124
486		30.99	809	660	477	35.3	17.6	124
491		30.88	806	654	480	35.1	17.7	124



Proj: I90  
 File: PN18  
 Desc: ICE- 80-S:.OED

File Name = PN18.Q00  
 BL# 5 to 895 16-Dec-97

Pg3

BL#	depth ft	CSX ksi	FMX kips	RMX kips	RA2 kips	EMX kips-ft	VMX ft/sec	BLC bl/ft
496		30.84	805	658	458	35.0	17.6	124
501		30.72	802	657	457	35.2	17.5	124
506		30.88	806	659	482	34.6	17.6	124
511		30.76	803	665	488	34.9	17.5	124
516		30.84	805	667	489	35.5	17.5	124
521		30.95	808	662	493	35.9	17.6	124
526		30.68	801	659	491	35.0	17.5	124
531		30.80	804	658	493	34.9	17.3	124
536		30.65	800	660	494	34.9	17.3	124
540	136.00	31.26	816	663	492	36.4	17.8	124
545		30.61	799	653	496	35.1	17.3	151
550		30.42	794	649	496	35.2	17.3	151
555		30.45	795	645	487	34.2	17.1	151
560		30.22	789	642	490	34.6	16.8	151
565		29.92	781	645	492	33.9	16.7	151
570		29.96	782	646	496	34.7	16.7	151
575		30.45	795	652	492	34.8	17.1	151
580		30.68	801	650	489	35.4	17.1	151
585		30.88	806	664	493	36.1	17.2	151
590		30.26	790	651	487	34.9	17.0	151
595		30.53	797	659	494	35.5	17.1	151
600		30.07	785	659	492	34.1	16.8	151
605		29.50	770	650	491	33.3	16.4	151
610		30.03	784	646	488	34.2	16.5	151
615		30.03	784	658	497	34.2	16.6	151
620		29.77	777	641	485	33.8	16.2	151
625		30.15	787	650	489	33.8	16.1	151
630		30.11	786	648	486	34.8	16.6	151
635		29.73	776	640	477	34.4	16.4	151
640		29.50	770	640	482	33.9	16.3	151
645		29.69	775	644	481	34.0	16.5	151
650		30.03	784	652	489	34.5	16.6	151
655		30.45	795	659	494	35.3	17.0	151
660		30.38	793	650	491	34.9	17.1	151
665		29.88	780	643	491	34.0	16.6	151
670		29.50	770	640	495	33.7	16.4	151
675		30.49	796	646	501	35.2	17.0	151
680		30.26	790	654	497	35.3	17.1	151
685		30.30	791	642	501	35.3	17.2	151
690		29.38	767	628	485	33.4	16.4	151
691	137.00	30.38	793	641	492	35.7	17.1	151
696		30.19	788	648	494	35.8	17.1	189
701		30.19	788	642	494	35.4	17.1	189
706		30.68	801	639	485	36.3	17.3	189
711		30.26	790	638	493	34.8	16.9	189
716		29.99	783	639	500	34.9	16.8	189
721		30.15	787	642	477	35.5	17.0	189
726		30.65	800	652	500	35.4	17.2	189
731		30.49	796	652	507	35.5	17.3	189
736		30.15	787	643	500	35.2	16.9	189
741		30.61	799	647	489	36.5	17.0	189
746		30.38	793	643	481	35.1	16.6	189



Proj: I90  
 Pile: PN18  
 Desc: ICE- 80-S:.OED

FileName = PN18.Q00  
 BL# 5 to 895 16-Dec-97

Pg4

BL#	depth ft	CSX ksi	FMX kips	RMX kips	RA2 kips	EMX kips-ft	VMX ft/sec	BLC bl/ft
751		30.61	799	644	485	36.4	17.2	189
756		30.22	789	637	506	36.2	16.9	189
761		30.80	804	642	502	36.7	17.2	189
766		31.07	811	644	513	37.1	16.9	189
771		30.68	801	650	503	36.3	16.4	189
776		29.80	778	630	495	34.9	16.4	189
781		30.61	799	649	497	36.5	16.6	189
786		30.65	800	638	505	36.2	16.3	189
791		30.30	791	636	501	36.4	16.6	189
796		29.88	780	634	503	35.3	16.4	189
801		30.68	801	646	509	36.5	16.9	189
806		30.42	794	646	509	36.0	16.6	189
811		30.15	787	641	501	35.5	16.4	189
816		30.15	787	641	507	36.4	16.7	189
821		30.88	806	656	511	37.3	17.0	189
826		30.30	791	644	511	35.7	16.4	189
831		30.45	795	647	511	36.2	16.3	189
836		30.72	802	654	509	36.8	16.6	189
841		30.03	784	648	511	35.0	16.2	189
846		30.42	794	647	511	36.1	16.3	189
851		30.45	795	654	513	35.9	16.4	189
856		30.53	797	648	511	35.9	16.4	189
861		30.19	788	646	507	35.2	16.1	189
866		30.45	795	653	511	36.0	16.3	189
871		29.99	783	642	508	34.5	16.1	189
876		29.96	782	650	517	34.7	16.3	189
880	138.00	30.49	796	651	517	35.5	16.5	189
885		30.03	784	648	513	34.3	16.2	189
890		30.22	789	648	506	35.1	16.6	189
895	138.08	30.26	790	646	507	35.1	16.7	189

STOP: 10:00:13

DRIVE TIME SUMMARY 16-Dec-97

DRIVE TIME SUMMARY 16-Dec-97				DRIVE	WAIT
-----				minutes	----
BN	5 ->	895, START	9:36:10 -> 10:00:03 STOP,	23.88	
-----				Total Time	23.88 minutes 0.00





I90

Pile: PN18 Blow: 890 Data: ICE- 80-S: OED

CAPWAP(R) Ver. 1996-2

CAPWAP FINAL RESULTS

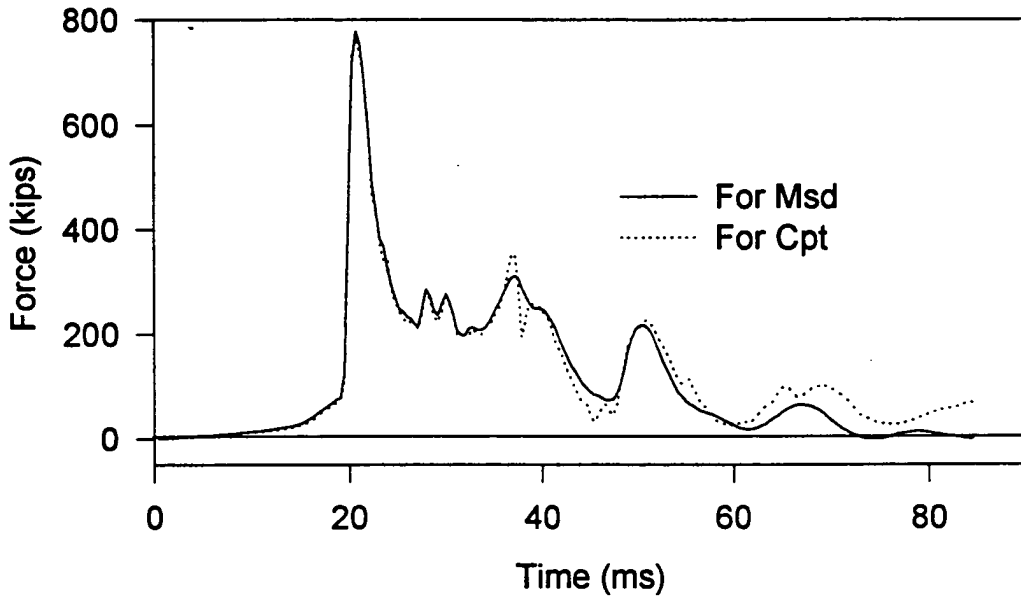
Total CAPWAP Capacity: 635.8; along Shaft 505.3; at Toe 130.5 kips  
 =====

Soil Sgmt No.	Dist. Below Gages ft	Depth Below Grade ft	Ru kips	Force in Pile at Ru kips	Sum of Ru kips	Unit Resist. w. Respect to Depth kips/ft	Resist. Area kips/f2	Smith Factor s/ft	Quake inch
				635.8					
1	10.0	4.0	2.4	633.4	2.4	.36	.08	.116	.200
2	16.7	10.7	3.4	630.0	5.8	.50	.11	.116	.200
3	23.4	17.4	1.8	628.2	7.6	.27	.06	.116	.200
4	30.1	24.1	.1	628.0	7.8	.02	.00	.116	.200
5	36.8	30.8	2.0	626.0	9.8	.30	.06	.116	.200
6	43.5	37.5	4.5	621.5	14.3	.67	.14	.116	.200
7	50.2	44.2	4.8	616.7	19.1	.71	.15	.116	.200
8	56.9	50.9	5.6	611.1	24.7	.84	.18	.116	.200
9	63.6	57.6	9.2	602.0	33.8	1.37	.29	.116	.200
10	70.3	64.3	12.1	589.9	45.9	1.81	.38	.116	.200
11	77.0	71.0	10.3	579.5	56.2	1.54	.32	.116	.200
12	83.7	77.7	5.6	574.0	61.8	.83	.18	.116	.200
13	90.4	84.4	3.2	570.7	65.0	.48	.10	.116	.200
14	97.1	91.1	4.8	566.0	69.8	.71	.15	.116	.200
15	103.8	97.8	8.0	558.0	77.8	1.20	.25	.116	.200
16	110.5	104.5	12.3	545.6	90.1	1.84	.39	.116	.200
17	117.2	111.2	20.0	525.6	110.2	2.99	.63	.116	.200
18	123.9	117.9	33.6	491.9	143.8	5.02	1.06	.116	.200
19	130.6	124.6	62.4	429.6	206.2	9.31	1.96	.116	.200
20	137.3	131.3	119.9	309.7	326.0	17.89	3.76	.116	.200
21	144.0	138.0	179.2	130.5	505.3	26.76	5.63	.116	.200
Average Skin Values			24.1			3.66	.76	.116	.200
Toe			130.5				5.00	.018	.138

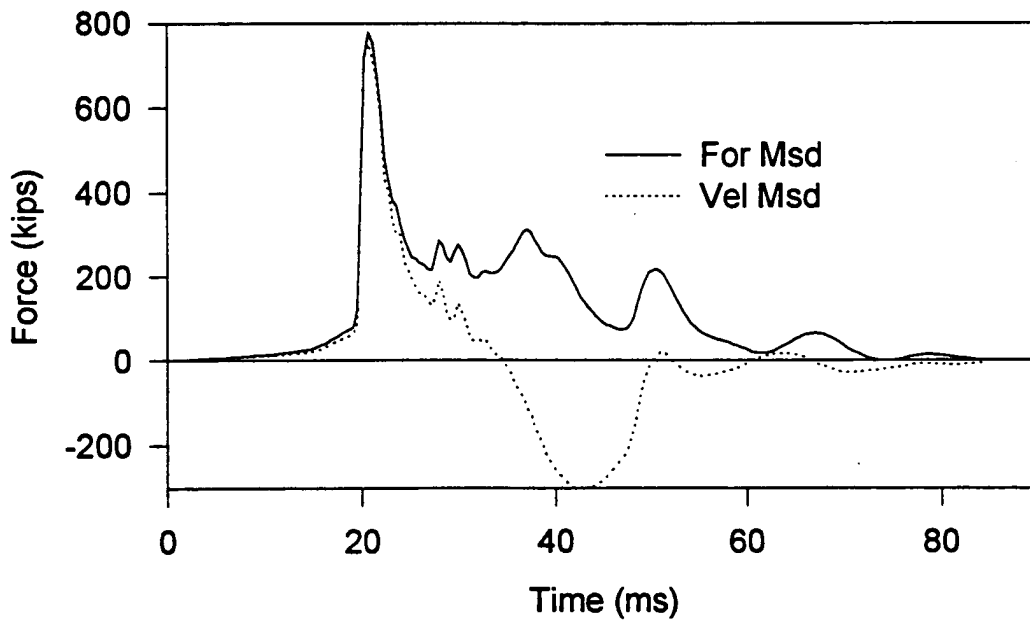
Soil Model Parameters/Extensions

	Skin	Toe
Case Damping Factor	1.264	.050
Unloading Level (% of Ru)	1	
Soil Plug Weight (kips)		.18





**Measured and Computed Force of Pile PN18 ( Blow 890 )**



**Measured Force and Velocity of Pile PN18 ( Blow 890 )**



I90

File: PN18 Blow: 890

Data: ICE- 80-S: OED

CAPWAP(R) Ver. 1996-2

## EXTREMA TABLE

Pile Sgmt No.	Dist. Below Gages ft	max. Force kips	min. Force kips	max. Comp. Stress kips/in2	max. Tension Stress kips/in2	max. Trnsfd. Energy kips-ft	max. Veloc. ft/s	max. Displ. in
1	3.3	773.9	.0	29.652	.000	34.10	16.3	.946
2	6.7	775.7	.0	29.720	.000	34.22	16.2	.934
3	10.0	777.3	.0	29.782	.000	34.11	16.2	.923
4	13.4	772.8	.0	29.610	.000	33.65	16.1	.911
5	16.7	774.5	.0	29.676	.000	33.52	16.1	.899
6	20.1	766.8	.0	29.381	.000	32.91	16.0	.886
7	23.4	767.8	.0	29.419	.000	32.78	16.0	.874
8	26.8	763.4	.0	29.249	.000	32.41	15.9	.861
9	30.1	764.1	.0	29.277	.000	32.28	15.9	.849
10	33.5	765.3	.0	29.323	.000	32.13	15.9	.836
11	36.8	767.2	-3.1	29.394	-.117	31.98	15.8	.823
12	40.2	764.7	-7.4	29.300	-.283	31.54	15.7	.808
13	43.5	767.5	-8.9	29.407	-.341	31.33	15.6	.792
14	46.9	758.9	-8.4	29.078	-.321	30.54	15.5	.775
15	50.2	762.0	-12.6	29.197	-.482	30.27	15.5	.757
16	53.6	753.4	-14.3	28.866	-.548	29.41	15.4	.737
17	56.9	758.7	-16.0	29.068	-.612	29.18	15.3	.721
18	60.3	749.6	-16.3	28.721	-.623	28.35	15.1	.705
19	63.6	756.5	-18.8	28.986	-.721	28.11	15.0	.688
20	67.0	739.9	-19.1	28.347	-.732	26.38	14.3	.669
21	70.3	746.7	-26.5	28.608	-1.015	26.55	14.7	.640
22	73.7	722.3	-28.6	27.674	-1.097	25.01	14.6	.629
23	77.0	727.1	-30.9	27.860	-1.185	24.82	14.4	.614
24	80.4	705.4	-30.5	27.028	-1.170	23.66	14.4	.598
25	83.7	708.7	-38.5	27.155	-1.474	23.44	14.3	.582
26	87.1	698.1	-44.3	26.749	-1.699	22.74	14.2	.566
27	90.4	701.7	-51.4	26.884	-1.968	22.51	14.1	.550
28	93.8	697.9	-56.1	26.739	-2.150	21.99	14.0	.532
29	97.1	702.9	-60.2	26.930	-2.307	21.71	13.9	.514
30	100.5	697.3	-62.8	26.718	-2.406	21.03	13.8	.494
31	103.8	704.3	-70.5	26.986	-2.703	20.70	13.7	.474
32	107.2	693.7	-74.6	26.580	-2.858	19.91	13.5	.458
33	110.5	703.6	-80.2	26.957	-3.073	19.66	13.3	.441
34	113.9	687.6	-79.9	26.344	-3.060	18.62	13.1	.423
35	117.2	702.1	-84.6	26.901	-3.240	18.33	12.8	.404
36	120.6	677.1	-83.1	25.942	-3.184	16.92	12.5	.385
37	123.9	700.1	-86.9	26.825	-3.331	16.59	12.1	.364
38	127.3	661.5	-81.2	25.346	-3.111	14.71	11.5	.344
39	130.6	703.2	-84.5	26.941	-3.239	14.36	10.9	.324
40	134.0	629.8	-72.3	24.131	-2.769	11.71	10.1	.304



I90

Pile: PN18 Blow: 890

Data: ICE- 80-S: OED

CAPWAP(R) Ver. 1996-2

EXTREMA TABLE

Pile Sgmt No.	Dist. Below Gages ft	max. Force kips	min. Force kips	max. Comp. Stress kips/in <sup>2</sup>	max. Tension Stress kips/in <sup>2</sup>	max. Trnsfd. Energy kips-ft	max. Veloc. ft/s	max. Displ. in
41	137.3	647.8	-75.7	24.822	-2.900	11.39	9.5	.285
42	140.7	454.7	-49.7	17.423	-1.905	7.53	10.6	.270
43	144.0	414.8	-47.9	15.892	-1.824	2.37	11.1	.255
Absolute	10.0 123.9			29.782	-3.331	(T= (T=	21.1 ms) 52.8 ms)	

